MONASH University

Optimization of Metabolic Syndrome Induction in Rats for the Investigation of Metabolic Effects and Mechanisms of Ellagitannin Geraniin

Cheng Hong Sheng

Bachelor of Science (Honours)

A thesis submitted for the degree of Doctor of Philosophy at

Monash University Malaysia in 2018

School of Science

Copyright notice

ABSTRACT

Metabolic syndrome is characterized by the concomitant manifestation of central obesity, insulin resistance, high blood pressure and dyslipidemia. Its widespread prevalence warrants more effective therapeutic strategies that can simultaneously improve multiple metabolic risks. One candidate is ellagitannin geraniin (or geraniin), which is a polyphenolic compound isolated from the rind of rambutan (*Nephelium lappaceum*). This project aimed to investigate the metabolic effects and possible mechanism of geraniin using diet-induced metabolic syndrome animal models. To induce metabolic syndrome, post-weaning (three-week old) and adult (eight-week old) rats were fed with either control, high-fat or high-fat-high-sucrose diets. A significant interplay between the developmental stages and types of high-calorie diets was noted. Within eight weeks, high-fat diet induced all features of metabolic syndrome in post-weaning rats, but not in adult rats. Compared to high-fat diet, high-fat-high-sucrose diet performed better in terms of metabolic syndrome induction among the adult rats but merely caused increased weight gain and hypertension. Compared to adult rats, post-weaning rats had faster weight gain, more abdominal fat, higher in fasting plasma glucose, increased hepatic steatosis and overexpression of *peroxisome proliferator-activated receptors* (*PPAR*) α and γ genes by more than 14- and 17-fold respectively. Post-weaning rats on high-fat diet was selected as the model for the study of geraniin due to consistent and successful disease induction. The effects of geraniin was compared to tocotrienol-rich fraction isolated from palm oil and metformin. Treatment with geraniin at a daily dosage of 25 mg/kg for four weeks via oral administration (dosage selected based on a pilot study) exhibited remarkable ameliorative effects against multiple metabolic abnormalities. At the end of the four-week treatment, geraniin was found to reduce the central adiposity, systolic and diastolic blood pressure, fasting blood glucose, circulating triglycerides and non-HDL cholesterols besides lowering the severity of hepatic steatosis. The geraniin-dependent reduction of fasting blood glucose was comparable to metformin, although the former failed to improve the fasting glucose tolerance. In terms of the redox homeostasis and inflammatory response, treatment with geraniin effectively normalized the myeloperoxidase activity, advanced glycation end products (AGE) and interleukin-1β in the blood plasma. These benefits were also observed in rats treated with metformin and tocotrienol-rich fraction. The AGE-lowering effect of geraniin was coupled with a 2.7-fold downregulation of *Receptor for Advanced Glycation End Product* (*RAGE*) in the liver and

1.8-fold upregulation of the *endogenous secretory RAGE* (*esRAGE*) genes in the abdominal adipose tissues compared to the rats on high-fat diet, suggesting a potent inhibitory effect on the AGE-RAGE axis. By comparing the hepatic transcriptomes, it was found that geraniin suppressed the expression of genes for lipid and steroid hormone metabolism which were otherwise, overexpressed by chronic high-fat feeding. Geraniin also downregulated numerous nuclear-encoded mitochondrial genes responsible for electron transport chain, respiratory protein complexes, ATP synthase, mitochondrial membrane and matrix. The mitochondrial modulatory effect of geraniin is a novel discovery and could be the primary mechanism for the observed health benefits. In conclusion, supplementation of geraniin mitigated almost all the pathological phenotypes of metabolic syndrome induced by high-fat diet. Such a pleiotropic effect makes it a promising candidate for metabolic syndrome therapy. Future research should focus on the interaction between geraniin, mitochondria and pathogenesis or recovery of MetS.

Publications during enrolment

Accepted/Published Journal Articles

1. Cheng HS, Yaw HP, Ton SH, Choy SM, Kong JMXF, Abdul Kadir K (2016). Glycyrrhizic acid prevents high calorie diet−induced metabolic aberrations despite the suppression of peroxisome proliferator-activated receptor γ expression. *Nutrition* **32**: 995-1001.
2. Cheng HS, Ton SH, Abdul Kadir K (2017). Ellagitannin geraniin: a review of the natural sources, biosynthesis, pharmacokinetics and biological effects. *Phytochemistry Reviews* **16**: 159-193.
3. Cheng HS, Ton SH, Phang SCW, Tan JBL, Abdul Kadir K (2017). Increased susceptibility of post-weaning rats on high-fat diet to metabolic syndrome. *Journal of Advanced Research* **8**: 743-752.
4. Cheng HS, Ton SH, Tan JBL, Abdul Kadir K (2017). The ameliorative effects of a tocotrienol-rich fraction on the AGE-RAGE axis and hypertension in high-fat-diet-fed rats with metabolic syndrome. *Nutrients* **9**: 984.
5. Cheng HS, Ton SH, Abdul Kadir K (2017). Therapeutic agents targeting at AGE-RAGE axis for the treatment of diabetes and cardiovascular disease: A review of clinical evidence. *Clinical Diabetes and Research* **1**: 16-34.

Submitted/Under review Journal Articles

1. Cheng HS, Phang SCW, Ton SH, Abdul Kadir K, Tan JBL (2018). Purified ingredient-based high-fat diet is superior to chow-based equivalent in the induction of metabolic syndrome. *Manuscript submitted for publication*.

Conference abstracts/proceedings

1. Cheng HS, Ton SH, Abdul Kadir K (2016). Metabolic syndrome model in rats: Comparison of different high calorie diets and developmental stages. Poster session presented at *Monash Science Symposium 2016*, 21st to 23rd November, Subang Jaya, Malaysia.
2. Cheng HS, Ton SH, Tan JBL, Abdul Kadir K (2017). Anti-metabolic syndrome and anti-advanced glycation end product properties of ellagitannin geraniin in rats on high-fat diet. Oral session presented at *International Congress of Diabetes and Metabolism*, 28th to 30th September, Seoul, Korea.
3. Cheng HS, Ton SH, Tan JBL, Palanisamy UD, Abdul Kadir K (2018) Hepatic transcriptomics analysis unveiled the mechanism underlying the protective effects of ellagitannin geraniin against lipid dysregulation and hepatic steatosis. Oral session presented at *6th Seoul International Congress of Endocrinology and Metabolism*, 19th to 22nd April, Seoul, Korea.

Thesis including published works declaration

I hereby declare that this thesis contains no material which has been accepted for the award of any other degree or diploma at any university or equivalent institution and that, to the best of my knowledge and belief, this thesis contains no material previously published or written by another person, except where due reference is made in the text of the thesis.

This thesis includes two original papers published in peer reviewed journals. The core theme of the thesis is biochemistry and pharmacognosy. The ideas, development and writing up of all the papers in the thesis were the principal responsibility of myself, the student, working within the School of Science under the supervision of Dr. Joash Tan Ban Lee, Dr. Ton So Ha and Prof. Khalid Abdul Kadir.

The inclusion of co-authors reflects the fact that the work came from active collaboration between researchers and acknowledges input into team-based research.

In the case of Chapter 1 (Section 1.4) and Chapter 2, my contribution to the work involved the following:

Thesis Chapter	Publication Title	Status	Nature and % of student contribution	Co-author name(s) Nature and % of Co-author's contribution*	Co-author(s), Monash student Y/N*
1	Ellagitannin geraniin: a review of the natural sources, biosynthesis, pharmacokinetics and biological effects	Published	80%. Idea conception, data mining, literature review and manuscript writing.	1) Dr. Ton So Ha Idea conception and manuscript proofreading and editing. 10%. 2) Prof. Khalid Abdul Kadir Idea conception and manuscript proofreading and editing. 10%.	No
2	Increased susceptibility of post-weaning rats on high-fat diet to metabolic syndrome	Published	65%. Idea conception, experiment design, data collection, data analysis and manuscript writing.	1) Dr. Ton So Ha Idea conception, experimental design, manuscript preparation and editing. 10%. 2) Prof. Khalid Abdul Kadir Idea conception, experimental design, manuscript preparation and editing. 10%. 3) Dr. Joash Tan Ban Lee Idea conception, data analysis, manuscript preparation and editing. 10%. 4) Ms. Sonia Phang Chew Wen Data collection, manuscript preparation and editing. 5%.	No

I have renumbered sections of submitted or published papers in order to generate a consistent presentation within the thesis.

Student signature:  **Date: 29th May 2018**

The undersigned hereby certify that the above declaration correctly reflects the nature and extent of the student's and co-authors' contributions to this work. In instances where I am not the responsible author I have consulted with the responsible author to agree on the respective contributions of the authors.

Main Supervisor signature: 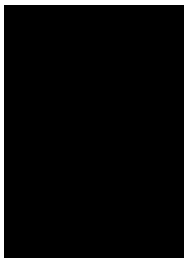 **Date: 30th May 2018**

ACKNOWLEDGEMENTS

The completion of this doctoral dissertation is impossible without the thoughtful assistance and support from many individuals. I hereby would like to express my earnest gratitude and acknowledge all of their contributions.

First and foremost, I would like to express my sincere appreciation to my principal supervisor, Dr. Joash Tan Ban Lee, my former supervisor, Dr. Ton So Ha as well as my co-supervisor, Prof. Khalid Abdul Kadir. Throughout my candidature, my supervisory team has provided unwavering support to my research project. Their timely advice, relentless dedication and extensive scientific knowledge are the key to my accomplishment. I could not have asked for a better supervisory team for my doctorate journey. Their professionalism, strong expertise and positive attitude have also inspired me to be a better scientist and excel at my work.

I would also like to extend my heartfelt gratitude to Assoc. Prof. Uma Devi Palanisamy and her lab members. Their work about ellagitannin geraniin serves as the cornerstone of many aspects of my PhD project. Despite not being a member of my supervisory team, Assoc. Prof. Uma Devi was extremely generous to help me set up many experiments throughout my project.

My genuine thanks also goes to Mr. Andrew Leong Kum Loong, the Principal Technical Officer as well as Mr. Zulkhaili Zainal Abidin, the Technical Officer of the Animal Facility, Monash University Malaysia. Their service and technical support on the animal handling and care have helped me to a remarkably great extent to complete the project. I would also like to acknowledge all the technical officers and lab management office of the School of Science for always being kind and enthusiastic to offer help. I also want to thank the administrative staffs of the School Research Office and School of Science for their outstanding administrative work that has ensured the smooth progress of my PhD candidature.

Next, the project would not be a reality without the funding sources. I would like to gratefully acknowledge the Ministry of Science, Technology and Innovation as well as the School of Science, Monash University Malaysia for the invaluable research funding. I am also very honoured to be a recipient of the Graduate Research Merit Scholarship provided by Monash University Malaysia.

The financial support of the campus has helped me tremendously in the journey to pursue my personal goal to be a scientist.

I am also deeply grateful to all my great lab mates, colleagues and friends; special mention to Mr. Hikari Oh Kan Fu, Ms. Athena Ng Xin Hui, Ms. Janet Tan Jia Yin and Ms. Sonia Phang Chew Wen for being ever-ready to lend a helping hand. Your overwhelming compassion and thoughtfulness to share any information and resources never fail to amaze me. Not forgetting all the interesting discussions, positive encouragement and fun we had throughout my PhD journey, for which I thank you all. Your presence has made my research life more pleasant and enjoyable.

Most importantly, I am forever in debt to all of my family members for their inexhaustible patience, ceaseless support and unconditional love. These are the crucial elements that keep me going for all these times. Thanks for patiently waiting for me to slowly crawl up the "PhD Mountain" and constantly motivating me to move forward. To my lovely sisters, Chia Lea and Chia Fang, you are my best listeners when I need to vent about my stressful work. Also, to my fiancé and true love, Sin Pei, I would like to thank you for being with me through every ups and downs. You are the source from which I draw my strength and happiness during difficult times. I am truly blessed for having all of you in my life.

Last but not the least, I would like to express my most sincere and genuine appreciation to my beloved parents, Mr. Cheng Soo Jin and Mrs. Goh Sei Hwei. I could never come this far without all your sacrifices, nurtures and guidance. Your constant supports and belief in me lay a strong foundation for me to courageously chase my childhood dream. I have no words to express my gratitude and love for both of you. I know I can never repay the slightest bits of your sacrifices and efforts for making me who I am today, but I hope with this doctoral thesis, I can make you proud.

I dedicate this thesis to both of you.

List of Supervisors

Main Supervisor

Dr. Joash Tan Ban Lee
School of Science
Monash University Malaysia
Jalan Lagoon Selatan
47500 Bandar Sunway
Selangor, Malaysia.

Co-Supervisors

Dr. Ton So Ha
School of Science
Monash University Malaysia
Jalan Lagoon Selatan
47500 Bandar Sunway
Selangor, Malaysia.

Professor Khalid Abdul Kadir
Jeffrey School of Medicine and Health Sciences
Monash University Malaysia
Jalan Lagoon Selatan
47500 Bandar Sunway
Selangor, Malaysia.

Table of Contents

List of Tables

List of Figures

Abbreviations

ABTS	2,2'-azino-bis(3-ethylbenzothiazoline-6-sulphonic acid)	**DEG**	Differentially expressed gene
ACE	Angiotensin converting enzyme	***Elovl***	*Elongation of very long chain fatty acids*
Acsl	*Acyl-CoA synthetase long-chain family member*	**eNOS**	Endothelial nitric oxide synthase
Adh7	*Alcohol dehydrogenase 7*	**ERK 1/2**	Extracellular signal-regulated protein kinase 1/2
AGE	Advanced glycation end product	***esRAGE***	*Endogenous secretory receptor for advanced glycation end product*
AMPK	AMP-activated protein kinase	***Fabp***	*Fatty acid binding protein*
ANOVA	Analysis of variance	**FRP**	Ferric reducing power
AOPP	Advanced oxidation protein products	**GLP-1**	Glucagon-like peptide 1
ARB	Angiotensin II receptor blockers	**H&E**	Hematoxylin and eosin
Bac	*β-actin*	**HbA1c**	Glycated hemoglobin A1c
BHA	Butylated hydroxyanisole	**HDL**	High-density lipoprotein
BHT	Butylated hydroxytoluene	**HFD**	High-fat diet
BMI	Body-mass index	**HFSD**	High-fat-sucrose diet
cAMP	Cyclic AMP	**HMG-CoA**	3-hydroxy-3-methyl-glutaryl-coenzyme A
CCB	Calcium channel blocker	**HOMA%β**	Homeostatic model assessment of β-cell function
CD	Control diet	**HOMA%S**	Homeostatic model assessment of insulin sensitivity
CHOP	C/EBP homologous protein	**HPLC**	High performance liquid chromatography
ChREBP	Carbohydrate-responsive element-binding protein	***Hprt1***	*Hypoxanthine phosphoribosyltransferase 1*
CVD	Cardiovascular disease	***HSD17B***	*17β-hydroxysteroid dehydrogenase*
Ddhd1	*DDHD domain containing 1*	**ICAM**	Intercellular adhesion molecule

IDF	International Diabetes Federation	**qPCR**	Quantitative polymerase chain reaction
IL	Interleukin	***RAGE***	*Receptor for advanced glycation end product*
JAK-STAT	Janus kinase-signal transducers and activators of transcription	**RNS**	Reactive nitrogen species
KEGG	Kyoto Encyclopedia of Genes and Genomes	**ROS**	Reactive oxygen species
LCMS	Liquid chromatography mass spectrometry	**rWAT**	Retroperitoneal white adipose tissue
LCMS-MS	Liquid chromatography-tandem mass spectrometry	***SdhA***	*Succinate dehydrogenase complex flavoprotein subunit A*
LDL	Low-density lipoprotein	**SEM**	Standard error of the mean
LXRα	Liver X receptor α	**SHR**	Spontaneously hypertensive rat
MAPK	Mitogen-activated protein kinase	**SPSS**	Statistical Package for the Social Sciences
MetS	Metabolic syndrome	**SREBP**	Sterol regulatory element binding protein
NAFLD	Non-alcoholic fatty liver disease	**StAR**	Steroidogenic acute regulatory protein
NFκB	Nuclear factor κB	**T2DM**	Type 2 diabetes mellitus
Nrf2	Nuclear factor erythroid 2-related factor 2	**TFAM**	Mitochondrial transcription factor A
		TNF-α	Tumor necrosis factor-α
OGTT	Oral glucose tolerance test	**TRF**	Tocotrienol-rich fraction
ORAC	Oxygen radical antioxidant capacity	**UPR^{mt}**	Mitochondrial unfolded protein response
PCA	Principal component analysis	**VCAM-1**	Vascular cell adhesion protein-1
PI3K-Akt	Phosphatidyl inositol 3-kinase-protein kinase B	**VLDL**	Very low-density lipoprotein
PPAR	*Peroxisome proliferator-activated receptor*	**WHO**	World Health Organization

CHAPTER 1

Introduction and Objectives

1. INTRODUCTION

1.1. An Overview of Metabolic Syndrome

Gone are the days when the survival of mankind is constantly challenged by under-nutrition, starvation, pandemics and infectious diseases; in this day and age, the majority of global mortality incidence is inflicted by so-called modern risk factors, namely high blood pressure, tobacco use, high blood glucose levels, sedentary lifestyle and obesity, particularly in developed and developing countries [1]. While obesity has raised much public concern and awareness, another related clinical entity - metabolic syndrome (MetS), has stayed out of the public eye [2, 3]. Essentially, MetS describes a collection of several metabolic anomalies including central obesity, hypertension, glucose intolerance and dyslipidaemia. Such a clustering of symptoms was first reported by a Swedish clinician named Kylin back in 1923, who found the co-occurrence of hypertension, hyperglycaemia and hyperuricemia in his patients [4]. Six decades later, a similar set of metabolic abnormalities have taken different names such as Metabolic Syndrome [5], Syndrome X [6], The Deadly Quartet [7] and Insulin Resistance Syndrome [8]. From late 1990's to 2000's, some of the most notable progresses in the clinical aspects of MetS happened, whereby several international diagnostic criteria were put forth, refined and established so as to better characterize the condition. In the following subsections, we will explore different facets of MetS to understand its current status and highlight the necessity of MetS research.

1.1.1. Clinical definition of metabolic syndrome

Instead of a diagnosis, MetS started as a clinical observation when it was realized that a number of cardiovascular risk factors appeared to co-manifest in individuals with impaired glucose tolerance and type 2 diabetes mellitus (T2DM) [6]. Insulin resistance was believed to be the key component that connected all the risk factors [6]. These risk factors, including hypertension, hyperinsulinaemia, glucose intolerance, increased triglyceride and reduced high-density lipoprotein (HDL) cholesterol, together with central obesity, later became the key hallmarks and diagnostic features of MetS (**Figure 1.1**).

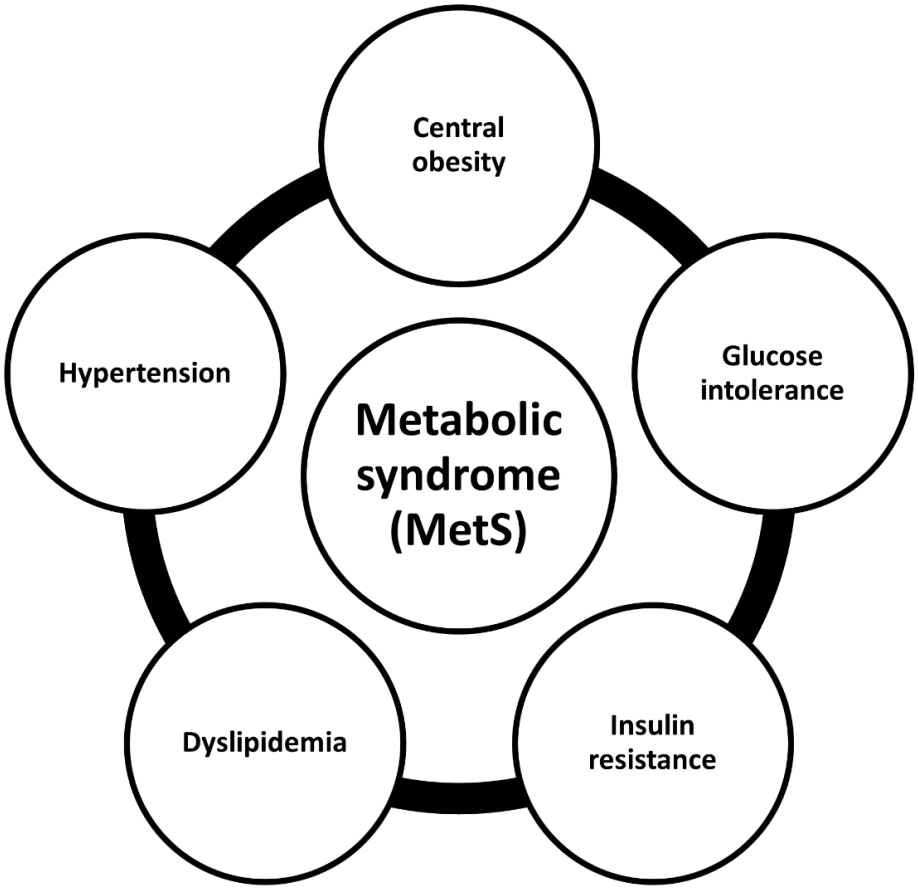

Figure 1.1: Key clinical features of metabolic syndrome.

The first official definition of MetS was published by World Health Organization (WHO) [9]. Subsequently, many international organizations and expert groups which included National Cholesterol Education Program Adult Treatment Panel III (NCEP ATP III) [10], American Association of Clinical Endocrinology [11], International Diabetes Federation (IDF) [12] as well as American Heart Association and the National Heart, Lung, and Blood Institute (AHA/NHLBI) [13] proposed their own or a modified version of diagnostic criteria. There were some disagreements on the cut points between different criteria, but an international collaboration was undertaken to devise a unified criteria for MetS that aimed to resolve discrepancies and facilitate the comparison of epidemiological data based on the same set of diagnostic criteria [14]. The clinical definitions of MetS proposed by different expert groups are summarized in **Table 1.1**. Even though the clinical utility of MetS is not indisputable [15], but increasing evidence suggests strong associations of MetS with various diseases other than CVD and T2DM; thus, highlighting the necessity to recognize individuals with such a risk factor clustering pattern.

Table 1.1: Diagnostic criteria and clinical definitions of metabolic syndrome.

Parameters	WHO (1999) [9]	NCEP ATP III (2001) [10]	AACE (2003) [11]	AHA/NHLBI (2005) [13]	IDF (2005) [12]		Harmonised (2009) [14]
Central obesity	BMI ≥ 30 kg/m^2 and/or	Not applicable			North American, European	Europids*, Middle East, Mediterranean, Sub-Saharan African	Asians, Central and South American
Male	Waist/hip ratio > 0.9	WC ≥ 102 cm		WC ≥ 102 cm	WC ≥ 102 cm	WC ≥ 94 cm	WC ≥ 90 cm
Female	Waist/hip ratio > 0.85	WC ≥ 88 cm		WC ≥ 88 cm	WC ≥ 88 cm	WC ≥ 80 cm	WC ≥ 80 cm
Blood pressure (systolic/diastolic)	≥ 140/90 mm Hg	≥ 130/85 mm Hg	≥ 130/85 mm Hg	≥ 130/85 mm Hg or Rx	≥ 130/85 mm Hg or Rx		
Fasting plasma glucose	IGT, IFG or T2DM	≥ 6.1 mmol/L	IGT or IFG	≥ 5.6mmol/L or Rx	≥ 5.6mmol/L or Rx or T2DM		
Plasma triglycerides	≥ 1.7 mmol/L	≥ 1.7 mmol/L	≥ 1.7 mmol/L	≥ 1.7 mmol/L or Rx	≥ 1.7 mmol/L or Rx		
HDL-C				Rx or	Rx or		
Male	< 0.9 mmol/L	< 1.03 mmol/L	< 1.03 mmol/L	< 1.03 mmol/L	< 1.03 mmol/L		
Female	< 1.0 mmol/L	< 1.29 mmol/L	< 1.29 mmol/L	< 1.29 mmol/L	< 1.29 mmol/L		
Microalbuminuria	Urinary albumin excretion rate ≥ 20µg/min or Albumin: creatinine ratio ≥ 30 mg/g	Not applicable	Not applicable	Not applicable	Not applicable		
Diagnostic criteria	T2DM, IGT and/or IR + any two or more of above	At least three of above	Individuals with risk factors† + at least two of above	At least three of above	Central obesity + any two or more of above		At least three of above

* For Europids or Caucasians, an increased risk of cardiovascular disease and diabetes mellitus occurs at waist circumferences of ≥ 94 in men and ≥ 80 cm in women, but the risk increases substantially at ≥ 102 cm in men and ≥ 88 cm in women. The latter thresholds are more commonly adapted in North American and European countries.

† Risk factors includes the following:

- Diagnosed with CVD, hypertension, PCOS, NAFLD or acanthosis nigricans; family history of T2DM, hypertension or CVD; history of gestational diabetes or glucose intolerance; non-Caucasian; sedentary lifestyle; overweight (BMI>25 kg/m^2); age > 40 years

BMI, body mass index; CVD, cardiovascular disease; HDL-C, high-density lipoprotein cholesterol; IFG, impaired fasting glucose; IGT, impaired glucose tolerance; IR, insulin resistance; NAFLD, non-alcoholic fatty liver disease; PCOS, polycystic ovarian syndrome; Rx, on medication; T2DM, type 2 diabetes mellitus; WC, waist circumference

1.1.2. Epidemiology and associated health risks of metabolic syndrome

According to Kaur (2014), the global prevalence of MetS could vary from <10% to as much as 84%, depending on the demographic variables of the studied population [16]. Nonetheless, most developing and developed countries reported a nationwide prevalence of about 20% to 30% among the adult population [17-19]. This is also in line with IDF's estimation which outlines that about a quarter of the world's adults have MetS [20]. What is worth mentioning is that the statistic is more than 10 years old. In fact, the prevalence of MetS has been escalating steadily in countries like India [21], China [22], South Korea [23] and the United States [24]. Therefore, the old statistic is likely to be an underestimation to the current state of MetS. Notwithstanding, MetS is undoubtedly a serious, ever-growing health concern around the world.

In Malaysia, MetS is also a dire health issue. Based on the IDF definition of MetS [12], close to two in every five Malaysian adults (37.1%) are affected by the condition [25]. It was a 14% increase compared to another study which reported a prevalence of 22.9% merely four years earlier [26]. Such a dramatic increment over a relatively short period of time suggests that the disorder is rapidly becoming out of control. The high incidence of MetS is also in concordant with the high prevalence of obesity. A recent nationwide survey reported that approximately half of the Malaysian adults are overweight while up to one fifth are obese [27, 28]. This means that more than 10 million Malaysian citizens are prone to obesity-/MetS-related complications. Such alarming trends clearly warrant immediate attention and drastic measures to contain and address the issues.

To add insult to injury, the global and local prevalence rates mentioned above exclude children and adolescent incidence, rendering the estimates unable to reflect the actual severity of the disorder. As a matter of fact, the prevalence of childhood obesity has also been rising steadily since 1980. As of 2013, roughly 13% of the children and adolescents worldwide (<20 years old) were overweight [29]. Considering the strong association between obesity and MetS, it is anticipated the prevalence of pediatric MetS is growing. However, current epidemiological studies in this aspect is limited. This is probably attributable to the ignorance to the issue and the lack of consensus on the definition of pediatric MetS. In this context, a systematic review of existing studies concluded a global MetS prevalence rate of 3.3% among the pediatric population, but the estimate is accompanied by a large variation, ranging from <1% to >19% [30,

31]. Locally, the predicted childhood MetS prevalence is about 2.6% [32, 33]. One recent study reported an exceedingly high incidence rate at 27.3% among the obese children [34]. Thus, the large discrepancy in the estimated global and local prevalence highlights the importance of more cross-sectional and longitudinal surveys for the determination of the true scenario and clinical relevance of childhood MetS.

1.1.3. Associated health risks of metabolic syndrome

By itself, MetS is simply a constellation of clinical manifestations caused by dysregulated metabolism. What is truly threatening is its association with a wide range of health complications and mortality. Most notably, individuals with MetS are twice more likely to develop CVD and up to 4.5 times more likely to have T2DM [35, 36]. Furthermore, MetS also significantly increases the risk of colorectal cancer in both men and women alike, besides independently enhancing the risk of liver and bladder cancers in men as well as endometrial, pancreatic, postmenopausal breast and rectal cancers in women [37]. Next, microalbuminuria is one of the diagnostic parameters in the earliest clinical definition of MetS. This suggests an adverse effect of MetS on the renal function. Indeed, there is concrete evidence for the strong association between MetS and chronic kidney disease [38]. Considering the high prevalence of obesity, MetS and T2DM in Malaysia, it is understandable why the prevalence of end stage renal disease is projected to double from 0.12% in 2015 to 0.26% in 2040 [39].

Apart from the peripheral organs, the central nervous system also appears to be affected by MetS. More explicitly, some studies concluded that MetS is linked to cognitive decline [40] and neurodegenerative diseases, namely Alzheimer's disease [41] and dementia [42]. Although the mechanistic links are unclear, the inflammatory state seems to be a common mediator of both disorders and thus, is postulated to play a crucial role in the crosstalk between MetS and cognitive impairment [43]. Not only is the cognitive function being affected, but MetS may also jeopardize psychological health. Multiple studies have concluded that MetS is a significant predisposing factor for the onset of major depressive disorder [44-46] while the evidence for other mental illnesses is limited. The interplay between MetS with the brain and mental dysfunction is a relatively new field whose pathogenesis is poorly understood. Nevertheless, a reexamination of the concept of MetS may be pertinent by taking the MetS-cognitive and MetS-psychological interactions into consideration to formulate a more comprehensive theory.

Some preliminary data demonstrated that MetS may also compromise reproductive function. In males, MetS tends to diminish semen quality by lowering the concentration, survival rate and motility of sperms [47]. A condition known as hypogonadism (as characterized by reduced total and free circulating testosterone levels) is also more common in men with MetS than those without [48]. On the contrary, elevated testosterone or hyperandrogenism, is observed more often in females with MetS [48]. Although the causation relationship between MetS and hyperandrogenism cannot be affirmed, increased testosterone has been demonstrated to arrest follicle maturation and ovulation [49]. Certain components of MetS, particularly obesity, are also associated with a number of pregnancy complications such as gestational diabetes, pre-eclampsia, preterm birth and perinatal death [50]. It is also becoming increasingly apparent that the nutritional and metabolic status of the mother can profoundly influence fetal growth and the likelihood of newborns to develop chronic diseases later in their lives via a mechanism known as fetal metabolic programming. Essentially, abnormal supply of nutrients during pregnancy, regardless of under- or over-nutrition, is speculated to trigger long-lasting epigenetic remodeling and modifications which affect the appetite control, energy balance regulation, lipid and glucose metabolism of the offspring [51]. Hence, all the evidence strongly accentuates the multifaceted negative effects of MetS on human reproduction.

To summarize, having MetS increases the risks of a wide range of health complications and all-cause mortality rate [35, 52]. Yet, it should be noted that health complications included here are some of the most well-established or most recent findings. The actual risks associated to MetS cannot be exhaustively listed and discussed. The vast variety of comorbidities unmistakably point out the devastating effects of MetS on our health.

1.1.4. Etiology and pathophysiology of metabolic syndrome

Like many chronic diseases, the onset of MetS is essentially governed by two major driving forces: environmental and genetic factors. It is widely believed that the environmental factors, which include sedentary lifestyle and unhealthy dietary behavior, play a predominant causative role. The disastrous health impacts of unhealthy diets have been long-established. According to large-scale studies, western dietary patterns high in processed meat, fried food, sweet and salty snacks is independently associated with increased risks of MetS [53], T2DM and coronary heart disease [54, 55] even after adjusting for other significant risks like demographic factors, smoking

and physical activity. Considering the high lipid and carbohydrate content, a western diet is bound to cause positive caloric balance. When coupled with sedentary lifestyle, even more unused calories are resulted. These excesses are eventually deposited in the body as fats, explaining why unhealthy dietary behavior and physical inactivity are more common in overweight and obese individuals [56]. Despite knowing that unhealthy eating is a major culprit to obesity and MetS, it is often hard to change our food preferences. In this context, recent discovery suggests that gut microbiota could in fact, manipulate our dietary behavior by exerting influences on the reward and satiety pathways, mood and sensory modulation; or even hijacking the vagus nerve to induce a sense of addiction towards certain foods that enhance the microbe fitness [57]. Hence, gut microbes could potentially sway our food preferences in such a way that we are constantly craving for high fat and/or high sugar foods, contributing to overeating and the onset of MetS.

On the other hand, genome-wide association studies allow us to explore the genetic aspects of MetS. Many genetic loci have been identified to link to obesity and phenotypes of MetS, each contributing a small but significant impact [58]. This strongly points out the polygenic nature of the metabolic disorder. Furthermore, the function of the susceptibility genes is also remarkably diverse, ranging from central regulation of food intake, satiety control, cellular growth and proliferation to lipid metabolism [58, 59]. The fact that genes responsible for central appetite regulation are implicated in concordance with the integral role of over-nutrition as the leading etiology of MetS. As such, based on our current understanding, MetS is a complex trait resulted from gene-environment interactions. Future research should aim to delineate these interactions in order to develop more effective strategies that can modify the risk for MetS.

As for the pathophysiology of MetS, an early hypothesis was that insulin resistance is the root cause of MetS [6]. More recent theory sees visceral obesity owing to prolonged over-nutrition, as the primary cause of MetS [60-62]. The latter is now widely accepted because of its coherence to the known etiologies of MetS besides being able to provide plausible explanation to the features and associated complications of MetS. Positive caloric balance, which is a combinatorial output of overeating, sedentary lifestyle and genetic predisposition, will lead to increased body fat. However, not all fat depots are created equal. For instance, compared to the subcutaneous adipose tissues, the visceral adipose tissues play a more proactive role as an endocrine organ to

exert metabolic modulation via the secretion of a wide variety of adipocytokines [63]. Abnormal adipocytokine secretion occurs when visceral adipocytes start to become enlarged (hypertrophy) due to chronic lipid influx. In this case, various detrimental adipocyte factors that can induce pro-inflammation, pro-thrombosis, vasoconstriction and insulin resistance are hyper-secreted while beneficial adipokines, most notably adiponectin, are markedly reduced [64]. Moreover, hypertrophic visceral adipose tissues are insensitive to insulin action and so, releasing more free fatty acids into the circulation which are known to cause hyperlipidemia and peripheral insulin resistance [65, 66]. Together, these pathological conditions of visceral adipose tissues observed in abdominal obesity are termed "adiposopathy" [61].

The deranged metabolism is further aggravated by the accumulation of lipids at atypical organs such as the liver, skeletal muscles, surrounding the heart or even the kidneys. Such an ectopic deposition of fats is attributable to the saturation of lipid storage at the adipose tissues and outflow of free fatty acids [67]. Hepatic and muscular intracellular lipid accumulation can induce local insulin resistance [68]. This directly impairs their ability to regulate circulating glucose and lipids, leading to chronic hyperglycemia and dyslipidemia. In the circulation, the aggregation of by-products and intermediates of lipid and glucose metabolites exacerbates oxidative stress and activates signaling cascades that ultimately lead to vascular damage and atherosclerotic processes [69]. Prolonged hyperglycemia also creates a hostile and stressful environment which compels the pancreatic β-cells to undergo dedifferentiation and revert to non-insulin-producing progenitor-like cells [70]. Over time, this will lead to insulin insufficiency and render the glucose level even more dysregulated. Conversely, intramyocardial ectopic fats are found to disrupt the heart structural integrity [71] whilst lipid accumulation in the renal sinus is associated with hypertension and chronic kidney disease [72], leading to heart and kidney failure, respectively. In short, ectopic fat depots bring about the devastating local and systemic effects that are consistent with the features of MetS. Hence, it is believed that this hypothesis underpins the true pathogenesis of MetS (**Figure 1.2**).

In summary, this section provides an overview about the history, diagnosis as well as the causes and effects of MetS. Existing epidemiological evidence strongly points out widespread prevalence of MetS all over the globe. Coupled with the chronic adverse health complications, MetS will cripple the economy, healthcare system and society in the foreseeable future. Thus,

further research about MetS is not only justified, but also absolutely imperative for us to devise more effective therapeutic and preventive strategies to combat the issues.

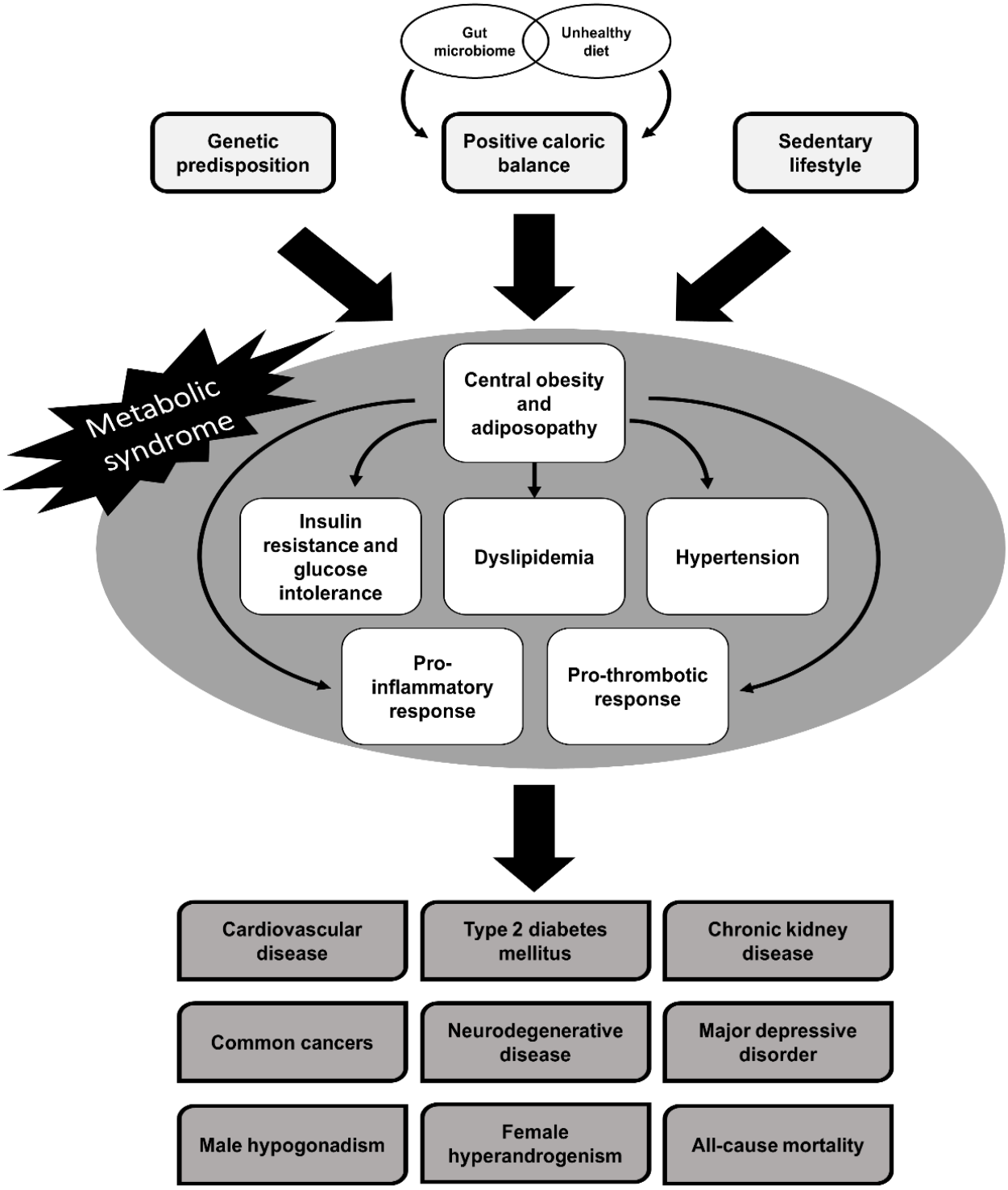

Figure 1.2: Etiology, pathophysiology and complications of metabolic syndrome.

1.2. Clinical Interventions of Metabolic Syndrome

Despite being promoted to a clinical entity for close to two decades, MetS is not very well embraced by a considerable portion of the medical community. One reason could be that the awareness of MetS is lacking, even among medical personnel [2, 3, 73]. However, strong linkages have been found between MetS with multiple chronic diseases. This strongly supports the necessity to diagnose and treat MetS as a whole. Therefore, this section will elaborate on the existing and prospective therapeutic strategies of MetS.

1.2.1. Conventional therapeutic approach of metabolic syndrome

The primary goal of MetS therapy is to prevent or delay the onset of T2DM and CVD. Considering the huge influence unhealthy dietary behavior and physical inactivity, lifestyle modification with a weight reduction goal often serves as the first-line intervention in premorbid individuals with MetS. For overweight people, the aim is to reduce body weight by 7% to 10% from baseline within six to 12 months via a combination of caloric restriction and increased physical activity [13]. A daily, moderate-intensity exercise session that lasts for 30 minutes is highly encouraged [74]. This should be accompanied by a reduction in calorie intake by 500 kcal to 1000 kcal per day to facilitate the utilization of the stored fats. In terms of the food choices, diets which are low in saturated fats, cholesterol, sodium and simple sugars while high in fruits, vegetables and whole grains are recommended. Different types of diets, namely low-carbohydrate, low-fat, Mediterranean and low-glycemic load regimens, have been suggested to confer weight-reducing effects. However, Wadden et al. (2012) concluded that the key determinant of weight loss is the calorie content instead of the macronutrient composition [75]. Hence, the choice of a diet should be based on the patient preference and compliance to ensure long term weight control.

Generally, MetS is considered as a premorbid condition in which pharmacological intervention is not indicated. However, in cases where intensive lifestyle modification fails, or when an individual has other pre-existing metabolic comorbidities, pharmacotherapy is needed. This means that the pharmacotherapy is initiated only when one or more risk factors have reached a true pathological level and so, the cut points are relatively higher compared to that of MetS (**Table 1.2**). Furthermore, the risk factors are treated independently. For example, a MetS patient

with an overly high circulating low-density lipoprotein (LDL)-cholesterol but borderline glucose and blood pressure levels do not require any treatment other than cholesterol-lowering medications. Such a therapeutic strategy also undermines the clinical utility of MetS because the diagnosis rarely modifies the treatment plan.

For adults, the most common pharmacological interventions for the risk factors of MetS is summarized in **Table 1.2**. Statins, or 3-hydroxy-3-methyl-glutaryl-coenzyme A (HMG-CoA) reductase inhibitors are used as the first-line cholesterol-lowering intervention. They are also often used in combination with fibrates, which are potent peroxisome proliferator-activated receptor (PPAR)-α, to treat hypertriglyceridemia [76]. On the other hand, there is no consensus on the first-line therapy for hypertension. Monotherapy with either diuretics, angiotensin converting enzyme (ACE) inhibitors, angiotensin II receptor blockers (ARBs) or calcium channel blockers (CCBs) are the primary choices [77] while anti-diabetic treatment is routinely initiated with metformin [78]. Combined therapy is not unusual to maintain the blood pressure and glucose targets in a long run.

Table 1.2: Criteria and pharmacotherapy for different risk factors of metabolic syndrome.

Risk factor	Components	Cut point	Types of Drugs
Atherogenic dyslipidemia	LDL-cholesterol	• High-risk patients >2.6 mmol/L • Moderate-risk patients > 3.4 mmol/L • Low-risk patients > 4.9 mmol/L	• Statins (first-line) • Fibrates • Nicotinic acid • Combined therapy of statin and fibrate/nicotinic acid
	Non-HDL-cholesterol*	• High-risk patients >3.4 mmol/L • Moderate-risk patients > 4.1 mmol/L • Low-risk patients > 4.9 mmol/L	
Elevated blood pressure	Systolic /diastolic blood pressure	• Without diabetes > 140/90 mm Hg • With diabetes > 130/80 mm Hg	• ACE inhibitors • ARBs • Diuretics • CCBs • β-blockers • Combined therapy
Elevated glucose	HbA_{1c}	> 6.5%	• Biguanides (first-line) • Sulphonylureas • Meglitinides • α-glucosidase inhibitors • TZDs • DPP4 inhibitors • SGLT2 inhibitors
	Fasting glucose	> 7.0 mmol/L	
	2-hr OGTT	> 11.1 mmol/L	

Prothrombotic state	-	When a patient is considered high risk for CVD.	• Low-dose aspirin

* Non-HDL-cholesterol is a secondary target. When the triglycerides > 5.65mmol/L or when the primary target (LDL-cholesterol) has been achieved but triglycerides > 2.26 mmol/L, the non-HDL-cholesterol level should be maintained within the goal.

ACE, angiotensin converting enzyme; ARB, angiotensin II receptor blocker; CCB, calcium channel blocker; CVD, cardiovascular disease; DPP4, dipeptidyl peptidase-4; HbA_{1c}, glycated hemoglobin A1c; HDL, high-density lipoprotein; LDL, low-density lipoprotein; OGTT, oral glucose tolerance test; SGLT2, sodium-glucose transport protein 2; TZD, thiazolidinedione

Information extracted from [13]

Even though such a treatment strategy has been proven very effective at reducing the risk of MetS-associated complications, it is accompanied by several drawbacks. Firstly, polypharmacy can have drug-drug interaction that exacerbates their adverse effects. Furthermore, patients are also less inclined to adhere to the treatment plan with the use of polypharmacy [79]. Collectively, these could lead to treatment failure, disease progression and hospitalization due to acute complications. It may be added that not all the aforementioned drugs are approved for use in pediatric patients because their safety profiles among the children and adolescents are not well-understood. Therefore, the long-term safety and effectiveness of conventional therapy among the pediatric population warrant further investigation. In summary, lifestyle modification together with polypharmacy is widely employed to treat MetS patients with high risk for CVD and T2DM. However, it is also associated with notable shortcomings besides being unable to address one of the key underlying pathology: abdominal obesity. Newer therapeutic strategies have been proposed to address some of these limitations.

1.2.2. Recent clinical advancements in metabolic syndrome therapy

Since the ectopic fat deposition plays an integral role in the pathogenesis of MetS (**Section 1.1.4**), alleviating abdominal obesity could potentially reverse the metabolic abnormalities. This also explains why the primary target of lifestyle modification is to induce weight loss. In fact, the use of anti-obesity drugs not only reduces body weight, but also improves various metabolic aberrations of MetS [80]. Some of the earliest weight-loss drugs are centrally acting sympathomimetics which were later superseded by serotonin-releasing agents. To date, many drugs from the two classes have been withdrawn from the market due to undesirable side effects. One exception is the extended release phentermine in combination with topiramate (anti-

convulsant) because the combined therapy confers greater efficacy at lower dosages which in turn, reduces the intolerance to or side effects of the drugs [81].

More recently, four new anti-obesity agents have been approved for body weight management, namely sibutramine, rimonabant, lorcaserin and orlistat. The first three of which are appetite suppressants. Nonetheless, due to severe adverse effects like cardiovascular risk and psychiatric issues, the clinical use of sibutramine and rimonabant has been banned. Unlike other anti-obesity agents mentioned above which primarily reduce appetite, orlistat is a pancreatic lipase inhibitor that hinders lipid absorption from the gastrointestinal tract [82]. Alongside with significant weight loss, treatment with orlistat also improved the blood pressure, glycemic control and lipid profiles [83, 84]. The side effects of orlistat such as abdominal discomfort, indigestion, steatorrhea and flatulence, are more tolerable and less detrimental compared to other anti-obesity drugs. This makes orlistat one of the most widely prescribed drugs for obese individuals

Prompt and substantial weight reduction can be achieved via bariatric surgery. Fundamentally, the procedure blocks nutrient absorption and/or restricts food intake via different approaches like reducing the stomach size, occupying intragastric capacity, bypassing the small intestine or a mixture of these procedures [85]. Currently, the operation is only performed on morbidly obese patients with a BMI>40 kg/m^2 or a BMI>35 kg/m^2 with comorbidities. The procedure not only causes tremendous weight loss, but also significantly improves the remission rate of T2DM, hypertension and dyslipidemia [86, 87]. However, the procedure is also associated with increased mortality and reoperation rates in addition to various post-operative complications like vomiting, reflux, nutritional and electrolyte anomalies [87]. The surgical cost is also a major hindrance. Therefore, after weighing the cost, risk and benefits, it is unlikely that the procedure can be a mainstream treatment of MetS.

In short, the ability of anti-obesity interventions to ameliorate various risk factors of MetS supports the causative role of central adiposity in the pathogenesis of MetS. What is truly attractive is their multifunctionality which can effectively improve several metabolic abnormalities with a single intervention. Such a criterion has become an important feature for many investigational drugs of MetS and obesity. Even though anti-obesity interventions are effective, each of the pharmacological and surgical approaches has its own drawbacks. Future research should aim to reduce the side effects in order to expand the clinical utility.

1.2.3. Investigational and prospective therapeutic agents of metabolic syndrome

In light of the limitations in both the conventional and recent therapeutic strategies of MetS, there is a large number of on-going research that attempts to discover and develop novel therapy for the disease. First and foremost, the success of anti-obesity agents on relieving MetS have driven ample research in this aspect. One example is by modulating the gastrointestinal satiation signals. Effective appetite stimulation and cessation is accomplished by a crosstalk between gastrointestinal tract and brain, which is also known as the gut-brain axis. This involves a number of anorexigenic (appetite suppression) and orexigenic (meal initiation) signaling peptides [88]. Presumably, enhancing the former while inhibiting the latter could trigger satiety and diminish meal size. One notable example of anorexigenic peptide is glucagon-like peptide 1 (GLP-1) which suppresses food intake and gastric emptying via the activation of GLP-1 receptor [89, 90]. Accordingly, many GLP-1 analogues such as exenatide, liraglutide and lixisenatide have demonstrated promising weight-reducing effect in clinical trials [91, 92]. Additionally, GLP-1 analogues have been widely used as glucose-lowering agents. Such a dual functionality confers additional health benefits, particularly to obese patients with T2DM, which makes the clinical prospect of GLP-1 analogues remarkable optimistic.

Chronic inflammation and elevated oxidative stress resulted from the ectopic fat accumulation are accountable to many MetS-associated pathological processes such as insulin resistance, atherosclerotic development and organ damage [93]. Hence, restoring the antioxidant defense and inhibiting inflammatory response could potentially delay the progression of the metabolic dysfunction. In the context of conventional antioxidants like vitamins A, C and D, the clinical evidence thus far does not support their beneficial effects on the prevention of CVD [94, 95]. However, the consumption of functional foods like green tea, cocoa, soy isoflavones and citrus products which are rich in polyphenols could resolve different risk factors in patients with MetS [96]. Apart from enhancing antioxidant capacity, some polyphenol-rich foods, green tea and berries in particular, also reduce body weight, LDL-cholesterol and triglyceride levels [97-99]. Current research on the polyphenol-rich functional foods is rather preliminary and does not provide concrete evidence about their protective effects on cardiometabolic endpoints like T2DM and CVD. Although they are unlikely to be the primary MetS therapy, polyphenol-rich

foods harbor the potential to serve as an adjunct nutritional therapy to potentiate the effects of other treatments.

In comparison to antioxidant therapy, anti-inflammatory therapy appears to be a better alternative. For instance, methotrexate, which is an anti-rheumatic drug for chronic inflammatory disorders, could lower the risks for CVD and myocardial infarction by 21% and 18%, respectively among patients with rheumatoid arthritis, psoriasis or polyarthritis [100]. This finding in turn; led to a large-scale clinical trial to investigate the impact of low-dose methotrexate on adverse cardiovascular events among CVD and/or T2DM patients [101]. To inhibit systemic inflammation, various monoclonal antibodies have been engineered to specifically block different pro-inflammatory cytokines like tumor necrosis factor α (TNF-α) [102], interleukin (IL)-1β [103] and IL-6 [104]. Whereas, some research groups use small molecules like salicylates [105, 106] and metformin [107] to modulate inflammatory signaling cascades, namely nuclear factor κB (NF-κB) and AMP-activated protein kinase (AMPK) pathways. All of these anti-inflammatory therapies have demonstrated promising beneficial metabolic effects, but the overall improvements seem to be rather modest [108]. Nevertheless, several clinical trials are currently underway to examine the effects of anti-inflammatory therapy on the onset of cardiovascular event and T2DM progression. The output of these studies will determine the eventual fate of anti-inflammatory therapy in the management of MetS-related complications.

Recent findings suggest a leading role of gut microbiome in the onset and progression of obesity and MetS [57]. This stimulates a heated discussion about the use of fecal microbiota transplantation to treat chronic metabolic diseases. Basically, fecal microbiota transplantation involves the transfer of the entire microbial population extracted from the fecal materials from a healthy individual to a sick recipient. At the moment, it is used to treat severe *Clostridium difficile*-associated diarrhea, a life-threatening gastrointestinal infection caused by abnormal microflora of the bowel and colonization of *C. difficile* [109]. Interestingly, a case study reported rapid weight gain in a *C. difficile* patient who received fecal microbiota from a healthy but overweight donor [110]. Similar obesity-inducing effect has been demonstrated in mice, but could be attenuated with concurrent low-fat, high-fruit/vegetable diet feeding and cohousing with lean mice [111]. Likewise, transplantation of gut microbiota from lean human donors also

successfully improved the insulin sensitivity of recipients with MetS [112]. These results strongly denote a horizontal transmissible interaction between diets and gut microbiome that can influence host biology and metabolism. The development of fecal microbiota transplantation as a MetS therapy is still in its infancy even though many preclinical studies have shown the crucial roles of gut microflora in all aspects of MetS, including hypertension, dyslipidemia, atherosclerosis, hepatic steatosis and insulin resistance [113]. The current task is to verify these claims with human trials.

Next, one of the biggest pitfalls of the conventional MetS therapeutic strategy is patient noncompliance issue due to polypharmacy. Conceptually, this can be minimized by having multifunctional medications that can improve multiple risk factors of MetS. There are two major ways to achieve this: (1) having a medication that combines multiple bioactive ingredients or the so-called "polypill" and (2) having an active drug with pleiotropic effects. The idea of using polypills that contain antihypertensive drugs, lipid-lowering agents, folic acid and aspirin to reduce the risk of CVD was put forth by Wald and Law (2003) [114]. Later on, such a notion was thought to be applicable for the treatment of T2DM and pre-diabetes with the incorporation of glucose-lowering medications into the polypill formulation [115]. To date, several randomized controlled trials have shown good tolerability and efficacy of polypills to reduce the occurrence of cardiovascular events among the people with high and moderate risk for CVD [116-118]. This is accompanied by improved patient adherence and reduced treatment cost [119, 120]. Essentially, polypills is a commendable concept and therapeutic strategy for multifaceted diseases, but the formulation should be modified to ensure tolerability and safety for the use in premorbid individuals.

Unlike polypills which may have inherent risk of drug-drug interaction, an active compound with pleiotropic effects can reverse multiple metabolic aberrations with negligible risk of such an interaction, making it comparatively a better choice. In this context, many existing medications like fibrates, statins [121] and ARBs [122] have demonstrated multiple beneficial effects to different aspects of MetS. This is attributable to their agonistic activity to PPARs which are nuclear receptors and transcription factors that play key regulatory roles in lipid and glucose homeostasis. Furthermore, many polyphenols such as resveratrol [123], quercetin [124] and epigallocatechin-3-gallate [125] have demonstrated excellent pleiotropic therapeutic effects on

MetS-associated anomalies in animal models. In fact, the compound of interest in the current project, ellagitannin geraniin, also belongs to the polyphenol group. Thus far, the investigations of polyphenols as multifunctional MetS therapy are mostly preclinical studies. However, the positive results are expected to motivate more intensive research to examine their viability and effectiveness in actual clinical settings.

Based on the investigational therapies, it is easily noticeable that the multifunctionality is a key feature which is highly sought after for the treatment of MetS. This was pointed out more than ten years ago as a vital element to effectively tackle polypharmacy-associated problems [126]. Indeed, realizing that MetS is essentially a multiplex risk factor, it is understandable to want a versatile drug that can efficaciously resolve all the metabolic anomalies at once. Desirably, a prospective MetS therapy should also have minimal adverse effects and be acceptable to people from all walks of life. For instance, albeit effective, the use of polypills in premorbid patients is rejected by a number of physicians due to the potential side effects [127]. Another example is the fecal microbiome transplantation which is deemed disgusting by many because of the perception about feces being unhygienic [128]. The reduced acceptance by either medical professionals or the general public could severely hinder their development. On the other hand, certain prospective therapeutic agents such as polyphenols and polyphenol-rich functional foods do show promising benefits and tolerability, but are not well-explored. Therefore, more research in this aspect could potentially unearth some exciting and clinically significant findings for the treatment of MetS.

In summary, looking at the conventional, recent and prospective therapeutic strategies of MetS, we are slowly transforming from alleviating individual risk factors to addressing the underlying pathology of MetS and treating it as a whole. That being said, physical activity and dietary monitoring remain as the best preventive strategies for MetS-associated complications and should be practiced by the young and old alike. In short, there is still a lot of room for improvement for the MetS intervention and hence, further studies in this field is clearly pertinent and warranted.

1.3. Challenges of Preclinical Metabolic Syndrome Research

As mentioned previously, both the current and prospective therapeutic strategies of MetS are associated with certain extent of limitations and imperfections. Therefore, more research is crucial to produce better, safer, more affordable and more easily acceptable MetS treatments. In this context, preclinical animal studies are widely performed to examine the toxicity, pharmacokinetics and pharmacodynamics of bioactive compounds which have demonstrated promising anti-MetS effects in cell-based studies. To fulfill the purpose, animals with MetS are needed. The selection of an appropriate MetS animal model or the establishment of a clinically-relevant disease model could in fact, be one of the most mind-boggling tasks at the beginning of a drug testing research project. Hence, in this section, we will discuss the commonly used animal models for MetS research and their pros and cons in order to put forward some key parameters for the establishment of a reliable MetS model for the present research project.

1.3.1. Common disease models for metabolic syndrome and obesity research

To establish a clinically-relevant disease model, animals are often subjected to the known etiology of the disease of interest. However, prior to the disease induction, researchers need to decide the demographic properties of the animal used, namely the species, strain, gender and age. Rodents like mice (*Mus musculus*) and rats (*Rattus norvegicus*) remain as the preferred choices for chronic disease studies like obesity, diabetes, hypertension and MetS because they are easy to handle and maintain, relatively inexpensive, have short lifespan and quick reproduction cycle, and most importantly, possess good resemblance with humans in terms of their genetic, metabolic and behavioral characteristics [129].

For rats, the most common strains used in obesity and MetS studies are Wister and Sprague Dawley rats while for mice, it is C57BL/6 mice [130]. Different obesity induction efficiency with high-fat diets (HFD) between strains has been noted for both species, but all the aforementioned strains demonstrated good susceptibility to a wide range of metabolic dysregulation [131, 132]. On the other hand, there is a gender bias in most biomedical research in which female animals are underused [133]. Most of the studies included in a recent review of MetS animal models are predominated by male animals [134]. Such a sex bias is driven by the concern that menstrual cycles may reduce the homogeneity of the study population and introduce

extra confounding effects into an experiment [135]. This could potentially result in poor generalizability of empirical findings, compromised understanding of disease biology and unanticipated drug responses among the underrepresented gender. Moreover, the starting age for MetS induction is also quite variable, but most studies employed young adult rodents of about six to eight weeks old [130, 134, 136]. Considering the growing prevalence of childhood obesity and MetS, there is a need to investigate if the existing models are appropriate for juvenile obesity research. Although these demographic characteristics could have a certain extent of influence on the MetS induction, to our best knowledge, the pathogenesis of MetS still holds true regardless of the species, strain, gender and starting age. Therefore, the selection criteria could also be based on extrinsic factors like the target human populations, costs and pre-existing facility and expertise.

As mentioned previously, the known etiology of MetS are genetic components, over-nutrition and sedentary lifestyle, the first two of which are widely manipulated to induce the metabolic disorder. Genetic models of MetS are pervasively used and well-accepted. Common examples are *ob/ob* mice, *db/db* mice, Zucker fatty rats, Zucker diabetic fatty rats and Koletsky rats, all of which have a loss-of-function mutation at the leptin or leptin receptor genes [134]. Due to the defective feedback mechanism of leptin signaling, the genetic models of MetS tend to exhibit hyperphagia and uncontrolled appetite, leading to rapid weight gain and other features of MetS. These genetic models can be purchased commercially and the development of MetS is well-characterized and highly reproducible. As a result, the time spent on disease induction is greatly shortened. Despite these benefits, the development of MetS caused by a single-gene disorder is inconsistent with the polygenic nature of MetS. Furthermore, in humans, congenital leptin deficiency caused by leptin gene mutations is extremely rare [137]. Therefore, it is questionable to generalize the findings coming from these models to whom leptin or leptin receptor deficiency does not play a role in the MetS pathogenesis. Another notable limitation of the genetic models is that they are unsuitable for drug testing of putative appetite control agents. This is because the leptin signaling defect seems to mask the effects of appetite suppressants, as exemplified in some studies wherein the hypophagic effect of sibutramine was abolished with the use of genetic models [138, 139]. Hence, even though genetic models are remarkably useful, they should be used with caution simply because obesity and MetS originated from monogenic defect is inconsistent with the true pathology and this potentially confounds the experimental findings.

Compared to genetic models, diet-induced MetS models are arguably better and more clinically relevant mimicries of MetS in humans. Indeed, without altering the genetic components, chronic high-calorie feeding simulates the over-nutrition behavior and consequently, leading to a wide variety of metabolic abnormalities when compared to the animals given low-calorie, healthier control diets (CDs). This is in concordance with the predominant causative role of positive caloric balance in the onset of MetS in humans. Numerous high-calorie diets which are enriched by lipids and/or carbohydrates can successfully induce MetS [136]. Some of the most popular formulated diets are those high in saturated fat, fructose, sucrose or a combination of these macronutrients. This is because increased dietary lipids and fructose markedly upregulates *de novo* lipogenesis and promotes ectopic lipid deposition, which in turn, leads to peripheral insulin resistance, inflammatory response, chronic oxidative stress insult, and progressive organ damage [140, 141]. The composition of these macronutrients can go as high as 70% of the total caloric content of MetS-inducing diets in contrast to CDs whose lipid and mono-/disaccharides content is often maintained at less than 10% [136]. These high-caloric diets, particularly for HFD, have a tremendous increase in the calorie density which will promote positive caloric balance upon prolonged consumption. In terms of the availability, there are many animal diet suppliers which can provide well-established high-calorie diets together with the paired CDs. This also facilitates inter-study comparisons provided that the same diets are used.

However, using dietary approach to induce MetS generally require a relatively long induction time, ranging from four weeks to six months [136]. Therefore, any strategy to reduce the induction time is highly desirable. Additionally, even with chronic high-calorie feeding, some animals would remain lean and are resistant to the obesogenic effect of high-calorie diets. This is in line with the polygenic and multifactorial nature of MetS. In a nutshell, high-calorie diets are useful and reliable to generate clinically-relevant MetS models. However, current diet formulations have some notable limitations which will be discussed in following section.

To recapitulate, the pros and cons of the common rodent MetS models have been outlined. Amongst these models, the diet-induced approach provides the closest resemblance to the manifestation of MetS found in population at large. Therefore, this method will be used to create the MetS models for the present study. In this context, the follow-up question would be: How to formulate an effective high-calorie diet for MetS induction? Interestingly, despite the enormous

amount of evidence to support the use of the model, there is little consensus on the diet formulation and limited understanding about the efficacy of different formulations. These questions will be further explored.

1.3.2. Common pitfalls of diet-induced metabolic syndrome models

As mentioned earlier, two notable disadvantages of diet-induced MetS models are long induction time and the possibility of induction failure due to the diet-resistant phenotype in a small proportion of animals. Furthermore, the use of self-formulated diets poses a huge issue – the inconsistency caused by a large variety of high-calorie diets being used, each with different preparation methods, compositions, formulations and nutritional values. The degree of dietary diversity is remarkably astounding; for instance, the lipid content in a HFD can range from 20% up to 60% of the total energy of the diet [130]. Likewise, the fructose-enriched diets have been prepared with either fructose or sucrose, by supplementation in either the solid foods or drinking liquid, at highly variable compositions which can go up to 70% of the total diet energy content or 10% (v/v) in the drinking water [136]. It is not unusual to combine the aforementioned approaches to create high-fat-high-sugar (fructose or sucrose) diets (HFSD) since it is believed to better mimic our dietary pattern. The diverse high-calorie diets render comparisons between different studies exceedingly difficult. Conversely, there are limited comparative studies that attempt to resolve the disease induction efficacy of different formulations. As a result, researchers often find it challenging to decide the diet of choice for speedy, reliable and cost-effective MetS induction without some pilot studies.

The issue of diet choice is further complicated by the use of animal chow or modified-chow based diets in MetS research. To elaborate, laboratory animal diets can be classified into two major types, namely chow and purified ingredient-based diets (expressed as chow diet and purified diet, respectively henceforth). Animal chow is primarily made up of agricultural products like wheat, corn, oat and soybean and so, it is naturally low in lipids, proteins and micronutrients. The actual composition of chow can exhibit significant variation the plant materials used which is dependent on the batches of the products, geographical regions of the suppliers and agricultural seasons [142]. Furthermore, their formulations are rarely disclosed, making it difficult to trace the true nutritional composition. On the contrary, purified diets are composed of well-defined macro- and micronutrients like casein, cornstarch, maltodextrose,

sucrose, cellulose, milk fat, supplemented with vitamins and minerals. There is a standardized formulation of purified diet for rodents [143]. The creation of high-calorie diets can be achieved by manipulating the composition of fats, starch, mono- and disaccharides. Knowing the formulation and ingredient used allows replication of the diets. Hence, in terms of reproducibility, purified diets are evidently superior to chow diets.

Surprisingly, the batch-to-batch variability is probably of the least concern when compared to other issues caused by the use of chow diets. To enhance the caloric density of a chow diet, some studies reported using modified chow-diet by mixing a large amount of fat or sugar to powdered chow [144-146]. This is convenient and cost-effective, but at the expense of the nutritional value of the diet because simply adding a certain macronutrient will markedly dilute the other nutrients. For example, enriching powdered chow with saturated fats in 1:1 ratio will virtually halve the composition of nutrients like proteins, vitamins and minerals, making their already-low content to go even lower. Prolonged deprivation of these essential nutrients could lead to unintended metabolic changes which are not in line with the onset of MetS despite successful obesity induction [142]. In addition, a small but significant portion of chow is composed of plant-derived phytochemicals which may confer protective effects against metabolic dysregulation. One example is phytoestrogen which is highly bioavailable and can prevent lipid and glucose dysregulation via the activation of AMPK pathway [147, 148]. Additionally, the anti-nutritional factors like trypsin inhibitors, phytic acids and phorbol esters are also the natural constituents of animal chow [149, 150]. These molecules can inhibit digestive enzymes and obstruct absorption, resulting in suboptimal nutrient uptake. Essentially, unlike purified diets in which phytoestrogen and anti-nutritional factors are almost non-existent, these phytochemicals in the chow may interfere the metabolism and disease induction besides introducing unaccounted confounding variables into the experiments.

Apart from that, the use of a mismatched CD is another common pitfall when diet-induced models are used in MetS research. To have a better understanding about this issue, we will first need to know the concept of matched CD. Assuming that you are trying to induce MetS in rats using a HFD, it is logical to adjust the relative amount of fat and carbohydrate without altering the composition of other micro- and macronutrients because other nutrients possess other physiological functions [142]. Therefore, in this case, a matched CD will have a low fat, high

carbohydrate content with the protein, fiber, vitamins and minerals contents being comparable to the HFD. Unfortunately, the use of properly matched CDs only made up a small portion (14%) of the high-impact preclinical MetS studies in 2007 [151]. One typical example of mismatched CD involves the use of purified high-calorie diet being matched to chow diet [152-154]. The two diets differ in both the nutritive and non-nutritive compositions, hence making it difficult to make sound comparison when they are used together in an experiment. Conversely, it is also rather common to come across studies that compare animals on a modified-chow diet to those on a chow diet [144-146]. As mentioned previously, mixing saturated fats or simple sugar to powdered chow will diminish protein and micronutrient contents. In cases like this, the observed metabolic derangements cannot be entirely attributable to the lipid or sugar enrichment, as the interference from protein or micronutrient insufficiency cannot be excluded. Furthermore, the presence of phytochemicals in the chow and modified-chow diets could potentially exacerbate the negative effects on the data interpretation of an experiment, particularly when a putative therapeutic agent is tested. This is because the possibility that the bioactive phytochemicals can interact with the putative drug cannot be eliminated. Such an interaction could lead to over- or underestimation of the treatment effect, depending on whether the compounds react in a synergistic or antagonistic manner. Hence, researchers who are unaware of the limitations of using mismatched CDs may unknowingly draw an inaccurate conclusion.

In summary, aside from the intrinsic limitations (long induction time and diet resistant phenotype) of diet-induced MetS models, the current experimental methodology is also associated with a number of notable pitfalls, namely the lack of standardized formulation for high-calorie diets, the use of chow- and modified-chow diets and mismatched CD. These issues have created a great deal of problems in MetS research such as infeasible inter-study comparisons, high brand-to-brand or batch-to-batch variability of the experimental diets and unaccounted confounding variables, all of which could collectively contribute to erroneous conclusions. In this context, the use of chow- and modified-chow diets should be discouraged. Additionally, more investigations that aim to directly compare different high-calorie diets as reported by Sumiyoshi et al. (2006), Sampey et al. (2011) and Bortolin et al. (2017) are undoubtedly valuable [155-157], not only because more information about the disease induction efficacy of different diets will be available, but would also lead to better MetS models to facilitate reliable bench-to-bedside translation.

1.3.3. Possible improvements to establish a better metabolic syndrome model?

Generally, it is of great interest of the research community to know which kinds of diets is superior in MetS induction so that less time and resources are invested to identify a reliable model at the research project startup stage. Due to the fat enrichment, HFD and HFSD tend to have higher caloric density compared to high-sugar diet, so they are more effective at inducing obesity [155, 158]. However, it is uncertain how good HFD is at disease induction relative to HFSD. As mentioned earlier, comparative studies are necessary to unravel the efficacy and differences between different formulations. Hence, it is pertinent to compare HFD to HFSD in an experiment together with a matched low-fat, low-sugar CD. The fat content can be formulated at 60% of the total energy content as this has been shown to be effective and pervasively used in many studies [134]. As for the simple sugars, both fructose and sucrose have been used, but the latter is the sole constituent of the table sugar, hence it could be a more clinically relevant option. The supplementation of additional simple sugars can be done by solid diet enrichment or in the form of sugar-sweetened water. In this context, sweetened beverage has been associated to higher calorie consumption in both humans and rats, probably due to its poor satiety response stimulation compared to solid foods [159-161]. To induce MetS, as much as 30% (v/v) sucrose water has been used, but generally, 10% sucrose water is sufficiently effective [136]. Accordingly, this comes down to a comparison between HFD (60% kcal) and HFSD (60% kcal fat + 10% sucrose water). An experiment with these diet formulations may shed some light on the relative efficacy of the two diets in MetS induction.

While diet formulation is a vital element to ensure successful disease modelling, the animal characteristics also play a crucial role. A common practice is to ensure that the parameters like the species, strain, gender and age are comparable within and between treatment groups to minimize variations. Incidentally, the effects of gender and age on disease induction is unclear. For the starting age in particular, rodents ranging from three- to 12-weeks old have been used in MetS study without a clear explanation for selecting a specific age [134]. However, based on very limited studies, it appears that younger rodents are more prone to metabolic dysregulation like increased weight gain and hypertension upon high-calorie feeding [162-164]. It is therefore hypothesized that juvenile, post-weaning rodents given high-calorie diet may allow faster MetS induction compared to adult rodents. Currently, this postulation is largely ungrounded, but it can

be argued based on two novel contributors to MetS: metabolic programming and gut microbiome. Briefly, metabolic programming depicts that nutritional insults like over-nutrition or starvation during fetal development and immediate postnatal stage could have a long-lasting obesogenic effect via epigenetic modifications [165, 166]. Metabolic abnormalities caused by fetal metabolic programming are aggravated by post-weaning high-fat feeding, implying that the epigenetic changes are probably modifiable by early childhood dietary pattern [167]. Furthermore, high-fat feeding right after weaning also shapes the gut microbiome very differently from those on CD [168]. The microbial population may be specialized in digesting fat-enriched foods. In comparison, the gut microflora of older animals may be well-adapted to the solid foods that they are exposed to (*eg.* chow diet), prior to an experiment. Both of these factors may influence the disease induction efficacy in animals, making it worthwhile to look into the effects of developmental stages on MetS modeling. Tentatively, juvenile rats on high-calorie diets could also serve as a model for pediatric obesity and MetS research to explore the differences from the adult counterparts.

As such, to put forth some key parameters which may lead to more prominent MetS features within a shorter time, the comparative studies using purified diets with different formulations and rats of different development stages are pertinent. The output of such studies can serve as a keystone for others to cut down their time and resources invested into disease modeling. Moreover, it is also interesting to investigate any differential outcomes caused by the factors and their interaction to understand the interplay between dietary behavior and developmental stages. This could prompt more drastic preventive strategies against MetS among the young ones.

1.4. A Remedy from the Mother Nature – Ellagitannin Geraniin

Up to this point, we have discussed about the severity of MetS, expected features of future MetS treatments and some of the challenges associated with preclinical drug screening of MetS. All these issues urge the necessity to dig deeper into the health problem in hopes that the threat can be annihilated. To accomplish this mission, there are many researchers working relentlessly, trying to engineer a novel therapy for obesity, MetS and their complications. Many of them attempt to seek possible solutions from the Mother Nature. As a matter of fact, close to 50% of the US Food and Drug Administration (FDA) approved drugs are originated from natural products and their derivatives or mimicries [169]. Many investigational phytochemicals have

demonstrated promising therapeutic against MetS [170]. For the current project, we propose ellagitannin geraniin (geraniin, in short), which is a hydrolysable tannin in the polyphenol superfamily, as a putative therapeutic agent for MetS. The chemical structure of geraniin is illustrated in **Figure 1.3**. The background information about geraniin, including its basic chemistry, natural sources, biosynthesis and pharmacological effects, has been summarized and published as a review article [171]. The review paper is included as **Section 1.4.1**, followed by a brief summary about the natural product and its relevance to MetS.

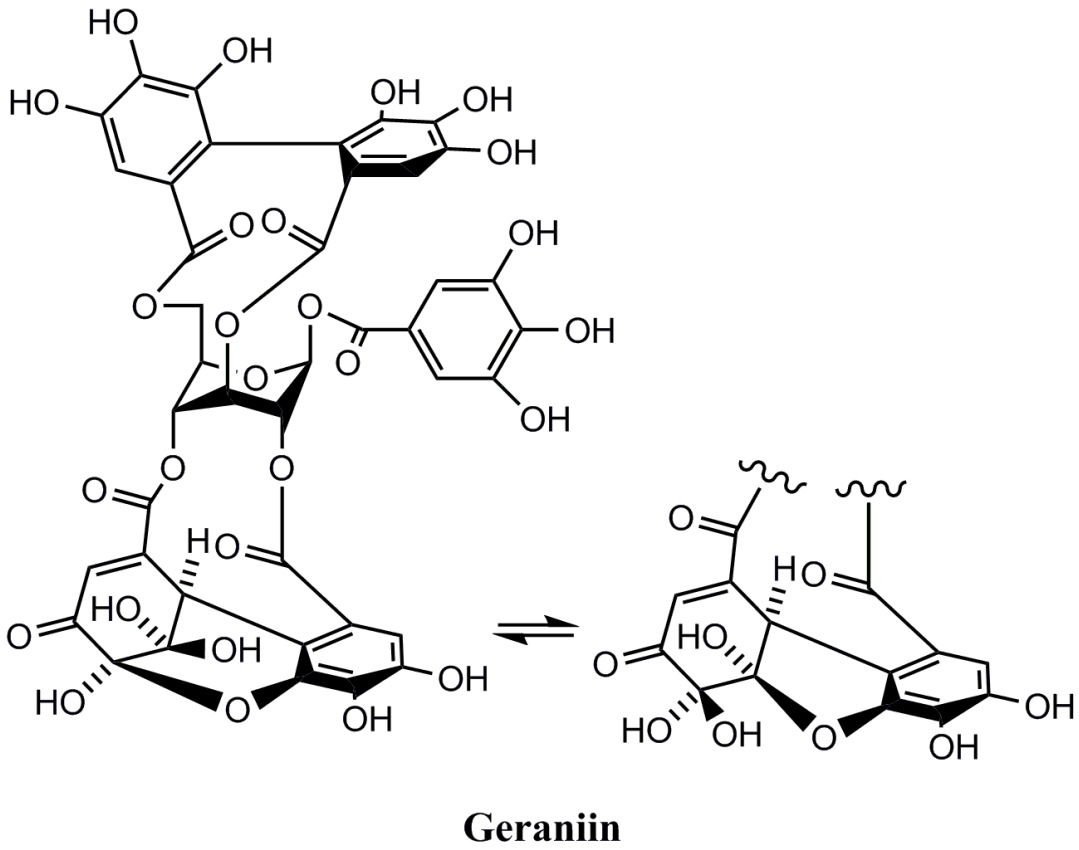

Figure 1.3: Chemical structure of ellagitannin geraniin.

1.4.1. Ellagitannin geraniin: A review of the natural sources, biosynthesis, pharmacokinetics and biological effects.

Phytochem Rev (2017) 16:159–193
DOI 10.1007/s11101-016-9464-2

Ellagitannin geraniin: a review of the natural sources, biosynthesis, pharmacokinetics and biological effects

Hong Sheng Cheng · So Ha Ton · Khalid Abdul Kadir

Received: 21 August 2015 / Accepted: 31 March 2016 / Published online: 7 April 2016

Abstract The discovery of the ellagitannin geraniin was made exactly 40 years ago. It is a secondary metabolite found in plants and is categorised as a hydrolysable tannin under the huge family of polyphenolic compounds. At present, the occurrence of geraniin has been verified in at least 71 plant species, many of which are used in traditional medicine. Hence, like other polyphenols, geraniin has also received widespread interest as a research focus to unearth its beneficial biological effects and therapeutic values apart from understanding its chemical properties, biosynthesis and interaction with the body system. Indeed, it has been demonstrated that geraniin possesses antioxidant, antimicrobial, anticancer, cytoprotective, immune-modulatory, analgesic properties besides exerting promising therapeutic effects on hypertension, cardiovascular disease and metabolic dysregulation. The objective of this review is to summarise the current knowledge about the basic chemistry, natural sources, isolation techniques, biosynthesis, pharmacokinetics and pharmacodynamics of geraniin. With reference to this information, the clinical significance, obstacles and future perspectives in geraniin research will also be scrutinised.

Keywords Antioxidants · Ellagic acid · Hydrolysable tannins · Polyphenols · Urolithins

H. S. Cheng (✉) · S. H. Ton
School of Science, Monash University Malaysia, Jalan Lagoon Selatan, 46150 Bandar Sunway, Selangor, Malaysia
e-mail: hsche19@student.monash.edu

K. Abdul Kadir
School of Medicine and Health Sciences, Monash University Malaysia, Jalan Lagoon Selatan, 46150 Bandar Sunway, Selangor, Malaysia

Abbreviations

DPPH	2,2-Diphenyl-1-picrylhydrazyl
IC_{50}	50 % inhibition concentration
5-LOX	5-Lipoxygenase
AGEs	Advanced glycation end products
ACE	Angiotensin-converting enzyme
COMT	Catechol-*O*-methyl transferase
CSF-1	Colony-stimulating factor-1
CYP1A1	Cytochrome P450 1A1
DHHDP	Dehydrohexahydrodiphenoyl
EV71	Enterovirus-71
ERK	Extracellular signal-regulated kinase
FRAP	Ferric reducing antioxidant power
GSH	Glutathione
Hsp90	Heat shock protein 90
HBV	Hepatitis B virus
HBeAg	Hepatitis B virus e antigen
HBsAg	Hepatitis B virus surface antigen
HSV	Herpes simplex virus
HHDP	Hexahydroxydiphenoyl
HPLC	High performance liquid chromatography
HIV	Human immunodeficiency virus
iNOS	Inducible nitric oxide synthase
LPS	Lipopolysaccharide

MIC	Minimum inhibitory concentration
NF-kB	Nuclear factor kB
Nrf2	Nuclear factor-erythroid 2-related factor 2
ORAC	Oxygen radical absorbance capacity
PGG	Pentagalloylglucose
PPAR	Peroxisome proliferator-activated receptor
PAI-1	Plasminogen activator inhibitor-1
RNS	Reactive nitrogen species
ROS	Reactive oxygen species
RANKL	Receptor activator of nuclear factor kB ligand
SOD	Superoxide dismutase
tPA	Tissue plasminogen activator
TGF	Transforming growth factor
TNF	Tumour necrosis factor
UDP	Uridine diphosphate

Introduction

Polyphenolic compounds which are secondary metabolites found ubiquitously in plants are probably among the most extensively studied phytochemicals. This is not only because of their pharmaceutical potential, but also due to their distinctive properties as food preservatives, natural colouring and flavouring agents as well as cosmetic products (Ignat et al. 2011). Polyphenolic compounds can be sub-divided into flavonoids, phenolic acids, tannins, stilbenes and lignans. In the tannin subgroup, there are generally three major classes, namely, hydrolysable tannins, non-hydrolyzable/condensed tannins and phlorotannins. Among the three classes, hydrolysable tannins are one of the earliest polyphenolic compounds that were subjected to quantitative and qualitative analysis about a century ago (Fisher 1914). In this context, it is also the class where the compound of interest in this review—the ellagitannin geraniin belongs.

The use of geraniin-containing herbs in folk medicine has been broadly documented. In Japan, *Geranium thunbergii* which has been long-known for its richness in geraniin, is certified as an official antidiarrheal drug (Luger et al. 1998). *Geranium bellum* which is known as "Pata de león" in Mexico, is used to treat fever, pain and gastrointestinal disorders (Velazquez-Gonzalez et al. 2014). Likewise, "amla" or fruits of *Phyllanthus emblica* are also used for similar ailments in addition to being a preventive measure for peptic ulcers and alopecia in India (Baliga and Dsouza 2011). Furthermore, in traditional Tibetan medicine, the roots of various *Geranium* spp. are collectively termed "*li ga dur*" and are used as an effective treatment for swelling in the limbs (Kletter and Kriechbaum 2001). *Geranium wilfordii* is also widely employed in traditional Chinese medicine for the therapy of rheumatism, osteoporosis and diarrhoea (Liu et al. 2010). Undeniably, the abundant occurrence of geraniin has been identified in a number of plant species, ranging from small flowering annual herbs to perennial woody shrubs or trees. At present, there is, yet very limited evidence to show its presence in fruits and vegetables. Nevertheless, considering the fact that ellagitannins have been discovered in different foods of plant origins like nuts, berries and grapes (Clifford and Scalbert 2000; Landete 2011), it is likely that geraniin may also exist in these functional foods.

Like many other polyphenolic compounds, geraniin is well-known for its potent antioxidant properties. Studies have shown that the antioxidant capacity of intact geraniin is at least fourfold to that of ascorbic acid while the metabolites of geraniin have displayed even more powerful antioxidant activities than geraniin itself (Ito 2011; Ishimoto et al. 2012). Aside from that, numerous biological activities have also been reported, including antihypertensive (Cheng et al. 1994; Lin et al. 2008), apoptotic (Lee et al. 2008), antiviral (Yang et al. 2007, 2012), liver protective (Londhe et al. 2012), anti-hyperglycaemic (Palanisamy et al. 2011a) and antidiabetic (Chung et al. 2014) activities. Hence, it is believed that geraniin may harbour therapeutic values which are worth investigating.

In this context, the aim of this review is to outline the properties of geraniin in terms of its chemistry, natural sources and available techniques for geraniin isolation and purification. Further discussion will also be carried out with reference to the current understanding of the pharmacological and biological effects of geraniin together with its putative mechanisms of action. This information may help to shed some light on the clinical significance of geraniin besides providing new perspectives in geraniin research.

Basic chemistry of the ellagitannin geraniin

The chemical formula of geraniin is $C_{41}H_{28}O_{27}$ with a molecular mass of 952.64 g/mol. Upon crystallization,

geraniin exists as a hydrate with a chemical formula of $C_{41}H_{28}O_{27}{\cdot}7H_2O$ (Okuda et al. 1982; Luger et al. 1998). Generally, ellagitannins are characterised as polyphenolic compounds with various numbers of hexahydroxydiphenoyl (HHDP) units attached to a sugar moiety. In addition, other acyl units like galloyl and sanguisorboyl moieties may also be found in ellagitannins. This gives a huge structural variety to ellagitannins because there are different combinations of acyl units to the sugar moiety and more importantly, due to the high tendency monomeric ellagitannins to form their dimeric or oligomeric counterparts (Niemetz and Gross 2005). Geraniin seems to be a typical ellagitannin since it is made up of common acyl moieties, namely a galloyl, a HHDP and a dehydrohexahydrodiphenoyl (DHHDP) group, esterified to a glucose molecule (Fig. 1).

Like many hydrolysable tannins, geraniin is water-soluble and readily undergoes hydrolysis in the presence of hot water, weak acids and weak bases. Under these treatments, the ester linkages will be hydrolysed and the HHDP and DHHDP units will undergo spontaneous rearrangement to yield water-insoluble, bislactone ellagic acids (Fig. 1) (Clifford and Scalbert 2000). Furthermore, geraniin can also precipitate water-soluble proteins and alkaloids. The reactivity is comparable to other tannins of similar molecular size (Okuda et al. 1985). Yet, unlike many tannins, geraniin gives almost no astringent mouth feeling (Okuda et al. 2009).

At aqueous state, the DHHDP unit of geraniin readily isomerises into a mixture of hydrated five- and six-membered hemiacetalic rings (Fig. 1). In addition, it is also exceedingly prone to chemical modifications. The DHHDP moiety can be oxidatively cleaved as exemplified by phyllanthusiins A, B and C which are some of the oxidative metabolites of geraniin (Fig. 2) (Yoshida et al. 1992). Moreover, the DHHDP moiety also allows geraniin to undergo condensation reactions with numerous compounds like ascorbic acid, acetone and *ortho*-phenylenediamine to form ascorgeraniin (elaeocarpusin), phyllanthusiin D and a phenazine derivative respectively (Fig. 2) (Okuda et al. 2009; Okuda and Ito 2011). These condensation products can be prepared under mild laboratory conditions without any enzymatic intervention, suggesting that some of these compounds may form naturally in plants (Okuda et al. 1986). Indeed, it has been shown that ascorgeraniin co-exists with geraniin in several plant species like *Geranium thunbergii* (Nonaka et al. 1986; Okuda et al. 1986) and *Euphorbia watanabei* (Amakura and Yoshida 1996) while an analog of ascorgeraniin, putranjivain A (Fig. 2) has also been successfully isolated from some euphorbiaceous plants (Lin et al. 1990a). Many of the aforementioned chemical reactions do not only occur under controlled procedures in the laboratory, but have also been observed in plants in the field (Klumpers et al. 1994; Viriot et al. 1994), clearly pointing out the high lability of geraniin.

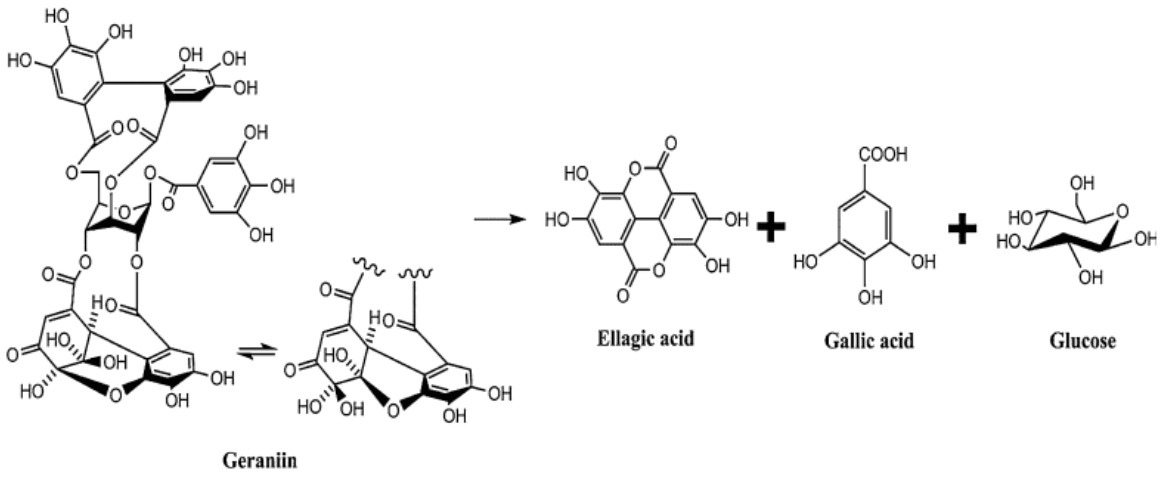

Fig. 1 Hydrolysis of geraniin

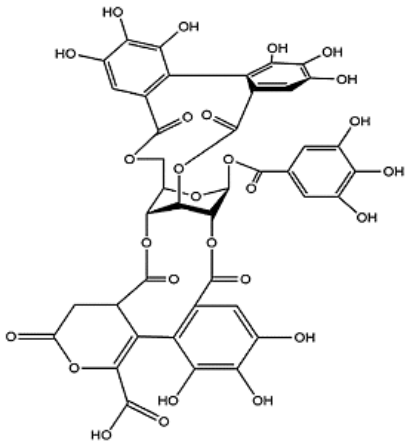

Phyllanthusiin A

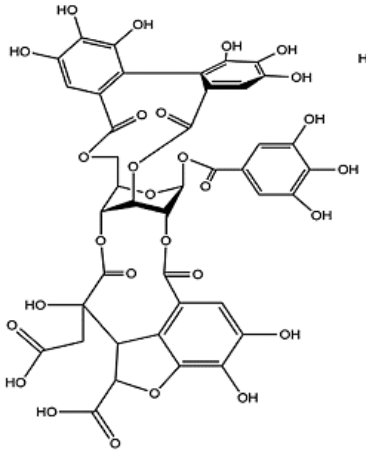

Phyllanthusiin B

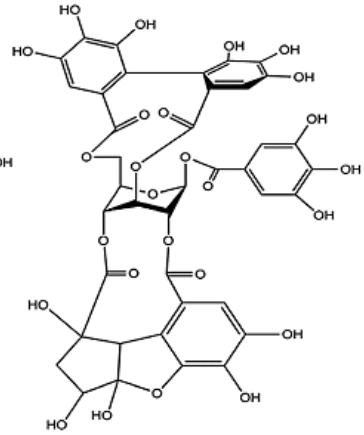

Phyllanthusiin C

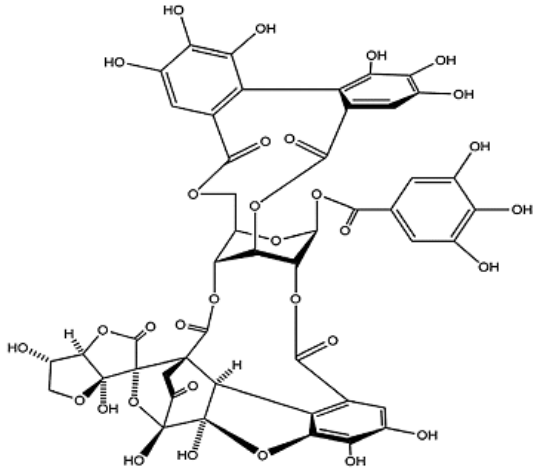

Ascorgeraniin (Elaeocarpusin)*

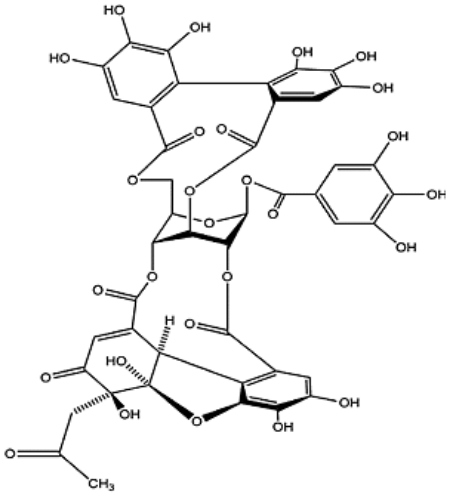

Phyllanthusiin D

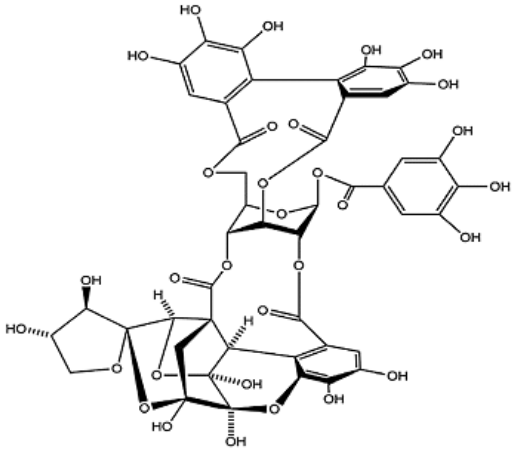

Putranjivain A (an analog of ascorgeraniin)*

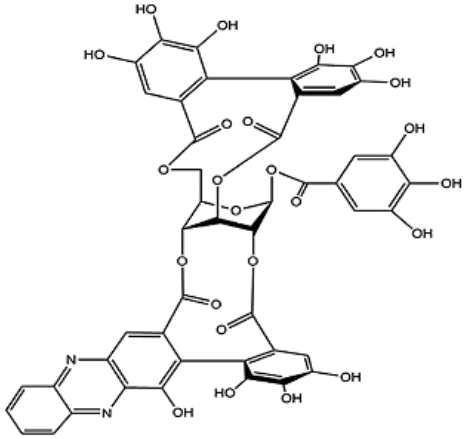

A phenazine derivative of geraniin

◀**Fig. 2** Chemically modified products of geraniin via oxidation (phyllanthusiins A, B, and C) and condensation with ascorbic acid (ascorgeraniin and putranjivain A), acetone (acetonyl-geraniin/phyllanthusiin D) and *ortho*-phenylenediamine (a phenazine derivative of geraniin). *Asterisk* the compound has been isolated from natural sources

Natural sources and isolation of the ellagitannin geraniin

The earliest documented attempt to extract the ellagitannin geraniin from plant species (*Geranium thunbergii*) can be traced back to mid-1970s by Okuda et al. (1975). However, at that time, the compound was simply termed Tannin 1 because it was one of the two major tannins found in the ethyl acetate fraction of *Geranium thunbergii* extract (Okuda et al. 1975). The official nomenclature, geraniin, was assigned to Tannin 1 in 1976, according to genus *Geranium* after its crystallization from *Geranium thunbergii* plant extracts (Okuda et al. 1976). Since then, the occurrence of geraniin has been confirmed in at least 71 different plant species from 26 genera and across 9 families which are summarised in Fig. 3. The prevalence of geraniin in a vast diversity of plant species suggests that it may be a key player in plant survival. In fact, various theories have been proposed to justify why plants invest their metabolic energy in tannin biosynthesis (Kraus et al. 2003), some of which include functions as herbivore deterrent (Butler 1989; Schultz 1989), pathogen defence (Field and Lettinga 1992; Schultz et al. 1992), ecological succession (Schimel et al. 1998), regulation of plant homeostasis (Scalbert 1991; Feucht and Treutter 1999), wound healing (Walkinshaw 1999) and resistance against abiotic stressors (Chalker-Scott and Krahmer 1989). Nonetheless, there is no conclusive remark about the exact function of each tannin in plants because empirical findings yield mixed results. Thus, the biological role of gerannin in plants also remains largely uncertain.

Generally, most of the screening work of geraniin distribution was done by Okuda et al. (1980) using high performance liquid chromatography (HPLC) of acetonitrile–water plant extracts. They ascertained the presence of geraniin in 41 plant species. The content of geraniin in different plants varies greatly, ranging from as low as 0.01 % in *Breynia nivosa* to more than 10 % in some *Geranium* spp. (Okuda et al. 1980). Based on Fig. 3, among the nine families in which geraniin-producing plants are found, Euphorbiaceae, Geraniaceae and Phyllanthaceae give rise to the highest number of such plant species. Geraniin-producing species are found most abundantly in the genus *Geranium*, in which 18 species were identified to date, followed closely by 15 *Euphorbia* spp. and 8 *Phyllanthus* spp. There is no distinctive geographical region for geraniin-producing plants since their habitat ranges from tropical to temperate areas. However, the synthesis of geraniin may be subjected to slight temporal variation (Okuda et al. 1980), notably for the plants in temperate areas probably due to the seasonal changes throughout the year.

As mentioned earlier, geraniin has been identified in both herbaceous and woody plants. The plant part used for geraniin extraction also varies considerably, including whole plant, leaf, herbaceous stem, tree bark, root, fruit skin and seed but the leaf is the most frequently used plant part, probably because it is easier to harvest, process and tends to give higher yield. Geraniin can also be extracted from fruit flesh of Indian gooseberry (*P. emblica*) (Liu et al. 2008, 2012b). This points to the likelihood of geraniin occurrence in other edible fruits. Aside from that, it is also worth highlighting that geraniin and other phenolic compounds have been isolated from suspension cell cultures of geraniin-synthesizing plants like *G. thunbergii* (Ishimaru and Shimomura 1991; Yazaki et al. 1991) and *S. sebiferum* (Neera and Ishimaru 1992; Neera et al. 1992). The yield of geraniin isolated from the hairy root culture was about 70 % of that extracted from the roots of the mother plant (Ishimaru and Shimomura 1991). However, certain conditions have been reported to enhance geraniin production of leaf callus cultures of *S. sebiferum*, including the use of Murashige-Skoog medium without NH_4NO_3, addition of 2,4-dichlorophenoxyacetic acid and benzyladenine to culture medium and placing the cultures under light (Neera et al. 1992). Such a cell culture system is undoubtedly useful for the studies of factors affecting geraniin biosynthesis. This will not only provide insight into the biological functionality of geraniin in plants, but also offer an alternative to manipulate the pathway for large-scale geraniin production, assuming the practical uses of geraniin are more prevalent in the future.

The reported percentage yield of ellagitannin geraniin extraction differs significantly (Table 1). This is attributable to both the difference of original geraniin content in the plant species and the diverse geraniin extraction and purification protocols. However, it is noted that *Geranium* spp. are more consistent in giving

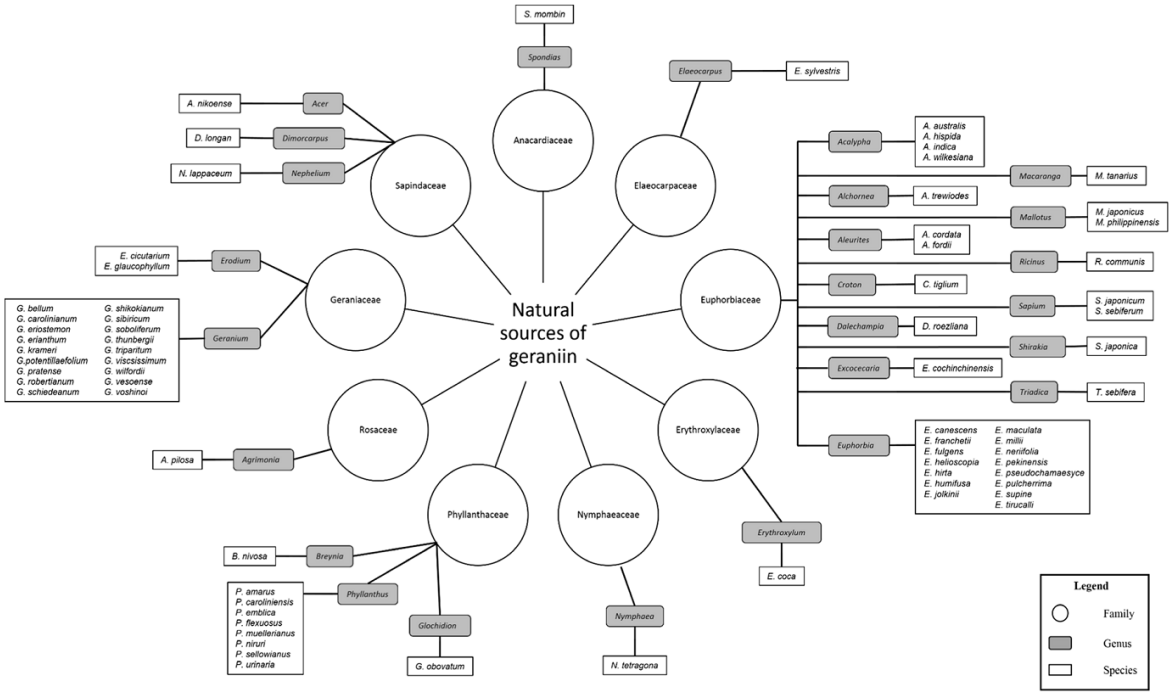

Fig. 3 Natural sources of the ellagitannin geraniin

higher percentage yield, suggesting that *Geranium* spp. are excellent natural sources of the compound. In terms of extraction techniques, conventional solvent extraction is commonly utilised. However, more recent techniques, particularly microwave-assisted extraction, has also been proven to be feasible to obtain geraniin from plant materials (Yang et al. 2010, 2013). To separate the plant crude extract, most research groups prefer gel filtration chromatography as the first step to obtain small molecule metabolites followed by further separation with reverse-phase column chromatography to obtain geraniin at a higher purity. Generally, extraction procedures involving intense heating should be avoided considering the high susceptibility of geraniin to be hydrolysed into corilagin, ellagic acid and gallic acid (Luger et al. 1998). The isolation techniques of geraniin from various plant materials and species are summarised in Table 1.

Biosynthesis of the ellagitannin geraniin

Thus far, there is no published literature specifically about the biosynthesis of ellagitannin geraniin. Nonetheless, most hydrolysable tannins seem to share a common precursor, 1,2,3,4,6-penta-*O*-galloyl-β-D-glucopyranose or pentagalloylglucose (PGG), suggesting that the synthesis of geraniin in plants may be somewhat similar. The biosynthesis of hydrolysable tannins has been summarised comprehensively in other reviews (Niemetz and Gross 2005; Gross 2008; Pouysegu et al. 2011).

The overview of ellagitannin biosynthesis is illustrated in Fig. 4. Briefly, PGG biosynthesis comprises two essential building blocks: β-D-glucose and gallic acid. The first step involves the esterification of gallic acid to glucose, yielding 1-*O*-galloyl-β-D-glucose or β-glucogallin. This process was first described by Gross (1983a) using transferases isolated from oak leaves and uridine diphosphate glucose (UDP-glucose) as the activated donor molecule. Strikingly, by using the same oak leaf enzyme preparations, it was later demonstrated that β-glucogallin possesses dual functionality as both the acyl donor and acyl acceptor for the formation of digalloylglucose without the need of additional cofactors (Gross 1983b). β-glucogallin remains as the principal acyl donor for higher degrees of esterification catalysed by β-glucogallin-dependent

Table 1 Isolation techniques and plant material used for geraniin extraction in different species

Family	Genus	Species	Plant part used	Extraction technique	Yield	References
Anacardiaceae	*Spondias*	*S. mombin*	Leaf and stem	Triplicate gel filtration chromatography of butanol-butanone (1:1) fraction of plant extract followed by reverse-phase column and gel filtration chromatography	1.7 g*	Corthout et al. (1991)
Elaeocarpaceae	*Elaeocarpus*	*E. sylvestris*	Leaf	Gel filtration chromatography of acetone–water (9:1) plant extract followed by subsequent gel filtration and reverse phase column chromatography	0.18 %†	Tanaka et al. (1986)
Euphorbiaceae	*Acalypha*	*A. hispida*	Leaf	Gel filtration chromatography of the butanol fraction of plant extract followed by thin layer chromatography	0.08 %‡	Adesina et al. (2000)
		A. indica	Whole plant	Gel filtration chromatography of the acetone–water (8:2) plant extract followed by successive chromatography with gel filtration and reverse phase column	0.07 %†	Ma et al. (1997)
		A. wilkesiana	Leaf	Gel filtration chromatography of the butanol fraction of plant extract followed by thin layer chromatography	0.10 %‡	Adesina et al. (2000)
	Euphorbia	*E. canescens*	Aerial part	Hide powder column chromatography was used to produce aqueous acetone fractions which were subjected to polyamide column chromatography and recrystallization	Not mentioned	Rakhimov et al. (2011)
		E. franchetii	Aerial part	Repeated silica gel column chromatography	Not mentioned	Rakhimov et al. (2011)
		E. hirta	Leaf	Reverse phase column chromatography of the butanol fraction of plant extract followed by serial gel filtration chromatography	0.02 %‡	Yoshida et al. (1988)
		E. humifusa	Leaf	Gel filtration chromatography of the ethyl acetate fraction of plant extract followed by gel filtration and reverse phase column chromatography	0.12 %‡	Yoshida et al. (1994)
	Macaranga	*M. tanarius*	Leaf	Gel filtration chromatography of acetone–water (7:3) plant extract followed by repeated reverse phase column and gel filtration chromatography	0.61 %‡	Lin et al. (1990b)
	Mallotus	*M. japonicus*	Leaf	Boiled water extraction for 20 min	1.2 %†	Tabata et al. (2008)
	Sapium	*S. japonicum*	Stem	Silica gel column chromatography of the ethyl acetate fraction of plant extract followed by gel filtration chromatography	0.002 %‡	Kang et al. (2006)
		S. sebiferum	Stem and callus	For stem tissues, acetone–water (8:2) extract was subjected to gel filtration chromatography followed by reverse-phase column and gel filtration chromatography For calli, the purification procedures were the same except for the solvent extraction in which acetone–water (9:1) solvent was used	0.21 % for stem†; 0.07–0.13 % for calli†	Neera and Ishimaru (1992), Neera et al. (1992)

Phytochem Rev (2017) 16:159–193

Table 1 continued

Family	Genus	Species	Plant part used	Extraction technique	Yield	References
Geraniaceae	*Erodium*	*E. cicutarium*	Aerial part	Reverse-phase column chromatography of the acidified (98 % formic acid) plant extract followed by recrystallization and then acetone-methanol (8:2) extraction	0.08 %‡	Fecka and Cisowski (2005)
		E. glaucophyllum	Unstated	Silica-gel column chromatography of the ether fraction of plant extract followed by repeated reverse-phase column chromatography	0.14 %‡	Gohar et al. (2003)
	Geranium	*G. bellum*	Aerial part	Gel filtration chromatography of the ethyl acetate fraction and methanol fractions of plant extract	0.70 %‡	Gayosso-De-Lucio et al. (2010)
			Aerial part	Gel filtration chromatography of the crude plant extract followed by silica gel column and reverse-phase column chromatography	3.46 %‡	Velazquez-Gonzalez et al. (2014)
		G. carolinianum	Aerial part	Silica gel column chromatography of the ethyl acetate plant extract followed by gel filtration chromatography	0.002 %‡	Li et al. (2008)
			Aerial part	Water extraction by reflux	Purification of geraniin was not done	Wu et al. (2011)
		G. potentillaefolium	Aerial part	Gel filtration chromatography of the ethyl acetate fraction and methanol fractions of plant extract	0.30 %‡	Gayosso-De-Lucio et al. (2010)
		G. pratense	Root	Reverse phase column chromatography of 80 % methanol plant extract and recrystallization	Not mentioned	Ushiki et al. (1998)
		G. schiedeanum	Aerial part	Gel filtration chromatography of the acetone–water (7:3) plant extract followed by reverse phase column chromatography	4.55 %‡ (Acetonylgeraniin was isolated instead of geraniin)	Gayosso-De-Lucio et al. (2014)
		G. sibiricum	Whole plant	Microwave-assisted enzymatic extraction	1.98 %‡	Yang et al. (2010)
			Whole plant	Microwave-assisted ethanol and low concentration acid extraction	4.52 %‡	Yang et al. (2013)
		G. thunbergii	Leaf	Droplet countercurrent chromatography of the ethyl acetate fraction of plant extract and repeated recrystallization	1.60 %†	Okuda et al. (1975, 1977)
			Callus	Gel filtration of the callus extract	0.04–0.65 %‡	Ishimaru and Shimomura (1991)

Table 1 continued

Family	Genus	Species	Plant part used	Extraction technique	Yield	References
			Callus	Gel filtration chromatography of the acetone–water (7:3) extract	Not mentioned	Yazaki et al. (1991)
			Whole plant	Silica gel column chromatography of the ethyl acetate fraction of plant extract followed by gel filtration chromatography	0.04 %‡	Youn and Jun (2013)
		G. viscosissimum	Aerial part	Soxhlet extraction with hexane first (to remove lipid) and then methanol	Not mentioned	Klocke et al. (1986)
		G. wilfordii	Unstated	Reverse-phase and normal-phase high speed counter-current chromatography of acetone–water (7:3) plant extract	Not mentioned	Liu et al. (2010)
			Unstated	Column chromatography with cross-linked 12 % agarose gel of acetone–water (7:3) plant extract	Not mentioned	Liu et al. (2011)
			Unstated	Liquid–liquid/solid three-phase high speed counter-current chromatography of acetone–water (7:3) plant extract	0.28 %‡	Liu et al. (2012a)
Nymphaeaceae	*Nymphaea*	*N. tetragona*	Leaf	Silica gel column chromatography of the ethyl acetate fraction of plant extract followed by gel filtration chromatography and silica gel preparative thin layer chromatography	0.29 %†	Kurihara et al. (1993)
			Root	Celite-loaded column chromatography of ethyl acetate fraction of plant extract followed by silica gel column, reverse phase column and gel filtration chromatography	0.04 %‡	Kang et al. (2011)
	Phyllanthus	*P. amarus*	Aerial part	Gel filtration chromatography of the acetone–water (7:3) plant extract followed by column chromatography	1.03 %‡	Foo and Wong (1992), Foo (1993), Foo (1995)
		P. caroliniensis	Whole plant	Silica gel column chromatography of the ethyl acetate plant extract followed by gel filtration chromatography	0.06 %‡	Filho et al. (1996)
		P. emblica	Leaf and branch	Aqueous plant extract was subjected to repeated gel filtration and silica gel column chromatography	0.02 %‡	Zhang et al. (2001)
			Fruit rind	Gel filtration chromatography of the ethyl acetate plant extract	0.01 %‡	Kumaran and Karunakaran (2006)
			Fruit flesh	Gel filtration chromatography of the ethyl acetate plant extract followed by reverse-phase HPLC	Not mentioned	Liu et al. (2008, 2012b)
		P. flexuosus	Leaf	Reverse phase column chromatography of the butanol fraction of plant extract followed by gel filtration chromatography	0.27 %‡	Yoshida et al. (1992)
		P. muellerianus	Leaf	Gel filtration chromatography of the ethyl acetate plant extract	1.2 %‡	Agyare et al. (2011), Ndjonka et al. (2012)

Table 1 continued

Family	Genus	Species	Plant part used	Extraction technique	Yield	References
		P. niruri	Unstated	Duplicate gel filtration chromatography of the butanol fraction of plant extract	0.23 %‡	Ueno et al. (1988)
			Leaf and stem	Gel filtration chromatography of the methanol plant extract followed by reverse phase column chromatography	0.79 %‡	Ishimaru et al. (1992)
			Aerial part	30 % ethanol and mild heat (60 °C) extraction for an hour	Not mentioned	Mahdi et al. (2011)
		P. sellowianus	Leaf and stem	Silica gel column chromatography of the ethyl acetate fraction of plant extract followed by gel filtration chromatography	0.009 %†	Miguel et al. (1996)
	P. urinaria	Whole plant		Gel filtration chromatography of acetone–water (4:1) plant extract followed by reverse phase column, gel filtration and silica gel column chromatography respectively	0.03 %†	Yang et al. (2007)
		Whole plant		Gel filtration chromatography of the acetone–water (7:3) plant extract followed by reverse phase column chromatography and recrystallization	0.04 %‡	Lin et al. (2008)
		Aerial part		30 % ethanol and mild heat (60 °C) extraction for an hour	Not mentioned	Mahdi et al. (2011)
Rosaceae	*Agrimonia*	*A. pilosa*	Whole plant	Reverse phase column chromatography of the acetone–water (7:3) plant extract followed by gel filtration chromatography and recrystallization	Not mentioned	Jin and Wang (2010)
Sapindaceae	*Acer*	*A. nikoense*	Leaf, bark, branch, timber	Each plant part was boiled in distilled water for 10 min	Purification of geraniin was not carried out	Okabe et al. (2001), Fujiki et al. (2003)
	Dimocarpus	*D. longan*	Seed	Soxhlet extraction of dried seeds to remove lipid content followed by resuspension in methanol and serial gel filtration chromatography	Purification of geraniin was not carried out	Sudjaroen et al. (2012)
	Nephelium	*N. lappaceum*	Fruit rind	Gel filtration chromatography of the methanol plant extract	Not mentioned	Thitilertdecha et al. (2010)
			Fruit rind	Reverse-phase column chromatography of the ethanol plant extract	0.15 %‡	Palanisamy et al. (2011a), Perera et al. (2012)

* Initial mass of the plant material used was not mentioned

† Fresh plant material was used

‡ Dried plant material was used

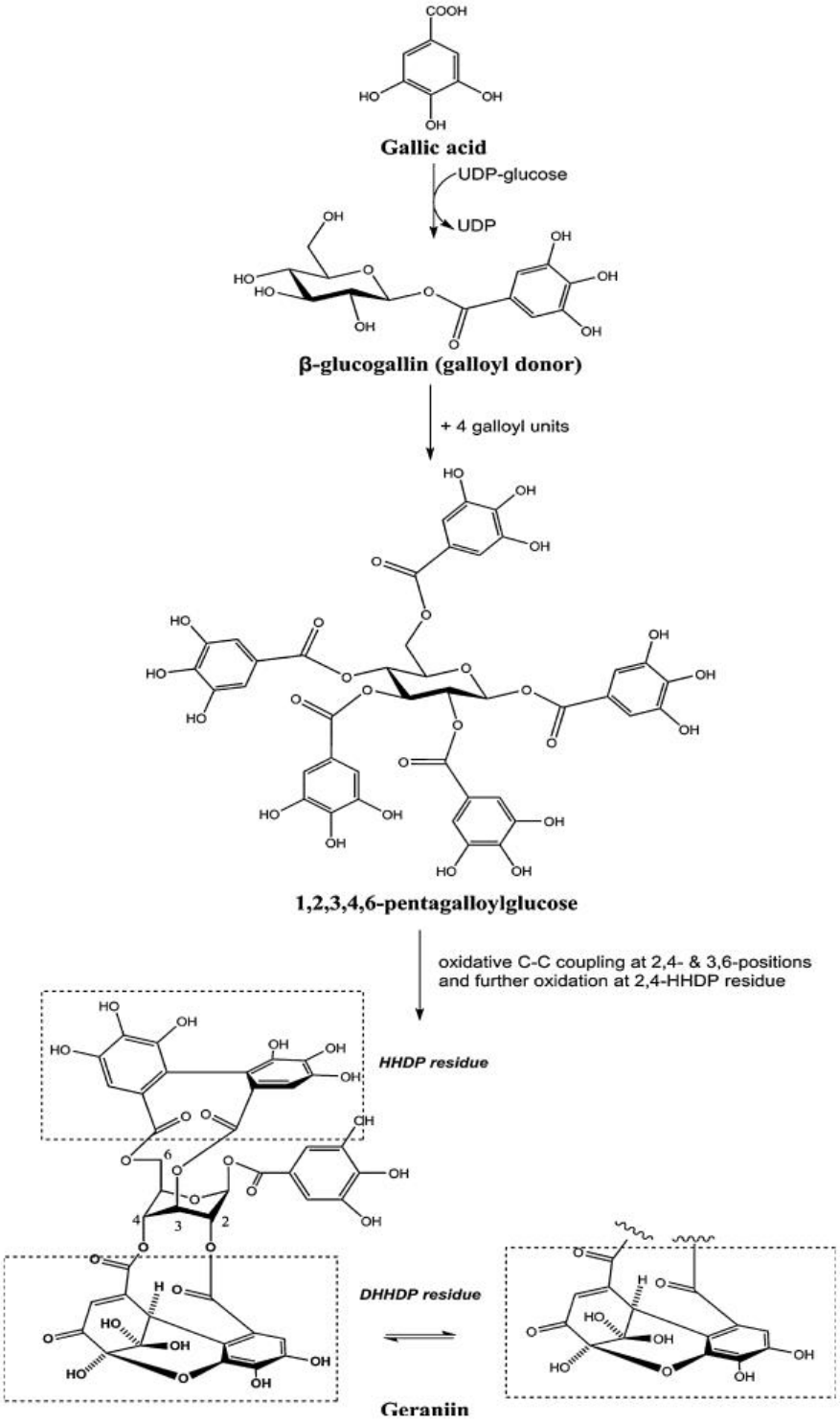

Fig. 4 Biosynthesis of the ellagitannin geraniin. *DHHDP* dehydrohexahydroxydiphenoyl, *HHDP* hexahydroxydiphenoyl, *UDP* uridine diphosphate

galloyltransferases up to PGG following a remarkably specific metabolic pattern (β-glucogallin → 1,6-digalloylglucose → 1,2,6-trigalloylglucose → 1,2,3,6-tetragalloylglucose → 1,2,3,4,6-pentagalloylglucose) (Schmidt et al. 1987; Cammann et al. 1989; Gross and Denzel 1991; Hagenah and Gross 1993). The highly selective acylation sequence of glucopyranosides suggests a combination of differential reactivity of primary and secondary hydroxyl groups, neighbour-activation effects and steric hindrance at work (Williams and Richardson 1967).

Subsequently, PGG acts as the immediate precursor for the formation of HHDP residues through oxidative biaryl coupling of adjacent galloyl units. Using radioactively-labelled PGG (Rausch and Gross 1996), the enzyme catalysing the oxidative C–C coupling was identified as one of the members from the group of laccase-type phenol oxidases (EC 1.10.3.2) and named "pentagalloylglucose: O_2 oxidoreductase" (Niemetz and Gross 2003). The HHDP moiety can be located at the 2,3-, 4,6-, 1,6-, 3,6- and/or 2,4-positions of the glucopyranose core (Immel and Khanbabaee 2000). In geraniin, it is postulated that the bridging HHDP units form at both the 2,4- and 3,6-positions of the glucopyranose ring in its $^1C_4$ conformation, followed by further oxidation of the 2,4-HHDP glucoside to yield a DHHDP residue (Pouysegu et al. 2011). The enzymatic catalysis of the HHDP residue oxidation, however, is not well-understood and thus, requires further investigation.

Pharmacokinetics and bioavailability of the ellagitannin geraniin

Existing evidence on the metabolism of geraniin upon oral ingestion is fairly limited, but the pharmacokinetic studies of other ellagitannins may help to provide a better overview for geraniin. Generally, intact geraniin is rarely found in the circulation after oral dosing. This is anticipated because of its large molar mass which does not facilitate simple diffusion very effectively and so, degradation of geraniin into smaller metabolites is crucial for the absorption. However, it is noteworthy that some of the large hydrolysable tannins like corilagin (M.W. 636 g/mol) and punicalagin (M.W. 1084 g/mol) do get absorbed and excreted at a small extent upon oral consumption in rats (Cerda et al. 2003; Ito 2011). In this context, the absorption and metabolism of geraniin may occur at two distinct regions of the gastrointestinal tract, namely (1) the stomach and proximal small intestine as well as (2) the distal small intestine and colon, the latter of which seems to play a more predominant role in the absorption. The proposed metabolism of geraniin into smaller metabolites is illustrated in Fig. 5.

Partial hydrolysis of geraniin produces corilagin while complete hydrolysis yields gallic acid and ellagic acid. All these hydrolytic products have been detected in serum and/or urine upon consumption of ellagitannin-rich functional food (Hodgson et al. 2000; Ito 2011), According to Seeram et al. (2006), in human subjects, the plasma concentration of ellagic acid peaked at about 1 h post oral administration of pomegranate juice which is high in ellagitannin content, suggesting that at least part of the ellagitannin are rapidly hydrolysed and absorbed in the stomach and/or small intestine. Daniel et al. (1991) demonstrated that it is in the small intestine that free ellagic acid is released from crude ellagitannin extract and the reaction is dependent on the mild alkaline pH in the small intestine and free from the interference of pancreatic enzymes and bile salts. In the same study, it was also shown that ellagitannin is relative stable under physiological gastric conditions. Although these findings are not established specifically based on geraniin, considering how most ellagitannins share similar basic chemistry, it is reasonable to extrapolate the information to geraniin. Absorption of free ellagic acid in small intestine is rather poor (<1 % of the total ingested amount) (Stoner et al. 2005). The absorption capacity is probably diminished by the high, irreversible binding of ellagic acid to macromolecules like proteins and DNA in the intestinal epithelium (Whitley et al. 2003).

Hydrolysis of geraniin as well as other catabolic reactions like decarboxylation and removal of hydroxyl groups continue in the large intestine where intestinal bacteria seem to play an integral role in the process. Various hydrolytic products including corilagin, ellagic acid, gallic acid and brevifolincarboxylic acid as well as decarboxylated products such as pyrogallol and brevifolin were found when geraniin was subjected to anaerobic incubation with rat fecal suspension (Ito 2011). Further incubation for more than 6 h affords various hydroxyl-6H-benzopyran-6-one derivatives (urolithins) (Ito et al. 2008; Ito 2011). The timing of urolithin production corresponds precisely to the upsurge of serum and urine urolithin

concentration which occur only after 6–12 h after single dosing of geraniin in rats (Ito et al. 2008; Ito 2011). This suggests that metabolites generated from intestinal microbial degradation of geraniin are subsequently absorbed into bloodstream at the large intestine. Nevertheless, not all the bacterial urolithin products are absorbed. Intestinal bacteria transform geraniin or ellagic acid into urolithins with different numbers of hydroxyl groups, ranging from monohydroxy-urolithin (urolithin B), dihydroxy-urolithin (urolithin A), trihydroxy-urolithin (urolithin C) up to tetrahydroxy-urolithin (urolithins D and E) (Ito et al. 2008; Garcia-Villalba et al. 2013), but only urolithins A, B and C are consistently found in the serum and urine (Cerda et al. 2004; Ito et al. 2008). Basically, intestinal bacteria-facilitated geraniin breakdown is a gradual process because complete clearance is not achieved even after 72 h (Ito et al. 2008). The hydrolysis reaction appears to be the rate-limiting reaction as conversion of ellagic acid to urolithins is much more efficient in comparison to conversion of ellagitannins to urolithins (Gonzalez-Barrio et al. 2011).

Another evidence that supports the involvement of colon microbes in geraniin metabolism is the marked interpersonal variation of the circulatory and excretory urolithins detected in human volunteers after drinking high-ellagitannin fruit juices (Seeram et al. 2006; Gonzalez-Barrio et al. 2010). Such an observation is attributable to the variability of colonic microbiota. In fact, not only does the urolithin profile show person-to-person differences, large inter-individual variations have also been detected in terms of the quantity of urolithins (Seeram et al. 2006), latency between ellagitannin ingestion and presence of urolithins in circulation (Gonzalez-Barrio et al. 2010) and the total urinary excretion of urolithin (Cerda et al. 2004), indicating how strong the dependence of ellagitannin geraniin metabolism is on the gut microflora.

As pointed out earlier, a number of metabolites, namely gallic acid, pyrogallol, ellagic acid and urolithins, are absorbed into the body. The metabolic pathways of these metabolites upon absorption is outlined in Fig. 6. Generally, compounds with ortho-dihydroxyl group will be swiftly methylated by the action of catechol-*O*-methyl transferase (COMT) to form a methyl ether group. In ellagic acid, there are two such groups and hence, two methyl moieties are added to form dimethylellagic acid. Gallic acid,

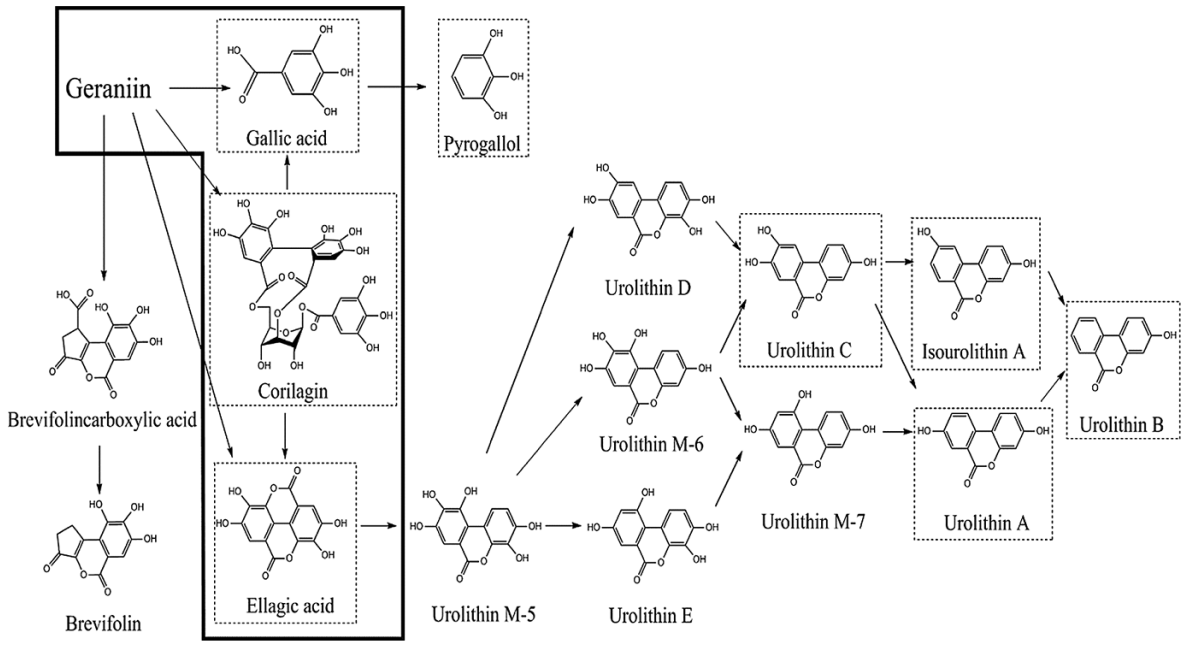

Fig. 5 Proposed metabolism of geraniin into different metabolites in the presence of intestinal microflora. Metabolic pathways highlighted by *solid line* may also take place in the stomach and/or proximal small intestine while the metabolites highlighted by *dotted line* are found in the serum or urine after the consumption of geraniin and other ellagitannins

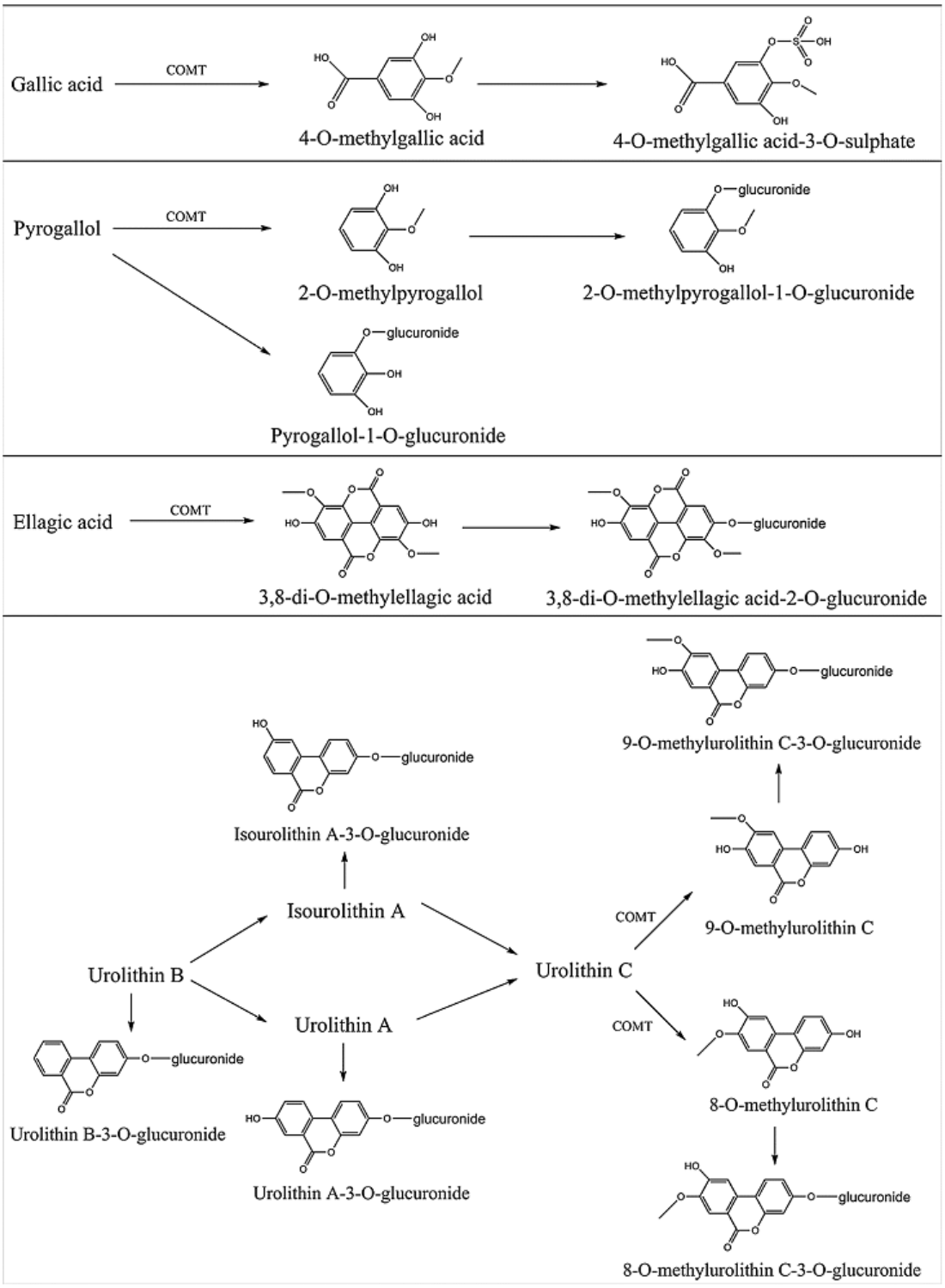

Fig. 6 Postulated metabolic pathways of metabolites originated from geraniin upon absorption into the body. *COMT* catechol-*O*-methyltransferase

pyrogallol and urolithin C can also be converted by COMT (Yasuda et al. 2000; Ito 2011). Aside from that, hydroxylation of urolithins A and B is also a likely in vivo metabolic process so that they become more susceptible to further conjugation and urinary excretion as evidenced by the escalated expression and activity of cytochrome P450 1A1 (CYP1A1) in ellagic acid-treated colon cancer cell lines (Gonzalez-Sarrias et al. 2009). Irrespective of methylation, virtually all the metabolites are subjected to sulphate or glucuronide conjugation. The conjugates are then delivered to either the liver or kidney for elimination.

No study has reported the detection of intact geraniin in the circulation or urine post oral administration. Absorption takes place after pH-induced hydrolysis and microbial transformation. Some metabolites, notably urolithins, display exceedingly good absorption efficacy whereas others like corilagin, gallic acid, ellagic acid and pyrogallol are absorbed to a much lesser extent (Ito 2011). The bioavailability of the metabolites, however, varies substantially. In rats, approximately 12.4 % of the total geraniin was excreted in urine as urolithins over 72 h (Ito et al. 2008) whereas in humans, the total urinary excretion of metabolites upon ellagitannin ingestion ranged from 0.7 to 52.7 % (Cerda et al. 2003). Once again, this reinforces the notion that the bioavailability is highly dependent on the bacterial composition of colonic microbiota. Despite the absorption, no evidence has shown the deposition of the metabolites in major organs like the adipose tissues, muscles, heart and brain. Accumulation of the metabolites in their conjugated form was detected in the liver and kidney (Espin et al. 2007). This shows the involvement of these organs in the elimination of geraniin metabolites. Indeed, a large amount and variety of urolithin conjugates were found in bile juice, confirming the active role of the hepatic drug clearance system in addition to urinary excretion (Espin et al. 2007). Such an enterohepatic circulation is held responsible for the long persistency of urolithins in the circulation.

In short, like other ellagitannins, there is limited evidence, showing that geraniin is bioavailable upon oral dosing. However, the compound is subjected to extensive degradation and metabolism mainly by the intestinal bacteria to afford various metabolites which are subsequently absorbed and persists in the body for a relatively long duration. These metabolites, particularly urolithins, may be the key players that account for the bioactivity of geraniin as well as other ellagitannins.

Biological effects of the ellagitannin geraniin

Over four decades of geraniin research, a large variety of bioactivities has been reported for the polyphenolic compound, ranging from antioxidant, antimicrobial, anticancer, anti-inflammatory, antihypertensive, anti-hyperglycaemic, antidiarrheal, anaesthetic to protective effects on different organs. Different approaches, including in vitro cell culture study, in vivo animal study as well as direct chemical and enzymatic assays have been employed to attain these findings. These bioactivities of geraniin are summarised in Table 2. Looking into these bioactive properties of geraniin may allow us to characterise the natural product and its mechanisms of action. The bioactivities of geraniin have also been summarised in a review by Perera et al. (2015).

Antioxidant properties

High antioxidant activity has been consistently reported in the crude extract of geraniin-rich plants. The crude ethanolic extract of *N. lappaceum* peels has a 2,2-diphenyl-1-picrylhydrazyl (DPPH) radical scavenging capacity comparable to that of vitamin C (Palanisamy et al. 2008). Such a powerful radical scavenging capacity has also been confirmed in the plant extract of the same (Thitilertdecha and Rakariyatham 2011) or different geraniin-rich plant species (Yang et al. 2010; Arina and Rohman 2013). Palanisamy et al. (2008) further tested the pro-oxidant capacity of the plant extract as some strong antioxidant agents, particularly vitamin C, also possess pro-oxidant properties through their interaction with catalytic metal ions to generate harmful radicals (Carr and Frei 1999). It was demonstrated that the peel extract of *N. lappeceum* has the lowest pro-oxidant capacity in comparison to vitamin C and α-tocopherol (Palanisamy et al. 2008). The pro-oxidant profile is similar to Emblica TM, a commercial antioxidant with exceedingly low pro-oxidant activity derived from the fruits of another geraniin-rich plant, *P. emblica* (Liu et al. 2008, 2012b). The consistency in the detection of strong antioxidant and low pro-oxidant activities of geraniin-rich plant extracts strongly suggest that geraniin may play an integral role to these bioactivities.

Table 2 Biological activities of the ellagitannin geraniin

Bioactivity	Experimental method	Mode of action/assay type	Effective concentration/dose	References
Antioxidant	In vitro biochemical assay	Scavenge 2,2-diphenyl-1-picrylhydrazyl (DPPH) radicals	0.31–18.7 μM*	Yokozawa et al. (1998), Xu et al. (2007), Lin et al. (2008), Liu et al. (2008), Thitilertdecha et al. (2010), Sudjaroen et al. (2012)
		Scavenge superoxide radicals	2.65 μM*	Lin et al. (2008)
		Scavenge hydroxyl radicals	0.11 μM*	Lin et al. (2008)
		Scavenge nitric oxide radicals	3.81 μM*	Kumaran and Karunakaran (2006)
		Oxygen radical absorbance capacity (ORAC)	1.95–3.80 mol-Trolox equivalent/mol	Ishimoto et al. (2012), Sudjaroen et al. (2012)
		Ferric reducing antioxidant power (FRAP)	92 μM (to give absorbance equal to 1 mM Fe(II) solution)	Sudjaroen et al. (2012)
		Xanthine oxidase inhibition	30.49 μM*	Lin et al. (2008)
		Lipid peroxidation inhibition	0.38–65.7 μM*	Liu et al. (2008), Thitilertdecha et al. (2010)
	H_2O_2-treated HepG2 cells	Reduce intracellular reactive oxygen species (ROS); increase glutathione level; promote Nrf2 nuclear translocation for upregulation of downstream detoxifying antioxidant genes	10–20 μM	Wang et al. (2015)
	SIN-1/AAPH-treated Hs68 cells	Scavenge nitric oxide, superoxide, peroxynitrite and peroxyl radicals	5–30 μM	Ling et al. (2012)
	CCl_4-induced acute liver damage rats	Enhance catalase activity and glutathione level and reduce malondialdehyde level in liver tissue homogenate	50 mg/kg/day; oral administration	Islam et al. (2008)
	S_{180} entity-tumor mice	Enhance superoxide dismutase activity and total antioxidant capacity and reduce malondialdehyde level in red blood cells	40–60 mg/kg/day; intragastric administration	Jin and Sun (2011)
Antibacterial	Disc diffusion method	*Aeromonas salmonicida*	500 μg; inhibitory zone-13 mm	Kurihara et al. (1993)
		Pseudomonas fluorescens	500 μg; inhibitory zone-14 mm	
		Streptomyces scabies	Not reported	Ushiki et al. (1998)
		Ralstonia solanacearum	0.5 μmol, inhibitory zone-19 mm	Ooshiro et al. (2011)
	Minimum inhibitory concentration (MIC) test	*Bacillus subtilis*	100 μg/mL	Adesina et al. (2000)
		Staphylococcus aureus	25 μg/mL	
		Escherichia coli	2.5 mg/mL	Gohar et al. (2003)

Table 2 continued

Bioactivity	Experimental method	Mode of action/assay type	Effective concentration/dose	References
		Staphylococcus aureus	3.16 mg/mL	
		Helicobacter pylori	6.25–25 μg/mL	Funatogawa et al. (2004)
Antiviral	In vitro biochemical assay	Inhibit RNA tumor virus reverse transcriptase	10–1000 μM	Kakiuchi et al. (1985)
		Inhibit CD4-gp120 binding	0.48 μg/mL*	Notka et al. (2004)
		Inhibit human immunodeficiency virus (HIV)-1 integrase	0.16 μg/mL*	Notka et al. (2004)
		Inhibit HIV-1 reverse transcriptase	1.8–14.6 μg/mL*	Notka et al. (2003, 2004)
		Inhibit HIV-1 protease	6.28 μg/mL*; 50 μg/mL (68–81 % inhibition	Xu et al. (2000), Notka et al. (2004)
	End-point dilution assay	Increase viral titre of *Coxsackie* B_2 and HSV (herpes simplex virus)-1 by 10^3-fold	50 μg/mL	Corthout et al. (1991)
	Hepatitis B virus (HBV)-producing MS-G2 cells	Inhibit HBV e (HBeAg) and surface (HbsAg) antigens	50 μM for 32.1 % and 46.6 % inhibition for HbsAg and HbeAg	Huang et al. (2003)
	HBV-producing HepG2 2.2.15 cells		200 μg/mL for 85.8 % and 63.7 % inhibition for HbsAg and HbeAg	Li et al. (2008)
	HIV-1-treated MT4 T-lymphoid cells	Inhibit HIV-1 replication	0.24–0.46 μg/mL*	Notka et al. (2003)
		Inhibit HIV-1 entry into cells	2.5 μg/mL for 70–75 % inhibition	
	Plaque assay of HSV-1 and -2-treated Vero cells	Inhibit HSV-1 infection	35 μM*	Yang et al. (2007)
		Inhibit HSV-2 infection	18.4 μM*	
	Plaque assay of enterovirus-71 (EV71)-treated rhabdomyosarcoma cells	Inhibit EV71 infection; reduce EV71 RNA replication	10 μg/mL*	Yang et al. (2012)
	Lethally EV71-infected mice	Prolong survival duration; reduce mortality rate	0.4–1.0 mg/kg/day for >35 % survival rate; intraperitoneal administration	
Antifungal	MIC test	*Candida pseudotropicalis*	2 mg/mL	Adesina et al. (2000)
		Candida albicans	1.99 mg/mL	Gohar et al. (2003)
Antiprotozoal	*Plasmodium falciparum*-infected human erythrocytes	Inhibit the growth of *P. falciparum*	11.19 μg/mL*	Ndjonka et al. (2012)
	Leishmania donovani-infected murine macrophages	Reduce the viability of intracellular amastigotes of *L. donovani*	0.4 μg/mL*	Kolodziej et al. (2001)

Phytochem Rev (2017) 16:159–193

Table 2 continued

Bioactivity	Experimental method	Mode of action/assay type	Effective concentration/dose	References
Anticancer	MK-1, HeLa and B16F10 cells	Inhibit tumour cell proliferation	9 μg/mL for MK-1 cells; 11 μg/mL for HeLa cells; 2 μg/mL for B16F10 cells†	Zhang et al. (2004)
	Human melanoma cells	Induce apoptosis	20–40 μM	Lee et al. (2008)
	HepG2 cells	Reduce tumour cell viability and upregulate p53 tumour suppressor gene expression	40 μM for 34 % in cell viability	Jin and Wang (2010)
	MCF-7 cells	Reduce tumour cell viability	13.2 μg/mL	Liu et al. (2011)
	HeLa and Jurkat cells	Reduce tumour cell viability; promote cell cycle arrest in G_2/M phase	0.76 μM for Jurkat cells; 5.1 μM for HeLa cells*	Vassallo et al. (2013)
	A549 lung cancer cells	Inhibit transforming growth factor (TGF)-β1-induced epithelial-mesenchymal transition, cell migration, invasion and anoikis resistance	15–20 μM	Ko (2015)
		Inhibit tumour cell proliferation; promote cell cycle arrest at S phase; induce apoptosis	12.75 μM*	Li et al. (2013)
	A549 xenograft tumours in nude mice	Inhibit tumour cell growth	10–20 mg/kg/day; oral administration for 54–72 % inhibition rate	
Immuno-modulatory	*Saccharomyces cerevisiae*-treated mouse macrophages	Enhanced phagocytosis and acid phosphatase activity of macrophages	Incubation in 2–20 μg/mL for 24 h	Ushio et al. (1991)
	Lipopolysaccharide (LPS)-activated murine macrophages	Inhibit LPS-induced IkB phosphorylation; inhibit NF-kB activity; inhibit activation of inducible nitric oxide synthase (iNOS)	30 μM	Pan et al. (2000)
	Murine macrophages	Induce the secretion of tumor necrosis factor (TNF)	0.7 μg/mL*	Kolodziej et al. (2001)
		Induce the release of interferon	0.3 μg/mL*	
	BALB/3T3 cells	Inhibit the release of TNF-α	43 μM*	Okabe et al. (2001), Fujiki et al. (2003)
	H. pylori-infected human gastric epithelial cells and murine macrophages	Downregulate the expression of 5-LOX, NF-kB, interleukin-8 and TNF-α	10 μM	Park et al. (2007)
Liver protection	In vitro biochemical assay	Inhibit lipid peroxidation	1.0–6.6 μg/mL*	Okuda et al. (1983)
	Ethanol-treated mouse liver slice culture	Prevent ethanol-induced cytotoxicity, reduce oxidative damage and inhibit apoptotic cell death	0.25 mM	Londhe et al. (2012)
	Peroxidised corn oil-treated rats	Improve lipid profile, liver function and inhibit lipid peroxidation	50–100 mg/kg/day; oral administration	Kimura et al. (1984)
	CCl_4-induced liver damage in rats		5–10 mg/kg/day; intramuscular administration	Nakanishi et al. (1999)

Table 2 continued

Bioactivity	Experimental method	Mode of action/assay type	Effective concentration/dose	References
Osteoprotective	Rat osteoclast cells	Reduce mature osteoclasts, pre-osteoclast, osteoclast fusion and bone resorption	0.01–10 nM	He et al. (2013)
	Mouse osteoclast cells	Inhibit the formation of osteoclasts and bone resorption	1.25–5 μM	Xiao et al. (2015)
	In vivo Ti-treated mouse calvaria model	Inhibit particle-induced osteolysis	1–4 mg/kg per 2 days; intraperitoneal administration	
	Bilaterally ovariectomized rats	Increase serum calcium, estradiol and calcitonin; modulate bone turnover biomarkers; prevent ovariectomy-induced bone loss	20–40 mg/kg/day; intragastric administration	Lu et al. (2015)
Neuroprotective	In vitro biochemical assay	Inhibit prolyl endopeptidase	0.069 μM*	Lee et al. (2007)
		Inhibit β-secretase	4.0 μM*	Youn and Jun (2013)
Radioprotective	In vitro biochemical assay	Inhibit γ-radiation-induced free radical liberation and DNA strand fragmentation	0.1 mM	Londhe et al. (2009)
	Chinese hamster lung fibroblast cells	Improve post irradiation cell viability; inhibit γ-radiation-induced apoptosis, cellular component damage and ROS generation; normalise antioxidant enzymes' activities	5 μg/mL	Kang et al. (2011)
	Mouse splenocytes	Inhibit γ-radiation-induced apoptosis and DNA damage; promote cell proliferation	1.6 μg/mL	Bing et al. (2013)
	Whole body irradiated mice	Inhibit γ-radiation-induced DNA damage in splenocytes; prevent the death of jejunal crypt cell	25 mg/kg; 17 h and 1 h prior to irradiation; intraperitoneal administration	
Antihypertensive	In vitro biochemical assay	Inhibit angiotensin-converting enzyme	13.22–400 μM*	Ueno et al. (1988), Lin et al. (2008)
	SHR and WKY rats	Lower arterial blood pressure	2–6 mg/kg; single dose; intravenous administration	Cheng et al. (1994)
	SHR rats	Lower systolic and diastolic blood pressure levels	5 mg/kg; single dose; oral administration	Lin et al. (2008)
Antihyperglycaemic and antidiabetic	In vitro biochemical assay	Inhibit α-glucosidase	0.92 μg/mL*	Palanisamy et al. (2011a)

Table 2 continued

Bioactivity	Experimental method	Mode of action/assay type	Effective concentration/dose	References
		Inhibit α-amylase	0.93 μg/mL*	
		Inhibit aldol reductase	7 μg/mL*	
		Inhibit advanced glycation end products formation	20 μg/mL	
	High fat diet-induced obese rats	Reduce white adipose tissue weight; improve glycaemic control and insulin sensitivity; improve lipid profile	50 mg/kg/day; oral administration	Chung et al. (2014)
Anticoagulant and antiplatelet	In vitro biochemical assay	Inhibit platelet aggregation induced by arachidonic acid, adenosine diphosphate, platelet activating factor and activated neutrophils	2.4 μM for AA-induced; 0.4 μM for ADP-induced; 1.1 μM for PAF-induced and 10.2 μM for activated neutrophil-induced*	Chen et al. (2012)
		Inhibit plasminogen activator inhibitor-1 (PAI-1)	10.48 μM	Yuan et al. (2012)
Analgesic and antinociceptive	Acetic acid-induced writhing/ abdominal constriction in mice	Reduce the number of writhing movements	10–30 mg/kg; single dose pretreatment; intraperitoneal administration	Miguel et al. (1996)
			5–25 mg/kg; single dose pretreatment; oral administration	Velazquez-Gonzalez et al. (2014)
Antidiarrheal	In vitro biochemical assay	Inhibit acetylcholine- and histamine-induced intestinal contractions	0.1–0.3 mg/mL	Kan and Taniyama (1992)
Wound healing	Primary human fibroblasts	Accelerate proliferation; enhance collagen synthesis	5 μM	Agyare et al. (2011)
	Human keratinocytes	Accelerate proliferation; induce keratinocyte differentiation	50–100 μM	
Gastric ulcer prevention	Acidified ethanol-induced gastric ulceration in rats	Inhibit back diffusion of acid; enhance gastric mucus production	10–100 mg/kg; single dose pretreatment; intragastric administration	Hung et al. (1995)

* IC_{50}

† GI_{50}

Indeed, using ferric reducing/antioxidant power (FRAP) assay, it is known that the antioxidant capacity of geraniin is about fivefold to sixfold more potent than L-ascorbic acid and trolox (Sudjaroen et al. 2012). Much of this antioxidant properties is probably attributable to its free radical scavenging ability towards numerous damaging radicals like DPPH radicals, superoxide radicals, hydroxyl radicals and nitric oxide radicals as shown in Table 2. Tabata et al. (2008) showed that geraniin is comparable to or even better than epigallocatechin gallate, a strong antioxidant found in green tea in terms of free radical scavenging (Tabata et al. 2008). Furthermore, to give an idea of how strong the radical scavenging activity of geraniin is, in most of the studies, the 50 % inhibition concentration (IC_{50}) of geraniin is about 7–14 times smaller than that of positive controls including ascorbic acid (Lin et al. 2008), butylated hydroxyanisole (BHA) (Liu et al. 2008) and butylated hydroxytoluene (BHT) (Lin et al. 2008), implying that geraniin is more effective at preventing oxidation than most of the widely used antioxidant food additives. In one particular study, it was even demonstrated that geraniin is about 87 times stronger than BHT in scavenging DPPH radicals (Thitilertdecha et al. 2010). The beneficial radical scavenging properties also confers cytoprotective effects in a human foreskin fibroblast cell line against oxidative and nitrosative stress-induced cell death (Ling et al. 2012). The mechanism of radical scavenging activity is not clearly characterised. However, it is generally accepted that most of the polyphenolic compounds scavenge free radicals via hydrogen atom transfer mechanism (Leopoldini et al. 2011; Meo et al. 2013). Phenolic compounds have a high tendency to donate a hydrogen atom to a radical, transforming the original radical into a harmless molecule, but itself to a phenoxyl radical (Leopoldini et al. 2011). Despite the formation of another radical, phenoxyl radicals are non-damaging because they have aromatic structures that facilitate resonance stabilization of the radical (Leopoldini et al. 2011). These phenoxyl radicals may further couple with another free radical to quench the reactivity of both radicals, a characteristic known as chain-breaking antioxidant activity. Such an activity has been reported in some of the natural polyphenols like catechin, quercetin and gallic acid (Roginsky 2003), but it is unsure whether the free radical scavenging activity of geraniin acts in a similar manner.

Apart from free radical scavenging activity, geraniin can also inhibit xanthine oxidase which is a reactive oxygen species (ROS)-generating enzyme (Lin et al. 2008). However, considering the protein-precipitating effect of geraniin, it is likely that the inhibitory effect may be caused by the precipitation of the enzyme (Sudjaroen et al. 2012). Geraniin also possesses an inhibitory effect on lipid peroxidation (Liu et al. 2008; Thitilertdecha et al. 2010). This may explain the reduction of malondialdehye level which an end product of the decomposition of certain lipid peroxidation products (Janero 1990) in animals after geraniin treatment (Islam et al. 2008; Jin and Sun 2011). In addition, geraniin treatment has been shown to enhance glutathione (GSH) levels as well as reduce intracellular ROS levels and cell death rates in a concentration- and time-dependent manner in human hepatocarcinoma cells exposed to hydrogen peroxide-induced oxidative stress (Wang et al. 2015). These beneficial effects might be due to geraniin-induced nuclear translocation of nuclear factor-erythroid 2-related factor 2 (Nrf2), which is a transcription factor responsible for the regulation of various detoxifying antioxidant genes, presumably via PI3K/AKT and ERK1/2 signalling pathways (Wang et al. 2015). Thus, aside from scavenging free radicals directly, at least in in vitro cell culture studies, the antioxidant activity of geraniin may also be augmented by its ability to trigger certain signalling pathways that eventually lead to the upregulation of antioxidant enzymes.

The antioxidant effect of geraniin has also been detected in tetrachloromethane (CCl_4)-induced acute liver failure rats (Islam et al. 2008) and sarcoma S_{180}-tumor cell-inoculated mice (Jin and Sun 2011) as evidenced by significant escalation in GSH and catalase activity in liver tissues for the former as well as increase in superoxide dismutase (SOD) activity in the red blood cells for the latter. These improvements in oxidative status were also associated with better outcomes like improved liver function and suppressed tumor growth in comparison to the untreated counterparts. As such, it is likely that the antioxidant activity of geraniin may be translated into therapeutic effects in certain diseases. However, our current understanding in this aspect is still limited and further investigation should be carried out to unearth the clinical potential of geraniin.

Antimicrobial activity

Crude extracts of geraniin-rich plants also display promising antimicrobial activity against some common human pathogens like *Staphylococcus aureus* and *Escherichia coli* (Thitilertdecha et al. 2008; Yang et al. 2013) as well as dengue virus 2 (Lee et al. 2013). Further investigations using purified geraniin from plant materials confirmed the antibacterial activities with a minimum inhibitory concentration (MIC) ranging from μg/mL to mg/mL (Table 2). Furthermore, Funatogawa et al. (2004) also demonstrated that most hydrolysable tannins, including geraniin, possess antibacterial activity against *Helicobacter pylori*. The activity is likely to be bactericidal because the number of viable cells decreased exponentially after prolonged exposure to another hydrolysable tannin, tellimagradin I. In the same study, Funatogawa et al. (2004) showed that hydrolysable tannins could disrupt liposomal membranes and subsequently, release the liposomal content in a dose-dependent manner. This may be one of the mechanisms of action which accounts for the bactericidal activity against *H. pylori*. The fact that most hydrolysable tannins exhibited similar effects on the growth of *H. pylori* and liposomal membranes disruption suggests that the antibacterial activity lies in the intrinsic properties of hydrolysable tannins. It is also worth mentioning that most of the antibacterial screening tests were not carried out at physiological gastric conditions, particularly acidic pH. As low pH is very likely to jeopardise the structural integrity of most hydrolysable tannins, further work is required to examine whether hydrolysable tannins, including geraniin, can retain its antibacterial properties against *H. pylori* under normal gastric conditions.

Based on Table 2, geraniin also demonstrates potent antiviral properties against some of the most devastating pathogenic viruses. Firstly, hepatitis B virus (HBV) is the major causative agent of acute and chronic liver diseases, of which the latter will lead to cirrhosis and is associated with increased risk of hepatocellular carcinoma (Tsukuma et al. 1993). In this context, geraniin intervention greatly reduced the liberation of HBV e (HBeAg) and surface (HBsAg) antigens from HBV-transfected cell lines (Huang et al. 2003; Li et al. 2008). Using in vitro enzymatic inhibition assays, geraniin also exhibited remarkable inhibitory effects on several enzymes of retroviral origin such as protease, integrase and most importantly, reverse transcriptase (Kakiuchi et al. 1985; Xu et al. 2000; Notka et al. 2004). Co-incubation of geraniin and human immunodeficiency virus (HIV) successfully inhibited virus uptake and replication in MT4-T-lymphoid cells, an outcome which is attributable to the blockade of CD4-gp120 binding by geraniin (Notka et al. 2003, 2004). Moreover, in the presence of small concentrations of geraniin, infection caused by human enterovirus 71 (EV71), herpes simplex virus (HSV) and Coxsackie B_2 was significantly reduced (Corthout et al. 1991; Yang et al. 2007, 2012). In one animal study (Yang et al. 2012), 1 mg/kg of geraniin was intraperitoneally administered to mice which were exposed to a lethal dose EV71. The outcome was astonishing. Geraniin treatment enhanced the survival rate of the mice by about 40 % besides extending the survival time and reducing the severity of the symptoms, strongly pointing out the in vivo therapeutic effect of geraniin against EV71.

In addition to antibacterial and antiviral activities, some studies also reported antifungal and antiprotozoal effects of geraniin. Geraniin treatment effectively inhibits the growth of *Candida pseudotropicalis* and *Candida albicans* at a MIC of 2 mg/mL (Adesina et al. 2000; Gohar et al. 2003). This is of paramount clinical importance because *Candida* spp. are the most common pathogens of fungal infection, principally among immunocompromised patients. When *Plasmodium falciparum*-infected erythrocytes were subjected to geraniin treatment, proliferation of *P. falciparum* was inhibited in a dose-dependent manner (Ndjonka et al. 2012). Moreover, geraniin therapy effectively impaired the viability of amastigotes of *Leishmania donovani* residing within murine macrophage cells at an IC_{50} of <0.4 μg/mL (Kolodziej et al. 2001). This is much more powerful than the clinically used antileishmanial drug, sodium stibogluconate (IC_{50}, 7.9 μg/mL). As such, the antifungal and antimalarial effects of geraniin undoubtedly merit further investigation to understand the precise mode of action and explore potential clinical significance, particularly in the treatment of candidiasis, malaria and leishmaniasis.

Apart from human pathogens, geraniin treatment also exerts antibacterial effects on plant bacteria in in vitro settings. For instance, when tested on *Streptomyces scabies*, which is a microorganism that causes common scab in potatoes, geraniin could reliably inhibit the growth of the potato pathogens (Ushiki

et al. 1998). A similar inhibitory effect was also observed against *Ralstonia solanacearum*, a plant pathogen that is capable of infecting a wide range of crops and eventually causing wilting and dying (Ooshiro et al. 2011) as well as fish pathogens like *Aeromonas salmonica* and *Pseudomonas fluorescens* (Kurihara et al. 1993). Thus, geraniin is not only valuable in fighting against some human infections, but also harbours incredible potential in agricultural aspects in term of disease prevention in large-scale crop plantations and fish farming.

Anticancer activity

Treatment with geraniin in a wide variety of cancer cell lines of both murine and human origins is able to impair the viability and impede the proliferation of the tumor cells. The anticancer activity of geraniin has also been recognised in one in vivo study using adenocarcinoma tumor cell xenografts onto nude mice (Li et al. 2013). Several mechanisms of action have been postulated to describe the anticancer properties of geraniin. Firstly, geraniin treatment induces apoptotic cell death of the cancer cells in a time- and dose-dependent pattern (Lee et al. 2008; Li et al. 2013). When being exposed to geraniin, the expression of Fas ligand is upregulated, promoting ligand-receptor interaction with Fas death receptor (Lee et al. 2008). This process initiates the pro-apoptotic signalling cascades, including the proteolysis of pro-caspase-8 to active caspase-8, liberation of cytochrome c from mitochondria into the cytoplasm, activation of caspase-9 and most importantly, caspase-3 (Lee et al. 2008; Li et al. 2013). Geraniin-facilitated induction of caspase 3 activity leads to apoptotic cell death by promoting DNA fragmentation, obstructing DNA repair besides inducing the cleavage of focal adhesion kinase which is an anti-apoptotic protein (Lee et al. 2008). It may be added that expression of the p53 tumor suppressor gene is also enhanced upon geraniin treatment (Jin and Wang 2010). Activated p53 will help to initiate programmed cell death. Furthermore, it will also promote cell cycle arrest which has been observed in certain geraniin-treated cancer cell lines (Li et al. 2013; Vassallo et al. 2013). Therefore, it is apparent that geraniin affects several pivotal signalling pathways in cell growth to interfere the proliferation and survival of malignant cells.

Secondly, the anti-cancer properties of geraniin are also linked to its interaction with heat shock protein 90 (Hsp90). Under physiological condition, Hsp90 is a chaperone protein that ensures proper protein folding to preserve precise biological activity, maintains protein structural integrity against environmental stresses and targets misfolded or non-functional proteins for proteolytic degradation (Neckers and Ivy 2003). In cancer cells, Hsp90 is imperative in prolonging cancer cell survival via the stabilization of oncoproteins (Solit and Rosen 2006). In this context, geraniin is able to bind to Hsp90 and triggers a dose-dependent inhibitory effect on the ATPase and chaperone activities of Hsp90 (Vassallo et al. 2013). This contributes to the reduction of the level of several client proteins of Hsp90 in tumour cells, including Raf-1, pAkt and EGFR which are active in cell fate determination like proliferation, differentiation, apoptosis and survival (Vassallo et al. 2013). The inhibitory effect of geraniin on Hsp90 is reported to be similar to that of 17-(allylamino)-17-demethoxygeldanamycin, an experimental drug which targets Hsp90 in cancer treatment (Vassallo et al. 2013). As such, it is believed that geraniin-dependent Hsp90 inhibition may be further exploited for the disruption of tumour progression.

One recent study reported that geraniin treatment may also be beneficial in the prevention of migration and metastasis of cancer cells (Ko 2015). In the study, transforming-growth factor β-1 (TGF-β1) was used to potentiate the metastatic properties of A549 lung cancer cells by inducing some of the key changes like morphological transformation from epithelial to mesenchymal phenotype, improved motility, enhanced invasiveness and resistance to anoikis which is a type of programmed cell death caused by the detachment of cells from the surrounding extracellular matrix (Ko 2015). All TGF-β1-induced metastatic processes are annihilated by geraniin treatment (Ko 2015). According to the evidence, geraniin may possess both tumoristatic and tumoricidal characteristics besides preventing malignant cell migration and these substantiate further exploration on the clinical use of geraniin as a cancer treatment.

Immuno-modulatory effect

The generation of free radicals is one of the most essential and fundamental process in our immune system. In small and regulated quantity, ROS and reactive nitrogen species (RNS) help to launch

cascades of immune responses to fend off pathogens and destroy malignant cells. On the contrary, uncontrolled overproduction of free radicals is responsible for the pathogenesis of a number of inflammatory and autoimmune diseases like cardiovascular disease, diabetes mellitus, Alzheimer's disease, Parkinson's disease and rheumatoid arthritis (Valko et al. 2007). As mentioned earlier, geraniin treatment confers antioxidant effect via its free radical scavenging capacity. This also allows geraniin to exert certain influences onto immune responses.

In this context, several studies have shown that treatment with geraniin on murine macrophages modulates the secretion of proinflammatory cytokines such as tumour necrosis factor (TNF), interleukin-8 and interferon (Kolodziej et al. 2001; Okabe et al. 2001; Fujiki et al. 2003; Park et al. 2007). The activities of some inflammatory mediator-producing enzymes like 5-lipoxygenase (5-LOX) and inducible nitric oxide synthase (iNOS) are also affected by the presence of geraniin (Pan et al. 2000; Park et al. 2007). Furthermore, in activated macrophages, geraniin compromises the activity of nuclear factor kB (NF-kB), which is a key signalling factor in cellular inflammatory response (Pan et al. 2000; Park et al. 2007). On the other hand, Ushio et al. (1991) demonstrated that geraniin-treated macrophages participated more actively in phagocytosis of yeasts in comparison to non-treated counterpart. Based on this evidence, geraniin appears to possess both the immuno-stimulating and immuno-suppressing effects. The dual functionality requires further clarification in order to utilise geraniin in the modulation of immune response.

Cytoprotective activity

Studies have also shown that treatment with geraniin may build a strong defensive barrier against chemical and radioactive assaults besides conferring protective effects for different tissues. One of the most significant cellular protective effect of geraniin is hepatoprotective activity. The liver plays an irreplaceable role in the detoxification and elimination of harmful drugs. Hence, despite the fact that the liver has an enormous regenerative capacity, long-term hepatocyte injury will inevitably lead to liver failure which is potentially fatal. Pretreatment with extracts from *Geranium schiedeanum*, which is a geraniin-rich plant decreased thioacetamide-induced hepatotoxicity by 66 % (Gayosso-de-Lucio et al. 2014). The beneficial effects of geraniin treatment in liver protection have been replicated in various in vitro and in vivo models of chemically-induced liver injury. Generally, geraniin helps to inhibit lipid peroxidation besides restoring liver function as evidenced by improved bilirubin level and aminotransferase activities which are deranged by liver toxins like peroxidised corn oil, tetrachloromethane and alcohol (Okuda et al. 1983; Kimura et al. 1984; Nakanishi et al. 1999; Londhe et al. 2012). The extent of programmed cell death in injured liver is also diminished by the presence of geraniin (Londhe et al. 2012).

The hepatoprotective activities are possibly related to the antioxidant effect because Londhe et al. (2012) reported significant changes in the activity of some key antioxidative enzymes in the liver, namely catalase, SOD, GSH peroxidase and GSH reductase. This is reasonable as the drug detoxification processes tend to release free radicals that pose tremendous oxidative and nitrosative stresses to the hepatocytes (Jaeschke et al. 2002). This causes liver damage which is further exacerbated by the activation of macrophages (Kupffer cells) and infiltration of neutrophils, leading to the onset of both necrotic and apoptotic cell death (Jaeschke et al. 2002; Jaeschke 2011). By removing free radicals and enhancing the activities of antioxidative enzymes, it is very likely that geraniin is able to protect the liver from the insults from hepatotoxins.

Recently, the osteoprotective effect of geraniin has been acknowledged. Co-incubation of geraniin and osteoclasts, which is a type of bone cells that cause bone resorption (breakdown of bone materials), results in a dose-dependent inhibitory effect on the differentiation and maturation of osteoclasts (He et al. 2013; Xiao et al. 2015). To understand the mechanism by which geraniin inhibits osteoclast differentiation, it is important to know that osteoclasts are developed from macrophages upon induction by TNF-related cytokine receptor activator of nuclear factor kB ligand (RANKL) and polypeptide growth factor colony-stimulating factor-1 (CSF-1) (Yasuda et al. 1998; Lacey et al. 1998). Treatment with geraniin markedly downregulates the expression of RANKL-induced osteoclast-specific genes, inhibits NF-kB and extracellular signal-regulated kinase (ERK) signalling pathways and suppresses the activity of key osteoclast

transcriptional factor, NFATc1 and c-Fos (Xiao et al. 2015). As a result, osteoclastogenesis is severely suppressed. This is directly translated into the reduction in bone resorption and particle-induced osteolysis in both in vitro and in vivo settings (He et al. 2013; Xiao et al. 2015). According to another in vivo study in which female rats were subjected to bilateral ovariectomy to simulate postmenopausal osteoporosis, geraniin treatment not only modulated a number of circulatory biomarkers which are involved in bone formation, resorption and remodelling, but also rescued low-estrogen-induced bone loss by maintaining bone density, mineral content and calcium content (Lu et al. 2015). In short, the osteoprotective effect of geraniin may have some practical uses in terms of ageing-related bone resorption, wear particle-induced peri-prosthetic osteolysis, postmenopausal osteoporosis as well as other degenerative bone diseases.

Furthermore, geraniin protects from cellular injury caused by ionising radiation, evidenced by the geraniin-mediated reduction in DNA fragmentation and cell death post exposure to γ-radiation (Londhe et al. 2009; Kang et al. 2011; Bing et al. 2013). Such a radioprotective effect is also observed in an in vivo study in which radiosensitive tissues like splenocytes and jejunal crypt cells are spared from the deleterious effects of whole body irradiation after geraniin pretreatment (Bing et al. 2013). This is attributable to the radical scavenging properties of geraniin because the upsurge of ROS level upon γ-radiation exposure is reversed by geraniin which minimises damage to vital intracelluler targets like proteins, membrane lipids and DNA (Londhe et al. 2009; Kang et al. 2011). As a result, the activation of proapoptotic signalling pathway is diminished by geraniin even after γ-irradiation (Bing et al. 2013).

Based on two preliminary studies, it is likely that geraniin may also exhibit neuprotective effects, particularly against Alzheimer's disease via the inhibition of prolyl endopeptidase (Lee et al. 2007) and β-secretase (Youn and Jun 2013). Prolyl endopeptidase is a serine protease that inactivates various neuropeptides via proteolysis. Exaggerated upregulation of prolyl endopeptidase in the hippocampus takes place in the pre-plaque phase (prior to β-amyloid plaque formation) in both senescence-accelerated (Fukunari et al. 1994) and amyloid precursor protein-transfected mice (Roßner et al. 2005) to induce a seemingly "accelerated aging" effect. This suggests that prolyl endopeptidase may be a major factor that contributes to initial cognitive impairment in aging progress and Alzheimer's pathogenesis. Secretase has long been known to play a predominant role in the formation of amyloid-β which accounts for cognitive impairments in Alzheimer's patients. Being able to inhibit these enzymes, geraniin seems to be an attractive compound to preserve cognitive capability. However, it should be noted that the studies by Lee et al. (2007) and Youn and Jun (2013) are enzymatic studies. Several issues, in particular the ability of geraniin to penetrate blood–brain barrier and the absorption by brain cells, require further investigations. In short, current evidence in this aspect is still limited.

Therapeutic effects in metabolic disorders

In vivo studies have shown that geraniin can effectively act as an antihypertensive agent even after a single dose of the polyphenolic compound (Cheng et al. 1994; Lin et al. 2008). The underlying mechanism is probably the inhibition of the angiotensin-converting enzyme (ACE) whose activity is to convert angiotensin I to II to promote vasoconstriction and aldosterone secretion (Ueno et al. 1988; Lin et al. 2008). By inhibiting ACE, geraniin treatment encourages vasorelaxation and lowers blood pressure. Geraniin may also interfere with the sympathetic pathway by reducing circulating noradrenaline in a dose-dependent manner (Cheng et al. 1994). The noradrenaline-lowering effect is not abolished by adrenalectomy, indicating that geraniin may directly interact with sympathetic nerve terminals to either reduce noradrenaline release or enhance reuptake efficiency to prevent spillover (Cheng et al. 1994). In contrast, when acetonylgeraniin, a by-product of geraniin extraction in the presence of acetone, is used to treat spontaneous hypertensive rats (SHRs) with induced orthostatic hypotension, the orthostatic hypotension is prevented and the serum noradrenaline is elevated (Hsu et al. 1994). Like geraniin, the effects of acetonylgeranin remain unaffected by adrenalectomy (Hsu et al. 1994). Based on these findings, it can be deduced that the DHHDP unit in geraniin may be the functional group that interacts with the sympathetic nerve terminals because a slight structural modification by acetone is sufficient to reverse its impacts on blood pressure regulation and circulating noradrenaline level.

Crude extract from rambutan (*N. lappaceum*) peels which is rich in geraniin is effective in inhibiting carbohydrate hydrolysing enzymes: α-glucosidase and α-amylase (Palanisamy et al. 2011b). It was later confirmed that the inhibitory effect is due to geraniin (Palanisamy et al. 2011a). Therefore, geraniin has the potential to interrupt carbohydrate digestion and glucose absorption which subsequently suppresses postprandial hyperglycaemia. Furthermore, in vitro assays demonstrated that geraniin significantly inhibits aldol reductase activity and the formation of advanced glycation end products (AGEs), both of which play a crucial role in the onset of diabetic complications (Palanisamy et al. 2011a). For diabetic treatment, the crude plant extracts from geraniin-rich *P. nururi* and peels of *N. lappaceum* could normalise lipid profile and glycaemic status in streptozotocin-induced diabetic rodents (Rani and Kumar 2015; Muhtadi et al. 2015). In another study, treatment with rambutan peel extract could control weight gain and inhibit adipocyte hypertrophy by interfering with the expression of peroxisome proliferator-activated receptor-γ (PPARγ), a key nuclear receptor for lipid metabolism and adipogenesis (Lestari et al. 2015). The beneficial health effects are indeed contributed by geraniin because in high-fat diet-induced obese rats, supplementation with geraniin also successfully ameliorates diet-induced metabolic dysregulations in glucose and lipid metabolisms besides significantly reducing visceral fat depots without notable side effect (Chung et al. 2014). Hence, considering the widespread prevalence of metabolic syndrome and type 2 diabetes mellitus, geraniin treatment may be employed to safely mitigate the metabolic dysfunction.

In addition, recent research shows that geraniin may help to prevent the formation of thrombus by inhibiting platelet aggregation (Chen et al. 2012). Chen et al. (2012) reported that geraniin is able to inhibit platelet aggregation induced by arachidonic acid, adenosine diphosphate and platelet activating factor in a dose-dependent way. Similar findings were found using an ex vivo study design in which platelets isolated from plasma of rabbits given intragastric 5 mg/kg of geraniin were used. Platelet aggregation induced by the three compounds was significantly inhibited at 60–120 min post geraniin administration (Chen et al. 2012). This points out that metabolites of geraniin, notably ellagic acid, may also possess antiplatelet aggregation activity. As the three compounds activate platelet aggregation via different mechanisms, it is assumed that the inhibitory effect of geraniin on platelet aggregation is non-selective. During thrombus formation, activated neutrophils will promote platelet activation and aggregation and in response, activated platelets will also encourage neutrophils rolling and adhesion to the thrombus-forming site (Kim et al. 2013). Such a platelet-neutrophil crosstalk is also abolished by geraniin (Chen et al. 2012). Furthermore, treatment with geraniin also inhibits the activity of plasminogen activator inhibitor-1 (PAI-1) (Yuan et al. 2012). As indicated by the name, PAI-1 is the principal inhibitor of tissue plasminogen activator (tPA) which is a major enzyme in blood clot breakdown and is clinically used to treat ischaemic stroke. By inhibiting PAI-1, geraniin is able to promote fibrinolysis to degrade blood clots. This is particularly useful for the treatment of thromboembolic events as well as atherosclerosis.

Analgesic and antinociceptive properties

Some geraniin-rich plants have been used in folk medicine as a pain reliever, indicating its potential analgesic and antinociceptive (inhibition of the pain perception) activity. Indeed, several studies reported that the plant extracts from the genus *Phyllanthus* has a potent, dose-dependent and long-lasting inhibitory effect on pain sensation (Santos et al. 1994, 1995). Furthermore, geraniin pretreatment given via both the oral route and intraperitoneal injection is able to reduce the writhing movements or abdominal contractions, which is interpreted as reduction in nociception, after acetic acid-induced abdominal pain in mice (Miguel et al. 1996; Velazquez-Gonzalez et al. 2014). However, geraniin is less effective in comparison to common analgesic agents, aspirin and acetaminophen (Miguel et al. 1996). Martini et al. (2000) demonstrated that geraniin could inhibit the binding of a GTP analogue to rat cerebral cortex membrane proteins. This implies that geraniin treatment has an inhibitory effect on the GTP-dependent G protein activation which is a critical step in the activity of G-protein coupled signal transduction. As a result, the activity of metabotropic glutamate receptor which is one of the many G-protein-coupled receptors and is responsible in pain perception, is also inhibited

(Montana and Gereau 2011). Thus, it is possible that geraniin may act as an analgesic drug by exerting a modulatory effect on the activation of metabotropic glutamate receptor in the glutaminergic excitatory pathways.

Other biological activities of geraniin

Although *G. thunbergii* which is a geraniin-rich plant has long been accepted as an official antidiarrheal drug in Japan, empirical findings supporting the antidiarrheal activity of geraniin is fairly limited. It is generally assumed that the antidiarrheal activity of geraniin is accountable to its astringency, a characteristic to shrink or constrict mucous membranes and body tissues (Ofuji et al. 1998), but the exact mechanism is not known. Based on Kan and Taniyama (1992), geraniin can decrease the contraction frequency of the small and large intestines when being subjected to contractile agents like histamine and acetylcholine. Such a modulatory effect on intestinal contractility may allow geraniin to exhibit antidiarrheal effect. Geraniin has also been shown to accelerate the progress of wound healing by stimulating the proliferation of fibroblasts and differentiation of keratinocytes (Agyare et al. 2011). It can also prevent gastric ulceration by inhibiting back diffusion of acid and inducing gastric mucus generation (Hung et al. 1995). Based on these findings, the traditional medicinal use of geraniin-rich plants in wound healing and the treatment of diarrhoea and peptic ulcer seems to be fairly justifiable. However, further investigations are highly encouraged to elucidate these bioactivities of geraniin.

Potential therapeutic significance, challenges and future research focus

Amazingly, a huge amount of insightful work has been conducted in attempts to understand the pharmacokinetics and pharmacodynamics of geraniin as well as the respective underlying mechanisms. Generally, it is assumed that geraniin is safe to be used on living tissues and organisms because to date, there is no acute toxicity or significant adverse effect which are remotely associated with the use of geraniin in both in vitro and in vivo studies. In most normal cell lines, geraniin can be tolerated at a considerably high concentration (up to 100 μM) without significantly jeopardising the cell viability (Agyare et al. 2011; Kang et al. 2011; Bing et al. 2013). In mice, 30 mg/kg of geraniin had been given intraperitoneally to facilitate full bioavailability and yet, no side effect was reported (Miguel et al. 1996). However, it is highly recommended to conduct a comprehensive risk assessment, at least in animal models, in order to examine the possible acute and chronic side effects of the natural compound. This information will be valuable when geraniin or its metabolites are tested in clinical settings.

Additionally, based on Table 2, geraniin possesses a wide variety of biological activities. A large portion of these findings are established according to the results from in vitro studies like biochemical or enzymatic assays and cell culture studies. Therefore, the conclusions from in vitro enzymatic assays should be analysed conscientiously. This is because, like other polyphenolic compounds, geraniin is a strong protein precipitant. In enzymatic assays, it will precipitate and denature proteins, rendering the tested enzymes non-functional. Although specific enzyme inhibitory effect cannot be ruled out, the fact that geraniin can suppress the activity of a number of structurally and functionally diverse enzymes like human digestive enzymes, enzymes from the central nervous system and of viral origin, strongly points out that non-selective inhibition due to protein precipitation is a more likely mechanism for the observed inhibitory effect. Clinically, the use of non-selective enzyme inhibitors is less appealing because it tends to interact with off-target enzymes, leading to undesirable side effects. Furthermore, as the enzyme inhibitory actions of geraniin are almost established exclusively based on in vitro studies, it is also uncertain whether the same effect can be replicated in vivo. Hence, for future phenolic compound research, it is advisable to take the protein precipitation effect into consideration, especially when studying enzyme inhibition.

In spite of the issue about in vitro enzymatic assays, most of the bioactivities of geraniin found in in vitro studies are reproducible using ex vivo or in vivo study designs, signifying that its biological effects are largely preserved even in complex physiological matrices. However, the evidence from in vivo studies is still limited. Also, for in vivo geraniin research, the most popular test objects are rodents and no human subject has been employed thus far. Hence, most of the

bioactivities are inferred based on animal studies and whether or not it will work as anticipated in human body is still unknown.

For in vivo animal study, the most widely employed mode of administrations are intraperitoneal and oral administration routes, of which the former ensures full bioavailability. Conversely, as outlined previously, oral ingestion of geraniin does not facilitate its absorption in the intact form. Therefore, it is increasingly recognised that the resulting bioactivities following oral intake of geraniin are attributable to the derivatives of geraniin such as ellagic acid and urolithins. In fact, a large number of studies have documented the anti-inflammatory, anticarcinogenic, antioxidant and antimicrobial effects of ellagic acid and urolithins (Landete 2011; Espin et al. 2013). Such a striking similarity in the biological functionality of the parental compound and its metabolites also suggests that these activities are due to a common intrinsic trait shared between these compounds which is unaffected by the degradation of geraniin. One likely speculation is the free radical scavenging activity which is found not only in geraniin and its metabolites, but also in many other polyphenolic compounds. This is because several biological effects of geraniin, namely antioxidant, cytoprotective and immunomodulatory effects, which are closely linked to the free radical scavenging properties are also consistently demonstrated in geraniin metabolites as well as other polyphenolic compounds.

Nevertheless, there are also some in vivo bioactivities which seem to implicate unique mechanisms that are independent from the antioxidant activity of geraniin, for instance, the therapeutic effect against metabolic dysregulation as well as anticoagulant, antiplatelet, analgesic and anticancer properties. Amongst these, the underlying mechanisms for anticancer effects are more clearly elaborated which involve the induction of apoptosis, destabilization of oncoprotein via Hsp90 interaction and inhibition of metastatic transformation. On the other hand, the discovery of the other bioactivities are relatively recent and the mechanisms are not explicitly defined, thus requiring further exploration. It may be added that the promising beneficial effects on metabolic dysfunction and anticoagulation are some of the most exciting features of geraniin as they can be further exploited for the therapy of some highly prevalent diseases, notably metabolic syndrome, type 2 diabetes mellitus and cardiovascular diseases. In short, due to the pleitropic effects, ellagitannin geraniin seems to be an attractive target drug in the treatment of multiple diseases but there are still a lot of uncertainties in the biological functionality of geraniin which are worth investigating.

One of the biggest challenges for the clinical application of geraniin is the low bioavailability upon oral ingestion, which is largely because of its large molecular size and is complicated by low solubility in gastric fluid (Elendran et al. 2015). To be considered as an oral drug candidate, effective formulation and transport system should be created to enhance the bioavailability of geraniin. Apart from that, isolation of geraniin from natural sources is a tedious and time-consuming procedure. Therefore, another challenge and prospective focus in geraniin research is to develop synthetic version of the hydrolysable tannin and its functional derivatives like ellagic acid and urolithins. Some of the subunits of geraniin like corilagin (Yamada et al. 2008), HHDP and DHHDP motifs (Pouysegu et al. 2011) have been chemically synthesized but there is no report about total synthesis of geraniin. The ability to chemically synthesise geraniin and its derivatives could offer several advantages such as bypassing the cumbersome isolation step, large-scale production of the compounds besides allowing the modifications of certain functional groups to enhance their bioactivities. Nonetheless, artificial synthesis of these compounds is only economically feasible if the practical applications and clinical values of geraniin are proven to be tremendous.

Conclusion

After almost 40 years of geraniin research, the science community has established a fundamental understanding of the hydrolysable tannin in terms of its natural sources, purification techniques, biosynthesis and pharmacokinetics. Additionally, like many other polyphenolic compounds, several promising and clinically significant bioactivities have also been discovered, making the ellagitannin geraniin an attractive research candidate so as to fully explore its therapeutic effects. Nevertheless, current evidence is still inadequate to support the clinical use of geraniin due to a few issues. Firstly, there is no thorough assessment about the potential short- and long-term harmful

impacts of geraniin ingestion, making the safety of geraniin consumption debatable. Next, the underlying mechanisms by which it exerts the observed beneficial effects remain largely mysterious. This aspect definitely requires more investigations because the knowledge of a drug's mechanism may not only facilitate better monitoring on the drug effects and prediction of the potential adverse effects, but also allow us to catch a glimpse into the complex pathogenesis of diseases like malignancy and metabolic dysfunction on which we could base to develop more effective drugs to tackle the target pathway. There is also a large room for improvement to optimise drug delivery and bioavailability if the hydrolysable tannin is to be considered as an oral medication. Last but not least, large-scale synthesis of geraniin is a must to ensure the feasibility of commercialization. Considering these challenges and predicaments, it can be said without fear of contradiction that we are still far from putting geraniin into actual clinical use and yet, the potent bioactivities found based on preliminary studies are a solid indicator that future input in geraniin research may be worthwhile after all.

Acknowledgments The work was supported by ScienceFund of Malaysia Ministry of Science, Technology and Innovation (MOSTI Grant No.: 02-02-10-SF0249) as well as internal grant from the School of Science, Monash University Malaysia.

Compliance with ethical standards

Conflict of interest The authors declare no conflict of interest.

References

Adesina SK, Idowu O, Ogundaini AO, Oladimeji H, Olugbade TA, Onawunmi GO, Pais M (2000) Antimicrobial constituents of the leaves of *Acalypha wilkesiana* and *Acalypha hispida*. Phytother Res 14:371–374

Agyare C, Lechtenberg M, Deters A, Petereit F, Hensel A (2011) Ellagitannins from *Phyllanthus muellerianus* (Kuntze) Exell.: geraniin and furosin stimulate cellular activity, differentiation and collagen synthesis of human skin keratinocytes and dermal fibroblasts. Phytomedicine 18:617–624

Amakura Y, Yoshida T (1996) Tannins and related polyphenols of Euphorbiaceous plants. XIV. Euphorbin I, a new dimeric hydrolysable tannin from *Euphorbia watanabei*. Chem Pharm Bull 44:1293–1297

Arina NB, Rohman A (2013) The phenolic contents and antiradical activity of Indonesian *Phyllantus urinaria* L. Int Food Res J 20:1119–1124

Baliga MS, Dsouza JJ (2011) Amla (*Emblica officinalis* Gaert), a wonder berry in the treatment and prevention of cancer. Eur J Cancer Prev 20:225–239

Bing SJ, Ha D, Kim MJ, Park E, Ahn G, Kim DS, Ko RK, Park JW, Lee NH, Jee Y (2013) Geraniin down regulates gamma radiation-induced apoptosis by suppressing DNA damage. Food Chem Toxicol 57:147–153

Butler LG (1989) Effects of condensed tannin on animal nutrition. In: Hemingway RW, Karchesy JJ (eds) Chemistry and significance of condensed tannins. Plenum Press, New York

Cammann J, Denzel K, Schilling G, Gross GG (1989) Biosynthesis of gallotannins: β-glucogallin-dependent formation of 1,2,3,4,6-pentagalloylglucose by enzymatic galloylation of 1,2,3,6-tetragalloylglucose. Arch Biochem Biophys 278:58–63

Carr A, Frei B (1999) Does vitamin C act as a pro-oxidant under physiological conditions? FASEB J 13:1007–1024

Cerda B, Llorach R, Ceron JJ, Espin JC, Tomas-Barberan FA (2003) Evaluation of the bioavailability and metabolism in the rats of punicalagin, an antioxidant polyphenol from pomegranate juice. Eur J Nutr 42:18–28

Cerda B, Espin JC, Parra S, Martinez P, Tomas-Barberan FA (2004) The potent *in vitro* antioxidant ellagitannins from pomegranate juice are metabolised into bioavailable but poor antioxidant hydroxyl-6H-dibenzopyran-6-one derivatives by the colonic microflora of healthy humans. Eur J Nutr 43:205–220

Chalker-Scott L, Krahmer RL (1989) Microscopic studies of tannin formation and distribution in plant tissues. In: Hemingway RW, Karchesy JJ (eds) Chemistry and significance of condensed tannins. Plenum Press, New York

Chen P, Li F, He B, Wu H, Yang J, Zhang X, Shen Z (2012) Effects of geraniin on platelet aggregation and interactions between platelets and neutrophils. J Kunming Med Univ 33:4–10

Cheng JT, Chang SS, Hsu FL (1994) Antihypertensive action of geraniin in rats. J Pharm Pharmacol 46:46–49

Chung APYS, Ton SH, Gurtu S, Palanisamy UD (2014) Ellagitannin geraniin supplementation ameliorates metabolic risks in high-fat-diet-induced obese Sprague Dawley rats. J Funct Foods 9:173–182

Clifford MN, Scalbert A (2000) Ellagitannins—nature, occurrence and dietary burden. J Sci Food Agric 80:1118–1125

Corthout J, Pieters LA, Claeys M, Vanden Berghe DA, Aj Vlietnck (1991) Antiviral ellagitannins from *Spondias mombin*. Phytochemistry 30:1129–1130

Daniel EM, Ratnayake S, Kinstle T, Stoner GD (1991) The effects of pH and rat intestinal contents on the liberation of ellagic acid from purified and crude ellagitannins. J Nat Prod 54:946–952

Elendran S, Lee WW, Prankerd R, Palanisamy UD (2015) The physicochemical properties of geraniin, a potential antihyperglycemic agent. Pharm Biol 8:1–8

Espin JC, Gonzalez-Barrio R, Cerda B, Lopez-Bote C, Rey AI, Tomas-Barberan FA (2007) Iberian pig as a model to clarify obscure points in the bioavailability and metabolism of ellagitannins in humans. J Agric Food Chem 55:10476–10485

Espin JC, Larrosa M, Garcia-Conesa T, Tomas-Barberan FA (2013) Biological significance of urolithins, the gut

microbial ellagic acid-derived metabolites: the evidence so far. Evid Based Complement Altern Med 2013:270418

Fecka I, Cisowski W (2005) Tannins and flavonoids from the *Erodium cicutarium* Herb. Z Naturforsch B 60:555–560

Feucht W, Treutter D (1999) The role of Flavan-3-ols and proanthocyanidins in plant defense. In: Dakshini KMM, Foy CL (eds) Principles and practices in plant ecology—allochemical interactions. CRC Press, Boca Raton

Field JA, Lettinga G (1992) Toxicity of tannic compounds to microorganisms. In: Hemingway RW, Laks PE (eds) Plant polyphenols. Synthesis, properties, significance. Plenum Press, New York

Filho VC, Santos AS, De Campos RO, Miguel OG, Yunes RA, Ferrari F, Messana I, Calixto JB (1996) Chemical and pharmacological studies of *Phyllanthus caroliniensis* in mice. J Pharm Pharmacol 48:1231–1236

Fisher E (1914) Synthesis of depsides, lichen-substances and tannins. J Am Chem Soc 36:1170–1201

Foo LY (1993) Amariin, a di-dehydrohexahydroxydiphenoyl hydrolysale tannin from *Phyllanthus amarus*. Phytochemistry 33:487–491

Foo LY (1995) Amariinic acid and related ellagitannins from *Phyllanthus amarus*. Phytochemistry 39:217–224

Foo LY, Wong H (1992) Phyllanthusiin D, an unusual hydrolysable tannin from *Phyllanthus amarus*. Phytochemistry 31:711–713

Fujiki H, Suganuma M, Kurusu M, Okabe S, Imayoshi Y, Taniguchi S, Yoshida T (2003) New TNF-α releasing inhibitors as cancer preventive agents from traditional herbal medicine and combination cancer prevention study with EGCG and sulindac or tamoxifen. Mutat Res 523–524:119–125

Fukunari A, Kato A, Sakai Y, Yoshimoto T, Ishiura S, Suzuki K, Nakajima T (1994) Colocalization of prolyl endopeptidase and amyloid β-peptide in brains of senescence-accelerated mouse. Neurosci Lett 176:201–204

Funatogawa K, Hayashi S, Shimomura H, Yoshida T, Hatano T, Ito H, Hirai Y (2004) Antibacterial activity of hydrolysable tannins derived from medicinal plants against *Helicobacter pylori*. Microbiol Immunol 48:251–261

Garcia-Villalba R, Beltran D, Espin JC, Selma MV, Tomas-Barberan FA (2013) Time course production of urolithins from ellagic acid by human gut microbiota. J Agric Food Chem 61:8797–8806

Gayosso-de-Lucio JA, Torres-Valencia JM, Cerda-Garcia-Rojas CM, Joseph-Nathan P (2010) Ellagitannins from *Geranium potentillaefolium* and *G. bellum*. Nat Prod Commun 5:531–534

Gayosso-De-Lucio J, Bautista M, Velazquez-Gonzalez C, De la O Arciniega M, Morales-Gonzalez JA, Benedi J (2014) Chemical composition and hepatotoxic effect of *Geranium schiedeanum* in a thioacetamide-induced liver injury model. Pharmacogn Mag 10(suppl S3):S574–S580

Gohar AA, Lahloub MF, Niwa M (2003) Antibacterial polyphenol from *Erodium glaucophyllum*. Z Naturforsch C 58:670–674

Gonzalez-Barrio R, Borges G, Mullen W, Crozier A (2010) Bioavailability of anthocyanins and ellagitannins following consumption of raspberries by healthy humans and subjects with an ileostomy. J Agric Food Chem 58:3933–3939

Gonzalez-Barrio R, Edwards CA, Crozier A (2011) Colonic catabolism of ellagitannins, ellagic acid, and raspberry anthocyanins: *in vivo* and *in vitro* studies. Drug Metab Dispos 39:1680–1688

Gonzalez-Sarrias A, Azorin-Ortuno M, Yanez-Gascon MJ, Tomas-Barberan FA, Garcia-Conesa MT, Espin JC (2009) Dissimilar *in vitro* and *in vivo* effects of ellagic acid and its microbiota-derived metabolites, urolithins, on the cytochrome P450 1A1. J Agric Food Chem 57:5623–5632

Gross GG (1983a) Partial purification and properties of UDP-glucose: vanillate 1-*O*-glucosyl transferase from oak leaves. Phytochemistry 22:2179–2182

Gross GG (1983b) Synthesis of mon-, di- and trigalloyl-β-D-glucose by β-glucogallin-dependent gallolytransferases from oak leaves. Z Naturforsch C 38:519–523

Gross GG (2008) from lignins to tannins: forty years of enzyme studies on the biosynthesis of phenolic compounds. Phytochemistry 69:3018–3031

Gross GG, Denzel K (1991) Biosynthesis of gallotannins. β-glucogallin-dependent galloylaytion of 1,6-digalloylglucose to 1,2,6-trigalloylglucose. Z Naturforsch C 46:389–394

Hagenah S, Gross GG (1993) Biosynthesis of 1,2,3,6-tetra-*O*-galloyl-β-D-glucose. Phytochemistry 32:637–641

He B, Hu M, Li SD, Yang XT, Lu YQ, Liu JX, Chen P, Shen ZQ (2013) Effects of geraniin on osteoclastic bone resorption and matrix metalloproteinase-9 expression. Bioorg Med Chem Lett 23:630–634

Hodgson JM, Morton LW, Puddey IB, Beilin LJ, Croft KD (2000) Gallic acid metabolites are markers of black tea intake in humans. J Agric Food Chem 48:2276–2280

Hsu FL, Lu FH, Cheng JT (1994) Influence of acetonylgeraniin, a hydrolysable tannin from *Euphoria longana*, on orthostatic hypotension in a rat model. Planta Med 60:297–300

Huang RL, Huang Yl OuJC, Chen CC, Hsu FL, Chang C (2003) Screening of 25 compounds isolated from *Phyllanthus* species for anti-human hepatitis B virus *in vitro*. Phytother Res 17:449–453

Hung CR, Chen JT, Neu SL (1995) Prophylactic effects of sucralfate and geraniin on ethanol-induced gastric mucosal damage in rats. Chin J Physiol 38:211–217

Ignat I, Volf I, Popa VI (2011) A critical review of methods for characterization of polyphenolic compounds in fruits and vegetables. Food Chem 126:1821–1835

Immel S, Khanbabaee K (2000) Atropdiastereoisomers of ellagitannin model compounds: configuration, conformation, and relative stability of D-glucose diphenoyl derivatives. Tetrahedron Asymmetry 11:2495–2507

Ishimaru K, Shimomura K (1991) Tannin production in hairy root culture of *Geranium thunbergii*. Phytochemistry 30:825–828

Ishimaru K, Yoshimatsu K, Yamakawa T, Kamada H, Shimomura K (1992) Phenolic constituents in tissue cultures of *Phyllanthus Niruri*. Phytochemistry 31:2015–2018

Ishimoto H, Tai A, Yoshimura M, Amakura Y, Yoshida T, Hatano T, Ito H (2012) Antioxdative properties of functional polyphenols and their metabolites assessed by an ORAC assay. Biosci Biotechnol Biochem 76:395–399

Islam A, Mazumder UK, Gupta M, Ghosal S (2008) Synergistic effects of geraniin and rutin in the antioxidant properties of major lignins in *Phyllanthus amarus*. Pharmacol Online 3:1024–1036

Ito H (2011) Metabolites of the ellagitannin geraniin and their antioxidant activities. Planta Med 77:1110–1115

Ito H, Iguchi A, Hatano T (2008) Identification of urinary and intestinal bacterial metabolites of ellagitannin geraniin in rats. J Agric Food Chem 56:393–400

Jaeschke H (2011) Reactive oxygen and mechanisms of inflammatory liver injury: present concepts. J Gastroenterol Hepatol 26:173–179

Jaeschke H, Gores GJ, Cederbaum AI, Hinson JA, Pessayre D, Lemasters JJ (2002) Mechanisms of hepatotoxicity. Toxicol Sci 65:166–176

Janero DR (1990) Malondialdehyde and thiobarbituric acid-reactivity as diagnostic indices of lipid peroxidation and peroxidative tissue injury. Free Radic Biol Med 9:515–540

Jin ZX, Sun RS (2011) Effects of geraniin in *Geranium sibiricum* L. on antioxidant function of S_{180} mice. Paper presented at the 2011 international conference on human health and biomedical engineering. Jilin Empire Garden Hotel Guohui Hall, China, 19–22 August 2011

Jin ZX, Wang BQ (2010) Induction of P53 genes in human hepatoma cells by geraniin. Paper presented at the 2010 3rd international conference on biomedical engineering and informatics. Yantai University, China, 16–18 October 2010

Kakiuchi N, Hattori M, Namba T, Nishizawa M, Yamagishi T, Okuda T (1985) Inhibitory effect of tannins on reverse transcriptase from RNA tumor virus. J Nat Prod 48:614–621

Kan S, Taniyama K (1992) Mechanism of inhibitory actions of *Geranium thunbergii*, tannic acid and geraniin on the motility of rat intestine. Shoyakugaku Zasshi 46:246–253

Kang SJ, Hong SS, Hwang BY, Ro JS, Lee KS, Towers GHN (2006) Phenolic compounds from the stems of *Sapium japonicum*. Nat Prod Sci 12:125–128

Kang KA, Lee IK, Zhang R, Piao MJ, Kim KC, Kim SY, Shin T, Kim BJ, Lee NH, Hyun JW (2011) Radioprotective effect of geraniin via the inhibition of apoptosis triggered by γ-radiation-induced oxidative stress. Cell Biol Toxicol 27:83–94

Kim KH, Barazia A, Cho J (2013) Real-time imaging of heterotypic platelet-neutrophil interactions on the activated endothelium during vascular inflammation and thrombus formation in live mice. J Vis Exp. doi:10.3791/50329

Kimura Y, Okuda H, Mori K, Okuda T, Arichi S (1984) Studies on the activities of tannins and related compounds from medicinal plants and drugs. IV. Effects of various extracts of Geranii Herba and geraniin on liver injury and lipid metabolism in rats fed peroxidised oil. Chem Pharm Bull 32:1866–1871

Kletter C, Kriechbaum M (2001) Li Ga Dur. In: Kletter C, Kriechbaum M (eds) Tibetan medicinal plants. Medpharm GmbH Scientific Publishers, Stuuttgart

Klocke JA, Wagenen BV, Balandrin MF (1986) The ellagitannin geraniin and its hydrolysis products isolated as insect growth inhibitors from semi-arid land plants. Phytochemistry 25:85–91

Klumpers J, Scalbert A, Janin G (1994) Ellagitannins in European oak wood: polymerization during wood ageing. Phytochemistry 36:1249–1252

Ko H (2015) Geraniin inhibits TGF-β1-induced epithelial-mesenchymal transition and suppresses A549 lung cancer migration, invasion and anoikis resistance. Bioorg Med Chem Lett 25:3529–3534

Kolodziej H, Kayser O, Kiderlen AF, Ito H, Hatano T, Yoshida T, Foo LY (2001) Antileishmanial activity of hydrolysable tannins and their modulatory effects on nitric oxide and tumour necrosis factor-α release in macrophages *in vitro*. Planta Med 67:825–832

Kraus TE, Dahlgren RA, Zasoski RJ (2003) Tannins in nutrient dynamics of forest ecosystems—a review. Plant Soil 256:41–66

Kumaran A, Karunakaran RJ (2006) Nitric oxide radical scavenging active components from *Phyllanthus emblica* L. Plant Foods Hum Nutr 61:1–5

Kurihara H, Kawabata J, Hatano M (1993) Geraniin, a hydrolysable tannin from *Nymphaea tetragona* Georgi (Nymphaeaceae). Biosci Biotechnol Biochem 57:1570–1571

Lacey DL, Timms E, Kelley MJ, Dunstan CR, Burgess T, Elliott R, Colombero A, Elliott G, Scully S, Hsu H, Sullivan J, Hawkins N, Davy E, Capparelli C, Eli A, Qian YX, Kaufman S, Sarosi I, Shalhoub V, Senaldi G, Guo J, Delaney J, Boyle WJ (1998) Osteoprotegerin ligand is a cytokine that regulates osteoclast differentiation and activation. Cell 93:165–176

Landete JM (2011) Ellagitannins, ellagic acid and their derived metabolites: a review about source, metabolism, functions and health. Food Res Int 44:1150–1160

Lee SH, Jun M, Choi JY, Yang EJ, Hur JM, Bae KH, Seong YH, Huh TL, Song KS (2007) Plant phenolics as prolyl endopeptidase inhibitors. Arch Pharm Res 30:827–833

Lee JC, Tsai CY, Kao JY, Kao MC, Tsai SC, Chang CS, Huang LJ, Kuo SC, Lin JK, Way TD (2008) Geraniin-mediated apoptosis by cleavage of focal adhesion kinase through up-regulation of Fas ligand expression in human melanoma cells. Mol Nutr Food Res 52:655–663

Lee SH, Tang YQ, Rathkrishnan A, Wang SM, Ong KC, Manikam R, Payne BJ, Jaganath IB, Sekaran SD (2013) Effects of cocktail of four local Malaysian medicinal plants (*Phyllanthus* spp.) against dengue virus 2. BMC Complement Altern Med 13:192

Leopoldini M, Russo N, Toscano M (2011) The molecular basis of working mechanism of natural polyphenolic antioxidants. Food Chem 125:288–306

Lestari SR, Djati MS, Rudijanto A, Fatchiyah F (2015) PPARγ expression by rambutan peel extract in obesity rat model-induced high-calorie diet. Asian Pac J Trop Biomed 5:812–817

Li J, Huang H, Zhou W, Feng M, Zhou P (2008) Anti-hepatitis B virus activities of *Geranium carolinianum* L. extracts and identification of the active components. Biol Pharm Bull 31:743–747

Li J, Wang S, Yin J, Pan L (2013) Geraniin induces apoptotic cell death in human lung adenocarcinoma A549 cells *in vitro* and *in vivo*. Can J Physiol Pharmcol 91:1016–1024

Lin JH, Ishimatsu M, Tanaka T, Nonaka G, Nishioka I (1990a) Tannins and related compounds. XCVI. Structures of macaranins and macarinins, new hydrolysable tannins possessing macaranoyl and tergalloyl ester groups, from the leaves of *Macaranga sinensis* (Baill.) Muell.-Arg. Chem Pharm Bull 38:1844–1851

Lin JH, Nonaka G, Nishioka I (1990b) Tannins and related compounds XCIV. Isolation and characterization of seven

new hydrolysable tannins from the leaves of *Macaranga tanarius* (L.) Muell. Et Arg. Chem Pharm Bull 38:1218–1223

Lin SY, Wang CC, Lu YL, Wu WC, Hou WC (2008) Antioxidant, antisemicarbazide-sensitive amine oxidase, and antihypertensive activities of geraniin isolated from *Phyllanthus urinaria*. Food Chem Toxicol 46:2485–2492

Ling LT, Saito Y, Palanisamy UD, Cheng HM, Noguchi N (2012) Cytoprotective effects of geraniin against peroxynitrite- and peroxyl radical-induced cell death via free radical scavenging activity. Food Chem 132:1899–1907

Liu X, Cui C, Zhao M, Wang J, Luo W, Yang B, Jiang Y (2008) Identification of phenolics in the fruit of emblica (*Phyllanthus emblica* L.) and their antioxidant activities. Food Chem 109:909–915

Liu D, Su Z, Wang C, Gu M, Xing S (2010) Separation and purification of hydrolysable tannin from *Geranium wilfordii* Maxim by reversed-phase and normal-phase high-speed counter-current chromatography. J Sep Sci 33: 2266–2271

Liu D, Ma Y, Wang Y, Su Z, Gu M, Janson JC (2011) One-step separation and purification of hydrolysable tannins from *Geranium wilfordii* Maxim by adsorption chromatography on cross-linked 12% agarose gel. J Sep Sci 34:995–998

Liu D, Ma Y, Gu M, Janson JC, Wang C, Xiao H (2012a) Liquid–liquid/solid three phase high-speed counter-current chromatography, a new technique for separation of polyphenols from *Geranium wilfordii* Maxim. J Sep Sci 35:2146–2151

Liu X, Zhao M, Wu K, Chai X, Yu H, Tao Z, Wang J (2012b) Immunomodulatory and anticancer activities of phenolics from emblica fruit (*Phyllanthus emblica* L.). Food Chem 131:685–690

Londhe JS, Devasagayam TPA, Foo LY, Ghaskadbi SS (2009) Radioprotective properties of polyphenols from *Phyllanthus amarus* Linn. J Radiat Res 50:303–309

Londhe JS, Devasagayam TPA, Foo LY, Shastry P, Ghaskadbi SS (2012) Geraniin and amariin, ellagitannins from *Phyllanthus amarus*, protect liver cells against ethanol induced cytotoxicity. Fitoterapia 83:1562–1568

Lu Y, He B, Zhang X, Yang R, Li S, Zhang Y, Yun Y, Yan H, Chen P, Shen Z (2015) Osteoprotective effect of geraniin against ovariectomy-induced bone loss in rats. Bioorg Med Chem Lett 25:673–679

Luger P, Weber M, Kashino S, Amakura Y, Yoshida T, Okuda T, Beurskens G, Dauter Z (1998) Structure of the tannin geraniin based on conventional X-ray data at 295 K and on synchrotron data at 293 and 123 K. Acta Crystallogr B 54:687–694

Ma YT, Chuang JI, Lin JH, Hsu FL (1997) Phenolics from *Acalypha indica*. J Chin Chem Soc 44:499–502

Mahdi ES, Noor AM, Sakeena MH, Abdullah GZ, Abdulkarim M, Abdul Sattar M (2011) Identification of phenolic compounds and assessment of *in vitro* antioxidants activity of 30% ethanolic extracts derived from two *Phyllanthus* species indigenous to Malaysia. Afr J Pharm Pharmacol 5:1967–1978

Martini LH, Souza CR, Marques PB, Calixto JB, Yunes RA, Souza DO (2000) Compounds extracted from *Phyllantus* and *Jatropha elliptica* inhibit the binding of [^{3}H] glutamate and [^{3}H]GMP-PNP in rat cerebral cortex membrane. Neurochem Res 25:211–215

Meo FD, Lemaur V, Cornil J, Lazzaron R, Duroux JL, Olivier Y, Trouillas P (2013) Free radical scavenging by natural polyphenols: atom versus electron transfer. J Phys Chem A 117:2082–2092

Miguel OG, Calixto JB, Santos ARS, Messana I, Ferrari F, Filho VC, Pizzolatti MG, Yunes RA (1996) Chemical and preliminary analgesic evaluation of geraniin and furosin isolated from *Phyllanthus sellowianus*. Planta Med 62:146–149

Montana MC, Gereau RW (2011) Metabotropic glutamate receptors as targets for analgesic: antagonism, activation, and allosteric modulation. Curr Pharm Biotechnol 12:1681–1688

Muhtadi, Primarianti AU, Sujono TA (2015) Antidiabetic activity of durian (*Durio zibethinus* Murr.) and rambutan (*Nephelium lappaceum* L.) fruits peels in alloxan diabetic rats. Procedia Food Sci 3:255–261

Nakanishi Y, Okuda T, Abe H (1999) Effects of geraniin on the liver in rats III-correlation between lipid accumulations and liver damage in CCl_4-treated rats. Nat Med 53:22–26

Ndjonka D, Bergmann B, Agyare C, Zimbres FM, Luersen K, Hensel A, Wrenger C, Liebau E (2012) *In vitro* activity of extracts and isolated polyphenols from West African medicinal plants against *Plasmodium falciparum*. Parasitol Res 111:827–834

Neckers L, Ivy SP (2003) Heat shock protein 90. Curr Opin Oncol 15:419–424

Neera S, Ishimaru K (1992) Tannin production in cell cultures of *Sapium sebiferum*. Phytochemistry 31:833–836

Neera S, Arakawa H, Ishimaru K (1992) Tannin production in *Sapium sebiferum* callus cultures. Phytochemistry 31:4143–4149

Niemetz R, Gross GG (2003) Oxidation of pentagalloylglucose to the ellagitannin, tellimagrandin II, by a phenol oxidase from *Tellima grandiflora* leaves. Phytochemistry 62:301–306

Niemetz R, Gross GG (2005) Enzymology of gallotannin and ellagitannin biosynthesis. Phytochemistry 66:2001–2011

Nonaka G, Morimoto S, Nishioka I (1986) Elaeocarpusin, a proto-type of geraniin from *Geranium thunbergii*. Chem Pharm Bull 34:941–943

Notka F, Meier GR, Wagner R (2003) Inhibition of wild-type human immunodeficiency virus and reverse transcriptase inhibitor-resistant variants by *Phyllanthus amarus*. Antivir Res 58:175–186

Notka F, Meier G, Wagner R (2004) Concerted inhibitory activities of *Phyllanthus amarus* on HIV replication *in vitro* and *ex vivo*. Antivir Res 64:93–102

Ofuji K, Hara H, Sukamoto T, Yamashita S (1998) Effects of an antidiarrhoeica containing an extract from geranium herb on astringent action and short-circuit current across jejunal mucosa. Nihon Yakurigaku Zasshi 111:265–275

Okabe S, Suganuma M, Imayoshi Y, Taniguchi S, Yoshida T, Fujiki H (2001) New TNF-α releasing inhibitors, geraniin and corilagin, in leaves of *Acer nikoense*, Megusurino-ki. Biol Pharm Bull 24:1145–1148

Okuda T, Ito H (2011) Tannins of constant structure in medicinal and food plants—hydrolysable tannins and polyphenols related to tannins. Molecules 16:2191–2217

Okuda T, Yoshida T, Mori K (1975) Constituents of *Geranium thunbergii* SIEB. et ZUCC. II. Ellagitannins. Yakugaku Zasshi 95:1462–1466

Okuda T, Mori K, Hayashi N (1976) Constituents of *Geranium thunbergii* SIEB. et ZUCC. III. Application of

determination methods of tannin activity with haemoglobin and of ellagitannin with nitrous acid. Yakugaku Zasshi 96:1143–1149

Okuda T, Yoshida T, Nayeshiro H (1977) Constituents of *Geranium thunbergii* SIEB. et ZUCC. IV. Ellagitannins. Structure of geraniin. Chem Pharm Bull 25:1862–1868

Okuda T, Mori K, Hatano T (1980) The distribution of geraniin and mallotusinic acid in the order geraniales. Phytochemistry 19:547–551

Okuda T, Yoshida T, Hatano T (1982) Constituents of *Geranium thunbergii* SIEB. et ZUCC. XII. Hydrated stereostructure and equilibration of geraniin. J Chem Soc Perkin Trans 1:9–14

Okuda T, Kimura Y, Yoshida T, Hatano T, Okuda H, Arichi S (1983) Studies on the activities of tannins and related compounds from medicinal plants and drugs. I. Inhibitory effects on lipid peroxidation in mitochondria and microsomes of liver. Chem Pharm Bull 31:1625–1631

Okuda T, Mori K, Hatano T (1985) Relationship of structures of tannins to the binding activities with haemoglobin and methylene blue. Chem Pharm Bull 33:1424–1433

Okuda T, Yoshida T, Hatano T, Ikeda Y, Shingu T, Inoue T (1986) Isolation of water-soluble tannins by centrifugal partition chromatography, and biomimetric synthesis of elaeocarpusin. Chem Pharm Bull 34:4075–4082

Okuda T, Yoshida T, Hatano T, Ito H (2009) Ellagitannins renewed the concept of tannins. In: Quideau S (ed) Chemistry and biology of ellagitannins: an underestimated class of bioactive plant polyphenols. World Scientific, Singapore

Ooshiro A, Kaji M, Katoh Y, Kawaide H, Natsume M (2011) Antibacterial activity of alkyl gallates and related compounds against *Ralstonia solanacearum*. J Pestic Sci 36:240–242

Palanisamy U, Ming CH, Masilamani T, Subramaniam T, Ling LT, Radhakrishnan AK (2008) Rind of the rambutan, *Nephelium lappaceum*, a potential source of natural antioxidants. Food Chem 109:54–63

Palanisamy UD, Ling LT, Manaharan T, Appleton D (2011a) Rapid isolation of geraniin from *Nephelium lappaceum* rind waste and its anti-hyperglycaemic activity. Food Chem 127:21–27

Palanisamy U, Manaharan T, Teng LL, Radhakrishnan AKC, Subramaniam T, Masilamani T (2011b) Rambutan rind in the management of hyperglycemia. Food Res Int 44:2278–2282

Pan MH, Lin-Shiao SY, Ho CT, Lin JH, Lin JK (2000) Suppression of lipopolysaccharide-induced nuclear factor-kB activity by theaflavin-3,3′-digallate from black tea and other polyphenols through down-regulation of IkB kinase activity in macrophages. Biochem Pharmacol 59:357–367

Park S, Han SU, Lee KM, Park KH, Cho SW, Hahm KB (2007) 5-LOX inhibitor modulates the inflammatory responses provoked by *Helicobacter pylori* infection. Helicobacter 12:49–58

Perera A, Appleton D, Ying LH, Elendran S, Palanisamy UD (2012) Large scale purification of geraniin from *Nephelium lappaceum* rind waste using reverse-phase chromatography. Sep Purif Technol 98:145–149

Perera A, Ton SH, Palanisamy UD (2015) Perspectives on geraniin, a multifunctional natural bioactive compound. Trends Food Sci Technol 44:243–257

Pouysegu L, Deffieux D, Malik G, Natangelo A, Quideau S (2011) Synthesis of ellagitannin natural products. Nat Prod Rep 28:853–874

Rakhimov RN, Abdulladzhanova NG, Kamev FG (2011) Phenolic compounds from *Euphorbia canescens* and *E. franchetii*. Chem Nat Compd 47:286–287

Rani S, Kumar B (2015) Efficacy of *Phyllanthus niruri* Linn. Extract in the management of type-2 diabetes mellitus associated hypercholesterolemia in mice diabetic model. Int J Curr Microbiol Appl Sci 4:507–513

Rausch H, Gross GG (1996) Preparation of [^{14}C]-labelled 1,2,3,4,6-penta-*O*-galloyl-β-D-glucose and related gallotannins. Z Naturforsch C 51:473–476

Roßner S, Schulz I, Zeitschel U, Schliebs R, Bigl V, Demuth H-U (2005) Brain prolyl endopeptidase expression in aging, APP transgenic mice and Alzheimer's disease. Neurochem Res 30:695–702

Roginsky V (2003) Chain-breaking antioxidant activity of natural polyphenols as determined during te chain oxidation of methyl linoleate in triton X-100 micelles. Arch Biochem Biophys 414:261–270

Santos ARS, Filho VC, Niero R, Viana AM, Moreno FN, Compos MM, Yunes RA, Calixto JB (1994) Analgesic effects of callus culture extracts from selected species of phyllanthus in mice. J Pharm Pharmacol 46:755–759

Santos ARS, Filho VC, Yunes RA, Calixto JB (1995) Analysis of the mechanisms underlying the antinociceptive effect of the extracts of plants from the genus *Phyllanthus*. Gen Pharm 26:1499–1506

Scalbert A (1991) Antimicrobial properties of tannins. Phytochemistry 30:3875–3883

Schimel JP, Cates RG, Ruess R (1998) The role of balsam poplar secondary chemicals in controlling soil nutrient dynamics through succession in the Alaskan taiga. Biogeochemistry 42:221–234

Schmidt SW, Denzel K, Schilliung G, Gross GG (1987) Enzymatic synthesis of 1,6-digalloylglucose from β-glucogallin by β-glucogallin: β-glucogallin 6-0-galloyltransferase from oak leaves. Z Naturforsch C 42:87–92

Schultz JC (1989) Tannin–insect interactions. In: Hemingway RW, Karchesy KK (eds) Chemistry and significance of condensed tannins. Plenum Press, New York

Schultz JC, Hunter MD, Appel HM (1992) Antimicrobial activity of polyphenols mediates plant–herbivore interactions. In: Hemingway RW, Laks PE (eds) Plant polyphenols. Synthesis, properties, significance. Plenum Press, New York

Seeram NP, Henning SM, Zhang Y, Suchard M, Li Z, Heber D (2006) Pomegranate juice ellagitannin metabolites are present in human plasma and some persist in urine for up to 48 hours. J Nutr 136:2481–2485

Solit DB, Rosen N (2006) Hsp90: a novel target for cancer therapy. Curr Top Med Chem 6:1205–1214

Stoner GD, Sardo C, Apseloff G, Mullet D, Wargo W, Pound V, Singh A, Sanders J, Aziz R, Casto B, Sun XL (2005) Pharmacokinetics of anthocyanins and ellagic acid in healthy volunteers fed freeze-dried black raspberries daily for 7 days. J Clin Pharmacol 45:1153–1164

Sudjaroen Y, Hull WE, Erben G, Wurtele G, Changbumrung S, Ulrich CM, Owen RW (2012) Isolation and characterization of ellagitannins as the major polyphenolic components

of Longan (*Dimocarpus longan* Lour) seeds. Phytochemistry 77:226–237

Tabata H, Katsube T, Tsuma T, Ohta Y, Imawaka N, Utsumi T (2008) Isolation and evaluation of the radical-scavenging activity of the antioxidants in the leaves of an edible plant, *Mallotus japonicus*. Food Chem 109:64–71

Tanaka T, Nonaka G, Nishioka I (1986) Tannins and related compounds. Part 37. Isolation and structure elucidation of elaeocarpusin, a novel ellagitannin from *Elaeocarpus sylvestris* var. Ellipticus. J Chem Soc Perkin Trans 1:369–376

Thitilertdecha N, Rakariyatham N (2011) Phenolic content and free radical scavenging activities in rambutan during fruit maturation. Sci Hortic 129:247–252

Thitilertdecha N, Teerawutgulrag A, Rakariyatham N (2008) Antioxidant and antibacterial activities of *Nephelium lappaceum* L. extracts. LWT Food Sci Technol 41:2029–2035

Thitilertdecha N, Teerawutgulrag A, Kilburn JD, Rakariyatham N (2010) Identification of major phenolic compounds from *Nephelium lappaceum* L. and their antioxidant activities. Molecules 15:1453–1465

Tsukuma H, Hiyama T, Tanaka S, Nakao M, Yabuuchi T, Kitamura T, Nakanishi K, Fujimoto I, Inoue A, Yamazaki H, Kawashima T (1993) Risk factors for hepatocellular carcinoma among patients with chronic liver disease. N Engl J Med 328:1797–1801

Ueno H, Horie S, Nishi Y, Shogawa H, Kawasaki M, Suzuki S, Hayashi T, Arisawa M, Shimizu M, Yoshizaki M, Morita N (1988) Chemical and pharmaceutical studies of medicinal plants in Paraguay. Geraniin, an angiotensin-converting enzyme inhibitor from "Paraparai Mi", *Phyllanthus Niruri*. J Nat Prod 51:357–359

Ushiki J, Tahara S, Hayakawa Y, Tadano T (1998) Medicinal plants for suppression soil-borne plant disease: II. Suppressive effect of *Geranium pratense* L. on common scab of potato and identification of the active compound. Soil Sci Plant Nutr 44:157–165

Ushio Y, Fang T, Okuda T, Abe H (1991) Modification changes in function and morphology of cultured macrophages by geraniin. Jpn J Pharmacol 57:187–196

Valko M, Leibfritz D, Moncol J, Cronin MTD, Mazur M, Telser J (2007) Free radicals and antioxidants in normal physiological functions and human disease. Int J Biochem Cell Biol 39:44–84

Vassallo A, Vaccaro MC, De Tommasi N, Paiz FD, Leone A (2013) Identification of the plant compound geraniin as a novel Hsp90 inhibitor. PLoS One 8:e74266

Velazquez-Gonzalez C, Carino-Cotes R, Gayosso de Lucio JA, Ortiz MI, Arciniega MDLO, Altamirano-Baez DA, Jumenes-Angeles L, Bautista-Avila M (2014) Antinociceptive and anti-inflammatory activities of *Geranium bellum* and its isolated compounds. BMC Complement Altern Med 14:506

Viriot C, Scalbert A, Herve du Penhoat CLM, Moutounet M (1994) Ellagitannins in woods of sessile oak and sweet chestnut dimerization and hydrolysis during wood ageing. Phytochemistry 36:1253–1260

Walkinshaw CH (1999) Constituent and induced tannin accumulations in roots of loblolly pines. In: Gross GG, Hemingway RW, Yoshida R, Branham S (eds) Plant polyphenols 2. Chemistry, biology, pharmacology, ecology. Kluwer/Plenum Publishers, New York

Wang P, Peng X, Wei ZF, Wei FY, Wang W, Ma WD, Yao LP, Fu YJ, Zu YG (2015) Geraniin exerts cytoprotective effect against cellular oxidative stress by upregulation of Nrf2-mediated antioxidant enzyme expression via PI3K/AKT and ERK1/2 pathway. Biochim Biophys Acta 1850: 1751–1761

Whitley AC, Stoner GD, Darby MV, Walle T (2003) Intestinal epithelial cell accumulation of the cancer preventive polyphenol ellagic acid-extensive binding to protein and DNA. Biochem Pharmacol 66:907–915

Williams JM, Richardson AC (1967) Selective acylation of pyranosides-I. Benzoylation of methyl α-D-glycopyranosides of mannose, glucose and galactose. Tetrahedron 23: 1369–1378

Wu QY, Zhou Y, Jin X, Guan Y, Xu M, Liu LF (2011) Chromatographic fingerprint and the simultaneous determination of five bioactive components of *Geranium carolinianum* L. water extract by high performance liquid chromatography. Int J Mol Sci 12:8740–8749

Xiao F, Zhai Z, Jiang C, Liu X, Li H, Qu X, Ouyang Z, Fan Q, Tang T, Qin A, Gu D (2015) Geraniin suppresses RANKL-induced osteoclastogenesis *in vitro* and ameliorates wear particle-induced osteolysis in mouse model. Exp Cell Res 330:91–101

Xu HX, Wan M, Dong H, But PPH, Foo LY (2000) Inhibitory activity of flavonoids and tannins against HIV-1 protease. Biol Pharm Bull 23:1072–1076

Xu M, Zha ZJ, Xl Qin, Zhang XL, Yang CR, Zhang YJ (2007) Phenolic antioxidants from the whole plant of *Phyllanthus urinaria*. Chem Biodivers 4:2246–2252

Yamada H, Nagao K, Dokei K, Kasai Y, Michihata N (2008) Total synthesis of (−)-corilagin. J Am Chem Soc 130: 7566–7567

Yang CM, Cheng HY, Lin TC, Chiang LC, Lin CC (2007) The *in vitro* activity of geraniin and 1,3,4,6-tetra-*O*-galloyl-β-D-glucose isolated from *Phyllanthus urinaria* against herpes simplex virus type 1 and type 2 infection. J Ethnopharmacol 110:555–558

Yang YC, Li J, Zu YG, Fu YJ, Luo M, Wo N, Liu XL (2010) Optimization of microwave-assisted enzymatic extraction of corilagin and geraniin from *Geranium sibiricum* Linne and evaluation of antioxidant activity. Suppressive effect of *Geranium pratense* L. on common scab of potato and identification of the active compound. Food Chem 122:373–380

Yang Y, Zhang L, Fan X, Qin C, Liu J (2012) Antiviral effect of geraniin on human enterovirus 71 *in vitro* and *in vivo*. Bioorg Med Chem Lett 22:2209–2211

Yang YC, Yang ZW, Zhang ZH, Zu YG, Fu YJ (2013) Effect of acid hydrolysis in the microwave-assisted extraction of phenolic compounds from *Geranium sibiricum* Linne with the guidance of antibacterial activity. J Med Plant Res 7:819–830

Yasuda H, Shima N, Nakagawa N, Yamaguchi K, Kinosaki M, Mochizuki S, Tomoyasu A, Yano K, Goto M, Murakami A, Tsuda E, Morinaga T, Higashio K, Udagawa N, Takahashi N, Suda T (1998) Osteoclast differentiation factor is a ligand for osteoprotegerin/osteoclastogenesis-inhibitory factor and is identical to TRANCE/RANKL. Proc Natl Acad Sci USA 95:3597–3602

Yasuda T, Inaba A, Ohmori M, Endo T, Kubo S, Ohsawa K (2000) Urinary metabolites of gallic acid in rats and their

radical-scavenging effects on 1,1-diphenyl-2-picrylhydrazyl radical. J Nat Prod 63:1444–1446

Yazaki K, Yoshida T, Okuda T (1991) Tannin production in cell suspension cultures of *Geranium thunbergii*. Phytochemistry 30:501–503

Yokozawa T, Chen CP, Dong E, Tanaka T, Nonaka GI, Nishioka I (1998) Study on the inhibitory effect of tannins and flavonoids against the 1,1-diphenyl-2-picrylhydrazyl radical. Biochem Pharmcol 56:213–222

Yoshida T, Chen L, Shingu T, Okuda T (1988) Tannins and related polyphenols of Euphorbiaceous plants. IV. Euphorbins A and B, novel dimeric dehydroellagitannins from *Euphorbia hirta* L. Chem Pharm Bull 36:2940–2949

Yoshida T, Itoh H, Matsunaga S, Tanaka R, Okuda T (1992) Tannins and related polyphenols of Euphorbiaceous plants. IX. Hydrolysable tannins with $^{1}C_{4}$ glucose core from *Phyllanthus flexuosus* Muell. Arg Chem Pharm Bull 40:53–60

Yoshida T, Amakura Y, Liu YZ, Okuda T (1994) Tannins and related polyphenols of Euphorbiaceous plants. XI. Three new hydrolysable tannins and a polyphenol glucoside from *Euphorbia humifusa*. Chem Pharm Bull 42:1803–1807

Youn K, Jun M (2013) *In vitro* BACE1 inhibitory activity of geraniin and corilagin from *Geranium thunbergii*. Planta Med 79:1038–1042

Yuan X, Hu D, Zhu W, Xu X, Lu C (2012) Application of frontal affinity chromatography combined on-line with mass spectrometry to screening PAI-1 inhibitors from traditional Chinese medicine. Anal Methods 4:3744–3747

Zhang YJ, Abe T, Tanaka T, Yang CR, Kouno I (2001) Phyllanemblinins A-F, new ellagitannins from *Phyllanthus emblica*. J Nat Prod 64:1527–1532

Zhang YJ, Nagao T, Tanaka T, Yang CR, Okabe H, Kouno I (2004) Antiproliferative activity of the main constituents from *Phyllanthus emblica*. Biol Pharm Bull 27:251–255

1.4.2. Summary of ellagitannin geraniin and the rationale for investigating its anti-metabolic syndrome effect.

According to the review [171], ellagitannin geraniin can be found in at least 71 plant species, with comparatively higher abundance in *Geranium* spp. Like many polyphenols, geraniin also demonstrates a wide range of activities. In this context, our interest lies in its anti-MetS properties. It has been shown to lower blood pressure by acting as an ACE inhibitor and lowering noradrenaline level [172, 173]. In an *in vitro* assay, the natural product could prevent platelet aggregation and thrombus formation [174]. Another biochemical study reported potent inhibitory effect of geraniin on the carbohydrate hydrolyzing enzymes like α-glucosidase and α-amylase, which may disrupt glucose absorption [175]. This is augmented by the lipid- and glucose-lowering effects observed in streptozotocin-induced diabetic rats when they were treated with plant crude extracts rich in geraniin [176, 177]. By itself, geraniin is a powerful antioxidant whose reducing power and radical scavenging capability is at least fivefold and sevenfold stronger than ascorbic acid, respectively [173, 178]. In some cell-based studies, the phytochemicals also effectively attenuated inflammatory response by inhibiting NF-κB and cytokine secretion [179, 180]. All of these bioactivities are associated to MetS, hence indicating the possibility that geraniin could be useful in MetS therapy. Indeed, lowering multiple metabolic abnormalities should lead to an overall reduction of the risks for MetS-associated complications. Furthermore, such pleotropic health benefits are also in line with the key feature of the future MetS therapy – multifunctionality. As such, it may be worthwhile to investigate the impacts of geraniin treatment in MetS models.

1.5. The Aim of the Research Project

1.5.1. Problem statements

Many known bioactivities of ellagitannin geraniin are established mainly based on *in vitro* studies. Most of the beneficial effects have not been confirmed in *in vivo* animal studies. Even less work has been done pertaining to the aspect of chronic metabolic disorder. So far, there is only one study reporting that treatment with purified geraniin (>95%) led to improved insulin sensitivity, reduction of abdominal fat pads and lipid-lowering effect [181]. To our best knowledge, no clinical trial on the effects of geraniin or geraniin-rich plant extract has been

carried out. This points out that the pre-existing knowledge in terms of the metabolic effects of geraniin is inadequate. Its mechanism of action is also poorly explored. Without the data, it is unlikely to outline the prospect and clinical utility of geraniin as an intervention to MetS.

1.5.2. Hypothesis and research objectives

Taking the aforementioned problems into consideration, the aim of this research project is **to investigate the metabolic effects and mechanism of ellagitannin geraniin in MetS using diet-induced rat models**. It is hypothesized the treatment with ellagitannin geraniin can bring about positive impacts on the metabolic status which is otherwise, deranged by chronic high-calorie feeding. To test the hypothesis, a reliable and clinically-relevant MetS model is a must. Altogether, the project would attempt to answer the following **research questions**:

1. To achieve a better MetS model, are there any differences between different diet formulations (HFD vs. HFSD) and the developmental stages of rats (post-weaning vs. young adult) in terms of the MetS induction efficacy based on induction time and overall MetS features?

2. What are the metabolic effects of ellagitannin geraniin with reference to the physical changes (body weight and blood pressure), biochemical parameters (lipid and glucose homeostasis), oxidative stress, inflammatory response and histopathological changes?

3. What are the implicated metabolic pathway(s) that can lead to the observed metabolic changes (if any) upon treatment with ellagitannin geraniin?

These research questions would be answered if the following **research objectives** are achieved:

1. *To find out the optimal diet-developmental stage combination that leads to fast and reliable MetS induction in rats.*
2. *To examine the effects of ellagitannin geraniin on physical, biochemical and histological changes upon oral administration using the established diet-induced MetS model..*
3. *To explore the hepatic mRNA changes imposed by ellagitannin geraniin treatment via transcriptomic study with next generation sequencing in order to postulate the possible metabolic pathway(s) influenced by the natural compound.*

1.5.3. Implications and significance of the research project

Being able to fulfill all the objectives will result in several notable contributions to the fundamental understanding about MetS and geraniin besides propelling the practical application of the natural compound. Firstly, studying the interplay between developmental stage and the types of high-calorie diets using animals can provide more information about the interaction between the environmental factor and our intrinsic characteristics on the onset of MetS. The findings can potentially spark in-depth investigations about the pathogenesis and long-term risk prediction, particularly in childhood obesity and MetS. This may trigger more aggressive early preventive initiatives via the nutritional approach during the early developmental stage.

Furthermore, a comparative study facilitates the direct comparison of the MetS induction efficacy caused by different diet formulations and developmental stages. This can resolve some confusion about the optimal disease induction approach. The best case scenario is that we can identify a combination of diet formulation and age that can lead to full-blown MetS within a relatively short time. If proven to be replicable in other strains and rodent species, such a model will be of utmost importance for future MetS preclinical research because of the reduction in time and resources attributed to disease modeling.

At the current stage, our understanding about geraniin is not sufficiently convincing even to prompt clinical trials, not to mention the actual clinical application as a MetS therapy. A critical appraisal of its multifaceted metabolic effects and the underlying mechanism allows us to piece together a more comprehensive picture about the clinical usefulness of the natural product. Additionally, by looking into the implicated metabolic pathways, there is a chance that we may be able to recognize a new target pathway to tackle MetS.

In the present study, geraniin is extracted from the rind of rambutan (*Nephelium lappeceum*). The plant species is native to tropical Southeast Asia regions and can produce edible fruits seasonally which are processed into canned products. The inedible rambutan rind will be a waste from the food processing. Interestingly, geraniin is present in high abundance in the rambutan rind. Around 25% to 30% of the crude rind extract is composed of geraniin [175, 182]. Discovering the pharmaceutical value of geraniin will therefore create added commercial value to rambutan rind, potentially turning the plant waste into something useful.

CHAPTER 2

Establishment of Metabolic Syndrome Rat Model

2. ESTABLISHMENT OF THE DIET-INDUCED METABOLIC SYNDROME MODEL IN RATS

2.1. General overview

In the context of MetS, a model is expected to display most of the features of the disorder, including central obesity, hypertension, high blood glucose and dyslipidemia. Two approaches are widely utilized to achieve the criteria, namely genetic and diet-induced models, the latter of which is a close mimicry of MetS in human beings due to the fact that over-nutrition is the primary etiology of the disease [130]. Nevertheless, diet-induced MetS requires relatively long induction time. Some studies reported successful induction within a month [183-185], but more often it takes more than two months of high calorie feeding to ensure complete MetS features in rodents. Therefore, any strategy to shorten the induction time is highly appreciated as it can greatly conserve time and research resources. One possible way is by identifying an effective diet formulation that can consistently lead to fast disease onset. To date, there are a wide range of high-calorie diets being used to induce MetS, each with different preparation methods, formulations and nutritional compositions. It will be extremely useful to identify a specific formulation that has an advantageous edge over the rest in MetS induction.

In addition, the susceptibility of rats to diet-induced MetS is partly dependent on the developmental stage [162, 163, 186]. However, the optimal starting age at which high-calorie feeding can cause faster disease onset remains inconclusive mainly due to the mixed empirical findings. According to the concept of programmed MetS, nutritional insult caused by HFD during the early childhood stage could have long-lasting adverse metabolic effects [167]. Hypothetically, younger rats may be more vulnerable to diet-induced MetS, but further investigation is warranted to verify the speculation.

Incidentally, it is also interesting to look at the interplay between different diet formulations and the developmental stages in the optimization of MetS animal model creation. As such, this chapter describes a comparative study that examines the disease induction efficacy of two widely employed high-calorie diets (HFD and HFSD) at two developmental stages (post-weaning and young adult) in rats. The study has been published [187] and is included as **Section 2.5**.

2.2. Objectives of the study

The primary aim of this chapter is **to identify an optimal combination of the high-calorie diet and developmental stage for the establishment of diet-induced MetS in Sprague Dawley rats**. Preferably, the disease induction method should lead to consistent manifestation of most, if not all, of the key MetS features within a reasonably short duration.

To accomplish the aim, the following objectives need to be fulfilled:

- To examine the disease induction efficiency of two widely employed high-calorie diets, namely HFD and HFSD.
- To explore the influence of developmental stages (post-weaning and young adult) on the progression of MetS.
- To study the interaction of high-calorie diet and developmental stage in the induction of MetS.

2.3. Overview of the research methodology

The use and handling of animals in the research have been approved by Monash University Monash Research Platform Animal Ethics Committees (AEC approval no.: MARP/2015/060) in compliance to the Australian Code of Practice for the Care and Use of Animals for Scientific Purposes outlined by National Health and Medical Research Council. The experimental design of the study is illustrated in **Figure 2.1**. Briefly, post-weaning (n=6 per group) and adult (n=7 per group) Sprague Dawley (*Rattus norvegicus*) rats were randomly assigned into three groups which were subjected to different experimental diets: CD, HFD and HFSD, respectively for eight weeks. Physical measurements like body weight, food and water intake as well as blood pressure were determined throughout the experiment. At the end of the experiment, the rats were humanely sacrificed for the collection of blood and tissue specimens which were used for various biochemical, transcriptional and histological assays to examine the metabolic status of the rats. The detailed assay procedures are available in the published manuscript (**Section 2.5**).

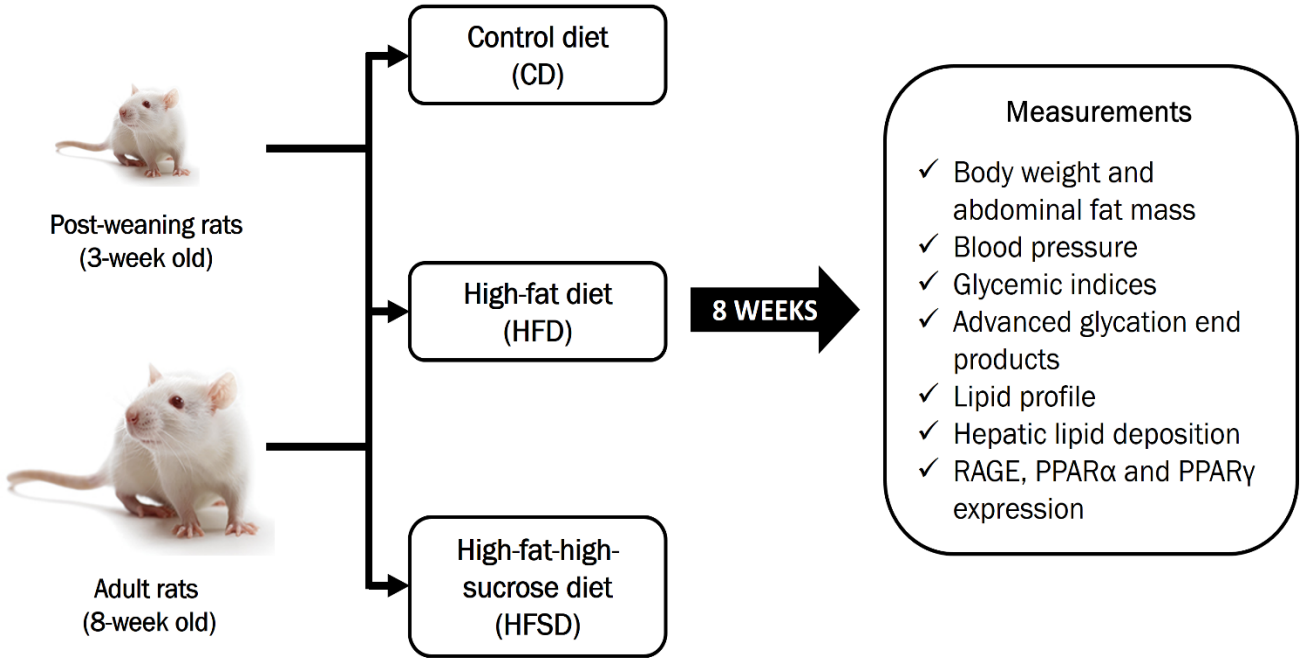

Figure 2.1: Experimental design of the animal study and the parameters measured throughout or at the end of the experiment. Total sample size is 39 Sprague Dawley rats (n=6 per group for post-weaning rats; n=7 per group for adult rats). CD, control diet; HFD, high-fat diet; HFSD, high-fat-high-sucrose diet; *PPAR*, peroxisome proliferator-activated receptor; *RAGE*, receptor for advanced glycation end product.

2.4. Key highlights of the study

The major findings as well as the conclusion presented in the manuscript are summarized in the following points:

- Developmental stage has a significant influence on many metabolic parameters related to MetS as evidenced by the increased weight gain and abdominal fat deposition in the post-weaning rats compared to adult rats. Post-weaning rats also had higher fasting plasma glucose, more hepatic lipid deposition, elevated expression of *RAGE* gene in abdominal fats and *PPARα* and *PPARγ* in the liver. Collectively, these metabolic abnormalities are indicative of the increased vulnerability of the post-weaning rats to MetS.
- Interplay between the developmental stage and types of high-calorie diet in the disease induction was noted. Among the post-weaning rats, HFD was the most effective diet that could lead to most MetS-related abnormalities. HFSD failed to promote weight gain and induce lipid and glucose dysregulation in the post-weaning rats. In another experiment done

by our group, the same purified ingredient-based HFD also performed better in MetS induction among the post-weaning rats compared to modified chow-based diet which was enriched by the same amount of saturated fats (**Appendix E1**-manuscript under review).

- In contrast, HFSD was more effective to induce metabolic anomalies in adult rats, which merely resulted in obesity and hypertension. The onset of elevated blood pressure in the adult rats on HFSD was also slower compared to post-weaning rats on either HFD or HFSD. HFD did not induce any remarkable changes to all the parameters in adult rats.
- In conclusion, post-weaning rats were more susceptible to MetS induced by high-calorie diets. In particular, post-weaning rats given HFD for eight weeks exhibited all crucial elements of MetS including central adiposity, increased blood pressure as well as lipid and glucose dysregulation. These metabolic aberrations were accompanied by hepatic steatosis and upregulated *PPARγ* expression in the liver and visceral adipose tissues. Hence, our results support that feeding post-weaning rats with HFD is a more effective and time-saving approach to establish a MetS model.

2.5. Published manuscript – Increased susceptibility of post-weaning rats on high-fat diet to metabolic syndrome

Journal of Advanced Research 8 (2017) 743–752

Contents lists available at ScienceDirect

Journal of Advanced Research

journal homepage: www.elsevier.com/locate/jare

Original Article

Increased susceptibility of post-weaning rats on high-fat diet to metabolic syndrome

Hong Sheng Cheng [a,*], So Ha Ton [a], Sonia Chew Wen Phang [b], Joash Ban Lee Tan [a], Khalid Abdul Kadir [b]

[a] School of Science, Monash University Malaysia, 46150 Bandar Sunway, Selangor, Malaysia
[b] School of Medicine and Health Sciences, Monash University Malaysia, 46150 Bandar Sunway, Selangor, Malaysia

GRAPHICAL ABSTRACT

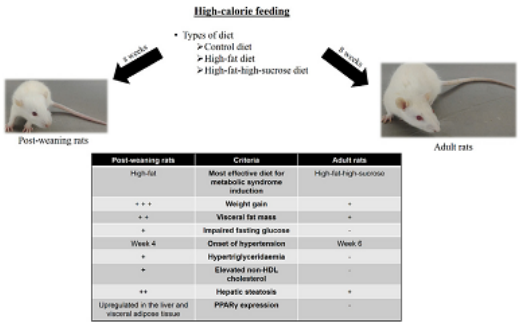

The effective high-calorie diet for metabolic syndrome induction is different between Sprague Dawley rats of different developmental stages. The post-weaning rats on high-fat diet for 8 weeks developed all phenotypes of metabolic syndrome while the adult rats on high-fat-high-sucrose diet merely became obese and hypertensive. The post-weaning rats on high-fat diet is a better and less time-consuming model for metabolic syndrome research.

ARTICLE INFO

Article history:
Received 23 July 2017
Revised 6 October 2017
Accepted 7 October 2017
Available online 9 October 2017

Keywords:
Dyslipidaemia
Hepatic steatosis
High-fat diet
Hypertension
Obesity
Peroxisome proliferator-activated receptor

ABSTRACT

The present study aimed to examine the effects of the types of high-calorie diets (high-fat and high-fat-high-sucrose diets) and two different developmental stages (post-weaning and young adult) on the induction of metabolic syndrome. Male, post-weaning and adult (3- and 8-week old, respectively) Sprague Dawley rats were given control, high-fat (60% kcal), and high-fat-high-sucrose (60% kcal fat + 30% sucrose water) diets for eight weeks (n = 6 to 7 per group). Physical, biochemical, and transcriptional changes as well as liver histology were noted. Post-weaning rats had higher weight gain, abdominal fat mass, fasting glucose, high density lipoprotein cholesterol, faster hypertension onset, but lower circulating advanced glycation end products compared to adult rats. This is accompanied by upregulation of peroxisome proliferator-activated receptor (PPAR) α and γ in the liver and receptor for advanced glycation end products (RAGE) in the visceral adipose tissue. Post-weaning rats on high-fat diet manifested all phenotypes of metabolic syndrome and increased hepatic steatosis, which are linked to increased hepatic and adipocyte PPARγ expression. Adult rats on high-fat-high-sucrose diet merely became obese and hypertensive within the same treatment duration. Thus, it is more effective and less time-consuming to induce metabolic syndrome in male post-weaning rats with high-fat diet compared to young adult

Peer review under responsibility of Cairo University.
* Corresponding author.
[redacted]

https://doi.org/10.1016/j.jare.2017.10.002

rats. As male rats were selectively included into the study, the results may not be generalisable to all post-weaning rats and further investigation on female rats is required.

Introduction

Metabolic syndrome (MetS) is a multiplex risk factors for cardiovascular disease and type 2 diabetes mellitus. The defining clinical criteria of MetS include central obesity, dyslipidaemia, hypertension, and glucose intolerance [1]. People with MetS are twice as likely to develop cardiovascular disease and up to five times as likely to become diabetic than those without the condition [2]. In addition, other comorbidities of MetS are also increasingly recognized, such as polycystic ovary syndrome [3], cancer [4], and cognitive degenerative disease [5]. MetS is deemed to be a worldwide health threat not only because of its devastating complications, but also due to the widespread global prevalence. In most developed and developing countries, approximately 20% of the adult population have MetS [6]. The statistic is undoubtedly an underestimation due to the exclusion of the rapidly-escalating paediatric and adolescent cases. Thus, studying the disease is crucial for us to propose potential solutions to this emerging epidemic.

One major challenge in MetS research is to create a clinically relevant disease model. In this context, metabolic dysfunction is commonly induced in rodents, particularly rats and mice, via different approaches, which include the use of genetic models like *ob*/*ob* and *db*/*db* mice as well as diet-induced models. The animal models of MetS are well-summarized by Panchal and Brown [7] and Aydin et al. [8]. Diet-induced models are usually preferred considering that over-nutrition is one of the key contributors to MetS. Nonetheless, the lack of standardised methodology for MetS induction results in a large variety of high-calorie diets being used, each with different preparation methods, formulations, and nutritional values. Some of the most popular diets are those high in saturated fat, fructose, sucrose or a combination of these macronutrients. This is because increased dietary lipid and fructose markedly upregulates *de novo* lipogenesis and promotes ectopic lipid deposition, which in turn, leads to peripheral insulin resistance, inflammatory response, chronic oxidative stress insult, and progressive organ damage [9,10]. Nonetheless, due to the diverse dietary compositions and feeding approaches, making comparisons between different diets and studies is often difficult. The issue of diet choice is further complicated by other concerns: purified ingredient-based diet versus chow-based diet [11], mismatched control diet [12], and feeding duration.

Additionally, other factors such as the animal species, strain, gender, and age should also be taken into consideration. Most studies employ male, adult rodents with a varying starting age. The feeding duration ranges from two to 18 weeks [8]. Given that the starting age could potentially influence the progression of MetS in both rodents [13,14] and humans [15], translating the experimental findings obtained from animal studies to mismatched age groups ought to be carried out cautiously. Furthermore, as mentioned earlier, the prevalence of metabolic syndrome among children and adolescents has drastically increased over recent years. Animal studies employing younger rats may be of interest since the experimental findings can potentially be applicable on paediatric population. Essentially, despite the extensive use of diet-induced models in MetS research, there are still a lot of unresolved issues and room for improvement to create better models.

Considering the vast diversity of determinants which may affect MetS progression, comparative animal studies are very useful for the optimisation of disease model creation. In the present study, we are particularly interested in the effects of age and dietary composition on the initiation of MetS. The other variables, such as the species, strain, and gender were kept constant by the use of male Sprague Dawley rats, which are one of the most commonly used animals in MetS research. The efficiency of two widely employed high-calorie diets (high-fat and high-fat-high-sucrose) in the induction of MetS in rats was examined. The differences in MetS progression that could be affected by the two developmental stages (post-weaning versus young adult) were also investigated. The findings will be discussed with reference to physical, biochemical, and transcriptional variables. The output of this study may help to put forward some key parameters for the establishment of a better MetS model.

Material and methods

Animal ethics and housing conditions

The use and handling of animals in the research have been approved by Monash University Monash Animal Research Platform Animal Ethics Committees (AEC approval No.: MARP/2015/060) in compliance to the Australian Code of Practice for the Care and Use of Animals for Scientific Purposes outlined by National Health and Medical Research Council. Thirty-nine male Sprague Dawley rats (Rattus norvergicus) including 18 post-weaning (3-week old) and 21 young adult (8-week old) were obtained from Monash University Malaysia Animal Facility. The rats were kept individually at 23 ± 1 °C with 12-h light/dark cycle. They were given ad libitum access to homemade purified ingredient-based diet and drinking water throughout the entire experiment.

Diet preparation, composition, and treatment

Both post-weaning and adult rats were randomly assigned into three groups (n = 6 for post-weaning rats and n = 7 for adult rats per group), which were provided with control diet (CD), high-fat

Table 1
Macronutrient composition and ingredients of control, high-fat and high-fat-high-sucrose diets.

Macronutrient	Control diet	High-fat diet	High-fat-high-sucrose diet
Protein (kcal%)	20	20	20
Carbohydrate (kcal%)	70	20	20
Lipid (kcal%)	10	60	60
Saturated (%)	36.6	57.9	57.9
Monounsaturated (%)	29.0	28.8	28.8
Polyunsaturated (%)	32.0	8.4	8.4
Trans (%)	1.8	3.6	3.6
Energy content (kcal/g)	3.9	5.3	5.3 + 1.2 kcal/mL from sucrose water
Ingredient	**Mass (g)**		
Casein	200	200	200
L-cystine	3	3	3
Corn starch	525.5	18	18
Maltodextrin	125	125	125
Sugar	50	50	50
Cellulose	50	50	50
Milk fat	20	245	245
Corn oil	25	25	25
AIN-93G Mineral mix	35	35	35
AIN-93-VX Vitamin mix	10	10	10
Choline bitartrate	2	2	2
t-butylhydroquinone	0.014	0.014	0.014
Additional supplement	–	–	30% (w/v) sucrose water

diet (HFD), and high-fat-high-sucrose diet (HFSD), respectively, for 8 weeks. The compositions of the diets, which were formulated based on AIN-93G diet [16] are shown in Table 1. All the ingredients, except for milk fat (Promac Enterprises Sdn. Bhd., Kuala Lumpur, Malaysia) and sucrose (MSM Malaysia Holdings Bhd., Kuala Lumpur, Malaysia), were purchased from MP Biomedical, Santa Ana, USA. The diets were prepared by mixing the ingredients thoroughly, followed by oven-baking for 10 min at 160 °C. For HFSD group, 30% (w/v) sucrose water was supplemented in addition to the HFD. The food and water were replenished every day. Body weight, food and water intake were measured daily.

Food was withdrawn while sucrose water of the HFSD group was replaced with tap water 12 h prior to humane sacrifice. The rats were euthanized by exsanguination via cardiac puncture under the influence of ketamine (75 mg/kg) and xylazine hydrochloride (10 mg/kg) administered intraperitoneally. Blood samples were collected in tubes with 0.5 M ethylenediaminetetraacetic acid (EDTA). Plasma was obtained by centrifugation of the blood samples at 4 °C, 2000×*g* for 20 min. The supernatant (plasma) was snap frozen in liquid nitrogen and stored at −80 °C until further use. About 1 cm × 1 cm of the liver tissues were excised and stored in 10% neutral buffered formalin for fixation and histology. Retroperitoneal white adipose tissue (rWAT) and liver were harvested promptly, snap frozen in liquid nitrogen and stored at −80 °C.

Blood pressure measurement

Systolic and diastolic blood pressure was measured with Mouse and Rat Tail Cuff Blood Pressure System (IITC Life Sciences, Los Angeles, USA). The rats were placed into a plastic restrainer one at a time to restrict their movement throughout the measurement. A tail-cuff with a pulse transducer was applied onto the tail of the restrained rats. The rat was then placed into a well-ventilated chamber equilibrated at 32 °C for 15–20 min to facilitate the dilatation of caudal arteries. Next, the triplicate readings of the systolic and diastolic blood pressure were recorded. The procedure was performed before the experiment (Week 0) and every two weeks (Week 2, 4, 6, and 8).

Biochemical assays

The glycaemic parameters and lipid profile at the end of the eight-week treatment were measured. Fasting plasma glucose was determined using Trinder's glucose oxidase test while fasting plasma insulin was determined using Mercodia Ultrasensitive Rat Insulin ELISA (Mercodia, Uppsala, Sweden). Based on the fasting plasma glucose and insulin levels, homeostasis model assessment of the insulin resistance (HOMA-IR), β-cell function (HOMA %β), and insulin sensitivity (HOMA %S) were evaluated using HOMA calculator [17]. Glycated haemoglobin A1c (HbA1c) and advanced glycation end product (AGE) levels were determined with Rat Haemoglobin A1c (HbA1c) kit (Crystal Chem, Downers Grove, USA) and OxiSelect™ Advanced Glycation End Product (AGE) Competitive ELISA kit (Cell Biolabs, San Diego, USA), respectively. Circulating triglyceride, total cholesterol (TC), and free fatty acid (FFA) levels were measured using Randox TR1607 Triglycerides, CH200 Cholesterol and FA115 Non-esterified Fatty Acids kits (Randox, Dublin, UK). Chylomicron, low density lipoprotein (LDL) and very low density lipoprotein (VLDL) were precipitated from the plasma specimens using Randox CH203 HDL-cholesterol Precipitant kit (Randox, Dublin, UK) and the remaining fraction was subjected to CH200 Cholesterol kit for the determination of high density lipoprotein (HDL)-cholesterol. Non HDL-cholesterol was calculated by subtracting HDL-cholesterol from TC. All assays with commercial kits were performed in duplicate according to the manufacturers' instructions.

RNA extraction and cDNA synthesis

Total RNA extraction of the liver was conducted using Qiagen RNeasy Mini Kit (Qiagen, Hilden, Germany), whereas that of rWAT was isolated with Tri-RNA reagent (Favorgen, Ping-Tung, Taiwan) and Qiagen RNeasy Mini Kit. The concentration and purity of the RNA were determined by measuring the absorbance at 260 nm and 280 nm with Infinite® 200 PRO (TECAN, Zürich, Switzerland). RNA integrity was examined with agarose gel electrophoresis to check 18S and 28S ribosomal RNA. RNase-free DNase I (ThermoFisher Scientific, Waltham, USA) treatment was performed prior to cDNA synthesis, which was carried out with Qiagen Omniscript Reverse Transcription Kit (Qiagen, Hilden, Germany).

Quantitative PCR (qPCR)

Rotor-Gene Q (Qiagen, Hilden, Germany) was used to carry out qPCR of peroxisome proliferator-activated receptors (PPAR) α and γ, lipoprotein lipase (LPL), and receptor for advanced glycation end product (RAGE) of the liver and adipose tissue. Hypoxanthine phosphoribosyltransferase 1 (HPRT1) and β-actin, which have been demonstrated to express stably in the target tissues, were selected as the reference genes for normalisation of the target genes [18]. JumpStart™ Taq ReadyMix (Sigma-Aldrich, St. Louis, USA) was used for the qPCR reactions. All primers and hydrolysis probes were synthesised by First BASE Laboratories, Malaysia. The nucleotide sequences of the primers and hydrolysis probes are outlined in Table 2. Normalised Ct or ΔCt values of the genes of interest were calculated using the following formula:

$$\Delta Ct = \text{average of } (Ct_{reference\ genes} - Ct_{gene\ of\ interest})$$

Tissue processing and histology

The well-fixed liver specimens were subjected to conventional tissue processing and embedded in paraffin wax. Thin sections (5 μm) were produced and stained with haematoxylin and eosin (H&E) to visualise the morphology. Three microscopic images at 200× magnification for each rat were captured with Nikon Eclipse

Table 2
Nucleotide sequences of the primers and hydrolysis probes.

Target gene	Nucleotide sequence (5′ → 3′)		
	Forward primer	Reverse primer	Hydrolysis probe
β-actin[a]	GTA TGG GTC AGA AGG ACT CC	GTT CAA TGG GGT ACT TCA GG	[TET] CCT CTC TTG CTC TGG GC [BHQ1]
HPRT1[a]	CTG GAA AGA ACG TCT TGA TTG	GTA TCC AAC ACT TCG AGA GG	[6FAM] AGC CCC AAA /[ZEN]/ATG GTT AAG GTT GCA AG [Iowa Black® FQ]
RAGE	CCC TGA CCT GTG CCA TCT CT	GGG TGT GCC ATC TTT TAT CCA	[6FAM] CCC AGC CTC CCC CTC AAA TCC A [BHQ1]
PPARα	TGT GGA GAT CGG CCT GGC CTT	CCG GAT GGT TGC TCT GCA GGT	[6FAM] TGC AGG AGG GGA TTG TGC ACG TGC TCA [BHQ1]
PPARγ	CCC TGG CAA AGC ATT TGT AT	GGT GAT TTG TCT GTT GTC TTT C	[6FAM] TCC TTC CCG CTG ACC A [BHQ1]
LPL	CAG CAA GGC ATA CAG GTG	CGA GTC TTC AGG TAC ATC TTA C	[6FAM] TTC TCT TGG CTC TGA CC [BHQ1]

HPRT1, hypoxanthine phosphoribosyltransferase 1; LPL, lipoprotein lipase; PPAR, peroxisome proliferator-activated receptor; RAGE, receptor for advanced glycation end product.
[a] Denotes reference genes.

TS100 (Nikon, Tokyo, Japan) and analysed with ImageJ to calculate the area of steatosis in the liver [19].

Statistical analysis

Statistical analysis was performed using Statistical Package for the Social Sciences (SPSS) 22.0. Dependent variables with repeated measures like cumulative weight gain and blood pressure were analysed using mixed model ANOVA using "time" as the within-subjects factor while "age" and "types of diets" as the between-subjects factors. Intergroup comparisons of other variables, including calorie intake, rWAT mass, glycaemic indices, lipid profile, and ΔCt values were analysed with two-way ANOVA with "age" and "types of diets" as the between-subjects factors. Pairwise comparisons were performed with Bonferroni correction. The level of statistical significance was pre-determined at $P \leq 0.05$.

Results

Differential obesity-inducing effects of HFD and HFSD on the post-weaning and adult rats

The initial weight of the rats within the same age groups, namely the post-weaning rats (64.5 ± 2.0 g, 63.0 ± 1.7 g, and 64.0 ± 1.9 g for CD, HFD, and HFSD) and the adult rats (222.2 ± 3.9 g, 219.4 ± 5.6 g, and 217.7 ± 3.2 g for CD, HFD, and HFSD), were not significantly different from each other. However, the post-weaning and adult rats gained weight at varying rates when exposed to different types of high-calorie diets. Based on Fig. 1A and B, the post-weaning and adult rats fed on HFD and HFSD, respectively, were more prone to accelerated weight gain. For the post-weaning rats on HFD, weight gain increased by about 25% over a course of eight weeks compared to those on CD and HFSD. Similar trend was also observed in the adult rats on HFSD compared to those on CD and HFD. Furthermore, the post-weaning rats also gained weight much faster than the adult rats ($P < 0.001$) which could be partly attributed to growth.

Increased weight gain is associated with increased rWAT mass as illustrated in Fig. 1C. To elucidate, the rWAT fat depot was increased by more than 50% in the post-weaning rats on HFD compared to the control group. Similar trend was observed in the adult rats on HFSD. Thus, it is justified to say that these rats developed central obesity after feeding on the corresponding high-calorie diets for eight weeks. The rWAT mass (±SEM) of the post-weaning rats (11.91 ± 0.76 g) was significantly higher than that of the adult rats (9.49 ± 0.68 g) ($P = 0.024$), suggesting that younger rats may be more susceptible to obesity induction. Nevertheless, calorie intake per day was similar across all groups (Fig. 1D),

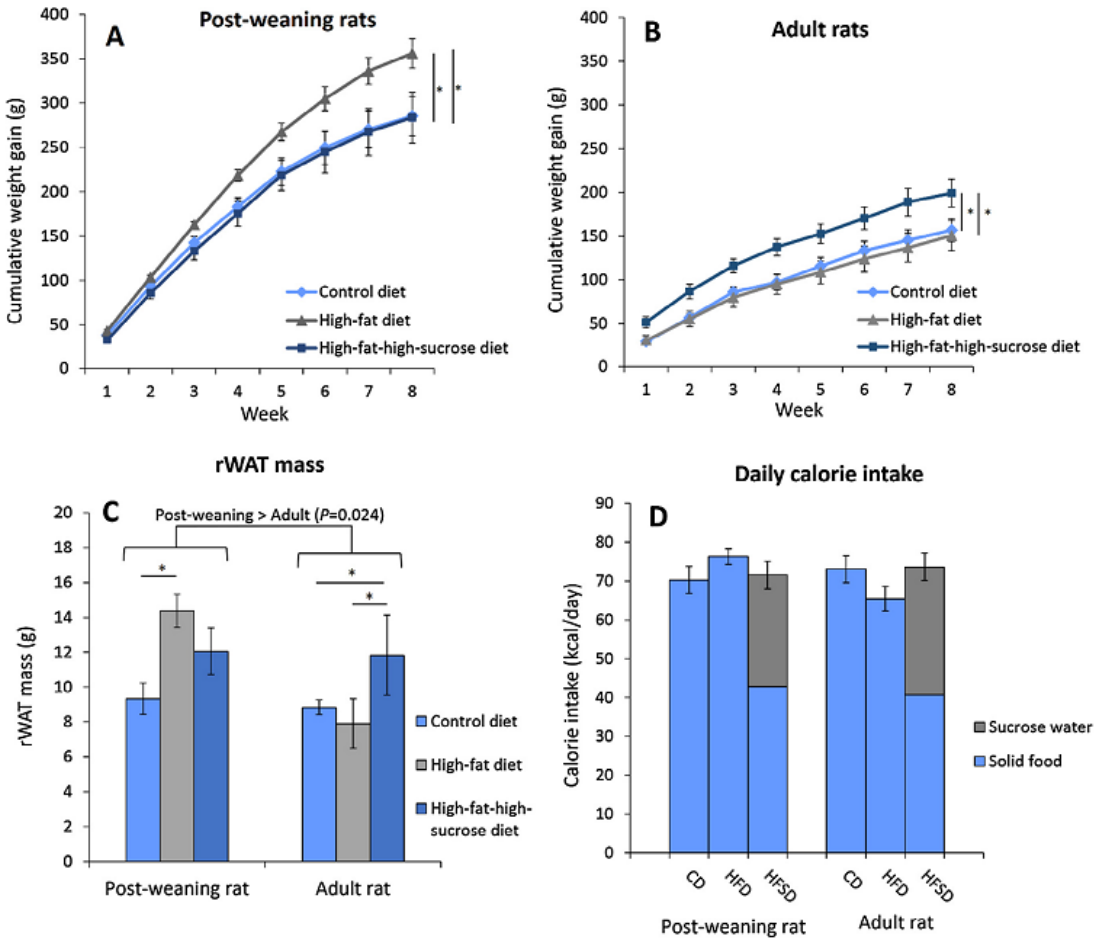

Fig. 1. Cumulative weight gain of the post-weaning (A) and adult rats (B) as well as the retroperitoneal white adipose tissue mass (C) and daily calorie intake (D) of the rats on different diets for eight weeks. Error bars indicate SEM. The sample size was n = 6–7 per group. * indicates $P < 0.05$ between groups. CD, control diet; HFD, high-fat diet; HFSD, high-fat-high-sucrose diet; rWAT, retroperitoneal white adipose tissue.

Table 3
Effects of HFD and HFSD on the consumption of food and water and glycaemic parameters of post-weaning and adult rats after eight-week long treatment.

Parameter	Post-weaning rat			Adult rat			Post-weaning rat vs Adult rat
	CD	HFD	HFSD	CD	HFD	HFSD	
Food intake (g/day)	18.11 ± 0.90	14.36 ± 0.37**	8.06 ± 0.77***,†††	18.82 ± 0.89	12.31 ± 0.59***	7.65 ± 0.52***,†††	*NS* (P = 0.330)
Water intake (mL/day)	21.59 ± 0.44	21.38 ± 0.73	23.71 ± 1.19	20.19 ± 0.90	19.70 ± 0.78	28.96 ± 1.17***,†††	*NS* (P = 0.552)
FPG (mmol/L)	5.52 ± 0.12	6.53 ± 0.15**	5.84 ± 0.21†	5.02 ± 0.18	5.12 ± 0.17	5.54 ± 0.20	Post-weaning > Adult (P < 0.001)
HbA1c (%)	3.81 ± 0.42	5.95 ± 0.51**	5.72 ± 0.63*	5.01 ± 0.31	5.73 ± 0.50	5.75 ± 0.32	*NS* (P = .378)
AGE (μg/mL)	61.23 ± 15.45	79.85 ± 5.62	43.48 ± 7.41†	104.56 ± 23.66	114.46 ± 17.81	61.85 ± 7.80†	Post-weaning < Adult (P = 0.011)
FPI (mU/L)	10.96 ± 1.95	5.69 ± 0.70	7.94 ± 1.06	6.51 ± 1.37	10.47 ± 3.46	8.91 ± 3.28	*NS* (P = 0.543)
HOMA-IR	1.26 ± 0.21	0.72 ± 0.10	0.82 ± 0.08	0.63 ± 0.16	0.87 ± 0.23	0.67 ± 0.19	*NS* (P = 0.158)
HOMA%β (%)	108.0 ± 12.9	40.8 ± 2.9**	63.8 ± 3.9	81.4 ± 17.5	80.0 ± 21.7	47.9 ± 8.0	*NS* (P = 0.917)
HOMA%S (%)	92.9 ± 19.9	132.4 ± 13.4	116.5 ± 13.2	129.0 ± 20.0	89.8 ± 14.2	119.3 ± 32.8	*NS* (P = 0.943)

Values are expressed as mean ± SEM. The sample size was n = 6–7 per group.
AGE, advanced glycation end products; CD, control diet; FPG, fasting plasma glucose; FPI, fasting plasma insulin; HbA1c, glycated haemoglobin A1c; HFD, high-fat diet; HFSD, high-fat-high-sucrose diet; HOMA %β, homeostasis model assessment of β-cell function; HOMA%S, homeostasis model assessment of insulin sensitivity; HOMA-IR, homeostasis model assessment of insulin resistance; *NS*, non-significant.
* P < 0.05 compared to CD.
** P < 0.01 compared to CD.
*** P < 0.001 compared to CD.
† P < 0.05 compared to HFD.
††† P < 0.001 compared to HFD.

indicating that the increased weight gain and rWAT mass were independent of calorie consumption. It is also worth mentioning that for the HFSD group, both the post-weaning and adult rats obtained more than two fifths of their daily calorie intake from the sucrose water. Carbohydrate preference over lipid was noted in adult rats as suggested by significant increase in the consumption of sucrose water (P < 0.001) (Table 3).

High calorie diets induced systolic and diastolic hypertension

Like the initial body weight, the starting systolic and diastolic blood pressure levels of the rats within the same age groups were comparable. Both the HFD and HFSD triggered systolic and diastolic hypertension (Fig. 2A, C) in the post-weaning rats. At the end of the experiment, the systolic blood pressure levels were

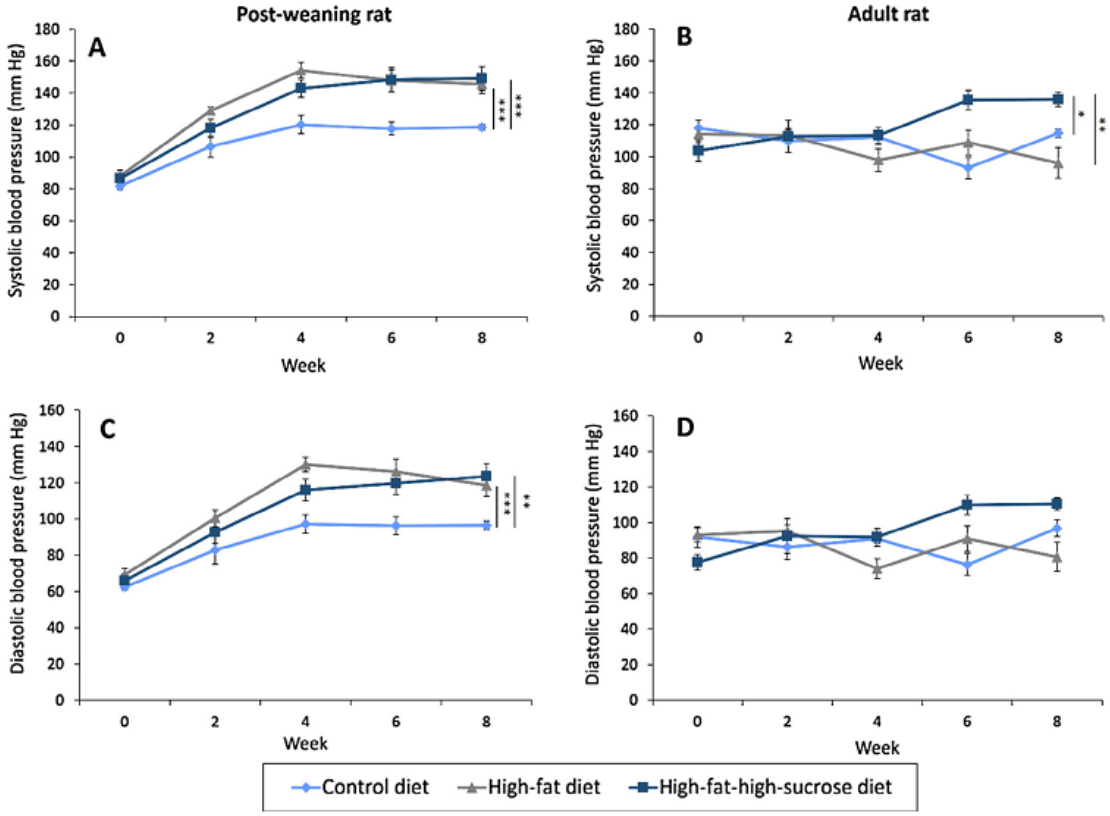

Fig. 2. Systolic and diastolic blood pressure of the post-weaning (A and C) and adult (B and D) rats on different diets over eight weeks. Error bars indicate SEM. The sample size was n = 6–7 per group. * indicates P < 0.05, ** indicates P < 0.01 and *** indicates P < 0.001 between groups.

146 ± 6 mmHg and 149 ± 7 mmHg in the HFD- and HFSD-treated post-weaning rats compared to 119 ± 2 mmHg in those on CD. Conversely, the diastolic blood pressure levels increased from 97 ± 2 mmHg in the CD group to 119 ± 6 mmHg and 124 ± 7 mmHg in the HFD and HFSD groups, respectively. The escalated blood pressure took place from week 4 onwards.

In contrast, the hypertensive effect of the high calorie diets was less prominent among the adult rats. Such an effect was observed only in the systolic blood pressure of those on HFSD whereby the blood pressure was elevated from 115 ± 3 mmHg in the CD group to 136 ± 4 mmHg in the HFSD group at the end of the experiment (Fig. 2B). The onset of the systolic hypertension occurred in week 6 which was slower compared to the post-weaning rats. In addition, no difference in the diastolic blood pressure of adult rats was detected (Fig. 2D). The results show that younger rats are more vulnerable to high-calorie diet-induced hypertension.

High-fat diet caused hyperglycaemia, dyslipidaemia and hepatic steatosis in the post-weaning rats

Based on Table 3, the food consumed per day was significantly lower in HFD- and HFSD-treated groups ($P < 0.001$). This was to compensate for the increased calorie content of the diets. The post-weaning rats given HFD became hyperglycaemic at the end of the experiment as demonstrated by the elevated fasting plasma glucose level compared to CD- and HFSD-treated rats. This is further supported by a significant increase in HbA1c % which is suggestive of chronic hyperglycaemia. The contributing factor could be an impairment in β-cell function as indicated by a 62% reduction in HOMA %β compared to the CD-treated rats. However, prolonged hyperglycaemia did not lead to increased circulating AGE level in the post-weaning rats on HFD. More surprisingly, compared to CD, HFSD significantly reduced plasma AGEs by 29% in the post-weaning rats.

On the other hand, the carbohydrate metabolism of the adult rats was mildly affected by the high calorie feeding because no difference was found between groups in terms of the glycaemic indices. Similar AGE-lowering effect of HFSD was also observed in the adult rats. Between different age groups, the post-weaning rats had significantly higher fasting plasma glucose level of 5.96 ± 0.11 mmol/L in comparison to 5.23 ± 0.10 mmol/L in the adult rats, suggesting that older rats are more resistant to metabolic derangement. However, the older rats had higher circulating AGEs (93.62 ± 8.16 μg/mL) compared to the young rats (61.52 ± 8.58 μg/mL) ($P = 0.011$), denoting a positive correlation between age and AGE accumulation.

The lipid profile is outlined in Table 4. Basically, post-weaning rats on HFD also developed hypertriglyceridaemia and elevated non-HDL cholesterol level at the end of experiment. Such adverse effects were not observed in adult rats on the high-calorie diets, implying that HFD is more effective in disrupting glucose and lipid homeostasis in the young rats. The dyslipidaemic condition of the post-weaning rats on HFD and HFSD is further augmented by the increased hepatic lipid deposition shown in Fig. 3. Even though the extent of fatty liver in adult rats on HFSD also increased by almost 100%, the difference did not reach statistical significance ($P = 0.085$) when compared to CD.

Unexpectedly, inter-diet group comparison shows that HFSD significantly reduced circulating TC compared to the CD- ($P = 0.043$) and HFD-treated rats ($P = 0.032$). Similarly, when the rats were fed with HFSD, HDL-cholesterol was also reduced in comparison to the CD- ($P < 0.001$) and HFD-treated rats ($P = 0.016$). Moreover, both high-calorie diets significantly lowered FFA level (±SEM) to 0.41 ± 0.05 mmol/L and 0.44 ± 0.05 mmol/L in HFD- ($P = 0.026$) and HFSD-treated rats ($P = 0.047$), respectively, compared to 0.61 ± 0.05 mmol/L in the control group.

Overexpression of rWAT RAGE and hepatic PPARs in the post-weaning rats

No difference in RAGE expression in the liver and rWAT was found (Fig. 4A, B). Nonetheless, rWAT RAGE expression of the post-weaning rats was upregulated twofold compared to the adult rats ($P = .005$). On the other hand, the post-weaning rats given HFD and HFSD significantly overexpressed PPARγ by more than fivefold in the rWAT compared to those on CD (Fig. 5A), but LPL expression remained unchanged (Fig. 5C). In the liver, PPARγ expression of the HFD-treated post-weaning rats also upregulated by 220% and 333% compared to the CD- and HFSD-treated rats. Additionally, hepatic lipid metabolism of the post-weaning rats was much more active than that of the adult rats because the PPARα and γ expression was increased by more than 14- and 17-fold, respectively in the young rats (Fig. 5B, D).

Discussion

Diets enriched with lipids and/or carbohydrates have been widely used to induce MetS in rodents with varying degrees of success at inducing the key symptoms, namely central obesity, hypertension, hyperglycaemia and dyslipidaemia [7,8]. In this study, we demonstrate that the interplay between the developmental stage of the rats and the types of diet plays a crucial role in disease induction. Three-week old post-weaning rats given HFD for eight weeks developed all the phenotypes of MetS whereas adult rats on HFSD merely became obese and hypertensive, making the former a more time-saving and cost-effective MetS model.

Although diet-induced obese model using post-weaning rats has been developed [20], comparative study between post-

Table 4
Effects of HFD and HFSD on the lipid profile and hepatic lipid deposition of post-weaning and adult rats after eight-week long treatment.

Parameter	Post-weaning rat			Adult rat			Post-weaning rat vs Adult rat
	CD	HFD	HFSD	CD	HFD	HFSD	
Triglycerides (mmol/L)	1.08 ± 0.07	1.88 ± 0.29*	1.15 ± 0.11	1.30 ± 0.19	0.95 ± 0.16	1.59 ± 0.17	*NS* ($P = 0.559$)
Total cholesterol (mmol/L)	1.80 ± 0.22	2.16 ± 0.20	1.59 ± 0.10	2.11 ± 0.21	1.79 ± 0.22	1.32 ± 0.07*	*NS* ($P = 0.493$)
HDL-cholesterol (mmol/L)	1.54 ± 0.18	1.17 ± 0.08	0.94 ± 0.09*	1.23 ± 0.21	1.12 ± 0.14	0.51 ± 0.07**,‖	Post-weaning > Adult ($P = 0.025$)
Non-HDL-cholesterol (mmol/L)	0.55 ± 0.10	1.12 ± 0.32*	0.71 ± 0.07	0.76 ± 0.05	0.58 ± 0.07	0.94 ± 0.09	*NS* ($P = 0.807$)
NEFA (mmol/L)	0.57 ± 0.05	0.38 ± 0.04	0.46 ± 0.07	0.66 ± 0.12	0.45 ± 0.07	0.42 ± 0.03*	*NS* ($P = 0.505$)
Hepatic lipid deposition (%)	1.95 ± 0.33	4.26 ± 0.33***	4.14 ± 0.64**	1.29 ± 0.17	1.80 ± 0.17	2.53 ± 0.33	Post-weaning > Adult ($P = 0.000$)

Values are expressed as mean ± SEM. The sample size was n = 6–7 per group.
CD, control diet; HFD, high-fat diet; HFSD, high-fat-high-sucrose diet; NEFA, non-esterified fatty acids; *NS*, non-significant.
* $P < 0.05$ compared to CD.
** $P < 0.01$ compared to CD.
*** $P < 0.001$ compared to CD.
‖ $P < 0.01$ compared to HFD.

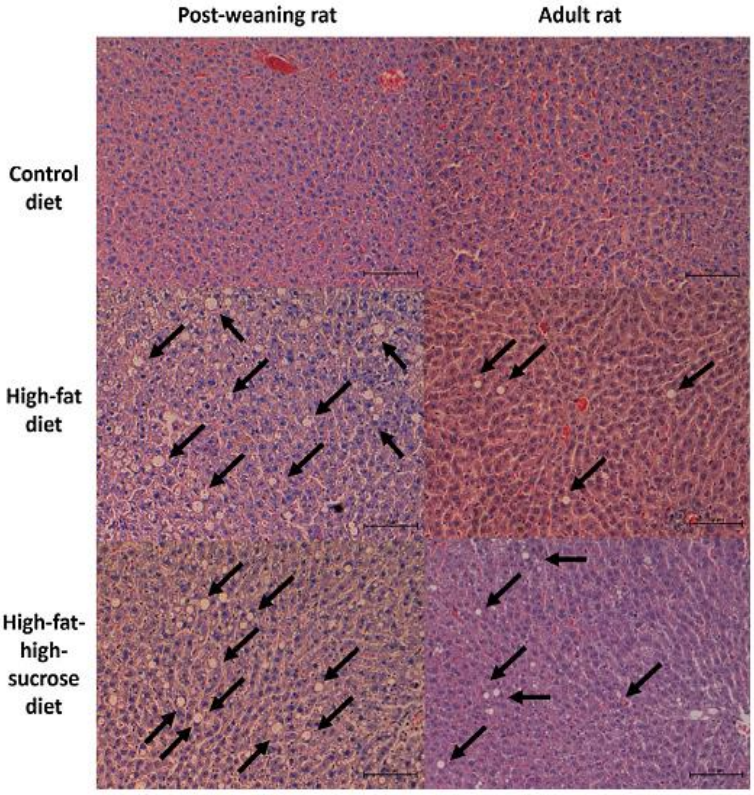

Fig. 3. Representative H&E-stained liver sections (x200 magnification) of the post-weaning and adult rats given different diets for eight weeks. The black arrows indicate the lipid deposition sites in the liver tissues. The sample size was n = 6–7 per group.

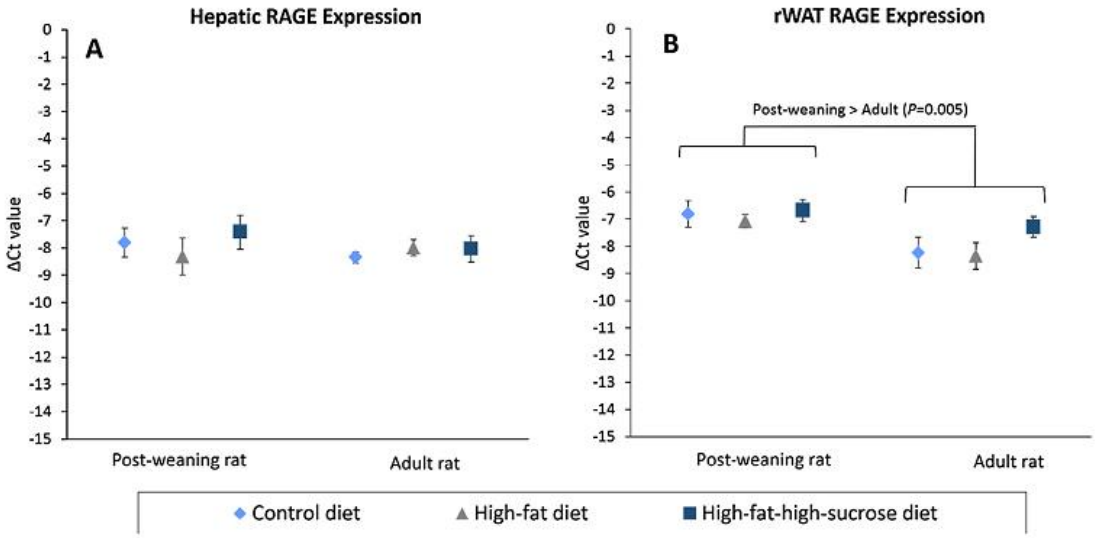

Fig. 4. Normalized Ct values (ΔCt) of RAGE expression in the liver (A) and rWAT (B) of the post-weaning and adult rats on different diets at the end of eight-week treatment. HPRT1 and β-actin were used as reference genes. Error bars indicate SEM. The sample size was 6–7 per group. RAGE, receptor for advanced glycation end products; rWAT, retroperitoneal white adipose tissue.

weaning rats and the commonly used young adult rats is rather limited. This study shows that post-weaning rats gained weight more rapidly to become centrally obese. This is accompanied by elevated systolic and diastolic blood pressure. In fact, increased susceptibility to hypertension upon HFD-feeding in younger rats has also been described previously [21]. Although the adult rats given HFSD diet also developed these features, the effects were relatively less severe (slower weight gain, lower rWAT mass and

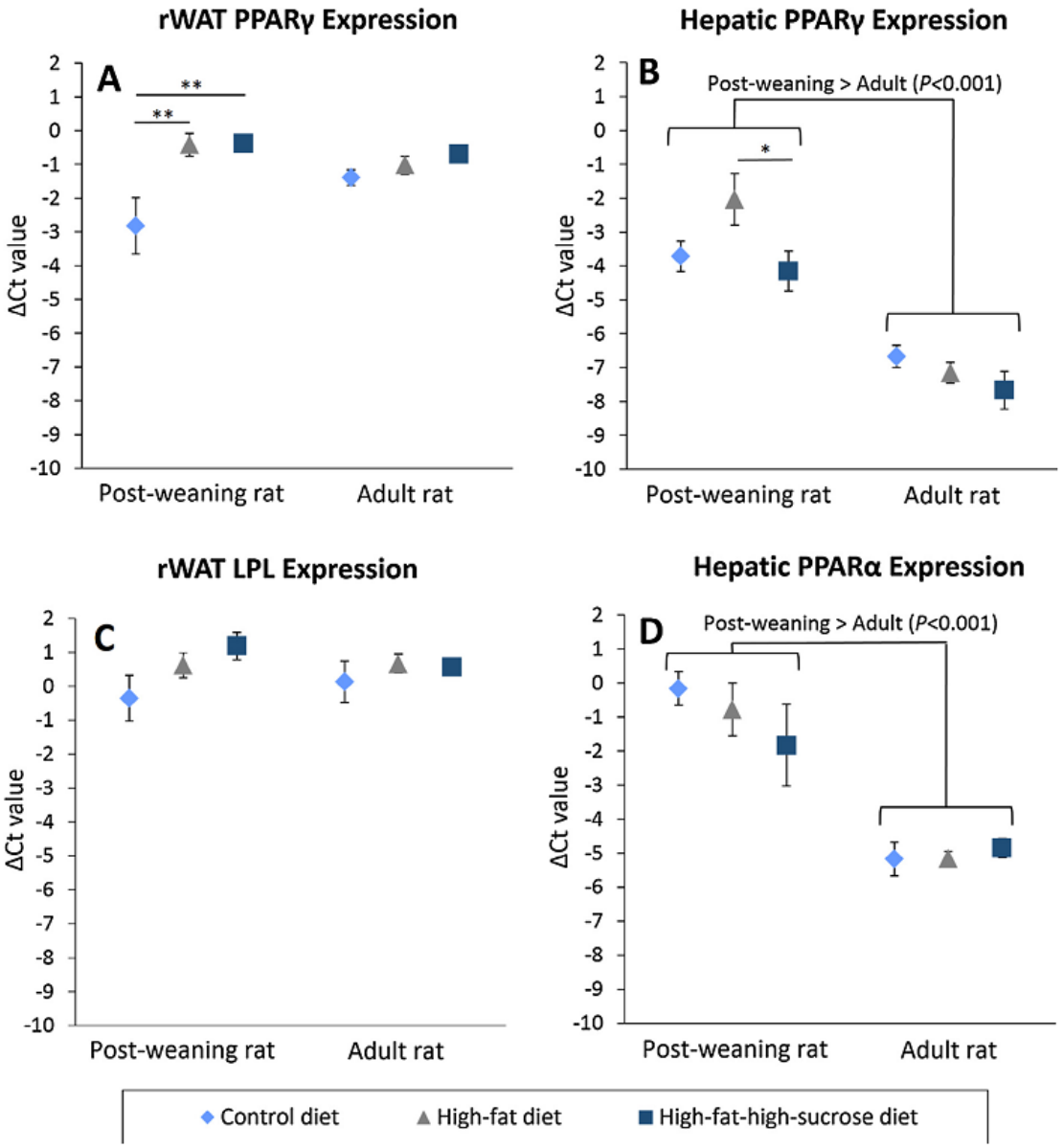

Fig. 5. Normalized Ct values (ΔCt) of PPARγ in the rWAT (A) and liver (B), LPL in the rWAT (C) and PPARα in the liver (D) of post-weaning and adult rats on different diets at the end of eight-week treatment. HPRT1 and β-actin were used as reference genes. Error bars indicate SEM. The sample size was 6–7 per group. * indicates $P < 0.05$, ** indicates $P < 0.01$ between groups. LPL, lipoprotein lipase; PPARα, peroxisome proliferator-activated receptor α; PPARγ, peroxisome proliferator-activated receptor γ; rWAT, retroperitoneal white adipose tissue.

delayed systolic hypertension onset). Furthermore, the post-weaning rats also developed impaired fasting glucose which could be caused by impaired β-cell function as indicated by low HOMA β %. In contrast, Pagliassotti and coworkers reported that older rats have reduced glucose disposal rate in the skeletal muscle and adipose tissues, thus, they are more susceptible to glucose intolerance due to insulin resistance [22]. This suggests that the development stage may affect the pathophysiology of glucose dysregulation. Even though insulin resistance is a major pathophysiology of glucose metabolic dysregulation in MetS, reduced β-cell function has also been identified as an important contributing factor, particularly in obese children and adolescents [23,24]. As such, our model could potentially be used to mimic childhood and adolescent MetS.

The overexpression of hepatic PPARα and γ, which is consistently found in obese murine models [25], was detected in the young rats. To elucidate, PPARα is primarily responsible for transcriptional regulation of the genes for fatty acid uptake and oxidation in the liver [26] whereas hepatic PPARγ is usually expressed at low levels but is markedly upregulated when there is an increased lipid flux into the liver [27]. This leads to an increased lipid accumulation in the liver which is also known as hepatic steatosis as observed in the post-weaning rats on HFD and HFSD in the present study. Increased liver steatosis could serve to modulate the triglyceride level and prevent ectopic fat deposition at other tissues [28] which may explain why the post-weaning rats on HFSD were able to maintain a normal lipid profile despite the severe hepatic steato-

sis. Normal hepatic PPARγ expression among the adult rats also suggests a state of lipid homeostasis, but the same cannot be said for the HFD-treated post-weaning rats.

In this study, post-weaning rats were selected to compare to adult rats because the young rats could be used to mimic childhood condition. Furthermore, the eight-week treatment covered Day 21 to Day 77 of their postnatal life which corresponds to the childhood, adolescence and early adulthood in human beings [29] and so, the onset of metabolic dysfunction in the post-weaning rats could potentially be used to model paediatric MetS. Additionally, considering their rapid growth and high basal metabolic rate, it is speculated that younger rats may be more sensitive to nutritional cues of the high-calorie diets. Indeed, we observed an immerse difference in term of the effectiveness of MetS induction between different developmental stages which strongly suggests an inherent metabolic regulatory difference. This may be linked to programmed MetS. Principally, the concept of programmed MetS suggests that nutritional insults (*eg.* starvation and overnutrition) during gestation [30] or immediate postnatal [31] may induce epigenetic modifications of key metabolic regulatory genes that substantially enhance the risk of metabolic diseases. Certain studies have demonstrated that the window for metabolic programming could extend into early childhood [32,33]. In this context, PPARs is known to be a key player in metabolic programming because a vast array of PPAR target genes, including *Hdac* and *Sirt7* which are both epigenetic regulators, are well-implicated in programmed metabolic syndrome [34]. This is in line with the expression assays of the present study which show the significant upregulation of PPARs in the liver of post-weaning rats but not the adult rats. Hence, programmed MetS could lend support to explain the susceptibility of post-weaning rats on HFD to the disorder, but further investigation on the epigenetic modification is warranted to explore the possible mechanism.

Apart from that, an age-dependent increase in the circulating AGE level was observed in spite of the elevated glucose level among the post-weaning rats, indicating a predominant role of ageing to AGE aggregation [35]. However, RAGE expression in the rWAT was discordant with AGE level. Such an upregulation of RAGE in the rWAT of post-weaning rats could be driven by other non-glycated peptide ligands. Studies have demonstrated the integral role of adipocyte RAGE in regulation of adiposity and atherosclerotic risk [36,37]. Therefore, enhanced adipocyte RAGE expression of the post-weaning rats could add another piece to the puzzle of their predisposition to MetS.

The daily calorie intake of the rats was relatively constant regardless of the age groups and the types of diet provided. This finding is consistent with previous study [38] and suggests that the observed metabolic perturbations are dependent on the components of the high-calorie diets, namely sucrose and lipids. The rats also showed a striking preference for carbohydrates over the lipids, as evidenced by the heavy reliance on the sucrose water in the HFSD group. As a result, the consumption of other macro- and micronutrients, most notably proteins, was substantially diluted (20% kcal in CD and HFD vs. 12% kcal in HFSD). The reduced protein intake may account for the lowering effect of cholesterol, FFA and AGE in the HFSD group simply because these parameters are dependent on the amount of transport proteins in the circulation.

Surprisingly, FFA level was lowered in both post-weaning and adult rats on high-calorie diets. This is consistent with a recent study which showed that FFA was significantly lowered in obese insulin resistant rodents [39]. This finding challenges the notion about the devastating insulin-desensitizing effect of FFA in obesity and MetS. In fact, Karpe et al. reviewed a number of clinical data and concluded that the causal relationship of increased systemic FFA and insulin resistance may not always be true [40]. Considering the emerging counter evidence, it may be wise to re-examined the role of circulating FFA in the pathogenesis of various metabolic disorders.

In the present study, even though the HFSD-treated rats consumed similar amount of calories, the protein intake was much less because of their dependence on sucrose-enriched water. This might lead to unintended metabolic changes due to protein malnutrition. Future studies should make sure the protein intake is comparable to the control group. Although the post-weaning rats seemed to be more vulnerable to MetS upon high-fat feeding, the impact of developmental stage cannot the fully elaborated without the rats of different ages namely, young, adult, middle- and old-aged. Further studies should also focus on the oxidative stress level, proinflammatory response, cytokine profile, sex and stress hormones so as to explore the possible mechanisms of the observed vulnerability.

Conclusions

To conclude, compared to the young adult rats which are commonly used in MetS study, the post-weaning rats were more vulnerable to metabolic dysfunctions. Notably, the post-weaning rats on HFD for eight weeks exhibited all key manifestations of MetS, including central obesity, systolic and diastolic hypertension, impaired fasting glucose, hypertriglyceridaemia, and elevated non-HDL cholesterol level. The expression of RAGE and PPARs were upregulated in the post-weaning rats compared to the adult rats, more so for those on HFD, leading to the postulation that nutritional insults during early childhood may have detrimental long-lasting effects on metabolism. Male, post-weaning rats on HFD will be a useful MetS model. However, the selective use of male post-weaning rats in this study limits the generalisation of the results to female rats. Thus, further studies should attempt to clarify the susceptibility of female post-weaning rats to MetS besides examining the pathophysiology of the model to explore the potential linkages with childhood obesity and MetS.

Acknowledgements

The work was supported by the Ministry of Science, Technology and Innovation, Malaysia (grant no.: 02-02-10-SF0249); and the School of Science, Monash University Malaysia. We would like to acknowledge Mr. Andrew Leong Kum Loong and Mr. Zulkhaili Zainal Abidin for their assistance in animal handling. We would also like to thank Mr. Derick Sim Kai Cheng and Ms. Lee Zhi Wei for their contribution to the project.

Conflict of interest

The authors have declared no conflict of interest.

Compliance with ethics requirements

All Institutional and National Guidelines for the care and use of animals (fisheries) were followed.

References

[1] Alberti KGMM, Eckel RH, Grundy SM, Zimmet PZ, Cleeman JI, Donato KA, et al. Harmonizing the metabolic syndrome. A joint interim statement of the International Diabetes Federation Task Force on Epidemiology and Prevention; National Heart, Lung, and Blood Institute; American Heart Association; World Heart Federation; International Atherosclerosis Society; and International Association for the Study of Obesity. Circulation 2009;120:1640–5.

[2] Ford ES. Risks for all-cause mortality, cardiovascular disease, and diabetes associated with the metabolic syndrome: a summary of the evidence. Diabetes Care 2005;28:1769–78.

[3] Baranova A, Tran TP, Birerdinc A, Younossi ZM. Systematic review: association of polycystic ovary syndrome with metabolic syndrome and non-alcoholic fatty liver disease. Aliment Pharmacol Ther 2011;33:801–14.
[4] Esposito K, Chiodini P, Colao A, Lenzi A, Giugliano D. Metabolic syndrome and risk of cancer: a systematic review and meta-analysis. Diabetes Care 2012;35:2402–11.
[5] Frisardi V, Solfrizzi V, Seripa D, Capurso C, Santamato A, Sancarlo D, et al. Metabolic-cognitive syndrome: a cross-talk between metabolic syndrome and Alzheimer's disease. Ageing Res Rev 2010;9:399–417.
[6] O'Neill S, O'Driscoll L. Metabolic syndrome: a closer look at the growing epidemic and its associated pathologies. Obes Rev 2015;16:1–12.
[7] Panchal SK, Brown L. Rodent models for metabolic syndrome research. J Biomed Biotechnol 2011;2011:351982.
[8] Aydin S, Aksoy A, Aydin S, Kalayci M, Yilmaz M, Kuloglu T, et al. Today's and yesterday's of pathophysiology: Biochemistry of metabolic syndrome and animal models. Nutrition 2014;30:1–9.
[9] Zlobine I, Gopal K, Ussher JR. Lipotoxicity in obesity and diabetes-related cardiac dysfunction. Biochim Biophys Acta 2016;1861:1555–68.
[10] Lim JS, Mietus-Snyder M, Valente A, Schwarz J-M, Lustig RH. The role of fructose in the pathogenesis of NAFLD and the metabolic syndrome. Nat Rev Gastroenterol Hepatol 2010;7:251–64.
[11] Warden CH, Fisler JS. Comparisons of diets used in animal models of high-fat feeding. Cell Metab 2008;7:277.
[12] Benoit B, Plaisancié P, Awada M, Géloën A, Estienne M, Capel F, et al. High-fat diet action on adiposity, inflammation, and insulin sensitivity depends on the control low-fat diet. Nutr Res 2013;33:952–60.
[13] Busserolles J, Mazur A, Gueux E, Rock E, Rayssiguier Y. Metabolic syndrome in the rat: females are protected against the pro-oxidant effect of a high sucrose diet. Exp Biol Med 2002;227:837–42.
[14] Ghezzi AC, Cambri LT, Botezelli JD, Ribeiro C, Dalia RA, de Mello MAR. Metabolic syndrome markers in wistar rats of different ages. Diabetol Metab Syndr 2012;4:16.
[15] Kuk JL, Ardern CI. Age and sex differences in the clustering of metabolic syndrome factors. Diabetes Care 2010;33:2457–61.
[16] Reeves PG. Components of the AIN-93 diets as improvements in the AIN-76A diet. J Nutr 1997;127:838S–41S.
[17] Levy JC, Matthews DR, Hermans MP. Correct homeostasis model assessment (HOMA) evaluation uses the computer program. Diabetes Care 1998;21:2191–2.
[18] Svingen T, Letting H, Hadrup N, Hass U, Vinggaard AM. Selection of reference genes for quantitative RT-PCR (RT-qPCR) analysis of rat tissues under physiological and toxicological conditions. PeerJ 2015;3:e855.
[19] Schneider CA, Rasband WS, Eliceiri KW. NIH Image to ImageJ: 25 years of image analysis. Nat Methods 2012;9:671–5.
[20] Lalanza JF, Caimari A, del Bas JM, Torregrosa D, Cigarroa I, Pallàs M, et al. Effects of a post-weaning cafeteria diet in young rats: metabolic syndrome, reduced activity and low anxiety-like behaviour. PLoS ONE 2014;9:e85049.
[21] Erdos B, Kirichenko N, Whidden M, Basgut B, Woods M, Cudykier I, et al. Effect of age on high-fat diet-induced hypertension. Am J Physiol Heart Circ Physiol 2011;301. H164–H72.
[22] Pagliassotti MJ, Gayles EC, Podolin DA, Wei Y, Morin CL. Developmental stage modifies diet-induced peripheral insulin resistance in rats. Am J Physiol Regul Integr Comp Physiol 2000;278:R66–73.
[23] Weiss R, Caprio S, Trombetta M, Taksali SE, Tamborlane WV, Bonadonna R. B-cell function across the spectrum of glucose tolerance in obese youth. Diabetes 2005;54:1735–43.
[24] Weigensberg MJ, Ball GDC, Shaibi GQ, Cruz ML, Goran MI. Decreased β-cell function in overweight Latino children with impaired fasting glucose. Diabetes Care 2005;28:2519–24.
[25] Memon RA, Tecott LH, Nonogaki K, Beigneux A, Moser AH, Grunfeld C, et al. Up-regulation of peroxisome proliferator-activated receptors (PPAR-α) and PPAR-γ messenger ribonucleic acid expression in the liver in murine obesity: Troglitazone induces expression of PPAR-γ-responsive adipose tissue-specific genes in the liver of obese diabetic mice. Endocrinology 2000;141:4021–31.
[26] Leone TC, Weinheimer CJ, Kelly DP. A critical role for the peroxisome proliferator-activated receptor α (PPARα) in the cellular fasting response: The PPARα-null mouse as a model of fatty acid oxidation disorders. Proc Natl Acad Sci U S A 1999;96:7473–8.
[27] Inoue M, Ohtake T, Motomura W, Takahashi N, Hosoki Y, Miyoshi S, et al. Increased expression of PPARγ in high fat diet-induced liver steatosis in mice. Biochem Biophys Res Commun 2005;336:215–22.
[28] Gavrilova O, Haluzik M, Matsusue K, Cutson JJ, Johnson L, Dietz KR, et al. Liver peroxisome proliferator-activated receptor γ contributes to hepatic steatosis, triglyceride clearance, and regulation of body fat mass. J Biol Chem 2003;278:34268–76.
[29] Sengupta P. The laboratory rat: relating its age with human's. Int J Prev Med 2013;4:624–30.
[30] Symonds ME, Sebert SP, Hyatt MA, Budge H. Nutritional programming of the metabolic syndrome. Nat Rev Endocrinol 2009;5:604–10.
[31] Patel MS, Srinivasan M. Metabolic programming due to alterations in nutrition in the immediate postnatal period. J Nutr 2010;140:658–61.
[32] Vickers MH, Breier BH, Cutfield WS, Hofman PL, Gluckman PD. Fetal origins of hyperphagia, obesity, and hypertension and postnatal amplification by hypercaloric nutrition. Am J Physiol Endocrinol Metab 2000;279. E83–E7.
[33] Tain Y-L, Sheen J-M, Yu H-R, Chen C-C, Tiao M-M, Hsu C-N, et al. Maternal melatonin therapy rescues prenatal dexamethasone and postnatal high-fat diet induced programmed hypertension in male rat offspring. Front Physiol 2015;6.
[34] Tain Y-L, Hsu C-N, Chan J. PPARs link early life nutritional insults to later programmed hypertension and metabolic syndrome. Int J Mol Sci 2016;17:20.
[35] Schleicher ED, Wagner E, Nerlich AG. Increased accumulation of the glycoxidation product N(epsilon)-(carboxymethyl)lysine in human tissues in diabetes and aging. J Clin Invest 1997;99:457–68.
[36] Ueno H, Koyama H, Shoji T, Monden M, Fukumoto S, Tanaka S, et al. Receptor for advanced glycation end-products (RAGE) regulation of adiposity and adiponectin is associated with atherogenesis in apoE-deficient mouse. Atherosclerosis 2010;211:431–6.
[37] Monden M, Koyama H, Otsuka Y, Morioka T, Mori K, Shoji T, et al. Receptor for advanced glycation end products regulates adipocyte hypertrophy and insulin sensitivity in mice. Diabetes 2013;62:478–89.
[38] Warwick ZS, Schiffman SS. Role of dietary fat in calorie intake and weight gain. Neurosci Biobehav Rev 1992;16:585–96.
[39] Jiang J, Wu Y, Wang X, Lu L, Wang L, Zhang B, et al. Blood free fatty acids were not increased in high-fat diet induced obese insulin-resistant animals. Obes Res Clin Pract 2016;10:207–10.
[40] Karpe F, Dickmann JR, Frayn KN. Fatty acids, obesity, and insulin resistance: time for a reevaluation. Diabetes 2011;60:2441–9.

CHAPTER 3

Metabolic Effects of Ellagitannin Geraniin

3. EFFECTS OF ELLAGITANNIN GERANIIN ON THE COMPONENTS OF METABOLIC SYNDROME IN RATS ON HIGH-FAT DIET

3.1. General overview

In recent years, the research of polyphenols in the aspect of chronic metabolic diseases is gaining momentum. Basically, polyphenols are chemical compounds that possess multiple phenol functional groups – a hydroxyl group (-OH) attached to an aromatic benzene ring. This distinctive chemical structure is accountable for their powerful antioxidant properties [188]. To date, more than 8000 plant polyphenols have been identified, but only a handful of them have been fully assessed for their bioactivities [189]. Even fewer have been tested in human subjects. Hence, the effectiveness of polyphenols on MetS is inconclusive due to limited studies and small sample size.

Like many other polyphenols, ellagitannin geraniin is not well-investigated despite its discovery more than 40 years ago [190]. Various herbs that are rich in geraniin have been used in traditional medicine of different cultures including Japan, Mexico, India and China to relieve a wide variety of symptoms, ranging from fever, edema, gastrointestinal discomfort to diarrhea [191-194]. More importantly, several preliminary studies have demonstrated the anti-hypertensive [172], anti-hyperglycemic [175], anti-inflammatory [179], anti-thrombotic [174] and insulin sensitizing [181] activities of geraniin. Such pleiotropic ameliorative effects on most of the MetS features does make it an interesting candidate as a multifunctional drug against the chronic disease. In terms of safety aspect, geraniin has minimal toxicity even at a considerably high dosage. For instance, in most normal cell lines, geraniin is well-tolerated up to 100 μM without jeopardizing the cell viability [195, 196]. This phytochemical compound has also been used in rats at 100 mg/kg for five days and 50 mg/kg for a month via oral administration without causing renal and hepatic dysfunction [181, 197]. Furthermore, the metabolism of geraniin upon oral consumption has been studied [198]. These insightful works about the toxicity and pharmacokinetics of ellagitannin geraniin allow us to emphasize on its bioactivities without worrying its safety profile.

Ellagitannin geraniin used in the present study was extracted and purified from the rind of *Nephelium lappaceum* (local name: rambutan). The plant is native to tropical Southeast Asia and seasonally produces edible fruits. Based on Perera et al. (2012), the crude ethanolic extract of rambutan rind contains approximately 21% of geraniin, which can be purified with a one-step reverse phase column chromatography [199]. Being able to isolate a natural product of potential pharmacological significance from an agricultural by-product is undoubtedly a commendable effort which may create added value to the crops.

In this chapter, the effects of ellagitannin geraniin in MetS will be elaborated. The metabolic effects of geraniin were compared to MetS rats treated with either metformin or tocotrienol-rich fraction (TRF), as well as untreated rats which were on either CD or HFD. Tocotrienols are subtypes of vitamin E which are well-known for its potent antioxidant capacity and inhibitory effect on the HMG-COA reductase [200, 201]. The TRF used in the present study is derived from palm oil and made up of 23.5% (*w/w*) α-tocotrienol, 43.2% γ-tocotrienol, 9.8% δ-tocotrienols and 23.5% α-tocopherol. Conversely, metformin which is primarily an anti-diabetic agent, has shown promising effectiveness in delaying the onset of MetS and T2DM [202, 203]. By comparing the metabolic effects of geraniin to TRF and metformin whose bioactivities have been characterized, it is possible to examine their relative effectiveness besides speculating if they share similar mode of action. Essentially, the findings of this study could unravel more insights into the biological activities and prospect of ellagitannin geraniin as a MetS therapy.

3.2. Objectives of the study

This chapter aims **to study the impacts of ellagitannin geraniin on the core features of MetS in Sprague Dawley rats on HFD**. To achieve the aim, the following research tasks have to be accomplished:

- To examine the extent of central obesity and adiposity.
- To investigate the systolic and diastolic blood pressure as well as levels of electrolytes in the blood circulation.
- To study the lipid and glucose metabolism based on biochemical markers in the blood circulation.
- To investigate the severity of hepatic steatosis.

- To compare the aforementioned physiological, biochemical and histopathological markers between different treatments to derive the efficacy of ellagitannin geraniin on MetS.

3.3. Methods and materials

3.3.1. Purification and identification of ellagitannin geraniin from *Nephelium lappaceum*

The isolation of ellagitannin geraniin from the peels of *Nephelium lappaceum* (rambutan) was performed in accordance to the protocol published by Perera et al. in 2012 [199]. The purity of the compound was examined with high performance liquid chromatography (HPLC) which depicted >95% purity (**Appendix A1**). Further identification of the compound was done with standard addition assay whereby purified geraniin was spiked with geraniin standard and analysed with HPLC to check if they share the same retention time. Structural confirmation was done with proton nuclear magnetic resonance (^{1}H-NMR), liquid chromatography-mass spectrometry (LCMS) and negative ionization mode liquid chromatography-tandem mass spectrometry (LCMS-MS). The ^{1}H-NMR spectrum of the purified geraniin was consistent with that reported by Gohar et al. in 2003 [204]. The LCMS *m/z* ratio of the isolated geraniin was 951 while the LCMS-MS *m/z* ratios of the geraniin fragments were 301, 463 and 933. These *m/z* ratios are consistent with previous studies [199, 205]. The results of the standard addition assay, ^{1}H-NMR, LCMS and LCMS-MS are available in **Appendices A1 to A3**.

3.3.2. Animal ethics and housing conditions

The use and handling of animals in the research have been approved by Monash University Monash Animal Research Platform Animal Ethics Committees (AEC approval no.: MARP/2015/060) in compliance to the Australian Code of Practice for the Care and Use of Animals for Scientific Purposes outlined by National Health and Medical Research Council. Male, post-weaning (3-week old) Sprague Dawley rats (*Rattus norvegicus*) of 45 g to 70 g were obtained from Monash University Malaysia Animal Facility. The rats were kept at 23 ± 1^0C with 2-hour light/dark cycle and given *ad libitum* access to homemade purified ingredient-based diets and tap water throughout the whole experiment.

3.3.3. Experimental design and treatment

The experimental design of the study is illustrated in **Figure 3.1**. Briefly, 34 post-weaning rats were randomly assigned into five different treatment groups (n= 6 to 7 per group): CD, HFD, metformin (Hovid, Malaysia), TRF (Hovid, Malaysia) and geraniin. Except for the rats in CD group which were given CD, others were given HFD for eight weeks to induce MetS. The disease modelling, dietary composition and ingredients are as described in **Section 2.3**. After eight weeks, the rats assigned to metformin, TRF and geraniin groups were given the respective treatments via oral gavage. The dosages are outlined in **Table 3.1**. All the compounds or drugs were suspended in 10% (w/v) glucose water prior to feeding to minimize animal resistance to the administration procedure [206]. The vehicle (10% glucose water) was also administered to the CD- and HFD-treated rats via the same approach. The treatment lasted for four weeks, during which the rats were given the pre-assigned diet.

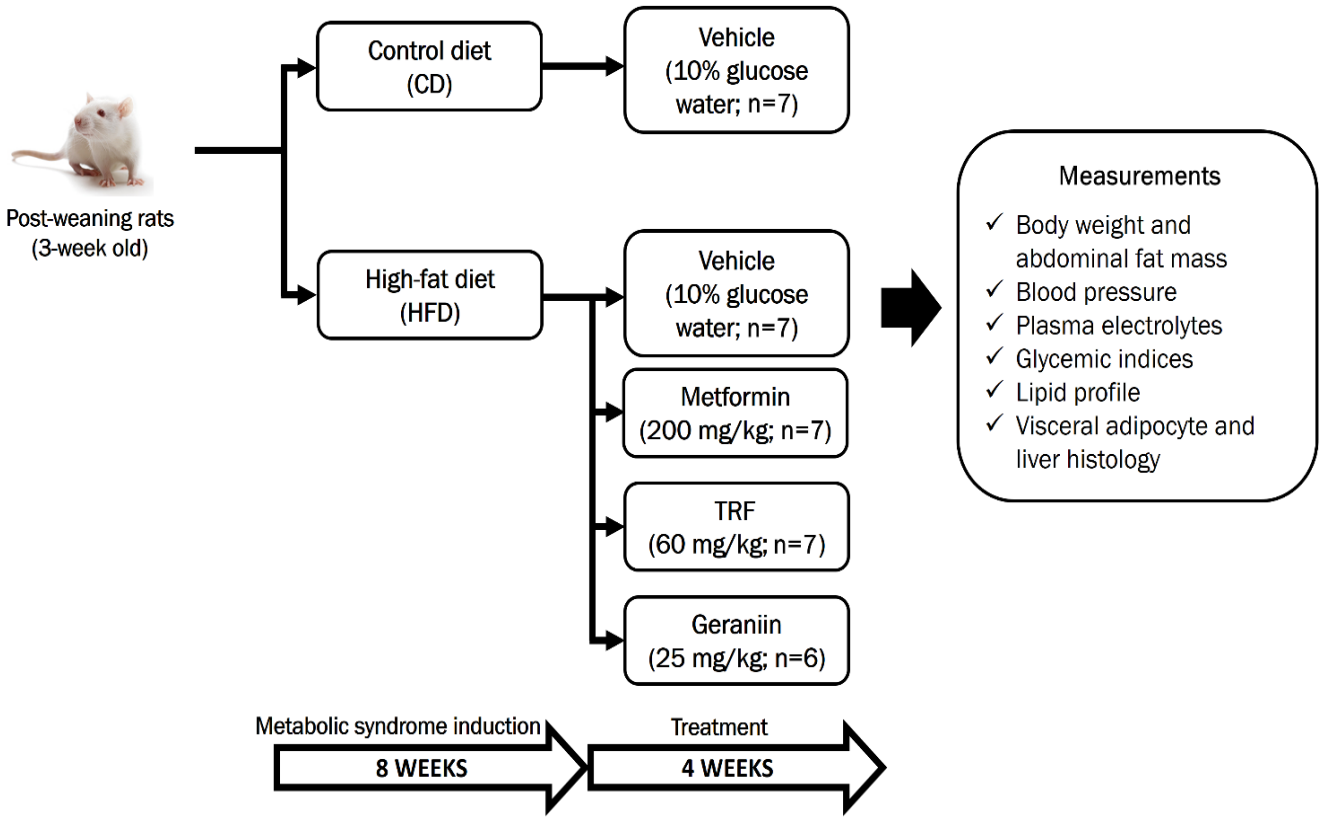

Figure 3.1: Experimental design to investigate the metabolic effects of ellagitannin geraniin in rats with HFD-induced metabolic syndrome.

Table 3.1: Dosage of the compounds or drugs used in the study.

Compound	Dosage	Reasons/References
Metformin	200 mg/kg/day	Calculated based on recommended human adult dosage (Lily & Godwin 2009) using the conversion factor suggested by United States Food and Drug Administration (2005) [203, 207]
Tocotrienol-rich fraction	60 mg/kg/day	Norazlina et al. (2002) and Ahmad et al. (2005) [208, 209]
Geraniin	25 mg/kg/day	Based on our in-house pilot study

The food and water were replenished daily. Body weight, food and water consumption were also measured daily. At the end of the experiment, the rats were subjected to 12-hour fasting prior to euthanasia with carbon dioxide. Blood samples from the posterior vena cava were collected in tubes containing 0.5M EDTA and swiftly centrifuged at 4ºC, 2000x *g* for 20 minutes to obtain the plasma. The plasma samples were then snap frozen in liquid nitrogen and stored at -80ºC until further use. Body tissues were excised and weighed. The liver and retroperitoneal white adipose tissues (rWAT) were stored in 10% (v/v) neutral buffered formalin for tissue fixation and histology.

3.3.4. Blood pressure measurement

Systolic and diastolic blood pressure was measured with Mouse and Rat Tail Cuff Blood Pressure System (IITC Life Sciences, USA). The rats were placed into a plastic restrainer one at a time to restrict their movement throughout the measurement. A tail-cuff with a pulse transducer was applied onto the tail of the restrained rats. The rat was then placed into a well-ventilated chamber equilibrated at 32ºC for 15 to 20 minutes to facilitate the dilatation of caudal arteries. Next, triplicate readings of the systolic and diastolic blood pressure were recorded. The procedure was performed once per week.

3.3.5. Determination of glycemic parameters and lipid components

Fasting blood glucose was determined with Accu-Chek® Performa glucometer (Roche Diagnostics, USA) whereas the fasting plasma insulin was determined using Mercodia Ultrasensitive Rat Insulin ELISA (Mercodia, Sweden). β-cell function (HOMA %β) and insulin sensitivity (HOMA %S) were evaluated using homeostatic model assessment (HOMA)

calculator [210]. Glycated hemoglobin A1c (HbA1c) was measured with Rat Hemoglobin A1c (HbA1c) kit (Crystal Chem, USA).

Triglyceride, total cholesterol and free fatty acid levels were determined using Randox TR1697 Triglycerides, CH200 Cholesterol and FA115 Non-esterified Fatty Acids kits (Randox, UK). Chylomicron, LDL and very low-density lipoproteins (VLDL) were precipitated from the plasma using Randox CH203 HDL-cholesterol Precipitant kit (Randox, UK) and the supernatant was subjected to CH200 Cholesterol kit for the determination of HDL-cholesterol. Non HDL-cholesterol was calculated by subtracting HDL-cholesterol from the total cholesterol. All analysis with the commercial kits were conducted in duplicates according to the manufacturers' instructions. The assay procedures and standard curves of the commercial kits are shown in **Appendices B1 to B6**.

3.3.6. Oral glucose tolerance test

Oral glucose tolerance test (OGTT) was performed before and after the compound treatment in Week 8 and 12. Prior to the test, the rats were deprived of food for 8 hours. After fasting, the basal blood glucose was measured with a glucometer. The rats were then given a glucose load of 2 g/kg as 40% (w/v) glucose solution via oral gavage. Blood glucose levels were measured at 30, 60, 90 and 120 minutes after the administration of the glucose load.

3.3.7. Plasma electrolyte levels

Atomic absorption spectrophotometry was used for the determination of plasma electrolyte levels. To measure the sodium and potassium concentrations, plasma specimens were diluted by 500 and 50 times respectively with distilled water. The concentration of the electrolytes was determined with PerkinElmer Atomic Absorption Spectrophotometer Analyst 100 (PerkinElmer, USA) using a sodium/potassium hollow cathode lamp. The wavelength was set at 589 nm and 766 nm for measuring sodium and potassium concentrations respectively. The actual concentration of the electrolytes was calculated based on the respective standard curves (**Appendices B7 and B8**).

3.3.8. Tissue processing and histology

Conventional tissue processing, which includes dehydration, clearing and infiltration of the liver and rWAT specimens with paraffin wax, was performed following formalin fixation. The tissues were then embedded in paraffin wax and stored at 4^{o}C. Thin sections (5μm) were produced and stained with hematoxylin and eosin (H&E) to visualize the morphology of the tissues. Nikon Eclipse TS100 (Nikon, Japan) was used to capture the microscopic images of the tissues. ImageJ was used to measure the adipocyte area of 200 to 300 adipocytes in the rWAT using the method published by Parlee et al. in 2014 [211]. Similarly, the software was also used to measure the area of fat vacuoles present in the liver based on the microscopic images [212].

3.3.9. Hepatic lipid extraction

Total lipid extraction of the liver tissues was carried out using the Folch method [213]. Briefly, 150 mg of the snap-frozen liver tissues were ground into powder and homogenized in 20mL of chloroform/methanol (2:1) mixture. The homogenates were vortexed for 1 minute and sonicated for 20 minutes. This was followed by centrifugation at 1000x *g* for 10 minutes. The supernatant was washed with 0.2 volume of water, vortexed for 1 minute and centrifuged at 1000x *g* for 5 minutes. The upper fraction was discarded. The remaining fraction was rinsed with 1 mL of methanol/water (1:1) mixture and centrifuged at 1000x *g* for 5 minutes. The upper fraction was removed, while the lower chloroform fraction that contained the total lipids was dried with a rotary evaporator. The hepatic total lipid extracts were weighed and then reconstituted in 1 mL of 1% (w/v) bovine serum albumin. The lipid extracts were subjected to a triglyceride assay with Randox TR1697 Triglycerides (Randox, UK).

3.3.10. Statistical analysis

Statistical analysis was performed was Statistical Package for the Social Sciences (SPSS) 22.0. Dependent variables with repeated measures such as the cumulative weight gain, food and calorie intake, blood pressure and pre- and post-treatment OGTT were analyzed with a mixed model analysis of variance (ANOVA) using “time” as the within-subjects factor and ‘treatment group’ as the between-subjects factor. The pairwise comparisons were performed with Bonferroni correction. Other variables were analyzed with one-way ANOVA followed by

Tukey's test. The level of statistical significance was set at $p \leq 0.05$. All the dependent variables are expressed in mean ± standard error of the mean (SEM) unless mentioned otherwise.

3.4. Results

3.4.1. Weight gain, visceral fat mass and morphology

The cumulative weight gain of the rats subjected to different treatments is illustrated in **Figure 3.2**. The initial body weight was comparable between groups (**Table 3.2**). Over a course of 12 weeks, the cumulative weight gain (± SEM) of the rats subjected to CD, HFD, metformin, TRF and geraniin were 317±7 g, 374±15 g, 337±16 g, 341±21 g and 349±10 g, respectively. Treatment with HFD alone increased the weight gain by 18% compared to CD alone. The obesogenic effect of the HFD became statistically significant from Week 7 onwards ($p<0.05$). None of the treatments with either metformin, TRF or geraniin significantly halted the accelerated weight gain induced by HFD ($p>0.05$), even though marginal reduction was noted.

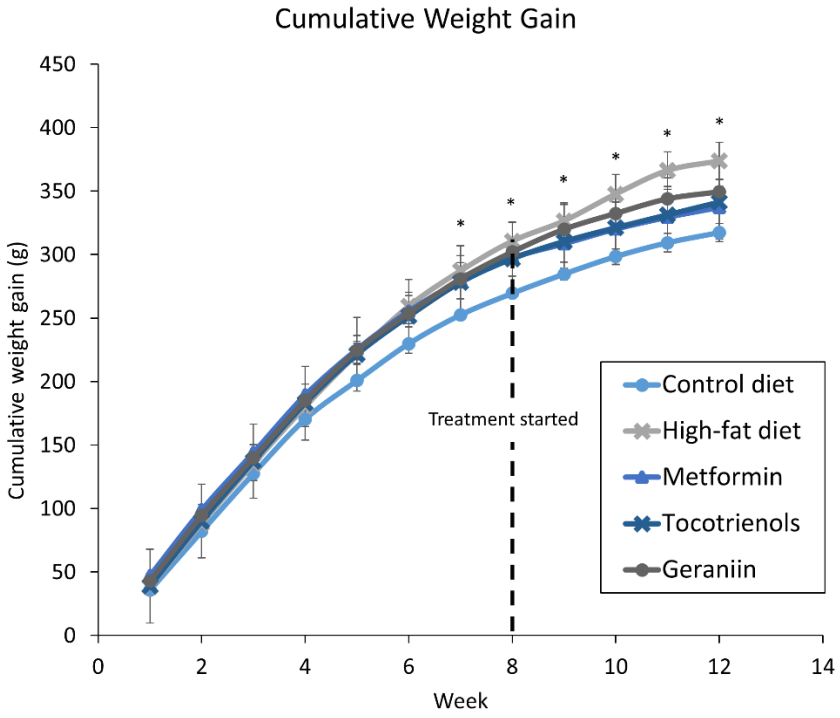

Figure 3.2: Cumulative weight gain of the rats assigned to different treatment groups over 12 weeks. Treatment with either metformin, TRF or geraniin started after 8 weeks of high-fat feeding as indicated by the black dotted line. Error bars indicate SEM. Sample size was n=6-7 per group. * $p<0.05$ between control and high-fat diet groups. TRF, tocotrienol-rich fraction.

Based on **Table 3.2**, the rats on CD had significantly higher food intake compared to the other groups throughout the entire experiment (p<0.05). This was to compensate for the lower caloric density of the CD, which explains the comparable calorie intake between groups. Furthermore, HFD also induced polydipsia. Prior to any therapeutic intervention, the rats on HFD increased their daily water consumption by 20% compared to those on CD. By the end of the experiment in Week 12, the extent of HFD-induced polydipsia worsened because the rats on HFD consumed almost 50% more water than those on CD regardless of the intervention. There was no significant change in the liver and kidney weight. The treatment effects of metformin, TRF and geraniin on food and water consumption as well as organ weight were unremarkable.

Table 3.2: Metadata related to weight gain and obesity of the rats assigned to different treatment groups.

Parameters	Treatment Group				
	Control diet	**High-fat diet**	**Metformin**	**TRF**	**Geraniin**
Initial body weight (g)	64 ± 6	63 ± 3	67 ± 3	63 ± 2	67 ± 2
Final body weight (g)	382 ± 10	437 ± 17*	404 ± 15	405 ± 20	416 ± 9
Food intake before Week 8 (g/day)	16.5 ± 0.2	13.1 ± 0.6***	13.0 ± 0.3***	12.4 ± 0.5***	12.4 ± 0.3***
Food intake after Week 8 (g/day)	17.1 ± 0.4	13.7 ± 0.6**	12.4 ± 0.5***	12.4 ± 0.7***	12.9 ± 0.4***
Calorie intake before Week 8 (kcal/day)	63.9 ± 0.9	69.5 ± 3.3	68.9 ± 1.8	66.1 ± 2.5	66.2 ± 1.7
Calorie intake after Week 8 (kcal/day)	66.5 ± 1.5	72.7 ± 3.4	66.0 ± 2.9	66.2 ± 3.9	68.4 ± 2.1
Water intake before Week 8 (mL/day)	18.5 ± 1.2	23.3 ± 0.9*	22.0 ± 0.8	20.1 ± 0.9	23.4 ± 0.5*
Water intake after Week 8 (mL/day)	19.9 ± 0.9	30.9 ± 2.4**	29.6 ± 2.6*	24.3 ± 1.3	31.5 ± 2.3**
Liver: Body weight ratio (%)	3.35 ± 0.05	3.74 ± 0.15	3.45 ± 0.04	3.71 ± 0.16	3.20 ± 0.09
Kidney: Body weight ratio (%)	0.73 ± 0.02	0.77 ± 0.02	0.69 ± 0.02	0.73 ± 0.02	0.74 ± 0.02

Values are expressed as mean ± SEM; * p<0.05, ** p<0.01 and *** p<0.001 compared to control diet.
TRF, tocotrienol-rich fraction.

The rWAT-to-body weight ratios (± SEM) were 2.53 ± 0.18%, 3.59 ± 0.28%, 3.93 ± 0.20%, 3.88 ± 0.20%, 3.28 ± 0.11% for the rats assigned to CD, HFD, metformin, TRF and geraniin treatment groups, respectively (**Figure 3.3**). HFD significantly increased the visceral fat depot by more than 40% compared to CD (p<0.05). Similar observation was also detected in metformin and TRF-treated rats. Conversely, the treatment with geraniin shows a mild reduction in visceral fat depot compared to HFD group, but the difference did not reach a statistical significance.

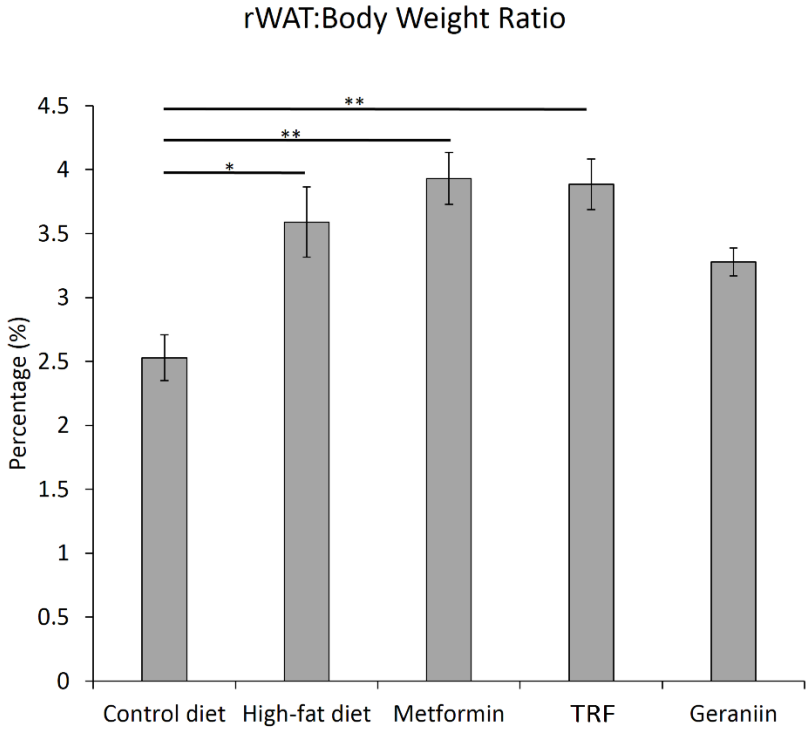

Figure 3.3: Retroperitoneal white adipose tissue weight-to-body weight ratio of the rats assigned to different treatment groups. The ratios are expressed in percentage. Error bars indicate SEM. Sample size was n=6-7 per group. * p<0.05 and ** p<0.01 between groups. rWAT, retroperitoneal white adipose tissue; TRF, tocotrienol-rich fraction.

The rWAT adipocyte sizes of rats on HFD were larger compared to those on CD (**Figure 3.4**). This condition, which is known as adipocyte hypertrophy, was also detected in metformin-treated rats, but was improved by TRF and geraniin. The observation was confirmed by the adipocyte areas quantified based on the microscopic images (**Figure 3.5**). The adipocyte areas (± SEM) were 4329 ± 341 μm^2, 5568 ± 331 μm^2, 6328 ± 357 μm^2, 4539 ± 432 μm^2 and 3692 ± 146 μm^2 for the rats subjected to CD, HFD, metformin, TRF and geraniin, respectively. HFD increased the average adipocyte size in the rWAT by more than 28%, although the difference did not reach a statistical significance (p=0.087). Treatment with geraniin, but not metformin and

TRF, normalized the morphological abnormality. The results show that chronic high-fat feeding induced rapid weight gain and central adiposity. None of the interventions with either metformin, TRF or geraniin conferred beneficial effects on weight control, but geraniin successfully ameliorated visceral adipocyte hypertrophy, which is a key feature of central adiposity.

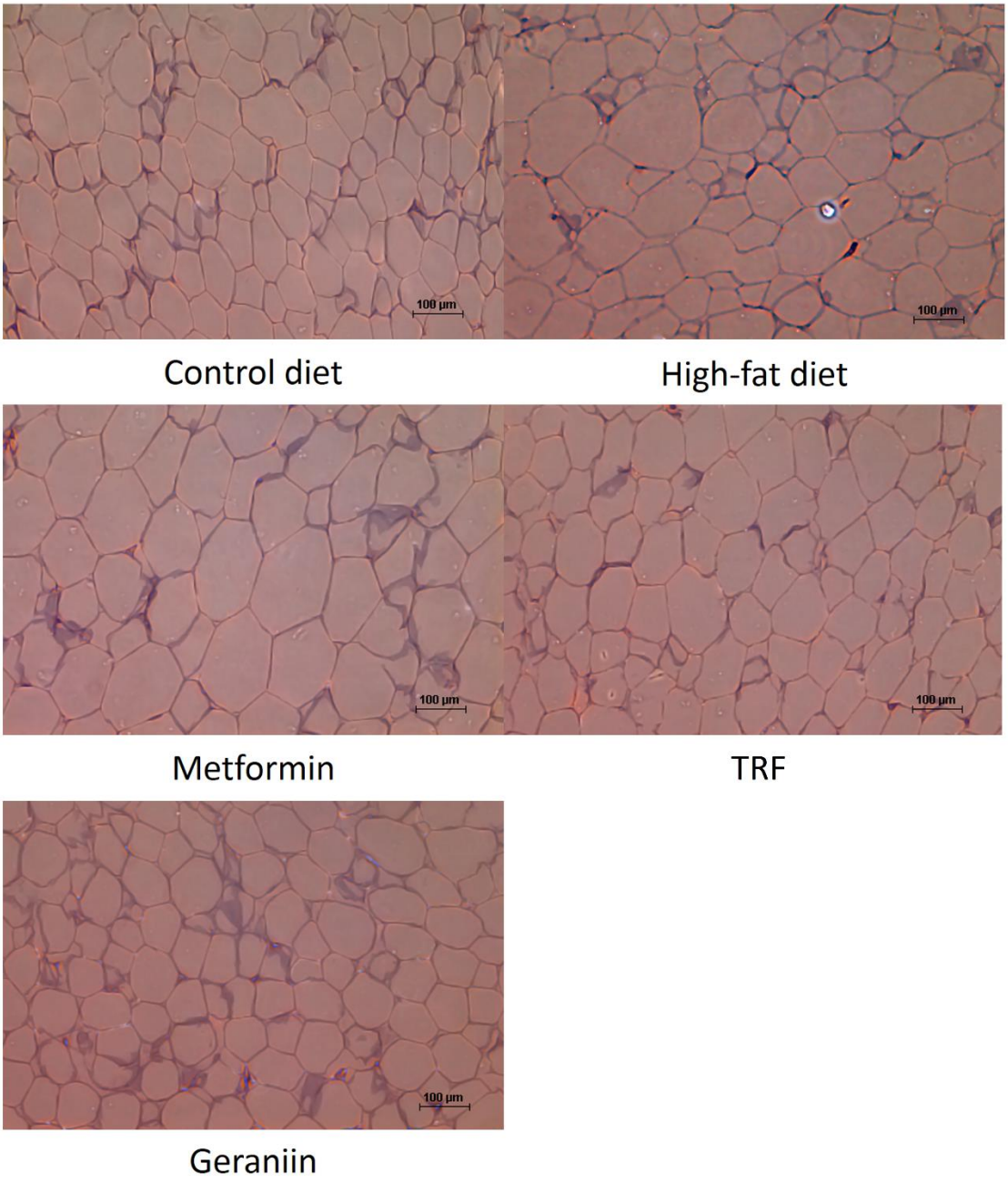

Figure 3.4: Representative microscopic images of the H&E-stained retroperitoneal white adipose tissues (x 100 magnification) of rats assigned to different treatment groups. TRF, tocotrienol-rich fraction.

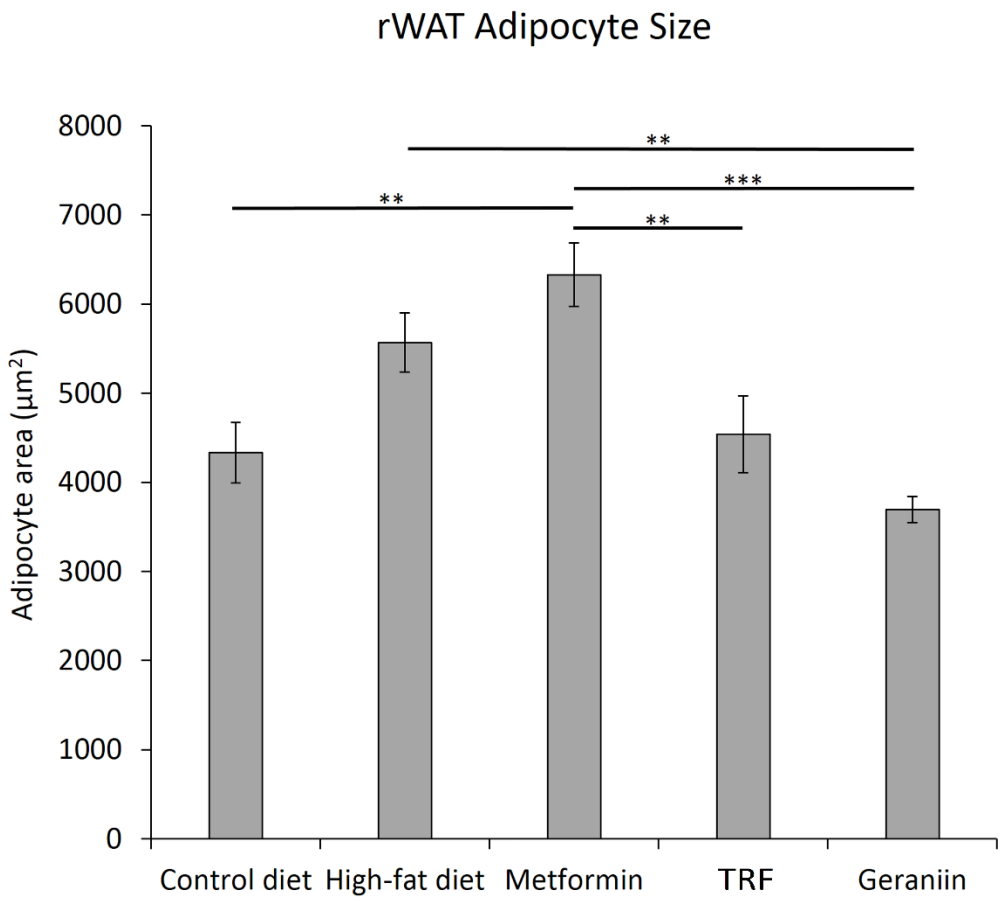

Figure 3.5: Adipocyte sizes of retroperitoneal white adipose tissues of the rats assigned to different treatment groups. The adipocyte areas were measured based on the microscopic images of the tissues and expressed in µm^2. Error bars indicate SEM. Sample size was n=6-7 per group. ** p<0.01 and *** p<0.001 between groups. rWAT, retroperitoneal white adipose tissue; TRF, tocotrienol-rich fraction.

3.4.2. Blood pressure and plasma electrolytes

The systolic and diatolic blood pressure levels are tabulated in **Table 3.3** and illustrated in **Figures 3.6 and 3.7** respectively. Essentially, HFD also significantly elevated the systolic blood pressure. The increased systolic blood pressure caused by HFD started from Week 3 onwards. In Week 8, all the rats on HFD were hypertensive before any intervention. One week into the treatment with TRF or geraniin, the rats showed comparable systolic blood pressure to the CD-treated rats. Such a blood pressure-lowering effect of TRF and geraniin persisted till the end of the experiment whereas the rats on HFD or treated with metformin remained hypertensive. The

blood pressuring-lowering effect of geraniin and TRF was also observed in the diastolic blood pressure (**Figure 3.7**).

Table 3.3: Systolic and diastolic blood pressure levels of the rats assigned to different treatment groups over 12 weeks.

Week	Treatment group					Treatment effect	Time effect	Interaction (Treatment* Time)
	CD	HFD	Metformin	TRF	Geraniin			
Systolic blood pressure								
0	87±2	83±1	89±2	87±2	89±2	Sig (p<0.001)	Sig (p<0.001)	Sig (p<0.001)
1	103±3	106±2	104±3	110±3	100±3			
2	119±4	122±3	116±4	129±5	115±5			
3	120±5	140±4*	136±5	145±5*	151±5**			
4	124±6	148±5*	143±6*	148±7*	146±7*			
5	116±6	149±5**	141±6*	146±6*	167±6***			
6	125±6	153±5**	144±6*	142±6*	156±6*			
7	123±3	145±3***	144±3**	149±4***	142±4**			
8	121±5	148±4**	143±5*	141±6*	145±6*			
9	122±3	141±2***	140±3**	128±3†	131±3			
10	122±6	149±5*	141±6*	137±6	122±6†			
11	117±4	145±3***	138±4**	128±4††	120±4†††			
12	118±3	139±2***	140±3***	119±3†††	114±3†††			
Diastolic blood pressure								
0	64±1	64±1	72±3	70±2	66±2	Sig (p<0.001)	Sig (p<0.001)	Sig (p<0.001)
1	73±2	79±2	80±2	82±4	72±3			
2	84±2	94±4	90±4	103±5*	81±3			
3	89±3	111±6*	110±7*	122±4*	112±5*			
4	93±4	118±6*	113±5*	122±7*	111±6*			
5	92±2	113±7*	116±7*	125±4*	125±6*			
6	95±3	119±5*	114±5*	110±4*	117±8*			
7	92±1	114±5**	115±4**	122±3***	115±2**			

8	87±2	117±5***	115±4**	114±4**	117±4**
9	90±1	110±3**	111±3**	101±5	102±4
10	94±2	117±7*	110±7	108±4	90±3†
11	83±1	110±4***	104±3**	94±4†	88±2††
12	84±2	104±3*	107±6**	94±6	86±1†

Values are expressed as mean ± SEM; * p<0.05, ** p<0.01 and *** p<0.001 compared to control diet group; † p<0.05, †† p<0.01 and ††† p<0.001 compared to high-fat diet group
CD, control diet; HFD, high-fat diet; TRF, tocotrienol-rich fraction.

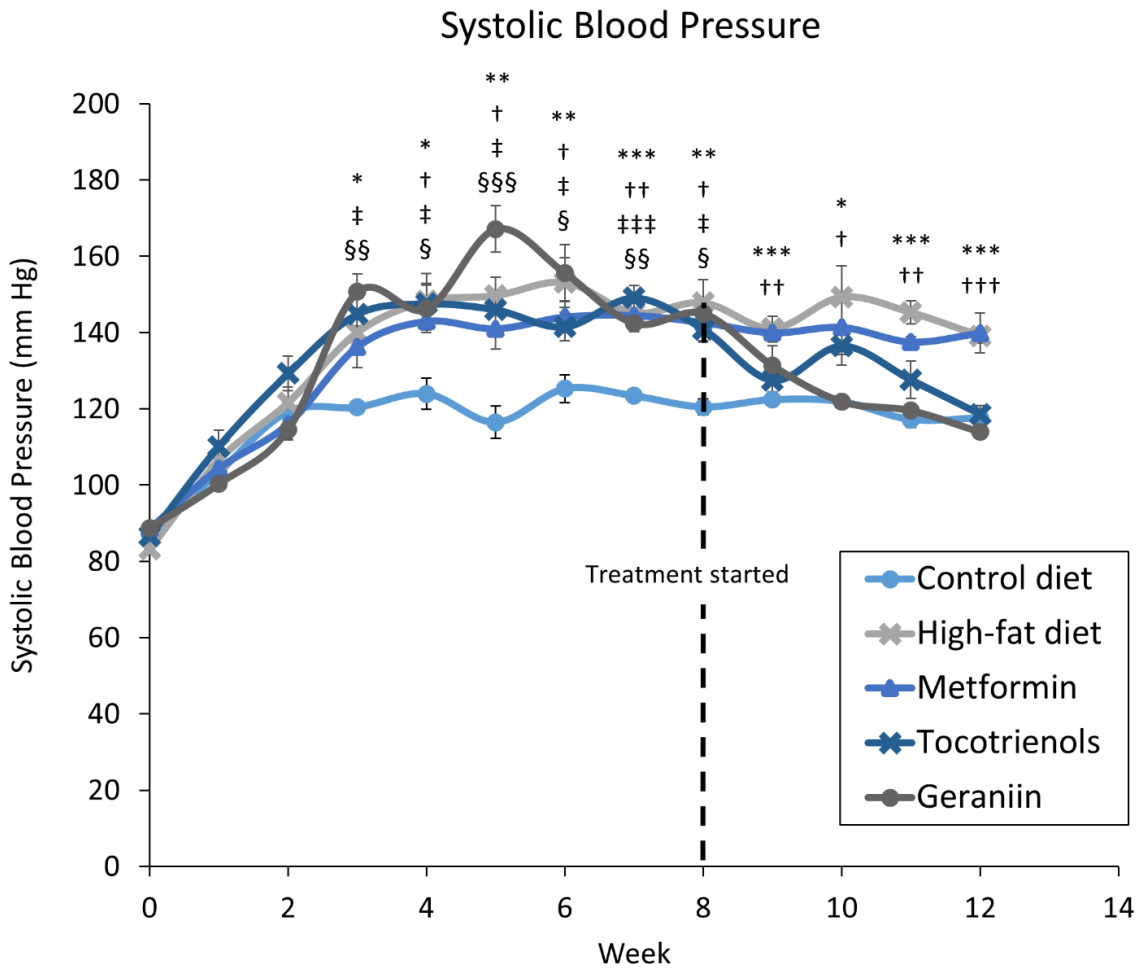

Figure 3.6: Systolic blood pressure of the rats assigned to different treatment groups over 12 weeks. Treatment with either metformin, TRF or geraniin started after 8 weeks of high-fat feeding as indicated by the black dotted line. Error bars indicate SEM. Sample size was n=6-7 per group. * p<0.05, ** p<0.01 and *** p<0.001 between high-fat and control diet groups; † p<0.05, †† p<0.01 and ††† p<0.001 between metformin and control diet groups; ‡ p<0.05 and ‡‡‡ p<0.001 between TRF and control diet groups; § p<0.05, §§ p<0.01 and §§§ p<0.001 between geraniin and control diet groups. TRF, tocotrienol-rich fraction.

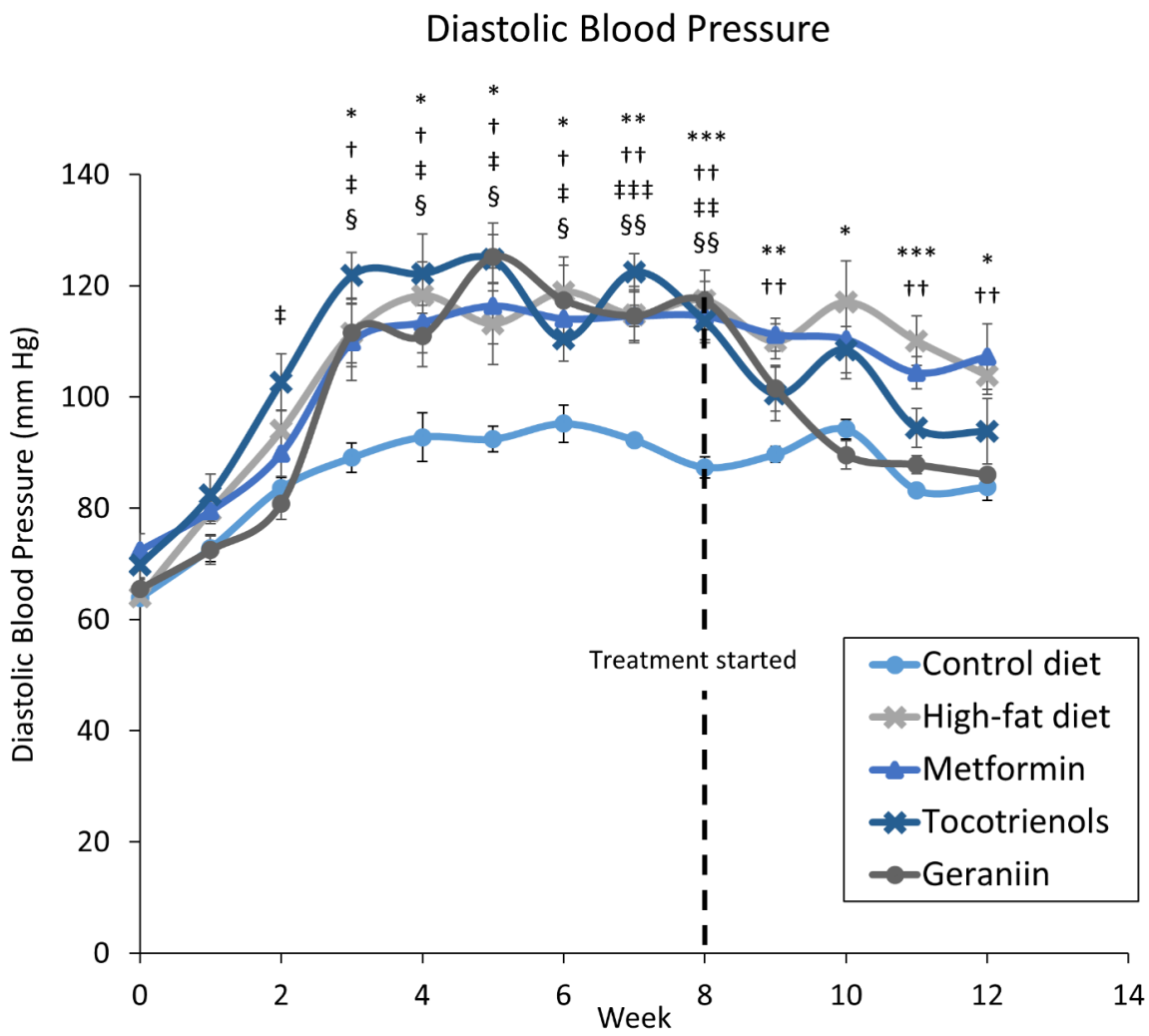

Figure 3.7: Diastolic blood pressure of the rats assigned to different treatment groups over 12 weeks. Treatment with either metformin, TRF or geraniin started after 8 weeks of high-fat feeding as indicated by the black dotted line. Error bars indicate SEM. Sample size was *n*=6-7 per group. * p<0.05, ** p<0.01 and *** p<0.001 between high-fat and control diet groups; † p<0.05 and †† p<0.01 between metformin and control diet groups; ‡ p<0.05, ‡‡ p<0.01 and ‡‡‡ p<0.001 between TRF and control diet groups; § p<0.05 and §§ p<0.01 between geraniin and control diet groups. TRF, tocotrienol-rich fraction.

The plasma sodium concentrations (± SEM) of the rats assigned to CD, HFD, metformin, TRF and geraniin were 126 ± 7 mEq/L, 159 ± 4 mEq/L, 147 ± 3 mEq/L, 160 ± 7 mEq/L and 147 ± 4 mEq/L, respectively (**Figure 3.8A**). The rats on HFD had 26% more sodium in the blood circulation compared to those on CD (p<0.01), but none of the treatments significantly reduced the plasma sodium level. The effect of the diets and interventions on plasma potassium concentration was unremarkable (**Figure 3.8B**).

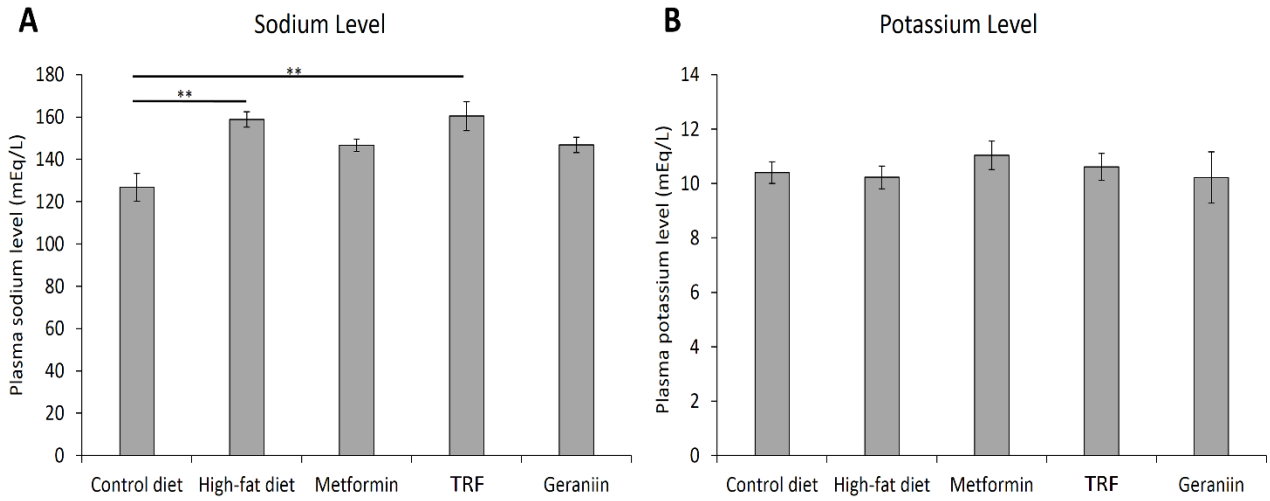

Figure 3.8: Plasma sodium **(A)** and potassium **(B)** levels of the rats assigned to different treatment groups. Error bars indicate SEM. Sample size was n=6-7 per group. ** p<0.01 between groups. TRF, tocotrienol-rich fraction.

3.4.3. Glucose and lipid metabolism

Prior to any treatment, the fasting blood glucose levels (± SEM) of the rats assigned to CD, HFD, metformin, TRF and geraniin were 5.7 ± 0.2 mmol/L, 6.7 ± 0.1 mmol/L, 6.2 ± 0.1 mmol/L, 6.5 ± 0.2 mmol/L and 6.6 ± 0.2 mmol/L, respectively (**Figure 3.9**). After the four-week treatment, the fasting blood glucose levels (± SEM) of the rats assigned to CD, HFD, metformin, TRF and geraniin were 5.5 ± 0.2 mmol/L, 6.4 ± 0.1 mmol/L, 5.4 ± 0.1 mmol/L, 6.3 ± 0.2 mmol/L and 5.7 ± 0.1 mmol/L, respectively (**Figure 3.9**). The result shows that HFD could impair the glucose homeostasis of the rats (p<0.001). Unlike TRF which did not have notable effect, treatment with either metformin or geraniin could reverse the diet-induced high blood glucose level.

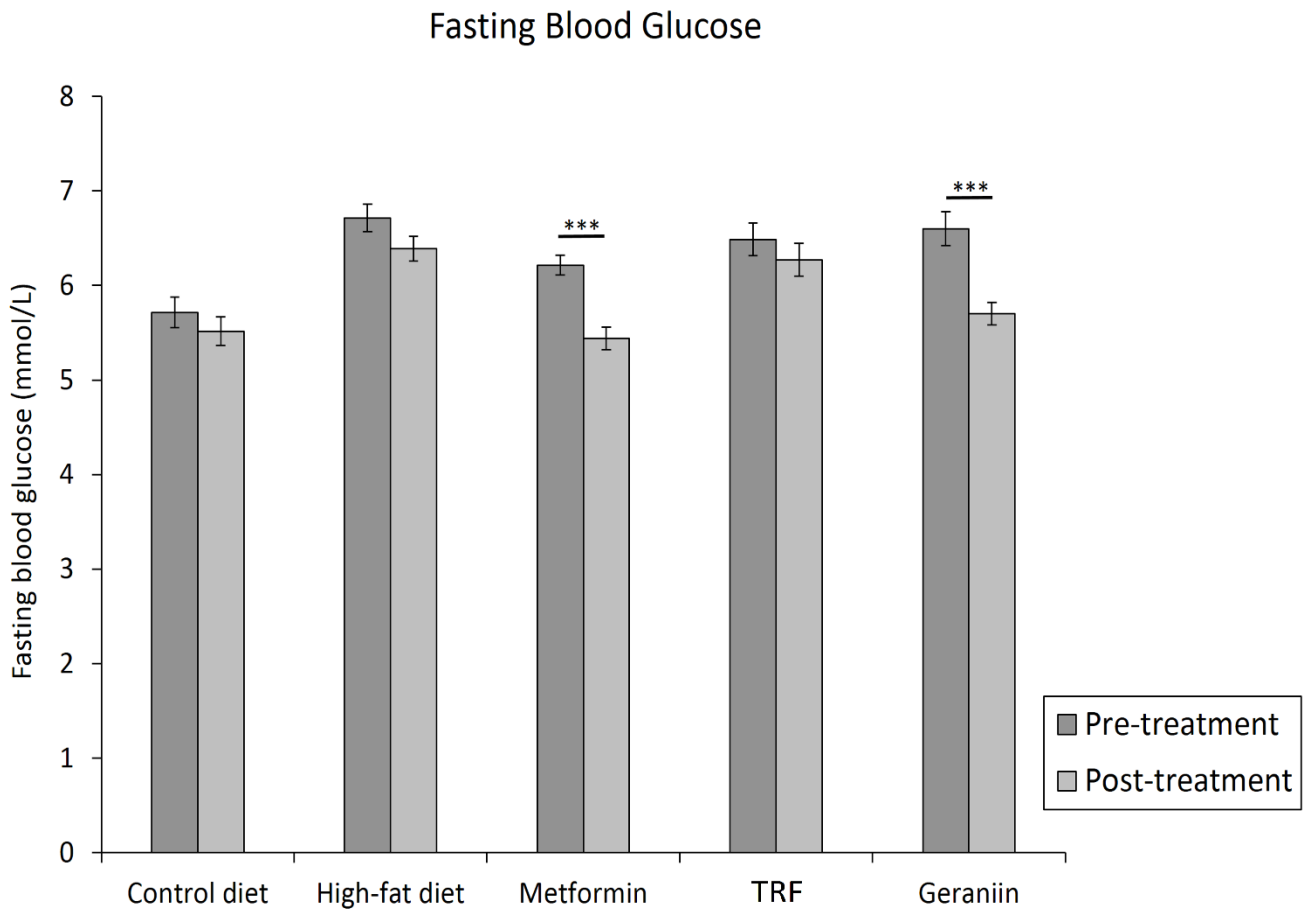

Figure 3.9: Fasting blood glucose levels of the rats before and after the experimental treatments. Error bars indicate SEM. Sample size was n=6-7 per group. *** p<0.001 between time points. TRF, tocotrienol-rich fraction.

The glucose-lowering effect of geraniin is supported by the HbA1c findings. The percentage of HbA1c (± SEM) of the rats assigned to CD, HFD, metformin, TRF and geraniin were 5.18 ± 0.07 %, 6.30 ± 0.13 %, 4.21 ± 0.24 %, 4.93 ± 0.24 % and 5.02 ± 0.17 %, respectively (**Figure 3.10**). The elevated HbA1c% of HFD-treated rats relative to CD-treated rats shows that long-term high-fat feeding could induce prolonged hyperglycemia (p<0.001). Similarly the glucose-lowering effect of metformin and geraniin is also reflected by a decline in the HbA1c% compared to HFD group (p<0.001). Surprisingly, although treatment with TRF did not improve the impaired fasting blood glucose, it managed to significantly lower the HbA1c level (p<0.001).

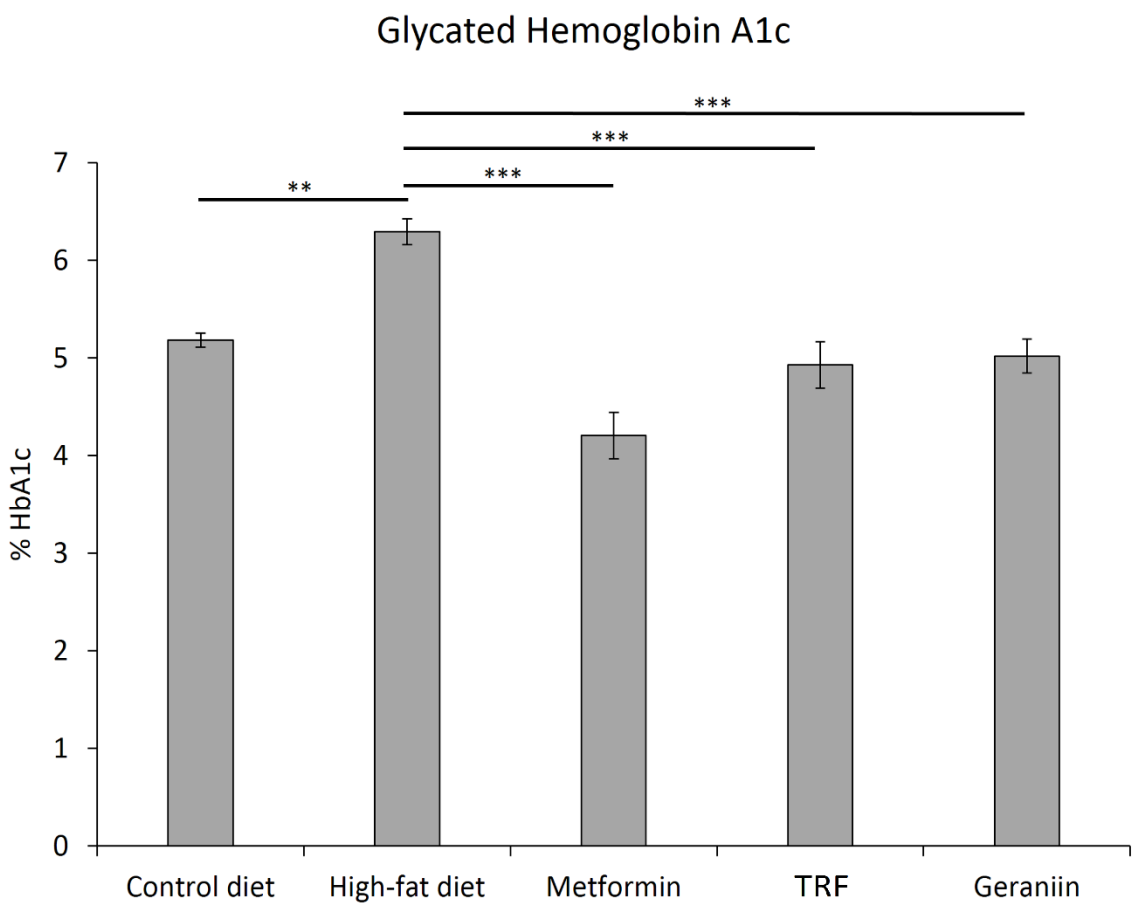

Figure 3.10: Glycated hemoglobin A1c of the rats assigned to different treatment groups. Error bars indicate SEM. Sample size was n=6-7 per group. ** p<0.01 and *** p<0.001 between groups. HbA1c, glycated hemoglobin A1c; TRF, tocotrienol-rich fraction.

Additionally, before any treatment, the area under curve of the OGTT (± SEM) of the rats assigned to CD, HFD, metformin, TRF and geraniin were 868 ± 25 min mmol/L, 944 ± 25 min mmol/L, 895 ± 21 min mmol/L, 952 ± 35 min mmol/L and 907 ± 24 min mmol/L, respectively (**Figure 3.11C**). After the four-week treatment, the area under curve of the OGTT (± SEM) of the rats assigned to CD, HFD, metformin, TRF and geraniin were 828 ± 13 min mmol/L, 984 ± 44 min mmol/L, 780 ± 15 min mmol/L, 935 ± 29 min mmol/L and 931 ± 16 min mmol/L, respectively (**Figure 3.11C**). Compared to the CD-treated rats, the area under curve of the OGTT of those on HFD increased by 16%, indicating the onset of impaired glucose tolerance (p<0.05). As anticipated, treatment with metformin successfully ameliorated the abnormal glucose disposal. Nonetheless, geraniin which was capable of normalizing the impaired fasting glucose and elevated HbA1c levels, failed to reverse the impaired glucose tolerance caused by HFD.

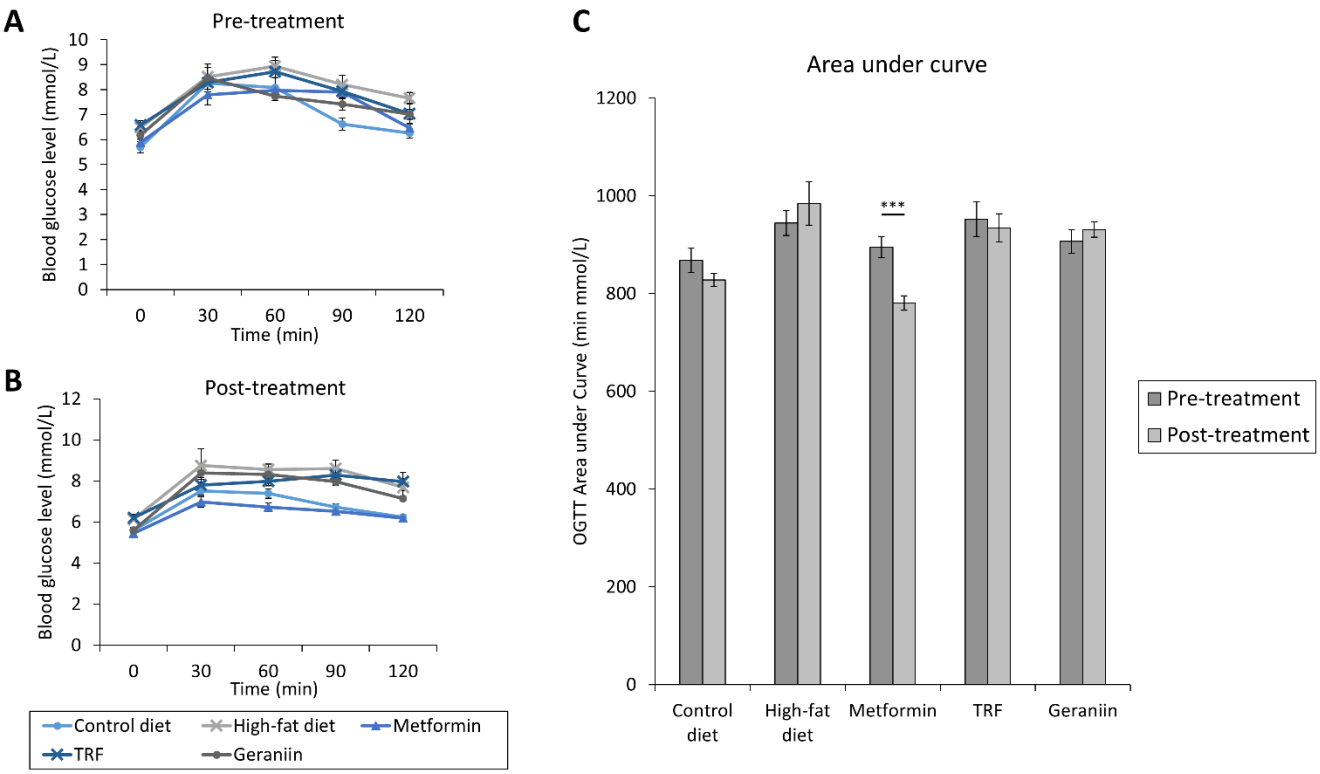

Figure 3.11: Oral glucose tolerance test of the rats before **(A)** and after **(B)** the experimental treatments. The area under curves are expressed in a bar plot **(C)**. Error bars indicate SEM. Sample size was *n*=6-7 per group. *** $p<0.001$ between time points. TRF, tocotrienol-rich fraction.

Despite the occurrence of impaired fasting glucose and impaired glucose tolerance in the rats on HFD, there was no notable change to the fasting plasma insulin. The fasting insulin levels (± SEM) of the rats assigned to CD, HFD, metformin, TRF and geraniin were 28.2 ± 2.3 mU/L, 24.6 ± 1.9 mU/L, 24.9 ± 1.8 mU/L, 24.8 ± 1.7 mU/L and 25.8 ± 3.1 mU/L (**Figure 3.12A**). When the HOMA indices were computed based on fasting blood glucose and fasting plasma insulin, the HOMA%S index (which indicates insulin sensitivity) was comparable across all treatment groups whilst the HOMA%β index (which indicates β-cell function) was compromised by close to 30% between HFD and CD groups ($p<0.05$) (**Figure 3.12B**). Metformin and geraniin appeared to reverse the impaired β-cell function, but the difference did not reach a statistical significance ($p>0.05$).

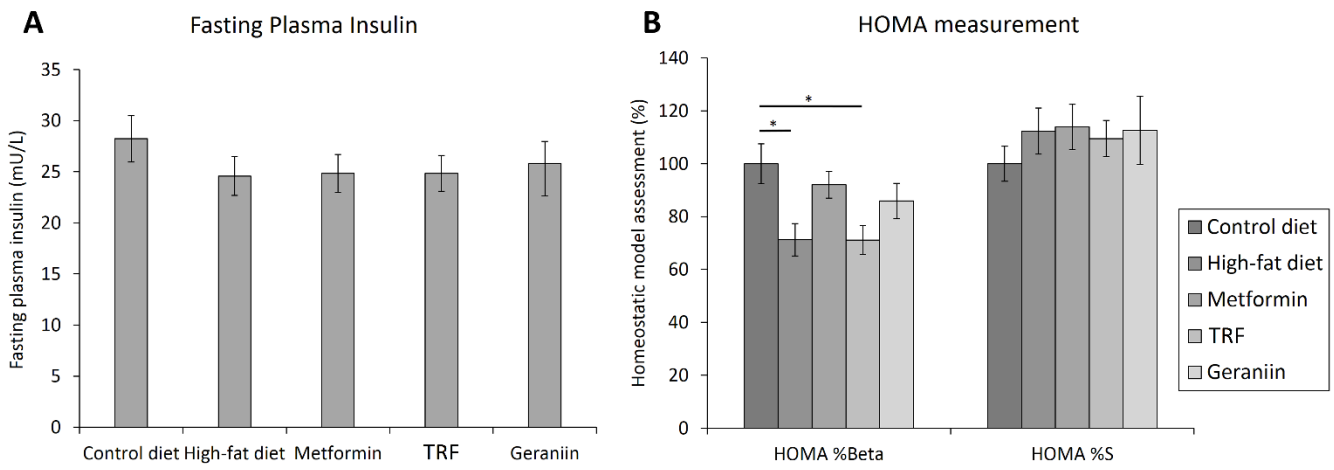

Figure 3.12: Fasting plasma insulin **(A)** and homeostatic model assessment **(B)** of the rats assigned to different treatment groups. Error bars indicate SEM. Sample size was n=6-7 per group. * p<0.05 between groups. HOMA, homeostatic model assessment; TRF, tocotrienol-rich fraction.

According to **Figure 3.13**, different treatments also have notable influence on the lipid profile, especially the triglycerides and non-HDL cholesterol. Essentially, HFD elevated the triglycerides by more than twofold compared to CD (p<0.001). The HFD-induced hypertriglyceridemia were not reversed by metformin or TRF. However, geraniin significantly lowered the triglycerides and non-HDL cholesterol to that comparable to the CD (p<0.01). Similar lowering effect on the non-HDL cholesterol was also observed in the rats treated with metformin or TRF (p<0.05). The other lipid components like total cholesterol, HDL-cholesterol and free fatty acids were comparable between the groups (p>0.05).

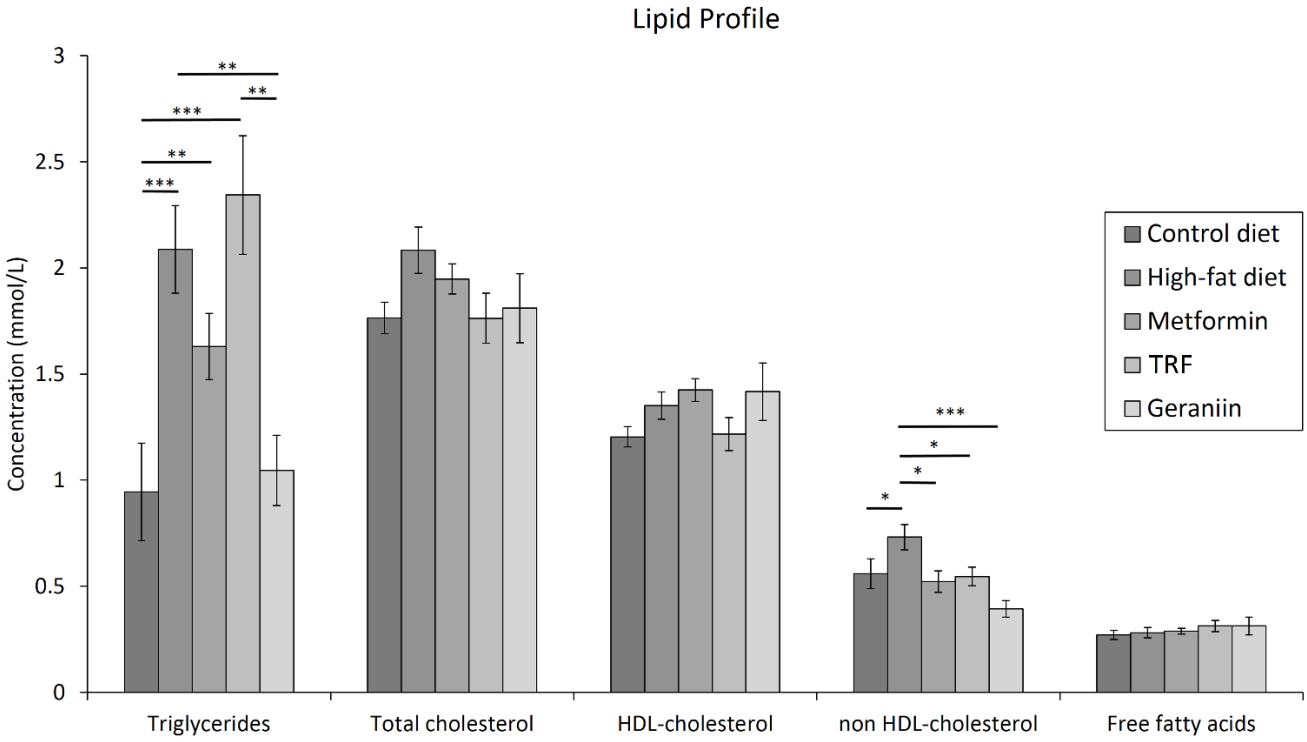

Figure 3.13: Lipid profile, including the triglycerides, total cholesterol, HDL-cholesterol, non-HDL cholesterol and free fatty acids of the rats assigned to different treatment groups. Error bars indicate SEM. Sample size was n=6-7 per group. * p<0.05, ** p<0.01 and *** p<0.001 between groups. HDL, high-density lipoprotein; TRF, tocotrienol-rich fraction.

3.4.4. Liver morphology and hepatic steatosis

Hyperlipidemia is often associated with the manifestation of abnormal lipid deposition in the liver, which is also known as hepatic steatosis. Based on **Figure 3.14**, there are more fat vacuoles in the liver of the rats on HFD compared to the other groups. When the rats were treated with CD, HFD, metformin, TRF and geraniin, the percentages of the fat vacuole area (± SEM) based on the microscopic images were 0.82 ± 0.13 %, 3.59 ± 0.26 %, 2.77 ± 0.25 %, 2.75 ± 0.31 % and 2.33 ± 0.20 %, respectively (**Figure 3.15A**). High-fat feeding resulted in a threefold increase in the hepatic lipid accumulation compared to CD group (p<0.001). Only with geraniin was the area of fat vacuoles reduced (p<0.01). Even so, it remained elevated compared to CD group (p<0.01).

To further confirm the extent of lipid deposition, the triglyceride levels in the hepatic lipid extracts were measured. The triglyceride concentrations in liver extracts (± SEM) of the rats assigned to CD, HFD, metformin, TRF and geraniin were 7.0 ± 0.4 µmol/g liver, 12.6 ± 1.1 µmol/g liver, 8.8 ± 1.6 µmol/g liver, 8.9 ± 0.8 µmol/g liver and 5.7 ± 1.0 µmol/g liver,

respectively (**Figure 3.15B**). The results agree with the trend observed in the percentages of fat vacuole area whereby HFD increased the hepatic lipid concentration significantly (p<0.01) while geraniin, but not metformin or TRF, effectively reduced the abnormality (p<0.01).

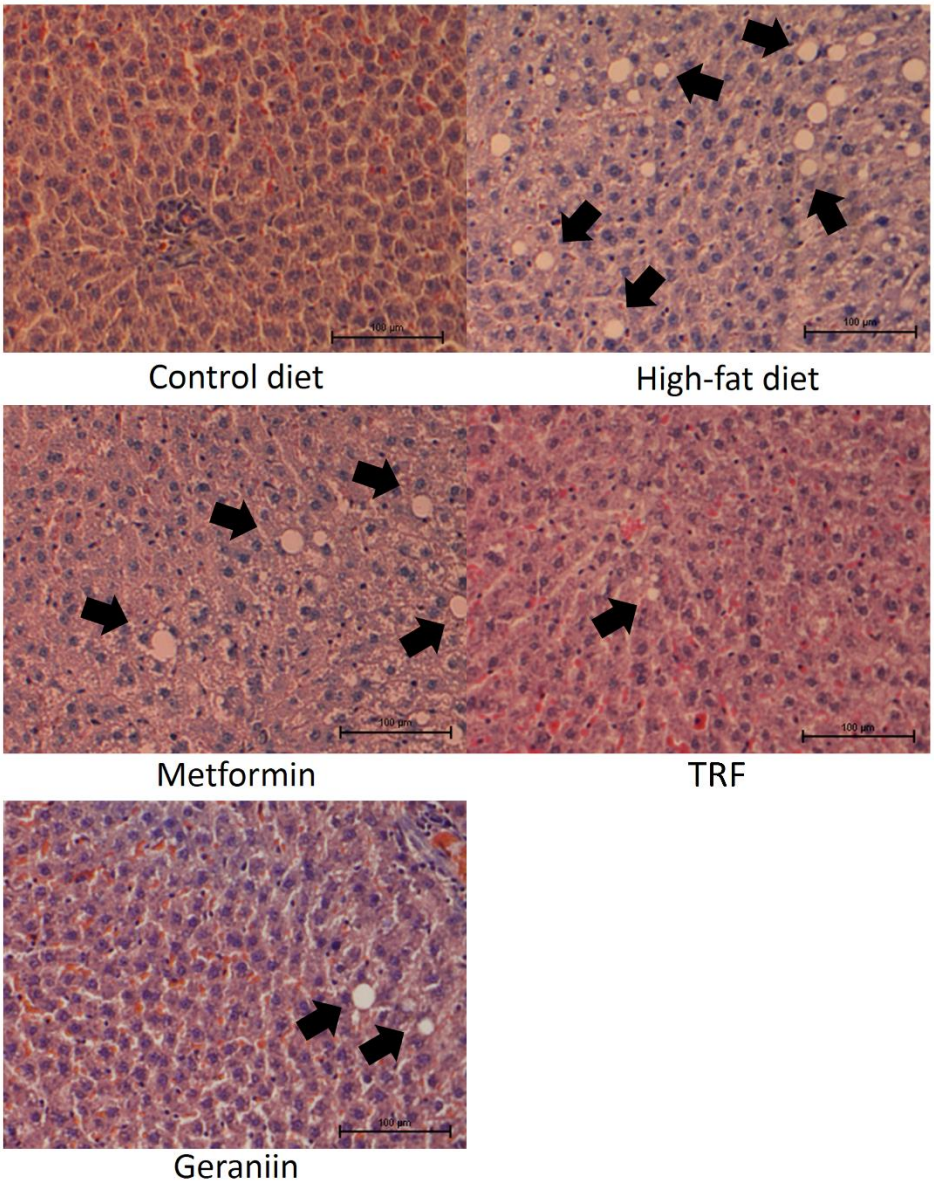

Figure 3.14: Representative microscopic images of the H&E-stained liver tissues (x 200 magnification) of rats assigned to different treatment groups. TRF, tocotrienol-rich fraction.

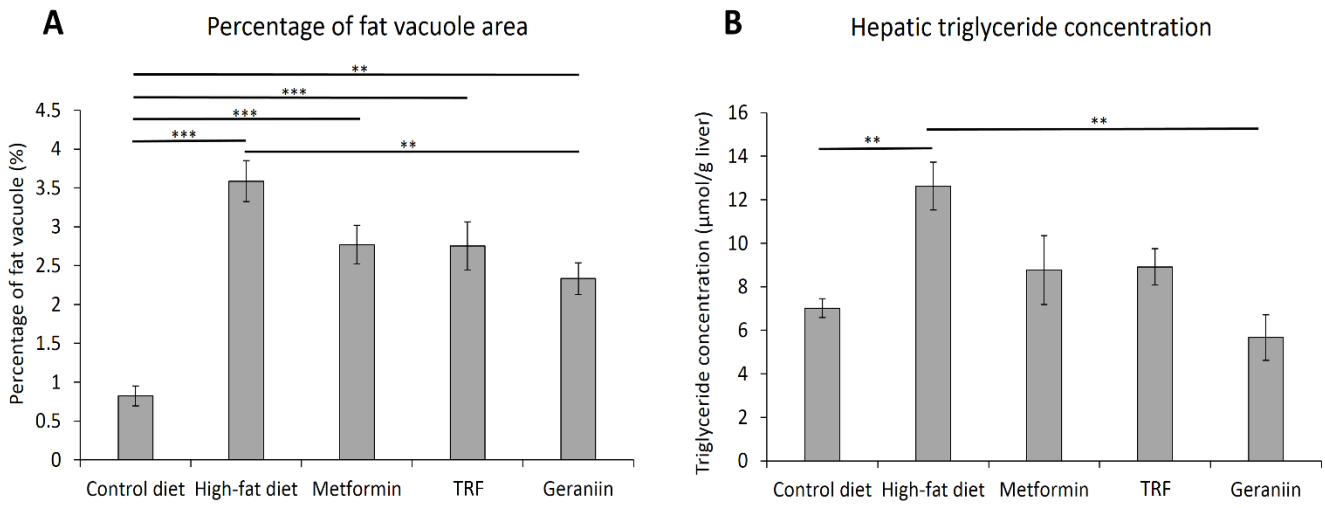

Figure 3.15: Percentage of fat vacuole area present in the liver microscopic images **(A)** and hepatic triglyceride concentration **(B)** of the rats assigned to different treatment groups. Error bars indicate SEM. Sample size was n=6-7 per group. ** p<0.01 and *** p<0.001 between groups. TRF, tocotrienol-rich fraction.

3.5. Discussion

In the present study, the rats on HFD for 12 weeks demonstrated all the clinical hallmarks of MetS, notably central obesity and adiposity, hypertension, hyperlipidemia, hyperglycemia together with hepatic steatosis. These HFD-induced metabolic aberrations are consistent with the observations reported in **Chapter 2**. On the other hand, treatment with ellagitannin geraniin at a daily dosage of 25 mg/kg for a month successfully alleviated most of the abnormalities. The natural product conferred anti-hypertensive, anti-hyperglycemic and lipid-lowering effects besides reducing the ectopic lipid deposition in the visceral adipose tissues and liver. The pleiotropic beneficial impacts on multiple risk factors do make geraniin a promising candidate for MetS pharmacotherapy.

Metformin, a proposed therapy for pre-diabetes and MetS [203, 214], effectively ameliorated the elevated fasting glucose, HbA1c and glucose intolerance. This is consistent with a recent clinical finding [215]. Even though both impaired fasting glucose and impaired glucose tolerance are indicative of abnormal glucose homeostasis, the associated underlying pathological processes are vastly different. To elaborate, impaired fasting glucose is predominantly attributable to compromised basal insulin secretion and hepatic glucose release, while impaired glucose tolerance is linked more closely to reduced postprandial insulin secretion and muscular insulin

resistance [216, 217]. The metformin-dependent lowering effect on the fasting blood glucose is predominantly due to the inhibition of hepatic gluconeogenesis [218]. Additionally, higher HOMA% β in metformin-treated rats was also observed, implying a restoration of the β-cell function at fasting condition which could further fortify the normal basal glucose homeostasis [219]. On the other hand, the underlying mechanism of metformin-induced improved glucose tolerance remains unclear. Lachin et al. (2007) proposed that such a health benefit is because of the combinatorial effects of reduced adiposity, fasting insulin and proinsulin [220]. Contradictorily, in the present study, treatment with metformin did not reduce the body weight, visceral fat mass and adipocyte hypertrophy. It is however, crucial to note that the clinical findings about the anti-obesity effect of metformin is inconclusive [221, 222]. Therefore, further investigation on this aspect is warranted.

Compared to metformin, geraniin exerted comparable beneficial effects on the fasting blood glucose, HbA1c and HOMA% β, but failed to reverse the abnormal glucose tolerance. The inherent pathological differences between impaired fasting glucose and impaired glucose tolerance suggest a selectivity of geraniin in terms of the target organ. Due to the inhibitory effect on the fasting glucose, the treatment with geraniin might preferentially influence the metabolic pathways in the liver upon oral consumption. This also coincides with the fact that most of the metabolites of geraniin, namely urolithins and ellagic acids, are heavily subjected to enterohepatic circulation [223]. Additionally, although certain geraniin metabolites in their conjugated forms are detected in the blood circulation after the consumption of ellagitannin-rich foods, none of them seem to accumulate in body tissues like the muscles, adipose tissues, lungs, liver, heart and kidneys [223]. Therefore, given the pharmacokinetic processes of geraniin, its bioactivities may be highly selective to a few organs, such as the liver, gallbladder and the gastrointestinal tract. It may be added that due to the relative short treatment period (4 weeks), measuring certain glycation products like fructosamine and glycated albumin could provide a better indication of the short-term glucose control in comparison to fasting blood glucose and HbA1c [224].

Unlike geraniin, the effect of metformin on hypertension, hypertriglyceridemia and hepatic steatosis was unremarkable. Nonetheless, a small extent of reduction in the hepatic lipid deposition despite the lack of statistical significance. Such a beneficial effect has been reported

in obese patients with T2DM and non-alcoholic fatty liver disease (NAFLD) [225]. It could be linked to the interaction of metformin with the mitochondrial respiratory chain complex I, AMPK as well as the transcriptional suppression of p160 steroid receptor coactivators 2 (SRC-2) in the liver [226, 227]. Nevertheless, Li et al. (2013) who performed a meta-analysis on the existing clinical trials, found no concrete evidence to support the therapeutic effects of metformin on NAFLD [228]. Thus, the effect of metformin on hepatic steatosis remains inconclusive.

Aside from that, TRF has demonstrated potent therapeutic effects on HFD-induced hypertension and hypercholesterolemia with negligible impacts on glycemic control, adiposity and hepatic steatosis. The anti-hypertensive activity is consistent with previous animal and clinical studies [229, 230]. Nevertheless, such an effect is not exclusive to tocotrienols, but is a common property of vitamin E as evidenced by similar hypotensive effect seen in α-tocopherol [229]. Since the blood pressure-lowering effect is a shared characteristic, the underlying mechanism could also be mutual. In this case, previous studies have reported that vitamin E can alleviate vascular oxidative stress and stimulate the aortic biosynthesis of prostacyclin, which in turn, results in vasodilation [229, 231, 232]. As such, the blood pressure-lowering effect of TRF may be attributable to antioxidant-dependent vasodilation.

Next, the cholesterol-lowering effect of TRF observed in the present study is also in line with several clinical trials [233-235]. Primarily, this is because of its inhibitory effect on the HMG-CoA reductase which is not present in tocopherols [200, 201]. In hypercholesterolemic patients with NAFLD, tocotrienols also conferred favorable effect on hepatic steatosis which could be linked to its cholesterol-lowering effect [236]. Muto et al. (2013) also identified that repressive effects of tocotrienols on the expression of hepatic sterol regulatory element binding protein 1c (SREBP-1c), C/EBP homologous protein (CHOP) and IL-1β [237]. Collectively, the downregulation of these genes could attenuate the progression of lipid accumulation and inflammation in the liver. However, in our study, the effect of TRF on hepatic steatosis was not prominent and so, further investigation in the hepato-protective effect of tocotrienols against diet-induced NAFLD is pertinent to attain a conclusive remark.

Basically, ellagitannin gerannin exhibited superior anti-hyperglycemic activity compared to TRF. Although several studies have reported the glucose-lowering effect of tocotrienols [238-

241], it was not detected in our study. Most of these studies used streptozotocin-induced diabetic rats as the disease model. The overt and severe diabetic status of the rats makes it more sensitive to minor therapeutic effects on the glycemic control. Furthermore, the selective toxicity of streptozotocin to pancreatic β-cells allow us to postulate that the glucose-lowering effect conferred by tocotrienols could be linked to improved β-cell function. Nonetheless, to date, there is no conclusive clinical evidence that supports the anti-hyperglycemic activity of tocotrienols in diabetic patients. Even though the fasting glucose level was not improved, supplementation with TRF significantly reduced the HbA1c level. This is because antioxidant agents like tocotrienols can donate hydrogen to the glycation interemediates, inhibiting the formation of Amadori products [242]. Despite the marginal effect on blood glucose control, TRF still exhibited striking blood pressure- and cholesterol-lowering activities, making it an interesting candidate as an adjunctive therapy in MetS. The results and findings about the effects on TRF in MetS presented in this chapter have been published and included in **Appendix E2** [243].

In our study, treatment with metformin mainly improved the glucose metabolism while TRF affected the blood pressure and cholesterol levels. These observations agree with the well-established bioactivities of the respective compounds. In comparison to metformin and TRF, geraniin clearly has more diverse metabolic effects. Moreover, due to the dissimilar metabolic activities between geraniin and TRF, it is presumed that the observed benefits of geraniin are not solely attributable to its antioxidant properties but instead, there are other independent mechanisms at play. Our findings about geraniin on MetS are consistent to a previous study which also concluded the favorable effects of the phytochemical on multiple metabolic risks in obese rats [181]. Both studies revealed significant glucose- and lipid-lowering effects of geraniin. However, Chung et al. (2014) also found that the supplementation of geraniin could improve insulin sensitivity in a dose-dependent manner which was not observed in our study [181]. Apart from these, what we added to the knowledge about geraniin are the inhibitory effects on HFD-induced hypertension and hepatic steatosis. Although the anti-hypertensive activity of geraniin has been reported with the use of spontaneously hypertensive rats (SHRs) [172, 173], our disease model is understandably more related to MetS due to their shared pathophysiology. As for the ameliorative effect on hepatic steatosis, to our best knowledge, this is the first time such a benefit of geraniin is reported.

Our understanding about the pharmacokinetics of geraniin depicts that the bioavailability of the compound is exceedingly low due to their large chemical structure and high polarity [244]. Like most ellagitannins, upon oral consumption, geraniin is subjected to extensive metabolism by the variable physiological pH along the gastrointestinal tract and gut microflora [244]. Consequently, a number of small metabolites are liberated, including the gallic acid, corilagin, ellagic acid, brevifolincarboxylic acid and a wide range of hydroxyl-dibenzopyranone derivatives (urolithins) [198]. These geraniin-derived metabolites are much more bioavailable than the parental compound itself. This is particularly true for urolithins whose maximum plasma concentration can reach up to 18.6 μM in healthy human subjects [245] in comparison to 1.8 μM for gallic acid [246] and 0.1 to 0.4 μM for ellagic acid [247, 248]. Owing to the higher bioavailability of geraniin-derived metabolites, it is widely accepted that the metabolites are the actual *in vivo* functional molecules. Indeed, many geraniin-derived metabolites also possess pleiotropic effects against metabolic anomalies. For instance, treatment with gallic acid or ellagic acid helps to maintain glucose and lipid homeostasis, control weight gain and reverse hepatic lipid accumulation in rodents on high-calorie diets [249-254].

Essentially, it is believed that the beneficial effects of geraniin on MetS are predominantly attributable to its key metabolites like ellagic acid, gallic acid and urolithins. This is mainly due to the limited bioavailability of geraniin upon oral consumption. Furthermore, based on existing evidence, the geraniin-derived metabolites also exhibit multifunctional effects against several metabolic risks as seen in the present study. As pointed out in a previous study [255], these metabolites may interact with each other to additively or even synergistically enhance the therapeutic effects. However, the underlying mechanism of these bioactivities require further investigation.

3.6. Summary and key highlights of the study

The major findings of the study presented in this chapter are summarized as follows:

- Treatment with geraniin at a daily dosage of 25 mg/kg did not reduce the increased weight gain and visceral fat depot caused by high-fat feeding, but could reduce the visceral adipocyte hypertrophy. On the contrary, the effects of metformin and TRF on these parameters were unremarkable.

- Geraniin and TRF significantly lowered the HFD-induced hypertension but failed to normalize the elevated sodium level. This suggests that the blood pressure-lowering activity of these molecules may be independent of the water and sodium regulation.
- In terms of the glucose metabolism, treatment with geraniin could ameliorate the impaired fasting glucose and elevated HbA1c, but not impaired glucose tolerance. On the other hand, TRF which had no effect on the glucose homeostasis, also significantly reduced the HbA1c. Metformin which is an anti-diabetic agent successfully improved the fasting glucose, glucose intolerance and HbA1c level.
- In terms of the lipid metabolism, treatment with geraniin effectively reversed the HFD-induced hypertriglyceridemia and increased non-HDL cholesterol level. Metformin and TRF failed to reverse the increased circulating triglycerides, but managed to lower the non-HDL cholesterol level.
- Unlike metformin and TRF which had marginal effect on the lipid accumulation in the liver, geraniin also ameliorated hepatic steatosis which is a liver complication of MetS.

In summary, treatment with geraniin successfully alleviated the core features of MetS induced by high-fat feeding. Such a pleiotropic effect against multiple metabolic dysregulations makes it a promising multifunctional therapy against MetS. Speculatively, geraniin-derived metabolites instead of the intact geraniin, are the functional *in vivo* molecules. Nevertheless, the molecular mechanism of geraniin as well as its metabolites remains largely undefined and so, future research in this aspect is highly encouraged.

CHAPTER 4

Effects of Ellagitannin Geraniin on Redox Balance and Inflammatory Response

4. EFFECTS OF ELLAGITANNIN GERANIIN ON THE OXIDATIVE STRESS AND INFLAMMATORY RESPONSE OF RATS WITH METABOLIC SYNDROME

4.1. General overview

Growing evidence supports that the oxidative stress and inflammatory response are also the crucial elements in the pathogenesis of obesity and MetS. Fundamentally, oxidative stress is a phenomenon caused by overwhelming generation of highly reactive molecules (so-called oxidants) which the protective mechanisms (so-called antioxidants) fail to eliminate. Examples of major oxidants are reactive oxygen species (ROS) and reactive nitrogen species (RNS) whereas common biological antioxidant defense mechanisms include enzymatic antioxidants like superoxide dismutase, glutathione peroxidase, glutathione reductase and catalase as well as non-enzymatic antioxidants like glutathione, vitamins C and E [256].

Under physiological condition, the reactive oxidants, especially ROS, serve as a vital signaling molecule in response to intra- and extracellular stimuli [257]. However, under a sustained stressful environment, the accumulation of ROS can trigger progressive tissue damage and organ dysfunction. Under over-nutrition state, the constant influx of oxidizable substrates trigger mitochondrial over-activity, which leads to an increased mitochondrial membrane potential and impaired oxidative phosphorylation, facilitating the interaction between electrons from the respiratory chain directly with oxygen to produce an excessive amount of ROS [258]. In peripheral organs, oxidative stress can severely alter their normal functions, as exemplified by ROS-induced suppression of insulin secretion and insulin resistance in pancreatic β-cells and adipocytes, respectively [259, 260]. The oxidative stress and progressive tissue damage are sensed as danger mediators which will in turn, activate various inflammatory signaling cascades [261]. In the adipose tissues, this process will trigger the release of a wide array of pro-inflammatory adipokines into the blood circulation as evidenced by elevated high-sensitivity C-reactive proteins, TNF-α, IL-6 and IL-18 in patients with MetS [262, 263]. In addition, the adipokines also possess a number of unfavorable properties that are well-implicated in the pathogenesis of MetS, including the stimulation of immune cell infiltration, insulin desensitization, atherogenicity and thrombogenesis [264]. While pro-inflammatory adipokines

are hyperactive, beneficial anti-inflammatory cytokines like adiponectin and IL-10 are substantially repressed in MetS patients [265]. Consequently, such imbalances of redox reactions and inflammatory/anti-inflammatory processes fueled by the positive caloric balance will collectively perpetuate the aggravation of various metabolic derangements.

One of the leading inflammatory pathways that has recently garnered the attention of the research community is the advanced glycation end products (AGEs) and receptor for advanced glycation end products (RAGE). Like HbA1c, the generation of AGE also involves Maillard reaction – the glycation of reducing sugars to macromolecules like proteins or lipids [266]. However, the formation of AGE is irreversible and influenced by oxidation processes, making it a long-term glycemic and oxidative stress biomarker [266]. Following the ligand binding of AGE to RAGE, a series of signaling pathways are activated, resulting in functional changes in terms of pro-inflammatory response, programmed cell death and cellular proliferation via the release of IL-6, TNF-α, IL-1α, vascular cell adhesion protein-1 (VCAM-1), intercellular adhesion molecule (ICAM) as well as pro-coagulant factors like thrombomodulin and tissue factor [267]. The pathological processes are well-implicated in the progression of chronic metabolic diseases, highlighting the vital role of AGE-RAGE axis in MetS and T2DM.

In this context, ellagitannin geraniin is known for its potent antioxidant capacity. Geraniin is four and seven times more effective than vitamins E and C respectively in attenuating biologically relevant peroxyl radicals [268]. Furthermore, the treatment with geraniin efficaciously alleviates the induction of NF-κB and secretion of several inflammatory cytokines in pathogen- or lipopolysaccharide-induced inflammatory cell models [179, 269]. The anti-glycative activity of geraniin has also been reported [175]. Collectively, these findings suggest that the natural product possesses remarkable antioxidant and anti-inflammatory effects, but whether such potency is conserved in *in vivo* MetS model is unclear. Moreover, the effect of geraniin on AGE-RAGE axis is not well-elaborated.

In this chapter, we looked into the effects of ellagitannin geraniin on the oxidative stress and inflammatory response in the MetS rat model. Using the experimental design as reported in **Chapter 3**, the effects of geraniin were compared to the treatments with either metformin or TRF to examine their relative efficacy in preserving the redox balance and attenuating inflammatory response. The output of the study would facilitate more in-depth understanding

about biological impacts of geraniin supplementation on redox reactions and inflammatory processes in the blood circulation and body tissues.

4.2. Objectives of the study

The objective of the study was to determine the effects of ellagitannin geraniin on the oxidative stress and inflammatory response on HFD-induced MetS in Sprague Dawley rats. To accomplish the aim, the following research tasks need to be fulfilled:

- To examine the oxidative stress biomarkers in the blood circulation, liver and adipose tissues
- To explore the accumulation of circulating AGE and activation of *RAGE* expression
- To investigate the extent of systemic inflammation by measuring the levels of circulating pro-inflammatory cytokines

4.3. Methods and materials

4.3.1. Experimental design and treatment

The blood and tissue specimens used in this chapter were taken from the experiment done in **Chapter 3**. The experimental design and treatment groups can be referred to **Section 3.3.3** and summarized in **Figure 4.1**. At the end of the experiment, the plasma fractions of the blood were retrieved, aliquoted to different tubes and snap frozen in liquid nitrogen. They were stored at -80^{o}C until required. Body tissues including the liver and rWAT were harvested, snap frozen in liquid nitrogen and stored at -80^{o}C for tissue lysate preparation and total RNA extraction.

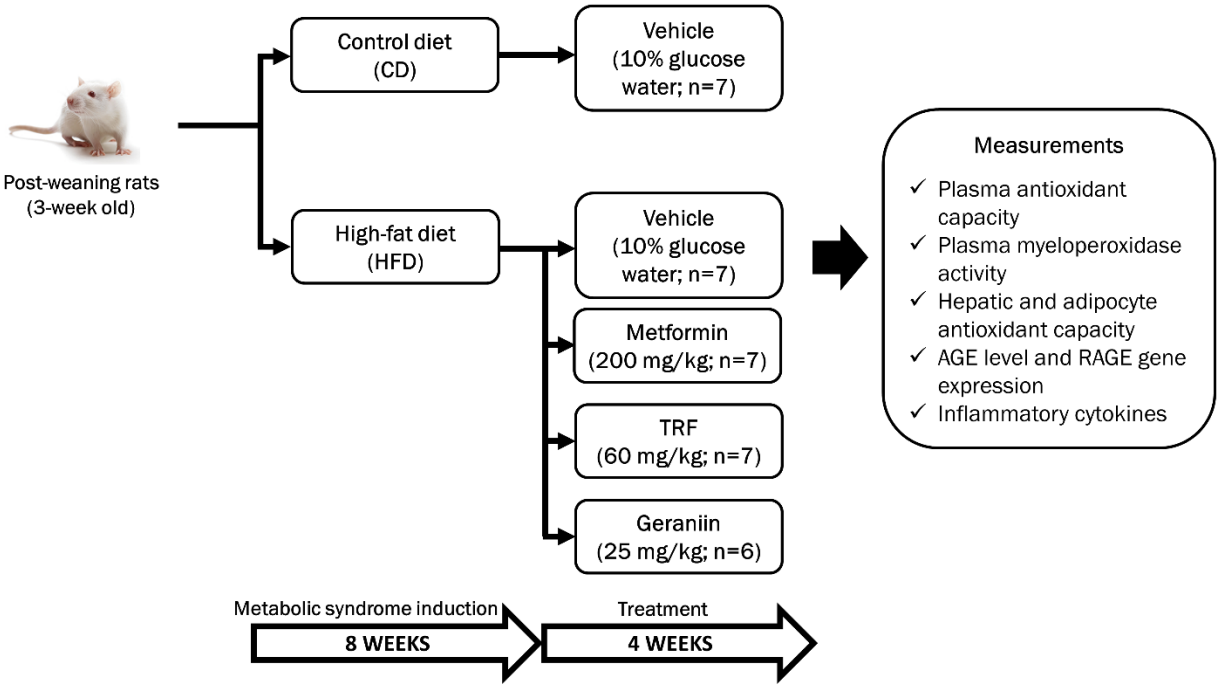

Figure 4.1: Experimental design to investigate the effects of ellagitannin geraniin on oxidative stress and inflammatory response in rats with HFD-induced MetS. AGE, advanced glycation end product; *RAGE*, receptor for advanced glycation end product; TRF, tocotrienol-rich fraction.

4.3.2. Determination of circulating oxidative stress biomarkers

Total plasma antioxidant capacity was measured with OxiSelect™ ORAC Activity Assay kit (Cell Biolabs, USA). The myeloperoxidase activity and AGE level in the plasma samples were determined with OxiSelect™ Myeloperoxidase Chlorination Activity Assay kit and OxiSelect™ Advanced Glycation End Product (AGE) Competitive ELISA kit (Cell Biolabs, USA) respectively. All analysis with the commercial kits were conducted in duplicates according to the manufacturers' instructions. The assay procedures and standard curves of the commercial kits are shown in **Appendices B9 to B11**.

4.3.3. Preparation of tissue lysates and Bradford assay

To prepare hepatic and rWAT tissue lysates, the tissues (30 mg for liver tissues; 100 mg for rWAT) were snap frozen with liquid nitrogen and ground to powder with a mortar and pestle. The powdered tissues were then transferred into a microcentrifuge tube and homogenized in 1

mL of cold lysis buffer. The homogenates were centrifuged at 10 000x *g* for 20 minutes at 4^{o}C. The supernatant was aliquoted into several microcentrifuge tubes and stored at -80^{o}C.

The concentration of proteins present in the tissue lysates were determined using Bradford protein assay (Sigma Aldrich, USA). The tissue lysates were diluted by 100 times. Then, 20 µL of the diluted tissue lysates were mixed with 200 µL of Bradford reagent. The absorbance at 595nm was measured while the protein concentration was calculated based on a bovine serum albumin (BSA) standard curve (**Appendix B12**).

4.3.4. Determination of redox status in the liver and rWAT

The redox status of the hepatic and rWAT tissue lysates were assessed with ferric reducing power (FRP) and 2,2'-azino-bis(3-ethylbenzothiazoline-6-sulphonic acid) (ABTS) radical scavenging assays. The protocols of the assays were based on a publication by Acharya (2017) [270].

For FRP assay, 30 µL of each tissue lysate was added to the wells in a 96-well plate in duplicates. Then, 90 µL of 0.2M phosphate buffer and 30 uL of 1% potassium ferricyanide were added and mixed with the tissue lysates. The mixtures were incubated in a water bath at 50^{o}C for 20 minutes. The reaction was stopped by adding 90 µL of 10% trichloroacetic acid. After that, the mixture was centrifuged at 1000x *g* for 10 minutes and 100 µL of the supernatant was retrieved and mixed with 100 µL of distilled water and 20 µL of 0.1% iron chloride. The mixture was incubated for another 15 minutes at room temperature. The absorbance at 750nm were measured. The reducing power of each tissue lysate was calculated based on an iron (II) sulphate standard curve followed by a correction with the protein content of the tissue lysates (**Appendix B13**).

For ABTS radical scavenging assay, 10 µL of each tissue lysate was added to the wells in a 96-well plate in duplicates. Then, 200 µL of ABTS reagent was added to the samples and mixed evenly. The mixtures were incubated in the dark for 5 minutes. The absorbance at 750nm was measured and the change in absorbance between blank and samples/standards was calculated. The radical scavenging capacity of each tissue lysate was determined based on an ascorbic acid standard curve followed by a corrected by the protein content of the tissue lysates (**Appendix B14**).

4.3.5. RNA extraction and cDNA synthesis

Total RNA of the rWAT was isolated with Tri-RNA reagent (Favorgen, Taiwan) followed by Qiagen RNeasy Mini kit (Qiagen, Germany) to clean up the RNA sample while that of the liver was extracted with Qiagen RNeasy Mini kit (Qiagen, Germany) directly. The concentration and purity of the RNA were determined by measuring the absorbance at 260nm and 280nm with Infinite® 200 PRO (TECAN, Switzerland). RNA integrity was examined with agarose gel electrophoresis to visualise the 18S and 28S ribosomal RNA. RNase-free DNase I (ThermoFisher Scientific, USA) treatment was performed prior to cDNA synthesis which was done with Qiagen Omniscript Reverse Transcription Kit (Qiagen, Germany).

4.3.6. Quantitative polymerase chain reaction (qPCR)

Rotor-Gene Q (Qiagen, Germany) was used to perform SYBR green-based qPCR of *RAGE* and endogenous secretory *RAGE* (*esRAGE*) in the liver and rWAT. The selected qPCR reaction master mix was TransStart Tip Green qPCR SuperMix (TransGen Biotech, China). Hypoxanthine phosphoribosyltransferase 1 (*Hprt1*), succinate dehydrogenase complex flavoprotein subunit A (*SdhA*) and β-actin (*Bac*) which demonstrate stable expression in the target tissues were selected as the endogenous reference genes for normalisation of the genes of interest [271]. The nucleotide sequences of the forward and reverse primers as well as the accession numbers are outlined in **Table 4.1**. PCR conditions and amplicon information are supplemented in **Appendix C**. Normalized Ct or ΔCt values of the genes of interest were calculated using the following formula:

$$\mathbf{\Delta Ct = average\ of\ Ct}_{\textit{reference genes}} \mathbf{- Ct}_{\textit{gene of interest}}$$

Table 4.1: Accession numbers, forward and reverse primers of the endogenous reference and target genes as well as amplicon size of the PCR products.

Target gene	Accession number	Nucleotide sequence (5'→ 3')		Amplicon size (bp)
		Forward primer	Reverse primer	
Bac*	NM_031144	GTA TGG GTC AGA AGG ACT CC	GTT CAA TGG GGT ACT TCA GG	81
Hprt1*	NM_012583	CTG GAA AGA ACG TCT TGA TTG	GTA TCC AAC ACT TCG AGA GG	146
SdhA*	NM_130428	GGC TTT CAC TTC TCT GTT GG	CCA CAG CAT CAA ACT CAT GG	103
RAGE	NM_053336	CGA GTC TAC CAG ATT CCT GGG	TCA CAA CTG TCC CTT TGC CA	175
esRAGE	GU164718	CAA TGT CCC CTG CCT CCA GA	TCA TCC TCA TGC CCT ACC TCA	200

* denotes endogenous reference genes.

Bac, β-actin; *esRAGE*, endogenous secretory receptor for advanced glycation end product; *Hprt1*, hypoxanthine phosphoribosyltransferase 1; *RAGE*, receptor for advanced glycation end product; *SdhA*, succinate dehydrogenase complex flavoprotein subunit A;

4.3.7. Determination of pro-inflammatory cytokines

Several inflammatory and anti-inflammatory cytokines in the plasma samples, including IL-1β, IL-6, IL-10, IL-18 and TNF-α were measured with LEGENDplex Rat Inflammation Panel (BioLegend, USA). The kit is a cytometric bead array that allows multiplex quantification of various cytokines and chemokines related to inflammatory response using fluorescence-encoded beads. The bead population classification and fluorescence signal were detected with a flow cytometer - BD FacsVerse (BD Biosciences, USA). The differentiation of the bead populations for different cytokines was carried out based on the forward scatter, side scatter and APC channels whereas the fluorescence intensity which is supposed to be positively correlated to the cytokine concentration was determined on PE channel. The flow cytometer setup and the assay which was performed in duplicates for each plasma sample were carried out according to the

manufacturer' instructions. The output data was analysed using BioLegend's LEGENDplex™ Data Analysis Software (BioLegend, USA) provided by the company to determine the concentrations of the cytokines in the plasma samples. The assay procedures and standard curves of each cytokines are shown in **Appendix B15**.

4.3.8. Statistical analysis

Statistical analysis was performed with SPSS 22.0. The variables were analyzed with one-way ANOVA followed by Tukey test for pairwise comparison. The level of statistical significance was pre-set at $p \leq 0.05$.

4.4. Results

4.4.1. Circulating oxidative stress markers

The plasma total antioxidant capacities (± SEM) of the rats assigned to CD, HFD, metformin, TRF and geraniin treatment groups were 3.08 ± 0.09 mM Trolox equivalent (TE), 2.55 ± 0.09 mM TE, 2.92 ± 0.15 mM TE, 3.14 ± 0.17 mM TE and 2.98 ± 0.09 mM TE, respectively (**Figure 4.2**). Chronic high-fat feeding caused a 17% reduction in the antioxidant capacity compared to the rats on CD (p<0.05). The plasma total antioxidant capacities of the rats treated with either metformin, TRF or geraniin were not significantly different from those on CD or HFD.

On the other hand, the myeloperoxidase activities (± SEM) of the rats assigned to CD, HFD, metformin, TRF and geraniin treatment groups were 0.65 ± 0.18, 2.06 ± 0.19, 0.50 ± 0.24 , 0.43 ± 0.29 and 0.45 ± 0.19 nmole/min/mL, respectively (**Figure 4.3**). To elaborate, myeloperoxidase which can generate reactive radicals during pathogenic infection, also serves as an oxidative stress biomarker in many chronic diseases [272]. In this study, the treatments with either metformin, TRF or geraniin successfully normalized the myeloperoxidase activity (p<0.001) which was otherwise, markedly enhanced by HFD (p<0.01). The observation indicates the antioxidant activity of the interventions.

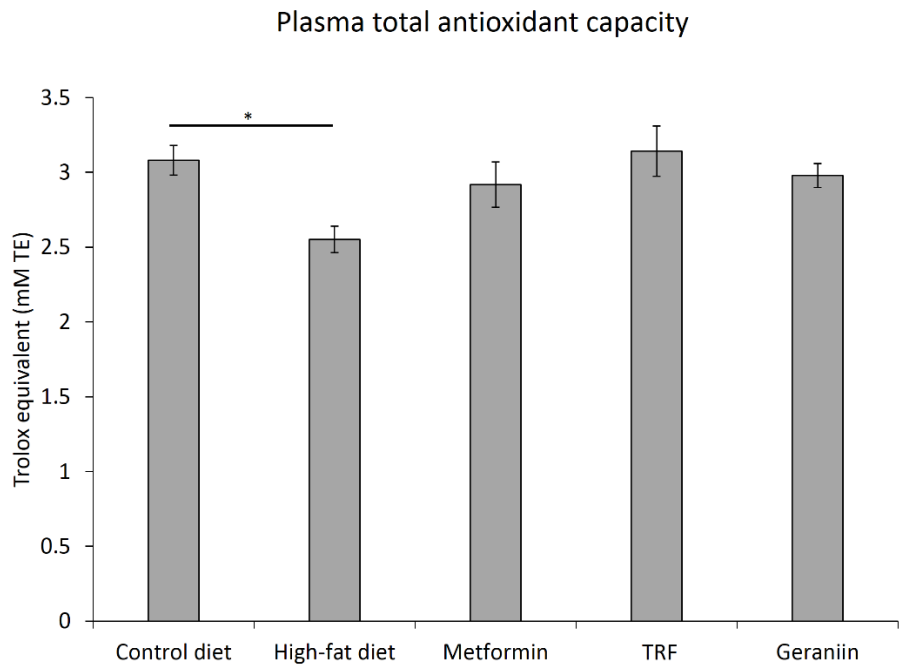

Figure 4.2: Plasma total antioxidant capacity of the rats assigned to different treatment groups based on oxygen radical antioxidant capacity (ORAC) assay. Error bars indicate SEM. Sample size was *n*=6-7 per group. * $p<0.05$ between groups. TE, Trolox equivalent; TRF, tocotrienol-rich fraction.

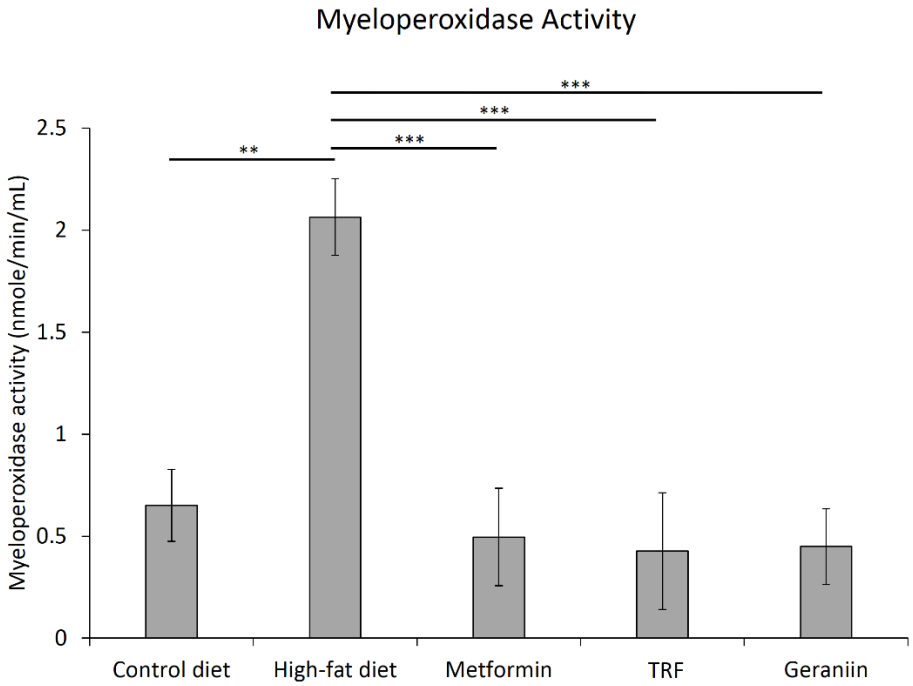

Figure 4.3: Myeloperoxidase activity of the rats assigned to different treatment groups. Error bars indicate SEM. Sample size was *n*=6-7 per group. ** $p<0.01$ and *** $p<0.001$ between groups. TRF, tocotrienol-rich fraction.

4.4.2. Hepatic and rWAT redox status

The total antioxidant capacities (± SEM) in the liver of the rats assigned to CD, HFD, metformin, TRF and geraniin treatment groups based on FRP assay were 2.87 ± 0.43 mmol Fe(II)/mg protein, 2.52 ± 0.16 mmol Fe(II)/mg protein, 1.78 ± 0.29 mmol Fe(II)/mg protein, 1.15 ± 0.10 mmol Fe(II)/mg protein and 2.03 ± 0.38 mmol Fe(II)/mg protein, respectively (**Figure 4.4A**). Compared to CD group, the rats on HFD showed a decline in hepatic antioxidant capacity regardless of the treatments, but only those treated with TRF reached a significant reduction relative to CD group. The hepatic antioxidant capacity of the rats with TRF supplementation was 60% lower than those on CD ($p<0.05$).

The total antioxidant capacity of the rWAT did not align with the trend observed in the liver. The rWAT total antioxidant capacities (± SEM) of the rats assigned to CD, HFD, metformin, TRF and geraniin treatment groups based on FRP assay were 13.29 ± 1.66 mmol Fe(II)/mg protein, 11.83 ± 1.94 mmol Fe(II)/mg protein, 10.09 ± 2.25 mmol Fe(II)/mg protein, 16.92 ± 1.88 mmol Fe(II)/mg protein and 20.27 ± 3.69 mmol Fe(II)/mg protein, respectively (**Figure 4.4B**). The supplementation with antioxidants like TRF and geraniin improved the antioxidant capacity in the rWAT by about 67% to 101% compared to the other groups. However, only the comparison between geraniin- and metformin-treated rats was significantly different ($p<0.05$).

The intracellular radical scavenging activity was assessed with ABTS assay. The hepatic radical scavenging activities (± SEM) of the rats assigned to CD, HFD, metformin, TRF and geraniin treatment groups were 16.53 ± 2.65 mM ascorbic acid/mg protein, 13.70 ± 1.835 mM ascorbic acid/mg protein, 12.70 ± 0.49 mM ascorbic acid/mg protein, 12.72 ± 0.70 mM ascorbic acid/mg protein and 13.53 ± 0.44 mM ascorbic acid/mg protein, respectively (**Figure 4.5A**). Conversely, the radical scavenging activities (± SEM) of the rWAT of rats assigned to CD, HFD, metformin, TRF and geraniin treatment groups were 21.17 ± 3.06 mM ascorbic acid/mg protein, 19.99 ± 2.23 mM ascorbic acid/mg protein, 18.94 ± 2.64 mM ascorbic acid/mg protein, 25.41 ± 3.12 mM ascorbic acid/mg protein and 24.61 ± 3.09 mM ascorbic acid/mg protein, respectively (**Figure 4.5B**). Although none of the comparison between groups in both tissues reached the statistical significance, the trend observed in ABTS assay of the tissue lysates is consistent with that of the FRP assay. More specifically, none of the treatment improved radical scavenging activity in the

liver whereas treatment with either TRF or geraniin, conferred some enhancement to the radical scavenging effect in the rWAT.

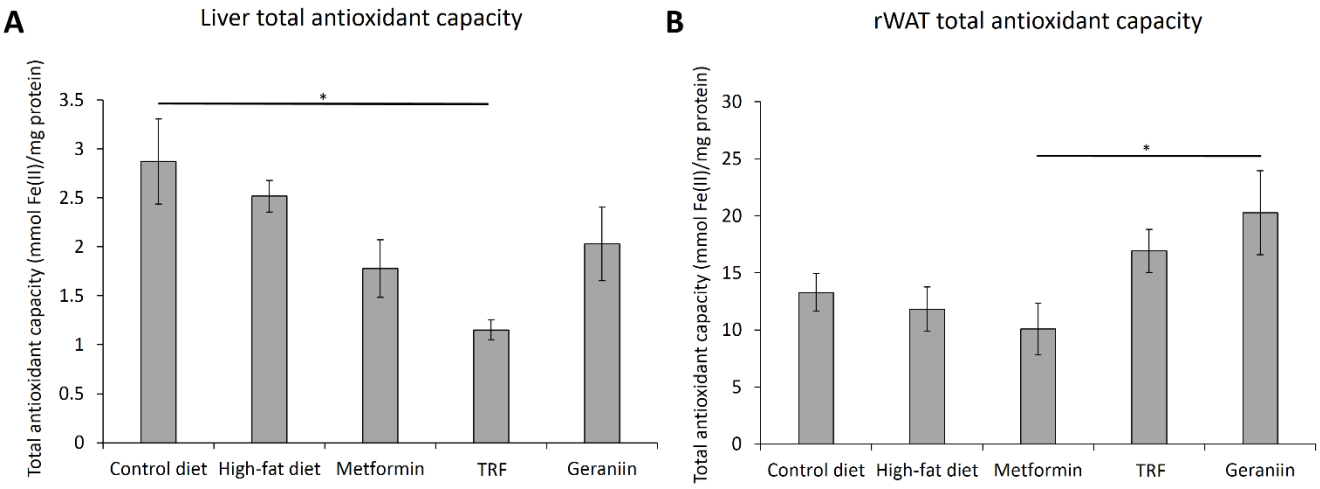

Figure 4.4: Total antioxidant capacity of the liver **(A)** and retroperitoneal white adipose tissues **(B)** of the rats assigned to different treatment groups based on ferric reducing power (FRP) assay. Error bars indicate SEM. Sample size was *n*=6-7 per group. * $p<0.05$ between groups. rWAT, retroperitoneal white adipose tissue; TRF, tocotrienol-rich fraction.

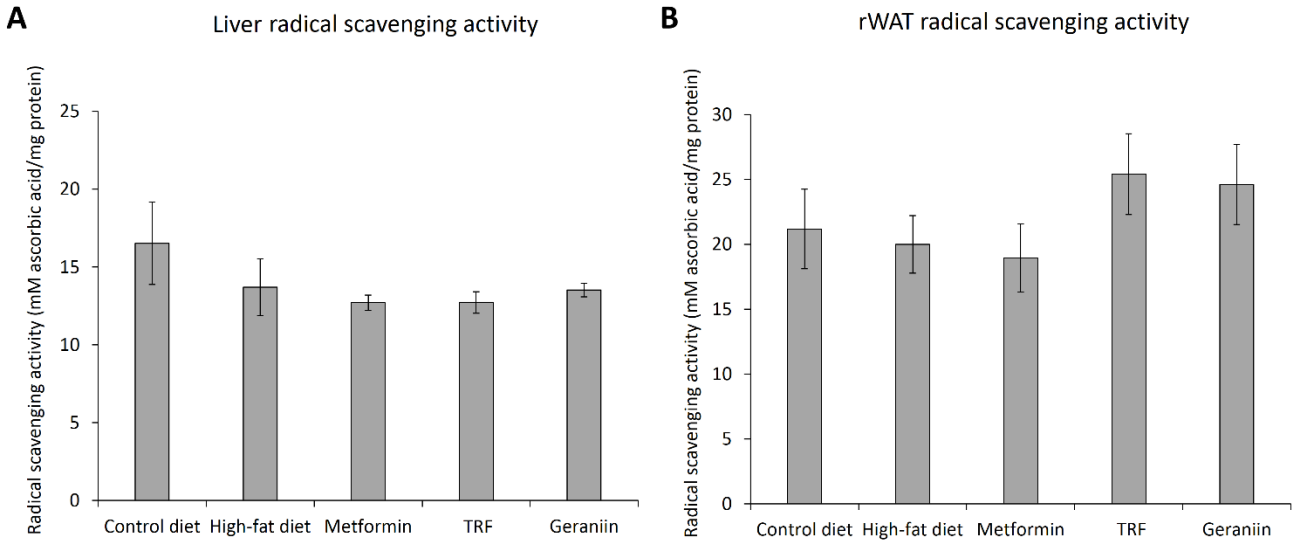

Figure 4.5: Radical scavenging capacity of the liver **(A)** and retroperitoneal white adipose tissue **(B)** of the rats assigned to different treatment groups based on 2,2'-azino-bis(3-ethylbenzothiazoline-6-sulphonic acid) (ABTS) assay. Error bars indicate SEM. Sample size was *n*=6-7 per group. rWAT, retroperitoneal white adipose tissue; TRF, tocotrienol-rich fraction.

4.4.3. AGE-RAGE axis

As for the AGE-RAGE axis, the circulating AGE concentrations (± SEM) of the rats assigned to CD, HFD, metformin, TRF and geraniin treatment groups were 13.06 ± 2.73 μg/mL, 52.92 ± 11.79 μg/mL, 7.40 ± 0.57 μg/mL, 7.21 ± 1.17 μg/mL and 2.70 ± 0.33 μg/mL, respectively (**Figure 4.6**). The circulating AGEs of the rats on HFD was four times higher than those on CD (p<0.001). Treatment with either metformin, TRF or geraniin alleviated the AGE aggregation in the blood circulation (p<0.001).

In line with the circulating AGE level, the hepatic *RAGE* mRNA was upregulated by 2.4-fold in the rats on HFD compared to those on CD (p <0.05). When the rats with MetS were treated with either metformin, TRF or geraniin for a month, the *RAGE* expression was downregulated by 2.3- to 3.1-fold and became comparable to the CD-treated rats (p<0.01) (**Figure 4.7A**). Aside from that, in the rWAT, the expression of *esRAGE* was downregulated by 2.3-fold comparing HFD- to CD-treated rats (p<0.01). This suppression of *esRAGE* in the rWAT was reversed by geraniin, but not metformin and TRF (p<0.05) (**Figure 4.8B**). The changes in gene expression of *RAGE* and *esRAGE* in the rWAT and liver, respectively were unremarkable (**Figures 4.7B and 4.8A**).

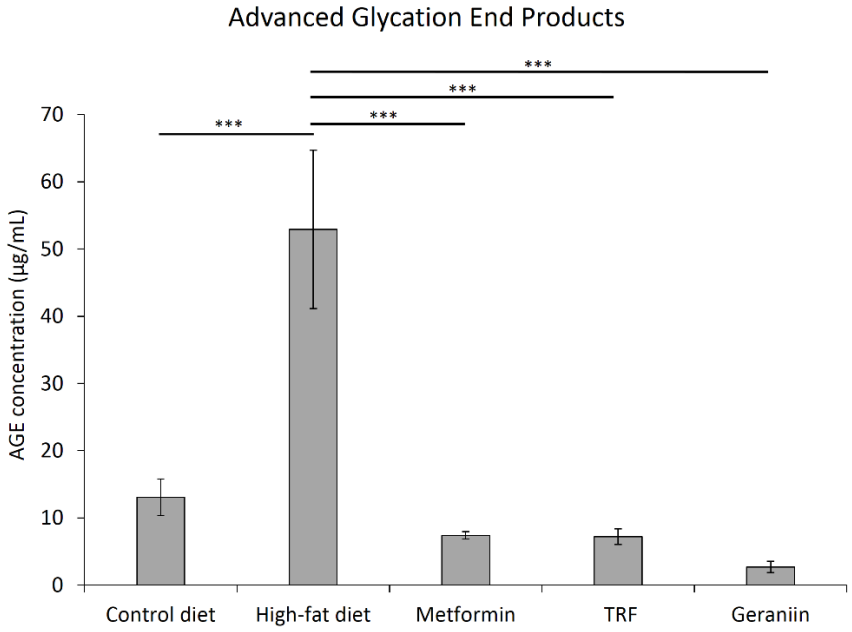

Figure 4.6: Advanced glycation end product concentration in the plasma of the rats assigned to different treatment groups. Error bars indicate SEM. Sample size was n=6-7 per group. *** p<0.001 between groups. AGE, advanced glycation end product; TRF, tocotrienol-rich fraction.

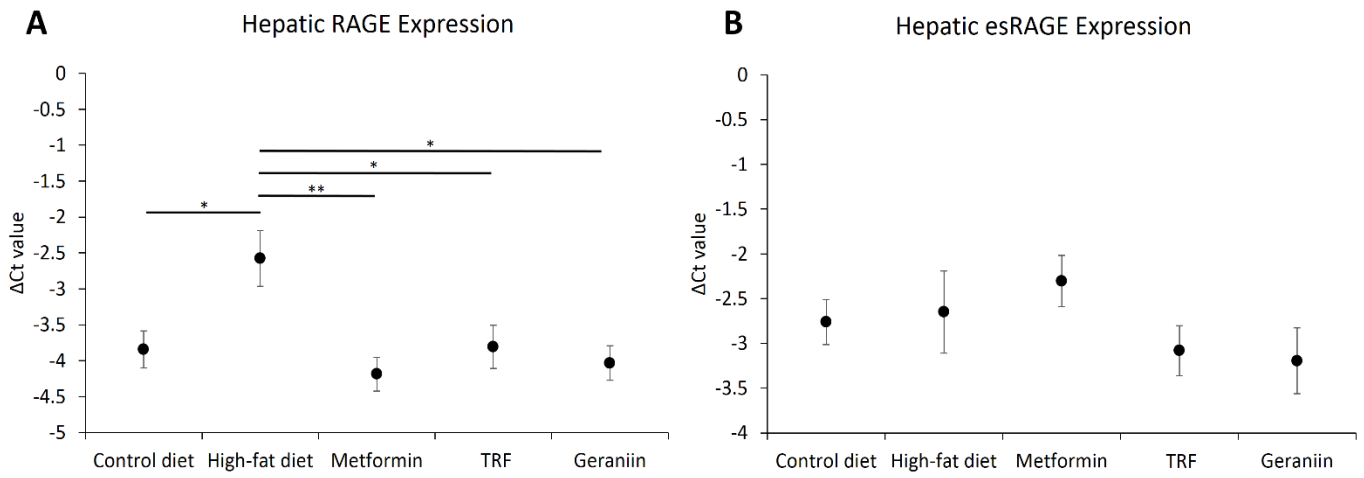

Figure 4.7: Normalized Ct values (ΔCt) of *RAGE* **(A)** and *esRAGE* **(B)** in the liver of the rats assigned to different treatment groups. Hypoxanthine phosphoribosyltransferase 1 (*Hprt1*), succinate dehydrogenase complex flavoprotein subunit A (*SdhA*) and β-actin (*Bac*) were used as the endogenous reference genes. Error bars indicate SEM. Sample size was *n*=6-7 per group. * $p<0.05$ and ** $p<0.01$ between groups. *esRAGE*, endogenous secretory receptor for advanced glycation end product; *RAGE*, receptor for advanced glycation end product; TRF, tocotrienol-rich fraction.

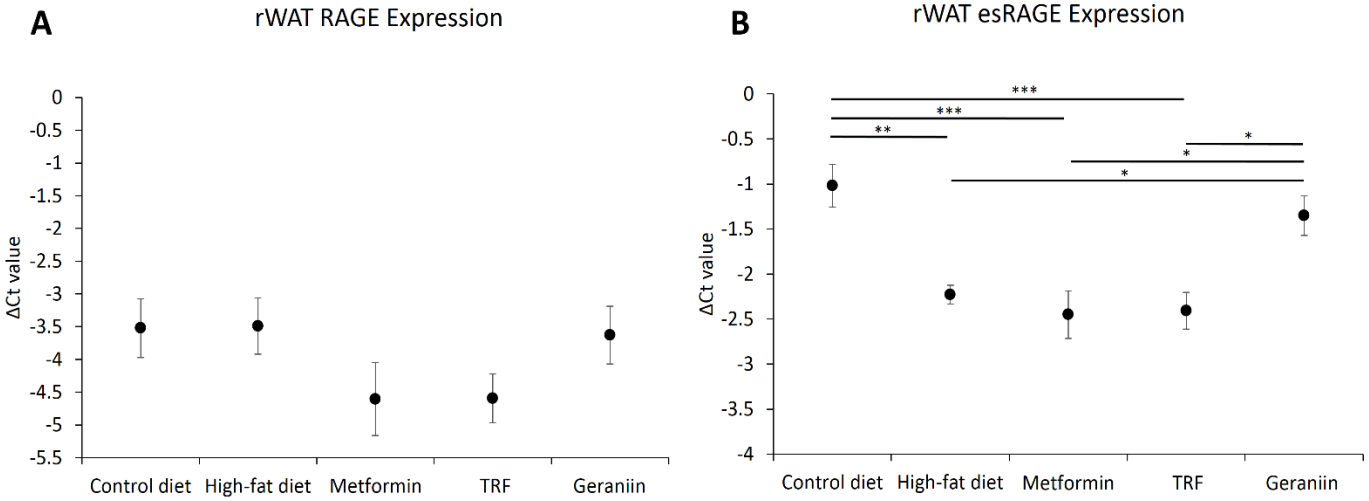

Figure 4.8: Normalized Ct values (ΔCt) of *RAGE* **(A)** and *esRAGE* **(B)** in the retroperitoneal white adipose tissues of the rats assigned to different treatment groups. Hypoxanthine phosphoribosyltransferase 1 (*Hprt1*), succinate dehydrogenase complex flavoprotein subunit A (*SdhA*) and β-actin (*Bac*) were used as the endogenous reference genes. Error bars indicate SEM. Sample size was *n*=6-7 per group. * $p<0.05$, ** $p<0.01$ and *** $p<0.001$ between groups. *esRAGE*, endogenous secretory receptor for advanced glycation end product; *RAGE*, receptor for advanced glycation end product; rWAT, retroperitoneal white adipose tissue; TRF, tocotrienol-rich fraction.

4.4.4. Circulating inflammatory cytokines

The circulating concentrations of five different cytokines, including IL-1β, IL-6, IL-10, IL-18 and TNF-α, are illustrated in **Figure 4.9**. Apart from IL-10 which is an anti-inflammatory cytokine, the other cytokines are closely associated to inflammatory response [273].

Notably, there was a 66% increase in the concentration of IL-1β in the rats on HFD relative to CD group ($p<0.05$). The elevated IL-1β was ameliorated by the treatment with either metformin, TRF or geraniin ($p<0.05$). HFD did not trigger the increase of other inflammatory cytokines like IL-6, IL-10, IL-18 and TNF-α in comparison to the CD group. Treatment with metformin significantly reduced the circulating IL-6 and TNF-α by more than half in comparison to the rats on HFD alone ($p<0.05$), whereas rats treated with TRF also exhibited a reduction in the circulating level of TNF-α compared to HFD group ($p<0.05$). Among the pro-inflammatory cytokines, only IL-18 remained unaffected by all the treatments. The concentration of IL-18 in the plasma was also the lowest amongst all the measured cytokines (<10 pg/mL). Expectedly, the rats on CD had the highest circulating IL-10 concentration, which is an anti-inflammatory cytokine. HFD significantly reduced IL-10 concentration by about 62% ($p<0.05$). The HFD-induced reduction in IL-10 was not improved with either metformin, TRF or geraniin ($p<0.05$).

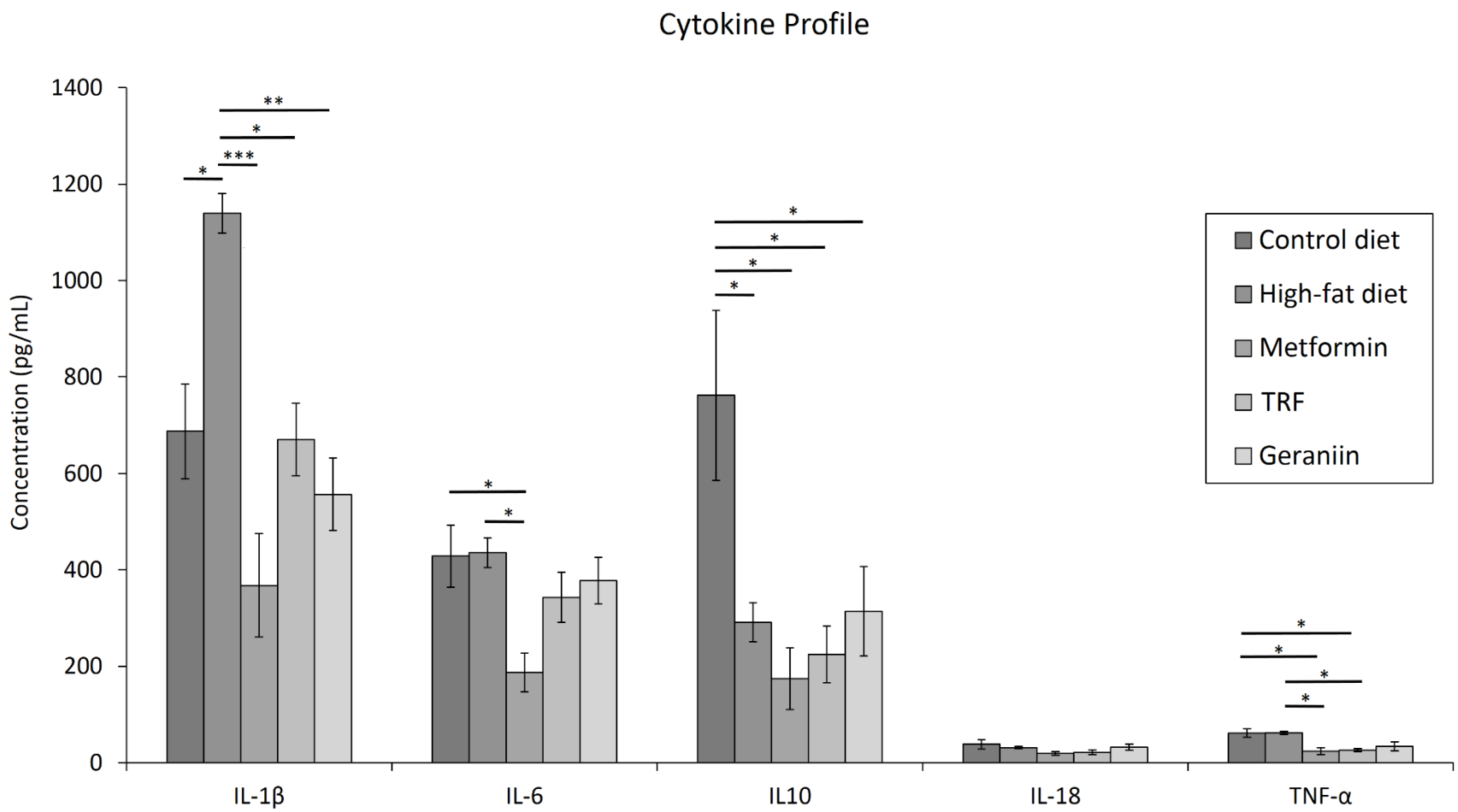

Figure 4.9: Circulating cytokine profiles, including the interleukin (IL)-1β, IL-6, IL-10, IL-18 and tumor necrosis factor-α (TNF-α) of the rats assigned to different treatment groups. Error bars indicate SEM. Sample size was n=6-7 per group. * p<0.05, ** p<0.01 and *** p<0.001 between groups. IL, interleukin; TNF-α, tumor necrosis factor-α; TRF, tocotrienol-rich fraction.

4.5. Discussion

In this study, the rats on HFD for 12 weeks exhibited impaired plasma antioxidant defense, activated AGE-RAGE axis and proinflammatory response. The impact of HFD on the intracellular oxidative stress level in the liver and rWAT was marginal. Despite some minor intergroup differences, in general, the treatment with either metformin, TRF or geraniin successfully restored the plasma total antioxidant capacity besides reducing circulating oxidative stress and proinflammatory biomarkers. The empirical findings support the pleiotropic therapeutic effects of geraniin in MetS, not only on the blood pressure regulation as well as lipid and glucose metabolism, but also the oxidative stress and inflammatory response induced by chronic high-fat consumption.

The devastating effects of HFD on the redox homeostasis have been extensively reported and reviewed [274]. Unhealthy dietary patterns with high lipid content can negatively influence the enzymatic and non-enzymatic antioxidant systems. In terms of the non-enzymatic antioxidant power, HFD could shift the redox status towards oxidative potential, weaken radical scavenging ability, promote ROS generation and lower the bioavailability of endogenous antioxidant components like glutathione, tetrahydrobiopterin and vitamin C [275-278]. Additionally, a high-calorie diet also impairs the normal function of common anti-oxidative enzymes like catalase, superoxide dismutase, glutathione peroxidase and glutathione reductase [279, 280]. This would further intensify the oxidative stress. In this context, our findings show that HFD disrupted the redox balance in the blood circulation to promote oxidative stress. This is marked by several indicators like ORAC assay of the plasma samples, the aggregation of AGE and myeloperoxidase activity. Interestingly, some of these oxidative biomarkers are also associated with multiple pathological processes. For instance, myeloperoxidase, which is an extracellular heme protein secreted by neutrophils during pathogenic invasion, is strongly linked to vascular inflammation and cardiovascular event [272]. On the other hand, the activation of AGE-RAGE axis is also associated to inflammatory response and various diabetic vascular complications [281]. More importantly, the pathological effects of AGE-RAGE overdrive are not limited to the endothelial tissues in blood vessel. RAGE is also expressed in hepatic stellate cells and hepatocytes [282]. The activation of hepatic RAGE upon ligand binding could trigger hepatic injury and fibrosis, contributing to the development of NAFLD [283-285]. In this study, since

RAGE overexpression (by 2.4-fold) was observed in the liver specimens of rats on HFD, the abnormality may contribute to the onset of MetS features observed.

In addition, it is also postulated that the pro-oxidant effect of HFD could be a crucial mediator of the pathogenesis of MetS and its complications. This is in line with a study which reported that the occurrence of uncontrolled ROS liberation upon high-fat feeding precedes the onset of dyslipidemia and inflammatory cytokine secretion [286]. Nevertheless, the elevated oxidative stress in the blood circulation was not reflected in the redox status in the liver and rWAT in the present study. This is due to the inherent differences between intra- and extracellular antioxidant defense systems in terms of the counter mechanism and pool of antioxidants. In the blood circulation, the redox balance is primarily maintained by three major mechanisms: antioxidative enzymes, chain-breaking antioxidants like vitamin E, glutathione and vitamin C and chelation of transition metals with binding proteins like ferritin, transferrin and caeruloplasmin [287, 288]. Although the relative importance of each mechanism is largely unclear, chain-breaking (non-enzymatic) antioxidants do play a critical role in offsetting the oxidative insults. Yet, once oxidized, many non-enzymatic antioxidants lose their original reducing properties. This results in impaired antioxidant defense which can be reversed by replenishing the antioxidant stock from exogenous sources or endogenous biosynthesis. Comparatively, in body tissues and cells, aside from the aforementioned antioxidant mechanisms, the modulation of redox balance is further fortified by nuclear factor erythroid 2-related factor 2 (Nrf2), autophagy and mitophagy to attenuate the release of ROS [289-291]. Hence, it can be said that the intracellular redox status is subjected to stricter regulation in comparison to the systemic redox balance. This makes the antioxidant capacity of the blood circulation more prone to drastic changes under the increased oxidative stress considering the relatively slow turnover of antioxidants.

Based on the results, treatment with geraniin could reverse the diet-induced impairment in the systemic redox balance. This is in parallel with the findings of a recent study that concluded the ameliorative effects of geraniin on enzymatic antioxidants and glutathione regenerative mechanism in obese rats [279]. The primary antioxidant mechanism of geraniin is similar to that of other phenolic compounds which is by transferring hydrogen atom to free radicals to nullify their reactivity, turning the radicals into harmless molecules [188]. Through the process, geraniin molecules are converted into non-damaging phenoxyl radicals due to the resonance stabilization

of the radicals conferred by the aromatic rings [188]. These phenoxyl radicals can also couple with each other to quench the radicals. This process can stop the chain reaction caused by a radical and so, is known as "chain-breaking antioxidant activity". Although geraniin is not absorbed in the intact form, its derivatives such as ellagic acid and gallic acid also exhibit incredible antioxidant power [292]. More importantly, the predominant bioactive geraniin-derived metabolites, urolithins are much more powerful in terms of the antioxidant properties compared to the parental compound [292]. Therefore, it is not surprising that the supplementation with geraniin can restore the redox homeostasis of blood circulation.

In addition, treatment with geraniin markedly reduced the activity of myeloperoxidase. As mentioned earlier, hyperactivity of myeloperoxidase is closely linked to cardiovascular dysfunction and atherogenesis [293, 294]. Even though the physiological function of myeloperoxidase is related to innate immunity against pathogens, many non-microbial molecules are also sensed by the immunity cells as dangerous signals by the pattern recognition receptors, resulting in the initiation of innate immunity response in the absence of microorganisms; a process which is also known as "sterile inflammation" [295]. Examples of the non-microbial stimuli include various damaged biomolecules resulted from oxidative stress and deranged metabolism such as AGE, oxidized LDL and β-amyloid peptides [296, 297]. Upon activation by these stimuli, the immunity cells like neutrophils and macrophages will secrete a wide variety of pro-oxidant and pro-inflammatory molecules to promote local oxidative and inflammatory state. One such molecule is myeloperoxidase which liberates hypochlorous radicals in order to eradicate pathogenic microorganisms [272]. However, under sterile inflammation conditions, the resultant pro-oxidant species could pose severe structural and functional damage to the local vascular tissues. The vascular dysfunction and inflammation is further exacerbated by the release of chemokines and chemoattractants that promote the recruitment and infiltration of other innate immunity cells, accelerating the onset of atherosclerotic lesions in MetS and diabetic patients [298-301]. In this context, myeloperoxidase is not only an oxidative stress biomarker, but also plays a pivotal role in atherogenesis. This is exemplified by myeloperoxidase knockout mice which showed remarkable resistance against diet-induced weight gain and insulin resistance [302]. In this study, all three interventions, namely metformin, TRF and geraniin, effectively mitigate the diet-induced myeloperoxidase hyperactivity, pointing out possible anti-atherogenic activity. Indeed, one recent study demonstrated that the dietary supplementation of high-purity

tocotrienols is highly effective against the formation of atherosclerotic lesions in atherosclerosis-prone mice [303]. Although thus far there is no direct evidence about the anti-atherogenic effect of geraniin, the consumption of polyphenol-rich diet is able to prevent some pathological processes associated to atherosclerosis [304]. In short, the inhibitory effect on myeloperoxidase activity conferred by metformin, TRF and geraniin is not only indicative of their ability to diminish oxidative stress in the blood circulation, but also the likelihood to protect vascular health.

Apart from that, geraniin supplementation also reduced the circulating AGE to the basal level. This is in parallel with the finding of an *in vitro* study [175]. Such an AGE-lowering effect was also observed in the rats treated with either metformin or TRF. The AGE reduction is accompanied by the transcriptional suppression of *RAGE* expression in the liver. For metformin, the inhibitory effect of AGE-RAGE axis has been reported in several clinical trials [305, 306]. Compared to placebo, metformin could reduce a number of glycation products including pentosidine, methylglyoxal, AGE and advanced oxidation protein products (AOPP) in diabetic patients [305, 306]. The reduction efficacy of glycation products was comparable to certain anti-diabetic agents like pioglitazone and repaglinide [307, 308], suggesting that the underlying mechanism of the AGE-lowering effect conferred by metformin is linked to its glucose-lowering properties. Simultaneous reduction of pro-inflammatory and pro-coagulant markers as well as cell adhesive molecules was also observed with the metformin therapy, many of which are modulated by AGE-RAGE-NF-κB signaling pathway [307]. This implies that the inhibition of AGE-RAGE axis induced by metformin is translated into anti-inflammatory and anti-thrombotic effects in diabetic patients.

Unlike metformin, TRF did not possess glucose-lowering effect. This has been revealed in previous studies [233, 309]. Thus, TRF is unable to inhibit AGE formation by reducing the precursor of glycation process, which is glucose. Instead, the inhibitory effect of TRF on the glycation process and AGE-RAGE axis is likely attributable to its antioxidant properties. To elucidate, the formation of AGE is initiated by a concentration-dependent glycation reaction of reducing sugars to amino groups in proteins or lipids, followed by a series of rearrangements or oxidation reactions [266]. Increased oxidative stress is known to accelerate the accumulation of dicarbonyls like glyoxal, methylglyoxal and 3-deoxyglucosone, which serve as reactive

intermediates to fuel the formation of AGE [310]. The oxidative stress can be countered by the antioxidant properties of tocotrienols; hence slowing down the generation of AGE independent of the glucose level. The AGE-lowering effect of TRF has also been shown clinically in the elderly [235]. This bioactivity, together with the cholesterol-lowering and antioxidant properties, is likely to improve cardiovascular health [311]. Therefore, TRF can potentially be exploited as an adjunct therapy for cardiovascular disease.

Ellagitannin geraniin, on the other hand, exerts anti-hyperglycemic and antioxidant properties. This is shown by the normalization of the fasting blood glucose and circulating oxidative stress markers, respectively. Considering that both actions disfavor AGE formation, the AGE-reducing activity of geraniin is likely to be a combinatory effect of the two bioactivities. More importantly, treatment with geraniin also induced the upregulation of *esRAGE* in certain tissues like rWAT, suggesting an additional AGE elimination mechanism. Essentially, esRAGE is the truncated form of RAGE without the cytosolic tail. Hence, in contrast to RAGE which is bound to the plasma membrane, esRAGE is secreted into the blood circulation to act as the decoy receptor for RAGE ligands [312]. The missing transmembrane domain and cytosolic signaling tail renders the esRAGE unbound to the cellular surface and thereby unable to trigger downstream signaling cascades. By scavenging the RAGE ligands in the circulation, esRAGE can assist their clearance and prevent them from RAGE ligand binding; subsequently attenuating the adverse effects of RAGE activation [313]. Thus, the inhibitory effect of geraniin on AGE-RAGE axis is likely attributable to its glucose-lowering action, antioxidant activity, as well as restoration of the *esRAGE* expression. Nonetheless, it is noted that the AGE level of the rats supplemented with geraniin was comparable to those treated with metformin or TRF. This implies the lack of additive or synergistic activity in modulating AGE level despite the presence of multiple AGE-inhibiting effects. Therefore, the possibility of one of the three AGE-lowering mechanisms functions being the predominant mechanism cannot be excluded.

Furthermore, HFD also activated the inflammatory response as indicated by the elevated circulating IL-1β. Like AGE-RAGE axis, the interaction of IL-1β with IL-1 receptors can potentiate various pathological processes in chronic metabolic diseases [314]. In this study, the HFD-induced increase in IL-1β was reversed by geraniin. The inhibitory effect of geraniin on cytokine release has also been shown in other inflammatory models like lipopolysaccharide-

induced acute lung injury and cisplatin-induced nephrotoxicity [315, 316]. The underlying mechanisms of the immune modulatory effect are attributable to the suppression of NF-κB and activation of Nrf2 signaling [269, 316]. Based on the results, treatment with geraniin can resolve the pro-inflammatory response caused by high-fat feeding. This observation further strengthens the pleiotropic beneficial effects of geraniin against MetS.

Like geraniin, supplementation with TRF also reversed the overly high concentration of IL-1β caused by HFD. Apart from that, the circulating TNF-α was also lowered by TRF. One recent study suggests the δ- and γ-tocotrienols are the functional subtypes of tocotrienols. Long-term consumption of these tocotrienol subtypes not only promotes their deposition in the heart, liver and adipose tissues, but also attenuates inflammatory cell infiltration into the liver and improves cardiovascular function [317]. Conversely, metformin also displays potent anti-inflammatory action as indicated by the reduction of multiple inflammatory markers, namely IL-1β, IL-6 and TNF-α. Such a biological effect have been widely reported [318]. Although it could have resulted from the improved glucose homeostasis, one clinical study demonstrates the anti-inflammatory effect of metformin irrespective of diabetes status [107]. This suggests that the anti-inflammatory action is an intrinsic property of metformin. This could be caused by the metformin-triggered AMPK activation, leading to downstream inhibition of NF-κB pathway [319]. In light of the anti-inflammatory activity, the potential use of metformin in other inflammatory diseases like inflammatory bowel disease and colitis-associated colon cancer is increasingly appreciated [320, 321].

Apart from increasing inflammatory cytokines in the blood circulation, chronic high-fat consumption also led to a decline in the anti-inflammatory cytokines like IL-10. Under physiological conditions, IL-10 serves as a host protective mechanism against exaggerated inflammatory responses upon microbial challenge by limiting inflammatory signaling cascades and cytokines [322]. Decreased circulating IL-10 level is commonly seen in people with insulin resistance, MetS and T2DM [323-326]. The macrophage response to IL-10 signaling is also dampened in the presence of hyperglycemia, further aggravating the inflammatory state [327]. However, in the present study, none of the treatments successfully restored the IL-10 level to the basal level. This points out that feeding on HFD has a long-lasting impact on IL-10 expression despite the reversal of redox homeostasis. Although the underlying mechanism for such an

observation is unclear, certain therapeutic strategies like physical exercise could ameliorate HFD-induced cardiomyopathy by promoting IL-10 elevation, signifying a beneficial role of the anti-inflammatory cytokine in chronic metabolic disease [328]. In short, treatment with either geraniin, TRF or metformin confers promising therapeutic effects to minimize inflammatory cytokines, but fails to recover the disruption to the anti-inflammatory cytokines caused by HFD.

One limitation of the study is the lack of actual quantification of the esRAGE in the plasma. In the present study, we demonstrated that *esRAGE* mRNA expression was enhanced in certain tissues by geraniin supplementation. Although this indicates a new AGE clearance mechanism that has not been previously discovered in geraniin, further verification of the circulating esRAGE with quantitative protein assays like western blot or ELISA is pertinent. This will allow us to examine if the alteration in the gene expression is truly translated into functional changes. On the other hand, we successfully demonstrated the threatening effects of HFD on the systemic redox balance and inflammatory response, together with the ameliorative effects of metformin, TRF and geraniin in these aspects. Nonetheless, we did not manage to link the impairments in the blood circulation to intracellular redox status. The incoherence could be due to disparities in terms of antioxidant pools and remedial mechanisms between intra- and extracellular condition. In this case, the feeding duration can be prolonged to precipitate a more severe form of oxidative stress and chronic inflammation in the body tissues. Furthermore, the measurement of circulating cytokines was done with cytometric bead arrays, which is a multiplex measurement method. Despite having good correlations with uniplex asssays like ELISA and western blot, multiplex assays might have possible cross-reactivity which may influence the specificity of the assays [329]. They are also known to be less robust when complex biological specimens like serum and plasma are used in the measurement [330]. Hence, further validation of the inflammatory cytokine results is required in future research. More importantly, additional investigation of the intracellular antioxidant and anti-inflammatory defense systems will also provide valuable information about biological effects of geraniin.

4.6. Summary and key highlights of the study

The crucial findings of the study presented in this chapter are summarized in the following:

- HFD significantly increased the biomarkers of oxidative stress and inflammatory response besides reducing anti-inflammatory cytokines in the blood circulation. The *RAGE* expression in the liver was also activated by HFD. This indicates that prolonged consumption of diet enriched by saturated fats could lead to increased oxidative stress and systemic inflammation.
- Treatment with either metformin, TRF or geraniin effectively ameliorated the HFD-induced oxidative stress, *RAGE* upregulation and inflammatory response. The three interventions differed in terms of the inhibitory effect on inflammatory cytokines. Specifically, metformin markedly reduced three inflammatory cytokines (IL-1β, IL-6 and TNF-α) whereas TRF and geraniin only lowered two (IL-1β and TNF-α) and one (IL-1β) pro-inflammatory cytokines in the blood circulation, respectively.
- Treatment with geraniin upregulated the expression of *esRAGE* in the rWAT. This implies an additional AGE-RAGE inhibitory mechanism via scavenging circulating AGEs and hindering AGE-RAGE ligand binding. The activity is not shared by metformin and TRF.
- The impact of HFD on intracellular redox balance in the liver and rWAT was minimal which is likely because of the sub-chronic disease progression. Treatment with antioxidants like TRF and geraniin did show a small improvement in the total antioxidant capacity of rWAT, but not in the liver. In general, the effect of treatment with either metformin, TRF or geraniin on the redox status in the liver and rWAT was marginal.

To summarize, treatment with geraniin not only restored the glucose and lipid homeostasis, but also normalized the circulating redox balance and inflammatory response which are otherwise, disrupted by high-fat feeding. Considering the critical role of oxidative stress and systemic low-grade inflammation in the progression of MetS, the observed beneficial bioactivities further reinforce the clinical prospect of ellagitannin geraniin as a multifunctional therapy against MetS and other related chronic metabolic diseases. However, the actual impact of geraniin on the intracellular redox homeostasis in different organs like the liver, adipose tissues and muscles remains to be clarified. Further validation of the inflammatory cytokines in the blood circulation and body tissues with more specific uniplex assays like ELISA is highly encouraged to establish the *in vivo* anti-inflammatory effect of geraniin.

CHAPTER 5

Underlying Mechanism of Ellagitannin Geraniin

5. HEPATIC TRANSCRIPTOMIC ANALYSIS UNVEILED THE MOLECULAR MECHANISM UNDERLYING THE PROTECTIVE EFFECTS OF ELLAGITANNIN GERANIIN AGAINST METABOLIC SYNDROME

5.1. General overview

The understanding about the molecular mechanism of geraniin is rather limited. According to several cell-based cancer studies, geraniin could modulate a number of signaling pathways like Nrf2, phosphatidyl inositol 3-kinase-protein kinase B (PI3K-Akt), extracellular signal-regulated protein kinase 1/2 (ERK 1/2), STAT3 and p38 MAPK to interrupt various malignant processes such as cancerous cell survival, growth, migration and invasion [331-334]. These signaling pathways also play a pivotal role in the pathophysiology of obesity and MetS. For instance, Nrf2 and PI3K-Akt pathways can modulate the inflammatory response and insulin signaling while MAPKs are implicated in adipocyte differentiation [335-337]. To date, there is no direct evidence that supports the activity of geraniin on these signaling pathways in obese or diabetic animal models. This makes our knowledge about geraniin somewhat superficial and incomprehensive. Thus, it is pertinent to explore its underlying mechanism in order to have a deeper understanding about the therapeutic effects of geraniin.

In the present study, the liver was selected for further investigation of the molecular mechanism because of three major reasons. First and foremost, based on our findings, many therapeutic effects of geraniin are associated with the liver, as exemplified by its ameliorative effects on hepatic steatosis and possibly hepatic insulin resistance. Secondly, many geraniin-derived metabolites are subjected to extensive enterohepatic circulation, which facilitates the persistent exposure of hepatocytes to these metabolites [223]. Lastly, the liver serves as the central hub for a wide range of metabolic processes including detoxification, metabolism of carbohydrates, lipids and proteins, biosynthesis of various circulating proteins as well as storage of numerous macro- and micronutrients. As such, examining the metabolic changes in the liver upon geraniin exposure can potentially unveil how geraniin confers the systemic beneficial effects in MetS.

Since the molecular targets of geraniin are largely unknown, an exploratory transcriptomic approach was used to pinpoint the potential mechanisms of geraniin action. Fundamentally, a

transcriptomic assay analyzes the complete set of RNA transcripts expressed by the genome, using high-throughput methods like microarray and next generation sequencing. Theoretically, this provides a snapshot of all gene expression which reflects the holistic metabolic state of certain tissues or cells under specific circumstances. Moreover, comparison of transcriptomes facilitates the identification of differentially expressed transcripts or genes, uncovering the alteration in molecular pathways in response to different treatments [338]. Considering that the cost of next generation sequencing has been greatly reduced over the years, the transcriptomic analysis by RNA sequencing is undeniably an invaluable tool for a mechanistic study.

Thus, this chapter describes one of the first attempts to elaborate the underlying mechanism of ellagitannin geraniin in MetS by studying its effects on the hepatic mRNA transcriptomes. By comparing the gene expression profile to untreated rats, the implicated metabolic pathways can be identified. The output of this analysis not only provides crucial information about the bioactivity of the natural product, but can potentially reveal new target pathways for MetS therapy.

5.2. Objectives of the study

This chapter aims to explore the molecular mechanism of ellagitannin geraniin in MetS by studying the liver mRNA transcriptomes using RNA sequencing approach. To attain this goal, the following research tasks need to be completed:

- To identify the differentially expressed genes (DEGs) between the hepatic transcriptomes of CD-, HFD- and geraniin-treated rats.
- To investigate the enriched molecular function of the DEGs with gene ontology enrichment analysis
- To outline the possible metabolic pathways affected by ellagitannin geraniin using Kyoto Encyclopedia of Genes and Genomes (KEGG) pathway analysis

5.3. Methods and materials

5.3.1. Experimental design and treatment

The tissue specimens used in this chapter were taken from the experiment done in **Chapter 3**. The experimental design and treatment groups can be referred to **Section 3.3.3**, but metformin- and TRF-treated groups were excluded from the transcriptomic analysis (**Figure 5.1**). This was because the comparisons of transcriptomes between these treatments and geraniin would not contribute to the main objective and their addition would complicate the transcriptomic data analysis. The liver tissues were quickly harvested upon dissection, snap frozen in the liquid nitrogen and stored at -80^{o}C for total RNA extraction.

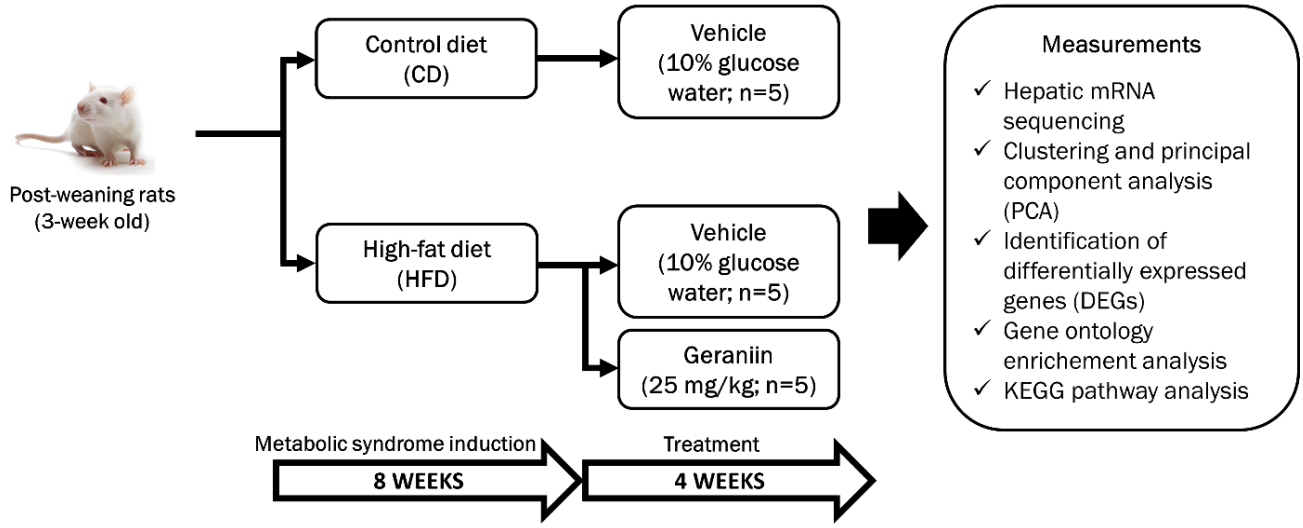

Figure 5.1: Experimental design for studying the molecular mechanism of ellagitannin geraniin with hepatic transcriptomic sequencing.

5.3.2. Total RNA extraction and quality control

Total RNA of the liver tissues from CD-, HFD- and geraniin-treated rats (n=5 per group) was isolated with Qiagen RNeasy Mini kit (Qiagen, Germany) and treated with RNase-free DNase I (ThermoFisher Scientific, USA) to eliminate genomic DNA contamination. Then, the total RNA samples were purified again with Qiagen RNease Mini kit to remove DNase I. For initial quality check, the RNA integrity was assessed with Agilent 2100 Bioanalyzer (Agilent Technologies, USA) while the concentration was measured with Qubit 2.0 Fluorometer (Life Technologies,

USA), both of which were performed by Monash University Malaysia Genomics Facility (Selangor, Malaysia).

5.3.3. Library preparation and sequencing

After the initial quality check, the purified total RNA samples were shipped out to Novogene (Beijing, China) which performed the mRNA enrichment, library preparation, library quality check and sequencing. Briefly, oligo dT beads were used to retrieve the mRNA transcripts from the total RNA samples. For library preparation, NEBNext® Ultra RNA Library Prep Kit for Illumina® (New England Biolabs, USA) was used for library preparation. The quality and concentration of the libraries was examined with Agilent 2100 Bioanalyzer, Qubit 2.0 Fluorometer and qPCR. Lastly, the libraries which were prepared from individual mRNA samples were subjected to multiplex sequencing (150bp paired-end) using Hiseq 4000 (Illumina, USA). Raw sequencing data were submitted to the NCBI sequence read archive (SRA) (Accession no.: SRP132230; Biosample: SAMN08408057-71; BioProject: PRJNA431835).

5.3.4. Sequencing data analysis and identification of differentially expressed genes

FastQC (version 0.11.5) was used for quality check of the raw and trimmed sequencing data [339]. Trimmomatic (version 0.36) was used to remove the adapter sequences present in the raw sequencing reads [340]. The rat (*Rattus norvegicus*) genome FASTA file (ftp://ftp.ensembl.org/pub/release-91/fasta/rattus_norvegicus/dna/Rattus_norvegicus.Rnor_6.0.dna.toplevel.fa.gz) and gene annotation GTF file (ftp://ftp.ensembl.org/pub/release-91/gtf/rattus_norvegicus/Rattus_norvegicus.Rnor_6.0.91.gtf.gz) were retrieved from Ensembl. HISAT2 (version 2.1.0) was used to build indexes and map the trimmed sequencing reads to the rat genome [341]. This is followed by the use of "union" mode of HTSeq (version 0.9.1) to generate gene-level read count data [342]. These bioinformatics analyses were carried out using a Linux-based workstation provided by Monash University Malaysia Genomics Facility. Differential expression analysis was carried out using DESeq2 (version 1.14.1) in R (version 3.3.2), in which the five biological replicates given the same treatment were analyzed as a group and compared to other treatment groups [343]. All the selected bioinformatics tools were the most up-to-date version at the time of the analyses being conducted. Variance stabilizing

transformation was used for exploratory analysis of the relationship between samples like principal component analysis (PCA). For the identification of differentially expressed genes (DEGs), the *p*-values were adjusted with Benjamini-Hochberg procedure. A false discovery rate (adjusted *p*-value) of <0.05 was set as the threshold for the selection of DEGs.

5.3.5. Gene ontology and KEGG pathway analysis

Gene ontology enrichment analysis was performed using Goseq (version 1.26.0) in R [344]. The analysis explored the enriched biological pathways, cellular components and molecular functions based on the DEGs between different treatments. The *p*-values were adjusted with Benjamini-Hochberg procedure. A false discovery rate (adjusted *p*-value) < 0.05 was set as the threshold for the enriched gene ontology. Overly long lists of statistically significant enriched gene ontology terms were further summarized with REVIGO to reduce functionally overlapping terms [345]. KEGG pathway analysis was conducted with DAVID Bioinformatics Resources 6.8 [346]. DAVID uses the modified Fisher Exact test to determine the statistical significance of each enriched pathway. The *p*- value <0.05 was set to select the enriched pathway. Selected pathways were visualized using Pathview [347].

5.3.6. Quantitative polymerase chain reaction (qPCR)

To assess the sequencing data, SYBR green-based qPCR with Rotor-Gene Q (Qiagen, Germany) was carried out. The RNA extraction and cDNA synthesis procedures can be referred to **Section 4.3.5**. The selected qPCR reaction master mix was TransStart Tip Green qPCR SuperMix (TransGen Biotech, China). The genes of interest were *PPARα*, *PPARγ*, alcohol dehydrogenase 7 (*Adh7*) and DDHD domain containing 1 (*Ddhd1*). The endogenous reference genes were *Hprt1*, *SdhA* and *Bac* while the normalization formula is as outlined in **Section 4.3.6**. The nucleotide sequences of the forward and reverse primers as well as the accession numbers are shown in **Table 5.1**. PCR conditions and amplicon information are provided in **Appendix C**.

Table 5.1: Accession numbers, forward and reverse primers of the endogenous reference and target genes as well as amplicon size of the PCR products.

Target gene	Accession number	Nucleotide sequence (5'→ 3')		Amplicon size (bp)
		Forward primer	Reverse primer	
Bac*	NM_031144	GTA TGG GTC AGA AGG ACT CC	GTT CAA TGG GGT ACT TCA GG	81
Hprt1*	NM_012583	CTG GAA AGA ACG TCT TGA TTG	GTA TCC AAC ACT TCG AGA GG	146
SdhA*	NM_130428	GGC TTT CAC TTC TCT GTT GG	CCA CAG CAT CAA ACT CAT GG	103
PPARα	NM_013196	TGT GGA GAT CGG CCT GGC CTT	CCG GAT GGT TGC TCT GCA GGT	100
PPARγ	NM_013124	CCC TGG CAA AGC ATT TGT AT	GGT GAT TTG TCT GTT GTC TTT C	100
Adh7	NM_134329	CTG CTT TTC ACT GGA CGG A	AAG GTG TGG GTT ATC AAC TGG	131
Ddhd1	NM_001033066	GCC AAA CTT TCT CAA CCC AG	GTA TGC TCG CTT TGC CAA TG	146

* denotes endogenous reference genes.

Adh7, alcohol dehydrogenase 7; *Bac*, β-actin; *Ddhd1*, DDHD domain containing 1; *Hprt1*, hypoxanthine phosphoribosyltransferase 1; *PPARα*, peroxisome proliferator-activated receptor α; *PPARγ*, peroxisome proliferator-activated receptor γ; *SdhA*, succinate dehydrogenase complex flavoprotein subunit A.

5.4. Results

5.4.1. Sequencing of rat hepatic mRNA transcriptomes

The average RNA Integrity Number (RIN) and concentration of the 15 total RNA samples were 6.05 and 967.8 ng/μL (**Appendix D**). The mRNA sequencing produced an average of 25.3 million raw paired-end reads per sample. With the number of biological replicates used in the study (n=5 per group), the sequencing depth can provide sufficient statistical power for a

differential expression analysis [348]. About 97.0% of the base calls were of Q20 (error probability = 1 in 100) and 92.5% of them were of Q30 (error probability = 1 in 1000). After quality control and trimming, an average of 24.5 million clean paired-end reads per sample were retained (**Figure 5.2**). Using HISAT2, 92.6% to 93.5% of the clean reads were mapped to the rat genome, of which close to 85% were map uniquely to one locus (**Figure 5.3**). Due to the "union" mode of HTSeq being used, only uniquely mapped reads were used for the gene-level read counting and downstream bioinformatics analysis.

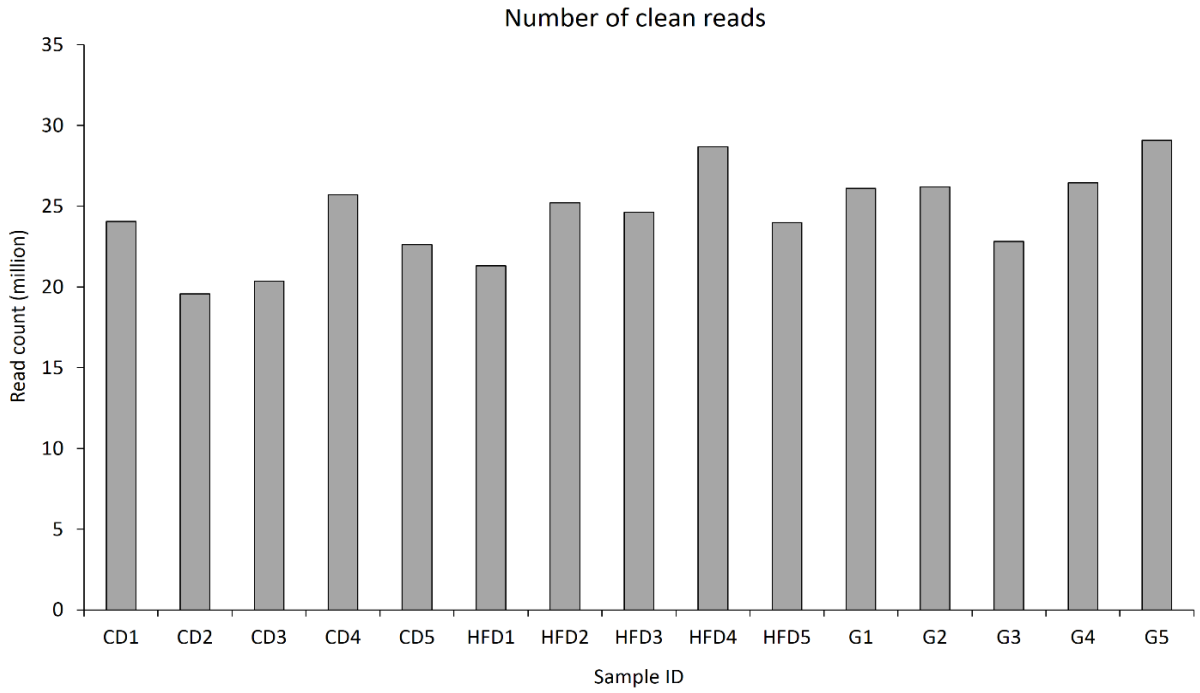

Figure 5.2: Number of clean paired-end reads of the mRNA sequencing after trimming. CD, control diet; G, geraniin; HFD, high-fat diet.

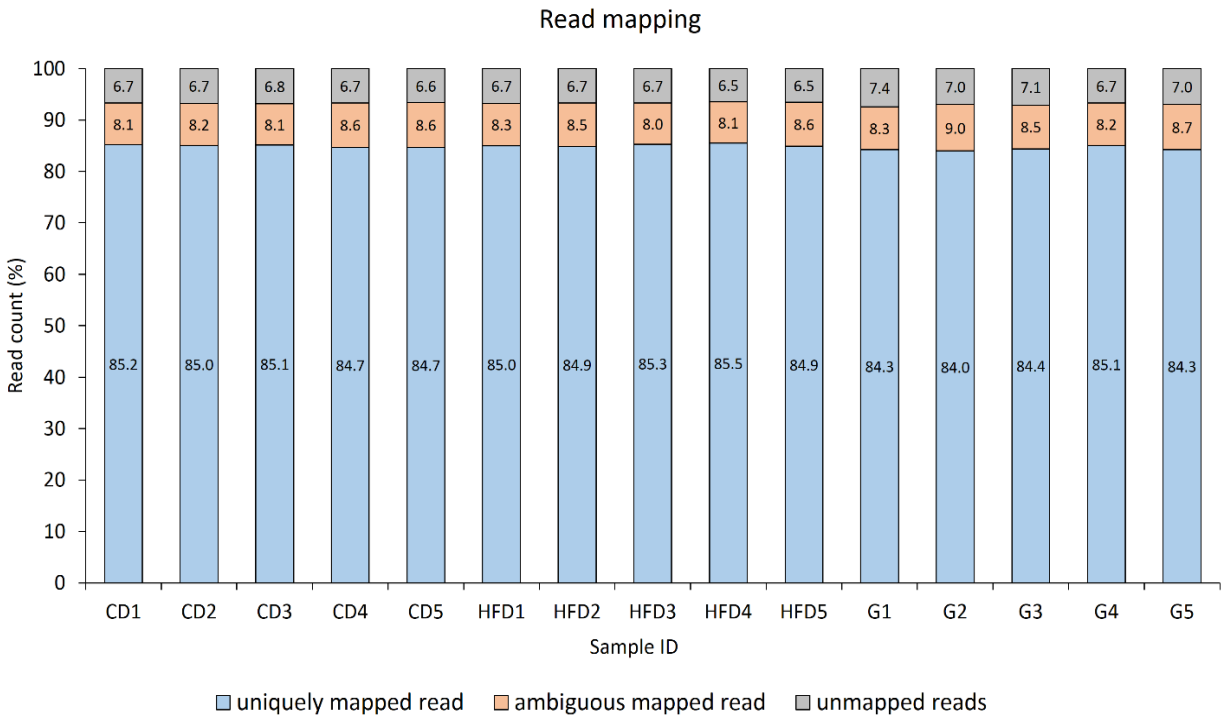

Figure 5.3: Proportion of the clean paired-end reads mapped to the rat genome uniquely, ambiguously or remained unmapped. The proportion is expressed as percentage and shown in the bar plot. CD, control diet; G, geraniin; HFD, high-fat diet.

5.4.2. Principal component analysis (PCA) and hierarchical clustering analysis

To visualize the grouping pattern of the sequencing data from different treatment groups, we performed a PCA using the transformed gene count data. Based on the PCA plot illustrated in **Figure 5.4**, the samples subjected to the same treatment appear to cluster together. The liver transcriptomes of the rats on HFD are more diverse compared to those on CD or treated with geraniin. This is supported by the hierarchical clustering analysis shown as a combination of heatmap and dendrogram in **Figure 5.5**. Based on the dendrogram, two major clusters are observed which separate CD-treated rats from those on HFD with or without geraniin treatment except for a sample from the HFD group which is more similar to the CD-treated rats. However, in general, the rats subjected to the same treatment shared higher similarity in terms of their hepatic transcriptomes compared to those with different treatments.

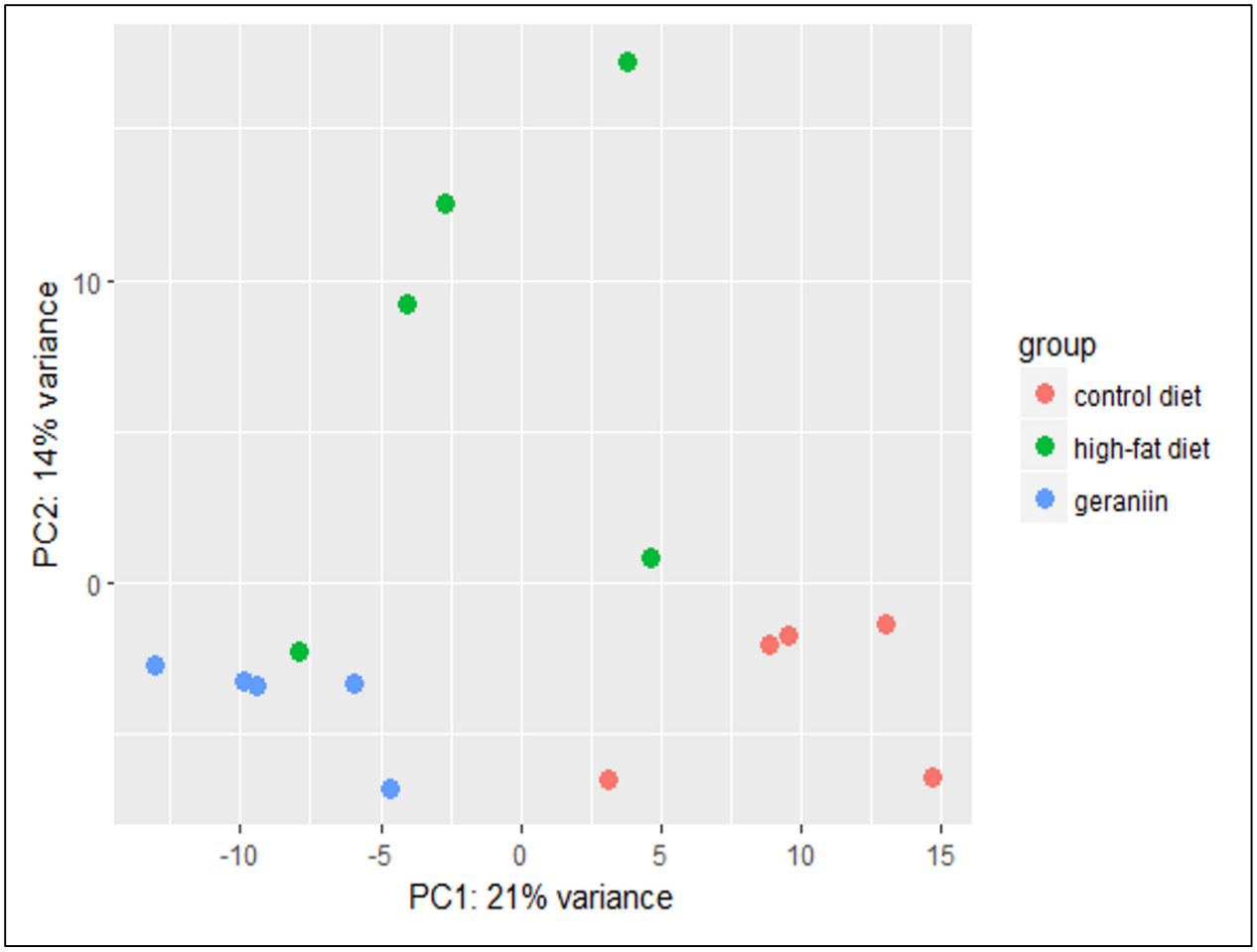

Figure 5.4: Principal component analysis to show the grouping pattern of the liver transcriptomes of the rats subjected to different treatments. The percentages of variance at the x- and y-axes indicate how much variance that can be explained by principal components (PC) 1 and 2, respectively.

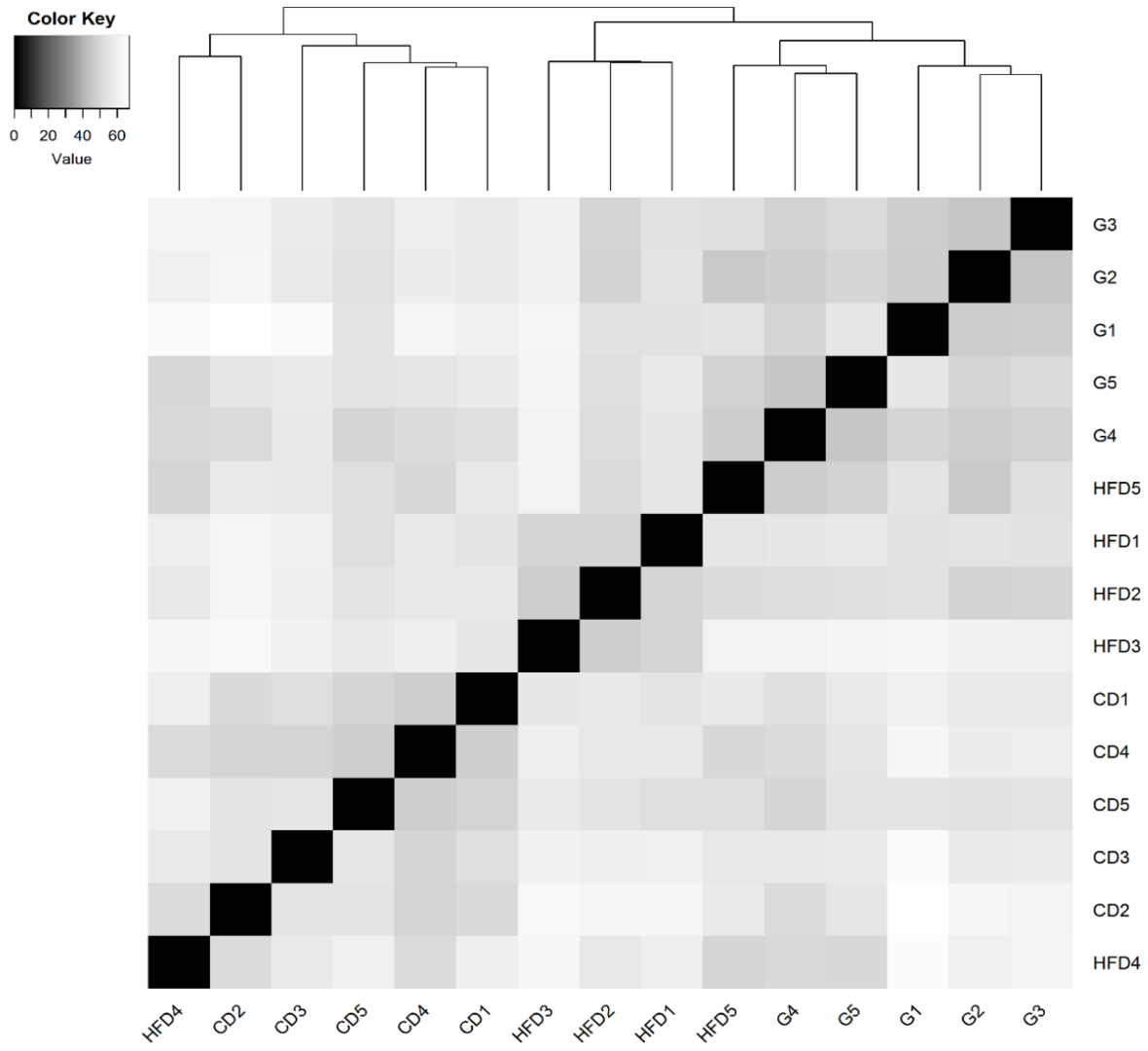

Figure 5.5: Hierarchy clustering analysis of the hepatic transcriptomes represented with a combination of a dendrogram (on top) and a heatmap. The dendrogram shows two major clusters that distinguish CD-treated rats from the rats of other treatment groups. The heatmap shows that the samples of the same treatment are more similar to each other (darker color) than to samples of other treatments (brighter color). CD, control diet; G, geraniin; HFD, high-fat diet.

5.4.3. Differentially expressed genes (DEGs)

Based on Deseq2, there were 554 DEGs (279 upregulated; 275 downregulated) between HFD and CD groups. Treatment with geraniin resulted in 553 DEGs (163 upregulated; 390 downregulated) compared to the rats on HFD. The top 40 DEGs (based on adjusted *p*-value) of

each comparison are summarized in **Tables 5.2 and 5.3** respectively. A Venn diagram of the two sets of DEGs revealed 94 overlapping DEGs (**Figure 5.6**). Most of the overlapping genes were either up- or downregulated by high-fat feeding, but were normalized by geraniin. Such a reverse expression pattern between HFD and geraniin groups is clearly visualized in **Figure 5.7**. Nevertheless, the overlapping DEGs compose about 20% of the total DEGs between geraniin and HFD-treated rats, indicating that majority of the genes modulated by geraniin are independent of the effects of high-fat feeding. The results not only demonstrate that geraniin could induce notable changes to the hepatic expression profiles, but also suggests the possibility of it having other independent molecular mechanisms.

Table 5.2: Overview of top 40 differentially expressed genes comparing the rats on high-fat diet to control diet.

Upregulated differentially expressed genes in the high-fat diet group relative to control diet group			
Gene Symbol	**Full Name**	**Fold Change**	**Adjusted *p*-value**
Ccdc146	Coiled-coil domain containing 146	3.09	8.95E-11
Cyp2c22	Cytochrome P450, family 2, subfamily c, polypeptide 22	2.62	1.27E-09
Slc6a6	Solute carrier family 6 member 6	2.50	1.93E-05
Gfra3	GDNF family receptor alpha 3	2.47	2.85E-07
Cxcl13	C-X-C motif chemokine ligand 13	2.36	7.24E-05
Gck	Glucokinase	2.33	9.20E-05
Ppard	Peroxisome proliferator-activated receptor delta	2.27	9.94E-05
Adamdec1	ADAM-like, decysin 1	2.26	1.29E-04
Tubb2a	Tubulin, beta 2A class IIa	2.24	7.98E-05
Ccdc141	Coiled-coil domain containing 141	2.24	2.13E-04
Acsl3	Aacyl-CoA synthetase long-chain family member 3	2.22	4.25E-11
Cyp7b1	Cytochrome P450, family 7, subfamily b, polypeptide 1	2.15	2.12E-04
Ptprn	Protein tyrosine phosphatase, receptor type, N	2.15	9.20E-05
RGD1305733	Similar to RIKEN cDNA 2900011O08	2.09	1.83E-04
Adam15	ADAM metallopeptidase domain 15	2.04	1.59E-10
Mk1	Mk1 protein	2.02	1.18E-10
Slc17a4	Solute carrier family 17, member 4	2.01	2.52E-05
Srebp1	Sterol regulatory element binding protein 1	1.91	2.80E-04
Trpm2	Transient receptor potential cation channel, subfamily M, member 2	1.83	7.08E-05

Cyp2c13	Cytochrome P450, family 2, subfamily c, polypeptide 13	1.81	1.83E-04
Arhgef19	Rho guanine nucleotide exchange factor 19	1.75	7.08E-05
Papd4	Poly(A) RNA polymerase D4, non-canonical	1.66	2.86E-10
Fggy	FGGY carbohydrate kinase domain containing	1.57	1.93E-05
Slc46a3	Solute carrier family 46, member 3	1.55	2.52E-05
Jmjd1c	Jumonji domain containing 1C	1.53	2.33E-04
Aadac	Arylacetamide deacetylase	1.52	1.39E-06
Syne2	Spectrin repeat containing nuclear envelope protein 2	1.50	2.71E-04
Downregulated differentially expressed genes in the high-fat diet group relative to control diet group			
Cyp17a1	Cytochrome P450, family 17, subfamily a, polypeptide 1	-3.26	6.09E-12
Ky	Kyphoscoliosis peptidase	-3.24	2.25E-10
Sdr16c6	Short chain dehydrogenase/reductase family 16C, member 6	-2.91	3.23E-08
Mycl	V-myc avian myelocytomatosis viral oncogene lung carcinoma derived homolog	-2.22	1.83E-04
Nampt	Nicotinamide phosphoribosyltransferase	-2.18	1.58E-04
Ptp4a1	Protein tyrosine phosphatase type IVA, member 1	-2.06	7.98E-05
Acot4	Acyl-CoA thioesterase 4	-2.03	1.20E-09
Got1	Glutamic-oxaloacetic transaminase 1	-1.87	1.66E-04
Cpt1a	Carnitine palmitoyltransferase 1A	-1.79	2.25E-09
Ppm1l	Protein phosphatase, Mg2+/Mn2+ dependent, 1L	-1.67	1.89E-04
Slc25a42	Solute carrier family 25, member 42	-1.62	2.16E-04
Sdsl	Serine dehydratase-like	-1.49	7.24E-05
Acot7	Acyl-CoA thioesterase 7	-1.49	1.51E-06

Table 5.3: Overview of top 40 differentially expressed genes comparing the high-fat diet treated rats with to those without geraniin supplementation.

Upregulated differentially expressed genes in the geraniin group relative to high-fat diet group			
Gene Symbol	**Full name**	**Fold Change**	**Adjusted *p*-value**
Slc30a3	Solute carrier family 30 member 3	2.42	9.81E-06
Fam169b	Family with sequence similarity 169, member B	2.21	2.13E-04
Rap1gap	Rap1 GTPase-activating protein	2.16	2.79E-04
Fam179a	Family with sequence similarity 179, member A	2.14	5.82E-04
Rtel1	Regulator of telomere elongation helicase 1	1.95	3.00E-04
Itgal	Integrin subunit alpha L	1.88	1.61E-04
Slc35c2	Solute carrier family 35 member C2	1.88	2.23E-05
Slc11a1	Solute carrier family 11 member 1	1.87	3.30E-05
Pitpnm1	Phosphatidylinositol transfer protein, membrane-associated 1	1.87	8.70E-08
Slc26a8	Solute carrier family 26 member 8	1.68	4.59E-04
Downregulated differentially expressed genes in the geraniin group relative to high-fat diet group			
Ddhd1	DDHD domain containing 1	-2.38	4.07E-05
Rps6	Ribosomal protein S6	-2.16	6.30E-04
Tcea3	Transcription elongation factor A3	-2.05	9.72E-07
Adh7	Alcohol dehydrogenase 7	-2.04	1.30E-03
Bche	Butyrylcholinesterase	-2.04	1.82E-04
C6	Complement C6	-1.88	1.73E-04
Golt1a	Golgi transport 1A	-1.83	4.21E-04
Leap2	Liver-expressed antimicrobial peptide 2	-1.79	2.58E-04
Fabp2	Fatty acid binding protein 2	-1.78	9.43E-03
Casp4	Caspase 4	-1.76	3.30E-05
Comt	Catechol-O-methyltransferase	-1.76	2.55E-04
Polr3k	RNA polymerase III subunit K	-1.66	4.20E-07
Fggy	FGGY carbohydrate kinase domain containing	-1.66	1.03E-06
Fabp1	Fatty acid binding protein 1	-1.55	1.90E-02
Mdh1	Malate dehydrogenase 1	-1.52	3.33E-05
Hspe1	Heat shock protein family E member 1	-1.51	4.53E-04

Dnajc3	DnaJ heat shock protein family (Hsp40) member C3	-1.51	6.88E-05
Ccng2	Cyclin G2	-1.49	5.87E-04
Uqcrb	Ubiquinol-cytochrome c reductase binding protein	-1.46	6.31E-07
Pgk1	Phosphoglycerate kinase 1	-1.46	6.88E-05
Akr1c3	Aldo-keto reductase family 1, member C3	-1.46	3.66E-04
Ttc23	Tetratricopeptide repeat domain 23	-1.46	6.20E-04
Aadac	Arylacetamide deacetylase	-1.46	4.71E-05
Ppdpf	Pancreatic progenitor cell differentiation and proliferation factor	-1.42	5.83E-04
Afm	Afamin	-1.42	4.58E-04
Cd164	CD164 molecule	-1.42	3.66E-04
Ndufv2	NADH:ubiquinone oxidoreductase core subunit V2	-1.41	8.97E-04
Tmem242	Transmembrane protein 242	-1.40	5.80E-04
Apoc3	Apolipoprotein C3	-1.40	1.82E-04
Apob	Apolipoprotein B	-1.33	3.37E-04

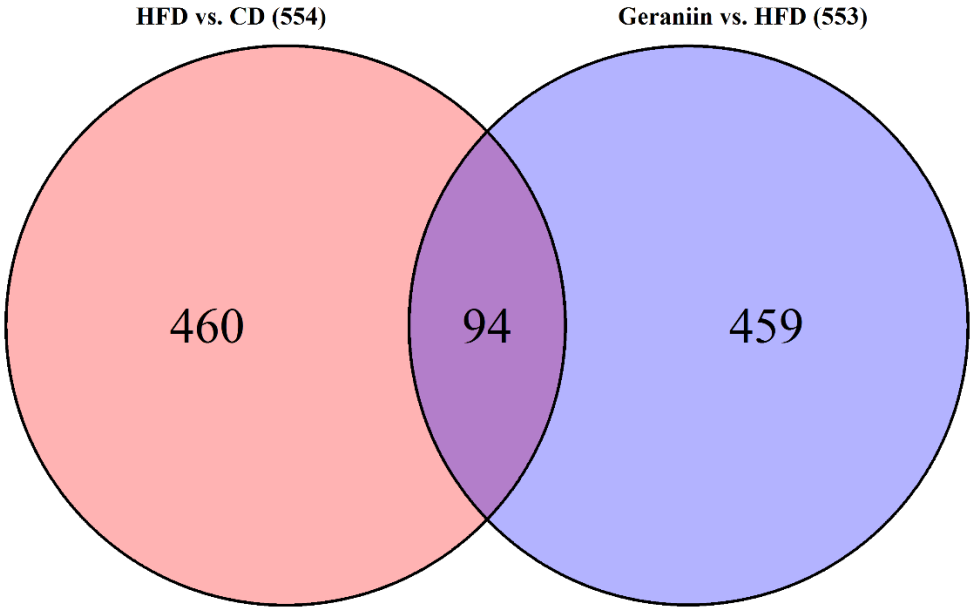

Figure 5.6: Venn diagram of the differentially expressed genes between two comparisons, **(i)** high-fat diet to control diet groups and **(ii)** geraniin to high-fat diet groups. The total number of differentially expressed genes found in each comparison are included in the parentheses.

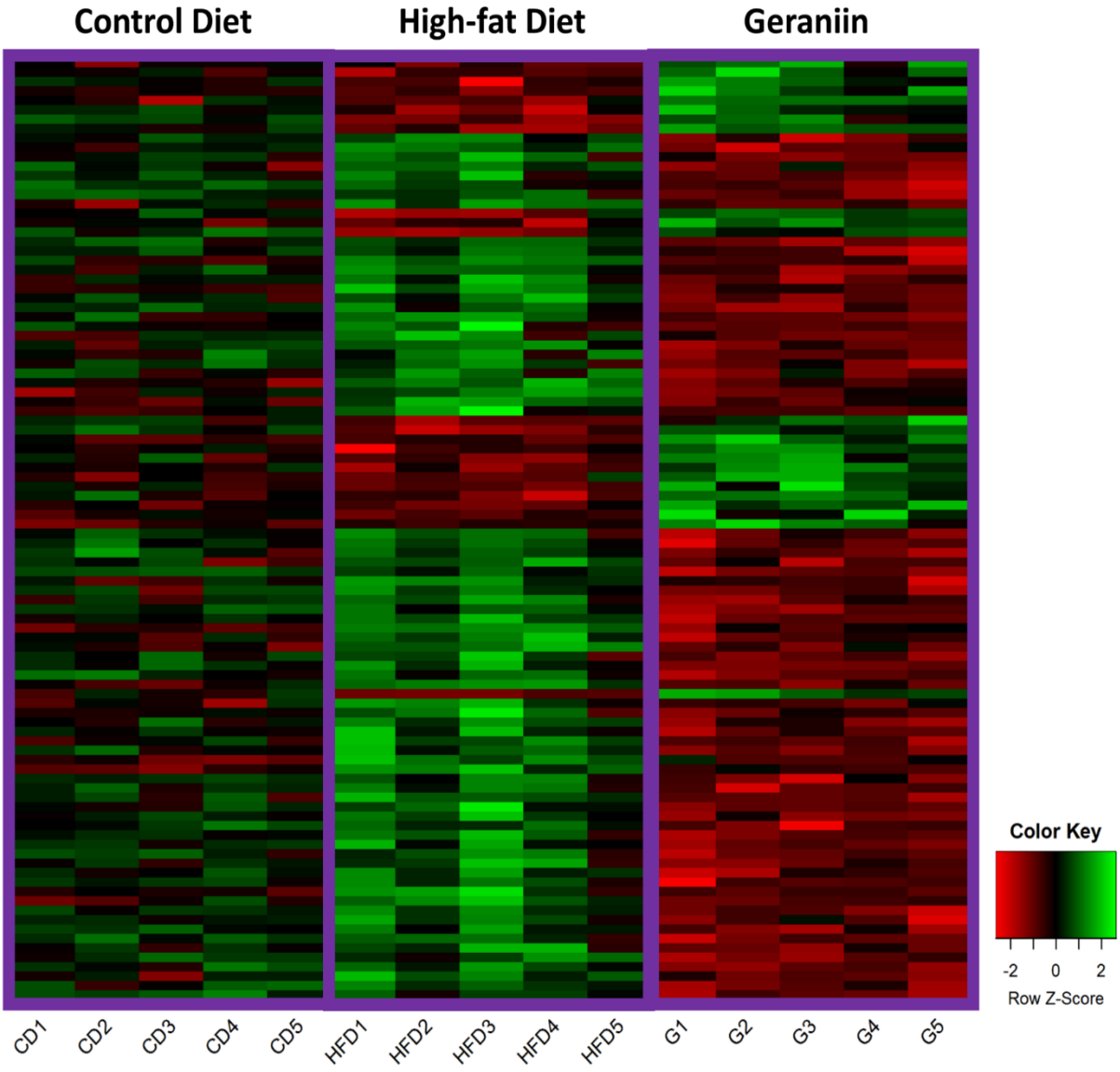

Figure 5.7: Heatmap of the top 100 most differentially expressed genes (with the smallest adjusted *p*-values) between geraniin- and high-fat diet-treated rats. Green color indicates upregulation while red color indicates downregulation relative to control diet group. CD, control diet; G, geraniin; HFD, high-fat diet.

5.4.4. Gene ontology and KEGG pathway analysis of DEGs

Using the DEGs obtained from Deseq2, gene ontology enrichment analysis was carried out to identify the activated or suppressed gene functions with different treatments. When comparing HFD to CD groups, most of the upregulated DEGs are linked to various lipid metabolic processes including the metabolism of organic acids, ketoacids, carboxylic acids and fatty acids

(**Figure 5.8**). Surprisingly, chronic high-fat feeding also induced the activation of steroid metabolism in the liver as exemplified by several enriched gene ontology terms like "steroid metabolic process", "steroid hydroxylase activity" and "aromatase activity" (**Figure 5.8**). On the contrary, the downregulated DEGs caused by HFD relative to CD groups resulted in only one significant gene ontology term – "small molecule metabolic process". Since none of the more specific terms were enriched, the suppressed functions caused by HFD in this study is inconclusive.

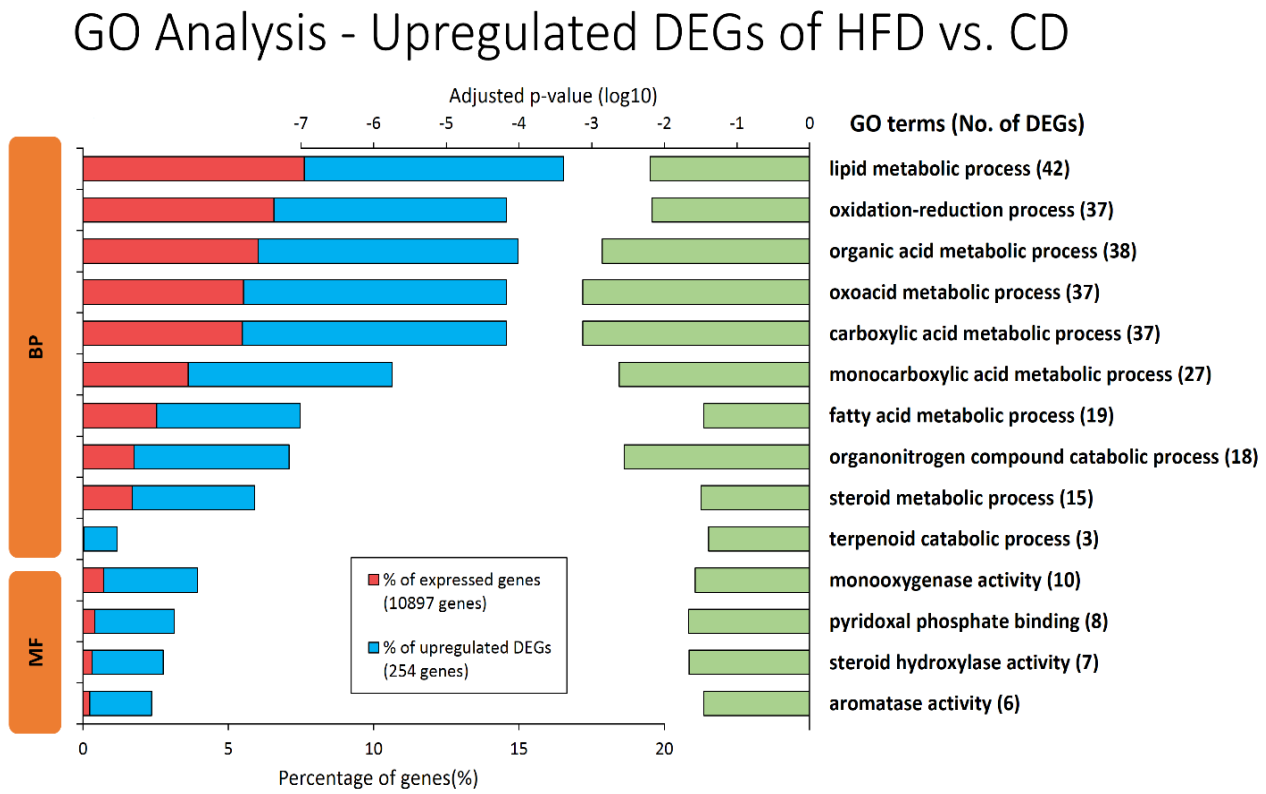

Figure 5.8: Gene ontology enrichment analysis of the upregulated differentially expressed genes induced by high-fat diet relative to control diet. Primary x-axis (bottom) indicates the percentage of genes for each gene ontology term at basal condition (red bars) and upon treatment with high-fat diet (blue bars) while the secondary x-axis (top) indicates the adjusted *p*-values (in log10 scale) of each comparison (green bars) between the basal and treatment conditions. The number of differentially expressed genes classified to each gene ontology term is shown in the parentheses. BP, biological pathway; CD, control diet; DEG, differentially expressed gene; HFD, high-fat diet; GO, gene ontology; MF, molecular function.

Similarly, the upregulated DEGs induced by geraniin in comparison to HFD group resulted in general gene ontology terms like "membrane part", "cell periphery" and "plasma membrane". As seen in **Figure 5.9**, most of the upregulated DEGs were involved in cellular components, of which close to 50% were associated with membrane components. The implicated membrane parts include the intrinsic and integral components of membrane as well as plasma membrane, implying that geraniin could affect the expression of certain membrane proteins. In addition to the cellular component gene ontology terms, approximately 9% of the upregulated genes induced by geraniin were responsible for the regulation of hepatic divalent cation homeostasis such as magnesium (Mg^{2+}), calcium (Ca^{2+}), cadmium (Cd^{2+}), nickel (Ni^{2+}) and zinc (Zn^{2+}).

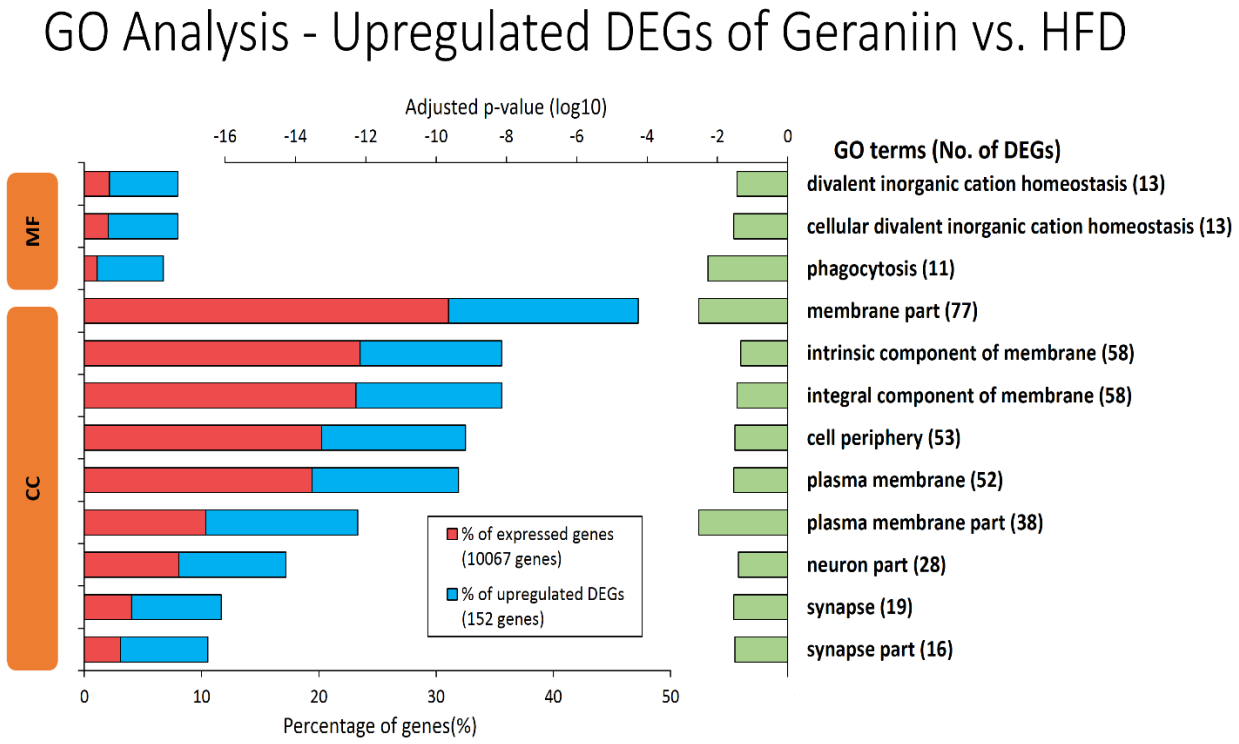

Figure 5.9: Gene ontology enrichment analysis of the upregulated differentially expressed genes induced by geraniin relative to high-fat diet group. Primary x-axis (bottom) indicates the percentage of genes for each gene ontology term at basal condition (red bars) and upon treatment with geraniin (blue bars) while the secondary x-axis (top) indicates the adjusted *p*-values (in log10 scale) of each comparison (green bars) between the basal and treatment conditions. The number of differentially expressed genes classified to each gene ontology term is shown in the parentheses.CC, cellular components; DEG, differentially expressed gene; HFD, high-fat diet; GO, gene ontology; MF, molecular function.

Because of the large number of downregulated DEGs between geraniin and HFD groups, the resultant enriched gene ontology terms are separated into three different illustrations (**Figures 5.10 to 5.12**) which represent the terms for biological pathways, cellular components and molecular functions, respectively. Based on **Figure 5.10**, many biological pathways involved in lipid and fatty acid metabolism were suppressed by the treatment with geraniin. The downregulated pathways include metabolic processes of organic acids, fatty acids, ketone, lipoproteins and carboxylic acids, of which many also overlap with the activated lipid metabolic processes caused by HFD. Furthermore, geraniin also significantly downregulated the genes responsible for steroid and cellular hormone metabolic processes. These findings suggest the ameliorative effects of geraniin on HFD-induced abnormal metabolic processes.

Aside from that, geraniin also repressed many biological pathways related to mitochondrial function such as "electron transport chain", "mitochondrial organization", "hydrogen ion transmembrane transport", and "regulation of cellular respiration" and "mitochondrial electron transport" (**Figure 5.10**). This suppressive activity of geraniin on mitochondrial function is more apparent in the cellular components gene ontology enrichment analysis. To elaborate, more than 80% of the downregulated DEGs caused by geraniin are related to membrane-bound organelles like mitochondria, endoplasmic reticulum and vesicles (**Figure 5.11**). Amongst these organelles, mitochondria are highly implicated because more than one third of the geraniin-induced downregulated DEGs are linked to mitochondria. The DEGs cover the mitochondrial matrix, membrane, ribosomes, respiratory chain complexes as well as ATP synthase complex (**Figure 5.11**). Likewise, in the molecular function gene ontology analysis, key mitochondrial activities like redox reaction, hydrogen transmembrane transportation, electron carrier activity, NADH dehydrogenase and succinate dehydrogenase activities were also overrepresented (**Figure 5.12**). Hence, based on the results, geraniin plays an influential role on the expression of mitochondrial-related genes.

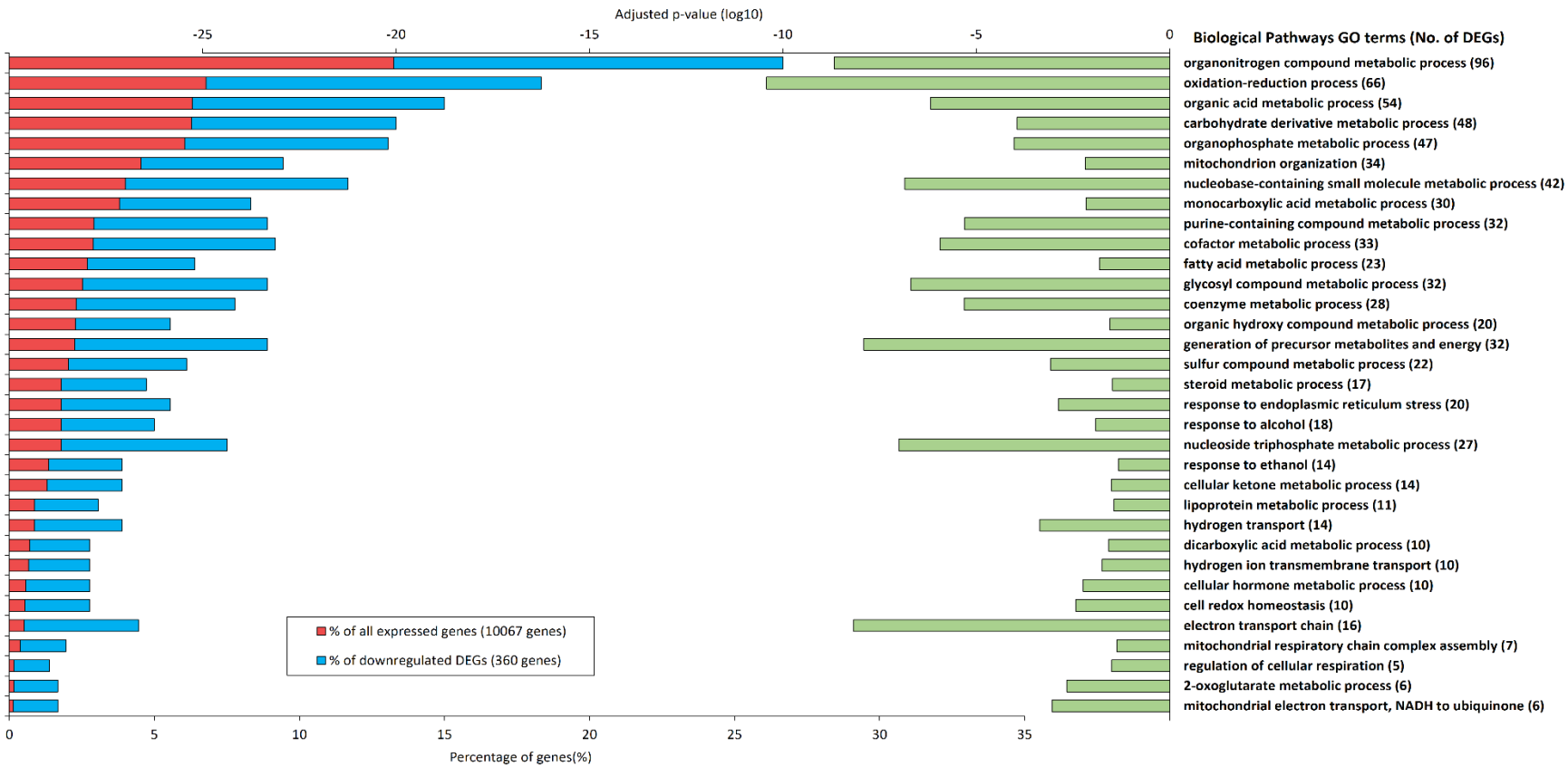

Figure 5.10: Gene ontology enrichment analysis of the biological pathways based on downregulated differentially expressed genes induced by geraniin relative to high-fat diet group. Primary x-axis (bottom) indicates the percentage of genes for each gene ontology term at basal condition (red bars) and upon treatment with geraniin (blue bars) while the secondary x-axis (top) indicates the adjusted *p*-values (in log10 scale) of each comparison (green bars) between the basal and treatment conditions. The number of differentially expressed genes classified to each gene ontology term is shown in the parentheses. DEG, differentially expressed gene; HFD, high-fat diet; GO, gene ontology.

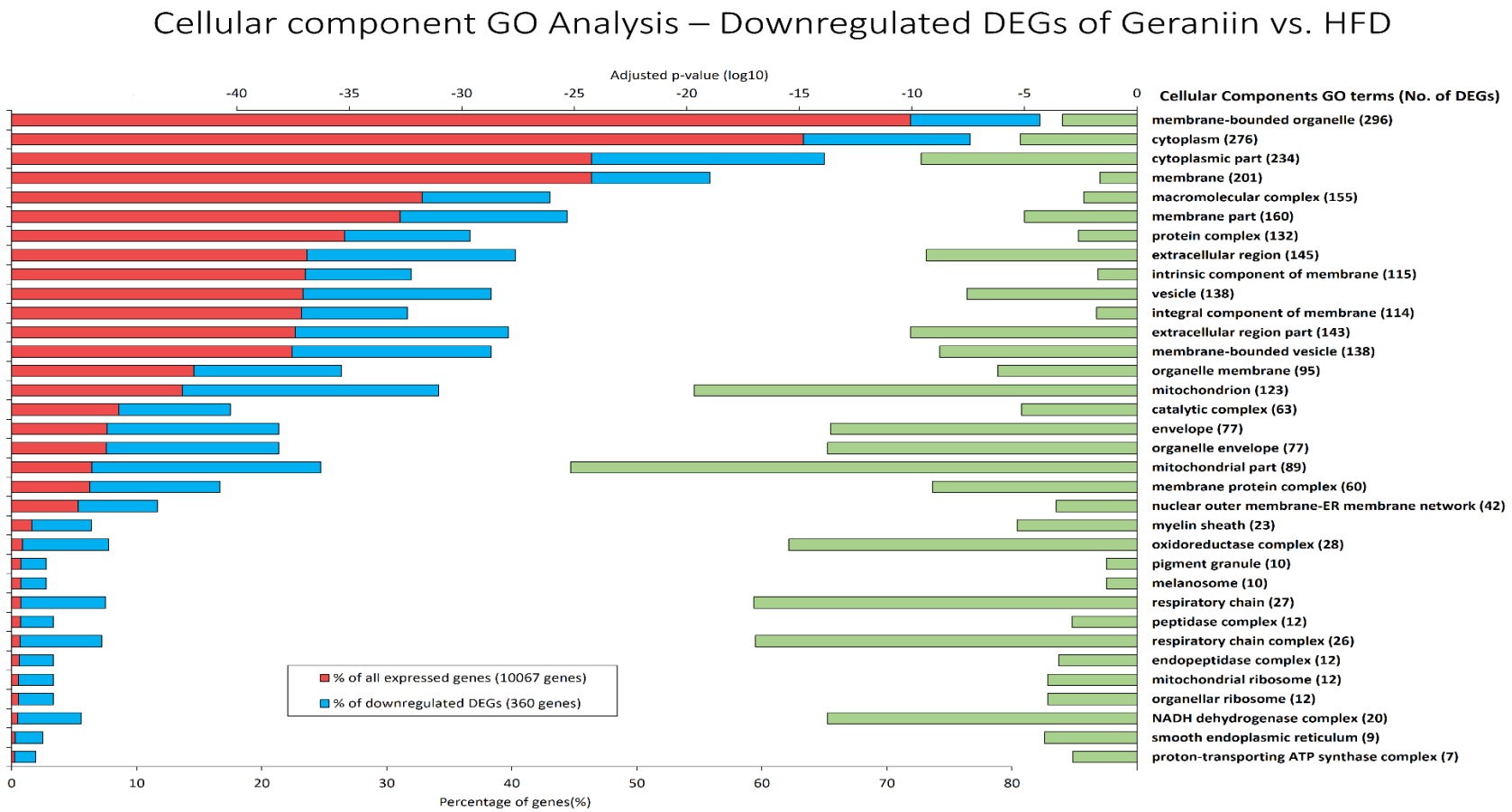

Figure 5.11: Gene ontology enrichment analysis of the cellular components based on downregulated differentially expressed genes induced by geraniin relative to high-fat diet group. Primary x-axis (bottom) indicates the percentage of genes for each gene ontology term at basal condition (red bars) and upon treatment with geraniin (blue bars) while the secondary x-axis (top) indicates the adjusted *p*-values (in log10 scale) of each comparison (green bars) between the basal and treatment conditions. The number of differentially expressed genes classified to each gene ontology term is shown in the parentheses. DEG, differentially expressed gene; HFD, high-fat diet; GO, gene ontology.

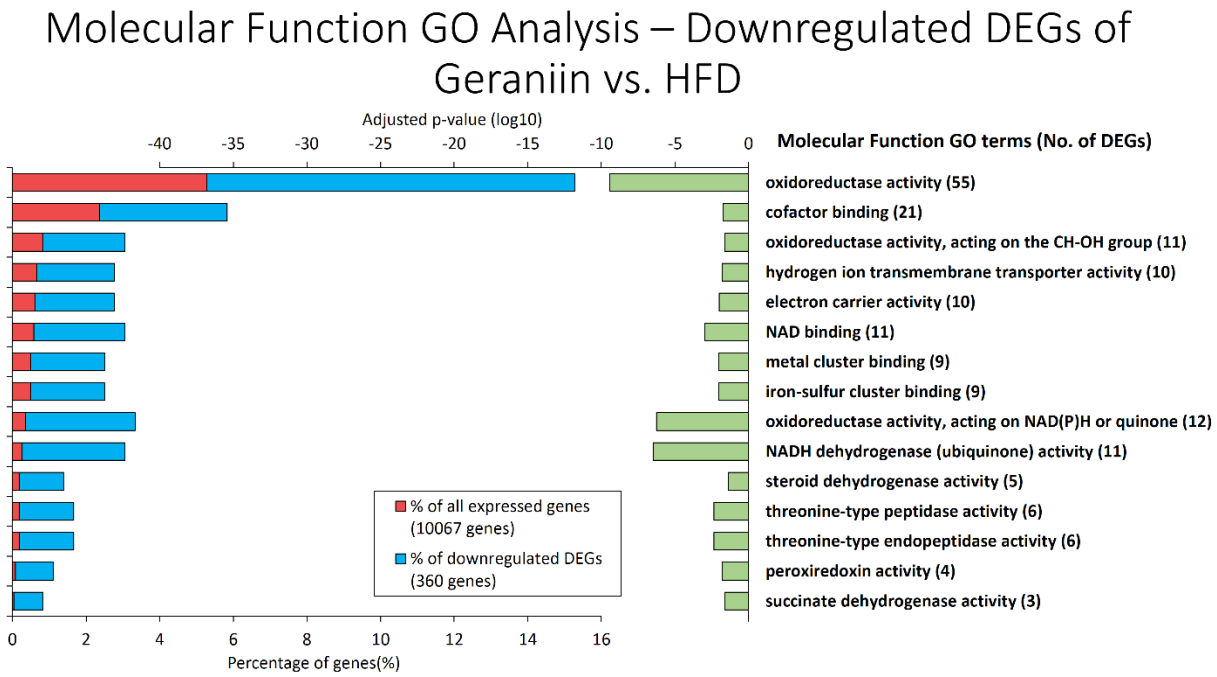

Figure 5.12: Gene ontology enrichment analysis of the molecular functions based on downregulated differentially expressed genes induced by geraniin relative to high-fat diet group. Primary x-axis (bottom) indicates the percentage of genes for each gene ontology term at basal condition (red bars) and upon treatment with geraniin (blue bars) while the secondary x-axis (top) indicates the adjusted *p*-values (in log10 scale) of each comparison (green bars) between the basal and treatment conditions. The number of differentially expressed genes classified to each gene ontology term is shown in the parentheses. DEG, differentially expressed gene; HFD, high-fat diet; GO, gene ontology.

Using the KEGG pathway analysis, "oxidative phosphorylation" was the most notable pathway over-represented by the suppressed DEGs caused by geraniin relative to HFD group. To visualize the suppressive effects of geraniin, DEGs between geraniin and HFD groups are mapped to the pathway. In **Figure 5.13**, it is evident that most of the genes or proteins that make up the protein complexes in the electron transport chain were downregulated by geraniin. This finding is in agreement with the gene ontology enrichment analysis and strongly suggests a modulatory effect of geraniin on the biological functions of mitochondria. Apart from oxidative phosphorylation, several metabolic pathways which are also suppressed by geraniin are summarized in **Table 5.4**.

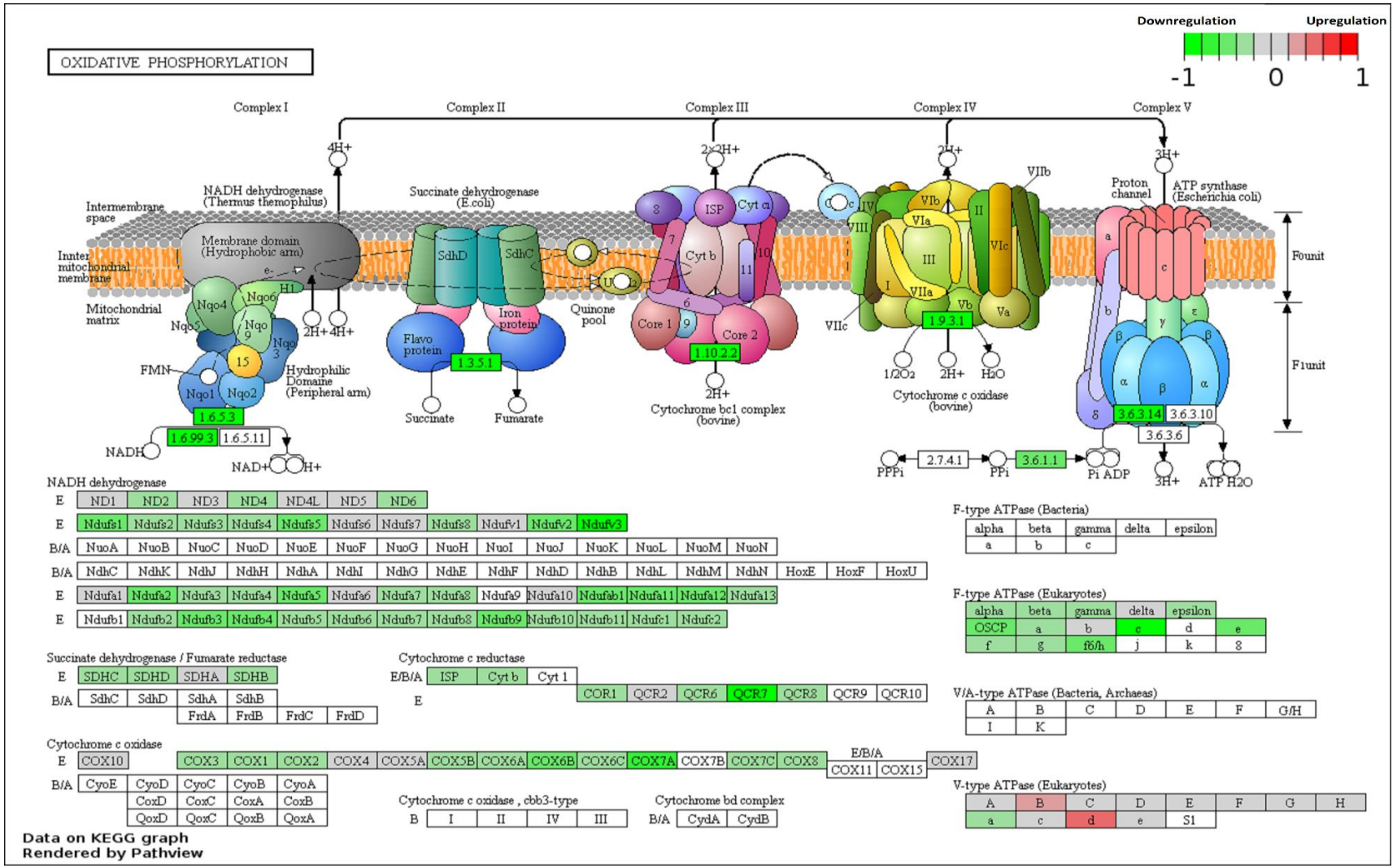

Figure 5.13: Differentially expressed genes induced by geraniin (relative to HFD-treated rats) mapped to the oxidative phosphorylation pathway. The subunits of major protein complexes involved in the pathway are illustrated in small square boxes and their expression levels are color coded (green – downregulation; red – upregulation; grey – unchanged; white – not expressed).

Table 5.4: KEGG pathways overrepresented by the downregulated differentially expressed genes of geraniin compared to high-fat diet groups.

Downregulated pathway	Number of DEGs involved in the KEGG term	Percentage of DEGs involved in the KEGG term (%)	Adjusted *p*-value
Oxidative phosphorylation	31	8.4	2.0×10^{-13}
Non-alcoholic fatty liver disease	27	7.3	6.3×10^{-9}
Metabolic pathways	83	22.4	1.2×10^{-8}
Citrate cycle (TCA cycle)	9	2.4	6.6×10^{-4}
Proteosome	10	2.7	2.4×10^{-3}
Protein processing in endoplasmic reticulum	18	4.9	6.8×10^{-3}
Biosynthesis of amino acids	11	3.0	1.2×10^{-2}
Carbon metabolism	14	3.8	1.2×10^{-2}

5.4.5. qPCR validation

Four genes which include *PPARα*, *PPARγ*, *Adh7* and *Ddhd1* were selected and subjected to qPCR to confirm if their expression patterns matched with the RNA sequencing data. *PPARα* and *γ* are linked to lipid metabolism whilst the expression of *Adh7* and *Ddhd1* were significantly affected by HFD and geraniin. Based on RNA sequencing result, the fold changes between HFD and CD groups for *PPARα*, *PPARγ*, *Adh7* and *Ddhd1* genes were -1.11, -1.03, 1.85 and 1.94-fold respectively ("-ve" sign denotes downregulation). On the other hand, the fold changes between geraniin and HFD groups for *PPARα*, *PPARγ*, *Adh7* and *Ddhd1* genes based on RNA sequencing data were 1.39, 1.19, -2.04 and -2.38 respectively. As seen in **Figure 5.14**, the gene expression patterns based on qPCR were consistent with the RNA sequencing-based transcriptomics analysis.

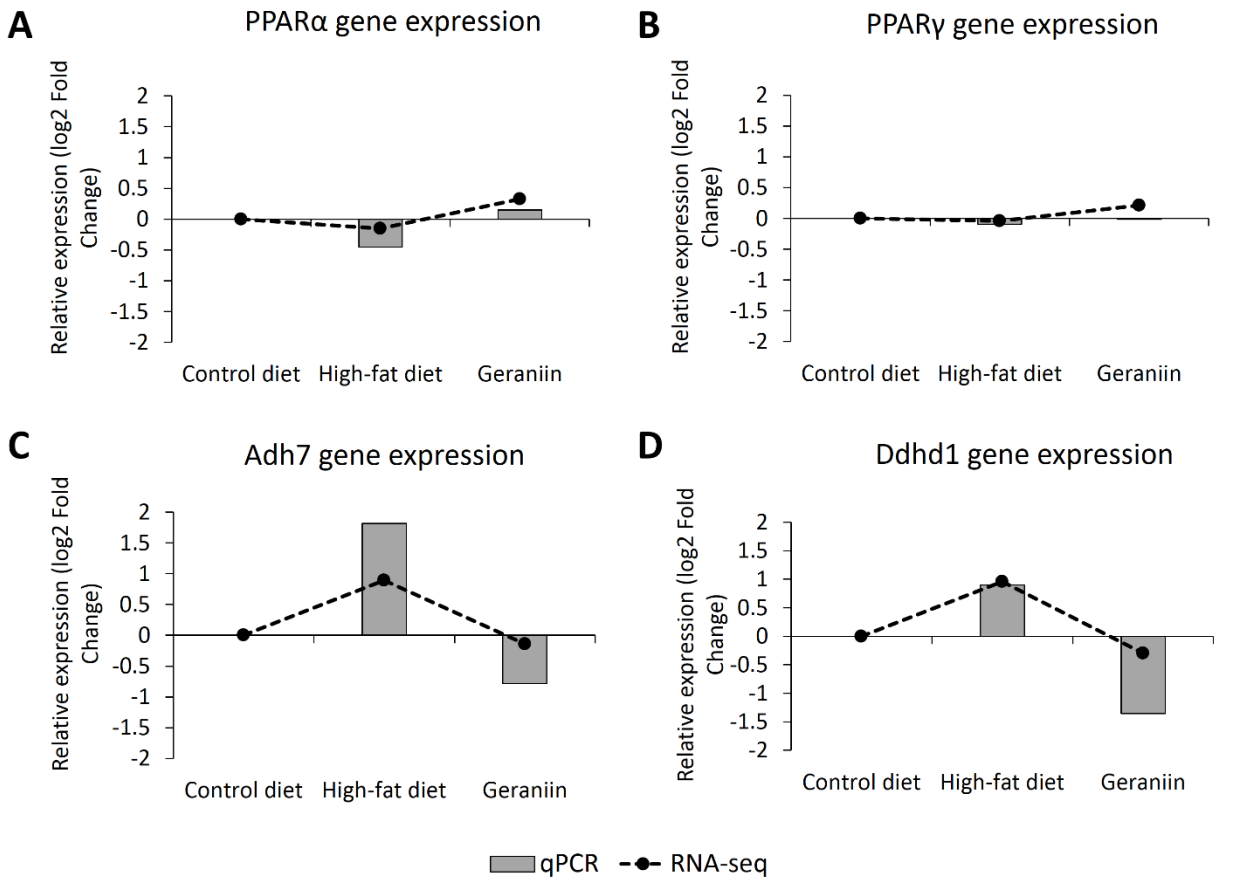

Figure 5.14: Comparison of the expression profiles of *PPARα* **(A)**, *PPARγ* **(B)**, *Adh7* **(C)** and *Ddhd1* **(D)** between RNA sequencing and qPCR. Sample size was *n*=5 per group for both RNA sequencing and qPCR assays. RNA-seq, RNA sequencing; qPCR, quantitative polymerase chain reaction.

5.5. Discussion

In the present study, transcriptomic analysis of the liver specimens from the rats treated with CD, HFD or geraniin was carried out to examine the molecular mechanism of geraniin in MetS. In general, our data demonstrates that treatment with geraniin significantly alters the expression of genes involved in mitochondrial structures and functions. To our knowledge, this is the first time such a modulatory effect of geraniin on mitochondria has been reported. This biological activity could potentially serve as the predominant mechanism that leads to the observed health benefits of geraniin in HFD-induced MetS.

The three treatments, namely CD, HFD and geraniin, resulted in three distinct clusters of the hepatic transcriptomes. This suggests that feeding on different diets as well as supplementation

with geraniin could induce distinctive influences to the expression profiles in the liver. Based on the grouping patterns, the transcriptomes originated from HFD and geraniin groups were more closely related to each other than with those from CD group. This is plausible given that the rats from both HFD and geraniin groups essentially fed on the same diets for the entire experiment. Furthermore, such a grouping pattern also points out that treatment with geraniin did not normalize all the transcriptional perturbations caused by HFD. Thus, the pleiotropic beneficial effects conferred by the natural product are attributable to selective biological pathways.

On the other hand, the hepatic transcriptomes of the rats on HFD showed a higher inter-group variation compared to the other two groups. In fact, various studies have reported a sizable inter-individual variability in terms of the weight gain and physiological changes after the exposure of high-calorie feeding to both rodents and humans [349-351]. The phenotypic differences are also reflected in the adipocyte and liver transcriptomes whereby several signaling cascades like the cAMP-dependent, AMPK as well as atherosclerosis signaling pathways were differentially expressed between C57BL/6J mice of different obesity susceptibility [352]. As such, considering the multifactorial properties of chronic diseases like obesity and MetS, it is not surprising to observe higher hepatic transcriptomic variability in response to HFD.

Compared to CD, HFD induced the overexpression of genes involved in lipid and fatty acid metabolic processes, likely because of the increased lipid influx after prolonged high-fat feeding. The finding is consistent with previous studies [353, 354]. Notably, one of the most upregulated genes is acyl-CoA synthetase 3 (*Acsl3*) whose function is to promote the formation of lipid droplet and VLDL [355, 356]. In the present study, *Acsl3* gene in the liver was upregulated by 2.22-fold. Knockdown of *Acsl3* in rat hepatocytes significantly suppressed the activity of several lipogenic transcription factors, including PPARγ, carbohydrate-responsive element-binding protein (ChREBP), sterol regulatory element-binding protein 1c (SREBP1c) and liver X receptor α (LXRα), signifying a vital role of the gene in hepatic lipogenesis [357]. Indeed, this is also confirmed in our study, whereby certain aforementioned transcription factor like *SREBP1* (upregulated by 1.91-fold) and *PPARδ* (upregulated by 2.27-fold) alongside with their targets genes were overexpressed in rats subjected to HFD. However, hepatic *PPARγ* gene of HFD-treated rats was not significantly upregulated compared to those on CD. This finding is not in line with that observed in the **Chapter 2**, in which *PPARγ* was highly expressed in post-weaning

rats on HFD relative to those on CD. It is worth mentioning that the hepatic *PPARγ* expression of the adult rats given high-calorie diets in the experiment described in **Chapter 2** also remained unchanged. This would suggest that the activation of hepatic *PPARγ* is probably age-dependent. Indeed, one study reported that the activation of *PPARγ* induced by ischemic stress differed significantly between ages, whereby the gene remained activated for a longer period of time in young mice, but not adult and old mice [358]. Such a prolonged activation of *PPARγ* could serve as a hepatoprotective mechanism in young rodents whose livers are relatively under-developed [358]. The age-dependent *PPARγ* activation may explain the lack of *PPARγ* overexpression in older rats (12 weeks) on HFD, but further investigation is required to verify the postulation. In short, the dysregulated lipid metabolism in the liver would explain the occurrence of hypertriglyceridemia in the blood circulation as well as the onset of NAFLD in the HFD-treated rats [359].

Furthermore, in the present study, the activation of hepatic steroid hormone metabolism was observed in rats on HFD. This has been consistently reported in other obese rodent models [360, 361]. Even though the liver is not a steroidogenic tissue, it actively participates in the conversion, inactivation and elimination of steroid hormones. The processes, which take place in the liver microsomes, are disrupted in people with chronic metabolic disorders [362]. For instance, in patients with NAFLD, the key regulatory genes in cholesterol and steroid metabolism like *SREBP2* and *steroidogenic acute regulatory protein* (*StAR*) are overexpressed up to 15-fold higher than normal individuals [363]. Similarly, the conversion of cortisone to cortisol, a process that affects the local concentration of active glucocorticoids (a type of chronic stress hormone), is also severely altered in the liver and subcutaneous adipose tissues of obese people [364]. In male Wistar rats, constant high-fat feeding led to reduced testosterone and increased 17β-estradiol concentrations in the blood circulation [361]. This coincides with our transcriptomic analysis which showed that genes involved in aromatase activity, namely cytochrome P450 families 2 and 3, were upregulated by HFD. The enhanced aromatase activity is also observed in other peripheral tissues like subcutaneous and gonadal adipose tissues in obese male mice [365]. Consequently, this could promote peripheral conversion of androgen to estrogen (*eg.* testosterone to 17β-estradiol) and result in obesity-related male hypogonadism [366, 367]. As such, based on the hepatic transcriptomic study, chronic high-fat feeding could interfere with the metabolic pathways of lipid and steroid hormones, contributing to the onset and progression of MetS.

The treatment with geraniin brought about significant changes to the hepatic transcriptomes. One implicated pathway is the lipid and fatty acid metabolism, as exemplified by the transcriptional suppression of several key genes involved in lipid transport and fatty acid elongation. In terms of lipid transport, notable geraniin-induced downregulated genes are fatty acid binding protein 1 and 2 (*Fabp1* & *Fabp2*) which were downregulated by 1.55- and 1.78-fold respectively. Fatty acid binding proteins are intracellular lipid chaperones that can interact reversibly with a wide array of hydrophobic ligands to facilitate lipid storage, trafficking, catabolism or signaling [368]. The types of ligands range from saturated and unsaturated fatty acids, cholesterols, bile acids to eicosanoids. Many studies have found a strong positive correlation between the levels of fatty acid binding proteins with various metabolic diseases such as obesity, MetS, diabetes mellitus, fatty liver disease, atherosclerosis and chronic kidney disease, implying a crucial role in the pathogenesis of the diseases [369-373]. This is further supported by the evidence from loss-of-function genetic models, in which *Fabp1* and *Fabp2* knockout mice are protected against the onset of HFD-induced obesity and hepatic steatosis [374-376]. The protective effect is accompanied by a change in primary energy substrate from lipids to carbohydrates, indicating the regulatory role of fatty acid binding proteins in lipid homeostasis [376]. Additionally, several selective inhibitors of fatty acid binding protein isoforms such as *Fabp 3*, *Fabp4* and *Fabp5* have also exhibit promising anti-atherosclerosis, anti-diabetes and anti-MetS effects [377]. These discoveries make them some of the most popular therapeutic candidates for chronic metabolic diseases in recent years. Hence, based on the evidence, it is speculated that geraniin-induced inhibitory effect on the expression of *Fabp1* and *Fabp2* expression could partly contribute to the amelioration of metabolic dysregulation.

Apart from lipid transportation, treatment with geraniin also inhibited the genes for fatty acid elongation like *Elovl2*, *Acsl3* and *Acsl5*. The crucial role of *Acsl3* in hepatic lipogenesis has been elaborated previously. Like *Acsl3*, *Acsl5* and *Elovl2* are also important mediators of triglyceride and fatty acid biosynthesis as well as lipid droplet formation [378, 379]. The ablation of *Elovl2* in mice results in remarkable resistance against diet-induced hepatic steatosis and weight gain, besides significantly reducing the body fat mass [380]. Likewise, whole-body abolishment of *Acsl5* not only reduces overall acyl CoA synthetase activity in the liver and brown adipose tissues by 50% and 37%, respectively, but also promotes energy expenditure and inhibits intestinal lipid absorption [381]. A number of the phenotypes detected in *Elovl2*, *Acsl3* and *Acsl5*

knockout mice were also observed in the rats supplemented with geraniin. Speculatively, geraniin-induced transcriptional inhibition of these genes could confer a protective barrier against the nutritional insult from chronic high-fat feeding via reduced ectopic fat deposition and *de novo* lipogenesis. The beneficial metabolic effect could be reinforced by the suppression of lipid trafficking, leading to the restoration of lipid and glucose homeostasis seen in geraniin-treated rats.

Based on the gene ontology enrichment analysis, the steroid metabolic process was the other metabolic pathway that was activated by HFD, but repressed by geraniin. The inhibitory effect appears to be selective to the gene expression of 17β-hydroxysteroid dehydrogenases (*HSD17B*) as evidenced by the downregulation of several isoforms of the genes including *HSD17B4, AKR1C3* (also known as *HSD17B5*), *HSD17B6* and *HSD17B12*. Principally, the primary physiological function of most HSD17B enzymes is to catalyze the inter-conversion of steroid hormones, namely estrogens and androgens, between their active and inactive forms in the presence of cofactors like $NAD(P)^+$ and NAD(P)H [382]. Certain isoforms also possess multifunctional properties and are involved in the metabolism of bile acids, fatty acids and cholesterols [383]. In this context, the proteins encoded by *HSD17B4* and *HSD17B6* are oxidative enzymes which catalyze the steroid hormone inactivation [384, 385] while those encoded by *AKR1C3* and *HSD17B12* are reductive enzymes that perform the reverse reaction [386, 387]. The bidirectional inhibition of steroid hormone inter-conversion caused by geraniin suggests an overall reduction in the steady-state levels of the local steroid hormones. Consequently, a number of steroid-dependent target genes like apolipoproteins B (*Apob*), apolipoprotein C1 (*Apoc1*) and C3 (*Apoc3*) were concomitantly downregulated with the treatment of geraniin [388]. These apolipoproteins are known for their strong association with numerous chronic metabolic disorders like dyslipidemia, MetS and coronary heart disease [389, 390]. Therefore, it is hypothesized that upon the treatment with geraniin, the transcriptional suppression of HSD17B isozymes in the liver could lead to downstream repression of apoliprotein expression, which in turn, ameliorated the lipid metabolic dysregulation such as hypertriglyceridemia and elevated non-HDL cholesterols in the blood circulation. Nevertheless, the current research paradigm of HSD17B enzymes emphasizes on its therapeutic potential for breast cancer, prostate cancer, acne and osteoporosis [391]. The implication of the enzymes in obesity and MetS is comparatively limited. However, emerging evidence does support the

pathological role of certain HSD17B isoforms in the onset of hepatic steatosis and diabetic-related skin degeneration, making the proteins an attractive target for MetS therapy [392, 393].

Interestingly, according to the liver transcriptome analysis, the supplementation of geraniin significantly downregulated many genes linked to mitochondrial function and structural composition such as the electron transport chain complexes, ATP synthase, mitochondrial membrane, matrix and ribosomes. This finding highlights a potent regulatory role of the natural product in mitochondrial function. To date, there is no direct proof about the effects of ellagitannin geraniin on the mitochondria. However, indirect evidence of such mitochondrial-modulating properties has been reported by recent studies about the predominant *in vivo* bioactive metabolites of geraniin – urolithins. For example, urolithin A has been shown to trigger mitophagy to hamper the deterioration of mitochondrial dysfunction; subsequently, leading to prolonged lifespan in *Caenorhabditis elegans* and improve motor function in mice with age-related muscular decline [394]. The regulatory effect of urolithin A on the expression of mitochondrial-related genes in the skeletal muscles has been confirmed again in a Phase I clinical study that employed healthy elderly people [395]. Furthermore, many well-known polyphenolic compounds such as resveratrol, quercetin, epigallocatechin-3-gallate and curcumin could also influence a myriad of mitochondrial events, ranging from mitochondrial biogenesis, mitochondrial membrane potential, electron transport chain, ATP synthesis and mitochondrial-mediated programmed cell death [396]. Considering that the mitochondrial-modulatory action appears to be a shared characteristic between various polyphenols, it is therefore, plausible to observe the regulatory effect on the expression of mitochondrial-related genes in geraniin and geraniin-derived metabolites.

In this context, the role of mitochondria in the pathophysiology of chronic metabolic diseases have been increasingly recognized. However, geraniin appears to suppress the expression of mitochondrial-related genes. It should be noted that mitochondrial dysfunction does not always reduce mitochondrial number. Some studies concluded a positive correlation between mitochondria proteins and DNA with BMI, whereby the circular mitochondrial genomes as well as mitochondrial citrate synthase activity were significantly increased in obese patients, especially among those without diabetes mellitus [397, 398]. This reflects a compensatory mechanism by increasing the number of mitochondria in response to the progression of

mitochondrial impairment caused by nutritional insults. On the contrary, site-specific reduction of mitochondrial count in the adipose tissues has been shown to be beneficial as it preserves insulin sensitivity and inhibits accelerated weight gain due to high-fat feeding in mice despite the occurrence of local mitochondrial stress [399]. These controversial findings point out that the mitochondrial number may not be an ideal indicator of the mitochondrial function (or dysfunction), at least under the circumstance of chronic metabolic diseases. As a matter of fact, several recent studies put forward the notion that the selective elimination of damaged mitochondria via mitophagy can effectively annihilate the pathogenic manifestations of mitochondrial dysfunction without jeopardizing the normal function of mitochondria [400-402]. Hence, by promoting the turnover of defective mitochondria, it may be more effective in restoring the collective physiological properties of the mitochondria and tissues than by enhancing the sheer number of mitochondria.

In relation to our transcriptomic results, it is believed that the geraniin-induced suppression of mitochondrial-related genes could help to ameliorate the perturbed metabolic processes caused by abnormal mitochondria in HFD-treated rats. Vernochet et al. (2012) concluded that reduced mitochondrial DNA copy number and proteins due to mitochondrial transcription factor A (TFAM) ablation in the adipose tissues of mice exceedingly elevates the oxygen consumption and protects against diet-induced obesity, insulin resistance and hepatosteatosis [399]. Furthermore, the selective downregulation of nuclear DNA-encoded mitochondrial genes could potentially alter the stoichiometric balance between nuclear- and mitochondrial-encoded proteins, particularly those that make up the oxidative phosphorylation complexes, resulting in a condition termed “mitonuclear protein imbalance” [403, 404]. In response to such an imbalance, mitochondria will activate the mitochondrial unfolded protein response (UPR^{mt}) to markedly enhance the synthesis of mitochondrial chaperones such as heat shock proteins [404, 405]. These mitochondrial chaperones are crucial for the maintenance of proper protein folding, assembly and function, which in turn, assists in the restoration of mitochondrial biogenesis and diminishes mitochondrial dysfunction [406]. In fact, mitonuclear protein imbalance followed by the UPR^{mt} activation acts as an integral mechanism to promote longevity in *C. elegans* [404]. On the contrary, loss of function of certain mitochondrial chaperone (*eg.* heat-shock protein 60) in the hypothalamus results in mitochondrial dysfunction, increased ROS production and the accelerated progression of insulin resistance [407]. As such, the suppression nuclear-encoded

mitochondrial genes observed in the present study could potentially induce the UPR^{mt} and confer an ameliorative effect on HFD-induced mitochondrial dysfunction.

On the other hand, the relationship between the transcriptional repression of mitochondrial genes and mitophagy is unclear because there was no noticeable change in the key mitophagic regulatory pathways like PINK/Parkin, BNIP3 and Nix as well as Fundc1 cascades [408]. Nonetheless, certain autophagy and mitophagy mediators like phosphatase and tensin homolog (*Pten*), double-stranded RNA-activated protein kinase-like endoplasmic reticulum kinase (*Perk*), transcription factor EB (*TFEB*), transcription factor E3 (*TFE3*) and autophagy protein 16 (*Atg16*) were significantly upregulated by the treatment with geraniin [409], revealing possible involvement of geraniin in the regulation of mitophagy.

Taken together, despite the growing evidence that supports the critical role of mitochondria in obesity, MetS and diabetes mellitus, the mechanisms underlying the regulation of mitochondrial dynamics, biogenesis and mitophagy remain convoluted and uncertain. As such, the impacts of ellagitannin geraniin on mitochondrial function in the presence of metabolic diseases undoubtedly warrant further clarification. The core finding of the present study is however, encouraging as it provides novel and solid evidence on the interaction between geraniin and the expression of mitochondrial-related genes, making it worthwhile for further exploration on its therapeutic effects on MetS via the modulation of mitochondrial function and dynamics.

One limitation of the present study is that the mRNA sequencing analysis was performed with only liver transcriptomes, mainly due to financial constraints. Without the transcriptomic analysis from other metabolically-active tissues like the skeletal muscles and adipose tissues, geraniin's ability to induce similar changes to the expression profile of these tissues remains inconclusive. Extrapolating the findings from purely hepatic transcriptomic analysis is impractical due to tissue-dependent differences in the expression profiles, particularly with respect to highly implicated pathway like mitochondrial function. Therefore, to explore the comprehensive picture of geraniin-induced systemic changes in the metabolic pathways, profiling the transcriptomes at various tissues is highly encouraged. Additionally, given our relatively small sample size (n=5 per group), the findings of transcriptomic study are principally exploratory. Moreover, as the mitochondrial-modulatory effect of geraniin was not anticipated prior to the experiment, the biomarkers related to mitochondrial dynamics such as morphological

changes, ATP production and ROS generation were not quantified. Hence, more investigations are warranted to delineate the interaction of geraniin with several metabolic pathways like lipid and steroid metabolism as well as mitochondrial activity in a more explicit manner.

5.6. Summary and key highlights of the study

The key findings of the experiment presented in this chapter are summarized as follows:

- Treatment with CD, HFD or supplementation with geraniin at a daily dosage of 25 mg/kg had induced significant changes to gene expression profile in the liver which resulted in unique transcriptomes according to the mRNA sequencing data.
- Compared to CD, chronic high-fat feeding triggered the overexpression of genes involved in fatty acid and lipid metabolism, most of which favors lipogenesis. These findings imply the activation of these processes due to elevated lipid uptake and influx, contributing to the onset of metabolic dysregulation in the MetS rat model.
- HFD also overexpressed the genes related to steroid metabolism, especially those linked to aromatase activity which is a key step in the conversion of androgens to estrogens. However, the role of HFD-dependent aromatase activation in the progression of obesity and MetS requires further investigation.
- Supplementation with geraniin successfully suppressed the overexpression of lipogenic genes induced by HFD. Furthermore, based on the gene ontology analysis, the natural product also played an inhibitory role on the steroid metabolic processes in the liver by downregulating genes from the HSD17B families. Collectively, the abnormal biochemical activities caused by HFD were reversed by the treatment with geraniin, contributing to the amelioration of MetS.
- Most notably, treatment with geraniin resulted in the suppression of mitochondrial-related genes in the liver. Pathway analysis revealed the involvement of the genes in various mitochondrial structures and biological functions, including electron transport chain, respiratory protein complexes, ATP synthase, membrane and matrix. Several mitophagy-related genes were also upregulated, suggesting potential regulatory effect of geraniin on selective clearance of defective mitochondria. As a result, the attenuation of mitochondrial

dysfunction may serve as the predominant mechanism of ellagitannin geraniin to reverse the devastating effects of HFD on glucose and lipid homeostasis in MetS.

In short, the hepatic transcriptomic study revealed the repression of geraniin on three metabolic pathways, namely lipid and fatty acid metabolism, steroid hormone metabolism and mitochondrial function, of which the first two were abnormally upregulated by high-fat feeding. By reversing the adverse impacts of HFD on the hepatic expression profile, geraniin could potentially restore the glucose and lipid homeostasis, leading to the observed health benefits in the MetS model. More importantly, treatment with geraniin also significantly downregulated the expression of numerous genes related to mitochondrial function besides upregulating mediators of mitophagy. To our best knowledge, this is a novel discovery. The finding indicates that geraniin could potentially modulate the clearance of damaged mitochondria which could lead to the recovery of optimal mitochondrial function and exert a protective barrier against nutritional insults caused by high-calorie diet. In this context, the mitochondrial dynamics remain as an exciting and yet, controversial aspects, particularly in the area of chronic metabolic diseases. Nonetheless, considering the exploratory nature of the transcriptomic study performed in the present study, further investigation is obligatorily necessary to elucidate the interaction of geraniin with the affected metabolic pathways and the possible implications.

CHAPTER 6

Conclusion and Future Work

6. CONCLUSION AND FUTURE WORK

6.1. Conclusion

To summarize, in the present project, several research tasks have been accomplished, including the creation of a diet-induced MetS model in rats, the investigation of the effects of ellagitannin geraniin in different aspects of metabolism, as well as the possible mechanisms to explain how geraniin improves health. In terms of the MetS model establishment, a remarkable interplay between the developmental stage of the rats and types of high-calorie diets was detected. Post-weaning rats (3-week old) on HFD for eight weeks displayed all the key features of MetS including increased weight gain, central adiposity, hyperglycemia, hypertension, dyslipidemia as well as increased ectopic lipid deposition in the liver. Unlike post-weaning rats, adult rats (8-week old) did not develop notable metabolic perturbation when feeding on HFD, but instead became obese and hypertensive (without glucose and lipid dysregulation) when feeding on HFSD. In general, compared to adult rats, post-weaning rats had overexpression of PPARα and PPARγ in the liver, which could contribute to the MetS susceptibility. As such, the enhanced vulnerability of post-weaning rats to MetS, particularly when feeding on HFD in comparison to HFSD, led to the manifestation of all crucial MetS-related abnormalities within a relatively short feeding duration. The disease induction approach was more effective and time-saving; therefore, it was selected as the disease model for the subsequent experiment.

Using the aforementioned MetS model, the metabolic effects of ellagitannin geraniin were examined. Treatment with geraniin at a dosage of 25 mg/kg/day for four weeks effectively normalized a wide range of metabolic anomalies induced by HFD, including hypertension, impaired fasting blood glucose, elevated HbA1c, hypertriglyceridemia and increased non-HDL cholesterols. The lipid deposition in the visceral adipose tissues and liver was also markedly reduced with geraniin supplementation. Furthermore, treatment with geraniin also restored the redox balance and lowered the IL-1β level in the blood circulation. The AGE level and hepatic *RAGE* expression was also inhibited by geraniin, alongside with an increase in *esRAGE* expression in the visceral adipose tissues, implying an AGE-lowering mechanism via AGE chelation and clearance. Based on the results, the oral consumption of geraniin could exert anti-

hypertensive, anti-hyperglycemic, lipid-lowering, anti-AGE-RAGE axis, anti-inflammatory and oxidative stress-reducing properties.

By comparison, the improvement on fasting glucose control and HbA1c conferred by geraniin was similar to metformin. Unlike metformin however, geraniin did not alleviate impaired glucose tolerance. Additionally, the ameliorative effects of geraniin on HFD-induced hypertension and increased non-HDL cholesterols was comparable to TRF, whose major composition: tocotrienols are a potent antioxidant and HMG-CoA reductase inhibitor. All three interventions, namely metformin, TRF and geraniin, were effective against increased oxidative stress and inflammatory response in the blood circulation. Notably, the positive impacts of geraniin on hypertriglyceridemia, hepatic steatosis and central adiposity were unmatched by the other two interventions. The range of beneficial bioactivities of geraniin on metabolism not only covers many features of MetS, but is also highly distinctive compared to metformin and TRF. This proposes a discrete underlying mechanism which is neither gluco- nor antioxidant-centric.

By studying the hepatic mRNA transcriptomes with next generation sequencing, it was revealed that daily supplementation of geraniin for a month could induce unique changes to the gene expression profile of the liver. A portion of the genes which were differentially (down)regulated by geraniin are linked to lipid and fatty acid metabolism as well as steroid hormones metabolism. These metabolic functions were transcriptionally activated by HFD, which could contribute to the progression of MetS. Hence, the geraniin-dependent suppression of these metabolic pathways could at least partly explain its ameliorative effects on HFD-induced metabolic dysregulation. Most notably, treatment with geraniin resulted in significant suppression of nuclear-encoded mitochondrial genes in the liver. These downregulated genes spanned over a wide range of mitochondrial structures and functions, particularly electron transport chain, respiratory protein complexes, ATP synthase as well as mitochondrial membrane and matrix. Certain genes involved in mitophagy were also upregulated by geraniin. The results suggest a modulatory effect of geraniin on mitochondrial function, which is a novel discovery about the natural product. By regulating the mitochondrial gene expression, geraniin can potentially influence the mitochondrial dynamics and biogenesis, which are highly implicated in the pathogenesis of MetS. The role of mitochondria in MetS and chronic metabolic diseases is a relatively new and exciting research focus. Further investigation is warranted to explicitly elaborate the interaction between geraniin and mitochondria as well as the downstream implications.

The findings of the research project are illustrated in **Figure 6.1**. One of the most significant highlights of the present study is the remarkable multifunctionality of ellagitannin geraniin. Indeed, treatment with geraniin mitigated almost all the pathological manifestations of MetS. Such a promising finding does make it a worthy therapeutic candidate for MetS and other related metabolic disorders. The exploration of the clinical prospect of geraniin could also be a baby step towards the introduction of multi-target MetS therapeutic approach. Apart from that, the comparative transcriptomic analysis not only points out the mitochondrial modulatory effect of geraniin, but also indicates the integral role of mitochondria in the pathology and recovery of MetS. This makes mitochondria an interesting target pathway for obesity and MetS therapy. Although mitochondrial biology is extensively studied, the implications of mitochondrial dynamics and dysfunction in obesity and MetS is a relative new research niche. Hence, the outputs of the present study could provide some indirect evidence to support the importance of mitochondrial research in chronic metabolic diseases, besides proposing a drug candidate from the natural sources – ellagitannin geraniin, for further investigation.

To conclude, chronic consumption of HFD could reliably induce all the core features of MetS in post-weaning rats within a relatively short duration (eight weeks). The consistency in disease induction outcomes coupled with the short induction time could enhance the time and cost efficiency, rendering it an excellent MetS model for studying the treatment effect of putative therapeutic agents. Using the disease model, it was discovered that treatment with ellagitannin geraniin at a daily dosage of 25 mg/kg via oral administration could reverse a wide array of metabolic abnormalities caused by high-fat feeding such as overly high fasting glucose and lipid components in the blood circulation, ectopic lipid deposition in the liver and abdominal adipose tissues, elevated systolic and diastolic blood pressure, high circulating oxidative stress and pro-inflammatory response. The explorative hepatic transcriptomic analysis revealed that geraniin could reverse the abnormal transcriptional activation of genes associated with lipid and steroid hormones metabolism. Moreover, geraniin also exerted notable modulatory effect on the mitochondrial gene expression in the liver, which could be the primary mechanism by which it confers the beneficial health impacts. Future research should focus on the elucidation of the relationship and interaction between geraniin, mitochondria and pathogenesis of MetS.

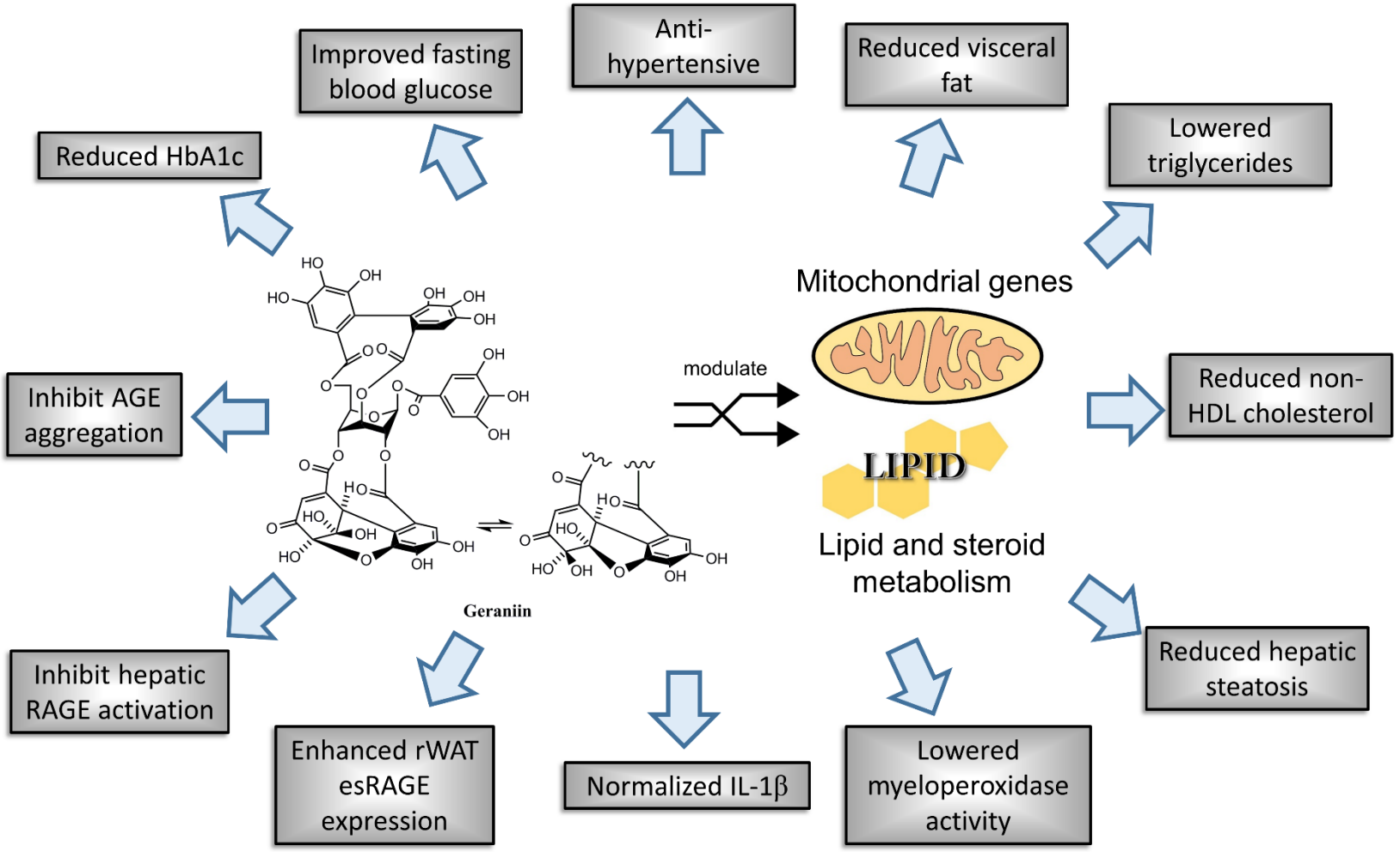

Figure 6.1: Summary of the key findings about the bioactivities and underlying mechanism of ellagitannin geraniin in MetS. AGE, advanced glycation end product; HnA1c, esRAGE, endogenous secretory receptor for advanced glycation end product; glycated hemoglobin A1c; HDL, high-density lipoprotein; IL-1β, interleukin 1β; RAGE, receptor for advanced glycation end product; rWAT, retroperitoneal white adipose tissues.

6.2. Future work

Following the outputs of the present study, there are a few exciting aspects that can be further explored to have a better understanding about the nature of MetS as well as the biological function of ellagitannin geraniin. First and foremost, pertaining to the MetS model used in this study, we observed an increased susceptibility of post-weaning rats to MetS when they were given HFD, but not HFSD. For adult rats, HFSD was more effective to induce metabolic dysregulation, albeit not all features of MetS. Such an observation suggests an inherent age-dependent disparity in terms of the metabolic regulation and processing of macronutrients. It is postulated that unusual nutritional experiences like under-nutrition and over-nutrition during rapid development stages like neonatal, perinatal and infancy periods could leave a long-lasting impact on the metabolism via epigenetic modification [410]. This phenomenon is termed "metabolic programming". In Sprague Dawley rats, maternal exposure to high-calorie diet during pregnancy significantly increased the risk for hyperphagia and obesity of the pups in the adult stage [411]. Similar predisposition is also observed when the rat pups are given milk enriched with high-calorie components [166]. The enhanced susceptibility as seen in our study proposes that the window for metabolic programming induced by nutritional insults can possibly extend beyond the gestational and perinatal stages. Therefore, further investigation could attempt to explore the epigenetic aspects of the MetS model, of which the output may be able to shed some light on the pathology of childhood obesity and MetS.

Next, it is established that the bioavailability of ellagitannin geraniin upon oral consumption is fairly limited. Based on the studies from other research groups, the biologically functional molecules are the metabolites of geraniin like gallic acid, ellagic acid, brevifolincarboxylic acid and a wide variety of urolithins [292, 412]. However, the geraniin-derived metabolites were not validated in the present study and so, whether they possess similar bioactivities and potency against MetS is unclear. Therefore, future work can aim to examine the metabolic effects of the major geraniin-derived metabolites using a similar experimental design as shown in the present study. This can facilitate the identification of the predominant biological active species (if any) besides revealing if the multifunctionality of geraniin is because of the combined effect of different metabolites that specifically improve different metabolic abnormalities, or whether the metabolites also exhibit pleiotropic health benefits. The outcome will consequently contribute to

a better understanding about the pharmacodynamics of geraniin and its metabolites, particularly in the aspect of chronic metabolic diseases.

Apart from that, based on the results, one of the most prominent effects with the oral supplementation of geraniin was the antihypertensive activity. The lowering effect on the systolic and diastolic blood pressure was observed as soon as one week into the intervention and persisted until the end of the experiment. The rapid improvement suggests the possibility of having a blood pressure-lowering mechanism which is independent of the regulation of lipid and glucose homeostasis. Thus far, the research about antihypertensive effect of geraniin is considerably preliminary. Even though the beneficial effect has been replicated in SHR rats, the true mechanism is not well-characterized [172, 173]. Our group found that supplementation of geraniin had no noticeable impact on the plasma electrolyte, aldosterone and renin levels (data not shown), thus suggesting limited influence of the natural product on the fluid and electrolyte homeostasis. Future research can consider other blood pressure-lowering mechanisms, namely vasodilation, sympathetic nervous system and chronic stress response, in order to unearth its clinical use as an antihypertensive agent.

The use of transcriptomic analysis by next generation sequencing revealed many interesting biological interactions of geraniin, including the novel mitochondrial modulatory properties. Nevertheless, since the analysis was performed only on the liver specimen, it is unclear if geraniin also confers similar regulatory effect in other tissues, particularly those that are well-implicated in MetS and obesity like the adipose tissues, skeletal muscles and pancreas. This should be carried out in future investigation. By studying the transcriptomes of multiple body tissues, the actual target of geraniin can be pinpointed; which will provide a more comprehensive insight into the overall effects of geraniin in MetS. Additionally, other high-throughput –omics techniques like proteomics and metabolomics are also exceedingly useful. Integrating datasets from several –omics analyses has become increasingly popular for the identification of metabolic pathways implicated in disease progression and drug response [413, 414]. Thus, a combinatory approach consisting of transcriptomics, proteomics and metabolomics can be utilized to understand and validate the molecular basis of geraniin and its metabolites in chronic metabolic diseases.

Finally, future research about geraniin in the aspect of MetS should elaborate its effect on mitochondrial biology such as the mitochondrial biogenesis, fusion and fission, dysfunction and selective degradation via mitophagy. This can be accomplished by examining the mitochondrial morphology, ATP output, ROS generation, key enzymes and transcription factors in mitophagy as well as mitonuclear protein stoichiometry. The outputs of these research tasks can provide a clearer picture of the affected phenotypes and pathways caused by geraniin that contribute to the consequent beneficial effects in MetS. By doing so, it is also probable to associate certain phenotypic changes of mitochondria to favorable outcomes in MetS, which will become a target pathway to improve the therapeutic strategy of the disease. More importantly, mitochondrial dynamics has been increasingly recognized as a modifiable factor in many degenerative diseases like aging, Alzheimer's disease and Parkinson's disease. Hence, understanding how geraniin affects the mitochondria may lay the foundation for its clinical application in the treatment of medical conditions other than obesity and MetS.

REFERENCES

REFERENCES

[1] World Health Organization (2009), *Global Health Risks: Mortality and Burden of Disease Attributable to Selected Major Risks*, World Health Organization, Geneva.
[2] Nádas J, Putz Z, Jermendy G, Hidvégi T (2007). Public awareness of the metabolic syndrome. *Diabetes Research and Clinical Practice* **76**: 155-156.
[3] Lewis SJ, Rodbard HW, Fox KM, Grandy S, for the SSG (2008). Self-reported prevalence and awareness of metabolic syndrome: findings from SHIELD. *International Journal of Clinical Practice* **62**: 1168-1176.
[4] Kylin E (1923). Studien ueber das Hypertonie-Hyperglyca "mie-Hyperurika" miesyndrom. *Zentralblatt fuer Innere Medizin* **44**: 105-127.
[5] Hanefeld M, Leonhardt W (1981). Das Metabolische Syndrom. *Dt Gesundh.-Wesen* **36**: 545-551.
[6] Reaven GM (1988). Role of insulin resistance in human disease. *Diabetes* **37**: 1595-1607.
[7] Kaplan NM (1989). The deadly quartet: Upper-body obesity, glucose intolerance, hypertriglyceridemia, and hypertension. *Archives of Internal Medicine* **149**: 1514-1520.
[8] Haffner SM, Valdez RA, Hazuda HP, Mitchell BD, Morales PA, Stern MP (1992). Prospective analysis of the insulin-resistance syndrome (Syndrome X). *Diabetes* **41**: 715-722.
[9] World Health Organization (1999), *Definition, Diagnosis and Classification of Diabetes mellitus and its Complications: Report of a WHO Consultation. Part 1, Diagnosis and Classification of Diabetes Mellitus*, World Health Organization, Geneva.
[10] Expert Panel on Detection Evaluation and Treatment of High Blood Cholesterol in Adults (2001). Executive summary of the third report of the national cholesterol education program (ncep) expert panel on detection, evaluation, and treatment of high blood cholesterol in adults (adult treatment panel III). *JAMA* **285**: 2486-2497.
[11] Einhorn D, Reaven GM, Cobin RH, Ford E, Ganda OP, Handelsman Y, et al. (2003). American College of Endocrinology position statement on the insulin resistance syndrome. *Endocrine Practice* **9**: 237-252.
[12] Alberti KGMM, Zimmet P, Shaw J (2005). The metabolic syndrome—a new worldwide definition. *The Lancet* **366**: 1059-1062.
[13] Grundy SM, Cleeman JI, Daniels SR, Donato KA, Eckel RH, Franklin BA, et al. (2005). Diagnosis and management of the metabolic syndrome: An American Heart Association/National Heart, Lung, and Blood Institute Scientific Statement. *Circulation* **112**: 2735-2752.
[14] Alberti KGMM, Eckel RH, Grundy SM, Zimmet PZ, Cleeman JI, Donato KA, et al. (2009). Harmonizing the metabolic syndrome: A joint interim statement of the International Diabetes Federation Task Force on Epidemiology and Prevention; National Heart, Lung, and Blood Institute; American Heart Association; World Heart Federation; International Atherosclerosis Society; and International Association for the Study of Obesity. *Circulation* **120**: 1640-1645.
[15] Kahn R, Buse J, Ferrannini E, Stern M (2005). The metabolic syndrome: Time for a critical appraisal. Joint statement from the American Diabetes Association and the European Association for the Study of Diabetes. *Diabetes Care* **28**: 2289-2304.
[16] Kaur J (2014). A comprehensive review on metabolic syndrome. *Cardiology Research and Practice* **2014**: 21.
[17] O'Neill S, O'Driscoll L (2015). Metabolic syndrome: a closer look at the growing epidemic and its associated pathologies. *Obesity Reviews* **16**: 1-12.
[18] Cornier M-A, Dabelea D, Hernandez TL, Lindstrom RC, Steig AJ, Stob NR, et al. (2008). The metabolic syndrome. *Endocrine Reviews* **29**: 777-822.

[19] Batsis JA, Nieto-Martinez RE, Lopez-Jimenez F (2007). Metabolic syndrome: From global epidemiology to individualized medicine. *Clinical Pharmacology and Therapeutics* **82**: 509-524.
[20] International Diabetes Federation (2006), *The IDF Consensus Worldwide Definition of the Metabolic Syndrome*, International Diabetes Federation, Brussels.
[21] Deedwania PC, Gupta R, Sharma KK, Achari V, Gupta B, Maheshwari A, et al. (2014). High prevalence of metabolic syndrome among urban subjects in India: A multisite study. *Diabetes and Metabolic Syndrome* **8**: 156-161.
[22] Li R, Li W, Lun Z, Zhang H, Sun Z, Kanu JS, et al. (2016). Prevalence of metabolic syndrome in mainland china: a meta-analysis of published studies. *BMC Public Health* **16**: 296.
[23] Lim S, Shin H, Song JH, Kwak SH, Kang SM, Won Yoon J, et al. (2011). Increasing prevalence of metabolic syndrome in Korea. The Korean National Health and Nutrition Examination Survey for 1998–2007. *Diabetes Care* **34**: 1323-1328.
[24] Aguilar M, Bhuket T, Torres S, Liu B, Wong RJ (2015). Prevalence of the metabolic syndrome in the united states, 2003-2012. *JAMA* **313**: 1973-1974.
[25] Wan Mohamud WN, Ismail Aa-S, Khir ASM, Ismail IS, Musa KI, Kadir KA, et al. (2012). Prevalence of metabolic syndrome and its risk factors in adult Malaysians: Results of a nationwide survey. *Diabetes Research and Clinical Practice* **96**: 91-97.
[26] Tan BY, Kantilal HK, Singh R (2008). Prevalence of metabolic syndrome among Malaysians using the International Diabetes Federation, National Cholesterol Education Program and Modified World Health Organization definitions. *Malaysian Journal of Nutrition* **14**: 65-77.
[27] Chan YY, Lim KK, Lim KH, Teh CH, Kee CC, Cheong SM, et al. (2017). Physical activity and overweight/obesity among Malaysian adults: findings from the 2015 National Health and morbidity survey (NHMS). *BMC Public Health* **17**: 733.
[28] Institute for Public Health Malaysia (2015), *National Health and Morbidity Survey 2015 (NHMS 2015). Vol. II: Non-Communicable Diseases, Risk Factors and Other Health Problems*, National Institutes of Health, Ministry of Health Malaysia, Kuala Lumpur.
[29] Ng M, Fleming T, Robinson M, Thomson B, Graetz N, Margono C, et al. (2014). Global, regional, and national prevalence of overweight and obesity in children and adults during 1980–2013: a systematic analysis for the Global Burden of Disease Study 2013. *The Lancet* **384**: 766-781.
[30] Tailor AM, Peeters PHM, Norat T, Vineis P, Romaguera D (2010). An update on the prevalence of the metabolic syndrome in children and adolescents. *International Journal of Pediatric Obesity* **5**: 202-213.
[31] Friend A, Craig L, Turner S (2012). The prevalence of metabolic syndrome in children: A systematic review of the literature. *Metabolic Syndrome and Related Disorders* **11**: 71-80.
[32] Narayanan P, Meng OL, Mahanim O (2011). Do the prevalence and components of metabolic syndrome differ among different ethnic groups? A cross-sectional study among obese Malaysian adolescents. *Metabolic Syndrome and Related Disorders* **9**: 389-395.
[33] Fadzlina A, Harun F, Nurul Haniza M, Al Sadat N, Murray L, Cantwell MM, et al. (2014). Metabolic syndrome among 13 year old adolescents: prevalence and risk factors. *BMC Public Health* **14**: S7.
[34] Hussain S, Men KK, Majid NA (2017). Comparison of the clinical and biochemical profile of metabolic syndrome between obese children below and above 10-years old attending paediatric clinic Hospital Universiti Sains Malaysia from 2006 to 2015. *Journal of the ASEAN Federation of Endocrine Societies* **32**: 132-138.

[35] Ford ES (2005). Risks for all-cause mortality, cardiovascular disease, and diabetes associated with the metabolic syndrome: A summary of the evidence. *Diabetes Care* **28**: 1769-1778.
[36] Gami AS, Witt BJ, Howard DE, Erwin PJ, Gami LA, Somers VK, et al. (2007). Metabolic syndrome and risk of incident cardiovascular events and death: A systematic review and meta-analysis of longitudinal studies. *Journal of the American College of Cardiology* **49**: 403-414.
[37] Esposito K, Chiodini P, Colao A, Lenzi A, Giugliano D (2012). Metabolic syndrome and risk of cancer: A systematic review and meta-analysis. *Diabetes Care* **35**: 2402-2411.
[38] Thomas G, Sehgal AR, Kashyap SR, Srinivas TR, Kirwan JP, Navaneethan SD (2011). Metabolic syndrome and kidney disease: A systematic review and meta-analysis. *Clinical Journal of the American Society of Nephrology* **6**: 2364-2373.
[39] Bujang MA, Adnan TH, Hashim NH, Mohan K, Kim Liong A, Ahmad G, et al. (2017). Forecasting the incidence and prevalence of patients with end-stage renal disease in Malaysia up to the year 2040. *International Journal of Nephrology* **2017**: 5.
[40] Rouch I, Trombert B, Kossowsky MP, Laurent B, Celle S, Ntougou Assoumou G, et al. (2014). Metabolic syndrome is associated with poor memory and executive performance in elderly community residents: The PROOF Study. *The American Journal of Geriatric Psychiatry* **22**: 1096-1104.
[41] Vanhanen M, Koivisto K, Moilanen L, Helkala EL, Hänninen T, Soininen H, et al. (2006). Association of metabolic syndrome with Alzheimer disease: A population-based study. *Neurology* **67**: 843-847.
[42] Raffaitin C, Gin H, Empana J-P, Helmer C, Berr C, Tzourio C, et al. (2009). Metabolic syndrome and risk for incident Alzheimer's disease or vascular dementia: The three-city study. *Diabetes Care* **32**: 169-174.
[43] Tang Y, Purkayastha S, Cai D (2015). Hypothalamic microinflammation: a common basis of metabolic syndrome and aging. *Trends in Neurosciences* **38**: 36-44.
[44] Takeuchi T, Nakao M, Nomura K, Inoue M, Tsurugano S, Shinozaki Y, et al. (2009). Association of the metabolic syndrome with depression and anxiety in Japanese men: A 1-year cohort study. *Diabetes/Metabolism Research and Reviews* **25**: 762-767.
[45] Pan A, Keum N, Okereke OI, Sun Q, Kivimaki M, Rubin RR, et al. (2012). Bidirectional association between depression and metabolic syndrome: A systematic review and meta-analysis of epidemiological studies. *Diabetes Care* **35**: 1171-1180.
[46] Koponen H, Jokelainen J, Keinänen-Kiukaanniemi S, Kumpusalo E, Vanhala M (2008). Metabolic syndrome predisposes to depressive symptoms: A population-based 7-year follow-up study. *Journal of Clinical Psychiatry* **69**: 178-182.
[47] Leisegang K, Udodong A, Bouic PJD, Henkel RR (2014). Effect of the metabolic syndrome on male reproductive function: a case-controlled pilot study. *Andrologia* **46**: 167-176.
[48] Brand JS, van der Tweel I, Grobbee DE, Emmelot-Vonk MH, van der Schouw YT (2011). Testosterone, sex hormone-binding globulin and the metabolic syndrome: a systematic review and meta-analysis of observational studies. *International Journal of Epidemiology* **40**: 189-207.
[49] Yang J-L, Zhang C-P, Li L, Huang L, Ji S-Y, Lu C-L, et al. (2010). Testosterone induces redistribution of Forkhead Box-3a and down-regulation of growth and differentiation Factor 9 messenger ribonucleic acid expression at early stage of mouse folliculogenesis. *Endocrinology* **151**: 774-782.
[50] Marchi J, Berg M, Dencker A, Olander EK, Begley C (2015). Risks associated with obesity in pregnancy, for the mother and baby: a systematic review of reviews. *Obesity Reviews* **16**: 621-638.

[51] Sookoian S, Gianotti TF, Burgueño AL, Pirola CJ (2013). Fetal metabolic programming and epigenetic modifications: a systems biology approach. *Pediatric Research* **73**: 531.
[52] Hui WS, Liu Z, Ho SC (2010). Metabolic syndrome and all-cause mortality: a meta-analysis of prospective cohort studies. *European Journal of Epidemiology* **25**: 375-384.
[53] Lutsey PL, Steffen LM, Stevens J (2008). Dietary intake and the development of the metabolic syndrome: The Atherosclerosis Risk in Communities Study. *Circulation* **117**: 754-761.
[54] Brunner EJ, Mosdøl A, Witte DR, Martikainen P, Stafford M, Shipley MJ, et al. (2008). Dietary patterns and 15-y risks of major coronary events, diabetes, and mortality. *The American Journal of Clinical Nutrition* **87**: 1414-1421.
[55] Iqbal R, Anand S, Ounpuu S, Islam S, Zhang X, Rangarajan S, et al. (2008). Dietary patterns and the risk of acute myocardial infarction in 52 countries: Results of the INTERHEART Study. *Circulation* **118**: 1929-1937.
[56] Kushner RF, Choi SW (2010). Prevalence of unhealthy lifestyle patterns among overweight and obese adults. *Obesity* **18**: 1160-1167.
[57] Alcock J, Maley CC, Aktipis CA (2014). Is eating behavior manipulated by the gastrointestinal microbiota? Evolutionary pressures and potential mechanisms. *Bioessays* **36**: 940-949.
[58] Fall T, Ingelsson E (2014). Genome-wide association studies of obesity and metabolic syndrome. *Molecular and Cellular Endocrinology* **382**: 740-757.
[59] Kraja AT, Vaidya D, Pankow JS, Goodarzi MO, Assimes TL, Kullo IJ, et al. (2011). A bivariate genome-wide approach to metabolic syndrome: STAMPEED Consortium. *Diabetes* **60**: 1329-1339.
[60] Grundy SM (2015). Adipose tissue and metabolic syndrome: too much, too little or neither. *European Journal of Clinical Investigation* **45**: 1209-1217.
[61] Bays HE (2009). "Sick fat," metabolic disease, and atherosclerosis. *The American Journal of Medicine* **122**: S26-S37.
[62] Després J-P, Lemieux I (2006). Abdominal obesity and metabolic syndrome. *Nature* **444**: 881.
[63] Matsuzawa Y (2009). The role of fat topology in the risk of disease. *International Journal of Obesity* **32**: S83.
[64] Maury E, Brichard SM (2010). Adipokine dysregulation, adipose tissue inflammation and metabolic syndrome. *Molecular and Cellular Endocrinology* **314**: 1-16.
[65] Kim JI, Huh JY, Sohn JH, Choe SS, Lee YS, Lim CY, et al. (2015). Lipid-overloaded enlarged adipocytes provoke insulin resistance independent of inflammation. *Molecular and Cellular Biology* **35**: 1686-1699.
[66] Horton JD, Shimomura I, Ikemoto S, Bashmakov Y, Hammer RE (2003). Overexpression of sterol regulatory element-binding protein-1a in mouse adipose tissue produces adipocyte hypertrophy, increased fatty acid secretion, and fatty liver. *Journal of Biological Chemistry* **278**: 36652-36660.
[67] Britton KA, Fox CS (2011). Ectopic fat depots and cardiovascular disease. *Circulation* **124**: e837-e841.
[68] Lara-Castro C, Garvey WT (2008). Intracellular lipid accumulation in liver and muscle and the insulin resistance syndrome. *Endocrinology and Metabolism Clinics of North America* **37**: 841-856.
[69] Teresa Vanessa F, Annamaria P, Pengou Z, Franco F (2013). Hyperglycemia-induced oxidative stress and its role in diabetes mellitus related cardiovascular diseases. *Current Pharmaceutical Design* **19**: 5695-5703.
[70] Talchai C, Xuan S, Lin Hua V, Sussel L, Accili D (2012). Pancreatic β cell dedifferentiation as a mechanism of diabetic β cell failure. *Cell* **150**: 1223-1234.

[71] Hankiewicz JH, Banke NH, Farjah M, Lewandowski ED (2010). Early impairment of transmural principal strains in the left ventricular wall after short-term, high-fat feeding of mice predisposed to cardiac steatosis. *Circulation: Cardiovascular Imaging* **3**: 710-717.
[72] Foster MC, Hwang S-J, Porter SA, Massaro JM, Hoffmann U, Fox CS (2011). Fatty kidney, hypertension, and chronic kidney disease: The Framingham Heart Study. *Hypertension* **58**: 784-790.
[73] Alam M, Nasreen S, Ullah E, Hussain A (2011). The awareness and prevalence of metabolic syndrome in medical community of Bahawalpur. *Oman Medical Journal* **26**: 26-28.
[74] Thompson PD, Buchner D, Piña IL, Balady GJ, Williams MA, Marcus BH, et al. (2003). Exercise and physical activity in the prevention and treatment of atherosclerotic cardiovascular disease: A statement from the Council on Clinical Cardiology (Subcommittee on Exercise, Rehabilitation, and Prevention) and the Council on Nutrition, Physical Activity, and Metabolism (Subcommittee on Physical Activity). *Circulation* **107**: 3109-3116.
[75] Wadden TA, Webb VL, Moran CH, Bailer BA (2012). Lifestyle modification for obesity: New developments in diet, physical activity, and behavior therapy. *Circulation* **125**: 1157-1170.
[76] Jellinger PS, Handelsman Y, Rosenblit PD, Bloomgarden ZT, Fonseca VA, Garber AJ, et al. (2017). American Association of Clinical Endocrinologists and American College of Endocrinology guidelines for management of dyslipidemia and prevention of cardiovascular disease. *Endocrine Practice* **23**: 1-87.
[77] Whelton PK, Carey RM, Aronow WS, Casey DE, Collins KJ, Dennison Himmelfarb C, et al. (2017). 2017 ACC/AHA/AAPA/ABC/ACPM/AGS/APhA/ASH/ASPC/NMA/PCNA guideline for the prevention, detection, evaluation, and management of high blood pressure in adults: A report of the American College of Cardiology/American Heart Association Task Force on Clinical Practice Guidelines. *Hypertension* DOI 10.1161/hyp.0000000000000065.
[78] Garber AJ, Abrahamson MJ, Barzilay JI, Blonde L, Bloomgarden ZT, Bush MA, et al. (2016). Consensus statement by the American Association of Clinical Endocrinologists and American College of Endocrinology on the comprehensive type 2 diabetes management algorithm-2016 executive summary. *Endocrine Practice* **22**: 84-113.
[79] Rollason V, Vogt N (2003). Reduction of polypharmacy in the elderly. *Drugs and Aging* **20**: 817-832.
[80] Hainer V, Hainerová IA (2012). Do we need anti-obesity drugs? *Diabetes/Metabolism Research and Reviews* **28**: 8-20.
[81] Alfaris N, Minnick AM, Hopkins CM, Berkowitz RI, Wadden TA (2015). Combination phentermine and topiramate extended release in the management of obesity. *Expert Opinion on Pharmacotherapy* **16**: 1263-1274.
[82] Heck AM, Yanovski JA, Calis KA (2000). Orlistat, a new lipase inhibitor for the management of obesity. *Pharmacotherapy: The Journal of Human Pharmacology and Drug Therapy* **20**: 270-279.
[83] Broom I, Wilding J, Stott P, Myers N, Group UKMS (2002). Randomised trial of the effect of orlistat on body weight and cardiovascular disease risk profile in obese patients: UK Multimorbidity Study. *International Journal of Clinical Practice* **56**: 494-499.
[84] Lindgärde F (2000). The effect of orlistat on body weight and coronary heart disease risk profile in obese patients: The Swedish Multimorbidity Study. *Journal of Internal Medicine* **248**: 245-254.
[85] Nguyen NT, Varela JE (2016). Bariatric surgery for obesity and metabolic disorders: state of the art. *Nature Reviews Gastroenterology and Hepatology* **14**: 160.

[86] Gloy VL, Briel M, Bhatt DL, Kashyap SR, Schauer PR, Mingrone G, et al. (2013). Bariatric surgery versus non-surgical treatment for obesity: a systematic review and meta-analysis of randomised controlled trials. *BMJ* **347**: f5934.
[87] Chang S, Stoll CT, Song J, Varela J, Eagon CJ, Colditz GA (2014). The effectiveness and risks of bariatric surgery: An updated systematic review and meta-analysis, 2003-2012. *JAMA Surgery* **149**: 275-287.
[88] Hussain SS, Bloom SR (2012). The regulation of food intake by the gut-brain axis: implications for obesity. *International Journal of Obesity* **37**: 625.
[89] Talsania T, Anini Y, Siu S, Drucker DJ, Brubaker PL (2005). Peripheral exendin-4 and peptide YY3–36 synergistically reduce food intake through different mechanisms in mice. *Endocrinology* **146**: 3748-3756.
[90] Abbott CR, Monteiro M, Small CJ, Sajedi A, Smith KL, Parkinson JRC, et al. (2005). The inhibitory effects of peripheral administration of peptide YY3–36 and glucagon-like peptide-1 on food intake are attenuated by ablation of the vagal–brainstem–hypothalamic pathway. *Brain Research* **1044**: 127-131.
[91] Vilsbøll T, Christensen M, Junker AE, Knop FK, Gluud LL (2012). Effects of glucagon-like peptide-1 receptor agonists on weight loss: systematic review and meta-analyses of randomised controlled trials. *BMJ* **344**: d7771.
[92] Tomlinson B, Hu M, Zhang Y, Chan P, Liu Z-M (2016). Investigational glucagon-like peptide-1 agonists for the treatment of obesity. *Expert Opinion on Investigational Drugs* **25**: 1167-1179.
[93] Klöting N, Blüher M (2014). Adipocyte dysfunction, inflammation and metabolic syndrome. *Reviews in Endocrine and Metabolic Disorders* **15**: 277-287.
[94] Myung S-K, Ju W, Cho B, Oh S-W, Park SM, Koo B-K, et al. (2013). Efficacy of vitamin and antioxidant supplements in prevention of cardiovascular disease: systematic review and meta-analysis of randomised controlled trials. *BMJ* **346**: f10.
[95] Fortmann SP, Burda BU, Senger CA, Lin JS, Whitlock EP (2013). Vitamin and mineral supplements in the primary prevention of cardiovascular disease and cancer: An updated systematic evidence review for the u.s. preventive services task force. *Annals of Internal Medicine* **159**: 824-834.
[96] Amiot MJ, Riva C, Vinet A (2016). Effects of dietary polyphenols on metabolic syndrome features in humans: a systematic review. *Obesity Reviews* **17**: 573-586.
[97] Chu S-l, Fu H, Yang J-x, Liu G-x, Dou P, Zhang L, et al. (2011). A randomized double-blind placebo-controlled study of Pu’er tea (普洱茶) extract on the regulation of metabolic syndrome. *Chinese Journal of Integrative Medicine* **17**: 492-498.
[98] Lehtonen HM, Suomela JP, Tahvonen R, Yang B, Venojärvi M, Viikari J, et al. (2011). Different berries and berry fractions have various but slightly positive effects on the associated variables of metabolic diseases on overweight and obese women. *European Journal of Clinical Nutrition* **65**: 394.
[99] Belcaro G, Ledda A, Hu S, Cesarone MR, Feragalli B, Dugall M (2013). Greenselect phytosome for borderline metabolic syndrome. *Evidence-Based Complementary and Alternative Medicine* **2013**: 7.
[100] Micha R, Imamura F, Wyler von Ballmoos M, Solomon DH, Hernán MA, Ridker PM, et al. (2011). Systematic review and meta-analysis of methotrexate use and risk of cardiovascular disease. *The American Journal of Cardiology* **108**: 1362-1370.
[101] Everett BM, Pradhan AD, Solomon DH, Paynter N, MacFadyen J, Zaharris E, et al. (2013). Rationale and design of the Cardiovascular Inflammation Reduction Trial: A test of the inflammatory hypothesis of atherothrombosis. *American Heart Journal* **166**: 199-207.e115.

[102] Stanley TL, Zanni MV, Johnsen S, Rasheed S, Makimura H, Lee H, et al. (2011). TNF-α antagonism with etanercept decreases glucose and increases the proportion of high molecular weight adiponectin in obese subjects with features of the metabolic syndrome. *The Journal of Clinical Endocrinology and Metabolism* **96**: E146-E150.
[103] Rissanen A, Howard CP, Botha J, Thuren T, for the Global I (2012). Effect of anti-IL-1β antibody (canakinumab) on insulin secretion rates in impaired glucose tolerance or type 2 diabetes: results of a randomized, placebo-controlled trial. *Diabetes, Obesity and Metabolism* **14**: 1088-1096.
[104] Schultz O, Oberhauser F, Saech J, Rubbert-Roth A, Hahn M, Krone W, et al. (2010). Effects of inhibition of interleukin-6 signalling on insulin sensitivity and lipoprotein (A) levels in human subjects with rheumatoid diseases. *PloS One* **5**: e14328.
[105] Kopp E, Ghosh S (1994). Inhibition of NF-kappa B by sodium salicylate and aspirin. *Science* **265**: 956-959.
[106] Baye E, Naderpoor N, Misso M, Teede H, Moran LJ, de Courten B (2017). Treatment with high dose salicylates improves cardiometabolic parameters: Meta-analysis of randomized controlled trials. *Metabolism* **71**: 94-106.
[107] Cameron AR, Morrison VL, Levin D, Mohan M, Forteath C, Beall C, et al. (2016). Anti-inflammatory effects of metformin irrespective of diabetes status. *Circulation Research* **119**: 652-665.
[108] Esser N, Paquot N, Scheen AJ (2015). Anti-inflammatory agents to treat or prevent type 2 diabetes, metabolic syndrome and cardiovascular disease. *Expert Opinion on Investigational Drugs* **24**: 283-307.
[109] Moayyedi P, Yuan Y, Baharith H, Ford A (2017). Faecal microbiota transplantation for *Clostridium difficile*-asscoiated diarrhoea: a systematic review of randomised controlled trials. *Medical Journal of Australia* **207**: 166-172.
[110] Alang N, Kelly CR (2015). Weight gain after fecal microbiota transplantation. *Open Forum Infectious Diseases* **2**: ofv004.
[111] Ridaura VK, Faith JJ, Rey FE, Cheng J, Duncan AE, Kau AL, et al. (2013). Gut microbiota from twins discordant for obesity modulate metabolism in mice. *Science* **341**: 1241214.
[112] Vrieze A, Van Nood E, Holleman F, Salojärvi J, Kootte RS, Bartelsman JFWM, et al. (2012). Transfer of intestinal microbiota from lean donors increases insulin sensitivity in individuals with metabolic syndrome. *Gastroenterology* **143**: 913-916.e917.
[113] de Groot PF, Frissen MN, de Clercq NC, Nieuwdorp M (2017). Fecal microbiota transplantation in metabolic syndrome: History, present and future. *Gut Microbes* **8**: 253-267.
[114] Wald NJ, Law MR (2003). A strategy to reduce cardiovascular disease by more than 80%. *BMJ* **326**: 1419.
[115] Kuehn BM (2006). "Polypill" could slash diabetes risks. *JAMA* **296**: 377-380.
[116] Malekzadeh F, Marshall T, Pourshams A, Gharravi M, Aslani A, Nateghi A, et al. (2010). A pilot double-blind randomised placebo-controlled trial of the effects of fixed-dose combination therapy ('polypill') on cardiovascular risk factors. *International Journal of Clinical Practice* **64**: 1220-1227.
[117] PILL Collaborative Group (2011). An international randomised placebo-controlled trial of a four-component combination pill ("Polypill") in people with raised cardiovascular risk. *PloS One* **6**: e19857.
[118] Yusuf S, Lonn E, Pais P, Bosch J, López-Jaramillo P, Zhu J, et al. (2016). Blood-pressure and cholesterol lowering in persons without cardiovascular disease. *New England Journal of Medicine* **374**: 2032-2043.

[119] Zomer E, Owen A, Magliano DJ, Ademi Z, Reid CM, Liew D (2013). Predicting the impact of polypill use in a metabolic syndrome population: An effectiveness and cost-effectiveness analysis. *American Journal of Cardiovascular Drugs* **13**: 121-128.
[120] Castellano JM, Sanz G, Peñalvo JL, Bansilal S, Fernández-Ortiz A, Alvarez L, et al. (2014). A polypill strategy to improve adherence: Results from the FOCUS project. *Journal of the American College of Cardiology* **64**: 2071-2082.
[121] Krysiak R, Gdula-Dymek A, Bachowski R, Okopień B (2010). Pleiotropic effects of atorvastatin and fenofibrate in metabolic syndrome and different types of pre-diabetes. *Diabetes Care* **33**: 2266-2270.
[122] Satoru Y (2011). Pleiotropic effects of ARB in metabolic syndrome. *Current Vascular Pharmacology* **9**: 158-161.
[123] Bagul PK, Middela H, Matapally S, Padiya R, Bastia T, Madhusudana K, et al. (2012). Attenuation of insulin resistance, metabolic syndrome and hepatic oxidative stress by resveratrol in fructose-fed rats. *Pharmacological Research* **66**: 260-268.
[124] Panchal SK, Poudyal H, Brown L (2012). Quercetin ameliorates cardiovascular, hepatic, and metabolic changes in diet-induced metabolic syndrome in rats. *The Journal of Nutrition* **142**: 1026-1032.
[125] Bose M, Lambert JD, Ju J, Reuhl KR, Shapses SA, Yang CS (2008). The major green tea polyphenol, (-)-epigallocatechin-3-gallate, inhibits obesity, metabolic syndrome, and fatty liver disease in high-fat–fed mice. *The Journal of Nutrition* **138**: 1677-1683.
[126] Grundy SM (2006). Drug therapy of the metabolic syndrome: minimizing the emerging crisis in polypharmacy. *Nature Reviews Drug Discovery* **5**: 295.
[127] Viera AJ, Sheridan SL, Edwards T, Soliman EZ, Harris R, Furberg CD (2011). Acceptance of a polypill approach to prevent cardiovascular disease among a sample of U.S. physicians. *Preventive Medicine* **52**: 10-15.
[128] Jayasinghe TN, Chiavaroli V, Holland DJ, Cutfield WS, O'Sullivan JM (2016). The new era of treatment for obesity and metabolic disorders: Evidence and expectations for gut microbiome transplantation. *Frontiers in Cellular and Infection Microbiology* **6**: 15.
[129] United Kingdom Home Office (2016), *Annual Statistics of Scientific Procedures on Living Animals Great Britain 2015*, United Kingdom Home Office, London.
[130] Panchal SK, Brown L (2011). Rodent models for metabolic syndrome research. *Journal of Biomedicine and Biotechnology* **2011**: 351982.
[131] Marques C, Meireles M, Norberto S, Leite J, Freitas J, Pestana D, et al. (2016). High-fat diet-induced obesity rat model: a comparison between Wistar and Sprague-Dawley rat. *Adipocyte* **5**: 11-21.
[132] Montgomery MK, Hallahan NL, Brown SH, Liu M, Mitchell TW, Cooney GJ, et al. (2013). Mouse strain-dependent variation in obesity and glucose homeostasis in response to high-fat feeding. *Diabetologia* **56**: 1129-1139.
[133] Beery AK, Zucker I (2011). Sex bias in neuroscience and biomedical research. *Neuroscience and Biobehavioral Reviews* **35**: 565-572.
[134] Wong SK, Chin K-Y, Suhaimi FH, Fairus A, Ima-Nirwana S (2016). Animal models of metabolic syndrome: a review. *Nutrition and Metabolism* **13**: 65.
[135] Wizemann TM, Pardue M-L (2001), *Exploring the Biological Contributions to Human Health: Does Sex Matter? ,* National Academy Press, Washington, DC.
[136] Aydin S, Aksoy A, Aydin S, Kalayci M, Yilmaz M, Kuloglu T, et al. (2014). Today's and yesterday's of pathophysiology: Biochemistry of metabolic syndrome and animal models. *Nutrition* **30**: 1-9.
[137] Mazen I, Amr K, Tantawy S, Farooqi IS, El Gammal M (2014). A novel mutation in the leptin gene (W121X) in an Egyptian family. *Molecular Genetics and Metabolism Reports* **1**: 474-476.

[138] Matsumoto K, Iijima H (2003). Sibutramine sensitivity assay revealed a unique phenotype of bombesin BB3 receptor-deficient mice. *European Journal of Pharmacology* **473**: 41-46.
[139] Day C, Bailey CJ (1998). Effect of the antiobesity agent sibutramine in obese-diabetic ob/ob mice. *International Journal of Obesity* **22**: 619.
[140] Zlobine I, Gopal K, Ussher JR (2016). Lipotoxicity in obesity and diabetes-related cardiac dysfunction. *Biochimica et Biophysica Acta (BBA) - Molecular and Cell Biology of Lipids* **1861**: 1555-1568.
[141] Lim JS, Mietus-Snyder M, Valente A, Schwarz J-M, Lustig RH (2010). The role of fructose in the pathogenesis of NAFLD and the metabolic syndrome. *Nature Reviews Gastroenterology and Hepatology* **7**: 251.
[142] Gajda AM, Pellizzon MA, Ricci MR, Ulman EA (2007). *Diet-induced metabolic syndrome in rodent models*. Retrieved 30 December, 2017, from https://www.alnmag.com/article/2008/04/diet-induced-metabolic-syndrome-rodent-models.
[143] Reeves PG (1997). Components of the AIN-93 diets as improvements in the AIN-76A diet. *The Journal of Nutrition* **127**: 838S-841S.
[144] Poudyal H, Panchal SK, Ward LC, Waanders J, Brown L (2012). Chronic high-carbohydrate, high-fat feeding in rats induces reversible metabolic, cardiovascular, and liver changes. *American Journal of Physiology-Endocrinology and Metabolism* **302**: E1472-E1482.
[145] Senaphan K, Kukongviriyapan U, Sangartit W, Pakdeechote P, Pannangpetch P, Prachaney P, et al. (2015). Ferulic Acid Alleviates Changes in a Rat Model of Metabolic Syndrome Induced by High-Carbohydrate, High-Fat Diet. *Nutrients* **7**: 5283.
[146] Suman RK, Ray Mohanty I, Borde MK, Maheshwari U, Deshmukh YA (2016). Development of an experimental model of diabetes co-existing with metabolic syndrome in rats. *Advances in Pharmacological Sciences* **2016**: 11.
[147] Brown NM, Setchell KDR (2001). Animal models impacted by phytoestrogens in commercial chow: Implications for pathways influenced by hormones. *Laboratory Investigation* **81**: 735.
[148] Cederroth CR, Vinciguerra M, Gjinovci A, Kühne F, Klein M, Cederroth M, et al. (2008). Dietary phytoestrogens activate AMP-activated protein kinase with improvement in lipid and glucose metabolism. *Diabetes* **57**: 1176-1185.
[149] Yacout M (2016). Anti-nutritional factors and its roles in animal nutrition. *Journal of Dairy, Veterinary and Animal Research* **4**: 00107.
[150] Nwala CO, Akaninwor JO, Monanu MO (2013). Nutritional studies on rats fed diets formulated from treated and raw samples of Jatropha Curcas seed. *International Journal of Engineering Science Invention* **2**: 14-19.
[151] Warden CH, Fisler JS (2007). Comparisons of diets used in animal models of high-fat feeding. *Cell Metabolism* **7**: 277.
[152] Yang Z-H, Miyahara H, Takeo J, Katayama M (2012). Diet high in fat and sucrose induces rapid onset of obesity-related metabolic syndrome partly through rapid response of genes involved in lipogenesis, insulin signalling and inflammation in mice. *Diabetology and Metabolic Syndrome* **4**: 32.
[153] Podrini C, Cambridge EL, Lelliott CJ, Carragher DM, Estabel J, Gerdin A-K, et al. (2013). High-fat feeding rapidly induces obesity and lipid derangements in C57BL/6N mice. *Mammalian Genome* **24**: 240-251.
[154] Zhou X, Han D, Xu R, Li S, Wu H, Qu C, et al. (2014). A model of metabolic syndrome and related diseases with intestinal endotoxemia in rats fed a high fat and high sucrose diet. *PloS One* **9**: e115148.

[155] Sumiyoshi M, Sakanaka M, Kimura Y (2006). Chronic intake of high-fat and high-sucrose diets differentially affects glucose intolerance in mice. *The Journal of Nutrition* **136**: 582-587.
[156] Sampey BP, Vanhoose AM, Winfield HM, Freemerman AJ, Muehlbauer MJ, Fueger PT, et al. (2011). Cafeteria diet is a robust model of human metabolic syndrome with liver and adipose inflammation: Comparison to high-fat diet. *Obesity* **19**: 1109-1117.
[157] Bortolin RC, Vargas AR, Gasparotto J, Chaves PR, Schnorr CE, Martinello KB, et al. (2017). A new animal diet based on human Western diet is a robust diet-induced obesity model: comparison to high-fat and cafeteria diets in term of metabolic and gut microbiota disruption. *International Journal of Obesity* DOI 10.1038/ijo.2017.225.
[158] Tang L-L, Tang X-H, Li X, Yu H-B, Xie Z-G, Liu X-Y, et al. (2014). Effect of high-fat or high-glucose diet on obesity and visceral adipose tissue in mice. *Acta Academiae Medicinae Sinicae* **36**: 614-619.
[159] Ramirez I (1987). Feeding a liquid diet increases energy intake, weight gain and body fat in rats. *The Journal of Nutrition* **117**: 2127-2134.
[160] DiMeglio DP, Mattes RD (2000). Liquid versus solid carbohydrate: effects on food intake and body weight. *International Journal of Obesity* **24**: 794.
[161] Mattes RD, Campbell WW (2009). Effects of food form and timing of ingestion on appetite and energy intake in lean young adults and in young adults with obesity. *Journal of the American Dietetic Association* **109**: 430-437.
[162] Erdos B, Kirichenko N, Whidden M, Basgut B, Woods M, Cudykier I, et al. (2011). Effect of age on high-fat diet-induced hypertension. *American Journal of Physiology-Heart and Circulatory Physiology* **301**: H164-H172.
[163] Pagliassotti MJ, Gayles EC, Podolin DA, Wei Y, Morin CL (2000). Developmental stage modifies diet-induced peripheral insulin resistance in rats. *American Journal of Physiology-Regulatory, Integrative and Comparative Physiology* **278**: R66-R73.
[164] Kesby JP, Kim JJ, Scadeng M, Woods G, Kado DM, Olefsky JM, et al. (2015). Spatial cognition in adult and aged mice exposed to high-fat diet. *PloS One* **10**: e0140034.
[165] Symonds ME, Sebert SP, Hyatt MA, Budge H (2009). Nutritional programming of the metabolic syndrome. *Nature Reviews Endocrinology* **5**: 604.
[166] Patel MS, Srinivasan M (2010). Metabolic programming due to alterations in nutrition in the immediate postnatal period. *The Journal of Nutrition* **140**: 658-661.
[167] Tain Y-L, Sheen J-M, Yu H-R, Chen C-C, Tiao M-M, Hsu C-N, et al. (2015). Maternal melatonin therapy rescues prenatal dexamethasone and postnatal high-fat diet induced programmed hypertension in male rat offspring. *Frontiers in Physiology* **6**: 377.
[168] Al K, Sarr O, Dunlop K, Gloor GB, Reid G, Burton J, et al. (2017). Impact of birth weight and postnatal diet on the gut microbiota of young adult guinea pigs. *PeerJ* **5**: e2840.
[169] Newman DJ, Cragg GM (2016). Natural products as sources of new drugs from 1981 to 2014. *Journal of Natural Products* **79**: 629-661.
[170] Cicero AFG, Colletti A (2016). Role of phytochemicals in the management of metabolic syndrome. *Phytomedicine* **23**: 1134-1144.
[171] Cheng HS, Ton SH, Abdul Kadir K (2017). Ellagitannin geraniin: a review of the natural sources, biosynthesis, pharmacokinetics and biological effects. *Phytochemistry Reviews* **16**: 159-193.
[172] Cheng J-T, Chang S-S, Hsu F-L (1994). Antihypertensive action of geraniin in rats. *Journal of Pharmacy and Pharmacology* **46**: 46-49.
[173] Lin S-Y, Wang C-C, Lu Y-L, Wu W-C, Hou W-C (2008). Antioxidant, anti-semicarbazide-sensitive amine oxidase, and anti-hypertensive activities of geraniin isolated from Phyllanthus urinaria. *Food and Chemical Toxicology* **46**: 2485-2492.

[174] Chen P, Li F, He B, Wu H, Yang J, Zhang X, et al. (2012). Effects of geraniin on platelet aggregation and interactions between platelets and neutrophils. *Journal of Kunming Medical University* **33**: 4-10.
[175] Palanisamy UD, Ling LT, Manaharan T, Appleton D (2011). Rapid isolation of geraniin from Nephelium lappaceum rind waste and its anti-hyperglycemic activity. *Food Chemistry* **127**: 21-27.
[176] Muhtadi, Primarianti AU, Sujono TA (2015). Antidiabetic activity of durian (Durio Zibethinus Murr.) and rambutan (Nephelium Lappaceum L.) fruit peels in alloxan diabetic rats. *Procedia Food Science* **3**: 255-261.
[177] Rani S, Kumar B (2015). Efficacy of Phyllanthus niruri Linn. extract in the management of type-2 diabetes mellitus associated hypercholesterolemia in mice diabetic model. *International journal of Current Microbiology and Applied Sciences* **4**: 507-513.
[178] Sudjaroen Y, Hull WE, Erben G, Würtele G, Changbumrung S, Ulrich CM, et al. (2012). Isolation and characterization of ellagitannins as the major polyphenolic components of Longan (Dimocarpus longan Lour) seeds. *Phytochemistry* **77**: 226-237.
[179] Park S, Han S-U, Lee K-M, Park KH, Cho SW, Hahm K-B (2007). 5-LOX inhibitor modulates the inflammatory responses provoked by Helicobacter pylori infection. *Helicobacter* **12**: 49-58.
[180] Fujiki H, Suganuma M, Kurusu M, Okabe S, Imayoshi Y, Taniguchi S, et al. (2003). New TNF-α releasing inhibitors as cancer preventive agents from traditional herbal medicine and combination cancer prevention study with EGCG and sulindac or tamoxifen. *Mutation Research/Fundamental and Molecular Mechanisms of Mutagenesis* **523-524**: 119-125.
[181] Chung APYS, Ton SH, Gurtu S, Palanisamy UD (2014). Ellagitannin geraniin supplementation ameliorates metabolic risks in high-fat diet-induced obese Sprague Dawley rats. *Journal of Functional Foods* **9**: 173-182.
[182] Thitilertdecha N, Teerawutgulrag A, Kilburn JD, Rakariyatham N (2010). Identification of major phenolic compounds from Nephelium lappaceum L. and their antioxidant activities. *Molecules* **15**: 1453.
[183] Barrios-Ramos J, Garduño-Siciliano L, Loredo-Mendoza M, G C-C, ME J-F, E M-B, et al. (2014). A quick model for the induction of metabolic syndrome markers in rats. *Internal Medicine* **4**: 137.
[184] Fujita Y, Maki K (2016). High-fat diet-induced obesity triggers alveolar bone loss and spontaneous periodontal disease in growing mice. *BMC Obesity* **3**: 1.
[185] Thirunavukkarasu V, Anitha Nandhini AT, Anuradha CV (2004). Lipoic acid attenuates hypertension and improves insulin sensitivity, kallikrein activity and nitrite levels in high fructose-fed rats. *Journal of Comparative Physiology B* **174**: 587-592.
[186] Catalano KJ, Bergman RN, Ader M (2005). Increased susceptibility to insulin resistance associated with abdominal obesity in aging rats. *Obesity Research* **13**: 11-20.
[187] Cheng HS, Ton SH, Phang SCW, Tan JBL, Abdul Kadir K (2017). Increased susceptibility of post-weaning rats on high-fat diet to metabolic syndrome. *Journal of Advanced Research* **8**: 743-752.
[188] Leopoldini M, Russo N, Toscano M (2011). The molecular basis of working mechanism of natural polyphenolic antioxidants. *Food Chemistry* **125**: 288-306.
[189] Pandey KB, Rizvi SI (2009). Plant polyphenols as dietary antioxidants in human health and disease. *Oxidative Medicine and Cellular Longevity* **2**: 270-278.
[190] Okuda T, Yoshida T, Mori K (1975). Constituents of *Geranium thunbergii* SIEB. et ZUCC. II. Ellagitannins. *Yakugaku Zasshi* **95**: 1462-1466.
[191] Baliga MS, Dsouza JJ (2011). Amla (Emblica officinalis Gaertn), a wonder berry in the treatment and prevention of cancer. *European Journal of Cancer Prevention* **20**: 225-239.

[192] Liu D, Su Z, Wang C, Gu M, Xing S (2010). Separation and purification of hydrolyzable tannin from Geranium wilfordii Maxim by reversed-phase and normal-phase high-speed counter-current chromatography. *Journal of Separation Science* **33**: 2266-2271.
[193] Luger P, Weber M, Kashino S, Amakura Y, Yoshida T, Okuda T, et al. (1998). Structure of the tannin geraniin based on conventional X-ray data at 295K and on synchroton data at 293 and 120K. *Acta Crystallographica* **54**: 687-694.
[194] Velázquez-González C, Cariño-Cortés R, Gayosso de Lucio JA, Ortiz MI, De la O Arciniega M, Altamirano-Báez DA, et al. (2014). Antinociceptive and anti-inflammatory activities of Geranium bellum and its isolated compounds. *BMC Complementary and Alternative Medicine* **14**: 506.
[195] Agyare C, Lechtenberg M, Deters A, Petereit F, Hensel A (2011). Ellagitannins from Phyllanthus muellerianus (Kuntze) Exell.: Geraniin and furosin stimulate cellular activity, differentiation and collagen synthesis of human skin keratinocytes and dermal fibroblasts. *Phytomedicine* **18**: 617-624.
[196] Bing SJ, Ha D, Kim MJ, Park E, Ahn G, Kim DS, et al. (2013). Geraniin down regulates gamma radiation-induced apoptosis by suppressing DNA damage. *Food and Chemical Toxicology* **57**: 147-153.
[197] Kimura Y, Okuda H, Mori K, Okuda T, Arichi S (1984). Studies on the activities of tannins and related compounds from medicinal plants and drugs. IV. Effects of various extracts of Geranii herba and geraniin on liver injury and lipid metabolism in rats fed peroxidized oil. *Chemical and Pharmaceutical Bulletin* **32**: 1866-1871.
[198] Ito H, Iguchi A, Hatano T (2008). Identification of urinary and intestinal bacterial metabolites of ellagitannin geraniin in rats. *Journal of Agricultural and Food Chemistry* **56**: 393-400.
[199] Perera A, Appleton D, Ying LH, Elendran S, Palanisamy UD (2012). Large scale purification of geraniin from Nephelium lappaceum rind waste using reverse-phase chromatography. *Separation and Purification Technology* **98**: 145-149.
[200] Khor HT, Chieng DY, Ong KK (1995). Tocotrienols inhibit liver HMG CoA reductase activity in the guinea pig. *Nutrition Research* **15**: 537-544.
[201] Müller L, Theile K, Böhm V (2010). In vitro antioxidant activity of tocopherols and tocotrienols and comparison of vitamin E concentration and lipophilic antioxidant capacity in human plasma. *Molecular Nutrition and Food Research* **54**: 731-742.
[202] Orchard TJ, Temprosa M, Goldberg R, et al. (2005). The effect of metformin and intensive lifestyle intervention on the metabolic syndrome: The diabetes prevention program randomized trial. *Annals of Internal Medicine* **142**: 611-619.
[203] Lily M, Godwin M (2009). Treating prediabetes with metformin: Systematic review and meta-analysis. *Canadian Family Physician* **55**: 363-369.
[204] Gohar Ahmed A, Lahloub Mohammed F, Niwa M (2003). Antibacterial Polyphenol from Erodium glaucophyllum. *Zeitschrift für Naturforschung C* **58**: 670.
[205] Tang Y-Q, Jaganath IB, Sekaran SD (2010). Phyllanthus spp. Induces Selective Growth Inhibition of PC-3 and MeWo Human Cancer Cells through Modulation of Cell Cycle and Induction of Apoptosis. *PloS One* **5**: e12644.
[206] Hoggatt AF, Hoggatt J, Honerlaw M, Pelus LM (2010). A spoonful of sugar helps the medicine go down: A novel technique to improve oral gavage in mice. *Journal of the American Association for Laboratory Animal Science* **49**: 329-334.
[207] United States Food and Drug Administration (2005). *Guidance for Industry: Estimating the Maximum Safe Starting Dose in Initial Clinical Trials for Therapeutics in Adult Healthy Volunteers*. Retrieved 30 January, 2018, from https://www.fda.gov/ohrms/dockets/98fr/02d-0492-gdl0002.pdf.

[208] Norazlina M, Ima-Nirwana S, Abdul Gapor MT, Abdul Kadir K (2002). Tocotrienols are needed for normal bone calcification in growing female rats. *Asia Pacific Journal of Clinical Nutrition* **11**: 194-199.
[209] Ahmad NS, Abdul Kadir K, Luke DA, Ima Nirwana S (2005). Tocotrienol offers better protection than tocopherol from free radical-induced damage of rat bone. *Clinical and Experimental Pharmacology and Physiology* **32**: 761-770.
[210] Levy JC, Matthews DR, Hermans MP (1998). Correct homeostasis model assessment (HOMA) evaluation uses the computer program. *Diabetes Care* **21**: 2191-2192.
[211] Parlee SD, Lentz SI, Mori H, MacDougald OA (2014). Quantifying size and number of adipocytes in adipose tissue. *Methods in Enzymology* **537**: 93-122.
[212] Schneider CA, Rasband WS, Eliceiri KW (2012). NIH Image to ImageJ: 25 years of image analysis. *Nature Methods* **9**: 671-675.
[213] Folch J, Lees M, Stanley GHS (1957). A simple method for the isolation and purification of total lipides from animal tissues. *Journal of Biological Chemistry* **226**: 497-509.
[214] Salpeter SR, Buckley NS, Kahn JA, Salpeter EE (2008). Meta-analysis: metformin treatment in persons at risk for diabetes mellitus. *The American Journal of Medicine* **121**: 149-157.e142.
[215] Aroda VR, Knowler WC, Crandall JP, Perreault L, Edelstein SL, Jeffries SL, et al. (2017). Metformin for diabetes prevention: insights gained from the Diabetes Prevention Program/Diabetes Prevention Program Outcomes Study. *Diabetologia* **60**: 1601-1611.
[216] Meyer C, Pimenta W, Woerle HJ, Van Haeften T, Szoke E, Mitrakou A, et al. (2006). Different mechanisms for impaired fasting glucose and impaired postprandial glucose tolerance in humans. *Diabetes Care* **29**: 1909-1914.
[217] Nathan DM, Davidson MB, DeFronzo RA, Heine RJ, Henry RR, Pratley R, et al. (2007). Impaired fasting glucose and impaired glucose tolerance: Implications for care. *Diabetes Care* **30**: 753-759.
[218] Hundal RS, Krssak M, Dufour S, Laurent D, Lebon V, Chandramouli V, et al. (2000). Mechanism by which metformin reduces glucose production in type 2 diabetes. *Diabetes* **49**: 2063-2069.
[219] Top W, Stehouwer C, Lehert P, Kooy A (2017). Metformin and β-cell function in insulin-treated patients with type 2 diabetes: A randomized placebo-controlled 4.3-year trial. *Diabetes, Obesity and Metabolism* DOI 10.1111/dom.13123.
[220] Lachin JM, Christophi CA, Edelstein SL, Ehrmann DA, Hamman RF, Kahn SE, et al. (2007). Factors associated with diabetes onset during metformin versus placebo therapy in the Diabetes Prevention Program. *Diabetes* **56**: 1153-1159.
[221] McDonagh MS, Selph S, Ozpinar A, Foley C (2014). Systematic review of the benefits and risks of metformin in treating obesity in children aged 18 years and younger. *JAMA Pediatrics* **168**: 178-184.
[222] Levri KM, Slaymaker E, Last A, Yeh J, Ference J, D'Amico F, et al. (2005). Metformin as treatment for overweight and obese adults: A systematic review. *The Annals of Family Medicine* **3**: 457-461.
[223] Espín JC, González-Barrio R, Cerdá B, López-Bote C, Rey AI, Tomás-Barberán FA (2007). Iberian pig as a model to clarify obscure points in the bioavailability and metabolism of ellagitannins in humans. *Journal of Agricultural and Food Chemistry* **55**: 10476-10485.
[224] Rogerio Tavares R, Maria Paula M, Joao Filipe R (2016). HbA1c, fructosamine, and glycated albumin in the detection of dysglycaemic conditions. *Current Diabetes Reviews* **12**: 14-19.
[225] Nar A, Gedik O (2009). The effect of metformin on leptin in obese patients with type 2 diabetes mellitus and nonalcoholic fatty liver disease. *Acta Diabetologica* **46**: 113-118.

[226] Madsen A, Bozickovic O, Bjune J-I, Mellgren G, Sagen JV (2015). Metformin inhibits hepatocellular glucose, lipid and cholesterol biosynthetic pathways by transcriptionally suppressing steroid receptor coactivator 2 (SRC-2). *Scientific Reports* **5**: 16430.
[227] Viollet B, Guigas B, Garcia NS, Leclerc J, Foretz M, Andreelli F (2012). Cellular and molecular mechanisms of metformin: an overview. *Clinical Science* **122**: 253-270.
[228] Li Y, Liu L, Wang B, Wang J, Chen D (2013). Metformin in non-alcoholic fatty liver disease: A systematic review and meta-analysis. *Biomedical Reports* **1**: 57-64.
[229] Koba K, Abe K, Ikeda I, Sugano M (1992). Effects of alpha-tocopherol and tocotrienols on blood pressure and linoleic acid metabolism in the spontaneously hypertensive rat (SHR). *Bioscience, Biotechnology, and Biochemistry* **56**: 1420-1423.
[230] Rasool AHG, Yuen KH, Yusoff K, Wong AR, Rahman ARA (2006). Dose dependent elevation of plasma tocotrienol levels and its effect on arterial compliance, plasma total antioxidant status, and lipid profile in healthy humans supplemented with tocotrienol rich vitamin E. *Journal of Nutritional Science and Vitaminology* **52**: 473-478.
[231] Chen X, Touyz RM, Park JB, Schiffrin EL (2001). Antioxidant effects of vitamins C and E are associated with altered activation of vascular NADPH oxidase and superoxide dismutase in stroke-prone SHR. *Hypertension* **38**: 606-611.
[232] Muharis SP, Top AGM, Murugan D, Mustafa MR (2010). Palm oil tocotrienol fractions restore endothelium dependent relaxation in aortic rings of streptozotocin-induced diabetic and spontaneously hypertensive rats. *Nutrition Research* **30**: 209-216.
[233] Baliarsingh S, Beg ZH, Ahmad J (2005). The therapeutic impacts of tocotrienols in type 2 diabetic patients with hyperlipidemia. *Atherosclerosis* **182**: 367-374.
[234] Qureshi AA, Sami SA, Salser WA, Khan FA (2002). Dose-dependent suppression of serum cholesterol by tocotrienol-rich fraction (TRF25) of rice bran in hypercholesterolemic humans. *Atherosclerosis* **161**: 199-207.
[235] Chin S-F, Ibahim J, Makpol S, Abdul Hamid NA, Abdul Latiff A, Zakaria Z, et al. (2011). Tocotrienol rich fraction supplementation improved lipid profile and oxidative status in healthy older adults: A randomized controlled study. *Nutrition and Metabolism* **8**: 42.
[236] Magosso E, Ansari MA, Gopalan Y, Shuaib IL, Wong J-W, Khan NAK, et al. (2013). Tocotrienols for normalisation of hepatic echogenic response in nonalcoholic fatty liver: a randomised placebo-controlled clinical trial. *Nutrition Journal* **12**: 166.
[237] Muto C, Yachi R, Aoki Y, Koike T, Igarashi O, Kiyose C (2013). Gamma-tocotrienol reduces the triacylglycerol level in rat primary hepatocytes through regulation of fatty acid metabolism. *Journal of Clinical Biochemistry and Nutrition* **52**: 32-37.
[238] Matough FA, budin SB, Hamid ZA, Rahman MA, Al-Wahaibi N, Mohammed J (2014). Tocotrienol-rich fraction from palm oil prevents oxidative damage in diabetic rats. *Sultan Qaboos University Medical Journal* **14**: e95-e103.
[239] Budin SB, Yusof KM, Idris MHM, Hamid ZA, Mohamed J (2011). Tocotrienol-rich fraction of palm oil reduced pancreatic damage and oxidative stress in streptozotocin-induced diabetic rats *Australian Journal of Basic and Applied Sciences* **5**: 2367-2374.
[240] Wan Nazaimoon W, Abdul Kadir K (2002). Tocotrienols-rich diet decreases advanced glycosylation end-products in non-diabetic rats and improves glycemic control in streptozotocin-induced diabetic rats. *Malaysian Journal of Pathology* **24**: 77-82.
[241] Wong W-Y, Poudyal H, Ward LC, Brown L (2012). Tocotrienols reverse cardiovascular, metabolic and liver changes in high carbohydrate, high fat diet-fed rats. *Nutrients* **4**: 1527.
[242] Akbar S, Bellary S, Griffiths HR (2011). Dietary antioxidant interventions in type 2 diabetes patients: a meta-analysis. *The British Journal of Diabetes & Vascular Disease* **11**: 62-68.

[243] Cheng HS, Ton SH, Tan JBL, Abdul Kadir K (2017). The ameliorative effects of a tocotrienol-rich fraction on the AGE-RAGE axis and hypertension in high-fat-diet-fed rats with metabolic syndrome. *Nutrients* **9**: 984.
[244] Garcia-Muñoz C, Vaillant F (2014). Metabolic fate of ellagitannins: Implications for health, and research perspectives for innovative functional foods. *Critical Reviews in Food Science and Nutrition* **54**: 1584-1598.
[245] Cerdá B, Espín JC, Parra S, Martínez P, Tomás-Barberán FA (2004). The potent in vitro antioxidantellagitannins from pomegranate juice aremetabolised into bioavailable but poorantioxidant hydroxy–6H–dibenzopyran–6–one derivatives by the colonic microfloraof healthy humans. *European Journal of Nutrition* **43**: 205-220.
[246] Shahrzad S, Aoyagi K, Winter A, Koyama A, Bitsch I (2001). Pharmacokinetics of gallic acid and its relative bioavailability from tea in healthy humans. *The Journal of Nutrition* **131**: 1207-1210.
[247] González-Sarrías A, García-Villalba R, Núñez-Sánchez MÁ, Tomé-Carneiro J, Zafrilla P, Mulero J, et al. (2015). Identifying the limits for ellagic acid bioavailability: A crossover pharmacokinetic study in healthy volunteers after consumption of pomegranate extracts. *Journal of Functional Foods* **19**: 225-235.
[248] Seeram NP, Lee R, Heber D (2004). Bioavailability of ellagic acid in human plasma after consumption of ellagitannins from pomegranate (Punica granatum L.) juice. *Clinica Chimica Acta* **348**: 63-68.
[249] Bak E-J, Kim J, Jang S, Woo G-H, Yoon H-G, Yoo Y-J, et al. (2013). Gallic acid improves glucose tolerance and triglyceride concentration in diet-induced obesity mice. *Scandinavian Journal of Clinical and Laboratory Investigation* **73**: 607-614.
[250] Chao J, Huo T-I, Cheng H-Y, Tsai J-C, Liao J-W, Lee M-S, et al. (2014). Gallic Acid Ameliorated Impaired Glucose and Lipid Homeostasis in High Fat Diet-Induced NAFLD Mice. *PloS One* **9**: e96969.
[251] Doan KV, Ko CM, Kinyua AW, Yang DJ, Choi Y-H, Oh IY, et al. (2015). Gallic acid regulates body weight and glucose homeostasis through AMPK activation. *Endocrinology* **156**: 157-168.
[252] Hsu C-L, Yen G-C (2007). Effect of gallic acid on high fat diet-induced dyslipidaemia, hepatosteatosis and oxidative stress in rats. *British Journal of Nutrition* **98**: 727-735.
[253] Panchal SK, Ward L, Brown L (2013). Ellagic acid attenuates high-carbohydrate, high-fat diet-induced metabolic syndrome in rats. *European Journal of Nutrition* **52**: 559-568.
[254] Yoshimura Y, Nishii S, Zaima N, Moriyama T, Kawamura Y (2013). Ellagic acid improves hepatic steatosis and serum lipid composition through reduction of serum resistin levels and transcriptional activation of hepatic ppara in obese, diabetic KK-Ay mice. *Biochemical and Biophysical Research Communications* **434**: 486-491.
[255] Spigoni V, Mena P, Cito M, Fantuzzi F, Bonadonna R, Brighenti F, et al. (2016). Effects on nitric oxide production of urolithins, gut-derived ellagitannin metabolites, in human aortic endothelial cells. *Molecules* **21**: 1009.
[256] Reuter S, Gupta SC, Chaturvedi MM, Aggarwal BB (2010). Oxidative stress, inflammation, and cancer: How are they linked? *Free Radical Biology and Medicine* **49**: 1603-1616.
[257] Jabs T (1999). Reactive oxygen intermediates as mediators of programmed cell death in plants and animals. *Biochemical Pharmacology* **57**: 231-245.
[258] Bhatti JS, Bhatti GK, Reddy PH (2017). Mitochondrial dysfunction and oxidative stress in metabolic disorders — A step towards mitochondria based therapeutic strategies. *Biochimica et Biophysica Acta (BBA) - Molecular Basis of Disease* **1863**: 1066-1077.

[259] Sakai K, Matsumoto K, Nishikawa T, Suefuji M, Nakamaru K, Hirashima Y, et al. (2003). Mitochondrial reactive oxygen species reduce insulin secretion by pancreatic β-cells. *Biochemical and Biophysical Research Communications* **300**: 216-222.
[260] Houstis N, Rosen ED, Lander ES (2006). Reactive oxygen species have a causal role in multiple forms of insulin resistance. *Nature* **440**: 944.
[261] Lugrin J, Rosenblatt-Velin N, Parapanov R, Liaudet L (2014). The role of oxidative stress during inflammatory processes. *Biological Chemistry* **395**: 203.
[262] Esposito K, Marfella R, Ciotola M, et al. (2004). Effect of a mediterranean-style diet on endothelial dysfunction and markers of vascular inflammation in the metabolic syndrome: A randomized trial. *JAMA* **292**: 1440-1446.
[263] Hung J, McQuillan BM, Chapman CML, Thompson PL, Beilby JP (2005). Elevated interleukin-18 levels are associated with the metabolic syndrome independent of obesity and insulin resistance. *Arteriosclerosis, Thrombosis, and Vascular Biology* **25**: 1268-1273.
[264] Marseglia L, Manti S, D'Angelo G, Nicotera A, Parisi E, Di Rosa G, et al. (2015). Oxidative stress in obesity: A critical component in human diseases. *International Journal of Molecular Sciences* **16**: 378.
[265] Choi KM, Ryu OH, Lee KW, Kim HY, Seo JA, Kim SG, et al. (2007). Serum adiponectin, interleukin-10 levels and inflammatory markers in the metabolic syndrome. *Diabetes Research and Clinical Practice* **75**: 235-240.
[266] Singh R, Barden A, Mori T, Beilin L (2001). Advanced glycation end-products: a review. *Diabetologia* **44**: 129-146.
[267] Xie J, Méndez JD, Méndez-Valenzuela V, Aguilar-Hernández MM (2013). Cellular signalling of the receptor for advanced glycation end products (RAGE). *Cellular Signalling* **25**: 2185-2197.
[268] Ishimoto H, Tai A, Yoshimura M, Amakura Y, Yoshida T, Hatano T, et al. (2012). Antioxidative properties of functional polyphenols and their metabolites assessed by an ORAC assay. *Bioscience, Biotechnology, and Biochemistry* **76**: 395-399.
[269] Pan MH, Lin-Shiau SY, Ho CT, Lin JH, Lin JK (2000). Suppression of lipopolysaccharide-induced nuclear factor-kappaB activity by theaflavin-3,3'-digallate from black tea and other polyphenols through down-regulation of IkappaB kinase activity in macrophages. *Biochemical Pharmacology* **59**: 357-367.
[270] Acharya K (2017). Simplified methods for microtiter based analysis of *in vitro* antioxidant activity. *Asian Journal of Pharmaceitics* **11**: S327-S335.
[271] Svingen T, Letting H, Hadrup N, Hass U, Vinggaard AM (2015). Selection of reference genes for quantitative RT-PCR (RT-qPCR) analysis of rat tissues under physiological and toxicological conditions. *PeerJ* **3**: e855.
[272] Anatoliotakis N, Deftereos S, Bouras G, Giannopoulos G, Tsounis D, Angelidis C, et al. (2013). Myeloperoxidase: Expressing inflammation and oxidative stress in cardiovascular disease. *Current Topics in Medicinal Chemistry* **13**: 115-138.
[273] Akdis M, Aab A, Altunbulakli C, Azkur K, Costa RA, Crameri R, et al. (2016). Interleukins (from IL-1 to IL-38), interferons, transforming growth factor β, and TNF-α: Receptors, functions, and roles in diseases. *Journal of Allergy and Clinical Immunology* **138**: 984-1010.
[274] Sies H, Stahl W, Sevanian A (2005). Nutritional, dietary and postprandial oxidative stress. *The Journal of Nutrition* **135**: 969-972.
[275] Yida Z, Imam MU, Ismail M, Ismail N, Ideris A, Abdullah MA (2015). High fat diet-induced inflammation and oxidative stress are attenuated by N-acetylneuraminic acid in rats. *Journal of Biomedical Science* **22**: 96.

[276] Walczewska A, Dziedzic B, Stepien T, Swiatek E, Nowak D (2010). Effect of dietary fats on oxidative-antioxidative status of blood in rats. *Journal of Clinical Biochemistry and Nutrition* **47**: 18-26.
[277] Vargas-Robles H, Rios A, Arellano-Mendoza M, Escalante BA, Schnoor M (2015). Antioxidative diet supplementation reverses high-fat diet-induced increases of cardiovascular risk factors in mice. *Oxidative Medicine and Cellular Longevity* **2015**: 9.
[278] Leighton F, Cuevas A, Guasch V, Pérez DD, Strobel P, San Martín A, et al. (1999). Plasma polyphenols and antioxidants, oxidative DNA damage and endothelial function in a diet and wine intervention study in humans. *Drugs Under Experimental and Clinical Research* **25**: 133-141.
[279] Chung APYS, Gurtu S, Chakravarthi S, Moorthy M, Palanisamy UD (2018). Geraniin protects high-fat diet-induced oxidative stress in Sprague Dawley rats. *Frontiers in Nutrition* **5**: 17.
[280] Jarukamjorn K, Jearapong N, Pimson C, Chatuphonprasert W (2016). A high-fat, high-fructose diet induces antioxidant imbalance and increases the risk and progression of nonalcoholic fatty liver disease in mice. *Scientifica* **2016**: 10.
[281] Yamagishi S-i, Nakamura N, Suematsu M, Kaseda K, Matsui T (2015). Advanced glycation end products: A molecular target for vascular complications in diabetes. *Molecular Medicine* **21**: S32-S40.
[282] Hideyuki H, Sho-ichi Y (2008). Advanced glycation end products (AGEs) and their involvement in liver disease. *Current Pharmaceutical Design* **14**: 969-972.
[283] Pereira ENGdS, Silvares RR, Flores EEI, Rodrigues KL, Ramos IP, da Silva IJ, et al. (2017). Hepatic microvascular dysfunction and increased advanced glycation end products are components of non-alcoholic fatty liver disease. *PloS One* **12**: e0179654.
[284] Leung C, Herath C, Jia Z, Andrikopoulos S, Brown B, Davies M, et al. (2016). Dietary advanced glycation end-products aggravate non-alcoholic fatty liver disease. *World Journal of Gastroenterology* **22**: 8026-8040.
[285] Yamagishi S-i, Matsui T (2015). Role of receptor for advanced glycation end products (RAGE) in liver disease. *European Journal of Medical Research* **20**: 15.
[286] Matsuzawa-Nagata N, Takamura T, Ando H, Nakamura S, Kurita S, Misu H, et al. (2008). Increased oxidative stress precedes the onset of high-fat diet–induced insulin resistance and obesity. *Metabolism* **57**: 1071-1077.
[287] Young IS, Woodside JV (2001). Antioxidants in health and disease. *Journal of Clinical Pathology* **54**: 176-186.
[288] Kurutas EB (2016). The importance of antioxidants which play the role in cellular response against oxidative/nitrosative stress: current state. *Nutrition Journal* **15**: 71.
[289] Nguyen T, Nioi P, Pickett CB (2009). The Nrf2-antioxidant response element signaling pathway and its activation by oxidative stress. *Journal of Biological Chemistry* **284**: 13291-13295.
[290] Filomeni G, De Zio D, Cecconi F (2014). Oxidative stress and autophagy: the clash between damage and metabolic needs. *Cell Death and Differentiation* **22**: 377.
[291] Kurihara Y, Kanki T, Aoki Y, Hirota Y, Saigusa T, Uchiumi T, et al. (2012). Mitophagy plays an essential role in reducing mitochondrial production of reactive oxygen species and mutation of mitochondrial DNA by maintaining mitochondrial quantity and quality in yeast. *Journal of Biological Chemistry* **287**: 3265-3272.
[292] Ito H (2011). Metabolites of the ellagitannin geraniin and their antioxidant activities. *Planta Medica* **77**: 1110-1115.
[293] Karakas M, Koenig W (2012). Myeloperoxidase production by macrophage and risk of atherosclerosis. *Current Atherosclerosis Reports* **14**: 277-283.

[294] Kataoka Y, Shao M, Wolski K, Uno K, Puri R, Murat Tuzcu E, et al. (2014). Myeloperoxidase levels predict accelerated progression of coronary atherosclerosis in diabetic patients: Insights from intravascular ultrasound. *Atherosclerosis* **232**: 377-383.
[295] Chen GY, Nuñez G (2010). Sterile inflammation: sensing and reacting to damage. *Nature Reviews Immunology* **10**: 826.
[296] Miller YI, Choi S-H, Wiesner P, Fang L, Harkewicz R, Hartvigsen K, et al. (2011). Oxidation-specific epitopes are danger-associated molecular patterns recognized by pattern recognition receptors of innate immunity. *Circulation Research* **108**: 235-248.
[297] Land WG (2015). The role of damage-associated molecular patterns (DAMPs) in human diseases Part II: DAMPs as diagnostics, prognostics and therapeutics in clinical medicine. *Sultan Qaboos University Medical Journal* **15**: e157-e170.
[298] Rocha VZ, Libby P (2009). Obesity, inflammation, and atherosclerosis. *Nature Reviews Cardiology* **6**: 399.
[299] Zernecke A, Weber C (2010). Chemokines in the vascular inflammatory response of atherosclerosis. *Cardiovascular Research* **86**: 192-201.
[300] Ishii M, Araki S, Goto M, Yamamoto Y, Kusuhara K (2016). CCL2 level is elevated with metabolic syndrome and CXCL10 level is correlated with visceral fat area in obese children. *Endocrine Journal* **63**: 795-804.
[301] Herder C, Haastert B, Müller-Scholze S, Koenig W, Thorand B, Holle R, et al. (2005). Association of systemic chemokine concentrations with impaired glucose tolerance and type 2 diabetes. *Results from the Cooperative Health Research in the Region of Augsburg Survey S4 (KORA S4)* **54**: S11-S17.
[302] Wang Q, Xie Z, Zhang W, Zhou J, Wu Y, Zhang M, et al. (2014). Myeloperoxidase deletion prevents high-fat diet–induced obesity and insulin resistance. *Diabetes* **63**: 4172-4185.
[303] Shibata A, Kobayashi T, Asai A, Eitsuka T, Oikawa S, Miyazawa T, et al. (2017). High purity tocotrienols attenuate atherosclerotic lesion formation in apoE-KO mice. *The Journal of Nutritional Biochemistry* **48**: 44-50.
[304] Cheng Y-C, Sheen J-M, Hu WL, Hung Y-C (2017). Polyphenols and oxidative stress in atherosclerosis-related ischemic heart disease and stroke. *Oxidative Medicine and Cellular Longevity* **2017**: 16.
[305] Chakraborty A, Chowdhury S, Bhattacharyya M (2011). Effect of metformin on oxidative stress, nitrosative stress and inflammatory biomarkers in type 2 diabetes patients. *Diabetes Research and Clinical Practice* **93**: 56-62.
[306] Esteghamati A, Eskandari D, Mirmiranpour H, Noshad S, Mousavizadeh M, Hedayati M, et al. (2013). Effects of metformin on markers of oxidative stress and antioxidant reserve in patients with newly diagnosed type 2 diabetes: A randomized clinical trial. *Clinical Nutrition* **32**: 179-185.
[307] Lund SS, Tarnow L, Stehouwer CDA, Schalkwijk CG, Teerlink T, Gram J, et al. (2008). Impact of metformin versus repaglinide on non-glycaemic cardiovascular risk markers related to inflammation and endothelial dysfunction in non-obese patients with type 2 diabetes. *European Journal of Endocrinology* **158**: 631-641.
[308] Mirmiranpour H, Mousavizadeh M, Noshad S, Ghavami M, Ebadi M, Ghasemiesfe M, et al. (2013). Comparative effects of pioglitazone and metformin on oxidative stress markers in newly diagnosed type 2 diabetes patients: A randomized clinical trial. *Journal of Diabetes and Its Complications* **27**: 501-507.
[309] Cicero AF, Rosticci M, Parini A, Morbini M, Urso R, Grandi E, et al. (2015). Short-term effects of a combined nutraceutical of insulin-sensitivity, lipid level and indexes of liver steatosis: a double-blind, randomized, cross-over clinical trial. *Nutrition Journal* **14**: 30.

[310] Turk Z (2010). Glycotoxines, carbonyl stress and relevance to diabetes and its complications. *Physiological Research* **59**: 147-156.
[311] Prasad K (2011). Tocotrienols and cardiovascular health. *Current Pharmaceutical Design* **17**: 2147-2154.
[312] Yan SF, Ramasamy R, Schmidt AM (2010). Soluble RAGE: Therapy and biomarker in unraveling the RAGE axis in chronic disease and aging. *Biochemical Pharmacology* **79**: 1379-1386.
[313] Schmidt AM (2015). Soluble RAGEs — Prospects for treating & tracking metabolic and inflammatory disease. *Vascular Pharmacology* **72**: 1-8.
[314] Ballak DB, Stienstra R, Tack CJ, Dinarello CA, van Diepen JA (2015). IL-1 family members in the pathogenesis and treatment of metabolic disease: Focus on adipose tissue inflammation and insulin resistance. *Cytokine* **75**: 280-290.
[315] Jiang L, Liu Y, He P, Chen J, Liu S, Tan N (2016). Geraniin ameliorates cisplatin-induced nephrotoxicity in mice. *Free Radical Research* **50**: 813-819.
[316] Zhu G, Xin X, Liu Y, Huang Y, Li K, Wu C (2017). Geraniin attenuates LPS-induced acute lung injury via inhibiting NF-κB and activating Nrf2 signaling pathways. *Oncotarget* **8**: 22835-22841.
[317] Wong W-Y, Ward LC, Fong CW, Yap WN, Brown L (2017). Anti-inflammatory γ- and δ-tocotrienols improve cardiovascular, liver and metabolic function in diet-induced obese rats. *European Journal of Nutrition* **56**: 133-150.
[318] Yoshifumi S (2015). Metformin and inflammation: Its potential beyond glucose-lowering effect. *Endocrine, Metabolic and Immune Disorders - Drug Targets* **15**: 196-205.
[319] Salminen A, Hyttinen JMT, Kaarniranta K (2011). AMP-activated protein kinase inhibits NF-κB signaling and inflammation: impact on healthspan and lifespan. *Journal of Molecular Medicine* **89**: 667-676.
[320] Koh SJ, Kim JM, Kim IK, Ko SH, Kim JS (2014). Anti‐inflammatory mechanism of metformin and its effects in intestinal inflammation and colitis‐associated colon cancer. *Journal of Gastroenterology and Hepatology* **29**: 502-510.
[321] Lee S-Y, Lee SH, Yang E-J, Kim E-K, Kim J-K, Shin D-Y, et al. (2015). Metformin ameliorates inflammatory bowel disease by suppression of the STAT3 signaling pathway and regulation of the between Th17/Treg balance. *PloS One* **10**: e0135858.
[322] Moore KW, Malefyt RdW, Coffman RL, O'Garra A (2001). Interleukin-10 and the Interleukin-10 Receptor. *Annual Review of Immunology* **19**: 683-765.
[323] Esposito K, Pontillo A, Giugliano F, Giugliano G, Marfella R, Nicoletti G, et al. (2003). Association of low interleukin-10 levels with the metabolic syndrome in obese women. *The Journal of Clinical Endocrinology and Metabolism* **88**: 1055-1058.
[324] van Exel E, Gussekloo J, de Craen AJM, Frölich M, Bootsma-van der Wiel A, Westendorp RGJ (2002). Low production capacity of interleukin-10 associates with the metabolic syndrome and type 2 diabetes: The Leiden 85-Plus Study. *Diabetes* **51**: 1088-1092.
[325] Straczkowski M, Kowalska I, Nikolajuk A, Krukowska A, Gorska M (2005). Plasma interleukin-10 concentration is positively related to insulin sensitivity in young healthy individuals. *Diabetes Care* **28**: 2036-2037.
[326] Leon-Cabrera S, Arana-Lechuga Y, Esqueda-León E, Terán-Pérez G, Gonzalez-Chavez A, Escobedo G, et al. (2015). Reduced systemic levels of IL-10 are associated with the severity of obstructive sleep apnea and insulin resistance in morbidly obese humans. *Mediators of Inflammation* **2015**: 9.
[327] Barry JC, Shakibakho S, Durrer C, Simtchouk S, Jawanda KK, Cheung ST, et al. (2016). Hyporesponsiveness to the anti-inflammatory action of interleukin-10 in type 2 diabetes. *Scientific Reports* **6**: 21244.

[328] Kesherwani V, Chavali V, Hackfort BT, Tyagi SC, Mishra PK (2015). Exercise ameliorates high fat diet induced cardiac dysfunction by increasing interleukin 10. *Frontiers in Physiology* **6**: 124.
[329] Leng SX, McElhaney JE, Walston JD, Xie D, Fedarko NS, Kuchel GA (2008). ELISA and multiplex technologies for cytokine measurement in inflammation and aging research. *The Journals of Gerontology: Series A* **63**: 879-884.
[330] Prabhakar U, Eirikis E, Reddy M, Silvestro E, Spitz S, Pendley C, et al. (2004). Validation and comparative analysis of a multiplexed assay for the simultaneous quantitative measurement of Th1/Th2 cytokines in human serum and human peripheral blood mononuclear cell culture supernatants. *Journal of Immunological Methods* **291**: 27-38.
[331] Wang P, Peng X, Wei Z-F, Wei F-Y, Wang W, Ma W-D, et al. (2015). Geraniin exerts cytoprotective effect against cellular oxidative stress by upregulation of Nrf2-mediated antioxidant enzyme expression via PI3K/AKT and ERK1/2 pathway. *Biochimica et Biophysica Acta (BBA) - General Subjects* **1850**: 1751-1761.
[332] Wang Y, Wan D, Zhou R, Zhong W, Lu S, Chai Y (2017). Geraniin inhibits migration and invasion of human osteosarcoma cancer cells through regulation of PI3K/Akt and ERK1/2 signaling pathways. *Anti-Cancer Drugs* **28**: 959-966.
[333] Ren Z, Zou W, Cui J, Liu L, Qing Y, Li Y (2017). Geraniin suppresses tumor cell growth and triggers apoptosis in human glioma via inhibition of STAT3 signaling. *Cytotechnology* **69**: 765-773.
[334] Zhai J-W, Gao C, Ma W-D, Wang W, Yao L-P, Xia X-X, et al. (2016). Geraniin induces apoptosis of human breast cancer cells MCF-7 via ROS-mediated stimulation of p38 MAPK. *Toxicology Mechanisms and Methods* **26**: 311-318.
[335] Bost F, Aouadi M, Caron L, Binétruy B (2005). The role of MAPKs in adipocyte differentiation and obesity. *Biochimie* **87**: 51-56.
[336] Zhang Z, Zhou S, Jiang X, Wang Y-H, Li F, Wang Y-G, et al. (2015). The role of the Nrf2/Keap1 pathway in obesity and metabolic syndrome. *Reviews in Endocrine and Metabolic Disorders* **16**: 35-45.
[337] Mackenzie R, Elliott B (2014). Akt/PKB activation and insulin signaling: a novel insulin signaling pathway in the treatment of type 2 diabetes. *Diabetes, Metabolic Syndrome and Obesity* **7**: 55-64.
[338] Hrdlickova R, Toloue M, Tian B (2017). RNA-Seq methods for transcriptome analysis. *Wiley Interdisciplinary Reviews: RNA* **8**: e1364.
[339] Andrews S (2010). *FastQC: A quality control tool for high throughput sequence data*. Retrieved 7 March, 2018, from https://www.bioinformatics.babraham.ac.uk/projects/fastqc/.
[340] Bolger AM, Lohse M, Usadel B (2014). Trimmomatic: a flexible trimmer for Illumina sequence data. *Bioinformatics* **30**: 2114-2120.
[341] Kim D, Langmead B, Salzberg SL (2015). HISAT: A fast spliced aligner with low memory requirements. *Nature Methods* **12**: 357.
[342] Anders S, Pyl PT, Huber W (2015). HTSeq—a Python framework to work with high-throughput sequencing data. *Bioinformatics* **31**: 166-169.
[343] Love MI, Huber W, Anders S (2014). Moderated estimation of fold change and dispersion for RNA-seq data with DESeq2. *Genome Biology* **15**: 550.
[344] Young MD, Wakefield MJ, Smyth GK, Oshlack A (2010). Gene ontology analysis for RNA-seq: accounting for selection bias. *Genome Biology* **11**: R14.
[345] Supek F, Bošnjak M, Škunca N, Šmuc T (2011). REVIGO summarizes and visualizes long lists of gene ontology terms. *PloS One* **6**: e21800.
[346] Huang DW, Sherman BT, Lempicki RA (2008). Systematic and integrative analysis of large gene lists using DAVID bioinformatics resources. *Nature Protocols* **4**: 44.

[347] Luo W, Pant G, Bhavnasi YK, Blanchard JSG, Brouwer C (2017). Pathview Web: user friendly pathway visualization and data integration. *Nucleic Acids Research* **45**: W501-W508.
[348] Liu Y, Zhou J, White KP (2014). RNA-seq differential expression studies: more sequence or more replication? *Bioinformatics* **30**: 301-304.
[349] Zhang LN, Morgan DG, Clapham JC, Speakman JR (2012). Factors predicting nongenetic variability in body weight gain induced by a high‐fat diet in inbred C57BL/6J mice. *Obesity* **20**: 1179-1188.
[350] Johannsen DL, Tchoukalova Y, Tam CS, Covington JD, Xie W, Schwarz J-M, et al. (2014). Effect of 8 weeks of overfeeding on ectopic fat deposition and insulin sensitivity: Testing the "adipose tissue expandability" hypothesis. *Diabetes Care* **37**: 2789-2797.
[351] Yang Y, Smith DL, Keating KD, Allison DB, Nagy TR (2014). Variations in body weight, food intake and body composition after long‐term high‐fat diet feeding in C57BL/6J mice. *Obesity* **22**: 2147-2155.
[352] Choi JY, McGregor RA, Kwon EY, Kim YJ, Han Y, Park JHY, et al. (2016). The metabolic response to a high-fat diet reveals obesity-prone and -resistant phenotypes in mice with distinct mRNA-seq transcriptome profiles. *International Journal of Obesity* **40**: 1452.
[353] Roberts MD, Mobley CB, Toedebush RG, Heese AJ, Zhu C, Krieger AE, et al. (2015). Western diet-induced hepatic steatosis and alterations in the liver transcriptome in adult Brown-Norway rats. *BMC Gastroenterology* **15**: 151.
[354] Renaud HJ, Cui JY, Lu H, Klaassen CD (2014). Effect of diet on expression of genes involved in lipid metabolism, oxidative stress, and inflammation in mouse liver–insights into mechanisms of hepatic steatosis. *PloS One* **9**: e88584.
[355] Fujimoto Y, Itabe H, Kinoshita T, Homma KJ, Onoduka J, Mori M, et al. (2007). Involvement of ACSL in local synthesis of neutral lipids in cytoplasmic lipid droplets in human hepatocyte HuH7. *Journal of Lipid Research* **48**: 1280-1292.
[356] Yao H, Ye J (2008). Long chain acyl-CoA synthetase 3-mediated phosphatidylcholine synthesis is required for assembly of very low density lipoproteins in human hepatoma Huh7 cells. *Journal of Biological Chemistry* **283**: 849-854.
[357] Bu SY, Mashek MT, Mashek DG (2009). Suppression of long chain acyl-CoA synthetase 3 decreases hepatic de novo fatty acid synthesis through decreased transcriptional activity. *Journal of Biological Chemistry* **284**: 30474-30483.
[358] Shin T, Kuboki S, Huber N, Eismann T, Galloway E, Schuster R, et al. (2008). Activation of peroxisome proliferator-activated receptor-γ during hepatic ischemia is age-dependent. *Journal of Surgical Research* **147**: 200-205.
[359] Geisler CE, Renquist BJ (2017). Hepatic lipid accumulation: cause and consequence of dysregulated glucoregulatory hormones. *Journal of Endocrinology* **234**: R1-R21.
[360] Waller-Evans H, Hue C, Fearnside J, Rothwell AR, Lockstone HE, Caldérari S, et al. (2013). Nutrigenomics of high fat diet induced obesity in mice suggests relationships between susceptibility to fatty liver disease and the proteasome. *PloS One* **8**: e82825.
[361] Krawczyńska A, Herman AP, Antushevich H, Bochenek J, Dziendzikowska K, Gajewska A, et al. (2017). Modifications of western-type diet regarding protein, fat and sucrose levels as modulators of steroid metabolism and activity in liver. *The Journal of Steroid Biochemistry and Molecular Biology* **165**: 331-341.
[362] Waxman DJ, Attisano C, Guengerich FP, Lapenson DP (1988). Human liver microsomal steroid metabolism: Identification of the major microsomal steroid hormone 6β-hydroxylase cytochrome P-450 enzyme. *Archives of Biochemistry and Biophysics* **263**: 424-436.
[363] Caballero F, Fernández A, De Lacy AM, Fernández-Checa JC, Caballería J, García-Ruiz C (2009). Enhanced free cholesterol, SREBP-2 and StAR expression in human NASH. *Journal of Hepatology* **50**: 789-796.

[364] Rask E, Olsson T, Soderberg S, Andrew R, Livingstone DEW, Johnson O, et al. (2001). Tissue-specific dysregulation of cortisol metabolism in human obesity. *The Journal of Clinical Endocrinology and Metabolism* **86**: 1418-1421.
[365] Polari L, Yatkin E, Martínez Chacón MG, Ahotupa M, Smeds A, Strauss L, et al. (2015). Weight gain and inflammation regulate aromatase expression in male adipose tissue, as evidenced by reporter gene activity. *Molecular and Cellular Endocrinology* **412**: 123-130.
[366] Makhsida N, Shah JAY, Yan G, Fisch H, Shabsigh R (2005). Hypogonadism and metabolic syndrome: Implications for testoterone therapy *The Journal of Urology* **174**: 827-834.
[367] Sánchez-Garrido MA, Ruiz-Pino F, Manfredi-Lozano M, Leon S, Garcia-Galiano D, Castaño JP, et al. (2014). Obesity-induced hypogonadism in the male: Premature reproductive neuroendocrine senescence and contribution of Kiss1-mediated mechanisms. *Endocrinology* **155**: 1067-1079.
[368] Furuhashi M, Hotamisligil GS (2008). Fatty acid-binding proteins: role in metabolic diseases and potential as drug targets. *Nature Reviews Drug Discovery* **7**: 489.
[369] Xu A, Wang Y, Xu JY, Stejskal D, Tam S, Zhang J, et al. (2006). Adipocyte fatty acid–binding protein is a plasma biomarker closely associated with obesity and metabolic syndrome. *Clinical Chemistry* **52**: 405-413.
[370] Graupera I, Coll M, Pose E, Elia C, Piano S, Solà E, et al. (2017). Adipocyte fatty-acid binding protein is overexpressed in cirrhosis and correlates with clinical outcomes. *Scientific Reports* **7**: 1829.
[371] Tso AWK, Xu A, Sham PC, Wat NMS, Wang Y, Fong CHY, et al. (2007). Serum adipocyte fatty acid–binding protein as a new biomarker predicting the development of type 2 diabetes: A 10-year prospective study in a Chinese cohort. *Diabetes Care* **30**: 2667-2672.
[372] Yeung DCY, Xu A, Cheung CWS, Wat NMS, Yau MH, Fong CHY, et al. (2007). Serum adipocyte fatty acid-binding protein levels were independently associated with carotid atherosclerosis. *Arteriosclerosis, Thrombosis, and Vascular Biology* **27**: 1796-1802.
[373] Kamijo-Ikemori A, Sugaya T, Kimura K (2006). Urinary fatty acid binding protein in renal disease. *Clinica Chimica Acta* **374**: 1-7.
[374] Newberry EP, Kennedy SM, Xie Y, Sternard BT, Luo J, Davidson NO (2008). Diet-induced obesity and hepatic steatosis in L-Fabp−/− mice is abrogated with SF, but not PUFA, feeding and attenuated after cholesterol supplementation. *American Journal of Physiology-Gastrointestinal and Liver Physiology* **294**: G307-G314.
[375] Vassileva G, Huwyler L, Poirier K, Agellon LB, Toth MJ (2000). The intestinal fatty acid binding protein is not essential for dietary fat absorption in mice. *The FASEB Journal* **14**: 2040-2046.
[376] Newberry EP, Xie Y, Kennedy SM, Luo J, Davidson NO (2006). Protection against western diet–induced obesity and hepatic steatosis in liver fatty acid–binding protein knockout mice. *Hepatology* **44**: 1191-1205.
[377] Wang Y-T, Liu C-H, Zhu H-L (2016). Fatty acid binding protein (FABP) inhibitors: a patent review (2012-2015). *Expert Opinion on Therapeutic Patents* **26**: 767-776.
[378] Kobayashi T, Zadravec D, Jacobsson A (2007). ELOVL2 overexpression enhances triacylglycerol synthesis in 3T3-L1 and F442A cells. *FEBS Letters* **581**: 3157-3163.
[379] Bu SY, Mashek DG (2010). Hepatic long-chain acyl-CoA synthetase 5 mediates fatty acid channeling between anabolic and catabolic pathways. *Journal of Lipid Research* **51**: 3270-3280.
[380] Pauter AM, Olsson P, Asadi A, Herslöf B, Csikasz RI, Zadravec D, et al. (2014). Elovl2 ablation demonstrates that systemic DHA is endogenously produced and is essential for lipid homeostasis in mice. *Journal of Lipid Research* **55**: 718-728.

[381] Bowman TA, O'Keeffe KR, D'Aquila T, Yan QW, Griffin JD, Killion EA, et al. (2016). Acyl CoA synthetase 5 (ACSL5) ablation in mice increases energy expenditure and insulin sensitivity and delays fat absorption. *Molecular Metabolism* **5**: 210-220.
[382] Marchais-Oberwinkler S, Henn C, Möller G, Klein T, Negri M, Oster A, et al. (2011). 17β-Hydroxysteroid dehydrogenases (17β-HSDs) as therapeutic targets: Protein structures, functions, and recent progress in inhibitor development. *The Journal of Steroid Biochemistry and Molecular Biology* **125**: 66-82.
[383] Moeller G, Adamski J (2009). Integrated view on 17beta-hydroxysteroid dehydrogenases. *Molecular and Cellular Endocrinology* **301**: 7-19.
[384] Biswas MG, Russell DW (1997). Expression, cloning and characterization of oxidative 17β- and 3α-hydroxysteroid dehydrogenases from rat and human prostate. *Journal of Biological Chemistry* **272**: 15959-15966.
[385] Rasiah KK, Gardiner-Garden M, Padilla EJD, Möller G, Kench JG, Alles MC, et al. (2009). HSD17B4 overexpression, an independent biomarker of poor patient outcome in prostate cancer. *Molecular and Cellular Endocrinology* **301**: 89-96.
[386] Luu-The V, Tremblay P, Labrie F (2006). Characterization of type 12 17β-hydroxysteroid dehydrogenase, an isoform of type 3 17β-hydroxysteroid dehydrogenase responsible for estradiol formation in women. *Molecular Endocrinology* **20**: 437-443.
[387] Jin Y, Penning TM (2007). Aldo-keto reductases and bioactivation/detoxication. *Annual Review of Pharmacology and Toxicology* **47**: 263-292.
[388] Ladias JA, Hadzopoulou-Cladaras M, Kardassis D, Cardot P, Cheng J, Zannis V, et al. (1992). Transcriptional regulation of human apolipoprotein genes ApoB, ApoCIII, and ApoAII by members of the steroid hormone receptor superfamily HNF-4, ARP-1, EAR-2, and EAR-3. *Journal of Biological Chemistry* **267**: 15849-15860.
[389] Onat A, Can G, Hergenç G, Yazıcı M, Karabulut A, Albayrak S (2007). Serum apolipoprotein B predicts dyslipidemia, metabolic syndrome and, in women, hypertension and diabetes, independent of markers of central obesity and inflammation. *International Journal of Obesity* **31**: 1119.
[390] Olivieri O, Bassi A, Stranieri C, Trabetti E, Martinelli N, Pizzolo F, et al. (2003). Apolipoprotein C-III, metabolic syndrome, and risk of coronary artery disease. *Journal of Lipid Research* **44**: 2374-2381.
[391] Poirier D (2010). 17β-Hydroxysteroid dehydrogenase inhibitors: a patent review. *Expert Opinion on Therapeutic Patents* **20**: 1123-1145.
[392] Cho M-K (2013). Decreased expression of type 5 17β-hydroxysteroid dehydrogenase (AKR1C3) protein identified in human diabetic skin tissue. *Annals of Dermatology* **25**: 423-427.
[393] Adam M, Heikelä H, Sobolewski C, Portius D, Mäki-Jouppila J, Mehmood A, et al. (2018). Hydroxysteroid (17β) dehydrogenase 13 deficiency triggers hepatic steatosis and inflammation in mice. *The FASEB Journal* DOI 10.1096/fj.201700914R fj.201700914R.
[394] Ryu D, Mouchiroud L, Andreux PA, Katsyuba E, Moullan N, Nicolet-dit-Félix AA, et al. (2016). Urolithin A induces mitophagy and prolongs lifespan in C. elegans and increases muscle function in rodents. *Nature Medicine* **22**: 879.
[395] Singh A, Andreux P, Blanco-Bose W, Ryu D, Aebischer P, Auwerx J, et al. (2017). Orally administered urolithin A is safe and modulates muscle and mitochondrial biomarkers in elderly. *Innovation in Aging* **1**: 1223-1224.
[396] Sandoval-Acuña C, Ferreira J, Speisky H (2014). Polyphenols and mitochondria: An update on their increasingly emerging ROS-scavenging independent actions. *Archives of Biochemistry and Biophysics* **559**: 75-90.
[397] Lindinger A, Peterli R, Peters T, Kern B, von Flüe M, Calame M, et al. (2010). Mitochondrial DNA content in human omental adipose tissue. *Obesity Surgery* **20**: 84-92.

[398] Bharadwaj MS, Tyrrell DJ, Leng I, Demons JL, Lyles MF, Carr JJ, et al. (2015). Relationships between mitochondrial content and bioenergetics with obesity, body composition and fat distribution in healthy older adults. *BMC Obesity* **2**: 40.
[399] Vernochet C, Mourier A, Bezy O, Macotela Y, Boucher J, Rardin Matthew J, et al. (2012). Adipose-specific deletion of TFAM increases mitochondrial oxidation and protects mice against obesity and insulin resistance. *Cell Metabolism* **16**: 765-776.
[400] Sarparanta J, Garcia-Macia M, Singh R (2017). Autophagy and mitochondria in obesity and type 2 diabetes. *Current Diabetes Reviews* **13**: 352-369.
[401] Wu W, Xu H, Wang Z, Mao Y, Yuan L, Luo W, et al. (2015). PINK1-Parkin-Mediated Mitophagy Protects Mitochondrial Integrity and Prevents Metabolic Stress-Induced Endothelial Injury. *PloS One* **10**: e0132499.
[402] Rovira-Llopis S, Bañuls C, Diaz-Morales N, Hernandez-Mijares A, Rocha M, Victor VM (2017). Mitochondrial dynamics in type 2 diabetes: Pathophysiological implications. *Redox Biology* **11**: 637-645.
[403] Zid BM, Rogers AN, Katewa SD, Vargas MA, Kolipinski MC, Lu TA, et al. (2009). 4E-BP Extends Lifespan upon Dietary Restriction by Enhancing Mitochondrial Activity in Drosophila. *Cell* **139**: 149-160.
[404] Houtkooper RH, Mouchiroud L, Ryu D, Moullan N, Katsyuba E, Knott G, et al. (2013). Mitonuclear protein imbalance as a conserved longevity mechanism. *Nature* **497**: 451.
[405] D'Amico D, Sorrentino V, Auwerx J (2017). Cytosolic proteostasis networks of the mitochondrial stress response. *Trends in Biochemical Sciences* **42**: 712-725.
[406] Mottis A, Jovaisaite V, Auwerx J (2014). The mitochondrial unfolded protein response in mammalian physiology. *Mammalian Genome* **25**: 424-433.
[407] Kleinridders A, Lauritzen HPMM, Ussar S, Christensen JH, Mori MA, Bross P, et al. (2013). Leptin regulation of Hsp60 impacts hypothalamic insulin signaling. *The Journal of Clinical Investigation* **123**: 4667-4680.
[408] Xiao F, Zhai Z, Jiang C, Liu X, Li H, Qu X, et al. (2015). Geraniin suppresses RANKL-induced osteoclastogenesis in vitro and ameliorates wear particle-induced osteolysis in mouse model. *Experimental Cell Research* **330**: 91-101.
[409] Ding W-X, Yin X-M (2012). Mitophagy: mechanisms, pathophysiological roles, and analysis. *Biological Chemistry* **393**: 547-564.
[410] Dyer JS, Rosenfeld CR (2011). Metabolic imprinting by prenatal, perinatal, and postnatal overnutrition: A review. *Seminars in Reproductive Medicine* **29**: 266-276.
[411] Chang G-Q, Gaysinskaya V, Karatayev O, Leibowitz SF (2008). Maternal high-fat diet and fetal programming: Increased proliferation of hypothalamic peptide-producing neurons that increase risk for overeating and obesity. *The Journal of Neuroscience* **28**: 12107-12119.
[412] Espin JC, Larrosa M, Garcia-Conesa MT, Tomas-Barberan F (2013). Biological significance of urolithins, the gut microbial ellagic acid-derived metabolites: The evidence so far. *Evidence-Based Complementary and Alternative Medicine* **2013**: 15.
[413] Meierhofer D, Weidner C, Sauer S (2014). Integrative analysis of transcriptomics, proteomics, and metabolomics data of white adipose and liver tissue of high-fat diet and rosiglitazone-treated insulin-resistant mice identified pathway alterations and molecular hubs. *Journal of Proteome Research* **13**: 5592-5602.
[414] Udhane SS, Legeza B, Marti N, Hertig D, Diserens G, Nuoffer J-M, et al. (2017). Combined transcriptome and metabolome analyses of metformin effects reveal novel links between metabolic networks in steroidogenic systems. *Scientific Reports* **7**: 8652.

Appendix

APPENDIX

Appendix A: Assessment of the Purity and Identity of Isolated Geraniin

Appendix A1: Purity and identity assessment with HPLC, LCMS and LCMS-MS

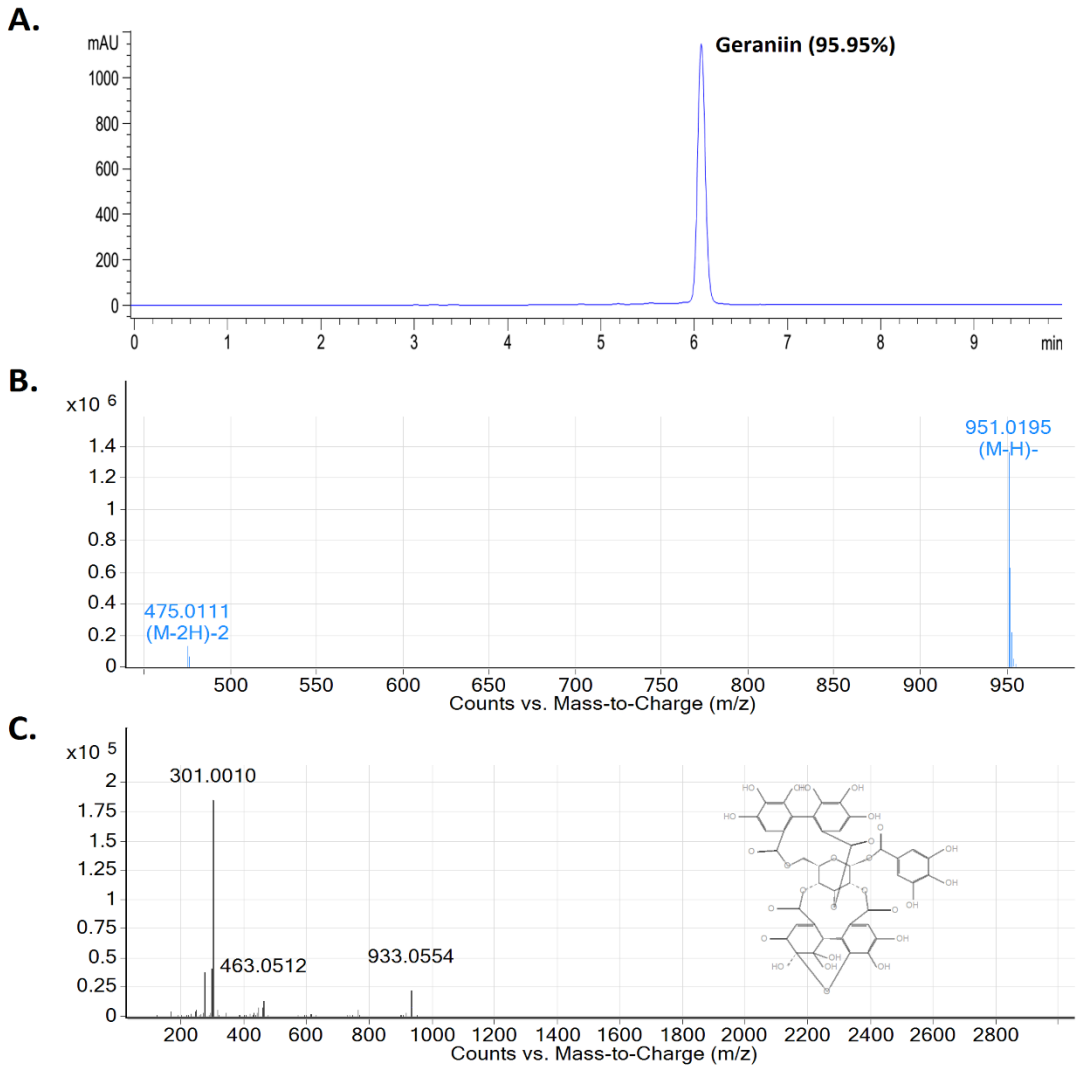

Figure A1: HPLC chromatogram **(A)** of purified geraiin from the rind of *Nephelium lappaceum* which shows a purity of 95.95%. The identity of the isolated compound was tested with negative ionization mode LCMS **(B)** and LCMS-MS **(C)**, both of which confirmed that the identity of geraniin based on the *m/z* ratios of the intact molecules and the fragmented derivatives.

Appendix A2: Identity confirmation with standard addition assay

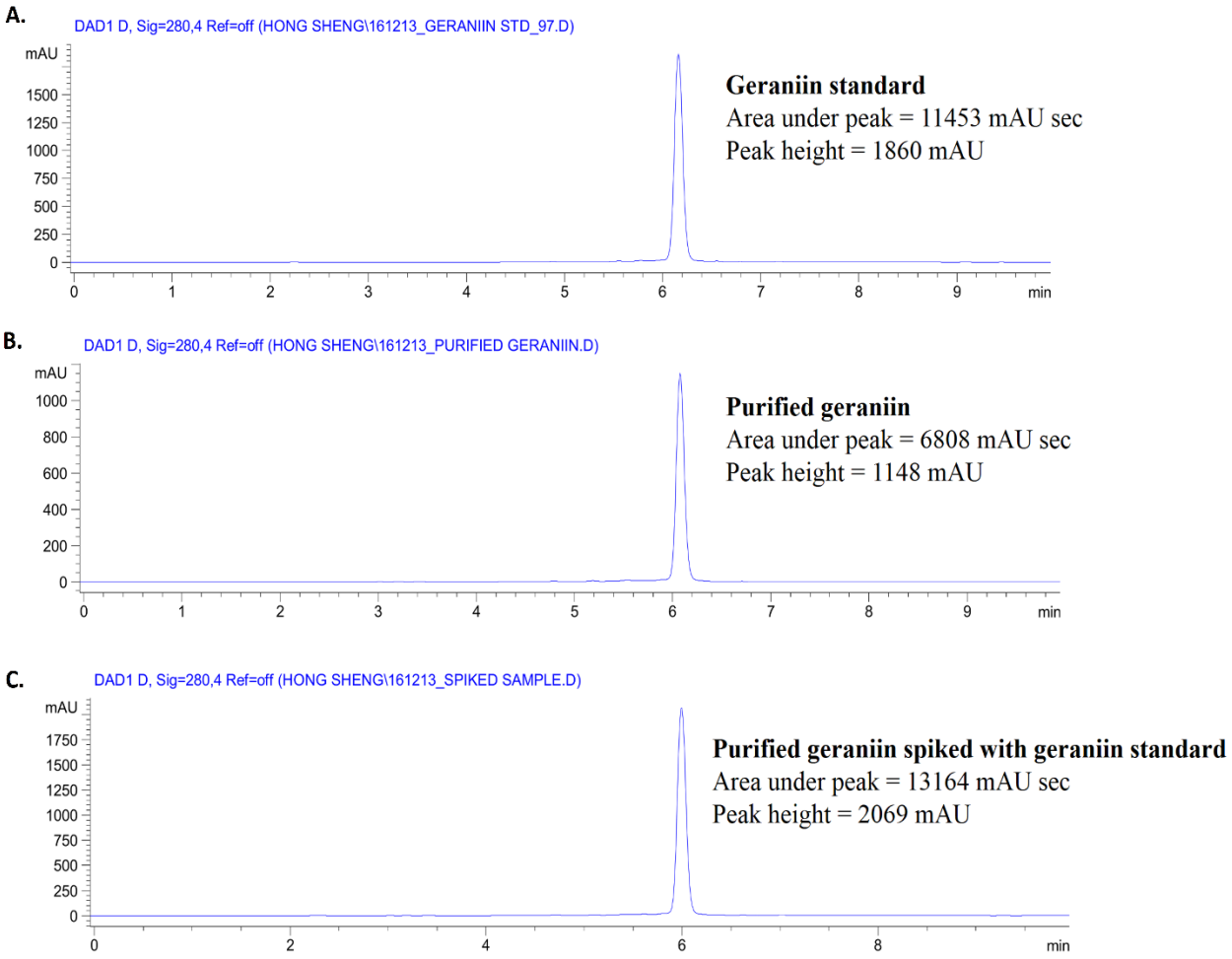

Figure A2: Standard addition assay of geraniin from the rind of *Nephelium lappaceum* using HPLC. The HPLC chromatograms of geraniin standard **(A)**, purified geraniin **(B)** and purified geraniin spiked with geraniin standard **(C)** are illustrated. The observation that purified geraniin and geraniin standard share the same retention time suggests that they are the same compound.

Appendix A3: Identity confirmation with ^{1}H-NMR

Functional groups	^{1}H-NMR chemical shift (300 MHz, DMSO-d6)	
	Purified geraniin	Gohar et al. (2003)
Glucose 1 2 3 4 5 6	 6.36 (1H, d) 5.34 (1H, d) 5.41 (1H, s) 5.22 (1H, s) 4.71 (1H, t) 4.39 (2H, m)	 6.35 (1H, d) 5.33 (1H, d) 5.39 (1H, s) 5.20 (1H, s) 4.70 (1H,t) 4.37 (2H, m)
Galloyl (Ring A) 2 & 6	 7.03 (2H, s)	 7.03 (2H, s)
HDDP (Rings B & C) 3 & 3’	 6.47, 6.79 (1H, s)	 6.45, 6.78 (1H, s)
DHHDP (Ring D) 3	 7.06 (1H, s)	 7.05 (1H, s)
DHHDP (Ring E) 1’ 3’	 4.89 (1H, s) 6.37 (1H, s)	 4.88 (1H, s) 6.38 (1H, s)

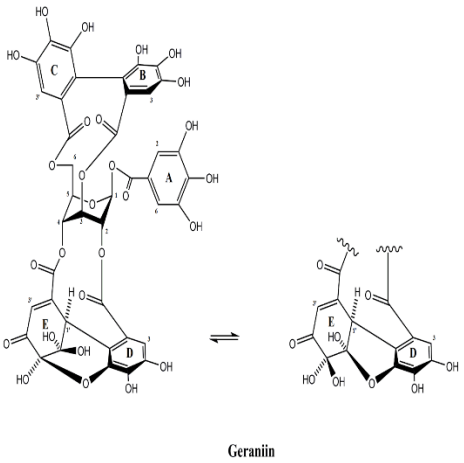

Figure A3: ^{1}H-NMR chemical shifts of geraniin from the rind of *Nephelium lappaceum* in comparison to published data by Gohar et al. (2003) [266].

Appendix B: Procedures and Standard Curves of Biochemical Assays

Appendix B1: Test procedure and standard curve of fasting plasma insulin

Table B1: Components and assay procedure of Mercodia Ultrasensitive Rat Insulin ELISA kit.

Mercodia Ultrasensitive Rat Insulin ELISA kit	**Materials and reagents provided:** • **96-well ELISA plate:** Coated with mouse monoclonal anti-insulin antibodies • **Calibrators 1-5:** Recombinant rat insulin standard solutions from 0.02 µg/L to 1.00 µg/L • **Enzyme Conjugate 11x:** Peroxidase conjugated mouse monoclonal anti-insulin antibodies • **Enzyme Conjugate Buffer** • **Wash Buffer 21x** • **Substrate TMB:** 3, 3', 5, 5' –tetramethylbenzidine in buffer • **Stop Solution:** 0.5M sulphuric acid
	Assay procedure: 1. Prepare 1x solutions of **Enzyme Conjugate** and **Wash Buffer**. 2. Pipette 25 µL each of **Calibrators** and samples into separate wells. 3. Add 100 µL **Enzyme Conjugate 1x** solution into each well. 4. Incubate the plate on a plate shaker (700-900 rpm) for 2 hours at room temperature. 5. Discard the mixture by inverting the plate over a sink. 6. Add 350 µL **Wash Buffer 1x** to each well. Discard the **Wash Buffer** and tap firmly several times against absorbent paper to remove excess liquid. Repeat this step 5 more times. 7. Add 200 µL **Substrate TMB** into each well. 8. Incubate 15 minutes at room temperature 9. Add 50 µL **Stop Solution** to each well and mix evenly 10. Read the absorbance at 450nm within 30 minutes. Based on the manufacturer's kit insert, the lowest detection limit of the assay is 0.02 µg/L. The intra- and inter-assay variations are 2.5% and 4.2% respectively.

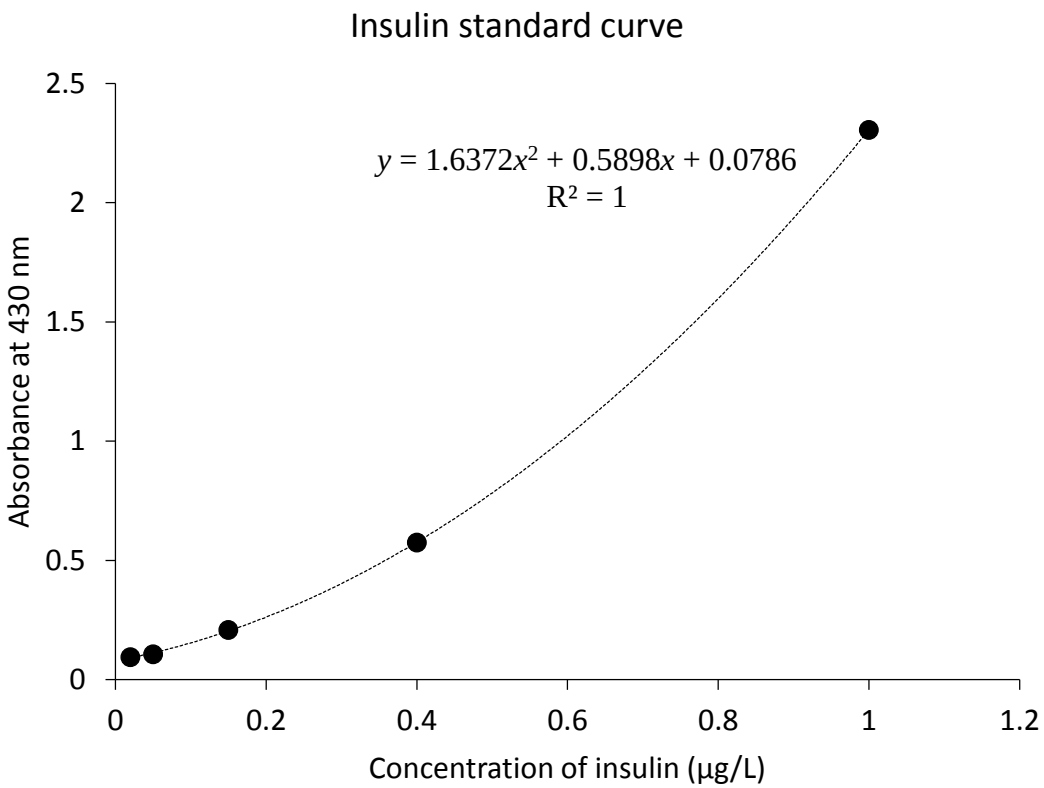

Figure B1: Standard curve of insulin from 0.02 µg/L to 1.00 µg/L at 430 nm. Error bars indicate the standard deviation of the absorbance values.

Appendix B2: Test procedure and standard curve of HbA1c

Table B2: Components and assay procedure of Rat Hemoglobin A1c kit.

<table>
<tr><td rowspan="2">Rat Hemoglobin A1c kit</td><td>Reagents provided:
Lysis Buffer
Reagent CC1a
Reagent CC1b
Reagent CC2
Calibrator 1: Lyophilized HbA1c standard. Upon reconstitution in 0.5 mL distilled water, the HbA1c % is 5.5%.
Calibrator 2: Lyophilized HbA1c standard. Upon reconstitution in 0.5 mL distilled water, the HbA1c % is 11.0%.</td></tr>
<tr><td>Assay procedure:
The kit is an enzymatic assay in which lysed whole blood samples are subjected to extensive protease digestion to release amino acids including glycated valines from the hemoglobin beta chains. Glycated valines then serves as substrates for specific valine oxidase (FVO) enzymes. The FVO specifically cleaves N-terminal valines and produces hydrogen peroxide which can be measured using a horseradish peroxidase catalyzed reaction with a suitable chromogen.
Transfer 62.5 µL of Lysis Buffer into separate microcentrifuge tubes
Add 5 µL of whole blood samples and Calibrators 1 and 2 into each tube and mix well.
Vortex the mixtures and incubate at room temperature for 10 minutes to lyse the red blood cells completely.
Add 112 µL of Reagent CC1a and 48 µL of Reagent CC1b into each well of a 96-well plate.
Add 25 µL of the lysates of whole blood samples and Calibrators into each well and mix well.
Place the plate in an incubator at 37ºC and allow it to equilibrate to the temperature over 5 minutes.
Measure the absorbance at 700nm (first reading).
Add 70 µL of Reagent CC2 and mix well.
Measure the absorbance at 700nm after 3 minutes at 37ºC (second reading).
Calculate the change in absorbance at 700nm using the following equation:
Δ abs @700nm = (Second reading – First reading) x $\frac{185}{255}$
Plot a standard curve with the change in absorbance against HbA1c% of Calibrators 1 and 2.</td></tr>
</table>

	Based on the manufacturer's kit insert, the linear range of the assay is 3.5% to 13.0%. The intra-assay variation is <10%.

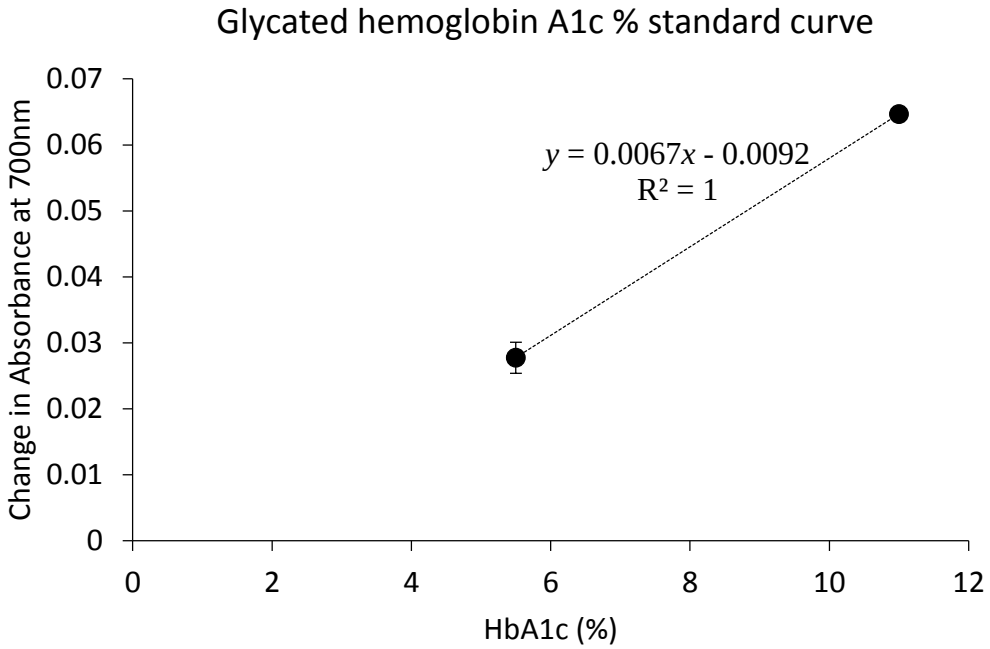

Figure B2: Standard curve of glycated hemoglobin A1C from 5.5% to 11% at 700 nm. Error bars indicate the standard deviation of the absorbance values. HbA1c, glycated hemoglobin A1c.

Appendix B3: Test procedure and standard curve of triglycerides

Table B3: Components and assay procedure of Randox TR1697 Triglycerides kit.

Randox TR1697 Triglycerides kit	**Materials and reagents provided:** • **Buffer R1a:** 40 mmol/L Pipes buffer (pH 7.4), 5.4 mmol/L 4-chlorophenol, 5 mmol/L magnesium ions, 1 mmol/L ATP, ≥ 0.5 U/mL peroxidase, ≥ 0.4 U/mL glycerol kinase, ≥ 1.5 U/mL glycerol-3-phosphate oxidase and 0.05% sodium azide • **Enzyme Reagent R1b:** 0.4 mmol/L 4-aminoantipyrine, ≥ 150 U/mL lipases and 0.05% sodium azide • **Calibrator:** Triglyceride standard solution at a concentration of 2.16 mmol/L
	Assay procedure: 1. Perform serial dilution to the **Calibrator** to prepare a set of standard solutions ranging from 0.27 mmol/L to 2.16 mmol/L. 2. Mix 250 µL of **Enzyme Reagent R1b** with 15 mL of **Buffer R1a** to become **Working Reagent R1.** 3. Transfer 1 mL of **Working Reagent R1** into separate microcentrifuge tubes. 4. Add 10 µL of plasma samples, blank (distilled water) and standard solutions into each tubes and mix well. 5. Incubate the mixtures for 10 minutes at 25°C. 6. Transfer 300 µL of the mixtures into different wells of a 96-well plate and measure the absorbance at 500nm. Based on the manufacturer's kit insert, the linear range of the assay is up to 11.4 mmol/L.

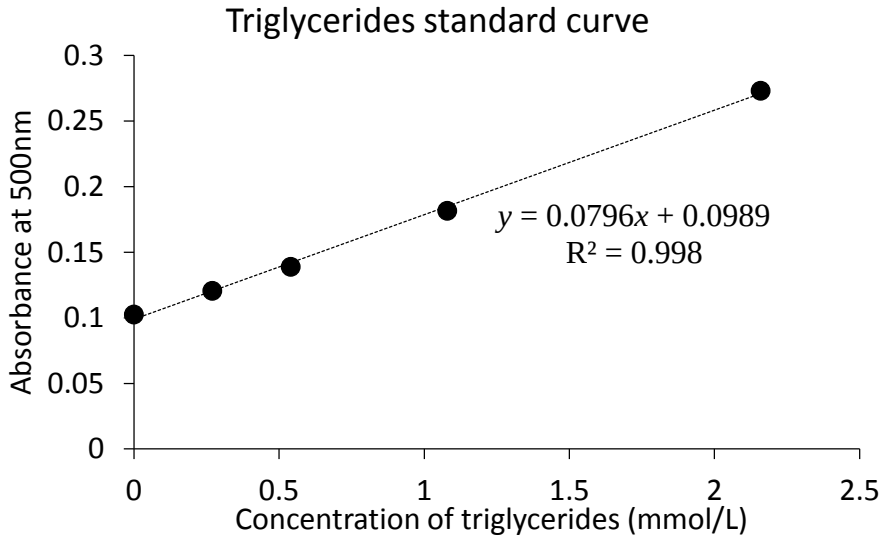

Figure B3: Standard curve of triglycerides from 0 mmol/L to 2.16 mmol/L at 500 nm. Error bars indicate the standard deviation of the absorbance values.

Appendix B4: Test procedure and standard curve of total cholesterols

Table B4: Components and assay procedure of Randox CH200 Cholesterol kit.

Randox CH200 Cholesterol kit	**Materials and reagents provided:** • **Reagent R1:** 80 mmol/L Pipes buffer (pH 6.8), 0.25 mmol/L 4-aminoantipyrine, 6 mmol/L phenol, ≥ 0.5 U/mL peroxidase, ≥ 0.15 U/mL cholesterol esterase, ≥ 0.10 U/mL cholesterol oxidase and 0.05% sodium azide • **Calibrator:** Cholesterol standard solution at a concentration of 5.33 mmol/L
	Assay procedure: 1. Perform serial dilution to the **Calibrator** to prepare a set of standard solutions ranging from 0.67 mmol/L to 5.33 mmol/L. 2. Transfer 1 mL of **Reagent R1** into separate microcentrifuge tubes. 3. Add 10 µL of plasma samples, blank (distilled water) and standard solutions into each tubes and mix well. 4. Incubate the mixtures for 10 minutes at 25°C. 5. Transfer 300 µL of the mixtures into different wells of a 96-well plate and measure the absorbance at 500nm. Based on the manufacturer's kit insert, the linear range of the assay is up to 17 mmol/L. The intra- and inter-assay variations are 1.99 % and 4.28 % respectively.

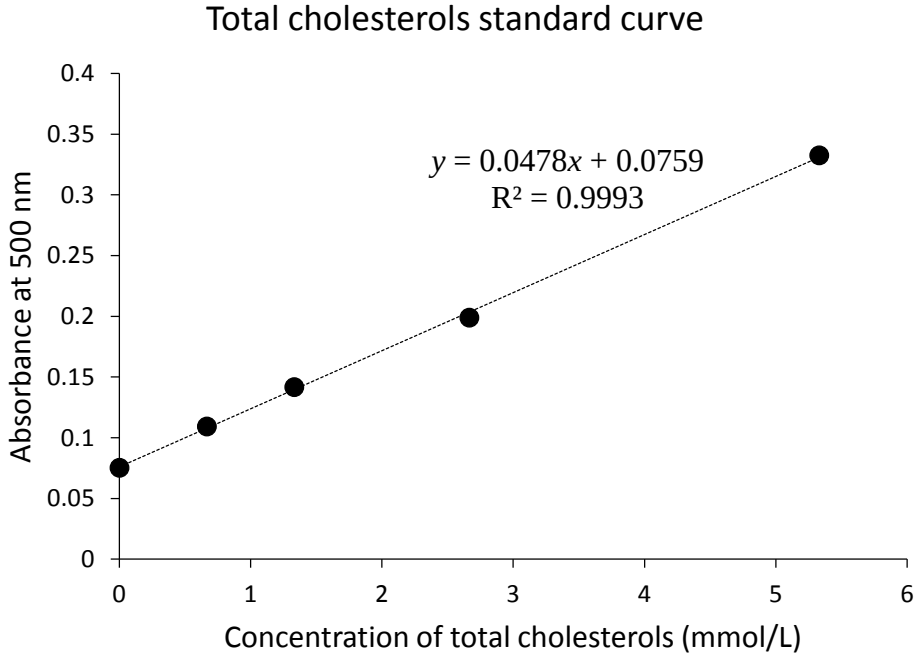

Figure B4: Standard curve of total cholesterols from 0 mmol/L to 5.33 mmol/L at 500 nm. Error bars indicate the standard deviation of the absorbance values.

Appendix B5: Test procedure and standard curve of HDL-cholesterols

Table B5: Components of Randox CH203 HDL-cholesterol Precipitant kit and the assay procedure of HDL-cholesterols.

Randox CH203 HDL-cholesterol Precipitant kit	**Materials and reagents provided:** • **Precipitation Reagent:** 0.55 mmol/L phosphotungstic acid, 25 mmol/L magnesium chloride
	Assay procedure: 1. Perform serial dilution to the **Calibrator** from **Appendix B4** to prepare a set of cholesterol standard solutions ranging from 0.67 mmol/L to 5.33 mmol/L. 2. Transfer 80 µL of **Precipitation Reagent** into separate microcentrifuge tubes. 3. Add 40 µL of plasma samples, blank (distilled water) and standard solutions into each tubes and mix well. 4. Incubate the mixtures for 10 minutes at 25ºC. 5. Centrifuge the tubes at 2000x *g* for 10 minutes. 6. Retrieve 50 µL of clear supernatant and mix with 500 µL of **Reagent R1** from **Appendix B4** in new microcentrifuge tubes. 7. Proceed to Steps 4 and 5 in **Appendix B4**

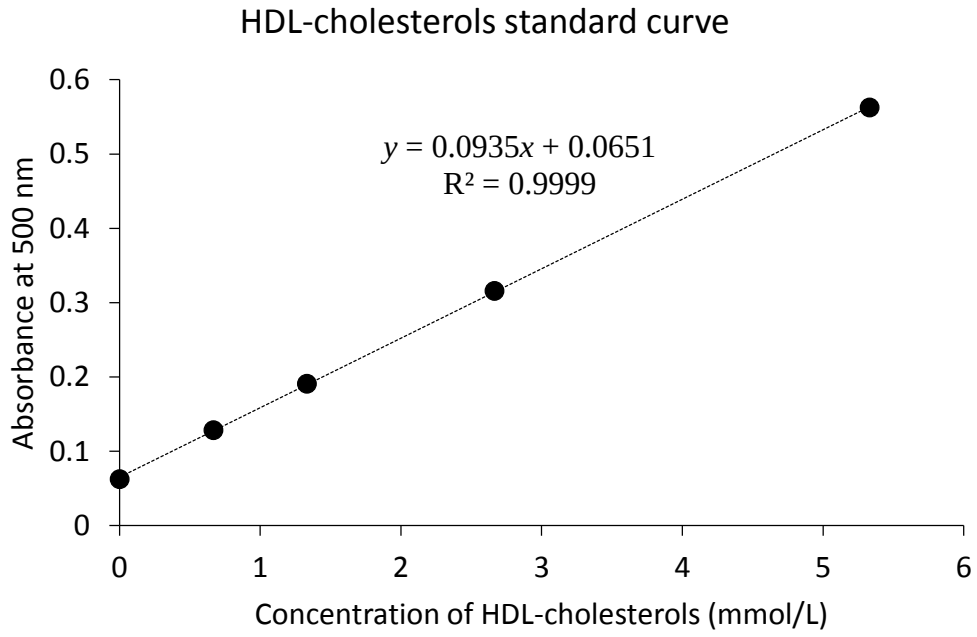

Figure B5: Standard curve of HDL-cholesterols from 0 mmol/L to 5.33 mmol/L at 500 nm. Error bars indicate the standard deviation of the absorbance values. HDL, high-density lipoprotein.

Appendix B6: Standard curve of free fatty acids

Table B6: Components and assay procedure of Randox FA115 Non-esterified Fatty Acids kit.

<table>
<tr><td rowspan="2">Randox FA115 Non-esterified Fatty Acids kit</td><td>Materials and reagents provided:
Buffer R1a: 0.04 mmol/L phosphate buffer (pH 6.9), 3 mmol/L magnesium chloride and surfactant
Enzyme/Coenzymes R1b: ≥ 0.3 U/mL acyl coenzyme A synthetase, ≥ 1.5 U/mL ascorbate oxidase, 0.9 mmol/L coenzyme A, 5.0 mmol/L ATP and 1.5 mmol/L 4-aminoantipyrine
Enzyme Diluent R2a: 0.3% (w/v) phenoxyethanol and surfactant
Reagent R2b: 10.6 mmol/L maleimide
Enzyme Reagent R2c: ≥ 10 U/mL acyl coenzyme A oxidase, 7.5 U/mL peroxidase and 1.2 mmol/L TOOS
Calibrator: Non-esterified fatty acid standard solution at a concentration of 1.05 mmol/L</td></tr>
<tr><td>Assay procedure:
Reconstitute one vial of Enzyme/Coenzymes R1b with 10 mL of Buffer R1a to produce Reagent R1.
Reconstitute one bottle of Reagent R2b with one bottle of Enzyme Diluent R2a, then transfer the mixture into one bottle of Enzyme Reagent R2c to produce Reagent R2.
Perform serial dilution to the Calibrator to prepare a set of non-esterified fatty acid standard solutions ranging from 0.13 mmol/L to 1.05 mmol/L.
Transfer 200 µL of Reagent R1 into separate microcentrifuge tubes.
Add 10 µL of plasma samples, blank (distilled water) and standard solutions into each tubes and mix well.
Incubate the mixtures for 5 minutes at 37ºC.
Add 400 µL of Reagent R2 into each tube.
Incubate the mixtures for another 5 minutes at 37ºC.
Transfer 250 µL of the mixtures into different wells of a 96-well plate and measure the absorbance at 550nm.
Based on the manufacturer’s kit insert, the linear range of the assay is up to 2.24 mmol/L. The intra-assay variation is 4.78 %.</td></tr>
</table>

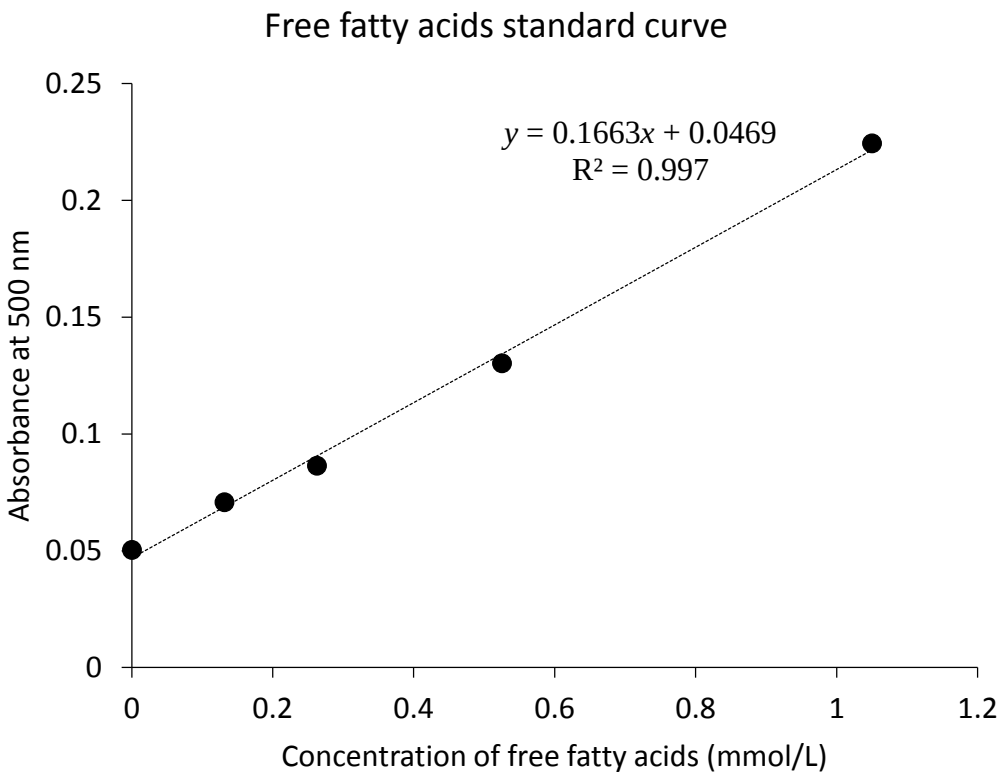

Figure B6: Standard curve of free fatty acids from 0 mmol/L to 1.05 mmol/L at 500 nm. Error bars indicate the standard deviation of the absorbance values.

Appendix B7: Standard curve of plasma sodium level

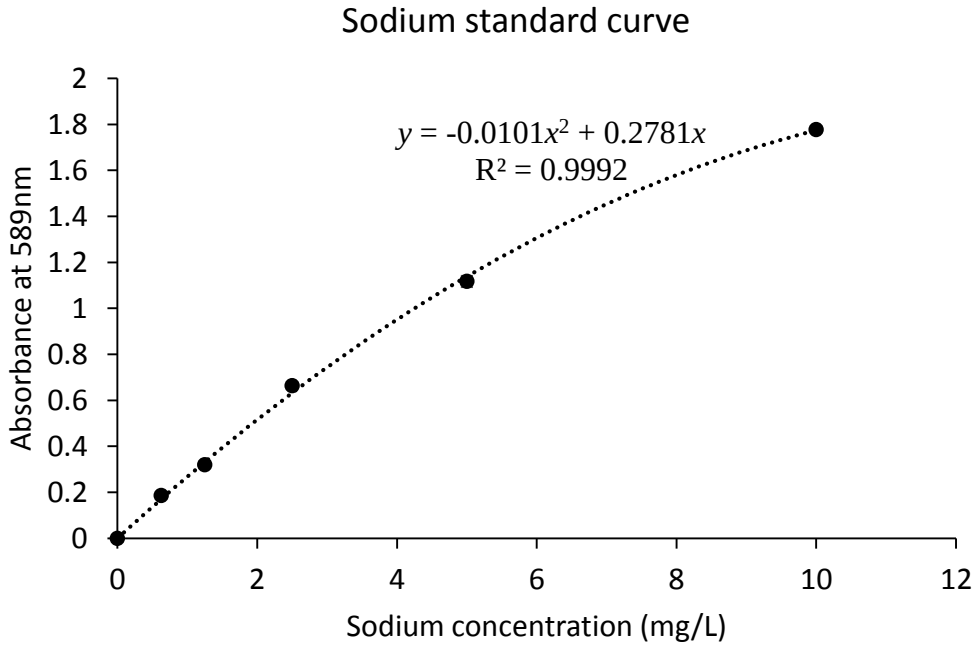

Figure B7: Standard curve of sodium from 0 mg/L to 10 mg/L at 589 nm. Error bars indicate the standard deviation of the absorbance values.

Appendix B8: Standard curve of plasma potassium level

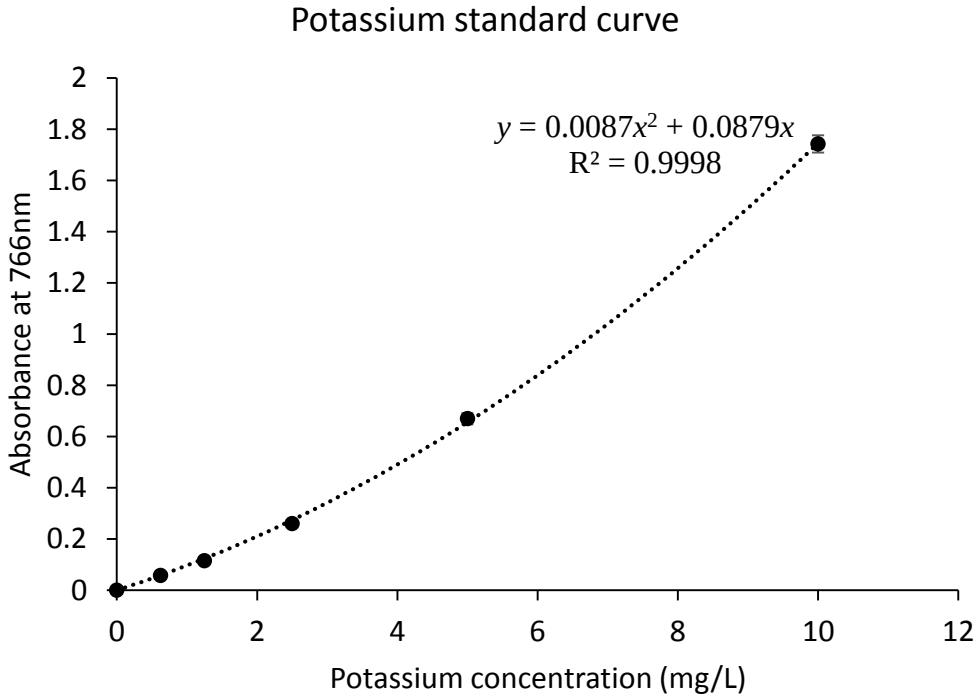

Figure B8: Standard curve of potassium from 0 mg/L to 10 mg/L at 766 nm. Error bars indicate the standard deviation of the absorbance values.

Appendix B9: Test procedure and standard curve of ORAC assay

Table B7: Components and assay procedure of OxiSelect™ Oxygen Radical Antioxidant Capacity (ORAC) Activity Assay kit.

OxiSelect™ Oxygen Radical Antioxidant Capacity (ORAC) Activity Assay kit	**Materials and reagents provided:** • **96-well microtiter plate:** Clear bottom black 96-well plate • **Fluorescein Probe 100x** • **Free Radical Initiator** • **Trolox Standard:** 5mM Trolox standard solution • **Assay Diluent 4x**
	Assay procedure: 1. Prepare 1x solution of **Assay Diluent** by diluting the 4x concentrate in deionized water. 2. Prepare 1x solution of **Fluorescein Probe** by diluting the 100x concentrate in 1x **Assay Diluent**. 3. Dilute plasma samples by 100-fold with **Assay Diluent.** 4. Perform serial dilution to the **Trolox Standard** with **Assay Diluent** to prepare a set of standard solutions ranging from 6.25 µM to 50 µM. 5. Prepare **Free Radical Initiator Solution** at a concentration of 80 mg/mL in 1x PBS right before use. 6. Add 25 µL of the standard solutions, blank (**Assay Diluent**) and samples to separate wells of a 96-well microtiter plate. 7. Add 150 µL of 1x **Fluorescein Probe** to each well and mix evenly. 8. Incubate the plate for 30 minutes at 37°C. 9. Add 25 µL of **Free Radical Initiator Solution** into each well and mix evenly. 10. Read the fluorescent intensity at 37°C with an excitation wavelength of 480nm and an emission wavelength of 520nm every 5 minutes for 60 minutes. 11. Calculate the area under curve (AUC) of each well followed by a correction with the AUC of the blank. 12. Construct the standard curve with the corrected AUC against the concentration of Trolox.

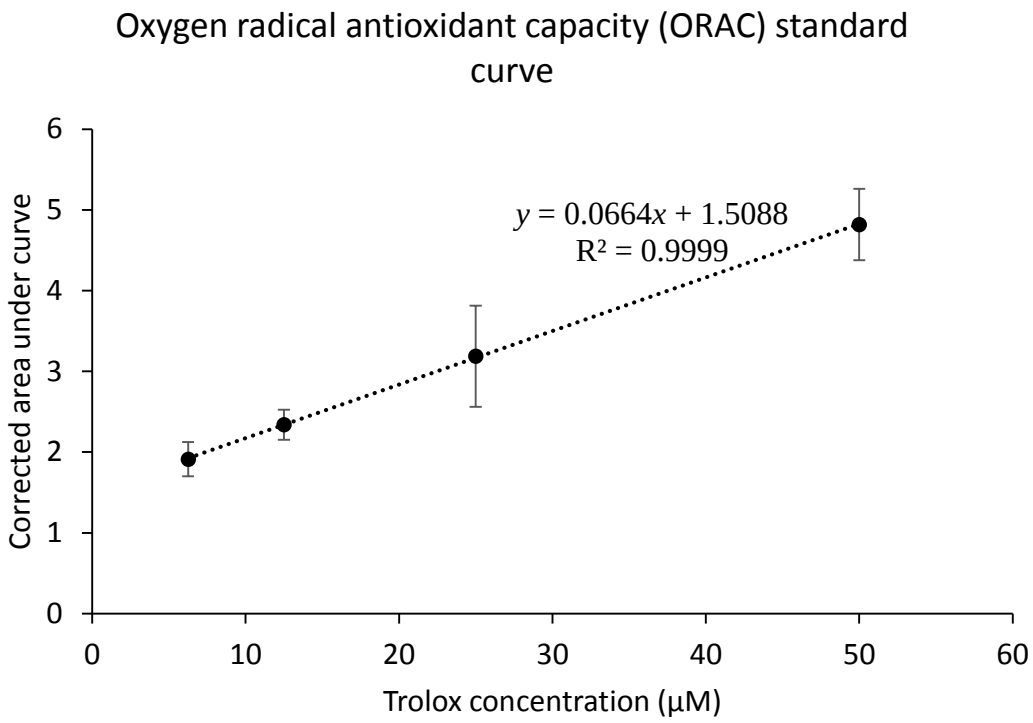

Figure B9: Standard curve of oxygen radical antioxidant capacity (ORAC) assay from 6.25 µM Trolox to 50 µM Trolox. Error bars indicate the standard deviation of the corrected area under curve.

Appendix B10: Test procedure and standard curve of myeloperoxidase activity

Table B8: Components and assay procedure of OxiSelect™ Myeloperoxidase Chlorination Activity Assay kit.

OxiSelect™ Myeloperoxidase Chlorination Activity Assay kit	**Materials and reagents provided:** • **8.82 M Hydrogen Peroxide** • **Chromogen Probe 100x** • **Assay Buffer 5x** • **TCEP Reagent 100x** • **Stop Solution 500x**
	Assay procedure: 1. Prepare 1x solution of **Assay Buffer** by diluting the 5x concentrate in deionized water. 2. Prepare **1mM Chromogen Working Solution** by diluting the 100x concentrates of **Chromogen Probe** and **TCEP Reagent** in 1x **Assay Buffer** (*e.g.* add 50 µL of **Chromogen Probe** and 50 µL of **TCEP Reagent** to 4.9 mL of 1x **Assay Buffer**). Keep the working solution in dark and at 4°C. 3. Prepare 1mM **Hydrogen Peroxide** in deionized water. 4. Prepare 1x **Stop Solution** by diluting the 500x concentrate in 1x **Assay Buffer** 5. Dilute the **1mM Chromogen Working Solution** to 333 µM and perform serial dilution to the 333 µM **Chromogen Working Solution** with **Assay Buffer** to prepare a set of standard solutions ranging from 42 µM to 333 µM. 6. Add 25 µL of the plasma samples to separate wells of a 96-well plate. 7. Add 25 µL of 1mM **Hydrogen Peroxide** to each well and mix evenly. 8. Incubate the plate for 60 minutes at room temperature. 9. Add 50 µL of 1x **Stop Solution** to each well and mix evenly 10. Incubate the plate for 10 minutes at room temperature. 11. Add 50 µL of 1mM **Chromogen Working Solution** into each well and mix evenly. Incubate for another 10 minutes at room temperature. 12. Transfer 150 µL of the standard solutions into new wells separately. 13. Read the absorbance at 405nm.

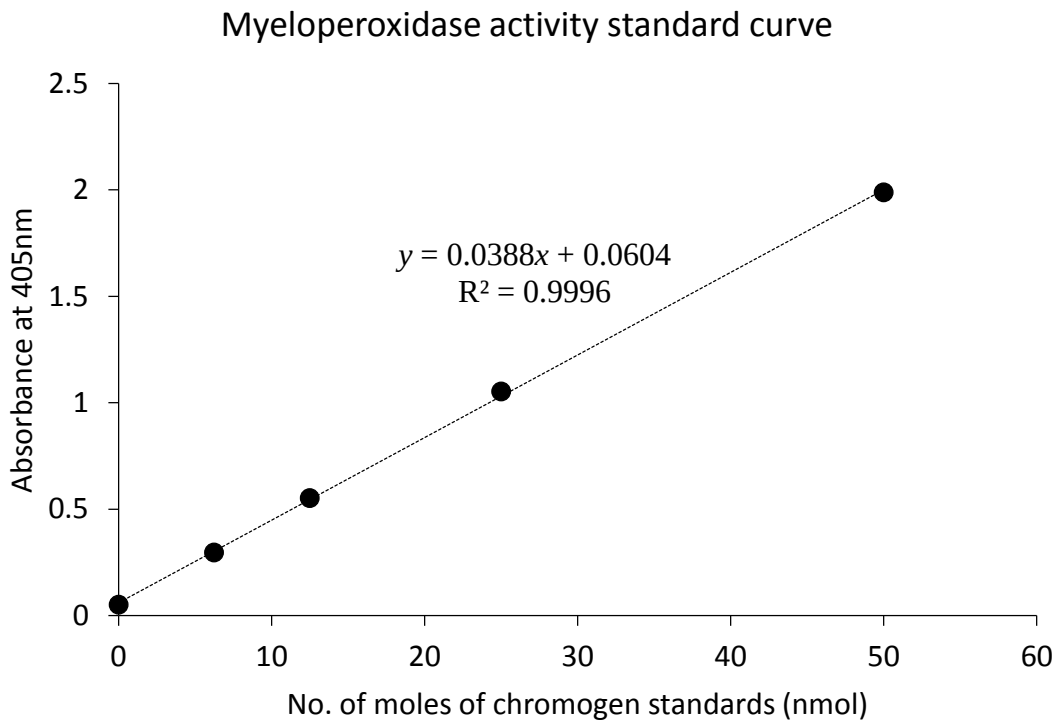

Figure B10: Standard curve of myeloperoxidase activity assay from 0 nmol to 50 nmol chromogen standards. Error bars indicate the standard deviation of the absorbance values.

Appendix B11: Test procedure and standard curve of advanced glycation end products

Table B9: Components and assay procedure of OxiSelect™ Advanced Glycation End Product ELISA kit.

OxiSelect™ Advanced Glycation End Product ELISA kit	**Materials and reagents provided:** • **96-well Protein Binding Plate** • **Anti-AGE Antibody 1000x** • **Secondary Antibody 1000x** • **Assay Diluent** • **Wash Buffer 10x** • **Substrate Solution** • **Stop Solution** • **AGE-BSA Standard:** AGE-BSA standard solution as a concentration of 1 mg/mL in PBS • **AGE Conjugate:** AGE conjugate at 1.0 mg/mL in PBS • **Conjugate Diluent 100x**
	Assay procedure: 1. Prepare 1x solution of **Conjugate Diluent** by diluting the 100x concentrate in PBS. 2. Dilute the 1mg/mL **AGE Conjugate** to 10 µg/mL in PBS. 3. Mix 10 µg/mL **AGE Conjugate** and 1x **Conjugate Diluent** at 1:1 ratio and transfer 100 µL of the mixture into separate wells of the **96-well Protein Binding Plate**. 4. Incubate the plate overnight at 4°C. Remove the mixture and wash twice with 1x PBS. Blot the plate dry on paper towels and add 200 µL of **Assay Diluent** to each well to block for 1 hour at room tempareture. Transfer the plate to 4°C and remover the **Assay Diluent** immediately before use. 5. Prepare 1x solution of the **Wash Buffer** with deionized water. 6. Prepare 1x solutions of **Anti-AGE** and **Secondary Antibodies** with **Assay Diluent** 7. Perform serial dilution to the **AGE-BSA Standard** with **Assay Diluent** to prepare a set of standard solutions ranging from 3.13 µg/mL to 100 µg/mL. 8. Add 50 µL of the plasma samples, standard solutions and blank (**Assay Diluent**) to separate wells of the **AGE Conjugate coated plate**. 9. Incubate at room temperature for 10 minutes on an orbital shaker (300 rpm). 10. Add 50 µL of 1x **Anti-AGE Antibody** to each well and mix evenly.

	11. Incubate the plate for 60 minutes at room temperature on an orbital shaker (300 rpm). 12. Wash the wells thrice with 250 µL of 1x **Wash Buffer** and blot dry. 13. Add 100 µL of 1x **Secondary Antibody** into each well and mix evenly. Incubate for another 60 minutes at room temperature on an orbital shaker (300 rpm). Wash the plate three times according to **Step 12**. 14. Add 100 µL of **Substrate Solution** to each well. Incubate the plate for 10 minutes at room temperature on an orbital shaker (300 rpm). 15. Add 100 µL of **Stop Solution** to each well. 16. Read the absorbance at 450nm.

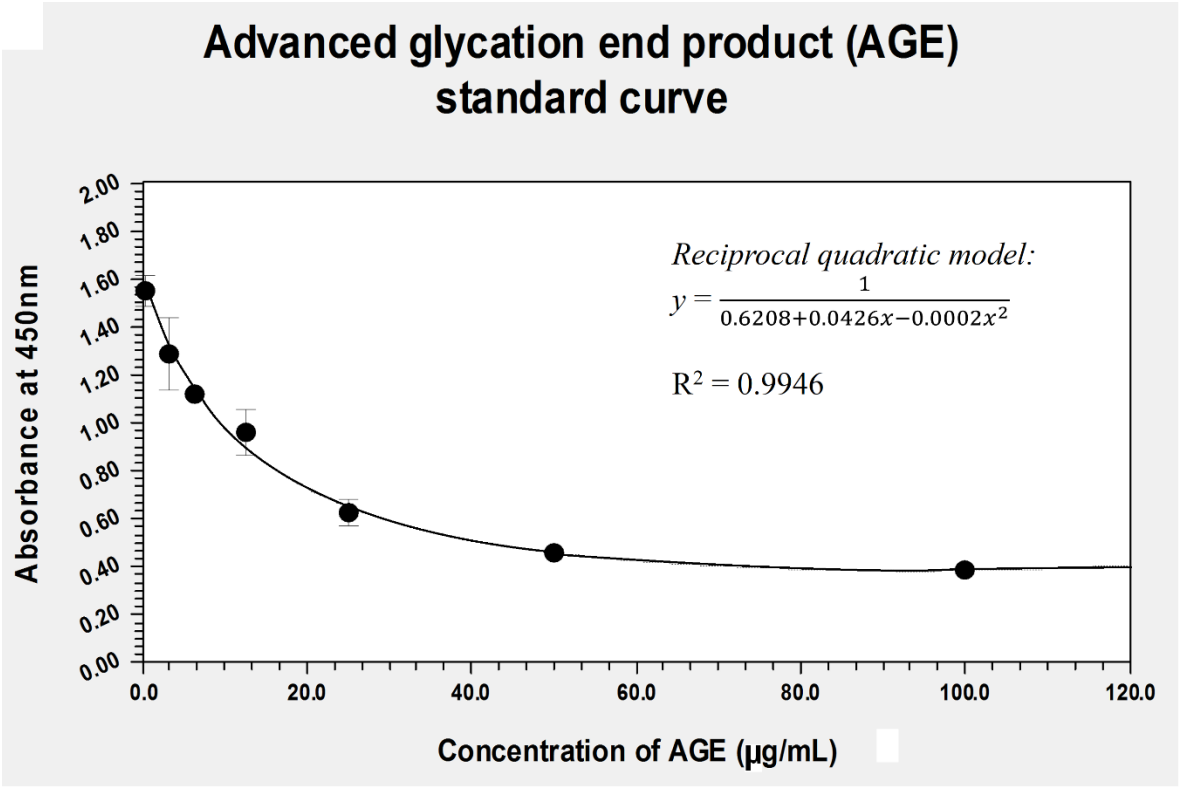

Figure B11: Standard curve of advanced glycation end products from 0 µg/mL to 100 µg/mL. Error bars indicate the standard deviation of the absorbance values.

Appendix B12: Standard curve of protein concentration

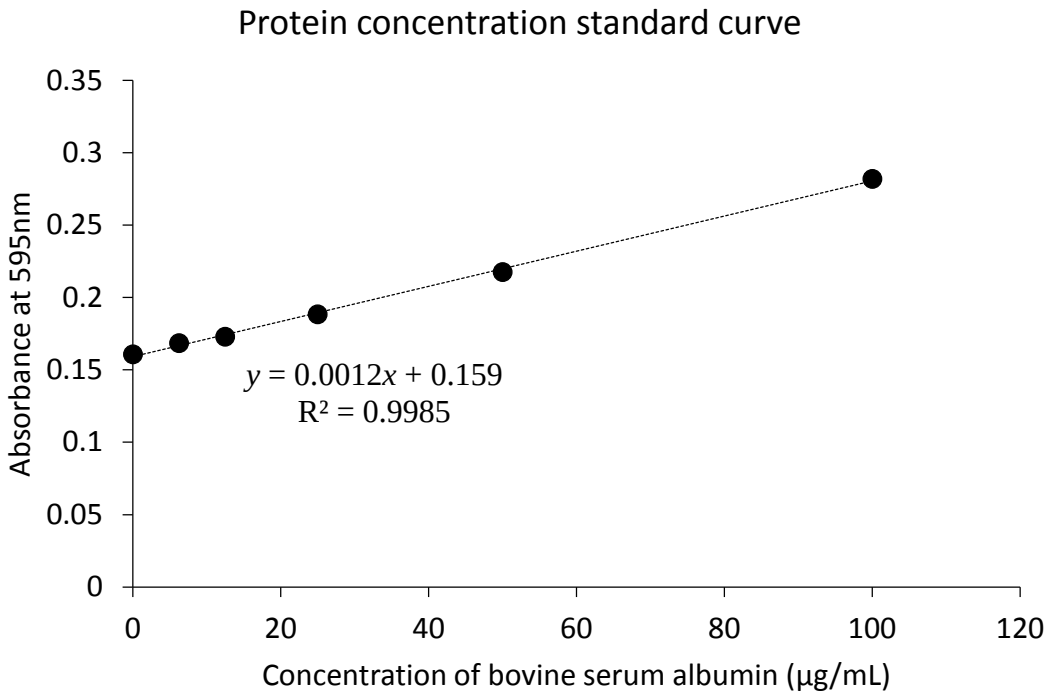

Figure B12: Standard curve of protein concentration from 0 µg/mL to 100 µg/mL. Error bars indicate the standard deviation of the absorbance values.

Appendix B13: Iron (II) sulphate standard curve of ferric reducing power (FRP) assay

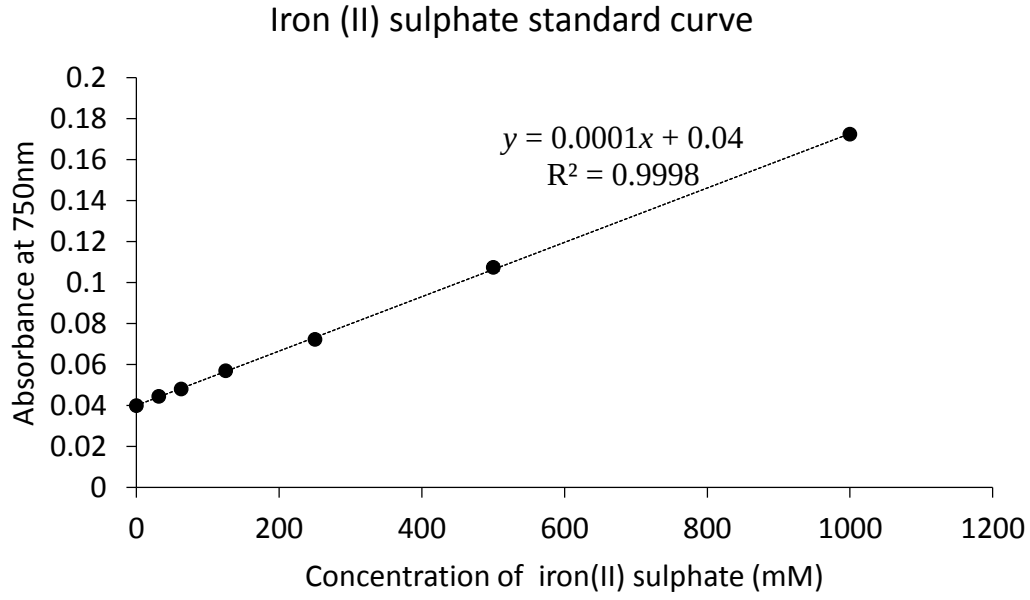

Figure B13: Standard curve of iron (II) sulphate from 0 mM to 1000 mM for FRP assay. Error bars indicate the standard deviation of the absorbance values.

Appendix B14: Standard curve of 2,2'-azino-bis(3-ethylbenzothiazoline-6-sulphonic acid) (ABTS) assay

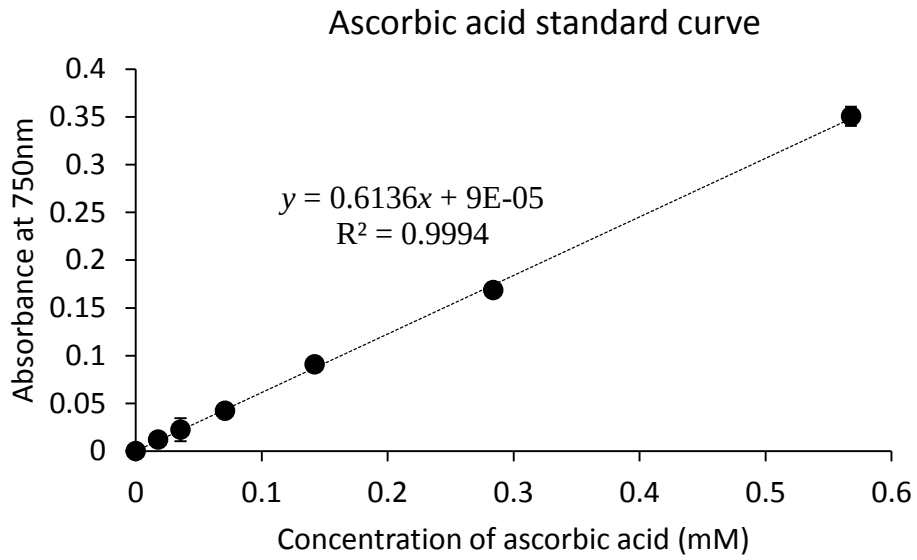

Figure B14: Standard curve of ascorbic acid from 0 mM to 0.57 mM for ABTS assay. Error bars indicate the standard deviation of the absorbance values.

Appendix B15: Test procedure and standard curves of LEGENDplex Rat Inflammation Panel for cytokine profiling

Table B10: Components and assay procedure of LEGENDplex Rat Inflammation Panel kit.

LEGENDplex Rat Inflammation Panel kit	**Materials and reagents provided:** • **96-well V-bottom plate** • **Lyophilized Matrix C** • **SA-PE Reagent** • **Assay Buffer** • **Wash Buffer 20x** • **Lyophilized Standard Cocktail** • **Capture Beads 13x:** Capture beads for IL-1β, IL-6, IL-10, IL-18 and TNF-α • **Detection Antibody**
	Assay procedure: 1. Prepare 1x solution of **Wash Buffer** with deionized water. 2. Prepare 1x solution of **Capture Bead Mixture** with **Assay Buffer**. 3. Reconstitute **Matrix C** in 10mL of **Assay Buffer**. 4. Reconstitute the **Standard Cocktail** in 250 µL of **Assay Buffer** and perform 4-fold serial dilution to the **Standard Cocktail** to prepare a set of standard solutions up to 4096-fold dilution. 5. Dilute plasma samples by 4-fold with **Assay Buffer**. 6. Add 25 µL of diluted plasma samples, blank (**Assay Buffer**) and standard solutions to separate of the **V-bottom plate**. 7. Add 25 µL of **Matrix C** to wells with blank and standard solutions. 8. Add 25 µL of **Assay Buffer** to wells with plasma samples. 9. Vortex the **Capture Bead Mixture** for 30 seconds and add 25 µL of the mixture to each well. 10. Seal the plate with a plate sealer and cover the plate with aluminum foil. Incubate the plate on a plate shaker (300 rpm) for 2 hours at room temperature. 11. Centrifuge the plate at 250x *g* for 5 minutes. 12. Discard the supernatant and blot the plate dry on paper towel. 13. Wash the plate with 200 µL of **Wash Buffer**. Shake the plate at 300 rpm for 1 minutes and repeat **Steps 11 and 12**. 14. Add 25 µL of **Detection Antibody** into each well. 15. Seal the plate with a plate sealer and cover the plate with aluminum foil. Incubate the plate on a plate shaker (300 rpm) for 1 hour at room temperature. 16. Add 25µL of **SA-PE Reagent** into each well.

	17. Seal the plate with a plate sealer and cover the plate with aluminum foil. Incubate the plate on a plate shaker (300 rpm) for 30 minutes at room temperature. 18. Repeat **Steps 11 and 12**. 19. Add 150 µL of **Wash Buffer** into each well. Resuspend the beads by pipetting. 20. Read the samples on a flow cytometer. Based on the manufacturer's kit insert, the intra- and inter-assay variations are 9.3% and 9.7% respectively.

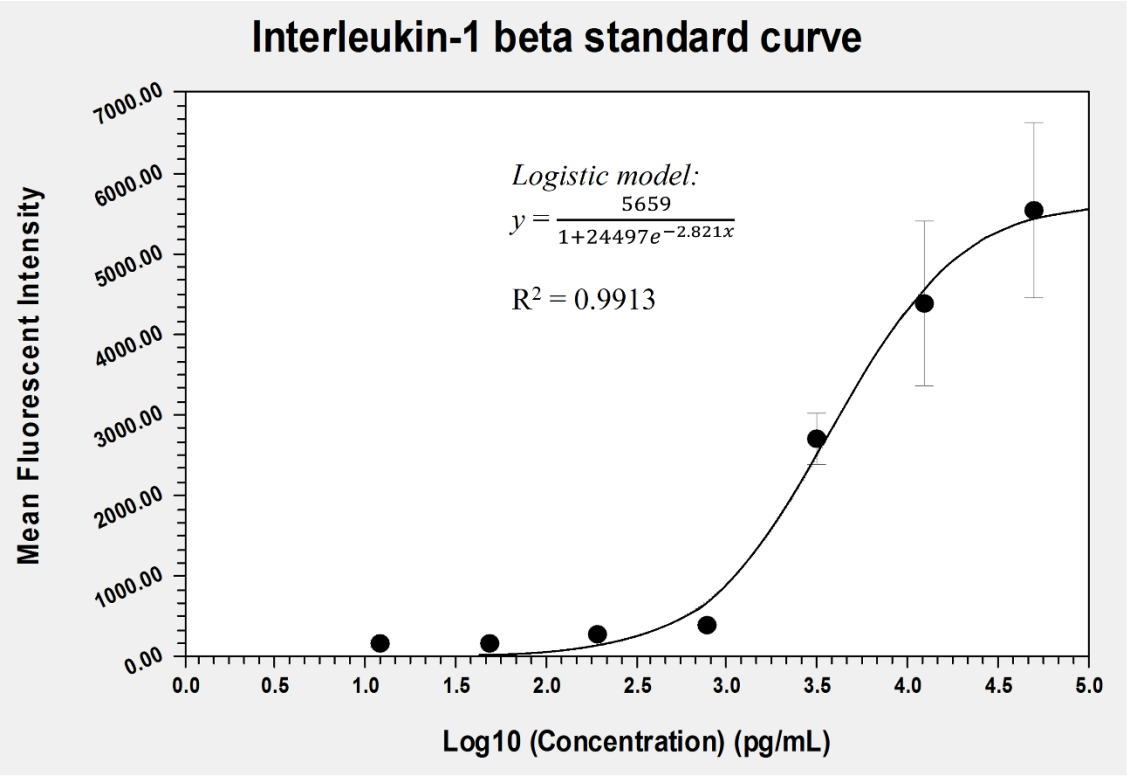

Figure B15: Standard curve of interleukin-1β from 12.2 pg/mL to 50000 pg/mL expressed in log10 scale. Error bars indicate the standard deviation of the absorbance values.

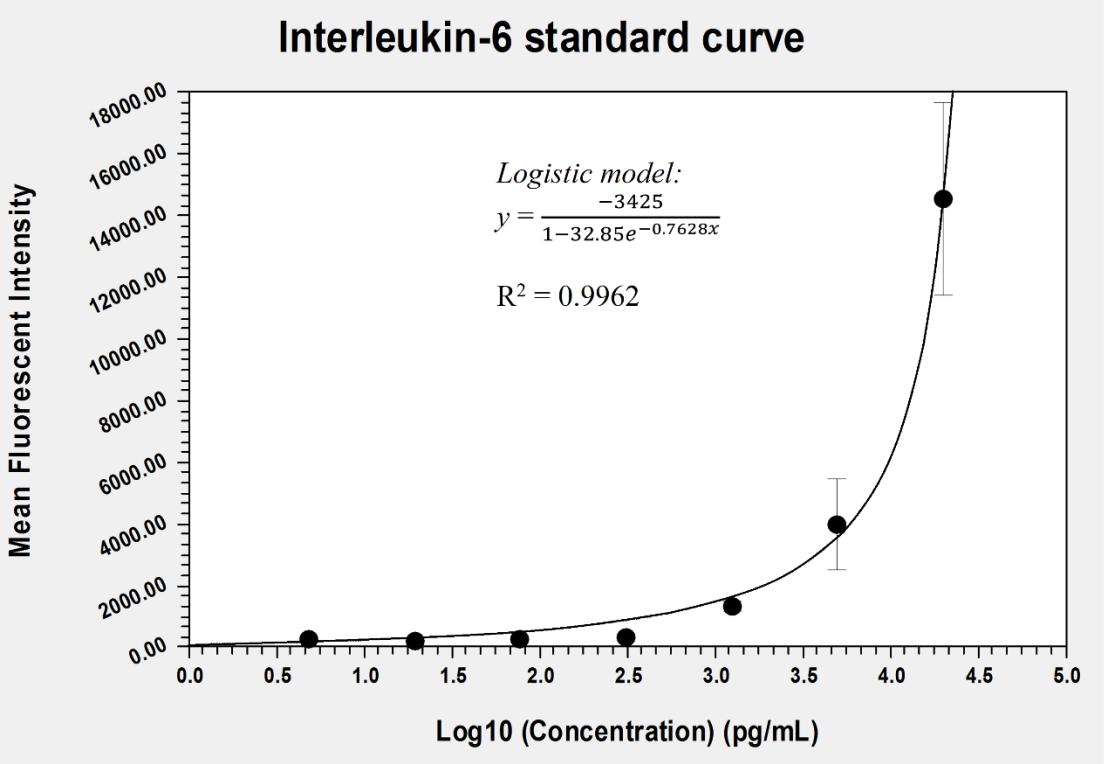

Figure B16: Standard curve of interleukin-6 from 4.88 pg/mL to 20000 pg/mL expressed in log10 scale. Error bars indicate the standard deviation of the absorbance values.

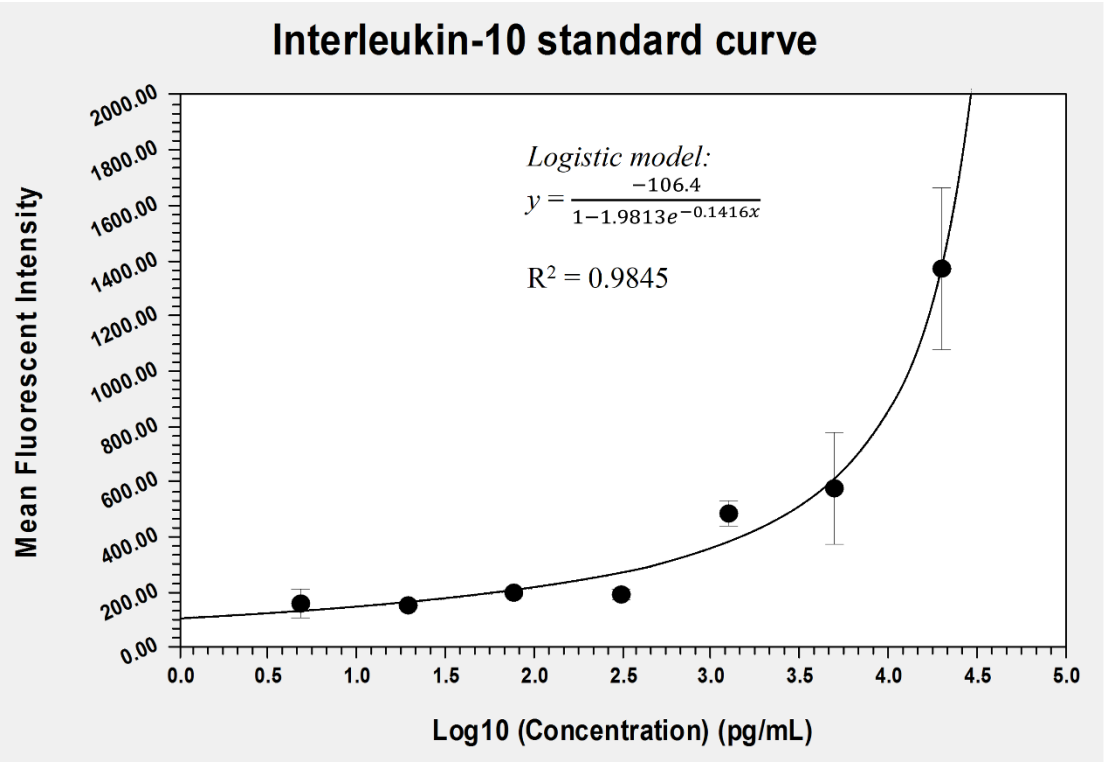

Figure B17: Standard curve of interleukin-10 from 4.88 pg/mL to 20000 pg/mL expressed in log10 scale. Error bars indicate the standard deviation of the absorbance values.

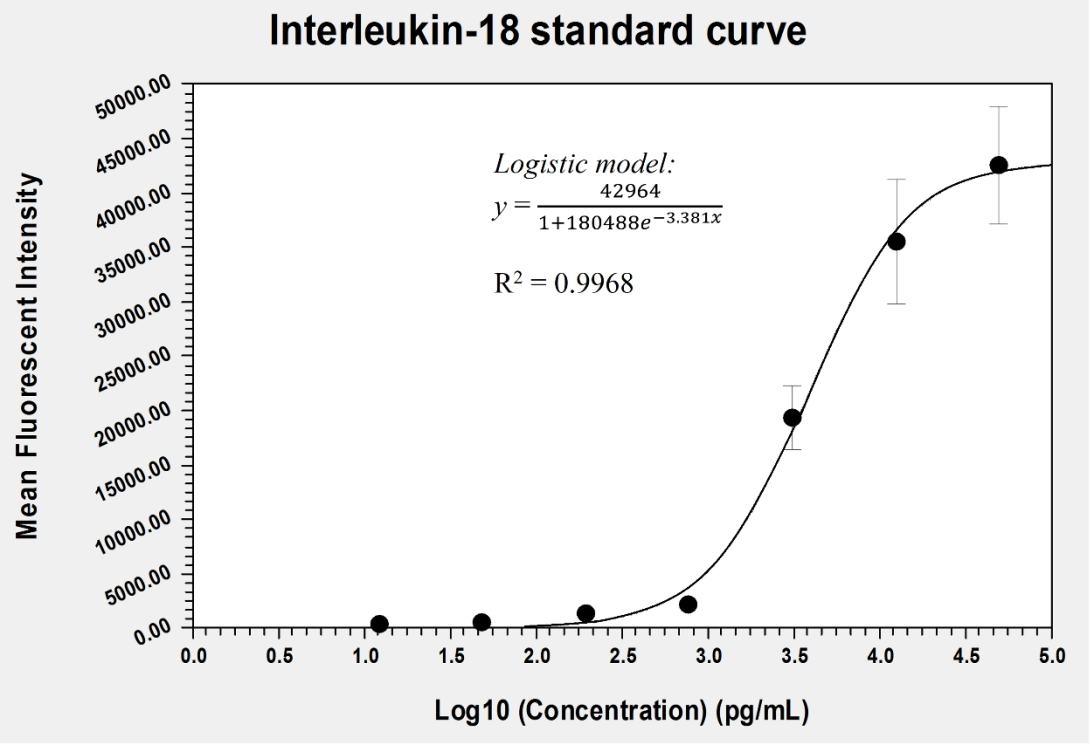

Figure B18: Standard curve of interleukin-18 from 12.2 pg/mL to 50000 pg/mL expressed in log10 scale. Error bars indicate the standard deviation of the absorbance values.

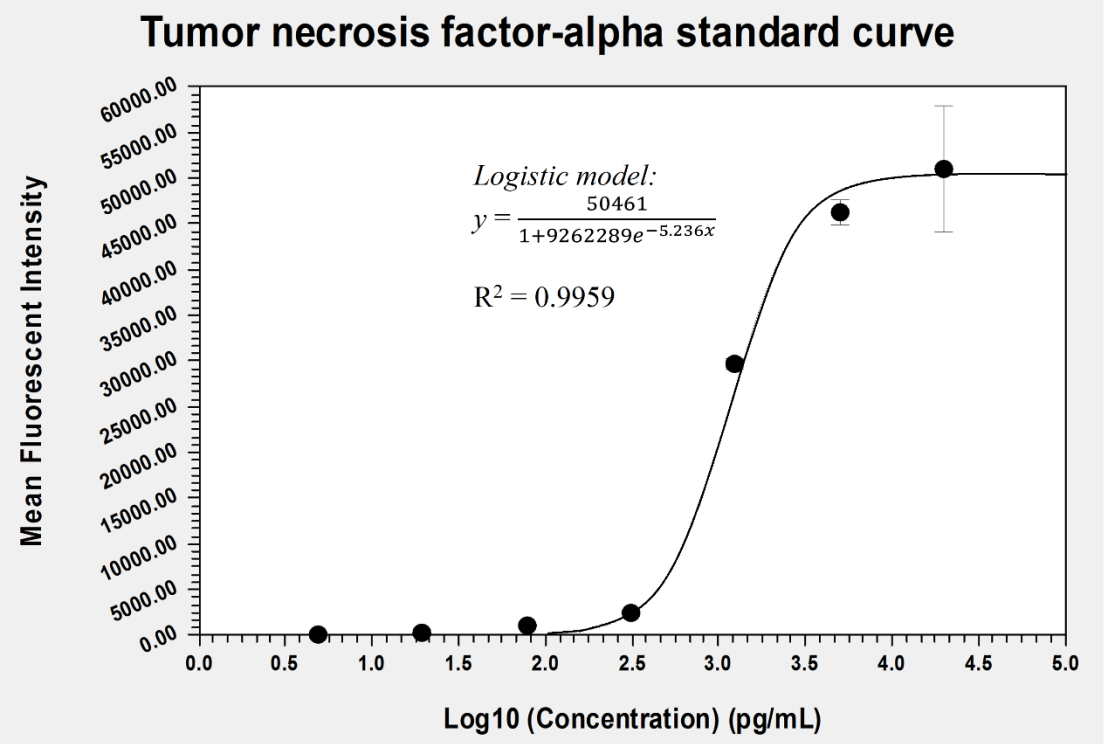

Figure B19: Standard curve of tumor necrosis factor-α from 4.88 pg/mL to 20000 pg/mL expressed in log10 scale. Error bars indicate the standard deviation of the absorbance values.

Appendix C: Quantitative polymerase chain reaction (qPCR) conditions and amplicon information

Appendix C1: Quantitative PCR (qPCR) condition

Table C1: Reaction mixture for qPCR of endogenous references and target genes.

Reagents	Volume per reaction (µL)	Final concentration
TransStart Tip Green qPCR SuperMix (2x concentrate)	12.5	1x
Forward primer (30 µM)	0.25	0.3 µM
Reverse primer (30 µM)	0.25	0.3 µM
cDNA template (0.05 µg/µL)	1.0	0.002 µg/µL
Rnase-free water	11	-
Total volume	**25**	

Table C2: Quantitative PCR condition of the endogenous reference and target genes.

Target gene	Initial denaturation	Denaturation	Annealing	Elongation	PCR efficiency
		(cycle for 35 times)			
*Bac**			48°C, 15 s		95.05%
*Hprt1**			47°C, 15 s		97.83%
*SdhA**			52°C, 15 s		92.54%
RAGE			53°C, 15 s		109.96%
esRAGE	94°C, 2 mins	94°C, 15 s	58°C, 15 s	72°C, 10s	94.74%
PPARα			66°C, 15 s		93.20%
PPARγ			54°C, 15 s		86.41%
Adh7			53°C, 15 s		101.55%
Ddhd1			53°C, 15 s		85.17%

* denotes endogenous reference genes

Adh7, alcohol dehydrogenase 7; *Bac*, β-actin; *Ddhd1*, DDHD domain containing 1; *Hprt1*, hypoxanthine phosphoribosyltransferase 1; *PPAR*, peroxisome proliferator-activated receptor; *RAGE*, receptor for advanced glycation end product; *SdhA*, succinate dehydrogenase complex flavoprotein subunit A; *esRAGE*, endogenous secretory receptor for advanced glycation end product.

Appendix C2: Primers and amplicons of the endogenous reference and target genes

***Rattus norvegicus β-actin* mRNA**
NCBI Reference Sequence: NM_031144.3

```
   1 gtcgagtccg cgtccacccg cgagtacaac cttcttgcag ctcctccgtc gccggtccac
  61 acccgccacc agttcgccat ggatgacgat atcgctgcgc tcgtcgtcga caacggctcc
 121 ggcatgtgca aggccggctt cgcgggcgac gatgctcccc gggccgtctt cccctccatc
 181 gtgggccgcc ctaggcacca gggtgtgatg gtgggtatgg gtcagaagga ctcctacgtg
 241 ggcgacgagg cccagagcaa gagaggcatc ctgaccctga agtaccccat tgaacacggc
 301 attgtcacca actgggacga tatggagaag atttggcacc acactttcta caatgagctg
 361 cgtgtggccc ctgaggagca ccctgtgctg ctcaccgagg cccctctgaa ccctaaggcc
 421 aaccgtgaaa agatgaccca gatcatgttt gagaccttca acaccccagc catgtacgta
 481 gccatccagg ctgtgttgtc cctgtatgcc tctggtcgta ccactggcat tgtgatggac
 541 tccggagacg gggtcaccca cactgtgccc atctatgagg gttacgcgct ccctcatgcc
 601 atcctgcgtc tggacctggc tggccgggac ctgacagact acctcatgaa gatcctgacc
 661 gagcgtggct acagcttcac caccacagct gagagggaaa tcgtgcgtga cattaaagag
 721 aagctgtgct atgttgccct agacttcgag caagagatgg ccactgccgc atcctcttcc
 781 tccctggaga agagctatga gctgcctgac ggtcaggtca tcactatcgg caatgagcgg
 841 ttccgatgcc ccgaggctct cttccagcct tccttcctgg gtatggaatc ctgtggcatc
 901 catgaaacta cattcaattc catcatgaag tgtgacgttg acatccgtaa agacctctat
 961 gccaacacag tgctgtctgg tggcaccacc atgtacccag gcattgctga caggatgcag
1021 aaggagatta ctgccctggc tcctagcacc atgaagatca agatcattgc tcctcctgag
1081 cgcaagtact ctgtgtggat tggtggctct atcctggcct cactgtccac cttccagcag
1141 atgtggatca gcaagcagga gtacgatgag tccggcccct ccatcgtgca ccgcaaatgc
1201 ttctaggcgg actgttactg agctgcgttt tacacccttt ctttgacaaa acctaacttg
1261 cgcaaaaaaa aaaaaaaaaa aaaaaaaaaa aaa
```

Figure C1: *Rattus norvegicus Bac* mRNA sequence (Accession number: NM_031144.3). Forward and reverse primers are highlighted in grey and indicated by the forward and backward arrows respectively.

***Rattus norvegicus Hprt1* mRNA**
NCBI Reference Sequence: NM_012583.2

```
   1 gcggtagcac ctcctccgcc agcttcctcc tcagaccgct tttcccgcga gccgaccggt
  61 tctgtcatgt cgaccctcag tcccagcgtc gtgattagtg atgatgaacc aggttatgac
 121 ctagatttat tttgcatacc taatcattat gctgaagatt tggaaaaggt gtttattcct
 181 catggactga ttatggacag gactgaaaga cttgctcgag atgtcatgaa ggagatggga
 241 ggccatcaca ttgtggccct ctgtgtgctg aaggggggct ataagttctt tgctgacctg
 301 ctggattaca ttaaagcgct gaatagaaat agtgataggt ccattcctat gactgtagat
 361 tttatcagac tgaagagcta ctgtaatgac cagtcaacgg gggacataaa agttattggt
 421 ggagatgatc tctcaacttt aactggaaag aacgtcttga ttgttgaaga tataattgac
 481 actggtaaaa caatgcagac tttgctttcc ttggtcaagc agtacagccc caaaatggtt
 541 aaggttgcaa gcttgctggt gaaaaggacc tctcgaagtg ttggatacag gccagacttt
 601 gttggatttg aaattccaga caagtttgtt gttggatatg cccttgacta taatgagcac
 661 ttcagggatt tgaatcatgt ttgtgtcatc agcgaaagtg gaaaagccaa gtacaaagcc
 721 taaaagacag cggcaagttg aatctacaag agtcctgttg atgtggccag taaagaacta
 781 gcagacgttc tagtcctgtg gccatctact tagtaaagct tttgcatgaa ccttctatga
 841 attttatggt ttttatttct agaaatgtct gttgctgcgt ccctttgat ttgcactatg
 901 agcctgtagg cagcctaccg tcaggtagat tgtcacttcc cttgtgagac agacagatct
 961 cttaaattac cactgttaaa taataatact gagattgtat ctgtaagaag gatttaaaaa
1021 gaagctgtat tagtttttta attggtattt taatttttat atattcagga gagaaagatg
1081 tgatattgtt aatttagaat agtctaaagc gctcagtttc atatcagtaa cagcatctaa
1141 gaggtttccc cagtggaata aacatgtttc agcagtgtga atcgttgtca accgttcctt
1201 ttaaatgcaa ataaatacat tctaaaaatt taaaaaaaaa aaaaaaaaaa aaaaaaaaaa
```

Figure C2: *Rattus norvegicus Hprt1* mRNA sequence (Accession number: NM_012583.2). Forward and reverse primers are highlighted in grey and indicated by the forward and backward arrows respectively.

***Rattus norvegicus SdhA* mRNA**
NCBI Reference Sequence: NM_130428.1

```
   1 cgcaagcgca gtctatcgct gaggcttgcg ggaaggcaaa catggccggg gttggcgcag
  61 tttcgagact tcttcgcggg cggcgcttgg ctctagctgg ggcgactcgt ggctttcact
 121 tctctgttgg tgagagcaag aaggcatccg ctaaagtttc agacgcgatt tctacccagt
 181 accccgtggt ggaccatgag tttgatgctg tggttgtagg tgcaggcggg gcaggcttgc
 241 gagctgcatt cggcctttct gaggcaggct ttaacacggc atgccttaca aagctctttc
 301 ctacccgctc acatactgtt gcagcacagg gaggtatcaa tgctgccctg gggaacatgg
 361 aagaggacaa ctggagatgg catttctatg acaccgtgaa aggctctgac tggctggggg
 421 atcaggatgc catccattac atgacagagc aagctcctgc ctccgtggtt gagctagaaa
 481 attacggtat gccgtttagc aggactgaag atgggaggat ttatcagcgt gcatttggtg
 541 gacagagcct caagttcggg aaaggcgggc aggcccatcg gtgttgctgt gtcgctgatc
 601 ggacgggcca ctcactctta cacaccttgt atggacgatc tctgcggtat gacaccagtt
 661 attttgtgga gtatttcgca ctggatcttc tgatggaaaa tggggagtgc cgtggtgtca
 721 ttgcactgtg catagaagat gggtccatac accgaataag agcaaagaac actattattg
 781 ctactggggg ctatgggcga acctacttca gctgtacttc tgcccacacc agcacagggg
 841 acggcacagc catggtcact cgggctggtt taccttgcca ggacttagaa tttgttcagt
 901 tccaccccac aggtatctat ggtgctggct gcctcatcac agaagggtgc cgtggagagg
 961 gaggcattct catcaacagc caaggcgaaa ggttcatgga gagatatgcc cctgttgcca
1021 aggacctagc atcaagagat gttgtgtctc gatccatgac tctcgagatc cgtgaaggaa
1081 gaggctgtgg ccctgagaag gatcacgtct acctgcagtt gcaccatctg ccccctgagc
1141 agctggccac gcgtctgcct gggatctcag agacggccat gatcttcgcc ggcgtggatg
1201 tcaccaagga gcccattcca gtccttccca ctgtgcatta caacatgggc gggattccca
1261 ctaactacaa gggacaggtg ctgaagcacg tgaacggcca ggatcagatt gtgcctggtc
1321 tgtacgcctg tggggaggct gcctgcgcct cagtgcatgg tgccaaccgg cttggagcaa
1381 actctctttt ggaccttgtc gtctttggcc gagcctgtgc cctgagcatt gcagaatctt
1441 gcaggcctgg agataaagtt cctccgatta aggcaaatgc tggagaagag tcggttatga
1501 atcttgacaa gttgagattt gctgatggaa gtgtaagaac atcagagctg cgcctcagca
1561 tgcagaagtc gatgcagagc catgccgccg tgttccgtgt gggaagtgtg ctgcaagaag
1621 gctgtgaaaa agtcagccag ctctatggag acctacagca tctgaagacg tttgacaggg
1681 gaatggtctg gaacacagac ctggtggaga cgctggagct gcagaatctg atgctgtgcg
1741 cactgcagac catatatggt gcggaagcac ggaaggagtc acggggagct catgccaggg
1801 aagattacaa ggtgcggatt gatgagtatg attactccaa gcccatcgag ggccagcaga
1861 agaagccatt tgcggaacac tggaggaagc acaccctctc atatgtggac accaagactg
1921 ggaaggttac tttggattac agacctgtta ttgacaagac cttgaatgag gctgactgtg
1981 ctactgtacc tcctgctatc cgttcctact gaaaaacctg acagctacag gaccagctta
2041 tgtgattata catcatagct tacctaggtt tcctctcata ctcgtcttgt taaaaatctg
2101 ctctcatgaa caaggagtca cttcacagat tatgatcaac agcttggcag tacttgatgt
2161 gagggactcg agttgcacca ttgtctctca ttcttgtgca gtgataaact ggtataattc
2221 ttaaatgatg tacaaacgaa caatctttta tttctaaata aaaccacata gtatttg
```

Figure C3: *Rattus norvegicus SdhA* mRNA sequence (Accession number: NM_130428.1). Forward and reverse primers are highlighted in grey and indicated by the forward and backward arrows respectively.

***Rattus norvegicus RAGE* mRNA**
NCBI Reference Sequence: NM_053336.2

```
   1 agccacagta ggaagtgggg cagacagaac caggagcctg ggaaggaagc accatgccaa
  61 cggggacagt agctagagcc tgggtactgg ttcttgctct gtggggagcc gtagctggtg
 121 gtcagaacat cacagcccgg atcggagagc cacttatgct gagctgtaag ggggccccta
 181 agaagccaac ccagaagcta gaatggaaac tgaacacagg aaggactgaa gcttggaagg
 241 tcctctctcc ccagggagac ccctgggaca gtgtggctcg aatcctcccc aatggttcac
 301 tcctccttcc agctatcgga attgtcgatg aggggacttt ccggtgtcgg gcaactaaca
 361 ggcttgggaa ggaggtcaag tccaactacc gagtccgagt ctaccagatt cctgggaagc
 421 cggaaattgt gaatcctgcc tctgaactca cagccaatgt ccctaataag gtggggacgt
 481 gtgtgtctga ggggagctac cctgcaggga cccttagctg gcacttggat gggaaacctc
 541 tgattcctga tggcaaaggg acagttgtga aggaggagac caggaggcac cctgagacgg
 601 gactcttcac gcttcggtca gagctcacag tgaccccagc ccaaggaggg accactccta
 661 cctattcctg cagcttcagc ctgggccttc ctcggcacag acccctgaac acagccccca
 721 tccagccccg agtcagggag cccctgcctc cagagggcat tcagctgttg gttgagcctg
 781 aaggtggaac agtcgctcct ggtgggaccg tgaccctgac ctgtgccatc tctgcccagc
 841 ctccccctca aatccactgg ataaaagatg gcacacccct gcccccttgcc cccagccctg
 901 tgctgctcct ccctgaggta gggcatgagg atgagggcat ctacagctgc gtggccaccc
 961 accctagcca tggacctcag gaaagccctc ctgtcaacat cagggtcaca gaaaccggtg
1021 atgaaggaca agctgcaggc tctgtggatg ggtctgggct gggaacgcta gccctggcct
1081 tagggatcct gggaggcctg ggaatagccg ctctgctcat tggggccatc ctgtggcgaa
1141 aacgacaacc cagactcgag gagaggaagg ccccagaaag ccaggaggac gaggaggaac
1201 gtgcagagct gaatcagtca gaggaagcgg aaatgccaga gaatggtgca gggggacctt
1261 aagagcgccc aggcaaaccc tgtctccttc agcttccgac ctcagctgtg ctggctccag
1321 acgagctccc ccactctacg atcccaattc aacctcgagc cactttcttc tccaaccaga
1381 gcccacatga tccatgctga gtaaacacct gacacatgtt aaaaaaaaaa aaaaaaaaaa
1441 aaa
```

Figure C4: *Rattus norvegicus RAGE* mRNA sequence (Accession number: NM_053336.2). Forward and reverse primers are highlighted in grey and indicated by the forward and backward arrows respectively.

***Rattus norvegicus esRAGE* mRNA**
NCBI Reference Sequence: GU164718.1

```
   1 agcctgggaa ggaagcacca tgccaacggg gacagtagct agagcctggg tactggttct
  61 tgctctgtgg ggtgagctat tcccaacccc accaactctc cccatcagct gccctgctcc
 121 catcccccca ggacctcttc tccctagaaa taccccctcc tgcccctgag actgggcacc
 181 acttcccaaa aacccaaacc taccctgccc tacacccacc agccctgcct ctctctcccc
 241 ttccaccctt ctacaatgat gttaccaccc aggagccgta gctggtggtc agaacatcac
 301 agcccggatc ggagagccac ttatgctgag ctgtaagggg gcccctagga agccaaccca
 361 gaagctagaa tggaaactga acacaggaag gactgaagct tggaaggtcc tctctcccca
 421 gggagacccc tgggacagtg tggctcgaat cctccccaat ggttcactcc tccttccagc
 481 tatcggaatt gtcgatgagg ggactttccg gtgtcgggca actaacaggc ttgggaagga
 541 ggtcaagtcc aactaccgag tccgagtcta ccgtaagggt tccaggccgt ggctaagtca
 601 ctttgcattt aacaaaaagc cttcatttac agcctccccc tcaaatccac tggataaaag
 661 atggcacacc cctgcccctt gcccccagcc ctgtgctgct cctccctggg gtagggcatg
 721 aggatgaggg catctacagc tgcgtggcca cccaccctag ccatggacct caggaaagcc
 781 ctcctgtcaa catcagggtc acagaaaccg gtgatgaagg acaagctgca ggctctgtgg
 841 atgggtctgg gctgggaacg ctagccctgg ccttagggat cctgggaggc ctgggaatag
 901 ccgctctgct cattggggcc atcctgtggc gaaaacgaca acccagactc gaggagagga
 961 aggccccaga aagccaggag gacgaggagg aacgtgcaga gctgaatcag tcagaggaag
1021 cggaaatgcc agagaatggt gcagggggac cttaagagcg cccaggcaaa ccctgtctcc
1081 ttcagcttcc gacctcagct gtgctggctc cagacgagct cccccactct acgatcccaa
1141 ttcaacctcg agccactttc ttctccaacc agagcccaca tgat
```

Figure C5: *Rattus norvegicus esRAGE* mRNA sequence (Accession number: GU164718.1). Forward and reverse primers are highlighted in grey and indicated by the forward and backward arrows respectively.

***Rattus norvegicus PPARα* mRNA**
NCBI Reference Sequence: NM_013196.1

```
   1 cgaactgtcc gctacttcga gtccccttga gcgccgtgtg ccggctctga acattggcgt
  61 tcgcagctgt tttgtgggct ggagggttcg tggagtcctg gaactgaagc gacgctgggt
 121 cctctggttg tccccttgag ggagggcaca cgagcgggga catcggggcg ctcccttccc
 181 acagcgtggt gcatttgggc gtaactcacc gggaggcgtt tcctgagacc ctcggggatc
 241 ttagaggcga gccaagactg aagttcaagg ccctgccttc cctgtgaact gacatttgtg
 301 actggtcaag ctcaggacac aagacgttgt catcacagat tggtgctctg tggcccgcct
 361 ggccacaacc attcaacatg gtggacacag agagccccat ctgtcctctc tccccacttg
 421 aagcagatga cctggaaagt cccttatctg aagaattctt acaagagatg ggaaacattc
 481 aagagatttc tcagtccctc ggagaggaga gttccggaag ctttagtttt gcggactacc
 541 agtacttagg gagctgtcca ggctcggagg gctctgtcat cacagacacc ctctctccag
 601 cttccagccc ctcctcagtc agctgccctg ctgtccccac cagtacagat gagtcccctg
 661 gcaatgcact gaacatcgag tgtcgaatat gtggggacaa ggcctcagga taccactatg
 721 gagtccacgc atgtgaaggc tgcaagggct tctttcggcg aactattcgg ctaaagctgg
 781 cgtacgacaa gtgtgatcga agctgcaaga ttcagaaaaa gaaccggaac aaatgccagt
 841 actgccgttt ccacaagtgc ctgtccgtcg ggatgtcaca caatgcaatc cgttttggaa
 901 gaatgccaag atctgagaaa gcaaaactga aggcagaaat ccttacctgt gaacacgatc
 961 tgaaagattc ggaaactgca gacctcaaat ctctggccaa gagaatccac gaagcctacc
1021 tgaagaactt caacatgaac aaggtcaagg cccgggtcat actcgcagga aagactagca
1081 acaatccgcc ttttgtcata catgacatgg agaccttgtg catggctgag aagacgcttg
1141 tggccaagat ggtagccaac ggcgttgaaa acaaggaggc agaggtccga ttcttccact
1201 gctgccagtg catgtccgtg gagaccgtca ccgagctcac ggaatttgcc aaggctatcc
1261 caggctttgc aaacttggac ttgaatgacc aggttacctt gctgaagtac ggtgtgtatg
1321 aagccatctt cacgatgctg tcctccttga tgaacaaaga cgggatgctg atcgcgtacg
1381 gcaatggctt catcacccga gagttcctaa agaacctgag gaagccattc tgcgacatca
1441 tggaacccaa gtttgacttc gctatgaagt tcaatgccct cgaactggat gacagtgaca
1501 tttccctttt tgtggctgct ataatttgct gtggagatcg gcctggcctt ctaaacatag
1561 gatacattga gaagttgcag gaggggattg tgcacgtgct caagctccac ctgcagagca
1621 accatccgga tgataccttt ctcttcccaa aactccttca aaaaatggtg gacctccggc
1681 agctggtcac ggagcatgcg cagctcgtgc aggtcatcaa gaagaccgag tcagacgcgg
1741 cgttgcaccc actgttgcaa gagatctaca gagacatgta ctgatttttc ctgagatggt
1801 aggccgttgc cactgttcag ggacctctga ggtctgcggc cccatacagg agagcaggga
1861 tttgcacaga tggcctccct ccttaccctt ggagatgaag agggctgagc ctaggcaatg
1921 caggctcctc ccacatcctt actttctgaa tgagcacttc taagacttcc tgctactgaa
1981 atggtggtga tcagaggcta gtaggattca gacaattaca gg
```

Figure C6: *Rattus norvegicus PPARα* mRNA sequence (Accession number: NM_013196.1). Forward and reverse primers are highlighted in grey and indicated by the forward and backward arrows respectively.

***Rattus norvegicus PPARγ* mRNA**
NCBI Reference Sequence: NM_013124.3

```
   1 gccttttcc tttaaccaac cgatctttta caagacacag acaaaacatc agtgggaatt
  61 aaggcaaatc tctgttttat gctgttatgg gtgaaactct gggagatcct cctgttgacc
 121 cagagcatgg tgccttcgct gatgcactgc ctatgagcac ttcacaagaa attaccatgg
 181 ttgacacaga gatgccattc tggcccacca acttcggaat cagctctgtg gacctctctg
 241 tgatggatga ccactcccat tcctttgaca tcaaaccctt taccacggtt gatttctcca
 301 gcatttctgc tccacactat gaagacatcc cgttcacaag agctgaccca atggttgctg
 361 attacaaata tgacctgaag ctccaagaat accaaagtgc gatcaaagta gagcctgcgt
 421 ccccgcctta ttattctgaa aaaacccaac tctacaacag gccacatgaa gagccttcaa
 481 actccctcat ggccatcgag tgccgagtct gtggggataa agcatcaggc ttccactatg
 541 gagtccatgc ttgtgaagga tgcaagggtt ttttccgaag aaccatccga ttgaagctta
 601 tttatgatag gtgtgatctt aactgtcgga tccacaaaaa gagtagaaat aaatgtcagt
 661 actgtcggtt tcagaagtgc cttgctgtgg ggatgtctca caatgccatc aggtttgggc
 721 gaatgccaca ggccgagaag gagaagctgt tggcggagat ctccagtgat atcgaccagc
 781 tgaacccaga gtctgctgat ctgcgagccc tggcaaagca tttgtatgac tcatacataa
 841 agtccttccc gctgaccaaa gccaaggcga gggcgatctt gacaggaaag acaacagaca
 901 aatcaccatt tgtcatctac gacatgaatt ccttaatgat gggagaagac aaaatcaagt
 961 tcaaacatat caccccccctg caggagcaga gcaaagaggt ggccatccgc atttttcaag
1021 ggtgccagtt tcgatccgtg gaagctgtgc aagagatcac agagtatgcc aaaaatatcc
1081 ctggtttcat taaccttgac ttgaatgacc aagtgactct gctcaagtat ggtgtccatg
1141 agatcatcta caccatgctg gcctccctga tgaataaaga tggagtcctc atatcagagg
1201 gacaaggatt catgaccagg gagttcctca aaagcctgcg gaagcccttt ggtgacttta
1261 tggagcctaa gtttgagttt gctgtgaagt tcaatgcact ggaattagat gacagtgact
1321 tggccatatt tatagctgtc attattctca gtggagaccg cccaggcttg ctgaacgtga
1381 agcccatcga ggacatccaa gacaacctgc tgcaggccct ggaactccag ctgaagctga
1441 accacccgga gtcctcccag ctgttcgcca aggtgctcca gaagatgaca gacctcaggc
1501 agattgtcac agagcacgtg cagctactgc atgtgatcaa gaagacggag acagatatga
1561 gccttcaccc tctgctccag gagatctaca aggacttgta ttagcagaaa agtcccagtc
1621 gctgacaaag tgttccttct atcgattgca ctattatttt gaggggaaaa aaatctgaca
1681 cctaagaaat ttactgtgaa aaaagcattt aaaaacaaaa agttttagaa catgatctat
1741 tttatgcata ttgtttataa agatacattt acaatttact tttaatatta aaaattacca
1801 cacta
```

Figure C7: *Rattus norvegicus PPARγ* mRNA sequence (Accession number: NM_013124.3). Forward and reverse primers are highlighted in grey and indicated by the forward and backward arrows respectively.

***Rattus norvegicus Adh7* mRNA**
NCBI Reference Sequence: NM_134329.1

```
   1 ccgtgcgtca gtcagaacac gttcctgttt gcagaccaca aacccaggaa agccaggatg
  61 gacactgctg gaaaagttat taagtgcaaa gcagctgtcc tatgggggac gaaccagccc
 121 ttctccattg aggacattga agtggcccca ccaaaggcta aggaagttcg tgttaagatt
 181 ttggccacgg gaatctgtgg cacagatgac cacgtgatca agggaacgat ggtgtctaag
 241 ttcccagtga ttgtgggaca cgaagcagtt gggattgtgg agagtgttgg agaagaggtc
 301 actacagtga gaccaggtga caaagtgatc cccctctttc taccacagtg tagagaatgc
 361 aacccctgcc gcaacccgga ggaaaatctc tgcattagga gcgacctgac aggccgtgga
 421 gtattggctg acggcacgac caggttcaca tgcaagggca aaccagtcca gcactttatg
 481 aacaccagca ccttcactga gtacacggtc ctggatgaat cctccgtagc taagattgat
 541 gccgaggctc ctcccgagaa agcctgcttg attggctgtg gattttccac tggttatggg
 601 gctgctgtta aaactgccaa ggtcagccct ggctccacct gtgctgtgtt tggcctggga
 661 ggagttggcc tgtcagtcgt catgggctgt aaagcggccg gcgcctcccg gatcatcgga
 721 attgacatca acaaggacaa atttcagaaa gccctggatg taggggccac agagtgtatc
 781 aatcccaggg acttcaccaa gcccatcagt gaggtgctgt cagacatgac aggcaacact
 841 gtccagtata cttttgaagt tatcgggcgc cttgagacca tggttgatgc cctctcatct
 901 tgccatatga actatgggac cagcgtggtg gtcggggctc ctccgtcagc caagatgctc
 961 agctatgacc caatgctgct tttcactgga cggacatgga agggctgcgt ctttggtggt
1021 tggaagagca gagatgatgt tcccaaattg gtgactgaat tcctggaaaa gaaatttgac
1081 ctgggccagt tgataaccca caccttgcct tttcataaca tcagtgaagg atttgaattg
1141 ctttattcag ggcaaagcat tcggactgtc ctgacatttt gagatccaga gagctgggtg
1201 ttctgtgctg ggcgaccgtg acctgaagcc ttgttcctga cagtgttctc tgatatcacg
1261 agtctgtctc agaaatgcca tgcagaggcc aggttgggga caagagagag aagctctaca
1321 gaggtttata aaccttcata tgtttagttt accgggtgcc tagcattagc agagaacagt
1381 aagagtaaat gttctagtct gcgttttcct aagacgataa ttctacactt cataagcata
1441 tacttggggt tccaatttgt tggaagaggg actgttttcc agaattttac cacaagttgt
1501 tgttacttaa aaacagacaa agcatgtcga gagatgtaga gaatacattt ttcaagagat
1561 ccccaccaaa gccacccgag ctctcattct gtttttcaac agaaacactt ttaaaaatgt
1621 tataaattaa cttgaattag attgtgaaat tgcacacata acttgattag attaagaaag
1681 aaagttggga aatttaaggg aagggcacgt tttttaatga ttaactttga aaattatcgt
1741 tatgtaattt agtgacatgg gggaagcaca tctgtgcctg gggatatcgt cagcgtttat
1801 taatataaag cacttttaca gtagcgatta cagatgaacc atagatataa ccacattggg
1861 atatttatga tattaaggtt aataaagtag aatgacaagt ccttaagggc atagtagtaa
1921 ctccatttaa catgaagatt attctcagat tgctttaact acaccagcct gtatctgcat
1981 ctgtctgtgg acatgtacac acacgtaata ttcattaaat tttcattgtg gtaaaagaaa
2041 aaaaaaaa
```

Figure C8: *Rattus norvegicus Adh7* mRNA sequence (Accession number: NM_134329.1). Forward and reverse primers are highlighted in grey and indicated by the forward and backward arrows respectively.

***Rattus norvegicus Ddhd1* mRNA**
NCBI Reference Sequence: NM_001033066.1

```
   1 gaaagattat aaagtccggg cccagagggc ggcggcatcg gatgcgcgtg tggcggaagc
  61 gccggcggca tgaactaccc cggccgcggc gccccacgga gccccgagcg taacggccgc
 121 ggcggcggtg cctgggagct aggctcggac gcggcgggcg tgttcggtgg cggcggctgc
 181 tgcttcgagc accagccggg tgacggcgtg ccgctgtcac tgctgcgcgc ggagccgctg
 241 cacctggcac cgggcgcgga cgacttgagc cacctggctc tggacccgtg cctcagcgac
 301 gagaactacg acttcagctc ggccgagtcg ggttcgtcgc tgcgctacta cagcgagggc
 361 gagagcgcgg gcggcggtag ctcttcttcg cctccgccgc cgctggtcgc tccgaactcg
 421 gggggcggcg gggcagcggg agggggaccc ggtgacagga agcgctcccg gccgggcggc
 481 tgcgccgctc ggcaccgcta cgaggtagtg acggagctgg gccccgagga ggtgcgctgg
 541 ttctacaagg aagacaagaa gacctggaag cccttcatcg gctacgactc tctgcgcatt
 601 gagctcgcct tccggagcct cctgcagacg acgggctctc gtgcccggtc ggcggaccgc
 661 gatggagacc gggtgtgcgg cccaacctct agcttcaggg aggacgacga ggaccgcgcc
 721 tgcggcttct gcccgcgcgc ggtggggcct gagccggaga tggaggagct ggtgaccatc
 781 gagcccgtgt gcgtgcgcgg cggcctctac gaggtggatg tcactcaagg agagtgctac
 841 ccggtatact ggaaccaggc cgataaaata ccagtgatgc gtggacagtg gtttatcgat
 901 ggcacttggc aacctctgga ggaagaagag agtaacttaa ttgagcaaga acatctcagt
 961 tgttttaggg gtcagcagat gcaagagaat tttgatattg aaatgtccaa atccatcgat
1021 ggaaaagacg ctgttcatag tttcaaactg agtcggaacc acgtggactg gcacagcatg
1081 gacgaggtct atctctacag tgacgcaaca acttccaaaa ttgcaagaac tgttacccag
1141 aaactggggt tttctaaagc ctccagcagt gggaccagac ttcacagagg ctacgtagaa
1201 gaagccacac tagaagacaa gccatcgcaa acttctcata ttgtgtttgt tgtgcacggc
1261 attggacaga agatggacca aggaagaatc atcaaaaaca cagccatgat gagagaggct
1321 gcaaggaaaa tagaagaaaa gcattttgcc aaccacgcaa cacacgttga gtttctacct
1381 gtggagtggc gatcgaagct tactcttgat ggagacactg ttgactccat cactcctgac
1441 aaggtgcggg gcctgaggga catgctcaac agcagcgcca tggacatcat gtactacacc
1501 agcccgctct acagggatga gctagttaaa ggccttcagc aagagctgaa tcgattatat
1561 tccctttttct gttcccggaa tccagacttt gaagagaaag ggggtaaagt ctcaatagtg
1621 tcccattcct tggggtgtgt aatcacttat gacatcatga tgggctggaa tccagttcga
1681 ctttatgagc agctgctgca gaaggaggag gagctgcctg acgagcggtg gatgagctac
1741 gaagagcggc atcttcttga tgagctctat atcactaaac ggcggctgag ggaaattgaa
1801 gatcggctgc atggattgaa ggcgccatcc ggctcacaaa cacctgcctt aaagtttaag
1861 gttgagaatt tcttctgtat gggatctccg ctagcagttt ttttagcatt acgcggcatc
1921 cgaccaggaa ataccggaag tcaagaccac attttaccta gagagatctg taaccgctta
1981 ctaaatattt ttcatcctac agacccagtg gcctacagat tagagccatt gattctgaaa
2041 cactacagca acatttctcc agtccagatc cactggtaca acacttcgaa ccctctacct
2101 tatgagcata tgaagccaaa ctttctcaac ccagcaaaag agcctacctc agcttcagag
2161 agtgagaaca tcgcagctat cccgagccct gtaacctccc cagtcttatc tcggcgccac
2221 tatggggaat ccataactaa cattggcaaa gcgagcatac tgggggctgc tagcattgga
2281 aaggggcttg gaggaatgtt gttctcaagg ttcggacggt cctccacacc acagccgtcg
2341 gagccatcta aggactcagc ggaagaggag aagaagcctg tctcttcacc ctccaccacc
2401 accgtggcca cgcagaccct gccgcacagc agctccggct tcctcgactc tgcattggaa
2461 ctggagcaca ggatcgactt cgaactcaga gaaggccttg tggagagccg ctattggtca
2521 gccgtcacgt cgcacactgc ctattggtca tccttggatg tcgctctttt tcttttaaca
2581 ttcatgtaca agcacgagca tgacagcgag gcaaagacca gcctagattc aatctgaact
2641 ctggacggat atgaatggcc caaaactttt ctgttaaaaa atgtgtcaag acatggagat
2701 tccaaggttc cggttttgtt aagggcaaga aatattttaa tttaaaagca ctttatttta
2761 tttttaaaag agaaaaaaac cacattttca gttctaaagg agttatttat gtttctgtca
2821 ttttgattga gtctagcaga gcccctgcag agaatcacca gagtggagtg tggtgggctt
2881 aggtgaactg catgaaggca gccatcacaa cccagttctc cagaggagcc taacgtaacg
2941 tattaaccaa aaggcgttac agcgctgacg tgcctgaagg ccagtccact ctgcaaagac
```

```
3001 tacaaggggg catcgtggct tctcgattct gcaaaggctt ctgtgcccac agttcctttg
3061 aaagaagagt atagcagatt ttaaatgtcc taaatttaac ttgttttgaa aagctaatgc
3121 taaaaagcaa tatttgaact actgtactta taatttatca tccctactta cttcagtgca
3181 ggaaacatgc ttaatgtctc ttttgccaca tctactctgt atcatgttga ggctcctttt
3241 tctcaaaact ccatctttgt aaatgagtag ctgatcctgt ggcgtaattt caggggtct
3301 ggggggttgg gttttgtttt tttgtttttg ttttttggt tttttggggt ttttttttg
3361 ttttggtttt ttttttgttt tatttttcat taaaaacatg gtttcacaaa aaaaaaaaaa
3421 aaaaaaaaaa aa
```

Figure C9: *Rattus norvegicus Ddhd1* mRNA sequence (Accession number: NM_001033066.1). Forward and reverse primers are highlighted in grey and indicated by the forward and backward arrows respectively.

Appendix C3: Agarose gel electrophoresis of qPCR products

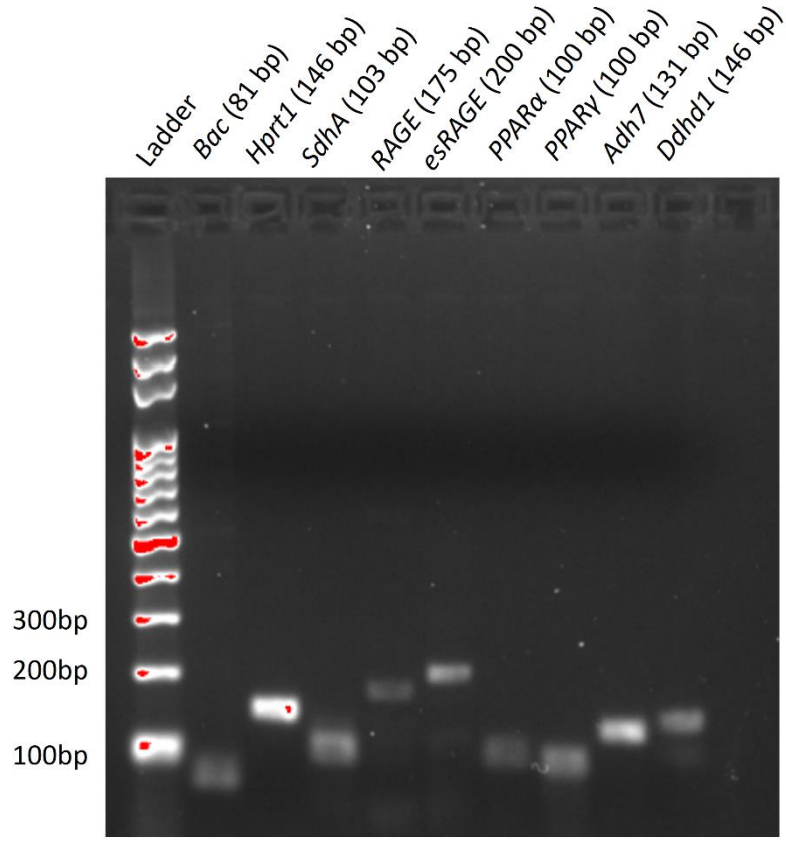

Figure C10: Agarose gel image of the qPCR products of endogenous references and target genes. The samples were run on a 2% agarose gel (1x TBE buffer) at 75V for 40 minutes. *Adh7*, alcohol dehydrogenase 7; *Bac*, β-actin; *Ddhd1*, DDHD domain containing 1; *Hprt1*, hypoxanthine phosphoribosyltransferase 1; *PPAR*, peroxisome proliferator-activated receptor; *RAGE*, receptor for advanced glycation end product; *SdhA*, succinate dehydrogenase complex flavoprotein subunit A; *esRAGE*, endogenous secretory receptor for advanced glycation end product.

Appendix D: Metadata of the hepatic RNA samples for transcriptomic analysis by next generation sequencing

Appendix D1: Purity, quality and integrity of the total RNA samples

Table D1: Concentration, purity and integrity of the total RNA samples prior to library preparation and sequencing.

Sample Identity	Concentration (ng/µL)	Abs 260/280	Abs 260/230	RNA integrity number
Control diet 1	868	1.99	2.14	6.8
Control diet 2	782	2.06	2.11	6.4
Control diet 3	944	2.06	2.18	6.7
Control diet 4	654	2.00	2.12	7.2
Control diet 5	1292	2.04	2.15	5.5
High-fat diet 1	836	2.06	2.14	4.8
High-fat diet 2	968	2.04	2.15	4.8
High-fat diet 3	970	2.11	2.19	4.0
High-fat diet 4	1204	2.09	2.21	6.5
High-fat diet 5	1158	2.08	2.18	6.7
Geraniin 1	1030	2.07	2.16	5.1
Geraniin 2	861	2.06	2.18	6.0
Geraniin 3	1110	2.08	2.12	5.9
Geraniin 4	850	2.06	2.05	7.5
Geraniin 5	990	2.00	2.12	6.8

Appendix D2: Agarose gel electrophoresis of the total RNA samples

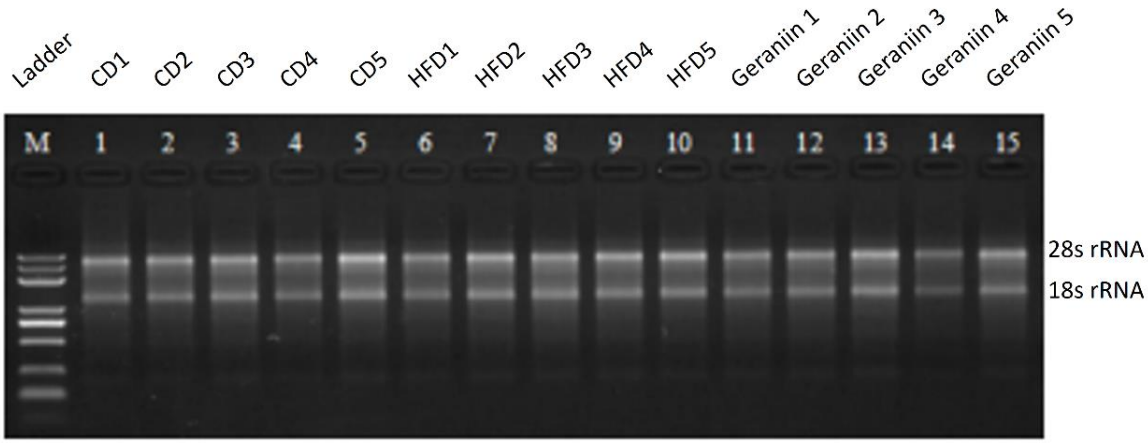

Figure D1: Agarose gel image of the hepatic RNA samples. The two clear bands are 18S (1.9 kb) and 28S (4.7 kb) rRNA. The samples were run in a 1% agarose gel (0.5x TBE buffer) at 180V for 16 minutes. CD, control diet; HFD, high-fat diet.

Appendix E: Published or submitted manuscripts

Appendix E1: Purified ingredient-based high-fat diet is superior to chow-based equivalent in the induction of metabolic syndrome

Journal of
Food Biochemistry

Purified ingredient-based high-fat diet is superior to chow-based equivalent in the induction of metabolic syndrome

Journal:	*Journal of Food Biochemistry*
Manuscript ID	JFBC-01-18-0077
Manuscript Type:	Full Article
Date Submitted by the Author:	31-Jan-2018
Complete List of Authors:	Cheng, Hong Sheng; Monash University - Malaysia Campus, School of Science Phang, Sonia Chew Wen; Monash University - Malaysia Campus, Jeffrey Cheah School of Medicine and Health Sciences Ton, So Ha; Monash University - Malaysia Campus, School of Science Abdul Kadir, Khalid; Monash University - Malaysia Campus, Jeffrey Cheah School of Medicine and Health Sciences Tan, Joash; Monash University Sunway Campus, School of Science
Keywords:	Diet-induced metabolic syndrome, dyslipidaemia, hypertension, impaired fasting glucose, insulin resistance, protein deficiency

Purified ingredient-based high-fat diet is superior to chow-based equivalent in the induction of metabolic syndrome

Cheng Hong Sheng[a], Phang Sonia Chew Wen[b], Ton So Ha[a], Abdul Kadir Khalid[b], Tan Joash Ban Lee[a*]

[a] *School of Science, Monash University Malaysia, 46150 Bandar Sunway, Selangor, Malaysia.*

[b] *School of Medicine and Health Sciences, Monash University Malaysia, 46150 Bandar Sunway, Selangor, Malaysia.*

[*] Corresponding author: Joash Tan Ban Lee; [redacted]

Abstract

The present study aimed to outline the physiological and metabolic disparity between chow- and purified ingredient-based high-fat diets and their efficacy in the induction of metabolic syndrome. Male, 3-week old Sprague Dawley rats were randomly assigned to chow-based control diet, chow-based high-fat diet, purified control diet and purified high-fat diet for 12 weeks. Physical and biochemical changes were documented. Chow-based diets, irrespective of the lipid content, resulted in significantly lower weight gain and organ weight compared to purified ingredient-based diets. Circulating insulin, total proteins, albumin and certain lipid components like the triglycerides, total cholesterol and HDL-cholesterol were also lower in the chow-based diet groups. Both chow- and purified high-fat diets induced central obesity, hypertension and hyperglycaemia, but the latter was associated with earlier onset of the metabolic aberrations and additionally, dyslipidaemia. In conclusion, purified high-fat diet is a better diet for metabolic syndrome induction in rats.

Practical Applications

Modelling metabolic syndrome is commonly accomplished with the use of chow- or purified ingredient-diets enriched with carbohydrates and/or lipids, but the differences and associated drawbacks are unclear. This study highlights that chow- or modified chow-based diets have a tendency to introduce unwanted metabolic changes which are inconsistent with the progression of metabolic syndrome. Thus, the use of these diets in metabolic disease study should be avoided. On the other hand, purified high-fat diet which can effectively induce the features of metabolic syndrome is highly recommended.

Keywords

Diet-induced metabolic syndrome, dyslipidaemia, hypertension, impaired fasting glucose, insulin resistance, protein deficiency

1. Introduction

Obesity and metabolic syndrome (MetS) are amongst some of the most prevalent global health concerns. In 2013, more than 35% of the world adult population were either overweight (BMI > 25 kg/m^2) or obese (BMI > 30 kg/m^2) (Ng *et al.* 2014), while the worldwide adult prevalence of MetS is approximately 25% (International Diabetes Federation 2006). Meanwhile, the prevalence of obesity and MetS among the children and adolescents is also ever-increasing (Ng, *et al.* 2014, Tailor *et al.* 2010). These health conditions are strongly linked to a number of non-communicable diseases such as type 2 diabetes, hypertension and coronary heart disease (Ford 2005, Park *et al.* 2012), which collectively contribute to more than 20% of the global premature deaths (under 70 years of age) (World Health Organization 2014). Considering the widespread prevalence and associated comorbidities, it goes without saying that obesity and MetS will continue bringing about massive economic and social burdens in the foreseeable future.

In light of this, obesity and MetS are extensively researched in the past few decades. Like many other biomedical studies, animal models (notably rodents such as mice and rats) play a crucial role in advancing our understanding about obesity and MetS. Primarily, a good experimental model should be able to fully and consistently mimic the human disease in order to facilitate reliable bench-to-bedside translation (Prabhakar 2012). Preferably, the model should also be easy to establish within a short duration and at a low economic cost.

In this context, a wide variety of approaches and models has been employed to study obesity and MetS, ranging from the loss-of-function genetic models (eg. *ob/ob* and *db/db* mice) as well as diet-, chemical- or even surgical-induced obese rodents (Lutz and Woods 2012, Panchal and Brown 2011). Diet-induced models may be better at mimicking the state of metabolic

dysfunctions in humans due to the multifactorial and polygenic nature of the disease. The diets used to induce obesity are generally enriched by lipids and/or carbohydrates (mainly sucrose or fructose) up to a total of 60% of the weight or the calorie content of the diets whereas the feeding duration typically ranges from one to six months (Wong *et al.* 2016).

Nonetheless, the use of diet-induced MetS models has several limitations. Most notably, the lack of a standardized disease induction methodology leads to a vast diversity of dietary compositions, preparation methods and nutritional values, rendering the comparison between studies difficult. In addition, the concern about the use of chow-based diets also arises because of batch-by-batch variability and non-disclosed formulation (Gajda *et al.* 2007). Chow-based diets possess high level of phytoestrogens which are highly bioavailable and confer beneficial effects on glucose and lipid metabolism (Brown and Setchell 2001, Cederroth *et al.* 2008). Furthermore, mixing animal chow with a large amount of fat or sugar will severely diminish the other essential nutrients, namely proteins, vitamins and minerals, thus resulting in unintended nutrient insufficiency which is not in line with the onset of MetS (Gajda, *et al.* 2007). The problem is further exacerbated by the mismatch between the control diets and the diets used to induce metabolic aberrations. Often, metabolic aberrations are induced by defined purified ingredient-based diet, but the control diet used is a chow-based diet. The huge differences in the dietary compositions tend to have a profound effect on the metabolism, causing misleading observations which are not accurately attributable to the high calorie consumption (Benoit *et al.* 2013). Despite the increasing awareness of these aforementioned issues, many recent studies still utilize chow-based diets supplemented with lipids and/or carbohydrates (Hao *et al.* 2015, Senaphan *et al.* 2015, Suman *et al.* 2016).

In this context, comparative studies that investigate the differential metabolic implications of chow- and purified ingredient-based diets are limited. As we have revealed that post-weaning rats given high-fat (60% kcal) diet led to earlier onset of MetS (Cheng *et al.* 2017), using the same model but with different dietary compositions, we would like to investigate the metabolic effects of chow- and purified ingredient-based high-fat diets. More importantly, this study aimed to outline the key differences between the two diets in the induction of MetS to promote careful formulation of the diets used in disease models establishment.

2. Materials and Methods

2.1. Animal ethics and housing conditions

The use and handling of animals in the study have been approved by Monash University Monash Animal Research Platform Animal Ethics Committees (AEC approval no.: MARP/2015/093) in compliance to the Australian Code of Practice for the Care and Use of Animals for Scientific Purposes outlined by National Health and Medical Research Council. Twenty eight male, three-week old post-weaning Sprague Dawley rats (*Rattus norvegicus*) were purchased from Monash University Malaysia Animal Facility. The rats were housed individually and kept at 23 ± 1^{0}C with 12-hour light/dark cycle. They had *ad libitum* access to food and tap water throughout the experiment.

2.2. Diet preparation, composition and treatment

The rats were randomized into four groups (n=7 per group) which were provided with chow-based control diet (Chow-CD), chow-based high-fat diet (Chow-HFD), purified ingredient-based control diet (Purified-CD) and purified ingredient-based high-fat diet (Purified-HFD) for 12

weeks. Chow-CD is a commercially available rat chow (Gold Coin, Selangor, Malaysia) while the purified ingredient-based diets were formulated based on AIN-93G diet with minor modifications (Reeves 1997). The macronutrient composition and ingredients of the experimental diets are outlined in Tables 1 and 2, respectively. All the purified ingredients were purchased from MP Biomedicals (Santa Ana, CA, USA), except for milk fat (Promac Enterprises Sdn. Bhd., Kuala Lumpur, Malaysia) and sucrose (MSM Malaysia Holdings Bhd., Kuala Lumpur, Malaysia). All the diets (except for Chow-CD which was ready-to-use), were prepared by mixing the ingredient thoroughly, followed by oven-baking for 10-20 minutes at 160^{o}C. The food and water were refilled daily whereas the body weight, food and water intake were measured daily.

At the end of the 12-week treatment, the rats were subjected to 12-hour fasting prior to euthanasia by exsanguination via cardiac puncture under the effect of ketamine (75 mg/kg) and xylazine hydrochloride (10 mg/kg) administered intraperitoneally. Blood samples were collected in tubes containing 0.5M EDTA. Plasma specimens were obtained by centrifugation at 4^{o}C, 2000x *g* for 20 minutes. The plasma was snap frozen in liquid nitrogen and stored at -80^{o}C until further use. Body organs including the liver, kidney and retroperitoneal white adipose tissue (rWAT) were harvested promptly, washed with phosphate buffered saline and weighed.

2.3. Blood pressure measurement

Systolic and diastolic blood pressure was measured with Mouse and Rat Tail Cuff Blood Pressure System (IITC Life Sciences, Los Angeles, CA, USA). Briefly, conscious rats were placed into a plastic restrainer one at a time to restrict their movement throughout the measurement. A tail-cuff with a pulse transducer was applied onto the tail of the restrained rats. The rat was then placed into a well-ventilated chamber equilibrated at 32^{o}C for 15 to 20 minutes

to facilitate the dilatation of caudal arteries. Next, the triplicate readings of the systolic and diastolic blood pressure were recorded. The procedure was performed once per week.

2.4. Glycaemic parameters

Fasting blood glucose was determined with Accu-Chek® Performa glucometer (Roche Diagnostics, Indianapolis, IN, USA) while fasting plasma insulin was determined using Mercodia Ultrasensitive Rat Insulin ELISA (Mercodia, Uppsala, Sweden). Homeostasis model assessment of the β-cell function (HOMA %β) and insulin sensitivity (HOMA %S) were calculated based on the fasting glucose and insulin levels (Levy *et al.* 1998) and expressed in percentage of the respective control groups. Glycated haemoglobin A1c (HbA1c) were determined with Rat Hemoglobin A1c (HbA1c) kit (Crystal Chem, Downers Grove, IL, USA). All measurements were done in duplicate.

2.5. Lipid profile

Circulating triglyceride and total cholesterol (TC) were determined with Randox TR1697 Triglycerides, CH200 Cholesterol (Randox, Dublin, UK) respectively. To determine high-density lipoprotein (HDL)-cholesterol level, the plasma specimens were mixed with Randox CH203 HDL-cholesterol Precipitant kit (Randox, UK) in 1: 2 ratio to precipitate chylomicron, low density lipoprotein (LDL)- and very low density lipoprotein (VLDL)-cholesterol. The mixture was centrifuged at 2000x *g* for 10 minutes. The supernatant which contained the HDL-cholesterol was retrieved and assayed for cholesterol content with CH200 Cholesterol kit. Non HDL-cholesterol was calculated by subtracting HDL-cholesterol from TC. All analysis by commercial kits were performed in duplicate according to the manufacturers' instructions.

2.6. Total plasma protein and albumin

The total plasma protein was determined using Bradford protein assay (Sigma Aldrich, St. Louis, USA). The plasma specimens were diluted by 1000 times followed by the addition of 10 volumes of the Bradford reagent. The absorbance at 595 nm was measured while the protein concentration was calculated based on a bovine serum albumin (BSA) standard curve (y = 0.0009x + 0.165).

The plasma albumin was determined using bromocresol green assay (Friendemann Schmidt, Parkwood, Australia) (Doumas *et al.* 1971). The plasma samples were diluted by two-fold. The diluted samples were then added to 100 volumes of the bromocresol green solution, mixed well and incubated at room temperature for 5 minutes. The absorbance at 645nm was measured whereas the albumin concentration was calculated based on a BSA standard curve (y=0.0013x + 0.3769).

2.7. Statistical analysis

All statistical tests were performed using Statistical Package for the Social Sciences (SPSS) 22.0. Dependent variables with repeated measures like the cumulative weight gain and blood pressure were analysed with mixed model ANOVA using “time” as the within-subjects factor and “types of diets (chow- or purified ingredient-based)” and “lipid content (CD or HFD)” as the between-subjects factor. Other variables were analysed with two-way ANOVA using “types of diets” and “lipid content” as the factors. Pairwise comparisons were performed with Bonferroni correction. The level of statistical significance was pre-determined at $p \leq 0.05$. All the results are presented as mean ± standard error of the mean.

3. Results

3.1. Weight gain and organ weight

The cumulative weight gain showed that the rats on high-fat diets had significant weight gain compared to those on control diets, regardless of the type of diets (chow- or purified ingredient-based) (Figure 1A). However, the onset of such an abnormally high weight gain was much earlier in Purified-HFD group (week 5) compared to Chow-HFD (week 11). Furthermore, the rats given purified ingredient-based diets were, in general, heavier than those on chow-based diets at any time point. More surprisingly, Purified-CD-treated rats gained more weight than Chow-HFD-treated rats over the course of the experiment. This suggests that the rats on chow-based diets were not as well-nourished as those on purified ingredient-based diets.

The rWAT weight was in line with the weight gain whereby the rats on high-fat diets had more visceral fat depot than those fed on control diets irrespective of the type of diets (Figure 1B). This supports obesity-inducing effect of high lipid consumption. Conversely, the rats on chow-based diets demonstrated significantly lower tissue weights not only of the rWAT, but also the kidney and liver (Figures 1C and D). Together with the weight gain data, these results signify a slower growth rate and reduced nourishment of the rats exposed to chow-based diet in comparison to those on purified ingredient-based diet.

3.2. Food and water intake

The feeding pattern may provide additional information to explain the weight gain and development. In this context, Figure 2A shows that the rats given high-fat diets consumed significantly less food per day. This food consumption difference was more notable in Purified-HFD (24% less) than in Chow-HFD (14% less) groups compared to their respective control

groups. This observation is plausible as the energy content of high-fat diets were higher than control diets due to the fortification with saturated fat. When the energy content was taken into consideration, it was found that Chow-HFD group consumed almost two-fifths more calories per day compared to Chow-CD group, while those on purified ingredient-based diets had comparable daily calorie consumption (Figure 2B). Moreover, treatment with chow-based diets led to lower calorie intake than purified ingredient-based diets, a result which is in agreement with the weight gain and organ weights. This points out that the retarded growth was attributable to the animal chow used in the diet preparation. The daily water intake between the rats on different types of diets also demonstrated very dissimilar pattern. The rats on Chow-CD consumed higher volume of water than those on Chow-HFD whereas the drinking pattern was reversed in those given purified ingredient-based diets (Figure 2C).

3.3. Systolic and diastolic blood pressure

Feeding on diets enriched with fat elevated the systolic blood pressure by approximately 15% from 117.35 ± 1.23 mm Hg to 134.48 ± 1.19 mm Hg (Figure 3A). Similar increase (89.1 ± 1.25 mm Hg to 105.20 ± 1.21 mm Hg) was also observed in the diastolic blood pressure (Figure 3B). The onset of the diet-induced hypertension took place about four weeks after the high-fat feeding. Such a hypertensive effect was strictly dependent on the fat content of the diets because the chow and purified ingredients did not have remarkable impact on the extent and onset of the hypertension.

3.4. Glycaemic parameters

We also looked into the effects of the diets on glucose metabolism. Treatment with Chow-HFD and Purified-HFD led to impaired fasting blood glucose compared to the respective control diets

(Figure 4A). The hyperglycaemic state was more chronic in the Purified-HFD group as evidenced by the elevated HbA1c, which is a biomarker of long-term glycaemic control. Although increased HbA1c was also observed in Chow-HFD-treated rats, the difference did not reach statistical significance (Figure 4C).

Astoundingly, unlike fasting blood glucose and HbA1c which were comparable between different types of diets, the rats that fed on chow- or purified ingredient-based diets exhibited vastly different levels of fasting plasma insulin. In fact, the fasting insulin level of chow-based diet-treated rats was suppressed by more than 10-fold (Figure 4B). High-fat feeding had no significant effect on the insulin level.

In addition, HOMA scores indicated different underlying mechanisms for the diet-induced hyperglycaemia in Purified-HFD and Chow-HFD groups. Essentially, the rats on Purified-HFD had lower HOMA%β (Figure 4D) while those on Chow-HFD had lower HOMA%S (Figure 4E) compared to their respective control diets. This suggests that the impaired fasting glucose of the former was caused by compromised β-cells function whereas that of the latter was due to insulin resistance.

3.5. Lipid profile

Treatment with different types of diets also triggered different extent of lipid metabolism dysregulation. Basically, Chow-HFD failed to induce any significant alteration to the lipid profile compared to Chow-CD. On the contrary, feeding on Purified-HFD caused a 136% increase in circulating triglyceride, 23% increase in TC and 39% increase in non HDL-cholesterol levels (Figures 5A, B and D). Evidently, Purified-HFD is more effective at inducing hyperlipidaemia. Apart from that, the rats on chow-based diets generally had lower lipid

components, namely triglyceride, TC and HDL-cholesterol in the circulation, as compared to those on purified ingredient-based diets (Figures 5A, B and C). In light of the stunted growth experienced by the chow-based diet-treated rats, such a hypolipidaemic effect may be indicative of a state of malnutrition.

3.6. Circulating protein and albumin

We further examined that total plasma protein and plasma albumin level to identify potential protein deficiency. Expectedly, the rats on chow-based diets had significantly lower total plasma protein (41.78 ± 0.966 g/L vs. 49.60 ± 0.925 g/L) and albumin (22.26 ± 2.33 g/L vs. 29.033 ± 2.33 g/L) compared to those on purified ingredient-based diets (Figures 6A and B). The declines in total plasma protein and albumin were about 19% and 30% respectively. Furthermore, Chow-CD led to even lower total plasma protein compared to the rats given Chow-HFD (Figure 6A). Collectively, this supports that hypothesis that chow-based diets led to a certain extent of protein insufficiency in comparison to purified ingredient-based diets.

4. Discussion

The present study points out several notable physical and metabolic differences between the diets prepared from either animal chow or purified ingredients. When the rats were exposed to chow-based diets irrespective of the fat content, they had slower growth rate, lower organ weights and significantly lower circulating levels of insulin, fat components and proteins compared to those on purified ingredient-based diets. These are the classic signs of malnutrition and protein insufficiency. Although it may be argued that the rats on purified ingredient-based diets were in fact, overly well-nourished, this argument is simply unlikely to be true because the growth curve of the rats given Purified-CD (about 4 g/day for 12 weeks) is more comparable to the reported

growth rate of male Sprague Dawley rats (Brower *et al.* 2015, Laaksonen *et al.* 2013). In contrast, the growth rate of the rats on Chow-CD was merely 2.43 g/day, which was much lower than anticipated. This strongly supports that chow-based diets were associated with stunted growth observed in the present study.

There are many contributing factors to such metabolic discrepancies between the two types of diets. Primarily, considering the comparable food intake between chow- and purified-ingredient diet-treated groups, it is hypothesized that the metabolisable energy of the chow was lower, thereby resulting in the poor nourishment. To clarify, metabolisable energy in this context is defined as the actual energy available from digestion of an animal feed, and is highly dependent on the digestibility of the food (Bielohuby *et al.* 2010). Compared to purified ingredient-based diets, chow diets have much lower digestibility and metabolisable energy (Bielohuby*, et al.* 2010). This is not unusual given the compositional complexity of animal chows unlike purified ingredient-based diets which contain readily digestible macronutrients like starch, maltodextrin and casein.

Furthermore, the types of indigestible fiber such as lignin, pectin and cellulose, could also affect the digestibility of other nutrients. As opposed to the diets formulated with purified ingredients whose content of indigestible fiber (usually cellulose) is well-defined, the composition of fiber in animal chow could vary considerably depending on the types of plant materials used for the pellet production. In this context, the presence of complex polysaccharides like lignin and pectin could significantly hamper the overall digestibility of food and crude protein whereas cellulose had the less effect (Chiou *et al.* 1998). Additionally, a small but significant portion of animal chow is composed of non-nutritive phytochemical compounds originated from the plant materials. Most notably are the anti-nutrients such as trypsin inhibitors, phytic acids and phorbol

esters, which are known to inhibit the digestive enzymes or obstruct absorption. The presence of anti-nutrients could also lead to slow growth rate due to their antagonistic effects on digestion (Nwala *et al.* 2013). Hence, when coupled with the lower metabolisable energy, the reduced digestion efficacy could explain the relatively poor nourishment of the rats on chow-based diets in comparison to those on purified ingredient-based diets. It is also noteworthy that these plant material-dependent constituents may exhibit diverse brand-to-brand, or even batch-to-batch variations, which will introduce unaccounted confounding variables into the experiments.

Protein insufficiency was also observed in the rats on chow-based diets as indicated by the decreased total plasma protein and albumin as well as lower transport protein-dependent parameters like triglycerides, TC and HDL-cholesterol. The findings are consistent with a previous study published by Solon-Biet et al. (2014) who also demonstrated that low-protein diets were associated with lowered TC, HDL- and LDL-cholesterol levels even when the lipid content of the diets was high (Solon-Biet *et al.* 2014). Since the differences exist only between chow- and purified ingredient-based diets but not within chow-based diets of variable fat content, this would explain why such a protein malnutrition remains largely unnoticed even though modified chow diets are widely used in experimental settings. The reduced protein level caused by chow-based diets consumption may potentially affect the metabolism which in turn, creates more confounding variables to disease modelling. Moreover, as some of the metabolic anomalies are not fully explained by high fat feeding but instead, by the ingredients of the diets, this may have profound effects on the assay results, rendering the conclusions inaccurate or even conflicting (Benoit*, et al.* 2013). Based on these arguments, chow-based diets are deemed inappropriate for the induction of obesity and MetS considering the high level of variability and the presence of significant confounding variables to the disease modelling.

Speaking of disease modelling, Purified-HFD is clearly superior to Chow-HFD in the induction of metabolic dysregulation. Feeding on Purified-HFD for 12 weeks resulted in all key hallmarks of MetS, namely central obesity, hypertension, hyperglycaemia and dyslipidaemia. Conversely, in the rats on Chow-HFD, not only was the lipid profile remained unaffected, but the onset of increased weight gain and impaired fasting glucose were also delayed. These differences can be linked to the greater digestibility of purified ingredient-based diets which led to increased nutrient uptake and consequently, a more chronic form of metabolic dysregulation. Aside from that, chow-based diets also contain phytoestrogens which are phytochemicals with estrogenic properties (Thigpen *et al.* 1999). Examples of phytoestrogens include isoflavones, lignans and coumestans. It is well-established that the consumption of phytoestrogens, particularly isoflavones, confers protective effects on the cardiovascular health and lipid homeostasis(Terzic *et al.* 2012, Wroblewski Lissin and Cooke 2000, Zhan and Ho 2005). This would therefore, elucidate why the rats on Chow-HFD did not develop dyslipidaemia despite the presence of other metabolic aberrations.

It may be added that Chow-HFD and Purified-HFD seemed to have very different mechanisms to induce hyperglycaemia. The former is linked to insulin resistance whereas the latter adversely affected the pancreatic β-cells function. Nevertheless, it is worth mentioning that treatment with purified ingredient-based diets in general, resulted in significantly higher fasting insulin compared to chow-based diets, even among the two control groups. This is also in line with previous studies(Apolzan and Harris 2012, Benoit*, et al.* 2013). It is speculated that Purified-CD might also trigger a certain extent of peripheral insulin resistance and hyperinsulinaemia as compared to Chow-CD (Benoit*, et al.* 2013), rendering us unable to distinguish the insulin resistant state of the rats on Purified-HFD. If Purified-HFD group were to be compared to Chow-

CD, the desensitization of insulin action caused by high-fat feeding would be evident(Huang *et al.* 2004, Yang *et al.* 2012). This again, reinforces the notion that conscientious selection and formulation of the experimental diets is of paramount importance, especially in insulin action and sensitivity study, in order to reach the correct conclusion.

One critical limitation of the present study is the variability in the nutritional composition between the four experimental diets. Unlike the clearly defined composition of purified ingredient-based diets, enriching rat chows with a large amount of lipids tremendously diluted the protein content (27% kcal to 12% kcal) as well as other micronutrients like vitamins and minerals. This may introduce additional impact on the metabolism and feeding behavior (Solon-Biet*, et al.* 2014) which are not in line with the pathogenesis of obesity and MetS. Likewise, the same concern is applicable in studies that employ modified chow-based diets for disease modelling. Next, milk fat, which is known to carry mostly saturated fat, was selected to increase the lipid content in both Chow- and Purified-HFD so as to accelerate the onset of metabolic dysfunction. Other lipid sources could have varying effects on the phenotypes of the disease (Buettner *et al.* 2006). Lastly, the starting age of the rats used in this study was three-week old. This was based our pilot study which demonstrated that post-weaning rats were more susceptible to MetS than adult rats (8-10 weeks old) when feeding on high-fat diet. Hence, in addition to lipid consumption, developmental stage may also have an effect on the progression of MetS. Such an interaction was not accounted in the present study.

To conclude, chow- and purified ingredient-based diets demonstrated some inherent discrepancies in the developmental and metabolic changes. Many of which were independent of, or had some degree of interaction with the overconsumption of dietary lipids, implying that the metabolic abnormalities observed particularly when Chow-HFD was used, were not fully

explained by the high-fat feeding , but rather by the inexplicit composition of the animal chow. Even though both HFDs were able to induce metabolic aberrations, Purified-HFD resulted in earlier onset of obesity, more severe dyslipidaemia and more chronic hyperglycaemia, making it a superior choice for MetS or obesity modelling. To our knowledge, this is one of the few studies that investigated the metabolic differences among chow- and purified ingredient-based diets. As the animal chow is a notable source of variability and confounding effects, the use of chow, particularly modified chow diets, should be strongly discouraged in metabolic disorders study.

References

Apolzan, J.W. and Harris, R.B.S. (2012). Differential effects of chow and purified diet on the consumption of sucrose solution and lard and the development of obesity. Physiology and Behavior, 105, 325-331.

Benoit, B., Plaisancié, P., Awada, M., Géloën, A., Estienne, M., Capel, F., Malpuech-Brugère, C., Debard, C., Pesenti, S., Morio, B., Vidal, H., Rieusset, J. and Michalski, M.-C. (2013). High-fat diet action on adiposity, inflammation, and insulin sensitivity depends on the control low-fat diet. Nutrition Research, 33, 952-960.

Bielohuby, M., Bodendorf, K., Brandstetter, H., Bidlingmaier, M. and Kienzle, E. (2010). Predicting metabolisable energy in commercial rat diets: physiological fuel values may be misleading. British Journal of Nutrition, 103, 1525-1533.

Brower, M., Grace, M., Kotz, C.M. and Koya, V. (2015). Comparative analysis of growth characteristics of Sprague Dawley rats obtained from different sources. Laboratory Animal Research, 31, 166-173.

Brown, N.M. and Setchell, K.D.R. (2001). Animal models impacted by phytoestrogens in commercial chow: Implications for pathways influenced by hormones. Laboratory Investigation, 81, 735-747.

Buettner, R., Parhofer, K.G., Woenckhaus, M., Wrede, C.E., Kunz-Schughart, L.A., Schölmerich, J. and Bollheimer, L.C. (2006). Defining high-fat-diet rat models: metabolic and molecular effects of different fat types. Journal of Molecular Endocrinology, 36, 485-501.

Cederroth, C.R., Vinciguerra, M., Gjinovci, A., Kühne, F., Klein, M., Cederroth, M., Caille, D., Suter, M., Neumann, D., James, R.W., Doerge, D.R., Wallimann, T., Meda, P., Foti, M., Rohner-Jeanrenaud, F., Vassalli, J.-D. and Nef, S. (2008). Dietary phytoestrogens activate AMP-activated protein kinase with improvement in lipid and glucose metabolism. Diabetes, 57, 1176-1185.

Cheng, H.S., Ton, S.H., Phang, S.C.W., Tan, J.B.L. and Abdul Kadir, K. (2017). Increased susceptibility of post-weaning rats on high-fat diet to metabolic syndrome. Journal of Advanced Research, 8, 743-752.

Chiou, P.W.-S., Yu, B. and Lin, C. (1998). The effect of different fibre components on growth rate, nutrient digestibility, rate of digesta passage and hindgut fermentation in domesticated rabbits. Laboratory Animals, 32, 276-283.

Doumas, B.T., Ard Watson, W. and Biggs, H.G. (1971). Albumin standards and the measurement of serum albumin with bromcresol green. Clinica Chimica Acta, 31, 87-96.

Ford, E.S. (2005). Risks for all-cause mortality, cardiovascular disease, and diabetes associated with the metabolic syndrome: A summary of the evidence. Diabetes Care, 28, 1769-1778.

Gajda, A.M., Pellizzon, M.A., Ricci, M.R. and Ulman, E.A. (2007). Diet-induced metabolic syndrome in rodent models. New Hampshire: Vicon Publishing Inc.

Hao, L., Lu, X., Sun, M., Li, K., Shen, L. and Wu, T. (2015). Protective effects of L-arabinose in high-carbohydrate, high-fat diet-induced metabolic syndrome in rats. Food and Nutrition Research, 59, 28886.

Huang, B.W., Chiang, M.T., Yao, H.T. and Chiang, W. (2004). The effect of high-fat and high-fructose diets on glucose tolerance and plasma lipid and leptin levels in rats. Diabetes, Obesity and Metabolism, 6, 120-126.

International Diabetes Federation (2006). The IDF Consensus Worldwide Definition of the Metabolic Syndrome. Brussels, Belgium: International Diabetes Federation.

Laaksonen, K., Nevalainen, T., Haasio, K., Kasanen, I., Nieminen, P. and Voipio, H.-M. (2013). Food and water intake, growth, and adiposity of Sprague-Dawley rats with diet board for 24 months. Laboratory Animals, 47, 245-256.

Levy, J.C., Matthews, D.R. and Hermans, M.P. (1998). Correct homeostasis model assessment (HOMA) evaluation uses the computer program. Diabetes Care, 21, 2191-2192.

Lutz, T.A. and Woods, S.C. (2012). Overview of Animal Models of Obesity. Current Protocols in Pharmacology, 58, 5.61.1-5.61.18.

Ng, M., Fleming, T., Robinson, M., Thomson, B., Graetz, N., Margono, C., Mullany, E.C., Biryukov, S., Abbafati, C., Abera, S.F., Abraham, J.P., Abu-Rmeileh, N.M.E., Achoki, T., AlBuhairan, F.S., Alemu, Z.A., Alfonso, R., Ali, M.K., Ali, R., Guzman, N.A., Ammar, W., Anwari, P., Banerjee, A., Barquera, S., Basu, S., Bennett, D.A., Bhutta, Z., Blore, J., Cabral, N., Nonato, I.C., Chang, J.-C., Chowdhury, R., Courville, K.J., Criqui, M.H., Cundiff, D.K., Dabhadkar, K.C., Dandona, L., Davis, A., Dayama, A., Dharmaratne, S.D., Ding, E.L., Durrani, A.M., Esteghamati, A., Farzadfar, F., Fay, D.F.J., Feigin, V.L., Flaxman, A., Forouzanfar, M.H., Goto, A., Green, M.A., Gupta, R., Hafezi-Nejad, N., Hankey, G.J., Harewood, H.C., Havmoeller,

R., Hay, S., Hernandez, L., Husseini, A., Idrisov, B.T., Ikeda, N., Islami, F., Jahangir, E., Jassal, S.K., Jee, S.H., Jeffreys, M., Jonas, J.B., Kabagambe, E.K., Khalifa, S.E.A.H., Kengne, A.P., Khader, Y.S., Khang, Y.-H., Kim, D., Kimokoti, R.W., Kinge, J.M., Kokubo, Y., Kosen, S., Kwan, G., Lai, T., Leinsalu, M., Li, Y., Liang, X., Liu, S., Logroscino, G., Lotufo, P.A., Lu, Y., Ma, J., Mainoo, N.K., Mensah, G.A., Merriman, T.R., Mokdad, A.H., Moschandreas, J., Naghavi, M., Naheed, A., Nand, D., Narayan, K.M.V., Nelson, E.L., Neuhouser, M.L., Nisar, M.I., Ohkubo, T., Oti, S.O., Pedroza, A., Prabhakaran, D., Roy, N., Sampson, U., Seo, H., Sepanlou, S.G., Shibuya, K., Shiri, R., Shiue, I., Singh, G.M., Singh, J.A., Skirbekk, V., Stapelberg, N.J.C., Sturua, L., Sykes, B.L., Tobias, M., Tran, B.X., Trasande, L., Toyoshima, H., van de Vijver, S., Vasankari, T.J., Veerman, J.L., Velasquez-Melendez, G., Vlassov, V.V., Vollset, S.E., Vos, T., Wang, C., Wang, X., Weiderpass, E., Werdecker, A., Wright, J.L., Yang, Y.C., Yatsuya, H., Yoon, J., Yoon, S.-J., Zhao, Y., Zhou, M., Zhu, S., Lopez, A.D., Murray, C.J.L. and Gakidou, E. (2014). Global, regional, and national prevalence of overweight and obesity in children and adults during 1980-2013: A systematic analysis for the Global Burden of Disease Study 2013. The Lancet, 384, 766-781.

Nwala, C.O., Akaninwor, J.O. and Monanu, M.O. (2013). Nutritional studies on rats fed diets formulated from treated and raw samples of Jatropha Curcas seed. International Journal of Engineering and Science Invention, 2, 14-19.

Panchal, S.K. and Brown, L. (2011). Rodent models for metabolic syndrome research. Journal of Biomedicine and Biotechnology, 2011, 351982.

Park, M.H., Falconer, C., Viner, R.M. and Kinra, S. (2012). The impact of childhood obesity on morbidity and mortality in adulthood: a systematic review. Obesity Reviews, 13, 985-1000.

Prabhakar, S. (2012). Translational research challenges: Finding the right animal models. Journal of Investigative Medicine, 60, 1141-1146.

Reeves, P.G. (1997). Components of the AIN-93 diets as improvements in the AIN-76A diet. Journal of Nutrition, 127, 838S-841S.

Senaphan, K., Kukongviriyapan, U., Sangartit, W., Pakdeechote, P., Pannangpetch, P., Prachaney, P., Greenwald, S. and Kukongviriyapan, V. (2015). Ferulic acid alleviates changes in a rat model of metabolic syndrome induced by high-carbohydrate, high-fat diet. Nutrients, 7, 6446-6464.

Solon-Biet, S.M., McMahon, A.C., Ballard, J.W.O., Ruohonen, K., Wu, L.E., Cogger, V.C., Warren, A., Huang, X., Pichaud, N., Melvin, R.G., Gokarn, R., Khalil, M., Turner, N., Cooney, G.J., Sinclair, D.A., Raubenheimer, D., Le Couteur, D.G. and Simpson, S.J. (2014). The ratio of macronutrients, not caloric intake, dictates cardiometabolic health, aging, and longevity in ad libitum-fed mice. Cell Metabolism, 19, 418-430.

Suman, R.K., Ray Mohanty, I., Borde, M.K., Maheshwari, U. and Deshmukh, Y.A. (2016). Development of an experimental model of diabetes co-existing with metabolic syndrome in rats. Advances in Pharmacological Sciences, 2016, 9463476.

Tailor, A.M., Peeters, P.H.M., Norat, T., Vineis, P. and Romaguera, D. (2010). An update on the prevalence of the metabolic syndrome in children and adolescents. International Journal of Pediatric Obesity, 5, 202-213.

Terzic, M., Micic, J., Dotlic, J., Maricic, S., Mihailovic, T. and Knezevic, N. (2012). Impact of phytoestrogens on serum lipids in postmenopausal women. Geburtshilfe und Frauenheilkunde, 72, 527-531.

Thigpen, J.E., Setchell, K.D.R., Ahlmark, K.B., Locklear, J., Spahr, T., Caviness, G.F., Goelz, M.F., Haseman, J.K., Newbold, R.R. and Forsythe, D.B. (1999). Phytoestrogen content of purified, open- and closed-formula laboratory animal diets. Comparative Medicine, 49, 530-536.

Wong, S.K., Chin, K.-Y., Suhaimi, F.H., Fairus, A. and Ima-Nirwana, S. (2016). Animal models of metabolic syndrome: a review. Nutrition and Metabolism, 13, 65.

World Health Organization (2014). Global Status Report on Noncommunicable Diseases 2014. Geneva: World Health Organization.

Wroblewski Lissin, L. and Cooke, J.P. (2000). Phytoestrogens and cardiovascular health. Journal of the American College of Cardiology, 35, 1403-1410.

Yang, Z.-H., Miyahara, H., Takeo, J. and Katayama, M. (2012). Diet high in fat and sucrose induces rapid onset of obesity-related metabolic syndrome partly through rapid response of genes involved in lipogenesis, insulin signalling and inflammation in mice. Diabetology & Metabolic Syndrome, 4, 32.

Zhan, S. and Ho, S.C. (2005). Meta-analysis of the effects of soy protein containing isoflavones on the lipid profile. American Journal of Clinical Nutrition, 81, 397-408.

Figure Captions

Figure 1: Cumulative weight gain (A) and the weight of retroperitoneal white adipose tissue (B), kidney (C) and liver (D) expressed in terms of the percentage of body weight (%) of the rats treated with different types of diets for 12 weeks. Sample size is n=7 per group. Error bars indicate SEM. * indicates $p<0.05$, ** indicates $p<0.01$ and *** indicates $p<0.001$ between groups. Square bracket indicates significant difference between chow- and purified ingredient-based diets. CD, control diet; HFD, high-fat diet; rWAT, retroperitoneal white adipose tissue.

Figure 2: Daily food (A), calorie (B) and water (C) intake of the rats treated with different types of diets for 12 weeks. Sample size is n=7 per group. Error bars indicate SEM. * indicates $p<0.05$, ** indicates $p<0.01$ and *** indicates $p<0.001$ between groups. Square bracket indicates significant difference between chow- and purified ingredient-based diets.

Figure 3: Systolic (A) and diastolic (B) blood pressure of the rats treated with different types of diets for 12 weeks. Sample size is n=7 per group. Error bars indicate SEM. *** indicates $p<0.001$ between groups. CD, control diet; HFD, high-fat diet.

Figure 4: Fasting blood glucose (A), fasting plasma insulin (B), glycated haemoglobin A1c (C), HOMA%β (D) and HOMA%S (E) of the rats treated with different types of diets for 12 weeks. Sample size is n=7 per group. Error bars indicate SEM. * indicates $p<0.05$, ** indicates $p<0.01$ and *** indicates $p<0.001$ between groups. Square bracket indicates significant difference between chow- and purified ingredient-based diets. HbA1c, glycated haemoglobin A1c; HOMA%β, homeostasis model assessment of β-cell function; HOMA %S, homeostasis model assessment of insulin sensitivity.

Figure 5: Triglyceride (A), total cholesterol (B), HDL-cholesterol (C) and non HDL-cholesterol (D) of the rats treated with different types of diets for 12 weeks. Sample size is n=7 per group. Error bars indicate SEM. * indicates $p<0.05$, ** indicates $p<0.01$ and *** indicates $p<0.001$ between groups. Square bracket indicates significant difference between chow- and purified ingredient-based diets. HDL, high density lipoprotein.

Figure 6: Total plasma protein (A) and plasma albumin (B) of the rats treated with different types of diets for 12 weeks. Sample size is n=7 per group. Error bars indicate SEM. * indicates $p<0.05$

and *** indicates $p<0.001$ between groups. Square bracket indicates significant difference between chow- and purified ingredient-based diets.

Table 1: Macronutrient composition and calorie content of the control and high-fat diets prepared with animal chow or purified ingredients

Macronutrient	Chow-based diets		Purified ingredient-based diets	
	Control	High-fat	Control	High-fat
Protein (kcal %)	27	12	20	20
Carbohydrate (kcal %)	64	28	70	20
Lipid (kcal%)	9	60	10	60
Energy content (kcal/g)	3.07	4.87	3.88	5.32

Table 2: Ingredients of the control and high-fat diets prepared with animal chow or purified ingredients.

Ingredient	Percentage/Amount		Ingredient	Mass (g)	
	Chow-based diets			Purified ingredient-based diets	
	Control	High-fat		Control	High-fat
Crude protein (min)	21%	15%	Casein	200	200
Nitrogen free extract	49%	34%	L-cystine	3	3
Crude fibre (max)	5.0%	3.5%	Corn starch	525.5	18
Crude fat (min)	3.0%	2.1%	Maltodextrin	125	125
Milk fat	-	30.3%	Sugar	50	50
Moisture (max)	13.0%	9.1%	Cellulose	50	50
Phosphorus (min)	0.6%	0.4%	Corn oil	25	25
Calcium (min)	0.8%	0.6%	Milk fat	20	245
Vitamin A	0.20 M.I.U/kg	0.14 M.I.U/kg	AIN-93G Mineral mix	35	35
Vitamin D_3	0.05 M.I.U/kg	0.03 M.I.U/kg	AIN-93-VX Vitamin mix	10	10
Vitamin E	0.03%	0.02%	Choline bitartrate	2	2
Other vitamins and mineral	Trace amount		t-butylhydroquinone	0.014	0.014

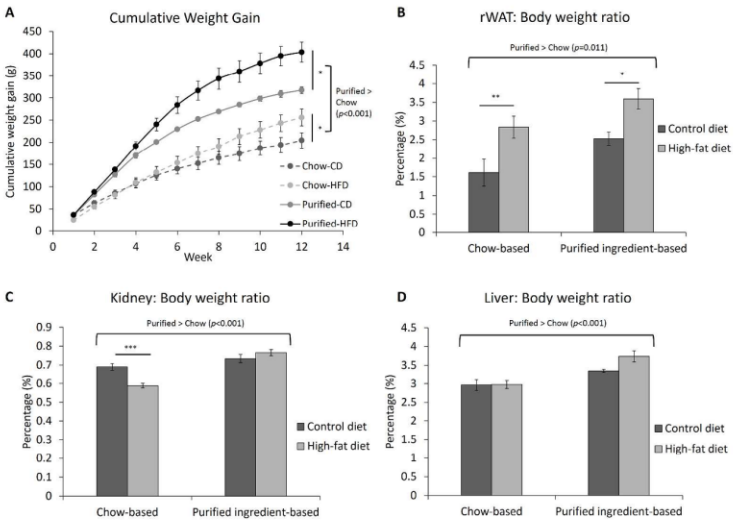

Figure 1: Cumulative weight gain (A) and the weight of retroperitoneal white adipose tissue (B), kidney (C) and liver (D) expressed in terms of the percentage of body weight (%) of the rats treated with different types of diets for 12 weeks. Sample size is n=7 per group. Error bars indicate SEM. * indicates p<0.05, ** indicates p<0.01 and *** indicates p<0.001 between groups. Square bracket indicates significant difference between chow- and purified ingredient-based diets. CD, control diet; HFD, high-fat diet; rWAT, retroperitoneal white adipose tissue.

1056x759mm (96 x 96 DPI)

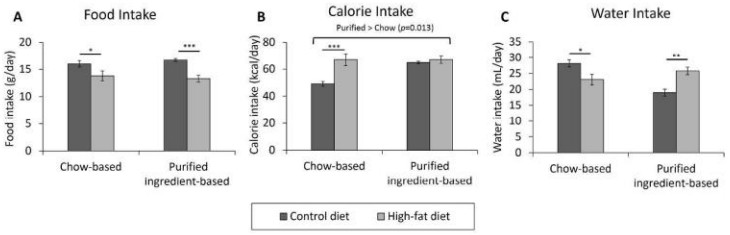

Figure 2: Daily food (A), calorie (B) and water (C) intake of the rats treated with different types of diets for 12 weeks. Sample size is n=7 per group. Error bars indicate SEM. * indicates p<0.05, ** indicates p<0.01 and *** indicates p<0.001 between groups. Square bracket indicates significant difference between chow- and purified ingredient-based diets.

1058x352mm (96 x 96 DPI)

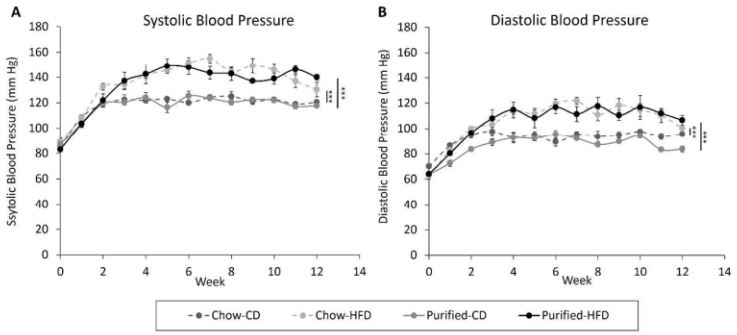

Figure 3: Systolic (A) and diastolic (B) blood pressure of the rats treated with different types of diets for 12 weeks. Sample size is n=7 per group. Error bars indicate SEM. *** indicates p<0.001 between groups. CD, control diet; HFD, high-fat diet.

1001x476mm (96 x 96 DPI)

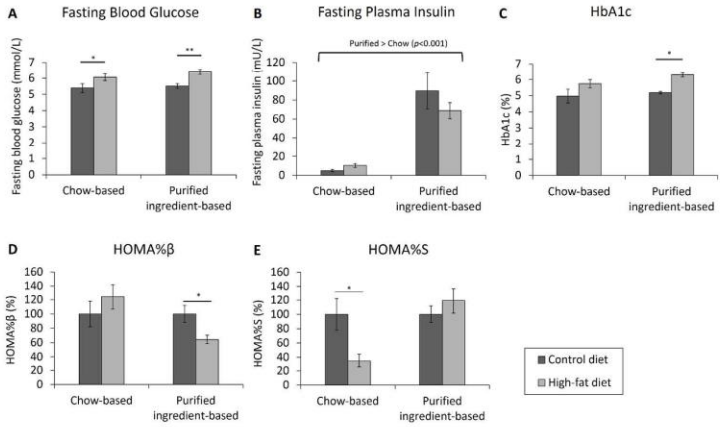

Figure 4: Fasting blood glucose (A), fasting plasma insulin (B), glycated haemoglobin A1c (C), HOMA%β (D) and HOMA%S (E) of the rats treated with different types of diets for 12 weeks. Sample size is n=7 per group. Error bars indicate SEM. * indicates p<0.05, ** indicates p<0.01 and *** indicates p<0.001 between groups. Square bracket indicates significant difference between chow- and purified ingredient-based diets. HbA1c, glycated haemoglobin A1c; HOMA%β, homeostasis model assessment of β-cell function; HOMA %S, homeostasis model assessment of insulin sensitivity.

1050x626mm (96 x 96 DPI)

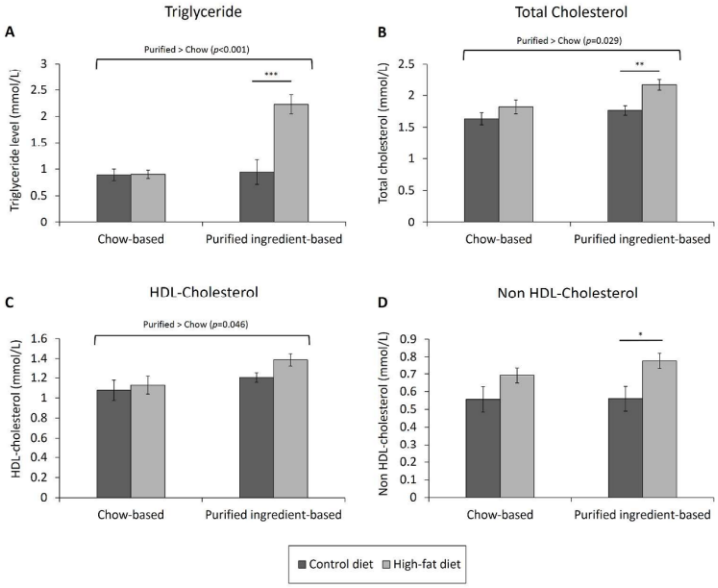

Figure 5: Triglyceride (A), total cholesterol (B), HDL-cholesterol (C) and non HDL-cholesterol (D) of the rats treated with different types of diets for 12 weeks. Sample size is n=7 per group. Error bars indicate SEM. * indicates p<0.05, ** indicates p<0.01 and *** indicates p<0.001 between groups. Square bracket indicates significant difference between chow- and purified ingredient-based diets. HDL, high density lipoprotein.

980x797mm (96 x 96 DPI)

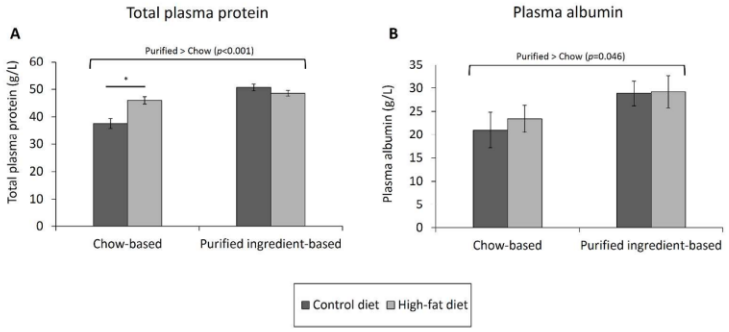

Figure 6: Total plasma protein (A) and plasma albumin (B) of the rats treated with different types of diets for 12 weeks. Sample size is n=7 per group. Error bars indicate SEM. * indicates $p<0.05$ and *** indicates $p<0.001$ between groups. Square bracket indicates significant difference between chow- and purified ingredient-based diets.

946x446mm (96 x 96 DPI)

Appendix E2: The ameliorative effects of a tocotrienol-rich fraction on the AGE-RAGE axis and hypertension in high-fat-diet-fed rats with metabolic syndrome

nutrients

MDPI

Article

The Ameliorative Effects of a Tocotrienol-Rich Fraction on the AGE-RAGE Axis and Hypertension in High-Fat-Diet-Fed Rats with Metabolic Syndrome

Hong Sheng Cheng [1,*], So Ha Ton [1], Joash Ban Lee Tan [1] and Khalid Abdul Kadir [2]

1 School of Science, Monash University Malaysia, Bandar Sunway, Selangor 46150, Malaysia; ton.soha2016@gmail.com (S.H.T.); tan.ban.lee@monash.edu (J.B.L.T.)
2 School of Medicine and Health Sciences, Monash University Malaysia, Bandar Sunway, Selangor 46150, Malaysia; khalid.kadir@monash.edu
* Correspondence: hong.cheng@monash.edu or hongsheng91cheng@gmail; Tel.: +60-1-0933-7034; Fax: +60-3-5514-6099

Received: 4 August 2017; Accepted: 1 September 2017; Published: 7 September 2017

Abstract: The clinical value of tocotrienols is increasingly appreciated because of the unique therapeutic effects that are not shared by tocopherols. However, their effect on metabolic syndrome is not well-established. This study aimed to investigate the effects of a tocotrienol-rich fraction (TRF) from palm oil in high-fat-diet-treated rats. Male, post-weaning Sprague Dawley rats were provided high-fat (60% kcal) diet for eight weeks followed by a TRF (60 mg/kg) treatment for another four weeks. Physical, metabolic, and histological changes were compared to those on control and high-fat diets respectively. High-fat feeding for eight weeks induced all hallmarks of metabolic syndrome. The TRF reversed systolic and diastolic hypertension, hypercholesterolemia, hepatic steatosis, impaired antioxidant defense, and myeloperoxidase hyperactivity triggered by the high-fat diet. It also conferred an inhibitory effect on protein glycation to reduce glycated hemoglobin A1c and advanced glycation end products (AGE). This was accompanied by the suppression of the receptor for advanced glycation end product (RAGE) expression in the liver. The treatment effects on visceral adiposity, glycemic control, triglyceride level, as well as peroxisome proliferator-activated receptor α and γ expression were negligible. To conclude, treatment with a TRF exhibited protective effects on the cardiovascular and liver health in addition to the amelioration of plasma redox imbalance and AGE-RAGE activation. Further investigation as a therapy for metabolic syndrome is therefore worthwhile.

Keywords: advanced glycation end product; cholesterol; hepatic steatosis; myeloperoxidase; peroxisome proliferator-activated receptor; vitamin E

1. Introduction

Being an important micronutrient and a powerful lipophilic antioxidant, vitamin E has received extensive research attention in the aspects of anti-inflammation, anti-cancer, chronic metabolic disorders, and neurodegenerative diseases ever since its discovery about a century ago [1–3]. Fundamentally, vitamin E can be divided into two major classes: tocopherols and tocotrienols, each with α, β, γ, and δ subtypes. Tocotrienols are differentiated from tocopherols by the presence of an unsaturated isoprenoid side chain with three double bonds. As α-tocopherol was the first natural form of vitamin E identified, it drew most of the research attention, rendering other isoforms, most notably tocotrienols, poorly understood.

Nevertheless, in recent years, the paradigm of vitamin E research has been shifting, whereby studies about tocotrienols are increasingly emphasized. In fact, many studies have reported that tocotrienols have

similar antioxidant capacity [4] and superior anti-cancer properties in comparison to tocopherols [5,6]. More importantly, tocotrienols also exhibit cholesterol-lowering [7], neuroprotective [8], and anti-aging [9] effects, which are not shared by tocopherols. The bioactivities of tocotrienols are summarized comprehensively in several review articles [10–12]. Several promising natural sources in which tocotrienols can be found in high abundance include oil palm, barley, and rice. The tocotrienol/tocopherol ratios are 1:1, 1.9:1, to 3:1 for rice bran oil, barley, and palm oil, respectively [11]. Therefore, identifying the medicinal uses of tocotrienols may create added value to these cultivated plants, which subsequently could be translated into economic growth.

On the other hand, given that elevated oxidative stress, low-grade systemic inflammation, and deranged lipid and glucose homeostasis are well-implicated in the pathogenesis of metabolic disorders like obesity, metabolic syndrome, type 2 diabetes mellitus, and cardiovascular disease, the known bioactivities of tocotrienols make it an appealing therapeutic candidate. Indeed, many recent studies have confirmed that treatment with tocotrienols or a tocotrienol-rich fraction (TRF) effectively ameliorated glucose dysregulation, hypercholesterolemia, hypertension, oxidative stress, as well as proinflammatory response in animal studies [13–17]. Despite the promising pre-clinical results, only the cholesterol-lowering and antioxidant effects have been consistently demonstrated in human studies [18–22], whereas other health benefits to humans like antihypertensive and antihyperglycemic activities remain inconclusive [21].

In this context, most of the bioactivities of tocotrienols are highly indicated in metabolic syndrome, but our pre-existing knowledge is established primarily based on diabetic animal models or hypercholesterolemic patients. Hypothetically, according to the known activities, tocotrienols or a TRF could potentially be a useful treatment of metabolic syndrome. Nonetheless, research on this aspect is rather limited. Considering the ever-increasing global prevalence of obesity and metabolic syndrome and promising value of tocotrienols, exploring the therapeutic effects and associated underlying mechanism of tocotrienols in obesity and metabolic syndrome is pertinent. Taken together, the present study aimed to examine the metabolic effects of tocotrienols in high-fat-diet-induced obese rats. The findings are discussed with reference to the physiological, biochemical, histopathological, and transcriptional alterations.

2. Materials and Methods

2.1. Animal Ethics and Housing Conditions

The use and handling of animals in the present study have been approved by Monash University Monash Animal Research Platform Animal Ethics Committees (AEC approval No.: MARP/2015/060) in compliance to the Australian Code of Practice for the Care and Use of Animals for Scientific Purposes outlined by National Health and Medical Research Council. Male, post-weaning (3-week-old) Sprague Dawley rats of 45–70 g were obtained from Monash University Malaysia Animal Facility. The rats were kept at 23 ± 1 °C with a 12 h light/dark cycle and given ad libitum access to homemade purified ingredient-based diets and tap water throughout the entire experiment.

2.2. Experimental Design and Treatment

Twenty-one post-weaning rats were randomized into three groups (n = 7 per group), namely control diet, high-fat diet, and TRF groups. Control diet group was treated with a low-fat (10% kcal) diet, while the high-fat diet and TRF groups were given a high-fat diet (60% kcal) for 8 weeks to induce metabolic syndrome. The diets were formulated based on AIN-93G diet [23], and their compositions are shown in Table 1.

Table 1. Macronutrient composition and ingredients of control and high-fat diets.

Macronutrient	Control Diet	High-Fat Diet
Protein (kcal %)	20	20
Carbohydrate (kcal %)	70	20
Lipid (kcal %)	10	60
Saturated (%)	36.6	57.9
Monounsaturated (%)	29.0	28.8
Polyunsaturated (%)	32.0	8.4
Trans (%)	1.8	3.6
Energy content (kcal/g)	3.9	5.3
Ingredient	Mass (g)	
Casein	200	200
L-cystine	3	3
Corn starch	525.5	18
Maltodextrin	125	125
Sugar	50	50
Cellulose	50	50
Milk fat	20	245
Corn oil	25	25
AIN-93G Mineral mix	35	35
AIN-93-VX Vitamin mix	10	10
Vitamin A	0.016	0.016
Vitamin B	0.092	0.092
Vitamin D	0.003	0.003
Vitamin E (α-tocopherol)	0.3	0.3
Vitamin K	0.001	0.001
Choline bitartrate	2	2
t-butylhydroquinone	0.014	0.014

After 8 weeks, the TRF group were treated with a 60 mg/kg commercially available TRF from palm oil known as Tocovid SupraBio^{TM} (Hovid, Ipoh, Malaysia) via oral gavage. The TRF is composed of 23.5% (*w*/*w*) α-tocotrienol, 43.2% γ-tocotrienol, 9.8% δ-tocotrienol, and 23.5% α-tocopherol. The dosage was selected based on a previous work [24]. The TRF was suspended in a 10% (*w*/*v*) glucose solution to minimize animal resistance to the administration procedure [25]. Control and high-fat diets groups were given the vehicle (a 10% glucose solution) via the same administration route. The treatment duration was 4 weeks, during which the rats were fed with the pre-assigned diets. The experimental design is illustrated in Figure 1.

The diets and water were refilled daily. Body weight, food, and water intake were also measured every day. At the end of the experiment, the rats were subjected to 12 h fasting prior to euthanasia with carbon dioxide. Blood samples were collected from the posterior vena cava and transferred into tubes with 0.5 M EDTA to avoid coagulation. The samples were then centrifuged immediately at 4 °C, 2000× *g* for 20 min to obtain the plasma specimens, which were snap-frozen in liquid nitrogen and stored at −80 °C until use. The liver, kidney, and retroperitoneal white adipose tissue (rWAT) were excised, washed with phosphate buffered saline (PBS), and weighed. Half of the liver and rWAT was snap-frozen and stored at −80 °C for RNA extraction and gene expression study, while the other half was stored in 10% (*v*/*v*) neutral buffered formalin for tissue fixation and histology.

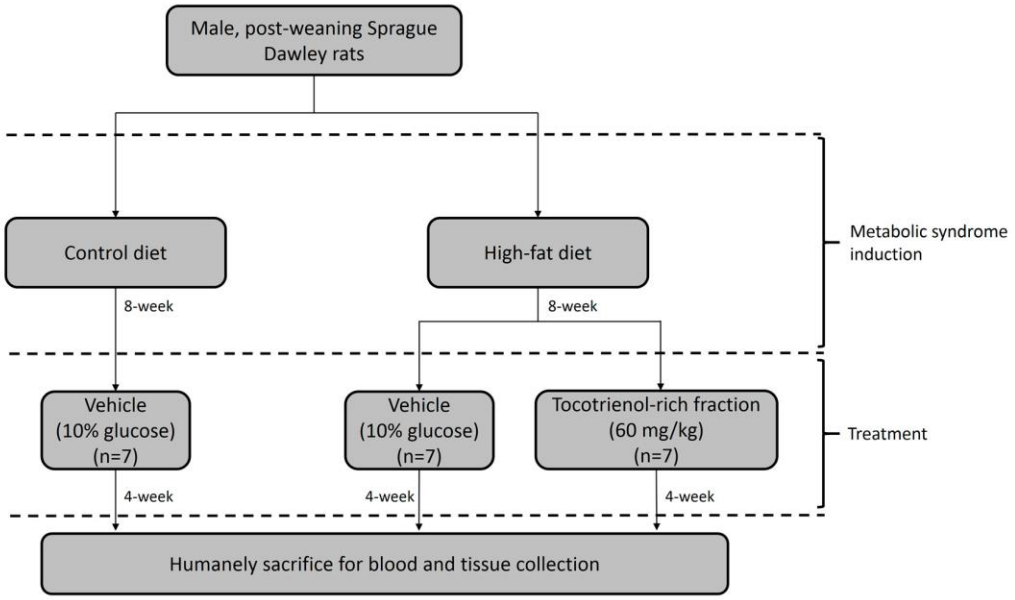

Figure 1. Experimental design of the present study.

2.3. Blood Pressure Measurement

Systolic and diastolic blood pressure was measured with Mouse and Rat Tail Cuff Blood Pressure System (IITC Life Sciences, Los Angeles, CA, USA). The rats were placed into a plastic restrainer one at a time to restrict their movement throughout the measurement. A tail-cuff with a pulse transducer was applied onto the tail of the restrained rats. The rat was then placed into a well-ventilated chamber equilibrated at 32 °C for 15–20 min to facilitate the dilatation of caudal arteries. Next, the triplicate readings of the systolic and diastolic blood pressure were recorded. The procedure was performed once per week.

2.4. Biochemical Assays

Fasting blood glucose was determined with Accu-Chek® Performa glucometer (Roche Diagnostics, Indianapolis, IN, USA), while fasting plasma insulin was measured using Mercodia Ultrasensitive Rat Insulin ELISA (Mercodia, Uppsala, Sweden). Homeostasis model assessment of the β-cell function (HOMA %β) and insulin sensitivity (HOMA %S) were calculated based on the fasting glucose and insulin levels [26] and expressed as a percentage of the control diet group. Glycated Hemoglobin A1c (HbA1c) and advanced glycation end products (AGEs) were quantified with the Rat Hemoglobin A1c (HbA1c) kit (Crystal Chem, Downers Grove, IL, USA) and the OxiSelect™ Advanced Glycation End Product (AGE) Competitive ELISA kit (Cell Biolabs, San Diego, CA, USA), respectively.

The lipid profile, including the triglyceride, total cholesterol (TC), and non-esterified fatty acid (NEFA) were measured with Randox TR1607 Triglycerides, CH200 Cholesterol, and FA115 Non-Esterified Fatty Acids kits (Randox, Dublin, UK). Chylomicron, low-density lipoprotein (LDL), and very low-density lipoprotein (VLDL) were precipitated from the plasma using the Randox CH203 HDL-cholesterol Precipitant kit (Randox, Dublin, UK), and the supernatant was subjected to the CH200 Cholesterol kit for the determination of high-density lipoprotein (HDL) cholesterol. Non-HDL-cholesterol was calculated by subtracting HDL cholesterol from total cholesterol.

Oxidative markers such as total plasma antioxidant capacity and myeloperoxidase activity were also measured with the OxiSelect™ ORAC Activity Assay kit and the OxiSelect™ Myeloperoxidase Chlorination Activity Assay kit (Cell Biolabs, San Diego, CA, USA) respectively. All analysis with the commercial kits was conducted in duplicates according to the manufacturers' instructions.

2.5. Oral Glucose Tolerance Test (OGTT)

OGTT was carried out before and after the treatment in Weeks 8 and 12. Food was suspended for 8 h prior to the measurement of fasting blood glucose level. This was the initial reading at 0 min. Then, they were given a glucose load of 2 g/kg as a 40% (*w*/*v*) glucose solution via oral gavage. Blood glucose levels were measured as 30, 60, 90, and 120 min after administration of the glucose load.

2.6. Plasma Electrolyte Levels

Atomic absorption spectrophotometry was used for the determination of plasma electrolyte levels. Plasma specimens were diluted by 500 and 50 times with distilled water for the measurement of sodium and potassium levels, respectively. The concentration of the electrolytes were determined with PerkinElmer Atomic Absorption Spectrophotometer Analyst 100 (PerkinElmer, Waltham, MA, USA) using a sodium/potassium hollow cathode lamp. The wavelength was set at 589 nm and 766 nm for measuring sodium and potassium concentrations, respectively. The actual concentration of the electrolytes was calculated based on a standard curve.

2.7. Tissue Processing and Histology

Conventional tissue processing, which includes dehydration, clearing, and infiltration of the liver and rWAT specimens with paraffin wax, was performed following formalin fixation. The tissues were then embedded in paraffin wax and stored at 4 °C. Thin sections (5 μm) were produced and stained with hematoxylin and eosin (H&E) to visualize the morphology of the tissues. Nikon Eclipse TS100 (Nikon, Tokyo, Japan) was used to capture the microscopic images of the tissues. ImageJ was used to measure the adipocyte size of the rWAT based on the method published by Parlee et al. (2014) [27].

2.8. Hepatic Lipid Extraction

Total lipid extraction of the liver tissues was carried out based on the Folch method [28]. Briefly, 150 mg of the snap-frozen liver tissues were ground into powder and homogenized in 20 mL of chloroform/methanol (2:1). The homogenates were vortexed for 1 min and sonicated for 20 min. This was followed by centrifugation at 1000× *g* for 10 min. The supernatant was washed with 0.2 volume of water, vortexed for 1 min, and centrifuged at 1000× *g* for 5 min. The upper fraction was discarded. The remaining fraction was rinsed with 1 mL of methanol/water (1:1) and centrifuged at 1000× *g* for 5 min. The upper fraction was removed, while the lower chloroform fraction that contained the total lipids was dried with a rotary evaporator. The hepatic total lipid extracts were weighed and then reconstituted in 1 mL of 1% (*w*/*v*) bovine serum albumin and subjected to a triglyceride assay with Randox TR1607 Triglycerides (Randox, Dublin, UK).

2.9. RNA Extraction and cDNA Synthesis

Total RNA of the rWAT was isolated with Tri-RNA reagent (Favorgen, Ping-Tung, Taiwan) followed by the Qiagen RNeasy Mini kit (Qiagen, Hilden, Germany) to clean up the RNA sample, while that of the liver was extracted with Qiagen RNeasy Mini kit directly. The concentration and purity of the RNA were determined by measuring the absorbance at 260 nm and 280 nm with Infinite® 200 PRO (TECAN, Zürich, Switzerland). RNA integrity was examined with agarose gel electrophoresis to check 18 S and 28 S ribosomal RNA. RNase-free DNase I (ThermoFisher Scientific, Waltham, MA, USA) treatment was performed prior to cDNA synthesis, which was performed with the Qiagen Omniscript Reverse Transcription Kit (Qiagen, Hilden, Germany).

2.10. Quantitative PCR (qPCR)

Rotor-Gene Q (Qiagen, Hilden, Germany) was used to perform SYBR green-based qPCR of receptor for advanced glycation end product (RAGE), soluble RAGE (sRAGE) peroxisome proliferator-activated receptors (PPARs) α and γ in the liver and rWAT. Hypoxanthine phosphoribosyltransferase 1 (HPRT1),

succinate dehydrogenase complex flavoprotein subunit A (SDHA), and β-actin (BAC), which demonstrate stable expression in the target tissues, were selected as the endogenous reference genes for normalization of the genes of interest [29]. The nucleotide sequences of the forward and reverse primers as well as the accession numbers are outlined in Table 2. PCR conditions are shown in Table S1. Normalized Ct/ΔCt values of the genes of interest were calculated using the following formula:

$$\Delta Ct = \text{average of } Ct_{\textit{reference genes}} - Ct_{\textit{gene of interest}} \quad (1)$$

Table 2. Accession numbers, forward and reverse primers of the endogenous reference, and target genes as well as amplicon size of the PCR products.

Target Gene	Accession Number	Nucleotide Sequence (5′→3′)		Amplicon Size (bp)
		Forward Primer	Reverse Primer	
β-actin *	NM_031144	GTA TGG GTC AGA AGG ACT CC	GTT CAA TGG GGT ACT TCA GG	80
HPRT1 *	NM_012583	CTG GAA AGA ACG TCT TGA TTG	GTA TCC AAC ACT TCG AGA GG	146
SDHA *	NM_130428	GGC TTT CAC TTC TCT GTT GG	CCA CAG CAT CAA ACT CAT GG	103
RAGE	NM_053336	CGA GTC TAC CAG ATT CCT GGG	TCA CAA CTG TCC CTT TGC CA	175
sRAGE	GUI164719	CAA TGT CCC CTG CCT CCA GA	TCA TCC TCA TGC CCT ACC TCA	200
PPARα	NM_013196	TGT GGA GAT CGG CCT GGC CTT	CCG GAT GGT TGC TCT GCA GGT	100
PPARγ	NM_013124	CCC TGG CAA AGC ATT TGT AT	GGT GAT TTG TCT GTT GTC TTT CC	100

* Endogenous reference genes; HPRT1: Hypoxanthine phosphoribosyltransferase 1; PPAR: peroxisome proliferator-activated receptor; RAGE: receptor for advanced glycation end product; SDHA: succinate dehydrogenase complex flavoprotein subunit A; sRAGE: soluble receptor for advanced glycation end product.

2.11. Statistical Analysis

Statistical analysis was performed with Statistical Package for the Social Sciences (SPSS) 22.0. Dependent variables with repeated measures such as the cumulative weight gain, food and calorie intake, blood pressure and pre- and post-treatment OGTT were analyzed with a mixed model ANOVA using "time" as the within-subjects factor and "treatment group" as the between-subjects factor. The pairwise comparisons were performed with Bonferroni correction. Other variables were analyzed with one-way ANOVA followed by Tukey's test. The level of statistical significance was pre-set at $p \leq 0.05$.

3. Results

3.1. Weight Gain and Adiposity

Figure 2A shows that the consumption of a high-fat diet, compared to the control diet, caused increased weight gain from Week 6 to the end of the experiment, while the TRF did not improve the weight control. The food intake of high-fat-diet- and TRF-treated rats was lower than that of the control diet group (Figure 2B). This was to compensate for the higher energy content of the high-fat diet, which explains the comparable calorie intake between all groups (Figure 2C).

High-fat diet increased the area of visceral adipocytes by more than 28%—a condition known as adipocyte hypertrophy (Figure 2D,E). Even though the TRF seems to reduce the adipocyte size, the difference did not reach statistical significance. The treatment also did not reduce the rWAT depot, which was otherwise increased by high-fat feeding by about 42% (Figure 2F). As such, high-fat diet led to the onset of central obesity and visceral adiposity, while treatment with the TRF has a limited effect on the condition.

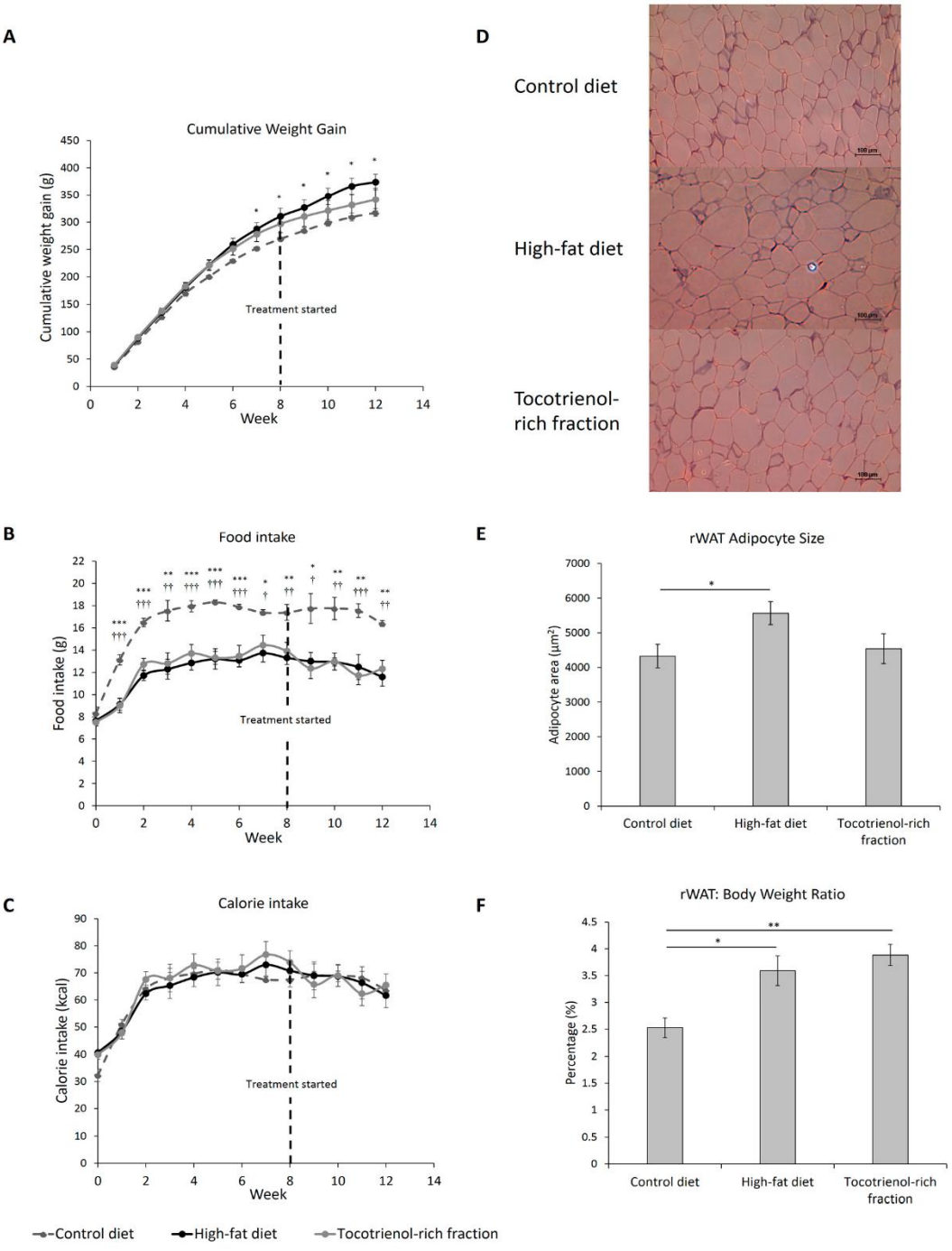

Figure 2. Cumulative weight gain (**A**), food intake (**B**), and calorie intake (**C**) of the rats assigned to different treatment groups. A tocotrienol-rich fraction was administered after 8 weeks of high-fat feeding, as indicated by the black dotted line. The representative images of the H&E-stained retroperitoneal white adipose tissues (×100 magnification) of each group are shown (**D**) and the average adipocyte areas are illustrated in bar plot (**E**). Retroperitoneal white adipose tissue weight-to-body weight ratio (**F**) was measured and expressed in percentage. Error bars indicate SEM. Sample size was $n = 7$ per group. For Figure 2A–C, *, **, *** Indicate $p < 0.05$, 0.01, 0.001 between control and high-fat diet groups; †, ††, ††† Indicate $p < 0.05$, 0.01, 0.001 between control diet and tocotrienol-rich fraction groups. For Figure 2E,F, * Indicates $p < 0.05$ and ** Indicates $p < 0.01$ between groups. rWAT: retroperitoneal white adipose tissue.

3.2. Blood Pressure and Electrolyte

Aside from central obesity, high-fat feeding caused a significant increase in systolic blood pressure compared to the control diet from Week 4 onwards (Figure 3A). The diastolic blood pressure followed a similar trend (Figure 3B). The hypertension was linked to increased fluid retention as indicated by the high-fat-diet-induced hypernatremia (158.74 ± 3.64 mEq/L vs. 126.73 ± 6.58 mEq/L) (Figure 3C). Interestingly, the TRF lowered the systolic and diastolic blood pressure gradually over four weeks. The difference in blood pressure between high-fat-diet- and TRF-treated groups became significantly different two weeks into treatment. Such an antihypertensive effect of the TRF seems to be independent from the water reabsorption mechanism as the elevated sodium level was not improved. Previous studies have suggested that the blood pressure-lowering effect may be linked to vitamin E-induced vasodilation [17,30]. The potassium level was not affected by the diets or the TRF (Figure 3D).

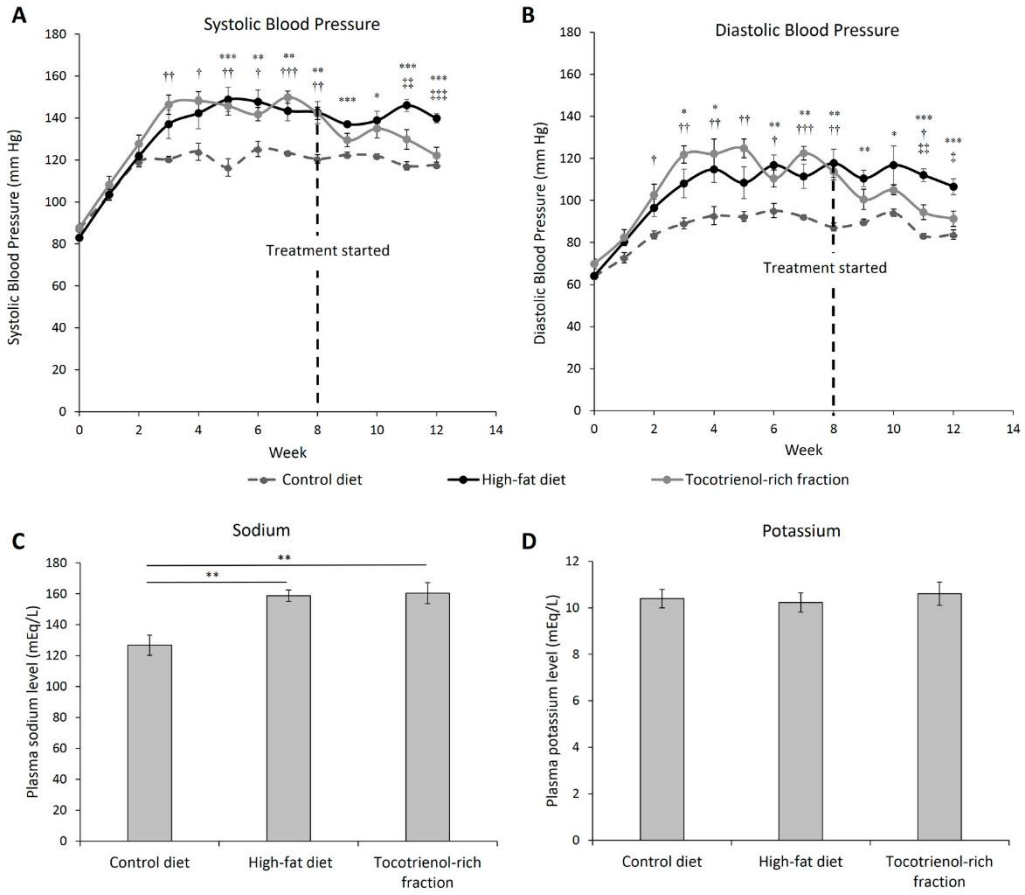

Figure 3. Systolic (**A**) and diastolic (**B**) blood pressure of the rats assigned to different treatment groups throughout 12 weeks. A tocotrienol-rich fraction was administered after 8 weeks of high-fat feeding as indicated by the black dotted line. Plasma sodium (**C**) and potassium (**D**) levels at the end of treatment was measured. Error bars indicate SEM. The sample size was $n = 7$ per group. For Figure 3A,B, *, **, *** Indicate $p < 0.05$, 0.01, 0.001 between and control and high-fat diet groups; †, ††, ††† Indicate $p < 0.05$, 0.01, 0.001 between the control diet and tocotrienol-rich fraction groups; ‡, ‡‡, ‡‡‡ Indicate $p < 0.05$, 0.01, 0.001 between the high-fat diet and tocotrienol-rich fraction groups. For Figure 3C, ** Indicates $p < 0.01$ between groups.

3.3. Glycemic Parameters and OGTT

Based on Table 3, high-fat consumption induced polydipsia, increased fasting blood glucose, and impaired β-cell function in addition to the impaired glucose tolerance, as shown in Figure 4A,B. These are the typical symptoms of diabetes mellitus. Treatment with the TRF failed to improve these abnormalities, suggesting that the fraction has minimal impact on glucose homeostasis.

Table 3. Food and water intake, organ weight, and glycemic indices of the rats given the control diet, the high-fat diet, and the TRF at the end of the eight-week treatment.

Parameters	Treatment Group		
	Control Diet	High-Fat Diet	Tocotrienol-Rich Fraction
Water intake (mL/day)	18.97 ± 1.07	25.14 ± 1.35 **	21.46 ± 0.99
Liver-to-body weight ratio (%)	3.35 ± 0.05	3.72 ± 0.13	3.71 ± 0.16
Kidney-to-body weight ratio (%)	0.73 ± 0.02	0.74 ± 0.01	0.73 ± 0.02
FBG (mmol/L)	5.51 ± 0.15	6.50 ± 0.14 **	6.27 ± 0.17 **
FPI (mU/L)	28.23 ± 2.27	25.54 ± 2.13	24.84 ± 1.74
HOMA%β (%)	100.00 ± 7.51	67.71 ± 5.89 **	71.11 ± 5.42 *
HOMA%S (%)	100.00 ± 6.61	106.32 ± 8.10	109.52 ± 6.88

Values are expressed as mean ± SEM; AUC: area under curve; FBG: fasting blood glucose; FPI: fasting plasma insulin; HOMA%S: homeostasis model assessment of insulin sensitivity; HOMA%β: homeostasis model assessment of β-cell function. * $p < 0.05$ and ** $p < 0.01$ compared to the control diet.

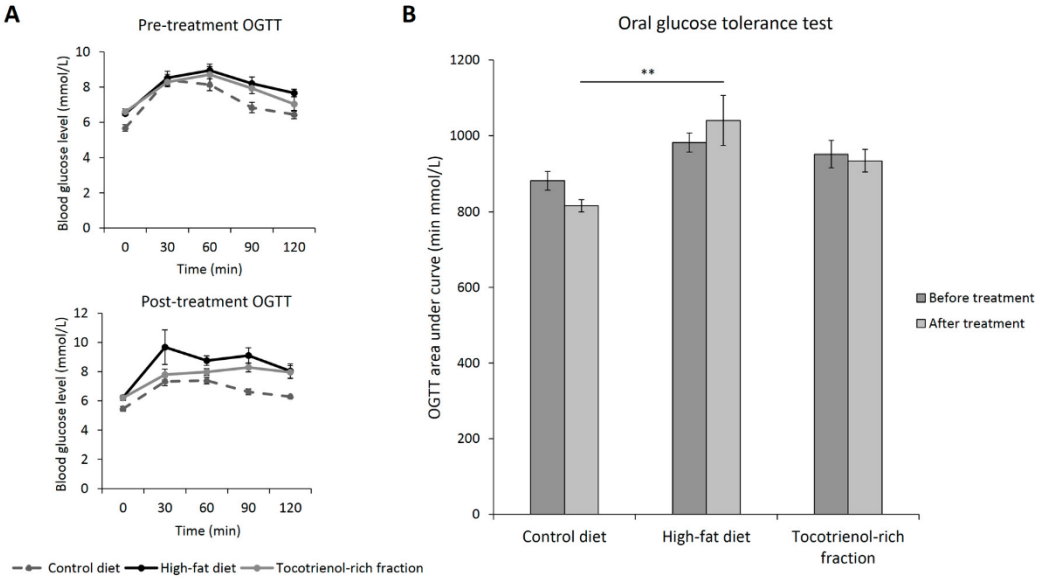

Figure 4. Oral glucose tolerance test before (Week 8) and after (Week 12) treatment (**A**). The AUCs are expressed in bar plot (**B**). Error bars indicate SEM. The sample size was $n = 7$ per group. ** Indicates $p < 0.01$ between groups. OGTT: oral glucose tolerance test.

3.4. Oxidative Stress Markers and AGE-RAGE Axis

Given that tocotrienols are strong antioxidants, we also examined the several oxidative stress biomarkers at the end of the experiment. It was revealed that the TRF was able to recover the plasma antioxidant capacity, which was otherwise crippled by the high-fat feeding by about 17% (Figure 5A). Furthermore, the activity of myeloperoxidase, a peroxidase enzyme that can promote oxidative stress, was elevated by more than twofold upon high-fat consumption. Such an exaggerated activation of myeloperoxidase was abolished with the treatment of the TRF (Figure 5B), which is in line with the plasma antioxidant capacity assay.

The TRF also successfully reduced protein glycation, as evidenced by the lowering effect on HbA1c (Figure 5C) and circulating AGE (Figure 5D). Although non-enzymatic glycation is a glucose-dependent process, the anti-glycative effect of the TRF seems to be glucose-independent because the treatment did not have a noticeable effect on glucose metabolism. It is postulated that the effect may be attributable to its antioxidant activity, as high oxidative stress could have otherwise promoted the formation of glycation products.

Additionally, considering such a drastic escalation of the circulating AGE level upon high-fat feeding and the AGE-lowering effect of the TRF, we endeavored to determine whether or not these changes modified the expression of RAGE in the liver and rWAT. Expectedly, hepatic RAGE expression was significantly upregulated 2.4-fold in the high-fat diet group. RAGE overexpression was nullified by the treatment with TRF, which is in concordance to the circulating AGE level (Figure 6A). RAGE expression in the rWAT was unaffected by the types of diet and the TRF (Figure 6C).

Apart from that, high-fat consumption also suppressed the expression of sRAGE in the rWAT 2.3-fold, which might lead to lower circulating sRAGE and consequently increased AGE accumulation. The TRF did not improve the downregulation of sRAGE (Figure 6D). On the other hand, neither the diets nor the TRF modified sRAGE expression in the liver (Figure 6B). The differential RAGE and sRAGE expression patterns between the liver and rWAT are indicative of a certain extent of tissue specificity in the expression of RAGE and its spliced variants.

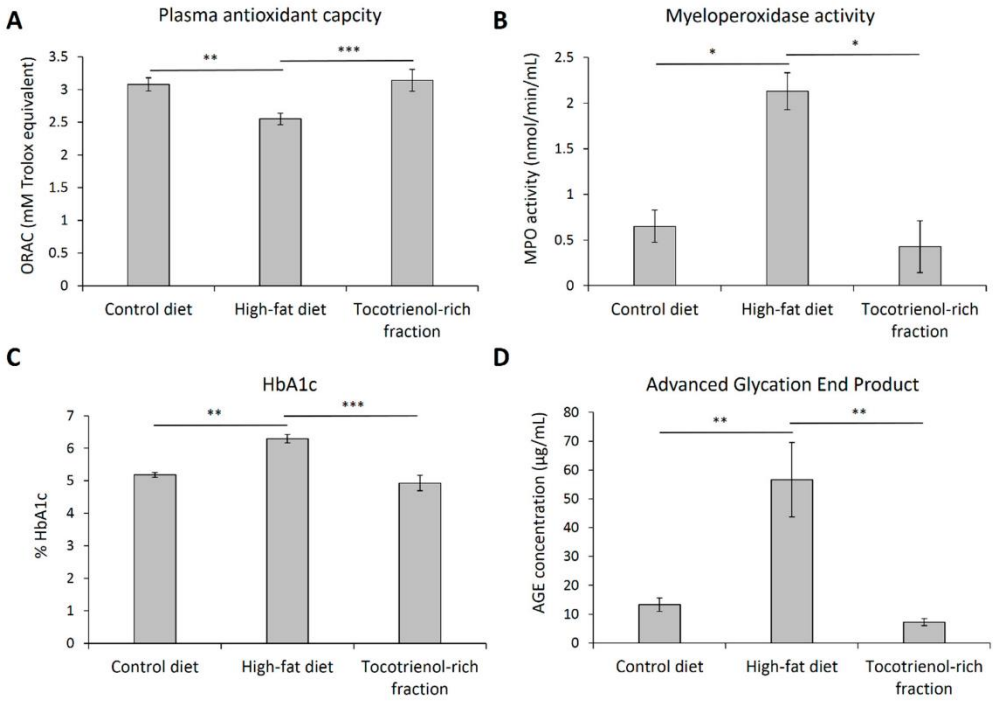

Figure 5. Total plasma antioxidant capacity (**A**), myeloperoxidase activity (**B**), glycated hemoglobin A1c (**C**), and advanced glycation end product (**D**) of the rats assigned to different treatment groups at the end of treatment. Error bars indicate SEM. The sample size was $n = 7$ per group. * Indicates $p < 0.05$, ** Indicates $p < 0.01$, and *** Indicates $p < 0.001$ between groups. AGE: advanced glycation end product; HbA1c: glycated hemoglobin A1c; MPO: myeloperoxidase; ORAC: oxygen radical absorbance capacity.

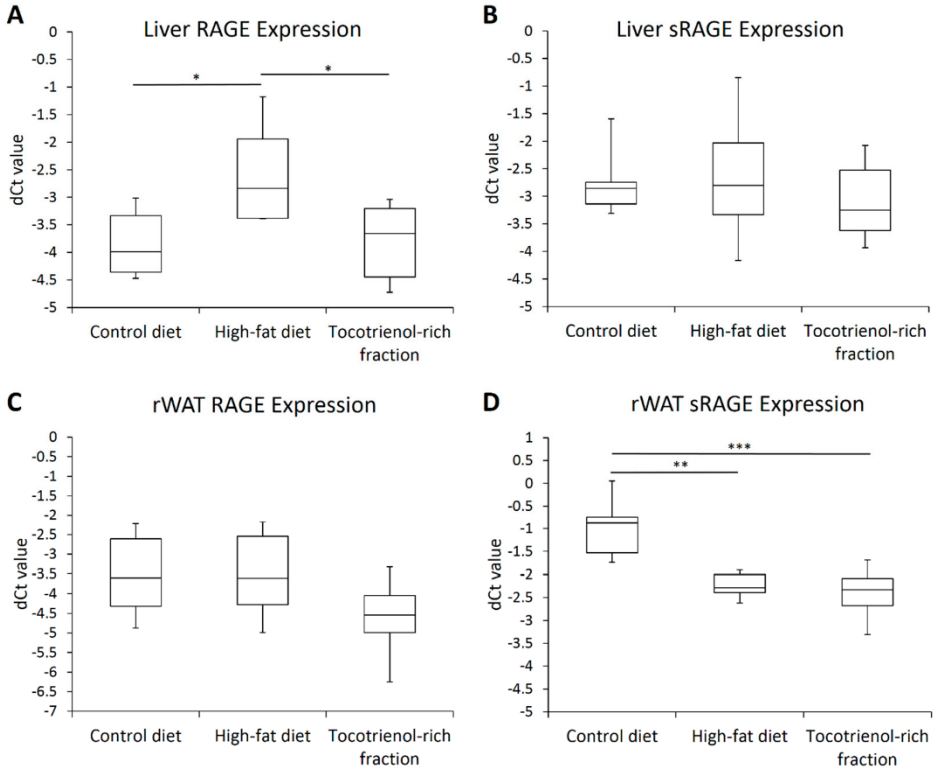

Figure 6. Box-and-whisker plots of normalized Ct values (dCt) of RAGE and sRAGE in the liver (**A**,**B**) as well as retroperitoneal adipose tissue (**C**,**D**) of the rats assigned to different treatment groups. Hypoxanthine phosphoribosyltransferase 1 (HPRT1), succinate dehydrogenase complex flavoprotein subunit A (SDHA), and β-actin (BAC) were used as the endogenous reference genes. Sample size was $n = 7$ per group. * Indicates $p < 0.05$, ** Indicates $p < 0.01$, and *** Indicates $p < 0.001$ between groups. RAGE: receptor for advanced glycation end product; sRAGE: soluble receptor for glycation end product; rWAT: retroperitoneal white adipose tissue.

3.5. Lipid Profile, Hepatic Steatosis, and PPAR Expression

Treatment with the TRF also reversed the high-fat-diet-induced hypercholesterolemia (Figure 7A). The total cholesterol and non HDL-cholesterol levels were reduced by the TRF by 19% and 29% respectively after the four-week treatment. However, the circulating triglyceride level remained elevated despite the administration of the TRF, indicating that the treatment is more specific on the cholesterol metabolism. Additionally, consumption of high-fat diet also triggered increased ectopic fat deposition in the liver (Figure 7B). Compared high-fat-diet-treated rats to those on control diet, the liver total lipids increased 3.6-fold from 0.08 ± 0.01 mg/mg liver to 0.28 ± 0.02 mg/mg liver whereas the hepatic triglycerides deposition also escalated from 7.02 ± 0.43 μmol/g liver to 12.63 ± 1.10 μmol/g liver. Treatment with the TRF did not lead to significant reduction of the total lipids (0.23 ± 0.01 mg/mg liver; $p = 0.063$), but did significantly reduce the triglycerides deposition to 8.92 ± 0.84 μmol/g liver (Figure 7C,D).

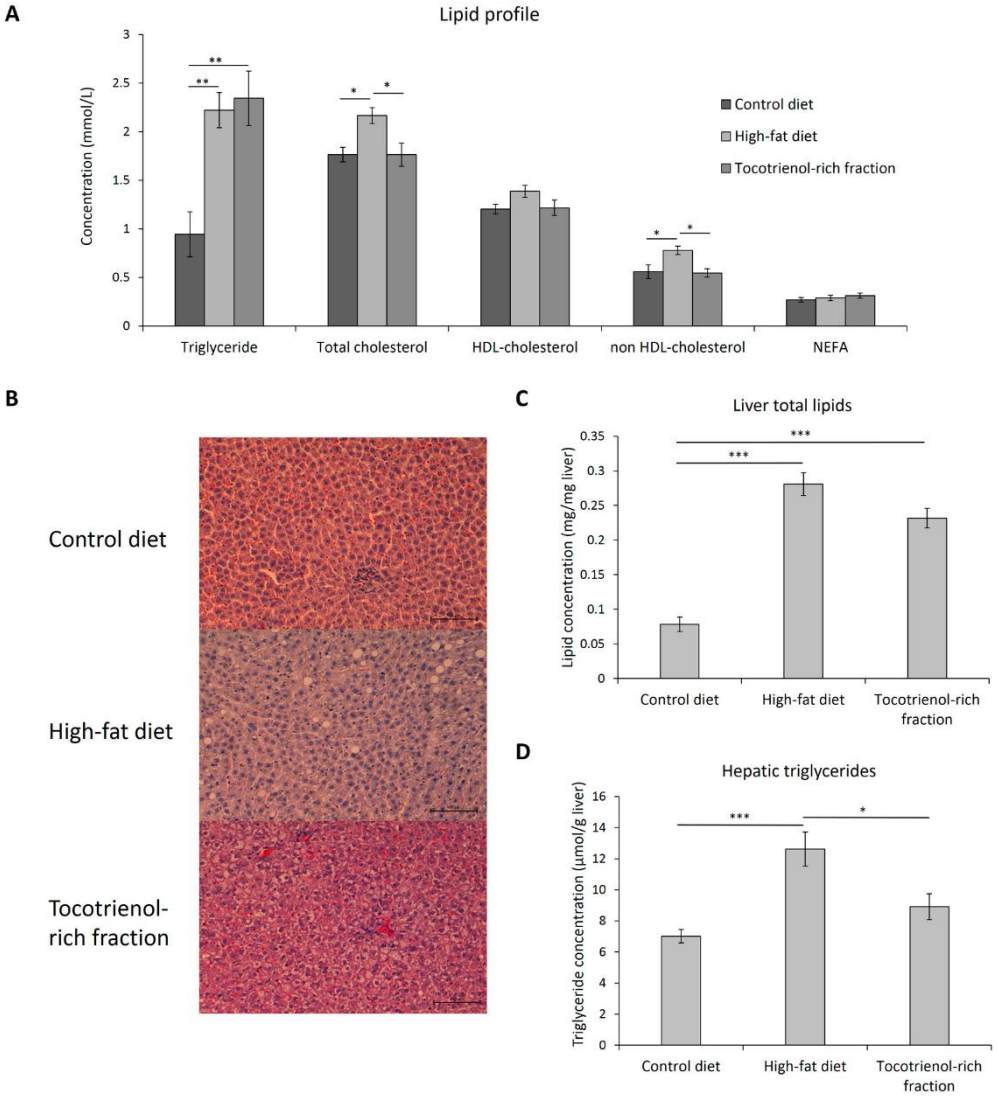

Figure 7. Lipid profile (**A**), including triglycerides, total cholesterol, HDL-cholesterol, non HDL-cholesterol and non-esterified free fatty acid levels of the rats assigned to different treatment groups at the end of treatment. The representative images of the H&E-stained liver tissue (x200 magnification) of each group are shown (**B**). The total lipids (**C**) and triglycerides (**D**) concentrations in the liver were quantified and illustrated in bar plots. Error bars indicate SEM. The sample size was $n = 7$ per group. * Indicates $p < 0.05$, ** Indicates $p < 0.01$ and *** Indicates $p < 0.001$ between groups. HDL, high density lipoprotein; NEFA, non-esterified fatty acid.

The results showed that the TRF has inhibitory effects on the lipid dysregulation. Since PPARs are the key regulators of lipid metabolism and adipogenesis, we also looked into the expression of PPARα and γ in our attempt to outline the underlying mechanism of the TRF. Basically, high-fat feeding suppressed the expression of PPARα in both the liver and rWAT 3.1- and 2.3-fold, respectively (Figure 8A,C). Transcriptional suppression of PPARα was not reversed by the TRF. The expression of PPARγ was unremarkable (Figure 8B,D).

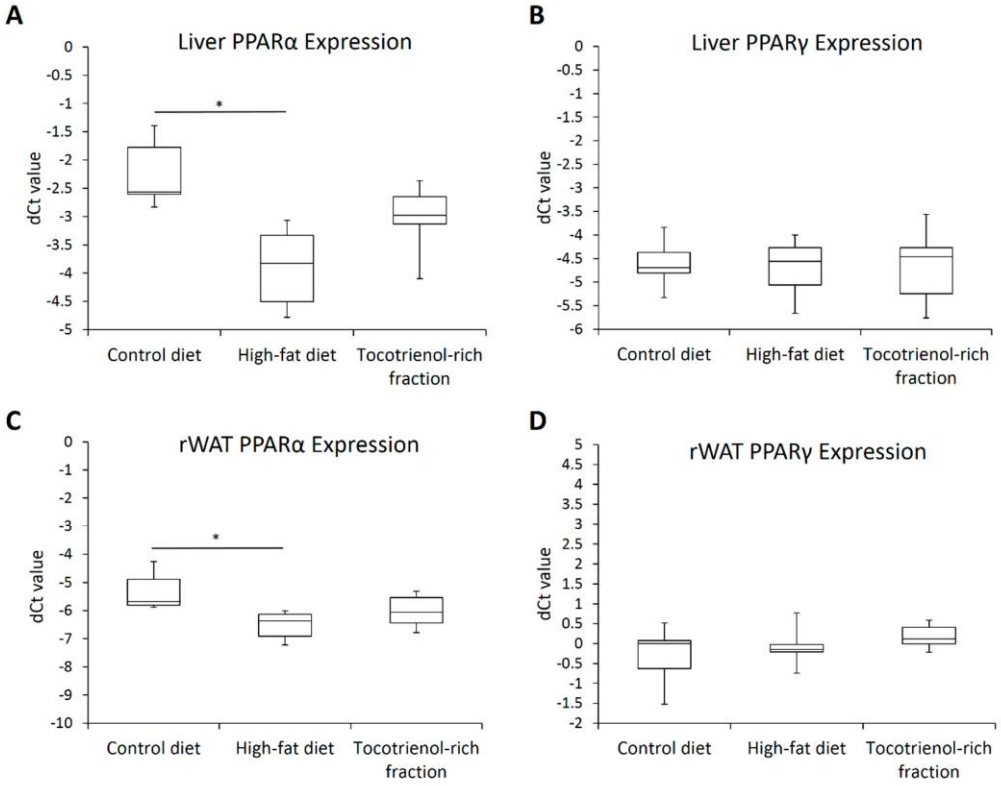

Figure 8. Box-and-whisker plots of normalized Ct values (dCt) of PPARα and PPARγ in the liver (**A**,**B**) as well as retroperitoneal adipose tissue (**C**,**D**) of the rats assigned to different treatment groups. Hypoxanthine phosphoribosyltransferase 1 (HPRT1), succinate dehydrogenase complex flavoprotein subunit A (SDHA), and β-actin (BAC) were used as the endogenous reference genes. Sample size was $n = 7$ per group. * Indicates $p < 0.05$ between groups. PPAR: peroxisome proliferator-activated receptor; rWAT: retroperitoneal white adipose tissue.

4. Discussion

In the present study, we demonstrated that a TRF can confer multiple beneficial effects on the rats on high-fat diet. After a four-week treatment of the fraction via oral administration at a daily dosage of 60 mg/kg, the rats showed significant improvements in terms of the blood pressure, cholesterol profile, ectopic fat deposition at the liver, and oxidative stress-related markers. Despite the unremarkable effect on glycemic control and central obesity, such multifunctionality of a TRF against metabolic syndrome still makes it an interesting candidate for further investigation and potential clinical use.

Our results pointed out that a TRF possesses remarkable antihypertensive activity. This is consistent with previous animal [17] and clinical studies [31]. Nevertheless, the effect is not exclusive to tocotrienol, but is a common property of vitamin E as evidenced by the comparable hypotensive effect of both α-tocopherol and α-tocopherol-tocotrienol mixture [17,32]. In this study, the diet-induced hypertension was linked to hypernatremia. This is in line with a previous study that indicated that a high-fat diet can promote sodium and water retention [33]. However, the TRF failed to reverse the elevated sodium level, implying that the antihypertensive effect is independent of the water and sodium reabsorption pathway. In fact, as the blood pressure-lowering activity is a shared characteristic between tocotrienols and tocopherols, the underlying mechanism should also be mutual. Previous studies have reported that vitamin E can alleviate vascular oxidative stress and stimulate the aortic biosynthesis of prostacyclin,

which has in turn resulted in vasodilation [17,30,34]. Thus, it is postulated that the antihypertensive effect of vitamin E is attributable to antioxidant-dependent vasodilation.

Although several studies have reported the glucose-lowering effect of tocotrienol [13,14,35,36], such an effect was not noticeable in the present study. It is worth mentioning that most of the aforementioned studies employed streptozotocin-induced diabetic rats whose hyperglycemia induction is dependent on the toxicity effect of streptozotocin on pancreatic β-cells. Tocotrienols have been shown to confer localized ameliorative effect on streptozotocin-induced cellular damage at the cerebral tissues by alleviating oxidative-nitrosative stress [37]. Furthermore, many studies that have reported the antihyperglycemic effect have either used tocotrienols pre-treatment prior to [35] or considerably fast treatment (~3 days) following [14–16] a streptozotocin challenge. This means that tocotrienols were introduced while the β-cells destruction caused by streptozotocin was still ongoing. In this context, tocotrienols are capable of reducing oxidative DNA damage [13,38,39]. Speculatively, this may protect the pancreatic β-cells from the insult of streptozotocin, which may in turn lead to a favorable glycemic profile. This may explain why we failed to detect improved glycemic control upon treatment with the TRF because extensive eradication of pancreatic β-cells, as is induced by streptozotocin, is uncommon in metabolic syndrome. Nonetheless, to our best knowledge, no clinical studies have demonstrated the glucose-lowering effect of tocotrienols in diabetic patients; hence, further investigation on this aspect is warranted. Future studies using streptozotocin-induced diabetic models should also evaluate the possible anti-streptozotocin activity of tocotrienols to eliminate the interference from the actual glucose-lowering effect.

As a powerful lipophilic antioxidant, treatment with the TRF also restored the total plasma antioxidant capacity in addition to abolishing myeloperoxidase hyperactivity. These findings show that the TRF could alleviate the oxidative stress in the systemic level [15,16]. Given that myeloperoxidase is highly implicated in atherogenesis [40,41], supplementation with a TRF could therefore prevent the development of atherosclerosis [42,43]. Additionally, a TRF also possesses anti-glycative activity, as has been shown by the reduction of HbA1c and AGE [35]. Although non-enzymatic glycation is thought to be a glucose-dependent process, it has long been known that increased oxidative stress could accelerate non-enzymatic glycation and promote the accumulation of glycated proteins and AGE precursors [44]. In the present study, the failure to reverse glycemic control and sRAGE expression points out that the TRF did not act on the glucose-dependent processes in the protein glycation as well as AGE detoxification, respectively. Therefore, such an anti-glycative activity of the fraction should be antioxidant-dependent [45]. Apart from that, we also demonstrated, for the first time, that the TRF could inhibit diet-induced transcriptional activation of RAGE in the liver. Such an AGE-RAGE inhibitory effect is complementary to its modulatory effect on the nuclear factor κB signaling cascade and certain proinflammatory cytokines [46]. Thus, the use of a TRF could potentially alleviate the proinflammatory response and potentiate the effects of other therapeutic agents in the treatment of metabolic syndrome and diabetes mellitus.

Next, treatment with the TRF also reversed the high-fat-diet-induced hypercholesterolemia by lowering total cholesterol and non-HDL cholesterol levels, which is in line with several clinical trials [19–21]. The cholesterol-lowering effect is due to the inhibitory effect of tocotrienols on β-hydroxy-β-methylglutaryl coenzyme A (HMG-CoA) reductase [7,47]. The normalized cholesterol profile also brought about significant improvement to hepatic steatosis. To date, the evidence for the hepato-protective effect of tocotrienols against diet-induced fatty liver is still limited. Two studies have been conducted using high-calorie diet-fed rats and hypercholesterolemic patients, respectively [36,48], both of which revealed a favorable effect of the TRF on hepatic lipid deposition. Mechanistically, high-fat feeding triggers the overexpression and hyperactivity of sterol regulatory element binding protein (SREBP)-2 and HMG-CoA reductase in the liver [49]. These abnormalities are effectively abolished by tocotrienols and thus contribute to hepato-protective activity [47,50].

Furthermore, high-fat feeding induced the transcriptional repression of PPARα in the liver and rWAT, which could also promote ectopic fat deposition because of the key regulatory roles of

PPARα in fatty acid β-oxidation [51]. The effect of the TRF on PPARα expression was unremarkable. Likewise, there was no change in the expression of hepatic and rWAT PPARγ. This points out that the ameliorative effects of the TRF on abnormal cholesterol profile and hepatic steatosis were PPAR-independent. In this case, even though the PPAR agonistic activity of tocotrienols has been demonstrated, it is established primarily through cell culture studies [43,52]. When the muscle tissues of TRF-treated mice were examined, there was no noticeable change in the expression of PPARs [52]. Together with the lack of PPAR activation in the liver and rWAT, in which PPARs are highly expressed, it is believed that in vivo PPAR agonistic activity of tocotrienols is marginal.

Lastly, our study was limited by the use of a TRF that contains 23.5% (*w*/*w*) of α-tocopherol. Therefore, possible interaction of the α-tocopherol cannot be excluded. Furthermore, we were also unable to differentiate the individual bioactivities of the four tocotrienol subtypes. With regard to the inhibition of HMG-CoA reductase, γ-tocotrienol is 30 times more effective than α- and δ-tocotrienols [53]. This signifies possible differences in the biological functionality of different tocotrienol isomers [54]. Nonetheless, this study, in general, is concordant with most clinical findings on diabetic and hypercholesterolemic patients [19,21] that show that tocotrienols have potent inhibitory effects on hypertension, hypercholesterolemia, and elevated oxidative stress, but have marginal effects on weight control and glucose metabolism. These beneficial effects support further study and the possible clinical use of a TRF as therapy for metabolic syndrome.

5. Conclusions

In conclusion, treatment with a TRF from palm oil for four weeks in rats with metabolic syndrome showed significant improvements in blood pressure, cholesterol profile, and systemic antioxidant defense in addition to a reduction in hepatic steatosis, proatherogenic markers such as myeloperoxidase, and proinflammatory markers such as advanced glycation end products. It was also demonstrated for the first time that a TRF can confer an inhibitory effect on RAGE transcriptional activation. Unlike as reported in previous studies, the treatment had minimal impact on glucose metabolism, PPAR expression, hypertriglyceridemia, and visceral adiposity. Further investigation on these aspects is warranted. As such, in light of the beneficial effects on cardiovascular health, lipid metabolism, redox balance, and anti-inflammation, a TRF is undoubtedly a promising candidate for metabolic syndrome therapy.

Supplementary Materials: The following are available online at www.mdpi.com/2072-6643/9/9/984/s1: Table S1: Quantitative PCR condition of the endogenous reference and target genes.

Acknowledgments: The work was funded by the Ministry of Science, Technology and Innovation, Malaysia (MOSTI grant: 02-02-10-SF0249) and an internal grant from the School of Science, Monash University Malaysia. We would like to express our deepest gratitude to Andrew Leong Kum Loong and Zulkhaili Zainal Abidin for their assistance in animal handling.

Author Contributions: Khalid Abdul Kadir and Ton So Ha designed the experiment. Cheng Hong Sheng performed the experiment and collected the data. Cheng Hong Sheng and Joash Tan Ban Lee analyzed the data. All authors took part in the manuscript preparation.

Conflicts of Interest: The authors declare no conflict of interest.

References

1. Pryor, W.A. Vitamin E and heart disease. *Free Radic. Biol. Med.* **2000**, *28*, 141–164. [CrossRef]
2. Ricciarelli, R.; Argellati, F.; Pronzato, M.A.; Domenicotti, C. Vitamin E and neurodegenerative diseases. *Mol. Aspects Med.* **2007**, *28*, 591–606. [CrossRef] [PubMed]
3. Jiang, Q. Natural forms of vitamin E: Metabolism, antioxidant, and anti-inflammatory activities and their role in disease prevention and therapy. *Free Radic. Biol. Med.* **2014**, *72*, 76–90. [CrossRef] [PubMed]
4. Müller, L.; Theile, K.; Böhm, V. In vitro antioxidant activity of tocopherols and tocotrienols and comparison of vitamin E concentration and lipophilic antioxidant capacity in human plasma. *Mol. Nutr. Food Res.* **2010**, *54*, 731–742. [CrossRef] [PubMed]

5. Gould, M.N.; Haag, J.D.; Kennan, W.S.; Tanner, M.A.; Elson, C.E. A comparison of tocopherol and tocotrienol for the chemoprevention of chemically induced rat mammary tumors. *Am. J. Clin. Nutr.* **1991**, *53*, 1068S–1070S. [PubMed]
6. Nesaretnam, K.; Meganathan, P.; Veerasenan, S.D.; Selvaduray, K.R. Tocotrienols and breast cancer: The evidence to date. *Genes Nutr.* **2012**, *7*, 3–9. [CrossRef] [PubMed]
7. Parker, R.A.; Pearce, B.C.; Clark, R.W.; Gordon, D.A.; Wright, J.J. Tocotrienols regulate cholesterol production in mammalian cells by post-transcriptional suppression of 3-hydroxy-3-methylglutaryl-coenzyme A reductase. *J. Biol. Chem.* **1993**, *268*, 11230–11238. [PubMed]
8. Khanna, S.; Roy, S.; Parinandi, N.L.; Maurer, M.; Sen, C.K. Characterization of the potent neuroprotective properties of the natural vitamin E α-tocotrienol. *J. Neurochem.* **2006**, *98*, 1474–1486. [CrossRef] [PubMed]
9. Adachi, H.; Ishii, N. Effects of tocotrienols on life span and protein carbonylation in Caenorhabditis elegans. *J. Gerontol. A Biol. Sci. Med. Sci.* **2000**, *55*, B280–B285. [CrossRef] [PubMed]
10. Sen, C.K.; Khanna, S.; Rink, C.; Roy, S. Tocotrienols: The emerging face of natural vitamin E. *Vitam. Horm.* **2007**, *76*, 203–261. [PubMed]
11. Aggarwal, B.B.; Sundaram, C.; Prasad, S.; Kannappan, R. Tocotrienols, the vitamin E of the 21st century: Its potential against cancer and other chronic diseases. *Biochem. Pharmacol.* **2010**, *80*, 1613–1631. [CrossRef] [PubMed]
12. Ahsan, H.; Ahad, A.; Iqbal, J.; Siddiqui, W.A. Pharmacological potential of tocotrienols: A review. *Nutr. Metab.* **2014**, *11*, 52. [CrossRef] [PubMed]
13. Budin, S.B.; Othman, F.; Louis, S.R.; Bakar, M.A.; Das, S.; Mohamed, J. The effects of palm oil tocotrienol-rich fraction supplementation on biochemical parameters, oxidative stress and the vascular wall of streptozotocin-induced diabetic rats. *Clinics* **2009**, *64*, 235–244. [CrossRef] [PubMed]
14. Siddiqui, S.; Rashid Khan, M.; Siddiqui, W.A. Comparative hypoglycemic and nephroprotective effects of tocotrienol rich fraction (TRF) from palm oil and rice bran oil against hyperglycemia induced nephropathy in type 1 diabetic rats. *Chem. Biol. Interact.* **2010**, *188*, 651–658. [CrossRef] [PubMed]
15. Siti Balkis, B.; Khairunnisa' Md, Y.; Muhd Hanis, M.I.; Zariyantey Abd, H.; Jamaludin, M. Tocotrienol-rich fraction of palm oil reduced pancreatic damage and oxidative stress in streptozotocin-induced diabetic rats. *Aust. J. Basic Appl. Sci.* **2011**, *5*, 2367–2374.
16. Matough, F.A.; Budin, S.B.; Hamid, Z.A.; Abdul Rahman, M.; Al-Wahaibi, N.; Mohammed, J. Tocotrienol-rich fraction from palm oil prevents oxidative damage in diabetic rats. *Sultan Qaboos Univ. Med. J.* **2014**, *14*, e95–e103. [CrossRef] [PubMed]
17. Koba, K.; Abe, K.; Ikeda, I.; Sugano, M. Effects of α-tocopherol and tocotrienols on blood pressure and linoleic acid metabolism in the spontaneously hypertensive rat (SHR). *Biosci. Biotechnol. Biochem.* **1992**, *56*, 1420–1423. [CrossRef] [PubMed]
18. Vafa, M.; Haghighat, N.; Moslehi, N.; Eghtesadi, S.; Heydari, I. Tocotrienols enriched canola oil can improve glycemic control and oxidative status of patients with type 2 diabetes mellitus: A randomized, double-blind, placebo-controlled trial. *J. Res. Med. Sci.* **2015**, *20*, 540–547. [CrossRef] [PubMed]
19. Qureshi, A.A.; Sami, S.A.; Salser, W.A.; Khan, F.A. Dose-dependent suppression of serum cholesterol by tocotrienol-rich fraction (TRF25) of rice bran in hypercholesterolemic humans. *Atherosclerosis* **2002**, *161*, 199–207. [CrossRef]
20. Chin, S.-F.; Ibahim, J.; Makpol, S.; Abdul Hamid, N.A.; Abdul Latiff, A.; Zakaria, Z.; Mazlan, M.; Mohd Yusof, Y.A.; Abdul Karim, A.; Wan Ngah, W.Z. Tocotrienol rich fraction supplementation improved lipid profile and oxidative status in healthy older adults: A randomized controlled study. *Nutr. Metab.* **2011**, *8*, 42. [CrossRef] [PubMed]
21. Baliarsingh, S.; Beg, Z.H.; Ahmad, J. The therapeutic impacts of tocotrienols in type 2 diabetic patients with hyperlipidemia. *Atherosclerosis* **2005**, *182*, 367–374. [CrossRef] [PubMed]
22. Cicero, A.F.; Rosticci, M.; Parini, A.; Morbini, M.; Urso, R.; Grandi, E.; Borghi, C. Short-term effects of a combined nutraceutical of insulin-sensitivity, lipid level and indexes of liver steatosis: A double-blind, randomized, cross-over clinical trial. *Nutr. J.* **2015**, *14*, 30. [CrossRef] [PubMed]
23. Reeves, P.G. Components of the AIN-93 diets as improvements in the AIN-76A diet. *J. Nutr.* **1997**, *127*, 838S–841S. [PubMed]

24. Ahmad, N.S.; Khalid, B.A.K.; Luke, D.A.; Ima Nirwana, S. Tocotrienol offers better protection than tocopherol from free radical-induced damage of rat bone. *Clin. Exp. Pharmacol. Physiol.* **2005**, *32*, 761–770. [CrossRef] [PubMed]
25. Hoggatt, A.F.; Hoggatt, J.; Honerlaw, M.; Pelus, L.M. A spoonful of sugar helps the medicine go down: A novel technique to improve oral gavage in mice. *J. Am. Assoc. Lab. Anim. Sci.* **2010**, *49*, 329–334. [PubMed]
26. Levy, J.C.; Matthews, D.R.; Hermans, M.P. Correct homeostasis model assessment (HOMA) evaluation uses the computer program. *Diabetes Care* **1998**, *21*, 2191–2192. [CrossRef] [PubMed]
27. Parlee, S.D.; Lentz, S.I.; Mori, H.; MacDougald, O.A. Quantifying size and number of adipocytes in adipose tissue. *Methods Enzymol.* **2014**, *537*, 93–122. [PubMed]
28. Folch, J.; Lees, M.; Stanley, G.H.S. A simple method for the isolation and purification of total lipides from animal tissues. *J. Biol. Chem.* **1957**, *226*, 497–509. [PubMed]
29. Svingen, T.; Letting, H.; Hadrup, N.; Hass, U.; Vinggaard, A.M. Selection of reference genes for quantitative RT-PCR (RT-qPCR) analysis of rat tissues under physiological and toxicological conditions. *PeerJ* **2015**, *3*, e855. [CrossRef] [PubMed]
30. Muharis, S.P.; Top, A.G.M.; Murugan, D.; Mustafa, M.R. Palm oil tocotrienol fractions restore endothelium dependent relaxation in aortic rings of streptozotocin-induced diabetic and spontaneously hypertensive rats. *Nutr. Res.* **2010**, *30*, 209–216. [CrossRef] [PubMed]
31. Rasool, A.H.G.; Yuen, K.H.; Yusoff, K.; Wong, A.R.; Rahman, A.R.A. Dose dependent elevation of plasma tocotrienol levels and its effect on arterial compliance, plasma total antioxidant status, and lipid profile in healthy humans supplemented with tocotrienol rich vitamin E. *J. Nutr. Sci. Vitaminol. (Tokyo)* **2006**, *52*, 473–478. [CrossRef] [PubMed]
32. Vasdev, S.; Gill, V.; Parai, S.; Longerich, L.; Gadag, V. Dietary vitamin E supplementation lowers blood pressure in spontaneously hypertensive rats. *Mol. Cell. Biochem.* **2002**, *238*, 111–117. [CrossRef] [PubMed]
33. Song, J.; Hu, X.; Shi, M.; Knepper, M.A.; Ecelbarger, C.A. Effects of dietary fat, NaCl, and fructose on renal sodium and water transporter abundances and systemic blood pressure. *Am. J. Physiol. Renal Physiol.* **2004**, *287*, F1204–F1212. [CrossRef] [PubMed]
34. Chen, X.; Touyz, R.M.; Park, J.B.; Schiffrin, E.L. Antioxidant effects of vitamins C and E are associated with altered activation of vascular NADPH oxidase and superoxide dismutase in stroke-prone SHR. *Hypertension* **2001**, *38*, 606–611. [CrossRef] [PubMed]
35. Wan Nazaimoon, W.M.; Khalid, B.A. Tocotrienols-rich diet decreases advanced glycosylation end-products in non-diabetic rats and improves glycemic control in streptozotocin-induced diabetic rats. *Malays. J. Pathol.* **2002**, *24*, 77–82. [PubMed]
36. Wong, W.-Y.; Poudyal, H.; Ward, L.C.; Brown, L. Tocotrienols reverse cardiovascular, metabolic and liver changes in high carbohydrate, high fat diet-fed rats. *Nutrients* **2012**, *4*, 1527. [CrossRef] [PubMed]
37. Tiwari, V.; Kuhad, A.; Bishnoi, M.; Chopra, K. Chronic treatment with tocotrienol, an isoform of vitamin E, prevents intracerebroventricular streptozotocin-induced cognitive impairment and oxidative-nitrosative stress in rats. *Pharmacol. Biochem. Behav.* **2009**, *93*, 183–189. [CrossRef] [PubMed]
38. Chin, S.-F.; Hamid, N.A.A.; Latiff, A.A.; Zakaria, Z.; Mazlan, M.; Yusof, Y.A.M.; Karim, A.A.; Ibahim, J.; Hamid, Z.; Ngah, W.Z.W. Reduction of DNA damage in older healthy adults by Tri E® Tocotrienol supplementation. *Nutrition* **2008**, *24*, 1–10. [CrossRef] [PubMed]
39. Taridi, N.M.; Yahaya, M.F.; Teoh, S.L.; Latiff, A.A.; Ngah, W.Z.W.; Das, S.; Mazlan, M. Tocotrienol rich fraction (TRF) supplementation protects against oxidative DNA damage and improves cognitive functions in Wistar rats. *Clin. Ter.* **2011**, *162*, 93–98. [PubMed]
40. Karakas, M.; Koenig, W. Myeloperoxidase production by macrophage and risk of atherosclerosis. *Curr. Atheroscler. Rep.* **2012**, *14*, 277–283. [CrossRef] [PubMed]
41. Kataoka, Y.; Shao, M.; Wolski, K.; Uno, K.; Puri, R.; Murat Tuzcu, E.; Hazen, S.L.; Nissen, S.E.; Nicholls, S.J. Myeloperoxidase levels predict accelerated progression of coronary atherosclerosis in diabetic patients: Insights from intravascular ultrasound. *Atherosclerosis* **2014**, *232*, 377–383. [CrossRef] [PubMed]
42. Qureshi, A.A.; Salser, W.A.; Parmar, R.; Emeson, E.E. Novel tocotrienols of rice bran inhibit atherosclerotic lesions in C57BL/6 ApoE-deficient mice. *J. Nutr.* **2001**, *131*, 2606–2618. [PubMed]
43. Li, F.; Tan, W.; Kang, Z.; Wong, C.-W. Tocotrienol enriched palm oil prevents atherosclerosis through modulating the activities of peroxisome proliferators-activated receptors. *Atherosclerosis* **2010**, *211*, 278–282. [CrossRef] [PubMed]

44. Baynes, J.W.; Thorpe, S.R. Role of oxidative stress in diabetic complications: A new perspective on an old paradigm. *Diabetes* **1999**, *48*, 1–9. [CrossRef] [PubMed]
45. Jain, S.K.; Palmer, M. The effect of oxygen radicals metabolites and vitamin E on glycosylation of proteins. *Free Radic. Biol. Med.* **1997**, *22*, 593–596. [CrossRef]
46. Kuhad, A.; Chopra, K. Attenuation of diabetic nephropathy by tocotrienol: Involvement of NFkB signaling pathway. *Life Sci.* **2009**, *84*, 296–301. [CrossRef] [PubMed]
47. Khor, H.T.; Chieng, D.Y.; Ong, K.K. Tocotrienols inhibit liver HMG CoA reductase activity in the guinea pig. *Nutr. Res.* **1995**, *15*, 537–544. [CrossRef]
48. Magosso, E.; Ansari, M.A.; Gopalan, Y.; Shuaib, I.L.; Wong, J.-W.; Khan, N.A.K.; Abu Bakar, M.R.; Ng, B.-H.; Yuen, K.-H. Tocotrienols for normalisation of hepatic echogenic response in nonalcoholic fatty liver: A randomised placebo-controlled clinical trial. *Nutr. J.* **2013**, *12*, 166. [CrossRef] [PubMed]
49. Wu, N.; Sarna, L.K.; Hwang, S.-Y.; Zhu, Q.; Wang, P.; Siow, Y.L.; O, K. Activation of 3-hydroxy-3-methylglutaryl coenzyme A (HMG-CoA) reductase during high fat diet feeding. *Biochim. Biophys. Acta* **2013**, *1832*, 1560–1568. [CrossRef] [PubMed]
50. Muto, C.; Yachi, R.; Aoki, Y.; Koike, T.; Igarashi, O.; Kiyose, C. Gamma-tocotrienol reduces the triacylglycerol level in rat primary hepatocytes through regulation of fatty acid metabolism. *J. Clin. Biochem. Nutr.* **2013**, *52*, 32–37. [CrossRef] [PubMed]
51. Kersten, S.; Seydoux, J.; Peters, J.M.; Gonzalez, F.J.; Desvergne, B.; Wahli, W. Peroxisome proliferator–activated receptor α mediates the adaptive response to fasting. *J. Clin. Investig.* **1999**, *103*, 1489–1498. [CrossRef] [PubMed]
52. Fang, F.; Kang, Z.; Wong, C. Vitamin E tocotrienols improve insulin sensitivity through activating peroxisome proliferator-activated receptors. *Mol. Nutr. Food Res.* **2010**, *54*, 345–352. [CrossRef] [PubMed]
53. Pearce, B.C.; Parker, R.A.; Deason, M.E.; Qureshi, A.A.; Wright, J.J.K. Hypocholesterolemic activity of synthetic and natural tocotrienols. *J. Med. Chem.* **1992**, *35*, 3595–3606. [CrossRef] [PubMed]
54. Wong, W.-Y.; Ward, L.C.; Fong, C.W.; Yap, W.N.; Brown, L. Anti-inflammatory γ- and δ-tocotrienols improve cardiovascular, liver and metabolic function in diet-induced obese rats. *Eur. J. Nutr.* **2017**, *56*, 133–150. [CrossRef] [PubMed]

Appendix F: Permission to reuse copyright content

Appendix F1: Permission to reuse content entitled "Ellagitannin geraniin: a review of the natural sources, biosynthesis, pharmacokinetics and biological effects"

SPRINGER NATURE LICENSE
TERMS AND CONDITIONS

May 18, 2018

This Agreement between Cheng Hong Sheng ("You") and Springer Nature ("Springer Nature") consists of your license details and the terms and conditions provided by Springer Nature and Copyright Clearance Center.

License Number	4351870814846
License date	May 18, 2018
Licensed Content Publisher	Springer Nature
Licensed Content Publication	Phytochemistry Reviews
Licensed Content Title	Ellagitannin geraniin: a review of the natural sources, biosynthesis, pharmacokinetics and biological effects
Licensed Content Author	Hong Sheng Cheng, So Ha Ton, Khalid Abdul Kadir
Licensed Content Date	Jan 1, 2016
Licensed Content Volume	16
Licensed Content Issue	1
Type of Use	Thesis/Dissertation
Requestor type	academic/university or research institute
Format	print and electronic
Portion	full article/chapter
Will you be translating?	no
Circulation/distribution	<501
Author of this Springer Nature content	yes
Title	The Metabolic Effects and Mechanism of Action of Ellagitannin Geraniin
Instructor name	Cheng Hong Sheng
Institution name	Monash University Malaysia
Expected presentation date	May 2018
Requestor Location	Cheng Hong Sheng Monash University Malaysia Jalan Lagoon Selatan Bandar Sunway Subang Jaya, Selangor 47500 Malaysia Attn: Cheng Hong Sheng
Billing Type	Invoice
Billing Address	Cheng Hong Sheng Monash University Malaysia Jalan Lagoon Selatan Bandar Sunway Subang Jaya, Malaysia 47500 Attn: Cheng Hong Sheng
Total	0.00 USD

ADDENDUM

Responses to Professor Yeo Chew Chieng's comments

Abstract

1. **Please rephrase the sentence to clarify the statement "Compared to high-fat diet, high-fat-high-sucrose diet performed better among the adult rats but merely caused increased weight gain and hypertension". What is meant by "performed better" in this context?**

   The term "performed better" refers to the efficiency of metabolic syndrome induction by using the diets enriched with different high-caloric macronutrients. To avoid confusion, the sentence has been modified to "*Compared to high-fat diet, high-fat-high-sucrose diet performed better in terms of metabolic syndrome induction among the adult rats but merely caused increased weight gain and hypertension.*"

2. **Add "...genes" to the end of "peroxisome proliferator-activated receptors (PPAR) α and γ..."; likewise in lines 27 and 28, you need to add "...genes" at the end of the italicized names (*RAGE* and *esRAGE*)**

   The word "genes" has been added accordingly at the respective sentences.

3. **Please explain why this particular dosage (25 mg/kg) was chosen. Also, please state how long was the treatment and when the ameliorative effects were observed following treatment.**

   The dosage (25 mg/kg/day) was selected based on a pilot study that used a range of geraniin concentrations from 12.5 to 100 mg/kg/day. We found no increase in the treatment effects based on simple tests like fasting blood glucose, blood pressure and fasting insulin levels beyond a daily dosage of 25 mg/kg and thus, the dosage was chosen for more in-depth investigation of its metabolic effects and underlying mechanisms. The rationale for the selection of dosages used in the study has been outlined in Table 3.1 (page 86). The duration of the oral administration was four weeks. Most of the treatment effects, except for certain measurements like body weight, blood pressure and oral glucose tolerance test, were measured at the end of the experiment. The aforementioned information has been added to the *Abstract* as shown in the following sentences, "*Treatment with geraniin at a daily dosage of 25 mg/kg for four weeks via oral administration (dosage selected based on a pilot study) exhibited remarkable ameliorative effects against multiple metabolic abnormalities. At the end of the four-week treatment, geraniin was found to reduce the*

central adiposity, systolic and diastolic blood pressure, fasting blood glucose, circulating triglycerides and non-HDL cholesterols besides lowering the severity of hepatic steatosis.

Chapter 1

4. **Section 1.1: I would add in a more cautionary phrase, "...particularly in the developed world" as undernutrition, starvation, and infectious diseases are still issues at large in the less developed world.**

   The phrase, "…particularly in developed and developing countries", has been added (page 2, Section 1.1).

5. **Please cite the relevant reference(s) in which the term adiposopathy" was used.**

   An existing citation (Bays 2009 *Am. J. Med.*, 122: S26-S37) [61] has been added to indicate the use of "adiposopathy" (page 9, paragraph 1, last line).

6. **Page 12, line 13: "...associated with...", and not "...associated to..."**

   The use of "…associated to…" has been changed to "…associated with…" (page 9, paragraph 2, line 13).

7. **Page 28, end of paragraph 1: "...which will be discussed in...", and not "...which will be discussion in..."**

   The word "discussion" has been corrected to "discussed" (page 21, paragraph 2, last line).

8. **Page 32, paragraph 2, lines 4 – 5: "These issues have created a great deal...", and not "These issues create in a great deal..."**

   The incorrect phrase "These issues create in a great deal…" has been corrected to "These issues have created a great deal…" (page 24, paragraph 2, line 5).

9. **Page 73, paragraph 1, line 6: "....there is only one study reporting that the treatment...", and not "...one study reported that treatment..."; line 10: ""...in terms of the metabolic effects..." (missing "of" in the sentence)**

   The word "reported" has been corrected to "reporting"; "of" has been added as suggested (page 63, Section 1.5.1, line 4).

10. **Page 75, end of paragraph 2: "...to tackle MetS", and not, "...to tackle of MetS" (delete "of")**

    The prepositions "of" has been removed (page 65, paragraph 3, last line).

Chapter 3

11. **Page 100: Figure 3.2 is suggested to be converted into a colour figure to ensure clarity for the different groups that were plotted onto the graph.**

    Figure 3.2 has been changed to a coloured figure (page 89).

12. **Page 105-106, Figures 3.6 and 3.7 are also suggested to be coloured; likewise for Figure 3.11 (A) and (B), page 110.**

    Figures 3.6, 3.7 and 3.11 (A) and (B) have been changed to coloured figures (pages 95, 96 and 100).

13. **Page 119, paragraph 3, line 5: As pointed out in "a certain study" or "certain studies"? Please provide the relevant citations to this study or these studies.**

    The sentence has been changed to "As pointed out in a previous study,…" and the relevant citation (Spigoni et al. 2016 *Molecules*, 21:1009) [255] has been added (page 108, paragraph 3, line 5).

Chapter 4

14. **Page 122, paragraph 2, line 5: please elaborate what is meant by "mitochondrial overdrive".**

    The term, "mitochondrial overdrive" means excessive mitochondrial activity. The term has been changed to "mitochondrial over-activity" to minimize confusion. Furthermore, the sentence has been rephrased to the following to elaborate the occurrence of mitochondrial over-activity and how this process leads to ROS generation

    "Under over-nutrition state, the constant influx of oxidizable substrates trigger mitochondrial over-activity, which leads to an increased mitochondrial membrane potential and impaired oxidative phosphorylation, facilitating the interaction between electrons from the respiratory chain directly with oxygen to produce an excessive amount of ROS [258]." (page 111, paragraph 2, line 4).

15. **Page 124, line 4: delete "which" in the sentence "....AGE-RAGE axis which is not well-elaborated"**

    The word, "which" has been removed (page 112, paragraph 3, last line).

16. **Page 129: it would be helpful at this stage to briefly describe the role of myeloperoxidase and the significance of the increase in its activity following HFD as this was not apparent in the Introduction to this Chapter.**

    The following sentence has been added to elaborate the role of myeloperoxidase, "*To elaborate, myeloperoxidase which can generate reactive radicals during pathogenic infection, also serves as an oxidative stress biomarker in many chronic diseases*." (page 118, Section 4.4.1, paragraph 2, line 3)

17. **Page 135, lines 3 – 4: citation is needed for the statement "IL-10, which is an anti-inflammatory cytokine, the other cytokines are closely associated to inflammatory response"**

    A citation (Akdis et al. 2016, *J. Allergy Clin. Immunol.*, 138: 984-1010) [273] has been added (page 124, paragraph 1, last line).

18. **Page 138, lines 2 – 3: how many folds was the *RAGE* overexpression observed in the liver specimens of rats on HFD? Please state here.**

    The *RAGE* expression was upregulated by 2.4-fold in the rats on HFD compared to those on CD. The fold change has been added (page 127, paragraph 1, line 1).

19. **Page 139: final lines – please provide citation(s) for the statement made here regarding myeloperoxidase hyperactivity.**

    Two citations (Karakas & Koenig 2012, *Curr. Atheroscler. Rep.*, 14: 277-283 and Kataoka et al. 2014 *Atherosclerosis*, 232: 377-383) [293, 294] have been added (page 128, paragraph 2, line 3).

Chapter 5

20. **Page 147, paragraph 1, line 5: "insulin antagonists", instead of "insulin antagonistic"**

    The phrase, "insulin antagonistic" has been changed to "insulin antagonists", but the entire paragraph has been removed in response to Comment 2 from Examiner #2.

21. **Page 148, paragraph 2, line 2: "...potential mechanisms of geraniin action" (add the word "action").**

    The word "action" has been added (page 135, paragraph 3, last line).

22. **Page 149, third objective: Should this be "To outline the possible metabolic pathways affected by ellagitannin geraniin...", instead? (Suggest adding in the underlined words, "possible" and "affected").**

    The words "possible" and "affected" have been added (page 136, Section 5.2, third bullet point).

23. **Page 149, 5.3.1: Metformin and TRF-treated groups were excluded from the RNASeq analysis because "they were not of interest with regards to the objectives of the mechanistic study"? This examiner is of the opinion that this statement needs to be rephrased by replacing "not of interest" with other more suitable phrase such as "they would not contribute to the main objective" and/or "their addition would complicate the transcriptomic data analyses".**

The sentence has been modified as follows, "*This was because the comparisons of transcriptomes between these treatments and geraniin would not contribute to the main objective and their addition would complicate the transcriptomic data analysis.*" (page 137, Section 5.3.1, line 3)

24. **Page 149, 5.3.2: was the total RNA obtained from each group of 5 rats pooled together or were they subjected to RNASeq individually? This has to be better clarified here. From the results presented (sections 5.4.1 and 5.4.2), it appeared that the RNASeq was performed on the total RNA extracted from the liver of each individual rat. However, from 5.4.4 onwards it appeared as though the analyses were carried out as per group of rats (CD, HFD and geraniin). Hence, for instance in Figure 5.14, were the RNASeq results presented from the average of the 5 rats per group or were they from a specific individual rat used to represent the group? Likewise, for the Gene Ontology analyses, were the RNASeq data analysed as a group? These need to be properly clarified.**

    The mRNA samples of the rats were subjected to RNAseq individually. Hence, for each group, there were five biological replicates, each with a distinct sequencing data. For the downstream bioinformatics analysis like the identification of differentially expressed genes between groups, gene ontology and KEGG pathway analysis, the sequencing data from each biological replicate under the same treatment were analysed as a group. Therefore, the differences between groups (*i.e.* differentially expressed genes) were established based on the average of the biological replicates within a group, instead of a specific individual rat. To clarify these points, the following sentences in Sections 5.3.3 and 5.3.4 have been modified.

    - *Lastly, the libraries <u>which were prepared from individual mRNA samples</u> were subjected to multiplex sequencing (150bp paired-end) using Hiseq 4000 (Illumina, USA)* (page 138, Section 5.3.3, line 7).
    - *Differential expression analysis was carried out using DESeq2 (version 1.14.1) in R (version 3.3.2), <u>in which the five biological replicates given the same treatment were analyzed as a group and compared to other treatment groups</u>* (page 138, Section 5.3.4, line 12).

25. **Page 169, 5.4.5: the manner by which the genes *PPARα, PPARγ, Adh7* and *Ddhd1* were chosen to validate the RNASeq data by using qRT-PCR needs to be better presented. Earlier sections of this chapter should highlight the expression levels of these genes as**

determined by RNASeq, which would then justify their validation using qRT-PCR. However, although *PPARα* and *PPARγ* were genes "linked" to lipid metabolism, their expression levels were more or less consistent across the CD, HFD and geraniin-treated rats as shown in Figure 5.14. How would these results reconcile with those presented in the earlier Chapter 2 where it was stated that "PPARγ expression of the HFD-treated post-weaning rats also upregulated by 220% and 333% compared to the CD- and HFSD-treated rats" (page 87 of the thesis; page 748 of the manuscript in *J. Adv. Res.* 8 (2017): 743-752). In Figure 5.14B, there was hardly any change in the expression levels of *PPARγ* in rats on HFD and treated with geraniin. Were the RNASeq results presented here the average of the particular group of rats or just from a single individual rat representing the group? This also needs to be clarified either in the text or the legend to Figure 5.14.

The relative gene expression levels between groups (expressed in fold change) for *PPARα*, *PPARγ*, *Adh7* and *Ddhd1* genes have been added to Section 5.4.5 to clarify the comparisons between qPCR and RNA sequencing results (page 157, Section 5.4.5, line 5). Like previous analysis, the RNA sequencing results were based on the average of all five biological replicates within the same group instead of a single individual rat. The sample sizes of each group has been added to the description of Figure 5.14 to avoid confusion (page 158).

Indeed, the inconsistency of the hepatic *PPARγ* expression between the experiments outlined in Chapters 2 and 5 is rather puzzling. However, the hepatic *PPARγ* expression of the adult rats given high-calorie diets in the experiment described in Chapter 2 also remained unchanged compared to the control group. This would suggest that the activation of hepatic *PPARγ* is probably age-dependent. Indeed, one study reported that the activation of *PPARγ* induced by ischemic stress differed significantly between ages, whereby the gene remained activated for a longer period of time in young mice, but not adult and old mice (Shin et al. 2008). Such a prolonged activation of *PPARγ* could serve as a hepatoprotective mechanism in young rodents whose livers are relatively under-developed. Even though the hepatic stressor used in our study is different, the age-dependent *PPARγ* activation may explain the lack of *PPARγ* overexpression in older rats (12 weeks) on HFD. However, further investigation is required to verify the postulation. The above explanation has been added to the Discussion (page 159, paragraph 3, line 12).

26. **Page 171, paragraph 3: to what extent is the upregulation of the *Acsl3* gene observed in the study? Was the upregulation consistent in all the rats within that particular group? Likewise, for the *SREBP1* and *PPARδ* genes, were the overexpression levels**

observed significant? The earlier paragraph stated that there was high transcriptomic variability in response to HFD. If that is the case, do the genes presented here consistently show up- or down-regulation in all the rats within a particular group, or are there variations observed within a group, i.e., where in some rats, there was upregulation in the genes whereas in other rats, downregulation was observed. This has to be stated with clarity here as well as earlier (as in the previous comments above).

The upregulation of *Acsl3*, *Srebp1* and *PPARδ* genes of HFD group relative to CD group were statistical significant (p<0.05). The fold changes were 2.22, 1.91 and 2.27-fold for *Acsl3*, *Srebp1* and *PPARδ* genes respectively. These fold changes have been added into the Discussion (page 159, paragraph 3, lines 5 and 11) as well as Table 5.2 (page 145). The expression of *Acsl3*, *Srebp1* and *PPARδ* genes were consistent and unaffected by the high transcriptomic variability in the HFD group. The upregulation of these genes were also consistently found in all the biological replicates in the HFD groups because the 95% confidence intervals for the fold change of *Acsl3, Srebp1* and *PPARδ* genes relative to CD group were 1.81 to 2.71-fold, 1.47 to 2.47-fold and 1.66 to 3.10-fold respectively. It should be noted that only genes that were differentially expressed between groups (p<0.05) were used for the downstream analysis and discussed in further details in the Discussion as mentioned in Section 5.3.5 (page 139, Section 5.3.5, line 3).

27. **Page 172, paragraph 2: how many folds were the *Fabp1* and *Fabp2* genes downregulated in the geraniin-treated rats?**

Fabp1 and *Fabp2* genes were downregulated by 1.55 and 1.78-fold in the geraniin-treated rats compared to those on HFD. The fold changes have been into the Discussion (page 161, paragraph 1, line 5) and Table 5.3 (page 147).

28. **Page 174, paragraph 3, lines 3 – 4: What is meant by "...positive correlation between mitochondrial proteins and DNA with BMI"? Please elaborate.**

The phrase "…positive correlation between mitochondrial proteins and DNA with BMI" means the amount of mitochondrial genomes as well as protein activity found specifically in mitochondria seemed to increase in people with higher BMI. The sentence has been modified as follows to provide clearer elaboration.

"*Some studies concluded a positive correlation between mitochondria proteins and DNA with BMI, whereby the circular mitochondrial genomes as well as mitochondrial citrate synthase activity were significantly increased in obese patients, especially among those without diabetes mellitus [397,398]. This reflects a compensatory mechanism by increasing*

the number of mitochondria in response to the progression of mitochondrial impairment caused by nutritional insults." (page 163, paragraph 3, line 4)

Chapter 6

29. **Page 181, end of paragraph 1: "...selected as the disease model for the subsequent experiments" (replace "following" with "subsequent"; experiments"–plural.**

    The word, "following" has been replaced with "subsequent". The word "experiment" remains as a singular noun because only one animal experiment was performed (page 169, paragraph 1, last line).

30. **Page 185, paragraph 2: "The biologically functional molecules are the metabolites of geraniin like gallic acid, ellagic acid, brevifolincarboxylic acid and a wide variety of urolinths", these molecules were not validated in this study but were obtained from previous papers. This should be stated clearly here.**

    The sentences have been rephrased (as follows) to clarify that the molecules were not tested in the present study.

    "*Based on studies from other research groups, the biologically functional molecules are the metabolites of geraniin like gallic acid, ellagic acid, brevifolincarboxylic acid and a wide variety of urolithins [292, 412]. However, the geraniin-derived metabolites were not validated in the present study and so, whether they possess similar bioactivities and potency as geraniin against MetS is unclear.*" (page 173, paragraph 2, line 2)

31. **Besides suggesting further transcriptomic work on other organs, there are also proteomics plus metabolomics work that could answer some of the questions posed by the results of this study.**

    The following sentences have been added to suggest the use of integrative –omics techniques, including transcriptomics, proteomics and metabolomics to understand and validate the molecular basis of geraniin.

    "*Additionally, other high-throughput –omics techniques like proteomics and metabolomics are also exceedingly useful. Integrating datasets from several –omics analyses has become increasingly popular for the identification of metabolic pathways implicated in disease progression and drug response [413, 414]. Thus, a combinatory approach consisting of transcriptomics, proteomics and metabolomics can be utilized to understand and validate the molecular basis of geraniin and its metabolites in chronic metabolic diseases.*" (page 174, paragraph 3, line 8)

Responses to Professor Lee Kok Onn's comments

Major Comments

1. **The thesis should not include within the main text PDFs of publications as part of the thesis. This is unacceptable. If the University of Monash accepts this, then perhaps another examiner can be found. There are two reasons:**
   - **The publications are multi-authored and thus indicate that these portions of the thesis are substantially contributed by the other co-authors, and thus should have no place within a thesis – which all candidates will state that this is all work done (intellectual and experimental) by the candidate themselves.**
   - **There is significant repetition within these publications of introduction, methods, discussion and references. The candidate must include only directly relevant material, with removal of all repetitive references, discussion, methods, etc.**

   The concerns of the examiner about the inclusion of published manuscripts in the thesis is reasonable and understandable. Essentially, this is a thesis including published works which is one of the thesis formats accepted by Monash University. All the guidelines required for a submission of thesis including published works have been fulfilled. A declaration (page IV) has also been made by me and my main supervisor to clarify the thesis format and contributions of every author to the publications. In this context, for a multi-authored publication to be included into the thesis, a student should have a substantial and significant contribution (>50%). This criterion has been fulfilled for both the included publications based on the declaration. I hope this could ease the examiner's concerns about my contribution to the published works.

   It is also understood that there are repetitive contents in the introduction, methods, discussion and references. Some of these information is necessary to link the publications to the theme of the thesis. In this case, Sections 1.4.2, 2.1, 2.3 and 2.4 have been revised to remove repetitive contents. The details about the modifications can be referred to the response to Comment 2.

2. **This thesis is very long, and contains significant amounts of irrelevant discussion and postulations that are NOT warranted or even related to the experimental results presented. The candidate must shorten the introduction and the discussion portions and remove the irrelevant and speculative discussions. The thesis can be shortened by half, and with only three quarters of the references. In this era of huge overload of**

scientific information, concise presentations are a requirement as evidence of scientific ability.

- The introduction (Chapter 1) has been greatly shortened by 10 pages (from 75 pages to 65 pages). The detailed information about the changes made is as follows:
  - Section 1.1.1 – Removed two paragraphs that describe the reasons that led to the definition of MetS by WHO and modifications of the MetS definitions over time.
  - Section 1.1.2 – Removed the first two introductory sentences in the first paragraph
  - Section 1.1.3 – Removed one sentence in the second paragraph that describes increased MetS rate among patients with psychiatric disorders.
  - Section 1.1.4 – Removed four introductory sentences about modern diets in the first paragraphs
  - Section 1.1.5 **–** The whole section which outlines the socioeconomic burdens of metabolic syndrome has been removed.
  - Section 1.2 – Removed two introductory sentences
  - Section 1.2.1 – Removed one sentence in the first and last paragraphs respectively that describes the therapy for pediatrics patients.
  - Section 1.2.2 – Removed detailed descriptions about anti-obesity agents like sympathomimetics, serotonin-releasing agents, sibutramine, rimonabant and lorcaserin in the first two paragraphs.
  - Section 1.2.3 – Removed two introductory sentences in the first paragraph as well as information about anorexigenic peptides other than GLP-1, sub-classes of polyphenols, definition of fecal microbiota transplantation, scepticism to "polypills", various PPAR receptors and redundant concluding remarks.
  - Section 1.3.1 – Removed information about uncommon rodent species as the models of chronic diseases in the first paragraph. Removed information about forced exercises to simulate physical activity in third paragraphs. Removed the entire paragraph about the use of cafeteria diet for MetS induction. Removed two paragraphs about chemically-induced MetS models.
  - Section 1.3.2 – Removed two introductory sentences in the first paragraph and one concluding sentence in the last paragraph.
  - Section 1.3.3 – Removed one paragraph about cafeteria diet.
  - Section 1.4 – Removed an introductory sentence and description about metformin
  - Section 1.4.2 – Removed an introductory paragraph

- Section 1.5.3 – Rephrased the elaborations about the usefulness of a reproducible MetS induction approach across different strains and species.

❖ Chapter 2 has been reduced by 1 page (16 pages to 15 pages).

- Section 2.1 – Removed three introductory sentences in the first paragraph
- Section 2.3 – Removed Table 2.1
- Section 2.4 – Removed elaborations about the experimental results and only included statements about the key findings.

❖ The page number of Chapter 3 remained unchanged (28 pages), but certain contents have been removed.

- Section 3.1 – Removed two introductory sentences in the first paragraph
- Section 3.5 – Removed three paragraphs about geraniin-derived metabolites with eNOS and bioactivities of urolithins.

❖ Chapter 4 has been reduced by 1 page (24 pages to 23 pages).

- Section 4.1 – Removed one introductory sentences in the first paragraph, some information about ROS and elaboration about AGE-RAGE axis and metabolic memory.
- Section 4.5 – Removed descriptions about Nrf2 and autophagy and detailed elaborations about IL-10.

❖ The page number of Chapter 5 remained unchanged (33 pages), but certain contents have been removed.

- Section 5.1 – Removed the first introductory paragraph
- Section 5.5 – Removed one paragraph about mitochondrial dysfunction and some elaborations about Sirt1 and its roles in mitochondrial function.

❖ Overall, 12 pages of contents have been removed from the thesis. The reference list has also been reduced from 506 to 414 citations.

3. **It is unclear how many experiments were done – were the animal groups of n=6 in Chapters 3 AND Chapter 4 the same experiment, or were the animals in Chapter 4 studied AFTER Chapter 3? Similarly with the experimental animals in Chapter 5 – were they the same animals as in Chapter 3 and 4 – or a whole different series. This has to be clearly stated in the thesis, and should be easily verifiable from the animals purchased, and animal housed in the University.**

   The experiment described in Chapters 3, 4 and 5 is the same experiment. Only one animal experimentation has been performed. The blood and tissue samples of the rats from

different groups were harvested for the assays outlined in the three chapters. The following sentence has been added to Sections 4.3.1 and 5.3.1 to clarify that the blood and tissue samples used in the respective chapters were harvested from the experiment done in Chapter 3.

- *The blood and tissue specimens used in this chapter were taken from the experiment done in Chapter 3.* (page 113, Section 4.3.1, line 1 & page 137, Section 5.3.1, line 1)

4. **The Appendix attached a publication in NUTRIENTS 2017. The figures are almost identical with the figures (with the Geraniin data omitted) in Chapter 3 of the thesis – e.g Figures 3.6 and 3.7, etc. However, the publication states that the number of animals per group was different. This discrepancy needs to be clarified, and verified.**
   There was a mistake with the sample size presented in Chapters 3 and 4. For CD, HFD, metformin and TRF groups, the sample size per group was n=7 whereas for geraniin group, the sample size was n=6. Fewer rats were used for geraniin group because the amount of geraniin isolated from the rambutan rind was limited. Therefore, the number of animals shown in Appendix E2 was correct. The incorrect information about the sample size in Figures 3.1 and 4.1 (pages 85 & 114) as well as those in the figure descriptions (Figures 3.2 to 3.15 and Figures 4.2 to 4.9) have been corrected.
5. **With the above serious concerns, if adequately clarified, the experimental work and results presented are clearly sufficient and clearly of a standard worthy of a PhD.**
   The comment is a statement about the standard of the thesis and no modification is required.

Detailed Comments on the Thesis

6. **The Title and Introduction of the Thesis does not reflect that a major portion of the work was in development of a model for study with different feeding dietary regimes. If the candidate feels that this is important enough for 1 attached PDF publication, and a whole chapter, perhaps the title and Abstract should be amended to reflect this.**
   The thesis title has been changed to "Optimization of Metabolic Syndrome Induction in Rats for the Investigation of Metabolic Effects and Mechanisms of Ellagitannin Geraniin". This is to reflect the development of a metabolic syndrome rat model. The key findings of the model establishment were included in the Abstract (page I, lines 7 to 15). The key challenges in the creation of diet-induced metabolic syndrome models have also been introduced in Introduction (page 19, Section 1.3).
7. **The Design of all the Experiments, in chapters 3, 4 and 5, should have included 2 doses (at least) of the compound being studied. It would make the evidence much more**

convincing if a dose effect was present in the results, rather than just a single comparative dose. Why and how was this dose chosen for this particular mouse MetS model – were there initial pilot experiments to choose this dose?

The dosage (25 mg/kg/day) was selected based on a pilot study that used a range of geraniin concentrations from 12.5 to 100 mg/kg/day. We found no increase in the treatment effects based on simple tests like fasting blood glucose, blood pressure and fasting insulin levels beyond a daily dosage of 25 mg/kg and thus, the dosage was chosen for more in-depth investigation of its metabolic effects and underlying mechanisms. The rationale for the selection of dosages used in the study has been outlined in Table 3.1 (page 86).

8. **There is NO comparison with previous studies. The candidate mentions that there was only 1 previous study – this should make it easier to compare the results. The Discussions hardly mention or refer to that. Any similarities or differences should then be discussed. Instead there are long speculative paragraphs which are not relevant to the results presented in each long discussion after the results. Example: eNOS was not measured, bioactivities were not studied – why have such a long discussion on these? Discussion should focus on the results presented, the interesting and puzzling findings.**

   The comparison between the present and previous studies were included in the in the original Discussion (page 107, paragraph 2, line 7**)**. To provide a comprehensive discussion, more detailed comparisons between the two studies have been added into the same paragraph. For instance, marked lipid-lowering and anti-hyperglycemic activities of geraniin were consistently found in both studies. However, the previous study reported an improvement of insulin sensitivity upon geraniin treatment, which was not found in our study (page 107, paragraph 2, line 9**)**. Paragraphs which are not related to the results (*e.g.* eNOS) have been removed. Detailed information about the modifications in Section 3.5 can be referred to the response to Comment 2.

9. **Chapter 3. Would another measure of glucose control e.g. Fructosamine or Glycated Albumin be more useful if the treatment duration was only 4 weeks? Was this considered by the candidate?**

   In this study, several indicators of glucose homeostasis have been used including fasting blood glucose, glycated hemoglobin (HbA1c) and oral glucose tolerance test. Even though the fructosamines and glycated albumins, which are glycation products that can reflect short-term glucose control, had not been considered in the study, the circulating concentration of a glycation product known as advanced glycation end product (AGE) was

measured and presented in Figure 4.6 (page 122). The AGE levels in the blood circulation can serve as a biomarker of glucose control and oxidative stress. Basically, the glucose control markers, particularly fasting blood glucose, HbA1c and AGE were in agreement with each other. Therefore, additional biomarkers may not be necessary. However, the suggestion to measure fructosamine or glycated albumin in order to determine short-term glucose control due to the relatively short treatment period has been added into Section 3.5 (page 105, paragraph 2, line 13**).**

10. **Chapter 3. Figure 3.9 compared to Figure 3.10. Does the magnitude of change in fasting glucose show some discrepancy with the magnitude of change in HbA1c? It would have been useful to have some discussion and attempt to discuss the differences.**
    For metformin- and geraniin-treated rats, the results of fasting blood glucose were in line with that of HbA1c whereby both glycemic indices were significantly reduced after the four-week treatment in comparison to the HFD group. These were mentioned and discussed in the original version (page 104, Section 3.5, paragraph 2, line 1 for metformin; page 105, paragraph 2, line 1 for geraniin). For TRF-treated rats, there was a significant decline in HbA1c, but not fasting blood glucose. Such a discrepancy is likely because of the antioxidant effect of tocotrienols which can inhibit the glycation reaction. The discussion about the observed discrepancy has been added (page 107, paragraph 1, line 7**)**.
11. **Chapter 3. Figures 3.6 and 3.7. Repeated measurements of Systolic and Diastolic Blood Pressure should ideally be assessed statistically by ANOVA for repeated measurements – as correctly stated in the Statistical methods. Why were only the individual time point differences given? The data in the text describing the differences should also be put in a table. As already stated in Comment 4 above, the figures look almost identical to the publication in NUTRIENTS 2017 in the Appendix but that was for n=7.**
    A new table (Table 3.3; page 94) has been added to tabulate the data of systolic and diastolic blood pressure levels. The *p*-values for the main effects (treatment group and time) and interaction (treatment group*time) resulted from the repeated measures ANOVA were also provided in the table. The sample size mentioned in Figures 3.6 and 3.7 was incorrect. The mistake has been rectified as mentioned in the response to Comment 4.
12. **Chapter 4. (Also in earlier Chapter 3 Methods). Multiplex measurements using single bead technology usually requires independent verification when an important difference in found. This is especially important if the values are close to either end of the range in the multiplex. Many laboratories have used multiplex as an initial**

screening tool, and then re-assayed using a good validated single compound assay. The candidate should perhaps discuss some of the limitations of the study, and not be too overenthusiastic throughout.

The limitations of the multiplex measurement technique used for cytokine profiling have been added (page 132, paragraph 2, line 13**)**. The suggestion to validate the cytokine results with more specific uniplex assays has also been added into the conclusion (page 133, last paragraph, line 8**)**.

13. **Chapter 5. Snapshots of Transcriptomes have as much value as snapshots of miRNA and Proteomic snapshots. With an n=5 the candidate should again discuss some of the limitations of the data presented. The comparison of changes would, at most, give suggestions for further hypothesis generation, and further experiments. It does not provide hard evidence for mechanisms of action for any new experimental compound. Conclusions should be much more restrained.**

    The limitations of the transcriptomic study performed in the present study have been added (page 165, paragraph 4, line 9**)**. The conclusion has also emphasized that the results generated from the transcriptomic study were exploratory and hence, further validation is necessary to provide solid evidence of the mechanism of geraniin (page 167, last paragraph, line 13**)**.

14. **The grammar and spelling is excellent throughout.**

    The comment is a statement which requires no modification.